Thu. May 30, 2019

[E] Poster | P (Space and Planetary Sciences)：P-EM Solar-Terrestrial Sciences, Space Electromagnetism & Space Environment

3:30 PM - 5:00 PM JST | 6:30 AM - 8:00 AM UTC | Poster Hall International Exhibition Hall8, Makuhari Messe_2

[P-EM15] Study of coupling processes in solar-terrestrial system

convener:Mamoru Yamamoto(Research Institute for Sustainable Humanosphere, Kyoto University), Yasunobu Ogawa(National Institute of Polar Research), Satonori Nozawa(Institute for Space-Earth Environment Research), Akimasa Yoshikawa(Department of Earth and Planetary Sciences, Kyushu University)

[PEM15-P01] Study on adaptive clutter rejection system using external receiving antennas for the MU radar

*Hiroyuki Hashiguchi[1], Issei Terada[1], Mamoru Yamamoto[1] (1.Research Institute for Sustainable Humanosphere, Kyoto University)

[PEM15-P02] Detached cusp aurora for southward IMF

*Kohei Takasu[1], Satoshi Taguchi[1], Keisuke Hosokawa[2] (1.Department of Geophysics, Graduate School of Science, Kyoto University, 2.Department of Communication Engineering and Informatics, University of Electro-Communications)

[PEM15-P03] Motion of the inverted-V structure during an isolated substorm

*Morio Tanaka[1], Satoshi Taguchi[1], Kohei Takasu[1], Tomokazu Oigawa[1], Keisuke Hosokawa[2] (1.Department of Geophysics, Graduate school of science, Kyoto University, 2.Department of Communication Engineering and Informatics, University of Electro-Communications)

[PEM15-P04] Observation and modeling of Na layer response to energetic particle precipitation

*Takuo T. Tsuda[1], Kyogo Takizawa[1], Ryo Tozu[1], Takuya Kawahara[2], Yoshimasa Tanaka[3], Mitsumu K. Ejiri[3], Takanori Nishiyama[3], Takuji Nakamura[3] (1.The University of Electro-Communications, 2.Shinshu University, 3.National Institute of Polar Research)

[PEM15-P05] Lidar data analysis of the sodium atoms in the thermosphere observed at Tromsoe, Norway

*Takuya Kawahara[1], Satonori Nozawa[2], Norihito Saito[3], Takuo T. Tsuda[4], Toru Takahashi[5], Testuya Kawabata[2], Miki Nishimura[1], Yoshitaka Kobayashi[1] (1.Faculty of Engineering, Shinshu University, 2.ISEE, Nagoya University, 3.RIKEN, Center for Advanced Photonics, 4.The University of Electro-Communications, 5.National Institute of Polar Research)

[PEM15-P06] Spatial-temporal distribution of anomalous enhancement of ambipolar diffusion coefficient observed by meteor radars installed in the polar region

*Toru Takahashi[1], Masaki Tsutsumi[1,2], Yasunobu Ogawa[1,2,3], Satonori Nozawa[3], Chris Hall[4], Hiroshi Miyaoka[1,2] (1.National Institute of Polar Research, 2.SOKENDAI, 3.Institute for Space-Earth Environmental Research, 4.TGO, The Arctic University of Norway)

[PEM15-P07] Progress of ICSWSE and MAGDAS project in recent years

*Shuji Abe[1], Akimasa Yoshikawa[2,1], Teiji Uozumi[1], Akiko Fujimoto[3] (1.International Center for Space Weather Science and Education, Japan, 2.Department of Earth and Planetary Sciences, Kyushu University, 3.Kyushu Institute of Technology)

[PEM15-P08] Status of GNU Radio Beacon Receiver 2 (GRBR2) development

*Mamoru Yamamoto[1], Mayumi Matsunaga[2], Roland Tsunoda[3] (1.Research Institute for Sustainable Humanosphere, Kyoto University, 2.Tokyo University of Technology, 3.SRI International)

[PEM15-P09] Statistical comparison between plasma bubble day-to-day variability and neutral atmosphere by using GPS scintillation and GAIA model

*Mamoru Yamamoto[1], Keigo Kono[1] (1.Research Institute for Sustainable Humanosphere, Kyoto University)

[PEM15-P10] Redevelopment of the MU radar transceiver-module control system

*Mamoru Yamamoto[1], Koki Kurokawa[1], Hiroyuki Hashiguchi[1] (1.Research Institute for Sustainable Humanosphere, Kyoto University)

[E] Poster | P (Space and Planetary Sciences)：P-EM Solar-Terrestrial Sciences, Space Electromagnetism & Space Environment

5:15 PM - 6:30 PM JST | 8:15 AM - 9:30 AM UTC | Poster Hall International Exhibition Hall8, Makuhari Messe_2

[P-EM15] Study of coupling processes in solar-terrestrial system

convener:Mamoru Yamamoto(Research Institute for Sustainable Humanosphere, Kyoto University), Yasunobu Ogawa(National Institute of Polar Research), Satonori Nozawa(Institute for Space-Earth Environment Research), Akimasa Yoshikawa(Department of Earth and Planetary Sciences, Kyushu University)

[PEM15-P01] Study on adaptive clutter rejection system using external receiving antennas for the MU radar

*Hiroyuki Hashiguchi[1], Issei Terada[1], Mamoru Yamamoto[1] (1.Research Institute for Sustainable Humanosphere, Kyoto University)

[PEM15-P02] Detached cusp aurora for southward IMF

*Kohei Takasu[1], Satoshi Taguchi[1], Keisuke Hosokawa[2] (1.Department of Geophysics, Graduate School of Science, Kyoto University, 2.Department of Communication Engineering and Informatics, University of Electro-Communications)

[PEM15-P03] Motion of the inverted-V structure during an isolated substorm

*Morio Tanaka[1], Satoshi Taguchi[1], Kohei Takasu[1], Tomokazu Oigawa[1], Keisuke Hosokawa[2] (1.Department of Geophysics, Graduate school of science, Kyoto University, 2.Department of Communication Engineering and Informatics, University of Electro-Communications)

[PEM15-P04] Observation and modeling of Na layer response to energetic particle precipitation

*Takuo T. Tsuda[1], Kyogo Takizawa[1], Ryo Tozu[1], Takuya Kawahara[2], Yoshimasa Tanaka[3], Mitsumu K. Ejiri[3], Takanori Nishiyama[3], Takuji Nakamura[3] (1.The University of Electro-Communications, 2.Shinshu University, 3.National Institute of Polar Research)

[PEM15-P05] Lidar data analysis of the sodium atoms in the thermosphere observed at Tromsoe, Norway

*Takuya Kawahara[1], Satonori Nozawa[2], Norihito Saito[3], Takuo T. Tsuda[4], Toru Takahashi[5], Testuya Kawabata[2], Miki Nishimura[1], Yoshitaka Kobayashi[1] (1.Faculty of Engineering, Shinshu University, 2.ISEE, Nagoya University, 3.RIKEN, Center for Advanced Photonics, 4.The University of Electro-Communications, 5.National Institute of Polar Research)

[PEM15-P06] Spatial-temporal distribution of anomalous enhancement of ambipolar diffusion coefficient observed by meteor radars installed in the polar region

*Toru Takahashi[1], Masaki Tsutsumi[1,2], Yasunobu Ogawa[1,2,3], Satonori Nozawa[3], Chris Hall[4], Hiroshi Miyaoka[1,2] (1.National Institute of Polar Research, 2.SOKENDAI, 3.Institute for Space-Earth Environmental Research, 4.TGO, The Arctic University of Norway)

[PEM15-P07] Progress of ICSWSE and MAGDAS project in recent years

*Shuji Abe[1], Akimasa Yoshikawa[2,1], Teiji Uozumi[1], Akiko Fujimoto[3] (1.International Center for Space Weather Science and Education, Japan, 2.Department of Earth and Planetary Sciences, Kyushu University, 3.Kyushu Institute of Technology)

[PEM15-P08] Status of GNU Radio Beacon Receiver 2 (GRBR2) development

*Mamoru Yamamoto[1], Mayumi Matsunaga[2], Roland Tsunoda[3] (1.Research Institute for Sustainable Humanosphere, Kyoto University, 2.Tokyo University of Technology, 3.SRI International)

[PEM15-P09] Statistical comparison between plasma bubble day-to-day variability and neutral atmosphere by using GPS scintillation and GAIA model

*Mamoru Yamamoto[1], Keigo Kono[1] (1.Research Institute for Sustainable Humanosphere, Kyoto University)

[PEM15-P10] Redevelopment of the MU radar transceiver-module control system

*Mamoru Yamamoto[1], Koki Kurokawa[1], Hiroyuki Hashiguchi[1] (1.Research Institute for Sustainable Humanosphere, Kyoto University)

[E] Poster | A (Atmospheric and Hydrospheric Sciences)：A-AS Atmospheric Sciences, Meteorology & Atmospheric Environment

1:45 PM - 3:15 PM JST | 4:45 AM - 6:15 AM UTC | Poster Hall International Exhibition Hall8, Makuhari Messe_1

[A-AS02] Advances in Tropical Cyclone Research: Past, Present, and Future

convener:Sachie Kanada(Nagoya University), Akiyoshi Wada(Department of Typhoon and Severe Weather Research, Meteorological Research Institute), Kosuke Ito(University of the Ryukyus), Yoshiaki Miyamoto(Faculty of Environment and Information Studies, Keio University)

[AAS02-P01] Numerical study on lightning frequency in a tropical cyclone

*Yousuke Sato[1,3], Yoshiaki Miyamoto[2,3], Tomita Hirofumi[3] (1.Department of Applied Energy, Nagoya University, 2.Faculty of Environment and Information Studies, Keio University, 3.RIKEN Center for Computational Science)

[AAS02-P02] **Sensitivity of Numerical Simulation of Typhoon Nepartak (2016) to Cloud Condensation Nuclei Concentration**

*Yu-De Wu[1], Jian-Liang Wang[1] (1.Dept. of Environmental Informational and Engineering, Chung Cheng Institute of Technology, National Defense University, Taiwan)

[AAS02-P03] Moisture Budget Analysis for Hurricane Precipitation on Texas

*Satoshi Iizuka[1], Naoki Sakai[1] (1.National Research Institute for Earth Science and Disaster Resilience)

[AAS02-P04] Remote response of a developing tropical cyclone over the western North Pacific to large-scale vapor transport from the Kuroshio in boreal fall

*Keita Fujiwara[1], Ryuichi Kawamura[2], Tetsuya Kawano[2] (1.Graduate School of Science, Kyushu University, 2.Faculty of Science, Kyushu University)

[AAS02-P05] Asymmetrically Intensifying Processes of a Category 4 Super Typhoon Lan (2017) during High Vertical Wind Shear

*Sachie Kanada[1], Akiyoshi Wada[2], Kazuhisa Tsuboki[1] (1.Nagoya University, 2.Meteorological Research Institute)

[AAS02-P06] Roles of preexisting oceanic condition and ocean coupling processes in the intensity prediction during the mature phase of Typhoon Trami (2018)

*Akiyoshi Wada[1] (1.Typhoon Research Department Meteorological Research Institute)

[AAS02-P07] Development and assessment of the probabilistic storm surge forecast system in Taiwan: Case Study of Typhoon Maria in 2018

*Chun-Wei Lin[1], Tso-Ren Wu[1], Yu-Lin Tsai[1], Shu-Chun Chuang[1], Chi-Hao Chu[2], Chuen-Teyr Terng[2] (1.Graduate Institute of Hydrological and Oceanic Sciences, National Central University, Chungli, Taiwan, 2.Marine Meteorology Center, Central Weather Bureau, Taipei, Taiwan)

[AAS02-P08] Basic Data Construction for a Typhoon Disaster Prevention Model : Analysis and Changes by El Nino and La Nina year

*HANA NA[1], Woo-Sik Jung[1] (1.Department of Atmospheric Environment Information Engineering, Atmospheric Environment Information Research Center, Inje University, Gimhae 50834, Korea)

[AAS02-P09] Basic Data Construction for a Typhoon Disaster Prevention Model : Analysis According to the Typhoon Path Type

*HANA NA[1], Woo-Sik JUNG[1] (1.Department of Atmospheric Environment Information Engineering, Atmospheric Environment Information Research Center, Inje University, Gimhae 50834, Korea)

[AAS02-P10] Basic Data Construction for a Typhoon Disaster Prevention Model : Monthly Characteristics of Typhoon Rusa, Maemi, Kompasu, and Bolaven

*HANA NA[1], Woo-Sik Jung[1] (1.Department of Atmospheric Environment Information Engineering, Atmospheric Environment Information Research Center, Inje University, Gimhae 50834, Korea)

[AAS02-P11] The mechanism of typhoon generated in the earth that rotates in the space where the solar wind blows

*Shinji Karasawa[1] (1.Miyagi National College of Technology Professor emeritus)

[E] Poster | A (Atmospheric and Hydrospheric Sciences)：A-AS Atmospheric Sciences, Meteorology & Atmospheric Environment

5:15 PM - 6:30 PM JST | 8:15 AM - 9:30 AM UTC | Poster Hall International Exhibition Hall8, Makuhari Messe_5

[A-AS02] Advances in Tropical Cyclone Research: Past, Present, and Future

convener:Sachie Kanada(Nagoya University), Akiyoshi Wada(Department of Typhoon and Severe Weather Research, Meteorological Research Institute), Kosuke Ito(University of the Ryukyus), Yoshiaki Miyamoto(Faculty of Environment and Information Studies, Keio University)

[AAS02-P01] Numerical study on lightning frequency in a tropical cyclone

*Yousuke Sato[1,3], Yoshiaki Miyamoto[2,3], Tomita Hirofumi[3] (1.Department of Applied Energy, Nagoya University, 2.Faculty of Environment and Information Studies, Keio University, 3.RIKEN Center for Computational Science)

[AAS02-P02] **Sensitivity of Numerical Simulation of Typhoon Nepartak (2016) to Cloud Condensation Nuclei Concentration**

*Yu-De Wu[1], Jian-Liang Wang[1] (1.Dept. of Environmental Informational and Engineering, Chung Cheng Institute of Technology, National Defense University, Taiwan)

[AAS02-P03] Moisture Budget Analysis for Hurricane Precipitation on Texas

*Satoshi Iizuka[1], Naoki Sakai[1] (1.National Research Institute for Earth Science and Disaster Resilience)

[AAS02-P04] Remote response of a developing tropical cyclone over the western North Pacific to large-scale vapor transport from the Kuroshio in boreal fall

*Keita Fujiwara[1], Ryuichi Kawamura[2], Tetsuya Kawano[2] (1.Graduate School of Science, Kyushu University, 2.Faculty of Science, Kyushu University)

[AAS02-P05] Asymmetrically Intensifying Processes of a Category 4 Super Typhoon Lan (2017) during High Vertical Wind Shear

*Sachie Kanada[1], Akiyoshi Wada[2], Kazuhisa Tsuboki[1] (1.Nagoya University, 2.Meteorological Research Institute)

[AAS02-P06] Roles of preexisting oceanic condition and ocean coupling processes in the intensity prediction during the mature phase of Typhoon Trami (2018)

*Akiyoshi Wada[1] (1.Typhoon Research Department Meteorological Research Institute)

[AAS02-P07] Development and assessment of the probabilistic storm surge forecast system in Taiwan: Case Study of Typhoon Maria in 2018

*Chun-Wei Lin[1], Tso-Ren Wu[1], Yu-Lin Tsai[1], Shu-Chun Chuang[1], Chi-Hao Chu[2], Chuen-Teyr Terng[2] (1.Graduate Institute of Hydrological and Oceanic Sciences, National Central University, Chungli, Taiwan, 2.Marine Meteorology Center, Central Weather Bureau, Taipei, Taiwan)

[AAS02-P08] Basic Data Construction for a Typhoon Disaster Prevention Model : Analysis and Changes by El Nino and La Nina year

*HANA NA[1], Woo-Sik Jung[1] (1.Department of Atmospheric Environment Information Engineering, Atmospheric Environment Information Research Center, Inje University, Gimhae 50834, Korea)

[AAS02-P09] Basic Data Construction for a Typhoon Disaster Prevention Model : Analysis According to the Typhoon Path Type

*HANA NA[1], Woo-Sik JUNG[1] (1.Department of Atmospheric Environment Information Engineering, Atmospheric Environment Information Research Center, Inje University, Gimhae 50834, Korea)

[AAS02-P10] Basic Data Construction for a Typhoon Disaster Prevention Model : Monthly Characteristics of Typhoon Rusa, Maemi, Kompasu, and Bolaven

*HANA NA[1], Woo-Sik Jung[1] (1.Department of Atmospheric Environment Information Engineering, Atmospheric Environment Information Research Center, Inje University, Gimhae 50834, Korea)

[AAS02-P11] The mechanism of typhoon generated in the earth that rotates in the space where the solar wind blows

*Shinji Karasawa[1] (1.Miyagi National College of Technology Professor emeritus)

[E] Poster | A (Atmospheric and Hydrospheric Sciences)：A-OS Ocean Sciences & Ocean Environment

10:45 AM - 12:15 PM JST | 1:45 AM - 3:15 AM UTC | Poster Hall International Exhibition Hall8, Makuhari Messe_2

[A-OS07] Climate variability and predictability on subseasonal to decadal timescales

convener:Takashi Mochizuki(Japan Agency for Marine-Earth Science and Technology), V Ramaswamy(NOAA GFDL), Doug Smith(Met Office), Yushi Morioka(Japan Agency for Marine-Earth Science and Technology)

[AOS07-P01] Changes in North American and European Heatwave Characteristics

*Szandra A. Peter[1], Ben Kirtman[1] (1.Rosenstiel School of Marine and Atmospheric Science)

[AOS07-P02] **The effects of the "New Climate" Warming on Western Mediterranean: Situation of the Recent Extreme Events**

*Mohammed-Said KARROUK[1] (1.Hassan II University of Casablanca)

[AOS07-P03] **Month-to-month Difference of the Western Pacific Subtropical High Simulated by CMIP5 Models**

*Xiao Dong[1], Renping Lin[1] (1.Institute of Atmospheric Physics)

[AOS07-P04] Potential regulation on the climatic effect of Tibetan Plateau heating by tropical air–sea coupling

*Ziqian Wang[1], Anmin Duan[2], Song Yang[1] (1.School of Atmospheric Sciences, Sun Yat-sen University, 2.Institute of Atmospheric Physics, Chinese Academy of Sciences)

[AOS07-P05] Intraseasonal variation of the South Asian high and its role in connecting the Indian and East Asian summer monsoons

*Wei Wei[1] (1.Sun Yat-sen University)

[AOS07-P06] Mean Surface Air Temperatures in Japan - Regional Classification and Interranual Variability

*Pascal Oettli[1], Masami Nonaka[1], Swadhin Behera[1] (1.Japan Agency for Marine-Earth Science and Technology)

[AOS07-P07] Inter-Annual Variability of the Indonesian Rainfall and Air-Sea Interaction over the Indian-Pacific Ocean Associated with Regime Shift

*Murni Ngestu Nurutami[1], Tadahiro Hayasaka[1] (1.Center for Atmospheric and Oceanic Studies, Graduate School of Science, Tohoku University)

[AOS07-P08] Exploring synoptic-scale drivers of interannual rainfall variability over Africa

*Piotr Wolski[1], Chris Jack[1], Waarith Abrahams[1], Stefaan Conradie[1] (1.University of Cape Town)

[AOS07-P09] **Effect of El Niño on the response ratio of Hadley circulation to different SST meridional structures**

*Juan Feng[1] (1.Beijing Normal University)

[AOS07-P10] **Novel data-driven approach for ENSO prediction**

*Dmitri Kondrashov[1], Evgeniy Loskutov[2], Andrei Gavrilov[2], Dmitry Mukhin[2], Alexander Feigin[2] (1.University of California, Los Angeles, United States, 2.Institute of Applied Physics of the Russian Academy of Sciences, Nizhny Novgorod, Russian Federation)

[AOS07-P11] Experimental seasonal climate prediction using CFES: Comparison with the SINTEX-F systems

*Nobumasa Komori[1], Bunmei Taguchi[2], Akira Kuwano-Yoshida[3,1], Takeshi Doi[1], Masami Nonaka[1] (1.Japan Agency for Marine-Earth Science and Technology, 2.Research Center for Advanced Science and Technology, The University of Tokyo, 3.Disaster Prevention Research Institute, Kyoto University)

[AOS07-P12] Exploring the SST error growth during ENSO developing phase by using BCC_CSM1.1(m)

*Ben Tian[1], Hongli Ren[1] (1.National Climate Center, China Meteorological Administration)

[AOS07-P13] Role of sea-ice initialization in climate predictability over the Weddell Sea

*Yushi Morioka[1], Takeshi Doi[1], Doroteaciro Iovino[2], Simona Masina[2], Swadhin Behera[1] (1.Japan Agency for Marine-Earth Science and Technology (JAMSTEC), 2.Centro Euro-Mediterraneo sui Cambiamenti Climatici (CMCC))

[AOS07-P14] Observed and hindcasted subdecadal variability of the tropical Pacific climate

*Takashi Mochizuki[1], Masahiro Watanabe[2] (1.Japan Agency for Marine-Earth Science and Technology, 2.Atmosphere-Ocean Research Institute, The University of Tokyo)

[E] Poster | A (Atmospheric and Hydrospheric Sciences)：A-OS Ocean Sciences & Ocean Environment

5:15 PM - 6:30 PM JST | 8:15 AM - 9:30 AM UTC | Poster Hall International Exhibition Hall8, Makuhari Messe_7

[A-OS07] Climate variability and predictability on subseasonal to decadal timescales

convener:Takashi Mochizuki(Japan Agency for Marine-Earth Science and Technology), V Ramaswamy(NOAA GFDL), Doug Smith(Met Office), Yushi Morioka(Japan Agency for Marine-Earth Science and Technology)

[AOS07-P01] Changes in North American and European Heatwave Characteristics

*Szandra A. Peter[1], Ben Kirtman[1] (1.Rosenstiel School of Marine and Atmospheric Science)

[AOS07-P02] **The effects of the "New Climate" Warming on Western Mediterranean: Situation of the Recent Extreme Events**

*Mohammed-Said KARROUK[1] (1.Hassan II University of Casablanca)

[AOS07-P03] **Month-to-month Difference of the Western Pacific Subtropical High Simulated by CMIP5 Models**

*Xiao Dong[1], Renping Lin[1] (1.Institute of Atmospheric Physics)

[AOS07-P04] Potential regulation on the climatic effect of Tibetan Plateau heating by tropical air–sea coupling

*Ziqian Wang[1], Anmin Duan[2], Song Yang[1] (1.School of Atmospheric Sciences, Sun Yat-sen University, 2.Institute of Atmospheric Physics, Chinese Academy of Sciences)

[AOS07-P05] Intraseasonal variation of the South Asian high and its role in connecting the Indian and East Asian summer monsoons

*Wei Wei[1] (1.Sun Yat-sen University)

[AOS07-P06] Mean Surface Air Temperatures in Japan - Regional Classification and Interranual Variability

*Pascal Oettli[1], Masami Nonaka[1], Swadhin Behera[1] (1.Japan Agency for Marine-Earth Science and Technology)

[AOS07-P07] Inter-Annual Variability of the Indonesian Rainfall and Air-Sea Interaction over the Indian-Pacific Ocean Associated with Regime Shift

*Murni Ngestu Nurutami[1], Tadahiro Hayasaka[1] (1.Center for Atmospheric and Oceanic Studies, Graduate School of Science, Tohoku University)

[AOS07-P08] Exploring synoptic-scale drivers of interannual rainfall variability over Africa

*Piotr Wolski[1], Chris Jack[1], Waarith Abrahams[1], Stefaan Conradie[1] (1.University of Cape Town)

[AOS07-P09] **Effect of El Niño on the response ratio of Hadley circulation to different SST meridional structures**

*Juan Feng[1] (1.Beijing Normal University)

[AOS07-P10] **Novel data-driven approach for ENSO prediction**

*Dmitri Kondrashov[1], Evgeniy Loskutov[2], Andrei Gavrilov[2], Dmitry Mukhin[2], Alexander Feigin[2] (1.University of California, Los Angeles, United States, 2.Institute of Applied Physics of the Russian Academy of Sciences, Nizhny Novgorod, Russian Federation)

[AOS07-P11] Experimental seasonal climate prediction using CFES: Comparison with the SINTEX-F systems

*Nobumasa Komori[1], Bunmei Taguchi[2], Akira Kuwano-Yoshida[3,1], Takeshi Doi[1], Masami Nonaka[1] (1.Japan Agency for Marine-Earth Science and Technology, 2.Research Center for Advanced Science and Technology, The University of Tokyo, 3.Disaster Prevention Research Institute, Kyoto University)

[AOS07-P12] Exploring the SST error growth during ENSO developing phase by using BCC_CSM1.1(m)

*Ben Tian[1], Hongli Ren[1] (1.National Climate Center, China Meteorological Administration)

[AOS07-P13] Role of sea-ice initialization in climate predictability over the Weddell Sea

*Yushi Morioka[1], Takeshi Doi[1], Doroteaciro Iovino[2], Simona Masina[2], Swadhin Behera[1] (1.Japan Agency for Marine-Earth Science and Technology (JAMSTEC), 2.Centro Euro-Mediterraneo sui Cambiamenti Climatici (CMCC))

[AOS07-P14] Observed and hindcasted subdecadal variability of the tropical Pacific climate

*Takashi Mochizuki[1], Masahiro Watanabe[2] (1.Japan Agency for Marine-Earth Science and Technology, 2.Atmosphere-Ocean Research Institute, The University of Tokyo)

[E] Poster | A (Atmospheric and Hydrospheric Sciences)：A-OS Ocean Sciences & Ocean Environment

3:30 PM - 5:00 PM JST | 6:30 AM - 8:00 AM UTC | Poster Hall International Exhibition Hall8, Makuhari Messe_4

[A-OS10] Atlantic climate variability, and its global impacts and predictability

convener:Ingo Richter(JAMSTEC Japan Agency for Marine-Earth Science and Technology), Hiroki Tokinaga(Research Institute for Applied Mechanics, Kyushu University), Noel S Keenlyside(Geophysical Institute Bergen), Carlos R Mechoso(University of California Los Angeles)

[AOS10-P01] The strengthening of Amazonian precipitation during the wet season driven by tropical sea surface temperature forcing

*Xinyue Wang[1], Xichen Li[1], Jiang Zhu[1], Clemente A S Tanajura[2] (1.Institute of Atmospheric Physics, Chinese Academy of Sciences, 2.Institute of Physics, Federal University of Bahia, Salvador, Brazil)

[AOS10-P02] **Linear inverse modeling of the tropical Atlantic**

*Ingo Richter[1], Ping Chang[2] (1.JAMSTEC Japan Agency for Marine-Earth Science and Technology, 2.Texas A&M University)

[AOS10-P03] Relationships Among Inter-model Spread and Biases in Tropical Atlantic Sea Surface Temperatures

Elsa - Mohino Harris[1], *Belen Rodriguez-Fonseca[1,2], Teresa - Losada[1], Irene - Polo[1], Roberto - Mechoso[3] (1.Department of Physics of the Earth and Astrophysics, Universidad Complutense de Madrid, 28040, Madrid, Spain. , 2.Institute of Geosciences IGEO,UCM-CSIC, 28040, Madrid, Spain., 3.Department of Atmospheric and Oceanic Sciences, UCLA, Los Angeles, USA)

[AOS10-P04] **Revisiting the CMIP5 Thermocline in the Equatorial Pacific and Atlantic Oceans**

Antonio - Castaño[1,2], Elsa - Mohino[1], *Belen Rodriguez-Fonseca[1,2], Teresa - Losada[1] (1.Department of Physics of the Earth and Astrophysics, Universidad Complutense de Madrid, 28040, Madrid, Spain., 2.Institute of Geosciences, IGEO, UCM-CSIC 28040, Madrid, Spain.)

[AOS10-P05] Lagged Effects of North Atlantic SST Anomalies on Weather in Remote Areas

*Natalia Gnatiuk[1], Timo Vihma[2], Leonid Bobylev[1] (1.Nansen International Environmental and Remote Sensing Centre, 2.Finnish Meteorological Institute)

[AOS10-P06] **SST anomalies in the northern tropical Atlantic as a negative feedback to ENSO development**

*Ingo Richter[1], Hiroki Tokinaga[2], Yu Kosaka[3], Takeshi Doi[1] (1.JAMSTEC Japan Agency for Marine-Earth Science and Technology, 2.Kyoto University, 3.University of Tokyo)

[E] Poster | A (Atmospheric and Hydrospheric Sciences)：A-OS Ocean Sciences & Ocean Environment

5:15 PM - 6:30 PM JST | 8:15 AM - 9:30 AM UTC | Poster Hall International Exhibition Hall8, Makuhari Messe_8

[A-OS10] Atlantic climate variability, and its global impacts and predictability

convener:Ingo Richter(JAMSTEC Japan Agency for Marine-Earth Science and Technology), Hiroki Tokinaga(Research Institute for Applied Mechanics, Kyushu University), Noel S Keenlyside(Geophysical Institute Bergen), Carlos R Mechoso(University of California Los Angeles)

[AOS10-P01] The strengthening of Amazonian precipitation during the wet season driven by tropical sea surface temperature forcing

*Xinyue Wang[1], Xichen Li[1], Jiang Zhu[1], Clemente A S Tanajura[2] (1.Institute of Atmospheric Physics, Chinese Academy of Sciences, 2.Institute of Physics, Federal University of Bahia, Salvador, Brazil)

[AOS10-P02] **Linear inverse modeling of the tropical Atlantic**

*Ingo Richter[1], Ping Chang[2] (1.JAMSTEC Japan Agency for Marine-Earth Science and Technology, 2.Texas A&M University)

[AOS10-P03] Relationships Among Inter-model Spread and Biases in Tropical Atlantic Sea Surface Temperatures

Elsa - Mohino Harris[1], *Belen Rodriguez-Fonseca[1,2], Teresa - Losada[1], Irene - Polo[1], Roberto - Mechoso[3] (1.Department of Physics of the Earth and Astrophysics, Universidad Complutense de Madrid, 28040, Madrid, Spain. , 2.Institute of Geosciences IGEO,UCM-CSIC, 28040, Madrid, Spain., 3.Department of Atmospheric and Oceanic Sciences, UCLA, Los Angeles, USA)

[AOS10-P04] **Revisiting the CMIP5 Thermocline in the Equatorial Pacific and Atlantic Oceans**

Antonio - Castaño[1,2], Elsa - Mohino[1], *Belen Rodriguez-Fonseca[1,2], Teresa - Losada[1] (1.Department of Physics of the Earth and Astrophysics, Universidad Complutense de Madrid, 28040, Madrid, Spain., 2.Institute of Geosciences, IGEO, UCM-CSIC 28040, Madrid, Spain.)

[AOS10-P05] Lagged Effects of North Atlantic SST Anomalies on Weather in Remote Areas

*Natalia Gnatiuk[1], Timo Vihma[2], Leonid Bobylev[1] (1.Nansen International Environmental and Remote Sensing Centre, 2.Finnish Meteorological Institute)

[AOS10-P06] **SST anomalies in the northern tropical Atlantic as a negative feedback to ENSO development**

*Ingo Richter[1], Hiroki Tokinaga[2], Yu Kosaka[3], Takeshi Doi[1] (1.JAMSTEC Japan Agency for Marine-Earth Science and Technology, 2.Kyoto University, 3.University of Tokyo)

[E] Poster | A (Atmospheric and Hydrospheric Sciences)：A-HW Hydrology & Water Environment

3:30 PM - 5:00 PM JST | 6:30 AM - 8:00 AM UTC | Poster Hall International Exhibition Hall8, Makuhari Messe_5

[A-HW22] Materials transport and nutrient cycles in watersheds; from headwaters to coastal seas

convener:Masahiro Kobayashi(Forestry and Forest Products Research Institute), Seiko Yoshikawa(Institute for Agro-environmental Sciences, National Agriculture and Food Research Organization), Jun Yasumoto(University of the Ryukyus, Faculty of Agriculuture), Adina Paytan(University of California Santa Cruz)

[AHW22-P01] Phosphate Enrichment Hampers Development of Juvenile Acropora digitifera Coral by Inhibiting Skeleton Formation

Mariko Iijima[1], *Yasumoto Ko[1], Jun Yasumoto[2], Mina Hirose[3], Mitsuru Jimbo[1], Shugo Watabe[1] (1.Kitasato University School of Marine Biosciences, 2.Faculty of Agriculture, University of the Ryukyus, 3.Tropical Technology Plus)

[AHW22-P02] Modeling chlorophyll-a concentration using remote sensing in shallow water systems: Comparison of sensors

*Assefa M Melesse[1], Tara Blakey[1], Mohammad Haji Gholizadeh[1], Mohd Manzar Abbas[1] (1.Florida International University)

[AHW22-P03] Dynamics in groundwater flow system with seasonal water table variation in a coastal and island

*Yusuke Tomozawa[1], Shin-ichi Onodera[1], Mitsuyo Saito[2] (1.Graduate School of Integrated Arts and Sciences Hiroshima University, 2.Graduate School of Environmental and Life Science, Okayama University)

[AHW22-P04] **The Tracing of Groundwater Contamination Sources in Indonesian Coastal Alluvial Groundwater using $\delta^{34}S$ and $\delta^{15}N$ Isotopes**

*Anna Fadliah Rusydi[1,4], Mitsuyo Saito[2], Seiichiro Ioka[3], Shin-ichi Onodera[1] (1.Graduate School of Integrated Arts and Sciences, Hiroshima University, Japan, 2.Graduate School of Environmental and Life Sciences, Okayama University, Japan, 3.Research Institute for Sustainable Energy, Hirosaki University, Japan, 4.Research Center for Geotechnology, Indonesian Institute of Sciences, Indonesia)

[AHW22-P05] Spatio-temporal dynamics of orthophosphate with implications for limitation of phytoplankton growth in north basin of Lake Biwa, Japan

*Xin Liu[1], Rong Yi[1], Masahiro Maruo[1], Syuhei Ban[1] (1.The University of Shiga Prefecture)

[AHW22-P06] Microbial phase analysis in aquifer of Ryukyu Limestone Zone using next generation sequencer

*Umi Murao[1], Jun Yasumoto[1], Yasumoto Ko[3], Mina Hirose[2], Nanami Mizusawa[3], Ryo Iguchi[4], Bam H.N. Razafindrabe[5], Syugo Watabe[3] (1.University of the Ryukyus, Faculty of Agriculuture Department of Regional Agricultural Engineering, 2.Tropical Tecnology Plus, 3.Kitasato University School of Marine Biosciences, 4.National Institute of Advanced Industrial Science and Technology, 5.University of the Ryukyus, Faculty of Agriculuture Department of Subtropical Agro-Environmental Sciences)

[AHW22-P07] Evaluation for temporal variation in groundwater inflow to the lagoons connected to Lake Biwa by radon (^{222}Rn) tracer analysis

*Mitsuyo Saito[1], Shin-ichi Onodera[2], Yusuke Tomozawa[2], Kunyang Wang[2], Syuhei Ban[3], Noboru Okuda[4] (1.Graduate School of Environmental and Life Science, Okayama University, 2.Graduate School of Integrated Arts and Sciences, Hiroshima University, 3.School of Environmental Sciences, The University of Shiga Prefecture, 4.Research Institute for Humanity and Nature)

[AHW22-P08] Br/Cl ratio characteristics of groundwater in coastal areas in Indonesia

*Seiichiro Ioka[1], Shin-ichi Onodera[2], Mitsuyo Saito[3], Anna Fadliah Rusydi[2,4] (1.Institute of Regional Innovation, Hirosaki University, Japan, 2.Graduate School of Integrated Arts and Sciences, Hiroshima University, Japan, 3.Graduate School of Environmental and Life Sciences, Okayama University, Japan, 4.Research Center for Geotechnology, Indonesian Institute of Sciences, Indonesia)

[AHW22-P09] Estimation of groundwater recharge and phosphorus transport under different precipitation conditions in a suburban catchment, using SWAT model

*Kunyang Wang[1,2], Shin-ichi Onodera[1], Mitsuyo Saito[3], Noboru Okuda[4], Takuya Okubo[5] (1.Graduate School of Integrated Arts and Science, Hiroshima University, 2.Capital Normal University, 3.Okayama University, 4.Research

Institute for Humanity and Nature, 5.University of the Shiga Prefecture)

[AHW22-P10] Losses of phosphorus with soil erosion and nitrate with groundwater recharge in an agricultural catchment, subtropical small island

*Shin-ichi Onodera[1], Mitsuyo Saito[2], Yang Cao[1], Anna Fadliah Rusydi[1], Hide Omae[3], Yoshiko Iizumi[4], Yusuke Tomozawa[1] (1.Graduate School of Integrated and Arts Sciences, Hiroshima University, 2.Graduate School of Environmental and Life Science, Okayama University, 3.JIRCAS TARF, 4.JIRCAS HQ)

[AHW22-P11] Phosphate solubilizing bacteria as an indicator of sediment phosphorus in freshwater lakes

*Sreekumari Kurissery[1], Katelynn Crawford[1], Nandakumar Kanavillil[1] (1.Lakehead University, Canada)

[AHW22-P12] A Study on the dynamics of various phosphate forms in soil and groundwater in Ryukyu limestone regions

*Masashi Nozaki[1], Jun Yasumoto[2], Yasumoto Ko[3], Hirose Mina[4], Iijima Mariko[3], Ryuichi Shinjo[5], Bam H.N. Razafindrabe[6] (1.University of The Ryukyus, Graduate School of Agriculture,, 2.University of the Ryukyus, Faculty of Agriculture, Department of Regional Agricultural Engineering, 3.Kitasato University School of Marine Biosciences, 4.Tropical Technology Plus, 5.Department of Physics and Earth Sciences, University of the Ryukyus, 6.University of the Ryukyus, Faculty of Agriculture, Department of Subtropical Agro-Environmental Sciences)

[AHW22-P13] Impacts of highly concentrated turbid water on the groundwater in the Tedori River alluvial fan, Japan

*Yoichi Fujihara[1], Shunsuke Chono[1], Keiji Takase[1], Eiji Ichion[1] (1.Department of Environmental Science, Ishikawa Prefectural University)

[AHW22-P14] Altitude effect of water stable isotopic ratio of ravine water and its contribution to groundwater in alluvial plains - Comparison in east and west side catchments of Lake Biwa –

*Yusuke Tomozawa[1], Kunyang Wang[1], Mitsuyo Saito[2], Syuhei Ban[3], Noboru Okuda[4], Shin-ichi Onodera[1] (1.Graduate School of Integrated Arts and Sciences Hiroshima University, 2.Graduate School of Environmental and Life Science, Okayama University, 3.School of Environmental Science, The University of Shiga Prefecture, 4.Research Institute for Humanity and Nature)

[AHW22-P15] Calculation of TN and TP concentration coefficients of river water for each land use by a simple watershed model.

*Seiko Yoshikawa[1], Donglai Ma[1,4], Tadamasa Saito[1,5], Kenji Matsumori[2], Yuko Itoh[3], Masahiro Kobayashi[3] (1.Institute for Agro-environmental Sciences, National Agriculture and Food Research Organization, 2.Western Region Agricultural Research Center, National Agriculture and Food Research Organization, 3.Forestry and Forest Products Research Institute, 4.Graduate school,Tsukuba University, 5.Faculty of Agriculture, Ibaraki University)

[AHW22-P16] **Possibility of nutrients transportation from littoral slope for enhancement of phytoplankton growth in north basin of Lake Biwa**

*Syuhei Ban[1], Rong YI[1], Xin Liu[1], Masahiro Maruo[1], Miki Sudo[1], Naoshige Goto[1], Jun Murase[2] (1.The University of Shiga Prefecture, 2.Nagoya University)

[AHW22-P17] SWAT model analysis for confirming the effects of crop growth on the suspended sediment concentration from a settling basin catchment on Ishigaki island

*Yang Cao[1], Shin-ichi Onodera[1], Mitsuyo Saito[2], Hide Omae[3], Yoshiko Iizumi[3] (1.Graduate School of Integrate Arts and Sciences, Hiroshima University, 2.Graduate School of Environmental and life Science, Okayama University, 3.Tropical Agriculture Research Front (TARF), Japan International Research Center for Agricultural Sciences (JIRCAS))

[AHW22-P18] Estimating the runoff of water, sediment, and nutrient using SWAT model in Kikuchi-river watershed, Kumamoto, and the influence of the forest

*Soichiro Fujii[1], Masahiko Kanamori[1], Yuko Nagano[1], Maki Kinoshita[2], Yuta Shimizu[3], Shin-ichi Onodera[4] (1.Japan Forest Technology Association, 2.PASCO Corporation, 3.Western Region Agricultural Research Center, National Agriculture and Food Research Organization, 4.Graduate School of Integrated and Arts Sciences, Hiroshima University)

[AHW22-P19] Atmospheric depositions on forest ecosystems in areas along the Sea of Japan

*Yuko Itoh[1], Keiji Takase[2], Yoichi Fujihara[2], Toru Okamoto[1] (1.Forestry and Forest Products Research Institute, Japan, 2.Ishikawa Prefectural University)

[AHW22-P20] Continuous and simultaneous flux measurement of N_2O and CO_2 from agricultural soil using a portable multi-turn time-of-flight mass spectrometer

*Noriko Nakayama[1], Yusuke Iwai[1], Yo Toma[2], Hiroshi Furutani[1], Ryusuke Hatano[3], Michisato Toyoda[1] (1.Osaka University, 2.Ehime University, 3.Hokkaido University)

[AHW22-P21] Effects of introduction of cyclic irrigation system on mass balances of SS and T-P in Lake Inbanuma, Chiba, Japan

*Tomijiro Kubota[1] (1.National Agriculture and Food Research Organization, Institute for Rural Engineering)

[E] Poster | A (Atmospheric and Hydrospheric Sciences)：A-HW Hydrology & Water Environment

5:15 PM - 6:30 PM JST | 8:15 AM - 9:30 AM UTC | Poster Hall International Exhibition Hall8, Makuhari Messe_9

[A-HW22] Materials transport and nutrient cycles in watersheds; from headwaters to coastal seas

convener:Masahiro Kobayashi(Forestry and Forest Products Research Institute), Seiko Yoshikawa(Institute for Agro-environmental Sciences, National Agriculture and Food Research Organization), Jun Yasumoto(University of the Ryukyus, Faculty of Agriculuture), Adina Paytan(University of California Santa Cruz)

[AHW22-P01] Phosphate Enrichment Hampers Development of Juvenile Acropora digitifera Coral by Inhibiting Skeleton Formation

Mariko Iijima[1], *Yasumoto Ko[1], Jun Yasumoto[2], Mina Hirose[3], Mitsuru Jimbo[1], Shugo Watabe[1] (1.Kitasato University School of Marine Biosciences, 2.Faculty of Agriculture, University of the Ryukyus, 3.Tropical Technology Plus)

[AHW22-P02] Modeling chlorophyll-a concentration using remote sensing in shallow water systems: Comparison of sensors

*Assefa M Melesse[1], Tara Blakey[1], Mohammad Haji Gholizadeh[1], Mohd Manzar Abbas[1] (1.Florida International University)

[AHW22-P03] Dynamics in groundwater flow system with seasonal water table variation in a coastal and island

*Yusuke Tomozawa[1], Shin-ichi Onodera[1], Mitsuyo Saito[2] (1.Graduate School of Integrated Arts and Sciences Hiroshima University, 2.Graduate School of Environmental and Life Science, Okayama University)

[AHW22-P04] **The Tracing of Groundwater Contamination Sources in Indonesian Coastal Alluvial Groundwater using $\delta^{34}S$ and $\delta^{15}N$ Isotopes**

*Anna Fadliah Rusydi[1,4], Mitsuyo Saito[2], Seiichiro Ioka[3], Shin-ichi Onodera[1] (1.Graduate School of Integrated Arts and Sciences, Hiroshima University, Japan, 2.Graduate School of Environmental and Life Sciences, Okayama University, Japan, 3.Research Institute for Sustainable Energy, Hirosaki University, Japan, 4.Research Center for Geotechnology, Indonesian Institute of Sciences, Indonesia)

[AHW22-P05] Spatio-temporal dynamics of orthophosphate with implications for limitation of phytoplankton growth in north basin of Lake Biwa, Japan

*Xin Liu[1], Rong Yi[1], Masahiro Maruo[1], Syuhei Ban[1] (1.The University of Shiga Prefecture)

[AHW22-P06] Microbial phase analysis in aquifer of Ryukyu Limestone Zone using next generation sequencer

*Umi Murao[1], Jun Yasumoto[1], Yasumoto Ko[3], Mina Hirose[2], Nanami Mizusawa[3], Ryo Iguchi[4], Bam H.N. Razafindrabe[5], Syugo Watabe[3] (1.University of the Ryukyus, Faculty of Agriculuture Department of Regional Agricultural Engineering, 2.Tropical Tecnology Plus, 3.Kitasato University School of Marine Biosciences, 4.National Institute of Advanced Industrial Science and Technology, 5.University of the Ryukyus, Faculty of Agriculuture Department of Subtropical Agro-Environmental Sciences)

[AHW22-P07] Evaluation for temporal variation in groundwater inflow to the lagoons connected to Lake Biwa by radon (^{222}Rn) tracer analysis

*Mitsuyo Saito[1], Shin-ichi Onodera[2], Yusuke Tomozawa[2], Kunyang Wang[2], Syuhei Ban[3], Noboru Okuda[4] (1.Graduate School of Environmental and Life Science, Okayama University, 2.Graduate School of Integrated Arts and Sciences, Hiroshima University, 3.School of Environmental Sciences, The University of Shiga Prefecture, 4.Research Institute for Humanity and Nature)

[AHW22-P08] Br/Cl ratio characteristics of groundwater in coastal areas in Indonesia

*Seiichiro Ioka[1], Shin-ichi Onodera[2], Mitsuyo Saito[3], Anna Fadliah Rusydi[2,4] (1.Institute of Regional Innovation, Hirosaki University, Japan, 2.Graduate School of Integrated Arts and Sciences, Hiroshima University, Japan, 3.Graduate School of Environmental and Life Sciences, Okayama University, Japan, 4.Research Center for Geotechnology, Indonesian Institute of Sciences, Indonesia)

[AHW22-P09] Estimation of groundwater recharge and phosphorus transport under different precipitation conditions in a suburban catchment, using SWAT model

*Kunyang Wang[1,2], Shin-ichi Onodera[1], Mitsuyo Saito[3], Noboru Okuda[4], Takuya Okubo[5] (1.Graduate School of Integrated Arts and Science, Hiroshima University, 2.Capital Normal University, 3.Okayama University, 4.Research

Institute for Humanity and Nature, 5.University of the Shiga Prefecture)

[AHW22-P10] Losses of phosphorus with soil erosion and nitrate with groundwater recharge in an agricultural catchment, subtropical small island

*Shin-ichi Onodera[1], Mitsuyo Saito[2], Yang Cao[1], Anna Fadliah Rusydi[1], Hide Omae[3], Yoshiko Iizumi[4], Yusuke Tomozawa[1] (1.Graduate School of Integrated and Arts Sciences, Hiroshima University, 2.Graduate School of Environmental and Life Science, Okayama University, 3.JIRCAS TARF, 4.JIRCAS HQ)

[AHW22-P11] Phosphate solubilizing bacteria as an indicator of sediment phosphorus in freshwater lakes

*Sreekumari Kurissery[1], Katelynn Crawford[1], Nandakumar Kanavillil[1] (1.Lakehead University, Canada)

[AHW22-P12] A Study on the dynamics of various phosphate forms in soil and groundwater in Ryukyu limestone regions

*Masashi Nozaki[1], Jun Yasumoto[2], Yasumoto Ko[3], Hirose Mina[4], Iijima Mariko[3], Ryuichi Shinjo[5], Bam H.N. Razafindrabe[6] (1.University of The Ryukyus, Graduate School of Agriculture,, 2.University of the Ryukyus, Faculty of Agriculture, Department of Regional Agricultural Engineering, 3.Kitasato University School of Marine Biosciences, 4.Tropical Technology Plus, 5.Department of Physics and Earth Sciences, University of the Ryukyus, 6.University of the Ryukyus, Faculty of Agriculture, Department of Subtropical Agro-Environmental Sciences)

[AHW22-P13] Impacts of highly concentrated turbid water on the groundwater in the Tedori River alluvial fan, Japan

*Yoichi Fujihara[1], Shunsuke Chono[1], Keiji Takase[1], Eiji Ichion[1] (1.Department of Environmental Science, Ishikawa Prefectural University)

[AHW22-P14] Altitude effect of water stable isotopic ratio of ravine water and its contribution to groundwater in alluvial plains - Comparison in east and west side catchments of Lake Biwa –

*Yusuke Tomozawa[1], Kunyang Wang[1], Mitsuyo Saito[2], Syuhei Ban[3], Noboru Okuda[4], Shin-ichi Onodera[1] (1.Graduate School of Integrated Arts and Sciences Hiroshima University, 2.Graduate School of Environmental and Life Science, Okayama University, 3.School of Environmental Science, The University of Shiga Prefecture, 4.Research Institute for Humanity and Nature)

[AHW22-P15] Calculation of TN and TP concentration coefficients of river water for each land use by a simple watershed model.

*Seiko Yoshikawa[1], Donglai Ma[1,4], Tadamasa Saito[1,5], Kenji Matsumori[2], Yuko Itoh[3], Masahiro Kobayashi[3] (1.Institute for Agro-environmental Sciences, National Agriculture and Food Research Organization, 2.Western Region Agricultural Research Center, National Agriculture and Food Research Organization, 3.Forestry and Forest Products Research Institute, 4.Graduate school,Tsukuba University, 5.Faculty of Agriculture, Ibaraki University)

[AHW22-P16] **Possibility of nutrients transportation from littoral slope for enhancement of phytoplankton growth in north basin of Lake Biwa**

*Syuhei Ban[1], Rong YI[1], Xin Liu[1], Masahiro Maruo[1], Miki Sudo[1], Naoshige Goto[1], Jun Murase[2] (1.The University of Shiga Prefecture, 2.Nagoya University)

[AHW22-P17] SWAT model analysis for confirming the effects of crop growth on the suspended sediment concentration from a settling basin catchment on Ishigaki island

*Yang Cao[1], Shin-ichi Onodera[1], Mitsuyo Saito[2], Hide Omae[3], Yoshiko Iizumi[3] (1.Graduate School of Integrate Arts and Sciences, Hiroshima University, 2.Graduate School of Environmental and life Science, Okayama University, 3.Tropical Agriculture Research Front (TARF), Japan International Research Center for Agricultural Sciences (JIRCAS))

[AHW22-P18] Estimating the runoff of water, sediment, and nutrient using SWAT model in Kikuchi-river watershed, Kumamoto, and the influence of the forest

*Soichiro Fujii[1], Masahiko Kanamori[1], Yuko Nagano[1], Maki Kinoshita[2], Yuta Shimizu[3], Shin-ichi Onodera[4] (1.Japan Forest Technology Association, 2.PASCO Corporation, 3.Western Region Agricultural Research Center, National Agriculture and Food Research Organization, 4.Graduate School of Integrated and Arts Sciences, Hiroshima University)

[AHW22-P19] Atmospheric depositions on forest ecosystems in areas along the Sea of Japan

*Yuko Itoh[1], Keiji Takase[2], Yoichi Fujihara[2], Toru Okamoto[1] (1.Forestry and Forest Products Research Institute, Japan, 2.Ishikawa Prefectural University)

[AHW22-P20] Continuous and simultaneous flux measurement of N_2O and CO_2 from agricultural soil using a portable multi-turn time-of-flight mass spectrometer

*Noriko Nakayama[1], Yusuke Iwai[1], Yo Toma[2], Hiroshi Furutani[1], Ryusuke Hatano[3], Michisato Toyoda[1] (1.Osaka University, 2.Ehime University, 3.Hokkaido University)

[AHW22-P21] Effects of introduction of cyclic irrigation system on mass balances of SS and T-P in Lake Inbanuma, Chiba, Japan

*Tomijiro Kubota[1] (1.National Agriculture and Food Research Organization, Institute for Rural Engineering)

[E] Poster | A (Atmospheric and Hydrospheric Sciences)：A-CG Complex & General

1:45 PM - 3:15 PM JST | 4:45 AM - 6:15 AM UTC | Poster Hall International Exhibition Hall8, Makuhari Messe_3

[A-CG34] Satellite Earth Environment Observation

convener:Riko Oki(Japan Aerospace Exploration Agency), Yoshiaki HONDA(Center for Environmental Remote Sensing, Chiba University), Yukari Takayabu(Atmosphere and Ocean Research Institute, the University of Tokyo), Tsuneo Matsunaga(Center for Global Environmental Research and Satellite Observation Center, National Institute for Environmental Studies)

[ACG34-P01] **Impact of usage of multiple-satellite sensors on accuracy of daily-mean sea surface wind data**

*Ayumi Koizumi[1], Masahisa Kubota[2], Kunio Kutsuwada[3], Hiroyuki Tomita[4], Tsutomu Hihara[5] (1.Tokai University, 2.Tokai University, Institute of Ocean Research and Development, 3.School of Marine Science and Technology, Tokai University, 4.Institute for Space-Earth Environmental, Nagoya University, 5.Japan Agency for Marine-Erth Science and Technology)

[ACG34-P02] Temperature and Size Variability of Warm Pools in the Global Oceans

*ChunYi Lin[1] (1.National Museum of Marine Science & Technology)

[ACG34-P03] Sea surface temperature from SGLI aboard the GCOM-C satellite of JAXA

*Yukio Kurihara[1], Kazunori Ogata[2], Hiroshi Murakami[2], Misako Kachi[2] (1.Tripli-I Co., Ltd., 2.JAXA EORC)

[ACG34-P04] Concept of small satellite UV/visible imaging spectrometer optimized for tropospheric NO_2 measurements in air quality monitoring

*Tamaki Fujinawa[1,5], Katsuyuki Noguchi[2], Akihiko Kuze[3], Andreas Richter[4], John P. Burrows[4], Andreas C. Meier[4], Tomohiro Sato[1], Takeshi Kuroda[1], Naohiro Yoshida[5], YASUKO KASAI[1,5] (1.National Institute of Information and Communications Technology, 2.Nara Women's University, 3.Japan Aerospace Exploration Agency, 4.University of Bremen, 5.Tokyo Institute of Technology)

[ACG34-P05] EarthCARE L2 algorithms for cloud and precipitation

*Kaori Sato[1], Hajime Okamoto[1], Hiroshi Ishimoto[2] (1.Research Institute for Applied Mechanics, Kyushu University, 2.Meteorological Research Institute)

[ACG34-P06] Analysis of the Surface Echo Characteristics Derived from GPM/DPR Wide Swath Observation Experiment

*Kosuke Yamamoto[1], Kinji Furukawa[1], Nobuhiro Takahashi[2], Takuji Kubota[1] (1.Japan Aerospace Exploration Agency, 2.Nagoya University)

[ACG34-P07] The Recent Results from the Global Precipitation Measurement (GPM) mission in Japan

*Riko Oki[1], Takuji Kubota[1], Kinji Furukawa[1], Yuki Kaneko[1], Moeka Yamaji[1], Kosuke Yamamoto[1], Toshio Iguchi[2], Yukari Takayabu[3] (1.Japan Aerospace Exploration Agency, 2.NICT, 3.the University of Tokyo)

[ACG34-P08] **Verification of Global Satellite Mapping of precipitation (GSMaP) for providing its error information**

*Moeka Yamaji[1], Takuji Kubota[1] (1.Earth Observation Research Center, Japan Aerospace Exploration Agency)

[ACG34-P09] Detection of the mixed phase top using the measured dual-frequency ratio of reflectivity with GPM/DPR

*Yuki Kaneko[1], Toshio Iguchi[2] (1.Japan Aerospace Exploration Agency, 2.National Institute of Information and Communications Technology)

[ACG34-P10] **Comparison between high frequency satellite rainfall estimation and APHRODITE-2 ground rain gauge observation**

*Hitoshi Hirose[1], Koichi Toyoshima[1], Atsushi Higuchi[1], Akiyo Yatagai[2], Natsuko Yasutomi[3] (1.Center for Environmental Remote Sensing, Chiba University, 2.Hirosaki University, 3.Disaster Prevention Research Institute, Kyoto University)

[ACG34-P11] Development of the high resolution GSMaP by the Himawari-8

*Tomoaki Mega[1], Tomoo Ushio[1] (1.Tokyo Metropolitan University)

[ACG34-P12] Preliminary results of on-orbit estimation for polarization sensitivity of GCOM-C/SGLI

*Risa Miyazaki[1], Hiroshi Murakami[1], Masahiro Hori[1] (1.Japan Aerospace Exploration Agency)

[ACG34-P13] Analysis of SGLI validation datas based on the effects of the growth and ground types for the AGB development

*Ryota Ishibashi[1], Koji KAJIWARA[1], Yoshiaki HONDA[1] (1.Center for environmental remote sensing, Chiba University)

[ACG34-P14] Remote sensing of aerosol optical properties and water-leaving radiance based on the optimal estimation approach

*Chong Shi[1], Teruyuki Nakajima[1], Makiko Hashimoto[1], Hideaki Takenaka[1] (1.Japan Aerospace Exploration Agency)

[ACG34-P15] Aerosol retrieval and PM2.5 from space using GOSAT/TANSO-CAI

*Makiko Hashimoto[1], Hideaki Takenaka[1], Teruyuki Nakajima[1], Akiko Higurashi[2] (1.Japan Aerospace Explortion Agency, 2.NIES)

[ACG34-P16] **Establishing a high resolution road fugitive dust emission inventory in Kaifeng City, China**

*Yiming Xu[1], Shili Liu[1], Xinyue Cao[1], Xianbao Shen[1], Zhiliang Yao[1] (1.Department of Environmental Science and Engineering, Beijing Technology and Business University)

[ACG34-P17] A Relationship between Diurnal Change Patterns of Land Surface Temperature and Spatial Configuration of the Osaka Metropolitan Area Captured by Himawari-8

*Yuhei Yamamoto[1], Hirohiko Ishikawa[1] (1.Disaster Prevention Research Institute, Kyoto University)

[E] Poster | A (Atmospheric and Hydrospheric Sciences)：A-CG Complex & General

5:15 PM - 6:30 PM JST | 8:15 AM - 9:30 AM UTC | Poster Hall International Exhibition Hall8, Makuhari Messe_12

[A-CG34] Satellite Earth Environment Observation

convener:Riko Oki(Japan Aerospace Exploration Agency), Yoshiaki HONDA(Center for Environmental Remote Sensing, Chiba University), Yukari Takayabu(Atmosphere and Ocean Research Institute, the University of Tokyo), Tsuneo Matsunaga(Center for Global Environmental Research and Satellite Observation Center, National Institute for Environmental Studies)

[ACG34-P01] **Impact of usage of multiple-satellite sensors on accuracy of daily-mean sea surface wind data**

*Ayumi Koizumi[1], Masahisa Kubota[2], Kunio Kutsuwada[3], Hiroyuki Tomita[4], Tsutomu Hihara[5] (1.Tokai University, 2.Tokai University, Institute of Ocean Research and Development, 3.School of Marine Science and Technology, Tokai University, 4.Institute for Space-Earth Environmental, Nagoya University, 5.Japan Agency for Marine-Erth Science and Technology)

[ACG34-P02] Temperature and Size Variability of Warm Pools in the Global Oceans

*ChunYi Lin[1] (1.National Museum of Marine Science & Technology)

[ACG34-P03] Sea surface temperature from SGLI aboard the GCOM-C satellite of JAXA

*Yukio Kurihara[1], Kazunori Ogata[2], Hiroshi Murakami[2], Misako Kachi[2] (1.Tripli-I Co., Ltd., 2.JAXA EORC)

[ACG34-P04] Concept of small satellite UV/visible imaging spectrometer optimized for tropospheric NO_2 measurements in air quality monitoring

*Tamaki Fujinawa[1,5], Katsuyuki Noguchi[2], Akihiko Kuze[3], Andreas Richter[4], John P. Burrows[4], Andreas C. Meier[4], Tomohiro Sato[1], Takeshi Kuroda[1], Naohiro Yoshida[5], YASUKO KASAI[1,5] (1.National Institute of Information and Communications Technology, 2.Nara Women's University, 3.Japan Aerospace Exploration Agency, 4.University of Bremen, 5.Tokyo Institute of Technology)

[ACG34-P05] EarthCARE L2 algorithms for cloud and precipitation

*Kaori Sato[1], Hajime Okamoto[1], Hiroshi Ishimoto[2] (1.Research Institute for Applied Mechanics, Kyushu University, 2.Meteorological Research Institute)

[ACG34-P06] Analysis of the Surface Echo Characteristics Derived from GPM/DPR Wide Swath Observation Experiment

*Kosuke Yamamoto[1], Kinji Furukawa[1], Nobuhiro Takahashi[2], Takuji Kubota[1] (1.Japan Aerospace Exploration Agency, 2.Nagoya University)

[ACG34-P07] The Recent Results from the Global Precipitation Measurement (GPM) mission in Japan

*Riko Oki[1], Takuji Kubota[1], Kinji Furukawa[1], Yuki Kaneko[1], Moeka Yamaji[1], Kosuke Yamamoto[1], Toshio Iguchi[2], Yukari Takayabu[3] (1.Japan Aerospace Exploration Agency, 2.NICT, 3.the University of Tokyo)

[ACG34-P08] **Verification of Global Satellite Mapping of precipitation (GSMaP) for providing its error information**

*Moeka Yamaji[1], Takuji Kubota[1] (1.Earth Observation Research Center, Japan Aerospace Exploration Agency)

[ACG34-P09] Detection of the mixed phase top using the measured dual-frequency ratio of reflectivity with GPM/DPR

*Yuki Kaneko[1], Toshio Iguchi[2] (1.Japan Aerospace Exploration Agency, 2.National Institute of Information and Communications Technology)

[ACG34-P10] **Comparison between high frequency satellite rainfall estimation and APHRODITE-2 ground rain gauge observation**

*Hitoshi Hirose[1], Koichi Toyoshima[1], Atsushi Higuchi[1], Akiyo Yatagai[2], Natsuko Yasutomi[3] (1.Center for Environmental Remote Sensing, Chiba University, 2.Hirosaki University, 3.Disaster Prevention Research Institute, Kyoto University)

[ACG34-P11] Development of the high resolution GSMaP by the Himawari-8

*Tomoaki Mega[1], Tomoo Ushio[1] (1.Tokyo Metropolitan University)

[ACG34-P12] Preliminary results of on-orbit estimation for polarization sensitivity of GCOM-C/SGLI

*Risa Miyazaki[1], Hiroshi Murakami[1], Masahiro Hori[1] (1.Japan Aerospace Exploration Agency)

[ACG34-P13] Analysis of SGLI validation datas based on the effects of the growth and ground types for the AGB development

*Ryota Ishibashi[1], Koji KAJIWARA[1], Yoshiaki HONDA[1] (1.Center for environmental remote sensing, Chiba University)

[ACG34-P14] Remote sensing of aerosol optical properties and water-leaving radiance based on the optimal estimation approach

*Chong Shi[1], Teruyuki Nakajima[1], Makiko Hashimoto[1], Hideaki Takenaka[1] (1.Japan Aerospace Exploration Agency)

[ACG34-P15] Aerosol retrieval and PM2.5 from space using GOSAT/TANSO-CAI

*Makiko Hashimoto[1], Hideaki Takenaka[1], Teruyuki Nakajima[1], Akiko Higurashi[2] (1.Japan Aerospace Explortion Agency, 2.NIES)

[ACG34-P16] **Establishing a high resolution road fugitive dust emission inventory in Kaifeng City, China**

*Yiming Xu[1], Shili Liu[1], Xinyue Cao[1], Xianbao Shen[1], Zhiliang Yao[1] (1.Department of Environmental Science and Engineering, Beijing Technology and Business University)

[ACG34-P17] A Relationship between Diurnal Change Patterns of Land Surface Temperature and Spatial Configuration of the Osaka Metropolitan Area Captured by Himawari-8

*Yuhei Yamamoto[1], Hirohiko Ishikawa[1] (1.Disaster Prevention Research Institute, Kyoto University)

[E] Poster | H (Human Geosciences)：H-TT Technology & Techniques

10:45 AM - 12:15 PM JST | 1:45 AM - 3:15 AM UTC | Poster Hall International Exhibition Hall8, Makuhari Messe_3

[H-TT19] Geographic Information Systems and Cartography

convener:Takashi Oguchi(Center for Spatial Information Science, The University of Tokyo), Yuji Murayama(Graduate School of Life and Environmental Sciences), Yoshiki Wakabayashi(Graduate School of Urban Environmental Sciences, Tokyo Metropolitan University)

[HTT19-P01] **Monitoring and Simulating Land Use/Cover Changes and its Impact on Land Surface Temperature in Sapporo City, Japan**

*RUCI WANG[1], YUJI MURAYAMA[1] (1.University of Tsukuba)

[HTT19-P02] **Spatiotemporal Variations of Land Cover/Use and Sustainable Urban Heat Island (UHI) Mitigation Strategies: A Case Study of Chinese Bay Megacities**

★Invited Papers

*Fei LIU[1], Yuji MURAYAMA[1] (1. University of Tsukuba)

[HTT19-P03] A LST Study of the Seoul Metropolitan City, South Korea, Based on Landsat Data (1996 – 2017)

*Prabath Priyankara[1,3], Manjula Ranagalage[1,4], DMSLB Dissanayake[1,4], Takehiro Morimoto[1,2], Yuji Murayama[1,2] (1.Graduate School of Life and Environmental Sciences, University of Tsukuba, Japan, 2.Faculty of Life and Environmental Sciences, University of Tsukuba, Japan, 3.Faculty of Agriculture, University of Ruhuna, Sri Lanka, 4.Faculty of Social Sciences and Humanities, Rajarata University of Sri Lanka, Sri Lanka)

[HTT19-P04] Improvement of GIS exercise classes using the GIS open educational resources based on questionnaire surveys

★Invited Papers

*Hiroyuki Yamauchi[1], Takashi Oguchi[1], Yuichi S. Hayakawa[2,1], Kotaro Iizuka[1] (1.Center for Spatial Information Science, The University of Tokyo, 2.Environmental Geography, Faculty of Environmental Earth Science, Hokkaido University)

[HTT19-P05] **The Development of COP for Tzu Chi Disaster Prevention System by Using QGIS-Taking 2018 Hualien Earthquake as an Example**

*kuan-wen tseng[1], Ming-Ta Tsai[1], Yun-Ching Wang[1], Ming-Chih Wang[1], Chien-Hsien Liu[1] (1.03-3809093)

[HTT19-P06] Comparative study on shape and distribution of landslides caused by the 2012 Northern Kyushu heavy rainfall and the 2016 Kumamoto earthquake in the Aso region, Kumamoto, Japan

*Yasutaka Haneda[1], Takashi Oguchi[2], Kotaro Iizuka[2], Hitoshi SAITO[3,2], Yuichi S. Hayakawa[4,2], Shoichiro Uchiyama[5] (1.Graduate School of Frontier Science, The University of Tokyo, 2.Center for Spatial Information Science, The University of Tokyo, 3.College of Economics, Kanto Gakuin University, 4.Faculty of Environmental Earth Science, Hokkaido University, 5.National Research Institute for Earth Science and Disaster Resilience)

[HTT19-P07] Using GIS and remote sensing to assess relationships between landslides and land cover changes in the Sanbagawa and Mikabu Belts, Shikoku, Japan

*Roxanne Lai[1], Takashi Oguchi[1] (1.University of Tokyo)

[HTT19-P08] **Analysis of Morphometric Parameters for Mountains Ranges and Landslides due to the July 2018 Heavy Rain in Western Japan Using GIS Data**

*Toshikazu Fukuba[1], Takashi Oguchi[2] (1.Department of Earth and Planetary Environmental Science, The University of Tokyo, 2.Center for Spatial Information Science, The University of Tokyo)

[HTT19-P09] Analyzing short-term topographic change in coastal sand dunes using UAS-SfM photogrammetry: A case study in Northern Kujukuri, Japan

*Seulgi Lee[1], Yasutaka Nakata[2], Kotaro Iizuka[3], Takashi Oguchi[3] (1.Graduate School of Frontier Sciences, The University of Tokyo, 2.Forest Research Department, Forestry Research Institute, Hokkaido Research Organization, 3.Center for Spatial Information Science, The University of Tokyo)

[HTT19-P10] **Responses of suspended sediment yield to precipitation, topography and dam control in the Yellow River Basin, China**

*Ruiqi Zhang[1], Takashi Oguchi[2] (1. Department of Natural Environmental Studies, Graduate School of Frontier Sciences, The University of Tokyo, 2.Center for Spatial Information Science, The University of Tokyo)

[E] Poster | H (Human Geosciences)：H-TT Technology & Techniques

5:15 PM - 6:30 PM JST | 8:15 AM - 9:30 AM UTC | Poster Hall International Exhibition Hall8, Makuhari Messe_16

[H-TT19] Geographic Information Systems and Cartography

convener:Takashi Oguchi(Center for Spatial Information Science, The University of Tokyo), Yuji Murayama(Graduate School of Life and Environmental Sciences), Yoshiki Wakabayashi(Graduate School of Urban Environmental Sciences, Tokyo Metropolitan University)

[HTT19-P01] **Monitoring and Simulating Land Use/Cover Changes and its Impact on Land Surface Temperature in Sapporo City, Japan**

*RUCI WANG[1], YUJI MURAYAMA[1] (1.University of Tsukuba)

[HTT19-P02] **Spatiotemporal Variations of Land Cover/Use and Sustainable Urban Heat Island (UHI) Mitigation Strategies: A Case Study of Chinese Bay Megacities**

★Invited Papers

*Fei LIU[1], Yuji MURAYAMA[1] (1. University of Tsukuba)

[HTT19-P03] A LST Study of the Seoul Metropolitan City, South Korea, Based on Landsat Data (1996 – 2017)

*Prabath Priyankara[1,3], Manjula Ranagalage[1,4], DMSLB Dissanayake[1,4], Takehiro Morimoto[1,2], Yuji Murayama[1,2] (1.Graduate School of Life and Environmental Sciences, University of Tsukuba, Japan, 2.Faculty of Life and Environmental Sciences, University of Tsukuba, Japan, 3.Faculty of Agriculture, University of Ruhuna, Sri Lanka, 4.Faculty of Social Sciences and Humanities, Rajarata University of Sri Lanka, Sri Lanka)

[HTT19-P04] Improvement of GIS exercise classes using the GIS open educational resources based on questionnaire surveys

★Invited Papers

*Hiroyuki Yamauchi[1], Takashi Oguchi[1], Yuichi S. Hayakawa[2,1], Kotaro Iizuka[1] (1.Center for Spatial Information Science, The University of Tokyo, 2.Environmental Geography, Faculty of Environmental Earth Science, Hokkaido University)

[HTT19-P05] **The Development of COP for Tzu Chi Disaster Prevention System by Using QGIS-Taking 2018 Hualien Earthquake as an Example**

*kuan-wen tseng[1], Ming-Ta Tsai[1], Yun-Ching Wang[1], Ming-Chih Wang[1], Chien-Hsien Liu[1] (1.03-3809093)

[HTT19-P06] Comparative study on shape and distribution of landslides caused by the 2012 Northern Kyushu heavy rainfall and the 2016 Kumamoto earthquake in the Aso region, Kumamoto, Japan

*Yasutaka Haneda[1], Takashi Oguchi[2], Kotaro Iizuka[2], Hitoshi SAITO[3,2], Yuichi S. Hayakawa[4,2], Shoichiro Uchiyama[5] (1.Graduate School of Frontier Science, The University of Tokyo, 2.Center for Spatial Information Science, The University of Tokyo, 3.College of Economics, Kanto Gakuin University, 4.Faculty of Environmental Earth Science, Hokkaido University, 5.National Research Institute for Earth Science and Disaster Resilience)

[HTT19-P07] Using GIS and remote sensing to assess relationships between landslides and land cover changes in the Sanbagawa and Mikabu Belts, Shikoku, Japan

*Roxanne Lai[1], Takashi Oguchi[1] (1.University of Tokyo)

[HTT19-P08] **Analysis of Morphometric Parameters for Mountains Ranges and Landslides due to the July 2018 Heavy Rain in Western Japan Using GIS Data**

*Toshikazu Fukuba[1], Takashi Oguchi[2] (1.Department of Earth and Planetary Environmental Science, The University of Tokyo, 2.Center for Spatial Information Science, The University of Tokyo)

[HTT19-P09] Analyzing short-term topographic change in coastal sand dunes using UAS-SfM photogrammetry: A case study in Northern Kujukuri, Japan

*Seulgi Lee[1], Yasutaka Nakata[2], Kotaro Iizuka[3], Takashi Oguchi[3] (1.Graduate School of Frontier Sciences, The University of Tokyo, 2.Forest Research Department, Forestry Research Institute, Hokkaido Research Organization, 3.Center for Spatial Information Science, The University of Tokyo)

[HTT19-P10] **Responses of suspended sediment yield to precipitation, topography and dam control in the Yellow River Basin, China**

*Ruiqi Zhang[1], Takashi Oguchi[2] (1. Department of Natural Environmental Studies, Graduate School of Frontier Sciences, The University of Tokyo, 2.Center for Spatial Information Science, The University of Tokyo)

[E] Poster | S (Solid Earth Sciences)：S-IT Science of the Earth's Interior & Techtonophysics

3:30 PM - 5:00 PM JST | 6:30 AM - 8:00 AM UTC | Poster Hall International Exhibition Hall8, Makuhari Messe_10

[S-IT25] Planetary cores: Structure, formation, and evolution

convener:Hidenori Terasaki(Graduate School of Science, Osaka University), Eiji Ohtani(Department of Earth and Planetary Materials Science, Graduate School of Science, Tohoku University), William F McDonough(University of Maryland College Park), George Helffrich(Earth-Life Science Institute, Tokyo Institute of Technology)

[SIT25-P01] Stratification of the Earth's core by SiO_2 crystallisation

*George Helffrich[1], Satoshi Kaneshima[2], Kei Hirose[1,3] (1.Earth-Life Science Institute, Tokyo Institute of Technology, 2.Earth and Planetary Sciences, Kyushu University, 3.Earth and Planetary Sciences Department, University of Tokyo)

[SIT25-P02] Relation between sound velocity and density for liquid iron alloys under Earth's core pressures by laser-shock compression

*Tatsuhiro Sakaiya[1], Tadashi Kondo[1], Hidenori Terasaki[1], Keisuke Shigemori[2], Yoichiro Hironaka[2] (1.Graduate School of Science, Osaka University, 2.Institute of Laser Engineering, Osaka University)

[SIT25-P03] Geochemical estimates of Earth's core heat content at the end of accretion

*Vincent Clesi[1], Renaud Deguen[1] (1.Laboratoire de Geologie de Lyon - Terre, Planètes, Environnement, Université Claude Bernard Lyon 1, CNRS, ENS-Lyon, 69622 Villeurbanne, France.)

[SIT25-P04] The effect of temperature on density of solid metals

*Asaka Kamiya[1], Hidenori Terasaki[1], Tadashi Kondo[1] (1.Osaka University)

[SIT25-P05] Phase relations in the Fe-Ni-Si system at high pressures and high temperatures

*Daijo Ikuta[1], Eiji Ohtani[1], Saori Kawaguchi[2], Naohisa Hirao[2], Yasuo Ohishi[2] (1.Department of Earth Science, Tohoku University, 2.JASRI)

[E] Poster | S (Solid Earth Sciences)：S-IT Science of the Earth's Interior & Techtonophysics

5:15 PM - 6:30 PM JST | 8:15 AM - 9:30 AM UTC | Poster Hall International Exhibition Hall8, Makuhari Messe_21

[S-IT25] Planetary cores: Structure, formation, and evolution

convener:Hidenori Terasaki(Graduate School of Science, Osaka University), Eiji Ohtani(Department of Earth and Planetary Materials Science, Graduate School of Science, Tohoku University), William F McDonough(University of Maryland College Park), George Helffrich(Earth-Life Science Institute, Tokyo Institute of Technology)

[SIT25-P01] Stratification of the Earth's core by SiO_2 crystallisation

*George Helffrich[1], Satoshi Kaneshima[2], Kei Hirose[1,3] (1.Earth-Life Science Institute, Tokyo Institute of Technology, 2.Earth and Planetary Sciences, Kyushu University, 3.Earth and Planetary Sciences Department, University of Tokyo)

[SIT25-P02] Relation between sound velocity and density for liquid iron alloys under Earth's core pressures by laser-shock compression

*Tatsuhiro Sakaiya[1], Tadashi Kondo[1], Hidenori Terasaki[1], Keisuke Shigemori[2], Yoichiro Hironaka[2] (1.Graduate School of Science, Osaka University, 2.Institute of Laser Engineering, Osaka University)

[SIT25-P03] Geochemical estimates of Earth's core heat content at the end of accretion

*Vincent Clesi[1], Renaud Deguen[1] (1.Laboratoire de Geologie de Lyon - Terre, Planètes, Environnement, Université Claude Bernard Lyon 1, CNRS, ENS-Lyon, 69622 Villeurbanne, France.)

[SIT25-P04] The effect of temperature on density of solid metals

*Asaka Kamiya[1], Hidenori Terasaki[1], Tadashi Kondo[1] (1.Osaka University)

[SIT25-P05] Phase relations in the Fe-Ni-Si system at high pressures and high temperatures

*Daijo Ikuta[1], Eiji Ohtani[1], Saori Kawaguchi[2], Naohisa Hirao[2], Yasuo Ohishi[2] (1.Department of Earth Science, Tohoku University, 2.JASRI)

[E] Poster | S (Solid Earth Sciences)：S-VC Volcanology

3:30 PM - 5:00 PM JST | 6:30 AM - 8:00 AM UTC | Poster Hall International Exhibition Hall8, Makuhari Messe_12

[S-VC34] Connecting magma dynamics in vent-conduit system with surface expression of volcanic eruption

convener:Takahiro Miwa(National research institute for earth science and disaster prevention), Nobuo Geshi(Geological Survey of Japan, The National Institute of Advanced Industrial Science and Technology)

[SVC34-P01] A new formulation of viscosity-included bubble nucleation rate in ascending magmas and re-estimation of bubble number density (2)

*Mizuki Nishiwaki[1], Atsushi Toramaru[2] (1.Department of Earth and Planetary Sciences, Graduate School of Sciences, Kyushu University, 2.Department of Earth and Planetary Sciences, Faculty of Sciences, Kyushu University)

[SVC34-P02] Kinetic delay of crystal growth controls plagioclase-basaltic melt apparent disequilibrium

*Ryoya Oida[1], Hidemi Ishibashi[1], ATSUSHI YASUDA[2], Natsumi Hokanishi[2] (1.Faculty of Science, Shizuoka University, 2.Earthquake Research Institute, University of Tokyo)

[SVC34-P03] **Eruptive trends and dynamics of remote volcanoes detected form space-based thermal data and SO_2 emissions: a comparative analysis of Stromboli, Batu Tara and Tinakula volcanoes**

*Corrado CIGOLINI[1], Marco Laiolo[1], Francesco Massimetti[1,2], Maurizio Ripepe[2], Diego Coppola[1] (1.Department of Earth Sciences, University of Torino, Italy, 2.Department of Earth Sciences, University of Firenze, Italy)

[SVC34-P04] The source depth of Strombolian explosions: a multiparametric approach and comparison

*Jacopo Taddeucci[1], Miguel Angel Alatorre-Ibarguengoitia[2], Valeria Cigala[3], Elisabetta Del Bello[1], Damien Gaudin[4], Ulrich Kueppers[4], Tullio Ricci[1], Valentino Salvatore[5], Piergiorgio Scarlato[1] (1.Istituto Nazionale di Geofisica e Vulcanologia, Rome, Italy, 2.Centro de Investigación en Gestión de Riesgo y Cambio Climático, Universidad de Ciencias y Artes de Chiapas, Tuxtla Gutiérrez, Mexico, 3.Department of Geosciences, Università degli Studi di Padova, Padua, Italy, 4.Department of Earth and Environmental Sciences. Ludwig-Maximilians-Universität (LMU). Munich, Germany, 5.Dipartimento di Scienze della Terra, Sapienza Università di Roma, Rome, Italy)

[SVC34-P05] Magmatic aggregate of basaltic ash particles

*Takahiro Miwa[1], Nobuo Geshi[2] (1.National research institute for earth science and disaster prevention, 2.National Institute of Advanced Industrial Science and Technology)

[SVC34-P06] Melt inclusion study on the eruption process of Izu-Omuroyama monogenetic volcano, Japan

Risako Hatada[1], *Hidemi Ishibashi[1], Yusuke Suzuki[2], ATSUSHI YASUDA[3], Natsumi Hokanishi[3] (1.Faculty of Science, Shizuoka University, 2.Izu Peninsula Geopark, 3.Earthquake Research Institute, University of Tokyo)

[SVC34-P07] Time-series variation in the textures of ejecta of the An'ei eruption, Izu-Oshima

*Yuya Ikenaga[1], Fukashi Maeno[1], ATSUSHI YASUDA[1] (1.Earthquake Research Institute, The University of Tokyo)

[SVC34-P08] The textural analysis of pumice from the Plinian eruption of Taupo volcano: implications for tube pumice

*Masatoshi Ohashi[1], Mie Ichihara[2], Fukashi Maeno[2], Ben Kennedy[3], Darren Gravley[3] (1.Department of Earth and Planetary Science, Graduate School of Science, The University of Tokyo, 2.Earthquake Research Institute, The University of Tokyo, 3.Department of Geological Sciences, The University of Canterbury)

[E] Poster | S (Solid Earth Sciences)：S-VC Volcanology

5:15 PM - 6:30 PM JST | 8:15 AM - 9:30 AM UTC | Poster Hall International Exhibition Hall8, Makuhari Messe_23

[S-VC34] Connecting magma dynamics in vent-conduit system with surface expression of volcanic eruption

convener:Takahiro Miwa(National research institute for earth science and disaster prevention), Nobuo Geshi(Geological Survey of Japan, The National Institute of Advanced Industrial Science and Technology)

[SVC34-P01] A new formulation of viscosity-included bubble nucleation rate in ascending magmas and re-estimation of bubble number density (2)

*Mizuki Nishiwaki[1], Atsushi Toramaru[2] (1.Department of Earth and Planetary Sciences, Graduate School of Sciences, Kyushu University, 2.Department of Earth and Planetary Sciences, Faculty of Sciences, Kyushu University)

[SVC34-P02] Kinetic delay of crystal growth controls plagioclase-basaltic melt apparent disequilibrium

*Ryoya Oida[1], Hidemi Ishibashi[1], ATSUSHI YASUDA[2], Natsumi Hokanishi[2] (1.Faculty of Science, Shizuoka University, 2.Earthquake Research Institute, University of Tokyo)

[SVC34-P03] **Eruptive trends and dynamics of remote volcanoes detected form space-based thermal data and SO_2 emissions: a comparative analysis of Stromboli, Batu Tara and Tinakula volcanoes**

*Corrado CIGOLINI[1], Marco Laiolo[1], Francesco Massimetti[1,2], Maurizio Ripepe[2], Diego Coppola[1] (1.Department of Earth Sciences, University of Torino, Italy, 2.Department of Earth Sciences, University of Firenze, Italy)

[SVC34-P04] The source depth of Strombolian explosions: a multiparametric approach and comparison

*Jacopo Taddeucci[1], Miguel Angel Alatorre-Ibarguengoitia[2], Valeria Cigala[3], Elisabetta Del Bello[1], Damien Gaudin[4], Ulrich Kueppers[4], Tullio Ricci[1], Valentino Salvatore[5], Piergiorgio Scarlato[1] (1.Istituto Nazionale di Geofisica e Vulcanologia, Rome, Italy, 2.Centro de Investigación en Gestión de Riesgo y Cambio Climático, Universidad de Ciencias y Artes de Chiapas, Tuxtla Gutiérrez, Mexico, 3.Department of Geosciences, Università degli Studi di Padova, Padua, Italy, 4.Department of Earth and Environmental Sciences. Ludwig-Maximilians-Universität (LMU). Munich, Germany, 5.Dipartimento di Scienze della Terra, Sapienza Università di Roma, Rome, Italy)

[SVC34-P05] Magmatic aggregate of basaltic ash particles

*Takahiro Miwa[1], Nobuo Geshi[2] (1.National research institute for earth science and disaster prevention, 2.National Institute of Advanced Industrial Science and Technology)

[SVC34-P06] Melt inclusion study on the eruption process of Izu-Omuroyama monogenetic volcano, Japan

Risako Hatada[1], *Hidemi Ishibashi[1], Yusuke Suzuki[2], ATSUSHI YASUDA[3], Natsumi Hokanishi[3] (1.Faculty of Science, Shizuoka University, 2.Izu Peninsula Geopark, 3.Earthquake Research Institute, University of Tokyo)

[SVC34-P07] Time-series variation in the textures of ejecta of the An'ei eruption, Izu-Oshima

*Yuya Ikenaga[1], Fukashi Maeno[1], ATSUSHI YASUDA[1] (1.Earthquake Research Institute, The University of Tokyo)

[SVC34-P08] The textural analysis of pumice from the Plinian eruption of Taupo volcano: implications for tube pumice

*Masatoshi Ohashi[1], Mie Ichihara[2], Fukashi Maeno[2], Ben Kennedy[3], Darren Gravley[3] (1.Department of Earth and Planetary Science, Graduate School of Science, The University of Tokyo, 2.Earthquake Research Institute, The University of Tokyo, 3.Department of Geological Sciences, The University of Canterbury)

[E] Poster | S (Solid Earth Sciences)：S-CG Complex & General

3:30 PM - 5:00 PM JST | 6:30 AM - 8:00 AM UTC | Poster Hall International Exhibition Hall8, Makuhari Messe_14

[S-CG50] Intraslab and intraplate earthquakes

convener:Saeko Kita(International Institute of Seismology and Earthquake Engineering, BRI), Tomohiro Ohuchi(Geodynamics Research Center, Ehime University), Marcel Thielmann(Bavarian Geoinstitute, University of Bayreuth), Ryo Okuwaki(Research Institute of Earthquake and Volcano Geology, Geological Survey of Japan, National Institute of Advanced Industrial Science and Technology)

[SCG50-P01] Changes in seismicity rate, stress orientations, and b-values before and after ETS events in the Philippine sea plate under Kii Peninsula

*Saeko Kita[1], Heidi Houston[2], Sachiko Tanaka[3], Youichi Asano[3], Takuo Shibutani[4], Naoki Suda[5] (1.Building Research Institute, 2.USC, 3.NIED, 4.DPRI, Kyoto University, 5.Hiroshima University)

[SCG50-P02] **Inhomogeneous conduit across slab controlled by intraslab stress heterogeneity in the Nankai subduction zone**

*Makoto Otsubo[1], Ayumu Miyakawa[2], Ikuo Katayama[3], Keishi Okazaki[4] (1.Geological Survey of Japan, Research Institute of Earthquake and Volcano Geology, 2.Geological Survey of Japan, Research Institute of Geology and Geoinformation, 3.Hiroshima University, 4.JAMSTEC)

[SCG50-P03] New insights into the mechanism of deep-focus earthquakes

*Ayako Tsuchiyama[1], Junichi Nakajima[1] (1.Tokyo Institute of Technology)

[SCG50-P04] Faulting in deforming harzburgite under wet conditions

*Tomohiro Ohuchi[1], Xinglin Lei[2], Yuji Higo[3], Yoshinori Tange[3], Takeshi Sakai[1] (1.Geodynamics Research Center, Ehime University, 2.National Institute of Advanced Industrial Science and Technology, 3.Japan Synchrotron Radiation Research Institute)

[SCG50-P05] Semi-brittle behavior of olivine single crystals under the conditions of Earth's mantle transition zone

Yoshihisa Naruse[1], *Tomohiro Ohuchi[1] (1.Geodynamics Research Center, Ehime University)

[SCG50-P06] High-pressure deformation experiments on peridotite gouges under hydrothermal conditions, using a deformation-DIA apparatus

*Maki Semba[1], Ken-ichi Hirauchi[1], Tomohiro Ohuchi[2], Katsuyoshi Michibayashi[3] (1.Department of Geosciences, Faculty of Science, Shizuoka University, 2.Geodynamics Research Center, Ehime University, 3.Department of Earth and Planetary Sciences, Nagoya university)

[SCG50-P07] Stable fault slip in antigorite-olivine aggregates at high pressures

Mai Ikehara[1], *Tomoaki Kubo[1], Takuya Iwasato[2], Yuji Higo[3], Masahiro Imamura[1], Yoshinori Tange[3] (1.Kyushu University, 2.Shin-Nippon Nondestructive Inspection Co., Ltd., 3.JASRI)

[SCG50-P08] Rheology and frictional instability of lawsonite in high pressure deformation experiments

*Rei Shiraishi[1], Jun Muto[1], Akihiro Tsunoda[2], Sando Sawa[1], Akio Suzuki[1] (1.Department of Earth Science, Graduate School of Science, Tohoku University, 2.Earthquake Research Institute, University of Tokyo)

[SCG50-P09] Grain Size Dependency of Olivine-Spinel Phase Transformational Mechanism Responsible for Deep-focus Earthquakes

*Sando Sawa[1], Jun Muto[1], Nobuyoshi Miyajima[2], Hiroyuki Nagahama[1] (1.Department of Earth Science, Tohoku University, 2.Bayerisches Geoinstitut, University of Bayreuth)

[SCG50-P10] **Seismicity and mineral destabilizations in the subducting mantle up to 6 GPa, 200 km depth**

*Thomas P. Ferrand[1] (1.Earthquake Research Institute)

[SCG50-P11] Receiver function imaging of subducting Pacific plate and mantle wedge under Japanese islands using denser network of stations

*HyeJeong Kim[1], Hitoshi Kawakatsu[1], Takeshi Akuhara[1], Masanao Shinohara[1] (1.Earthquake Research Institute, The University of Tokyo)

[SCG50-P12] Strong S-wave attenuation in the mantle wedge beneath the NE Japan and interpretations of high-frequency wave propagation path of intraslab earthquakes

*Takahiro Shiina[1,2], Kei Katsumata[2], Kiyoshi Yomogida[3], Aitaro Kato[1] (1.Earthquake Research Institute, The University of Tokyo, 2.Institute of Seismology and Volcanology, Graduate School of Science, Hokkaido University, 3.Graduate School of Science, Hokkaido University)

[E] Poster | S (Solid Earth Sciences)：S-CG Complex & General

5:15 PM - 6:30 PM JST | 8:15 AM - 9:30 AM UTC | Poster Hall International Exhibition Hall8, Makuhari Messe_26

[S-CG50] Intraslab and intraplate earthquakes

convener:Saeko Kita(International Institute of Seismology and Earthquake Engineering, BRI), Tomohiro Ohuchi(Geodynamics Research Center, Ehime University), Marcel Thielmann(Bavarian Geoinstitute, University of Bayreuth), Ryo Okuwaki(Research Institute of Earthquake and Volcano Geology, Geological Survey of Japan, National Institute of Advanced Industrial Science and Technology)

[SCG50-P01] Changes in seismicity rate, stress orientations, and b-values before and after ETS events in the Philippine sea plate under Kii Peninsula

*Saeko Kita[1], Heidi Houston[2], Sachiko Tanaka[3], Youichi Asano[3], Takuo Shibutani[4], Naoki Suda[5] (1.Building Research Institute, 2.USC, 3.NIED, 4.DPRI, Kyoto University, 5.Hiroshima University)

[SCG50-P02] **Inhomogeneous conduit across slab controlled by intraslab stress heterogeneity in the Nankai subduction zone**

*Makoto Otsubo[1], Ayumu Miyakawa[2], Ikuo Katayama[3], Keishi Okazaki[4] (1.Geological Survey of Japan, Research Institute of Earthquake and Volcano Geology, 2.Geological Survey of Japan, Research Institute of Geology and Geoinformation, 3.Hiroshima University, 4.JAMSTEC)

[SCG50-P03] New insights into the mechanism of deep-focus earthquakes

*Ayako Tsuchiyama[1], Junichi Nakajima[1] (1.Tokyo Institute of Technology)

[SCG50-P04] Faulting in deforming harzburgite under wet conditions

*Tomohiro Ohuchi[1], Xinglin Lei[2], Yuji Higo[3], Yoshinori Tange[3], Takeshi Sakai[1] (1.Geodynamics Research Center, Ehime University, 2.National Institute of Advanced Industrial Science and Technology, 3.Japan Synchrotron Radiation Research Institute)

[SCG50-P05] Semi-brittle behavior of olivine single crystals under the conditions of Earth's mantle transition zone

Yoshihisa Naruse[1], *Tomohiro Ohuchi[1] (1.Geodynamics Research Center, Ehime University)

[SCG50-P06] High-pressure deformation experiments on peridotite gouges under hydrothermal conditions, using a deformation-DIA apparatus

*Maki Semba[1], Ken-ichi Hirauchi[1], Tomohiro Ohuchi[2], Katsuyoshi Michibayashi[3] (1.Department of Geosciences, Faculty of Science, Shizuoka University, 2.Geodynamics Research Center, Ehime University, 3.Department of Earth and Planetary Sciences, Nagoya university)

[SCG50-P07] Stable fault slip in antigorite-olivine aggregates at high pressures

Mai Ikehara[1], *Tomoaki Kubo[1], Takuya Iwasato[2], Yuji Higo[3], Masahiro Imamura[1], Yoshinori Tange[3] (1.Kyushu University, 2.Shin-Nippon Nondestructive Inspection Co., Ltd., 3.JASRI)

[SCG50-P08] Rheology and frictional instability of lawsonite in high pressure deformation experiments

*Rei Shiraishi[1], Jun Muto[1], Akihiro Tsunoda[2], Sando Sawa[1], Akio Suzuki[1] (1.Department of Earth Science, Graduate School of Science, Tohoku University, 2.Earthquake Research Institute, University of Tokyo)

[SCG50-P09] Grain Size Dependency of Olivine-Spinel Phase Transformational Mechanism Responsible for Deep-focus Earthquakes

*Sando Sawa[1], Jun Muto[1], Nobuyoshi Miyajima[2], Hiroyuki Nagahama[1] (1.Department of Earth Science, Tohoku University, 2.Bayerisches Geoinstitut, University of Bayreuth)

[SCG50-P10] **Seismicity and mineral destabilizations in the subducting mantle up to 6 GPa, 200 km depth**

*Thomas P. Ferrand[1] (1.Earthquake Research Institute)

[SCG50-P11] Receiver function imaging of subducting Pacific plate and mantle wedge under Japanese islands using denser network of stations

*HyeJeong Kim[1], Hitoshi Kawakatsu[1], Takeshi Akuhara[1], Masanao Shinohara[1] (1.Earthquake Research Institute, The University of Tokyo)

[SCG50-P12] Strong S-wave attenuation in the mantle wedge beneath the NE Japan and interpretations of high-frequency wave propagation path of intraslab earthquakes

*Takahiro Shiina[1,2], Kei Katsumata[2], Kiyoshi Yomogida[3], Aitaro Kato[1] (1.Earthquake Research Institute, The University of Tokyo, 2.Institute of Seismology and Volcanology, Graduate School of Science, Hokkaido University, 3.Graduate School of Science, Hokkaido University)

[E] Poster | S (Solid Earth Sciences)：S-CG Complex & General

10:45 AM - 12:15 PM JST | 1:45 AM - 3:15 AM UTC | Poster Hall International Exhibition Hall8, Makuhari Messe_6

[S-CG51] Role of volatiles on Earth and planetary dynamics

convener:Takayuki Ishii(Bavarian Research Institute, University of Bayreuth), Eiji Ohtani(Department of Earth and Planetary Materials Science, Graduate School of Science, Tohoku University), Michihiko Nakamura(Division of Earth and Planetary Materials Science, Department of Earth Science, Graduate School of Science, Tohoku University), Bjorn Mysen(Geophysical Laboratory, Carnegie Inst. Washington)

[SCG51-P01] Permeability prediction of porous media with the finite difference Stokes solver LaMEM

*Philipp Eichheimer[1], Wakana Fujita[2], Marcel Thielmann[1], Anton Popov[3], Gregor Golabek[1], Boris Kaus[3], Maximilian Kottwitz[3] (1.Bayerisches Geoinstitut, University of Bayreuth, 2.Department of Earth Science, Tohoku University, Sendai, 3.Institute of Geosciences, Johannes Gutenberg University Mainz)

[SCG51-P02] Grain growth-induced fluid localization and permeability reduction

*Wakana Fujita[1], Michihiko Nakamura[1], Kentaro Uesugi[2] (1.Graduate School of Science, Tohoku University, 2.JASRI/SPring-8)

[SCG51-P03] Pargasite stability in the upper mantle at H_2O-undersaturated conditions

*Marija Putak Juricek[1], Hans Keppler[1] (1.BGI)

[SCG51-P04] **Constraining the water content at the top of the mantle transition zone with the elasticity of wadsleyite and olivine**

*Zhongqing Wu[1] (1.University of Science and Technology of China)

[SCG51-P05] ***Single crystal elasticity of Fe-bearing phase E by Brillouin spectroscopy***

*Niccolo Satta[1], Hauke Marquardt [2], Alexander Kurnosov[1], Tiziana Boffa Ballaran [1], Johannes Buchen[3], Catherine McCammon[1], Takaaki Kawazoe[4] (1.Bayerisches Geoinstitut, University of Bayreuth, 95440 Bayreuth, Germany, 2.Department of Earth Sciences, University of Oxford, South Parks Road, Oxford, UK., 3.Seismological Laboratory, California Institute of Technology, Pasadena, CA 91125, USA., 4.Department of Earth and Planetary Systems Science, Hiroshima University, Hiroshima 739-8526, Japan.)

[SCG51-P06] Discovery of two hexagonal phases in (Fe,Al)OOH under the P-T conditions of the deep lower mantle

*Lu Liu[1,2], Li Zhang[1], Hongsheng Yuan[1] (1.Center for High Pressure Science and Technology Advanced Research, 2.University of Science and Technology of China)

[SCG51-P07] **Effect of grid resolution on tectonic regimes in global-scale convection models**

*Enrico Marzotto[1], Marcel Thielmann[1], Gregor Golabek[1] (1.Bayerisches Geoinstitut)

[SCG51-P08] A 3-D crust and uppermost mantle electrical conductivity model of subduction zone beneath NE Japan

*Masahiro Ichiki[1,2], Toshiki Kaida[1], Yasuo Ogawa[3] (1.Graduate School of Science, Tohoku University, 2.International Research Institute of Disaster Science, 3.School of Science, Tokyo Institute of Technology)

[SCG51-P09] *The conditions of sublithospheric diamond formation constrained from ferric iron-rich exsolution from ferropericlase inclusions.*

*Caterina Melai[1], Daniel Frost[1], Tiziana Boffa Ballaran[1], Catherine McCammon[1] (1.Bayerisches Geoinstitute)

[SCG51-P10] **Probing the variation of the oxygen fugacity in diamond anvil cells using the Fe-Ir alloy as redox sensor**

*Serena Dominijanni[1], Catherine McCammon[1], Leonid Dubrovinsky[1], Dan Frost[1], Nobuyoshi Miyajima[1] (1.Bayerisches Geoinstitut)

[SCG51-P11] Goethite behavior at Earth's lower mantle conditions

*Egor Gennadievich Koemets[1], Maxim Bykov[1], George Aprilis[2], Timofey Fedotenko[2], Stella Chariton[1], Saiana Khandarkhaeva[1], Iuliia Koemets[1], Marcel Thielmann[1], Natalia Dubrovinsaia[2], Leonid Dubrovinsky[1] (1.BGI (Bayerisches Geoinstitut), Universität Bayreuth, Germany, 2.Material Physics and Technology at Extreme Conditions, Laboratory of Crystallography, Universität Bayreuth, Germany)

[SCG51-P12] The oxygen content of sulphides in the mantle and a geothermometer for diamond formation

*Sumith Abeykoon[1], Dan Frost[1], Vera Laurenz[1] (1.Bayerisches Geoinstitut, University of Bayreuth)

[E] Poster | S (Solid Earth Sciences)：S-CG Complex & General

5:15 PM - 6:30 PM JST | 8:15 AM - 9:30 AM UTC | Poster Hall International Exhibition Hall8, Makuhari Messe_27

[S-CG51] Role of volatiles on Earth and planetary dynamics

convener:Takayuki Ishii(Bavarian Research Institute, University of Bayreuth), Eiji Ohtani(Department of Earth and Planetary Materials Science, Graduate School of Science, Tohoku University), Michihiko Nakamura(Division of Earth and Planetary Materials Science, Department of Earth Science, Graduate School of Science, Tohoku University), Bjorn Mysen(Geophysical Laboratory, Carnegie Inst. Washington)

[SCG51-P01] Permeability prediction of porous media with the finite difference Stokes solver LaMEM

*Philipp Eichheimer[1], Wakana Fujita[2], Marcel Thielmann[1], Anton Popov[3], Gregor Golabek[1], Boris Kaus[3], Maximilian Kottwitz[3] (1.Bayerisches Geoinstitut, University of Bayreuth, 2.Department of Earth Science, Tohoku University, Sendai, 3.Institute of Geosciences, Johannes Gutenberg University Mainz)

[SCG51-P02] Grain growth-induced fluid localization and permeability reduction

*Wakana Fujita[1], Michihiko Nakamura[1], Kentaro Uesugi[2] (1.Graduate School of Science, Tohoku University, 2.JASRI/SPring-8)

[SCG51-P03] Pargasite stability in the upper mantle at H_2O-undersaturated conditions

*Marija Putak Juricek[1], Hans Keppler[1] (1.BGI)

[SCG51-P04] **Constraining the water content at the top of the mantle transition zone with the elasticity of wadsleyite and olivine**

*Zhongqing Wu[1] (1.University of Science and Technology of China)

[SCG51-P05] ***Single crystal elasticity of Fe-bearing phase E by Brillouin spectroscopy***

*Niccolo Satta[1], Hauke Marquardt [2], Alexander Kurnosov[1], Tiziana Boffa Ballaran [1], Johannes Buchen[3], Catherine McCammon[1], Takaaki Kawazoe[4] (1.Bayerisches Geoinstitut, University of Bayreuth, 95440 Bayreuth, Germany, 2.Department of Earth Sciences, University of Oxford, South Parks Road, Oxford, UK., 3.Seismological Laboratory, California Institute of Technology, Pasadena, CA 91125, USA., 4.Department of Earth and Planetary Systems Science, Hiroshima University, Hiroshima 739-8526, Japan.)

[SCG51-P06] Discovery of two hexagonal phases in (Fe,Al)OOH under the P-T conditions of the deep lower mantle

*Lu Liu[1,2], Li Zhang[1], Hongsheng Yuan[1] (1.Center for High Pressure Science and Technology Advanced Research, 2.University of Science and Technology of China)

[SCG51-P07] **Effect of grid resolution on tectonic regimes in global-scale convection models**

*Enrico Marzotto[1], Marcel Thielmann[1], Gregor Golabek[1] (1.Bayerisches Geoinstitut)

[SCG51-P08] A 3-D crust and uppermost mantle electrical conductivity model of subduction zone beneath NE Japan

*Masahiro Ichiki[1,2], Toshiki Kaida[1], Yasuo Ogawa[3] (1.Graduate School of Science, Tohoku University, 2.International Research Institute of Disaster Science, 3.School of Science, Tokyo Institute of Technology)

[SCG51-P09] *The conditions of sublithospheric diamond formation constrained from ferric iron-rich exsolution from ferropericlase inclusions.*

*Caterina Melai[1], Daniel Frost[1], Tiziana Boffa Ballaran[1], Catherine McCammon[1] (1.Bayerisches Geoinstitute)

[SCG51-P10] **Probing the variation of the oxygen fugacity in diamond anvil cells using the Fe-Ir alloy as redox sensor**

*Serena Dominijanni[1], Catherine McCammon[1], Leonid Dubrovinsky[1], Dan Frost[1], Nobuyoshi Miyajima[1] (1.Bayerisches Geoinstitut)

[SCG51-P11] Goethite behavior at Earth's lower mantle conditions

*Egor Gennadievich Koemets[1], Maxim Bykov[1], George Aprilis[2], Timofey Fedotenko[2], Stella Chariton[1], Saiana Khandarkhaeva[1], Iuliia Koemets[1], Marcel Thielmann[1], Natalia Dubrovinsaia[2], Leonid Dubrovinsky[1] (1.BGI (Bayerisches Geoinstitut), Universität Bayreuth, Germany, 2.Material Physics and Technology at Extreme Conditions, Laboratory of Crystallography, Universität Bayreuth, Germany)

[SCG51-P12] The oxygen content of sulphides in the mantle and a geothermometer for diamond formation

*Sumith Abeykoon[1], Dan Frost[1], Vera Laurenz[1] (1.Bayerisches Geoinstitut, University of Bayreuth)

[E] Poster | M (Multidisciplinary and Interdisciplinary)：M-IS Intersection

10:45 AM - 12:15 PM JST | 1:45 AM - 3:15 AM UTC | Poster Hall International Exhibition Hall8, Makuhari Messe_9

[M-IS03] Evolution and variability of the Asian monsoon in Cenozoic global climate changes

convener:Masanobu Yamamoto(Faculty of Environmental Earth Science, Hokkaido University), Ryuji Tada(Department of Earth and Planetary Science, Graduate School of Science, The Univeristy of Tokyo)

[MIS03-P01] Asian dust source variability since 10 Ma based on grain size specific mineral composition at IODP Site U1425 in the Japan Sea

*Mui Fa Alison Lee[1], Tomohisa Irino[1] (1.Faculty of Environmental Earth Science, Hokkaido University)

[MIS03-P02] Sources and formation environment of biomass burning products in Pliocene and Pleistocene marine sediments in the Japan Sea

*Song Lu[1], Youhei Yamashita[2], Tomohisa Irino[2] (1.Graduate School of Environmental Science, Hokkaido University , 2.Faculty of Environmental Earth Science, Hokkaido University)

[MIS03-P03] Variation of mineral dust flux in peat at a high moor on the Mt. Daisetsu during Holocene

*Tomohisa Irino[1], Keisuke Hirai[1], Osamu Seki[1], James Hooper[2], Samuel Marx[2] (1.Hokkaido University, 2.University of Wollongong)

[MIS03-P04] Variations in sea surface environments recorded by algal biomarkers in the Japan Sea off the western coast of Hokkaido (IODP Site U1422) over the last 250 ka

*Asako Suzuki[1], Ken Sawada[2], Satoshi Furota[3], Yaeko Igarashi[4], Tomohisa Irino[5] (1.Graduate School of Science, Hokkaido University, 2.Department of Earth and Planetary Sciences, Faculty of Science, Hokkaido University, 3.Japan Agency for Marine-Earth Science and Technology, 4.Institute for Paleoenvironment of Northern Regions, 5.Faculty of Environmental Earth Science, Hokkaido University)

[MIS03-P05] **Decadal oscillation in hydrogen stable isotope ratio of long chain fatty acids in Lake Suigetsu sediment core**

*Masaya Inagaki[1], Masanobu Yamamoto[1,2], Takeshi Nakagawa[3] (1.Graduate School of Environmental Science, Hokkaido University, 2.Faculty of Environmental Earth Science, Hokkaido University, 3.Research Center for Palaeoclimatology, Ritsumeikan University)

[MIS03-P06] **Amplitude modulation of sea surface temperature variability in the Bay of Bengal by 400-kyr eccentricity cycle**

*Masanobu Yamamoto[1], Yuko Tsuchiya[1], Steven Clemens[2] (1.Faculty of Environmental Earth Science, Hokkaido University, 2.Department of Earth, Planetary and Environmental Sciences, Brown University)

[E] Poster | M (Multidisciplinary and Interdisciplinary)：M-IS Intersection

5:15 PM - 6:30 PM JST | 8:15 AM - 9:30 AM UTC | Poster Hall International Exhibition Hall8, Makuhari Messe_34

[M-IS03] Evolution and variability of the Asian monsoon in Cenozoic global climate changes

convener:Masanobu Yamamoto(Faculty of Environmental Earth Science, Hokkaido University), Ryuji Tada(Department of Earth and Planetary Science, Graduate School of Science, The Univeristy of Tokyo)

[MIS03-P01] Asian dust source variability since 10 Ma based on grain size specific mineral composition at IODP Site U1425 in the Japan Sea

*Mui Fa Alison Lee[1], Tomohisa Irino[1] (1.Faculty of Environmental Earth Science, Hokkaido University)

[MIS03-P02] Sources and formation environment of biomass burning products in Pliocene and Pleistocene marine sediments in the Japan Sea

*Song Lu[1], Youhei Yamashita[2], Tomohisa Irino[2] (1.Graduate School of Environmental Science, Hokkaido University , 2.Faculty of Environmental Earth Science, Hokkaido University)

[MIS03-P03] Variation of mineral dust flux in peat at a high moor on the Mt. Daisetsu during Holocene

*Tomohisa Irino[1], Keisuke Hirai[1], Osamu Seki[1], James Hooper[2], Samuel Marx[2] (1.Hokkaido University, 2.University of Wollongong)

[MIS03-P04] Variations in sea surface environments recorded by algal biomarkers in the Japan Sea off the western coast of Hokkaido (IODP Site U1422) over the last 250 ka

*Asako Suzuki[1], Ken Sawada[2], Satoshi Furota[3], Yaeko Igarashi[4], Tomohisa Irino[5] (1.Graduate School of Science, Hokkaido University, 2.Department of Earth and Planetary Sciences, Faculty of Science, Hokkaido University, 3.Japan Agency for Marine-Earth Science and Technology, 4.Institute for Paleoenvironment of Northern Regions, 5.Faculty of Environmental Earth Science, Hokkaido University)

[MIS03-P05] **Decadal oscillation in hydrogen stable isotope ratio of long chain fatty acids in Lake Suigetsu sediment core**

*Masaya Inagaki[1], Masanobu Yamamoto[1,2], Takeshi Nakagawa[3] (1.Graduate School of Environmental Science, Hokkaido University, 2.Faculty of Environmental Earth Science, Hokkaido University, 3.Research Center for Palaeoclimatology, Ritsumeikan University)

[MIS03-P06] **Amplitude modulation of sea surface temperature variability in the Bay of Bengal by 400-kyr eccentricity cycle**

*Masanobu Yamamoto[1], Yuko Tsuchiya[1], Steven Clemens[2] (1.Faculty of Environmental Earth Science, Hokkaido University, 2.Department of Earth, Planetary and Environmental Sciences, Brown University)

[E] Poster | M (Multidisciplinary and Interdisciplinary)：M-IS Intersection

10:45 AM - 12:15 PM JST | 1:45 AM - 3:15 AM UTC | Poster Hall International Exhibition Hall8, Makuhari Messe_10

[M-IS04] Interdisciplinary studies on pre-earthquake processes

convener:Katsumi Hattori(Department of Earth Sciences, Graduate School of Science, Chiba University), JANN-YENQ Liu(Institute of Space Science, National Central University, Taiwan), Dimitar Ouzounov(Center of Excellence in Earth Systems Modeling & Observations (CEESMO) , Schmid College of Science & Technology Chapman University, Orange, California, USA), Qinghua Huang(Peking University)

[MIS04-P01] Statistical analysis and Evaluation of ULF seismo-magnetic phenomena at Kakioka, Japan, during 1983-2017

*Kei Takahashi[1], Katsumi Hattori[2], Peng Han[3] (1.Faculty of Science, Chiba University, 2.Graduate School of Science, Chiba University, 3.Southern University of Science and Technology, China)

[MIS04-P02] Pre-seismic anomalies on Earth's magnetic field and ionosphere electron density using Swarm data

*Amune Yamazaki[1], Katsumi Hattori[1], Rui Song[1] (1.Chiba University)

[MIS04-P03] Measurement of radon density in the atmosphere at Okayama, Kochi, Choshi and Kiyosumi, II

*Tohru Okabayashi[1], Kiyotaka Ninagawa[2], Isao Yamamoto[3], Katsumi Hattori[4], Chie Yoshino[4], Haruna Kojima[4], Nobuhiro Maeda (1.Department of Merical Risk and Crisis Management, Faculty of Risk and Crisis Management, Chiba Institute of Science, 2.Faculty of Science, Okayama University of Science, 3.Falcuty of Engineering, Okayama University of Science, 4.Graduate school of Science, Chiba University)

[MIS04-P04] Possible anomalous changes in solar quiet-daily geomagnetic variation *Sq* related to the 2011 off the Pacific coast of Tohoku earthquake (Mw 9.0)

*Xiaocan Liu[1], Katsumi Hattori[2,3], Peng Han[4], Huaran Chen[1] (1.Institute of geophysics China Earthquake Administrition, 2.Graduate School of Science, Chiba University, Chiba, Japan, 3. Center for Environmental Remote Sensing, Chiba University, Chiba, Japan, 4.Department of Earth and Space Sciences, Southern University of Science and Technology, ShenZhen, China)

[MIS04-P05] Co-seismic geomagnetic fluctuations and atmospheric disturbances during the 2018 M6.2 Hualien Earthquake

*Chun-Rong Chen[1], JANN-YENQ Liu[1] (1.Graduate Institute of Space Science, National Central University)

[MIS04-P06] Multi-sensor monitoring network for earthquake precursor study near subduction zone at Boso, Japan

*Katsumi Hattori[1], Chie Yoshino[1], WEIYUN XIE[2], Sanaka Saito[2], Haruna Kojima[2], Rui Song[2], Peng Han[3], Toru Mogi[4], Tada-nori Goto[5], Ichi Takumi[6], Hiroshi Yasukawa[7], Motoaki Mouri[8], Jun Izutsu[9], Tadashi Takano[10], Chihiro Yamanaka[11], Masashi Kamogawa[12], Yoshiaki Ando[13], JANN-YENQ Liu[14], Dimitar Ouzounov[15], Valery Tramutoli[16] (1.Department of Earth Sciences, Graduate School of Science, Chiba University, 2.Graduate School of Science and Engineering, Chiba University, 3.Southern University of Science and Technology, China, 4.Hokkaido University, 5.Kyoto University, 6.Nagoya Institute of Technology, 7.Aichi Prefectural University, 8.Aichi University, 9.Chubu University, 10.Nihon University, 11.Osaka University, 12.Tokyo Gakugei University, 13.The University of Electro-Communications, 14.National Central University, Taiwan, 15.Chapman University, US, 16.University of Basilicagta, Italy)

[MIS04-P07] Transient Effects in Atmosphere and Ionosphere Associated with 2018 Mw 7.5 Sulawesi Indonesia Earthquake and Triggered Tsunami and Volcano Activities

★Invited Papers

*Dimitar Ouzounov[1], Sergey Pulinets[2], Dmitry Davidenko[2], Alexander Rozhnoi[3], Maria Solovieva[3], Tiger Liu[4] (1.Center of Excellence in Earth Systems Modeling & Observations (CEESMO) , Schmid College of Science & Technology Chapman University, Orange, California, USA, 2.Space Research Institute, RAS, Moscow, Russia, 3.The Schmidt Institute of Physics of the Earth, RAS, Moscow, Russia, 4.Center for Astronautical Physics and Engineering, National Central University, Taoyuan City, Taiwan)

[MIS04-P08] Seismicity change and b value variation prior to the Wenchuan earthquake (*Ms 8.0*)

*Peng Han[1], Rui Wang[1], Ying Chang[1], Miao Miao[1], Haixia Shi[2], Lingyuan Meng[2], Xuemei Zhang[2], Weiyun Xie[3], Katsumi Hattori[3] (1.Southern University of Science and Technology, Shenzhen, China, 2.China Earthquake Networks

Center, Beijing 100045, China, 3.Chiba University, Chiba, Japan)

[E] Poster | M (Multidisciplinary and Interdisciplinary)：M-IS Intersection

5:15 PM - 6:30 PM JST | 8:15 AM - 9:30 AM UTC | Poster Hall International Exhibition Hall8, Makuhari Messe_35

[M-IS04] Interdisciplinary studies on pre-earthquake processes

convener:Katsumi Hattori(Department of Earth Sciences, Graduate School of Science, Chiba University), JANN-YENQ Liu(Institute of Space Science, National Central University, Taiwan), Dimitar Ouzounov(Center of Excellence in Earth Systems Modeling & Observations (CEESMO) , Schmid College of Science & Technology Chapman University, Orange, California, USA), Qinghua Huang(Peking University)

[MIS04-P01] Statistical analysis and Evaluation of ULF seismo-magnetic phenomena at Kakioka, Japan, during 1983-2017

*Kei Takahashi[1], Katsumi Hattori[2], Peng Han[3] (1.Faculty of Science, Chiba University, 2.Graduate School of Science, Chiba University, 3.Southern University of Science and Technology, China)

[MIS04-P02] Pre-seismic anomalies on Earth's magnetic field and ionosphere electron density using Swarm data

*Amune Yamazaki[1], Katsumi Hattori[1], Rui Song[1] (1.Chiba University)

[MIS04-P03] Measurement of radon density in the atmosphere at Okayama, Kochi, Choshi and Kiyosumi, II

*Tohru Okabayashi[1], Kiyotaka Ninagawa[2], Isao Yamamoto[3], Katsumi Hattori[4], Chie Yoshino[4], Haruna Kojima[4], Nobuhiro Maeda (1.Department of Merical Risk and Crisis Management, Faculty of Risk and Crisis Management, Chiba Institute of Science, 2.Faculty of Science, Okayama University of Science, 3.Falcuty of Engineering, Okayama University of Science, 4.Graduate school of Science, Chiba University)

[MIS04-P04] Possible anomalous changes in solar quiet-daily geomagnetic variation *Sq* related to the 2011 off the Pacific coast of Tohoku earthquake (Mw 9.0)

*Xiaocan Liu[1], Katsumi Hattori[2,3], Peng Han[4], Huaran Chen[1] (1.Institute of geophysics China Earthquake Administrition, 2.Graduate School of Science, Chiba University, Chiba, Japan, 3. Center for Environmental Remote Sensing, Chiba University, Chiba, Japan, 4.Department of Earth and Space Sciences, Southern University of Science and Technology, ShenZhen, China)

[MIS04-P05] Co-seismic geomagnetic fluctuations and atmospheric disturbances during the 2018 M6.2 Hualien Earthquake

*Chun-Rong Chen[1], JANN-YENQ Liu[1] (1.Graduate Institute of Space Science, National Central University)

[MIS04-P06] Multi-sensor monitoring network for earthquake precursor study near subduction zone at Boso, Japan

*Katsumi Hattori[1], Chie Yoshino[1], WEIYUN XIE[2], Sanaka Saito[2], Haruna Kojima[2], Rui Song[2], Peng Han[3], Toru Mogi[4], Tada-nori Goto[5], Ichi Takumi[6], Hiroshi Yasukawa[7], Motoaki Mouri[8], Jun Izutsu[9], Tadashi Takano[10], Chihiro Yamanaka[11], Masashi Kamogawa[12], Yoshiaki Ando[13], JANN-YENQ Liu[14], Dimitar Ouzounov[15], Valery Tramutoli[16] (1.Department of Earth Sciences, Graduate School of Science, Chiba University, 2.Graduate School of Science and Engineering, Chiba University, 3.Southern University of Science and Technology, China, 4.Hokkaido University, 5.Kyoto University, 6.Nagoya Institute of Technology, 7.Aichi Prefectural University, 8.Aichi University, 9.Chubu University, 10.Nihon University, 11.Osaka University, 12.Tokyo Gakugei University, 13.The University of Electro-Communications, 14.National Central University, Taiwan, 15.Chapman University, US, 16.University of Basilicagta, Italy)

[MIS04-P07] Transient Effects in Atmosphere and Ionosphere Associated with 2018 Mw 7.5 Sulawesi Indonesia Earthquake and Triggered Tsunami and Volcano Activities

★Invited Papers

*Dimitar Ouzounov[1], Sergey Pulinets[2], Dmitry Davidenko[2], Alexander Rozhnoi[3], Maria Solovieva[3], Tiger Liu[4] (1.Center of Excellence in Earth Systems Modeling & Observations (CEESMO) , Schmid College of Science & Technology Chapman University, Orange, California, USA, 2.Space Research Institute, RAS, Moscow, Russia, 3.The Schmidt Institute of Physics of the Earth, RAS, Moscow, Russia, 4.Center for Astronautical Physics and Engineering, National Central University, Taoyuan City, Taiwan)

[MIS04-P08] Seismicity change and b value variation prior to the Wenchuan earthquake (*Ms 8.0*)

*Peng Han[1], Rui Wang[1], Ying Chang[1], Miao Miao[1], Haixia Shi[2], Lingyuan Meng[2], Xuemei Zhang[2], Weiyun Xie[3], Katsumi Hattori[3] (1.Southern University of Science and Technology, Shenzhen, China, 2.China Earthquake Networks Center, Beijing 100045, China, 3.Chiba University, Chiba, Japan)

[E] Poster | M (Multidisciplinary and Interdisciplinary)：M-IS Intersection

3:30 PM - 5:00 PM JST | 6:30 AM - 8:00 AM UTC | Poster Hall International Exhibition Hall8, Makuhari Messe_19

[M-IS06] Conservation of geoparks, natural geosites and cultural heritage: weathering process and damage assessment

convener:Chiaki T. Oguchi(Institute for Environmental Science and Technology, Graduate School of Science and Engineering, Saitama University), Tetsuya Waragai(Graduate School of Science and Engineering, Nihon University), Kuniyasu Mokudai(Tohoku Gakuin University), Magdalini Theodoridou(School of Engineering, Cardiff University)

[MIS06-P01] The artistic qualities of religion reliefs in Taya-cave.Japan

*OGATA KEISUKE[1] (1.TSURUMI UNIVERSITY)

[MIS06-P02] Effect of stress concentration on the Weathering Mechanism of Sandstone Pillars of Angkor Wat, Cambodia by means of numerical simulation

*Takato Takemura[1], Tetsuya Waragai[2] (1.Nihon Univ., 2.Nihon University)

[MIS06-P03] Meaning to preserve evidence of large scale landslide

*Kuniyasu Mokudai[1], Hidekazu Sato[2] (1.Japan Geoservice Incorporated, 2.Mt. Kurikoma Area Geopark)

[E] Poster | M (Multidisciplinary and Interdisciplinary)：M-IS Intersection

5:15 PM - 6:30 PM JST | 8:15 AM - 9:30 AM UTC | Poster Hall International Exhibition Hall8, Makuhari Messe_36

[M-IS06] Conservation of geoparks, natural geosites and cultural heritage: weathering process and damage assessment

convener:Chiaki T. Oguchi(Institute for Environmental Science and Technology, Graduate School of Science and Engineering, Saitama University), Tetsuya Waragai(Graduate School of Science and Engineering, Nihon University), Kuniyasu Mokudai(Tohoku Gakuin University), Magdalini Theodoridou(School of Engineering, Cardiff University)

[MIS06-P01] The artistic qualities of religion reliefs in Taya-cave.Japan

*OGATA KEISUKE[1] (1.TSURUMI UNIVERSITY)

[MIS06-P02] Effect of stress concentration on the Weathering Mechanism of Sandstone Pillars of Angkor Wat, Cambodia by means of numerical simulation

*Takato Takemura[1], Tetsuya Waragai[2] (1.Nihon Univ., 2.Nihon University)

[MIS06-P03] Meaning to preserve evidence of large scale landslide

*Kuniyasu Mokudai[1], Hidekazu Sato[2] (1.Japan Geoservice Incorporated, 2.Mt. Kurikoma Area Geopark)

[E] Poster | M (Multidisciplinary and Interdisciplinary)：M-IS Intersection

3:30 PM - 5:00 PM JST | 6:30 AM - 8:00 AM UTC | Poster Hall International Exhibition Hall8, Makuhari Messe_20

[M-IS07] Astrobiology

convener:Hikaru Yabuta(Hiroshima University, Department of Earth and Planetary Systems Science), Seiji Sugita(Department of Earth and Planetary Science, Graduate School of Science Sciece, The University of Tokyo), Misato Fukagawa(National Astronomical Observatory of Japan), Fujishima Kosuke(Tokyo Institute of Technology, Earth-Life Science Institute)

[MIS07-P01] Exoplanets Revealed by High-Precision Infrared Doppler Technique Using IRD: Large Exploration for Planets around Cool M-type Stars Begins

*Masayuki Kuzuhara[1,3], Bunei Sato[4], Motohide Tamura[2,1,3], Takayuki Kotani[1,3,5], Nagayoshi Ohashi[3,6], Masashi Omiya[1,3], Teruyuki Hirano[4], Hiroki Harakawa[6,3,1], Wako Aoki[3,5], Norio Narita[2,1], Yasunori Hori[1,3], Akitoshi Ueda[3,5], Akihiko Fukui[2], Hiroyuki Tako Ishikawa[5,3], Ishizuka Masato[2], Takashi Kurokawa[1,7], Nobuhiko Kusakabe[1,3], Tomoyuki Kudo[6,3,1], Eiichiro Kokubo[3], Mihoko Konishi[1,3], Tadashi Nakajima[1,3,5], Jun Nishikawa[3,5,1], Masahiro Ogihara[3], Takuma Serizawa[7] (1.Astrobiology Center of NINS, 2.The University of Tokyo, Graduate School of Science, 3.National Astronomical Observatory of Japan, 4.Tokyo Institute of Technology, 5.SOKENDAI, 6.Subaru Telescope, 7.Tokyo University of Agriculture and Technology)

[MIS07-P02] Discrimination of organic compounds and mineral particles by fluorescent microscopy for the detection of Martian life.

*Tomoka Okada[1], Yoshitaka Yoshimura[2], Atsuo Miyakawa[3], Yuka Murano[3], Shin-ichi Yokobori[3], Akihiko Yamagishi[3], Kensei Kobayashi[1], Yoko Kebukawa[1] (1.YOKOHAMA National university, 2.Tamagawa University, 3.Tokyo University of Pharmacy and Life Sciences)

[MIS07-P03] Morphological and spectroscopic characteristics of organic matter in Banded Iron Formation, Barberton Greenstone Belt, South Africa

*Hiroki Amemiya[1], Ryo Nakajima[1], Yoko Ohtomo[1], Tsubasa Otake[1], Tsutomu Sato[1] (1.Division of sustainable Resources Engineering, Faculty of Engineering, Hokkaido University)

[MIS07-P04] Understanding peptide sequence selectivity on iron sulfide (FeS) nanoparticle surfaces

*Fujishima Kosuke[1], Norio Kitadai[1], Kenji Kasama[1] (1.Earth-Life Science Institute, Tokyo Institute of Technology)

[MIS07-P05] A process model of L-homochiral peptides formation initiated with L-alanine

*Toratane Munegumi[1], Taisuke Yamaga[1] (1.Department of Science Education, Naruto University of Education)

[MIS07-P06] Possible Formation of Amino Acids and Carboxylic Acids in Slightly-Reducing Primitive Earth Atmospheres

*Miei Kinoshita[1], Shintaro Ikeda[1], Kimitaka Kawamura[2], Bhagawati Kunwar[2], Hitoshi Fukuda[3], Yoshiyuki Oguri[3], Hiromi Shibata[4], Junichi Takahashi[1], Vladimir Airapetian[5], Yoko Kebukawa[1], Kensei Kobayashi[1] (1.Yokohama National University, 2.Chubu University, 3.Tokyo Institute of Technology, 4.Osaka University, 5.NASA Goddard SFC)

[MIS07-P07] Application of Machine learning and software development for initial analysis in the TANPOPO mission

*Kyoko Okudaira[1], Yuto Toda[1], Takashi Sonoke[1], Yuichi Yaguchi[1], Masashi Yoshida[1], Junya Imani[2], Satoshi Sasaki[3], Hajime Yano[4], Hirohide Demura[1], Makoto Tabata[5], Akihiko Yamagishi[6] (1.The University of Aizu, 2.YUKI Precision, 3.Tokyo University of Technology, 4.JAXA, 5.Chiba University, 6.Tokyo University of Pharmacy and Life Science)

[MIS07-P08] Structure analysis of the hyper velocity impact tracks of the particles captured by silica aerogel on the International Space Station

*Mizuho Nishi[1], Akira Tsuchiyama[1], Hajime Yano[2], Hikaru Yabuta[3], Kyoko Okudaira[4], Junya Matsuno[1], Masayuki Uesugi[5], Uesugi Kentaro[5], Nakano Tukasa[6], Takaaki Noguchi[7], MITA Hajime[8], Akihiko Yamagishi[9] (1.Kyoto University, 2.Institute of Space and Astronautical Science, Japan Aerospace Exploration Agency, 3.Hiroshima University, 4.The University of Aizu, 5.JASRI/SPring-8, 6.National Institute of Advanced Industrial Science and Technology, 7.Kyusyu University, 8.Fukuoka Institute of Technology, 9.Tokyo University of Pharmacy and Life Science)

[MIS07-P09] High-Angular-Resolution Observations of Protoplanetary Disks

*Misato Fukagawa[1] (1.National Astronomical Observatory of Japan)

[MIS07-P10] Characterization of high molecular weight amino acid precursors formed in interstellar ice analog

*Soushi Kuramoto[1], Tomohito Sato[1], Hitoshi Fukuda[2], Yoshiyuki Oguri[2], Kotaro Kondo[2], Hiromi Shibata[3], Yoko Kebukawa[1], Kensei Kobayashi[1], Satoshi Yoshida[4] (1.Yokohama National University, 2.Tokyo Institute of Technology, 3.University of Osaka, 4.National Institutes for Quantum Radiological Science and Technology)

[MIS07-P11] Theoretical elucidation of prebiotic formation processes into nucleobases

*Yu Komatsu[1,2], Taiki Suzuki[1,2] (1.Astrobiology Center, 2.National Astronomical Observatory of Japan)

[MIS07-P12] Formation Process of A Glycine's Precursor Candidate, CH3NH2

*Taiki Suzuki[1,2], Liton Majumdar[3], Masatoshi Ohishi[2] (1.National Institutes of Natural Sciences Astrobiology Center, 2.National Astronomical Observatory of Japan, 3.NASA Jet Propulsion Laboratory (JPL))

[MIS07-P13] Numerical study on the stellar atmosphere & wind of Cool Stars

*Takahito Sakaue[1], Kazunari Shibata[1] (1.Kyoto University)

[MIS07-P14] Design of space exposure experiments of organic matter in Tanpopo 2

*Takuya Yokoo[1], tomohito sato[1], Itsuki Sakon[2], Kazumichi Nakagawa[3], Hajime Yano[4], Miki Nakayama[5], Hajime Mita[5], Yoko Kebukawa[1], Kensei Kobayashi[1] (1.Yokohama National University, 2.University of Tokyo, 3.Kobe University, 4.JAXA, 5.Fukuoka Institute of Technology)

[E] Poster | M (Multidisciplinary and Interdisciplinary)：M-IS Intersection

5:15 PM - 6:30 PM JST | 8:15 AM - 9:30 AM UTC | Poster Hall International Exhibition Hall8, Makuhari Messe_37

[M-IS07] Astrobiology

convener:Hikaru Yabuta(Hiroshima University, Department of Earth and Planetary Systems Science), Seiji Sugita(Department of Earth and Planetary Science, Graduate School of Science Sciece, The University of Tokyo), Misato Fukagawa(National Astronomical Observatory of Japan), Fujishima Kosuke(Tokyo Institute of Technology, Earth-Life Science Institute)

[MIS07-P01] Exoplanets Revealed by High-Precision Infrared Doppler Technique Using IRD: Large Exploration for Planets around Cool M-type Stars Begins

*Masayuki Kuzuhara[1,3], Bunei Sato[4], Motohide Tamura[2,1,3], Takayuki Kotani[1,3,5], Nagayoshi Ohashi[3,6], Masashi Omiya[1,3], Teruyuki Hirano[4], Hiroki Harakawa[6,3,1], Wako Aoki[3,5], Norio Narita[2,1], Yasunori Hori[1,3], Akitoshi Ueda[3,5], Akihiko Fukui[2], Hiroyuki Tako Ishikawa[5,3], Ishizuka Masato[2], Takashi Kurokawa[1,7], Nobuhiko Kusakabe[1,3], Tomoyuki Kudo[6,3,1], Eiichiro Kokubo[3], Mihoko Konishi[1,3], Tadashi Nakajima[1,3,5], Jun Nishikawa[3,5,1], Masahiro Ogihara[3], Takuma Serizawa[7] (1.Astrobiology Center of NINS, 2.The University of Tokyo, Graduate School of Science, 3.National Astronomical Observatory of Japan, 4.Tokyo Institute of Technology, 5.SOKENDAI, 6.Subaru Telescope, 7.Tokyo University of Agriculture and Technology)

[MIS07-P02] Discrimination of organic compounds and mineral particles by fluorescent microscopy for the detection of Martian life.

*Tomoka Okada[1], Yoshitaka Yoshimura[2], Atsuo Miyakawa[3], Yuka Murano[3], Shin-ichi Yokobori[3], Akihiko Yamagishi[3], Kensei Kobayashi[1], Yoko Kebukawa[1] (1.YOKOHAMA National university, 2.Tamagawa University, 3.Tokyo University of Pharmacy and Life Sciences)

[MIS07-P03] Morphological and spectroscopic characteristics of organic matter in Banded Iron Formation, Barberton Greenstone Belt, South Africa

*Hiroki Amemiya[1], Ryo Nakajima[1], Yoko Ohtomo[1], Tsubasa Otake[1], Tsutomu Sato[1] (1.Division of sustainable Resources Engineering, Faculty of Engineering, Hokkaido University)

[MIS07-P04] Understanding peptide sequence selectivity on iron sulfide (FeS) nanoparticle surfaces

*Fujishima Kosuke[1], Norio Kitadai[1], Kenji Kasama[1] (1.Earth-Life Science Institute, Tokyo Institute of Technology)

[MIS07-P05] A process model of L-homochiral peptides formation initiated with L-alanine

*Toratane Munegumi[1], Taisuke Yamaga[1] (1.Department of Science Education, Naruto University of Education)

[MIS07-P06] Possible Formation of Amino Acids and Carboxylic Acids in Slightly-Reducing Primitive Earth Atmospheres

*Miei Kinoshita[1], Shintaro Ikeda[1], Kimitaka Kawamura[2], Bhagawati Kunwar[2], Hitoshi Fukuda[3], Yoshiyuki Oguri[3], Hiromi Shibata[4], Junichi Takahashi[1], Vladimir Airapetian[5], Yoko Kebukawa[1], Kensei Kobayashi[1] (1.Yokohama National University, 2.Chubu University, 3.Tokyo Institute of Technology, 4.Osaka University, 5.NASA Goddard SFC)

[MIS07-P07] Application of Machine learning and software development for initial analysis in the TANPOPO mission

*Kyoko Okudaira[1], Yuto Toda[1], Takashi Sonoke[1], Yuichi Yaguchi[1], Masashi Yoshida[1], Junya Imani[2], Satoshi Sasaki[3], Hajime Yano[4], Hirohide Demura[1], Makoto Tabata[5], Akihiko Yamagishi[6] (1.The University of Aizu, 2.YUKI Precision, 3.Tokyo University of Technology, 4.JAXA, 5.Chiba University, 6.Tokyo University of Pharmacy and Life Science)

[MIS07-P08] Structure analysis of the hyper velocity impact tracks of the particles captured by silica aerogel on the International Space Station

*Mizuho Nishi[1], Akira Tsuchiyama[1], Hajime Yano[2], Hikaru Yabuta[3], Kyoko Okudaira[4], Junya Matsuno[1], Masayuki Uesugi[5], Uesugi Kentaro[5], Nakano Tukasa[6], Takaaki Noguchi[7], MITA Hajime[8], Akihiko Yamagishi[9] (1.Kyoto University, 2.Institute of Space and Astronautical Science, Japan Aerospace Exploration Agency, 3.Hiroshima University, 4.The University of Aizu, 5.JASRI/SPring-8, 6.National Institute of Advanced Industrial Science and Technology, 7.Kyusyu University, 8.Fukuoka Institute of Technology, 9.Tokyo University of Pharmacy and Life Science)

[MIS07-P09] High-Angular-Resolution Observations of Protoplanetary Disks

*Misato Fukagawa[1] (1.National Astronomical Observatory of Japan)

[MIS07-P10] Characterization of high molecular weight amino acid precursors formed in interstellar ice analog

*Soushi Kuramoto[1], Tomohito Sato[1], Hitoshi Fukuda[2], Yoshiyuki Oguri[2], Kotaro Kondo[2], Hiromi Shibata[3], Yoko Kebukawa[1], Kensei Kobayashi[1], Satoshi Yoshida[4] (1.Yokohama National University, 2.Tokyo Institute of Technology, 3.University of Osaka, 4.National Institutes for Quantum Radiological Science and Technology)

[MIS07-P11] Theoretical elucidation of prebiotic formation processes into nucleobases

*Yu Komatsu[1,2], Taiki Suzuki[1,2] (1.Astrobiology Center, 2.National Astronomical Observatory of Japan)

[MIS07-P12] Formation Process of A Glycine's Precursor Candidate, CH3NH2

*Taiki Suzuki[1,2], Liton Majumdar[3], Masatoshi Ohishi[2] (1.National Institutes of Natural Sciences Astrobiology Center, 2.National Astronomical Observatory of Japan, 3.NASA Jet Propulsion Laboratory (JPL))

[MIS07-P13] Numerical study on the stellar atmosphere & wind of Cool Stars

*Takahito Sakaue[1], Kazunari Shibata[1] (1.Kyoto University)

[MIS07-P14] Design of space exposure experiments of organic matter in Tanpopo 2

*Takuya Yokoo[1], tomohito sato[1], Itsuki Sakon[2], Kazumichi Nakagawa[3], Hajime Yano[4], Miki Nakayama[5], Hajime Mita[5], Yoko Kebukawa[1], Kensei Kobayashi[1] (1.Yokohama National University, 2.University of Tokyo, 3.Kobe University, 4.JAXA, 5.Fukuoka Institute of Technology)

[E] Poster | M (Multidisciplinary and Interdisciplinary)：M-AG Applied Geosciences

10:45 AM - 12:15 PM JST | 1:45 AM - 3:15 AM UTC | Poster Hall International Exhibition Hall8, Makuhari Messe_11

[M-AG38] Satellite Land Physical Processes Monitoring at Medium/High/Very High Resolution

convener:Jean-Claude Roger(University of Maryland College Park), Shinichi Sobue(Japan Aerospace Exploration Agency), Eric Vermote(NASA Goddard Space Flight Center)

[MAG38-P01] Improving the AVHRR LTDR BRDF correction

*Jose Luis Villaescusa[1,2], Belen Franch[1,2], Jean-Claude Roger[1,2], Eric Vermote[2] (1.University of Maryland College Park, 2.NASA Goddard Space Flight Center)

[MAG38-P02] Winter wheat yield model based on remote sensing data

*Belen Franch[1,2], Eric Vermote[2,1], Sergii Skakun[1,2], Jean-Claude Roger[1,2], Inbal Becker-Reshef[1], Chris Justice[1] (1.Department of Geographical Sciences, University of Maryland, 2.NASA Goddard Space Flight Center)

[MAG38-P03] Agricultural monitoring from Optical and SAR data

*Andrés Eduardo Santamaría-Artigas[1,2], Sergii Skakun[1,2], Belen Franch[1,2], Jean-Claude Roger[1,2], Eric Vermote[2] (1.University of Maryland College Park, 2.NASA Goddard Space Flight Center)

[MAG38-P04] **Eco-hydrological modeling using field-based and Earth Observations to assess water use efficiency and support agricultural water resources management**

pierre Guillevic[2,1], *Jean-Claude Roger[1,2] (1.University of Maryland, College Park, USA, 2.NASA Goddard Space flight Center, Greenbelt, USA)

[MAG38-P05] Detecting and quantifying forest dynamics using SAR time-series data in Indonesia

*Pedro Rodriguez-Veiga[1,2,3], Narumasa Tsutsumida[3] (1.Centre for Landscape and Climate Research, University of Leicester, Leicester, UK, 2.NERC National Centre for Earth Observation (NCEO), Leicester, UK, 3.Graduate School of Global Environmental Studies, Kyoto University, Japan)

[E] Poster | M (Multidisciplinary and Interdisciplinary)：M-AG Applied Geosciences

5:15 PM - 6:30 PM JST | 8:15 AM - 9:30 AM UTC | Poster Hall International Exhibition Hall8, Makuhari Messe_43

[M-AG38] Satellite Land Physical Processes Monitoring at Medium/High/Very High Resolution

convener:Jean-Claude Roger(University of Maryland College Park), Shinichi Sobue(Japan Aerospace Exploration Agency), Eric Vermote(NASA Goddard Space Flight Center)

[MAG38-P01] Improving the AVHRR LTDR BRDF correction

*Jose Luis Villaescusa[1,2], Belen Franch[1,2], Jean-Claude Roger[1,2], Eric Vermote[2] (1.University of Maryland College Park, 2.NASA Goddard Space Flight Center)

[MAG38-P02] Winter wheat yield model based on remote sensing data

*Belen Franch[1,2], Eric Vermote[2,1], Sergii Skakun[1,2], Jean-Claude Roger[1,2], Inbal Becker-Reshef[1], Chris Justice[1] (1.Department of Geographical Sciences, University of Maryland, 2.NASA Goddard Space Flight Center)

[MAG38-P03] Agricultural monitoring from Optical and SAR data

*Andrés Eduardo Santamaría-Artigas[1,2], Sergii Skakun[1,2], Belen Franch[1,2], Jean-Claude Roger[1,2], Eric Vermote[2] (1.University of Maryland College Park, 2.NASA Goddard Space Flight Center)

[MAG38-P04] **Eco-hydrological modeling using field-based and Earth Observations to assess water use efficiency and support agricultural water resources management**

pierre Guillevic[2,1], *Jean-Claude Roger[1,2] (1.University of Maryland, College Park, USA, 2.NASA Goddard Space flight Center, Greenbelt, USA)

[MAG38-P05] Detecting and quantifying forest dynamics using SAR time-series data in Indonesia

*Pedro Rodriguez-Veiga[1,2,3], Narumasa Tsutsumida[3] (1.Centre for Landscape and Climate Research, University of Leicester, Leicester, UK, 2.NERC National Centre for Earth Observation (NCEO), Leicester, UK, 3.Graduate School of Global Environmental Studies, Kyoto University, Japan)

[E] Poster | M (Multidisciplinary and Interdisciplinary)：M-AG Applied Geosciences

3:30 PM - 5:00 PM JST | 6:30 AM - 8:00 AM UTC | Poster Hall International Exhibition Hall8, Makuhari Messe_25

[M-AG40] CTBT IMS Technologies for Detecting Nuclear Explosion and Their Applications to Earth Science

convener:Nurcan Meral Ozel(Comprehensive Nuclear-Test-Ban Treaty Organization), Hiroyuki Matsumoto(Japan Agency for Marine-Earth Science and Technology), Yosuke Naoi(Japan Atomic Energy Agency)

[MAG40-P01] Overview of the Japanese National Data Centre-1 (NDC-1)

*RYOHEI EMURA[1], Takayuki Otsu[1], Toyomi Sakamoto[1], Soshi Iwata[1], Takanari Fujii[1], Mami Nogami[1], Makiko Iwakuni[1], Masashi Motohashi[1] (1.Japan Weather Association)

[MAG40-P02] Challenging to utilize the infrasound technologies for civil and science application

*Masashi Motohashi[1], Nobuo Arai[2], Takayuki Otsu[1], Mami Nogami[1], Makiko Iwakuni[1], Ryohei Emura[1] (1.Japan Weather Association, 2.Disaster Mitigation Research Center, Nagoya Unicersity)

[MAG40-P03] CTBT IMS hydroacoustic signal detections from the Ioto volcanic island in the northwest Pacific Ocean

*Hiroyuki Matsumoto[1,2], Mario Zampolli[1], Georgios Haralabus[1], Jerry Stanley[1], James Mattila[1], Nurcan Meral Ozel[1] (1.Comprehensive Nuclear-Test-Ban Treaty Organization (CTBTO), 2.Japan Agency for Marine-Earth Science and Technology (JAMSTEC))

[MAG40-P04] Installation of a floating hydrophone system within the SOFAR channel

*Hiroko Sugioka[1], Masayuki Obayashi[2] (1.Kobe University, 2.JAMSTEC)

[MAG40-P05] Fin whale signals observed at S-net seismic stations

*Takeshi Nakamura[1], Ryoichi Iwase[2] (1.National Research Institute for Earth Science and Disaster Resilience, 2.Japan Agency for Marine-Earth Science and Technology)

[MAG40-P06] Implementation of integrated observation from seafloor through atmosphere – past, current, and future plans

*Keisuke Ariyoshi[1], Akira Nagano[1], Hiroyuki Matsumoto[1], Nurcan Meral Ozel[2] (1.Japan Agency for Marine-Earth Science and Technology, 2.Comprehensive Nuclear-Test-Ban Treaty Organization)

[E] Poster | M (Multidisciplinary and Interdisciplinary)：M-AG Applied Geosciences

5:15 PM - 6:30 PM JST | 8:15 AM - 9:30 AM UTC | Poster Hall International Exhibition Hall8, Makuhari Messe_45

[M-AG40] CTBT IMS Technologies for Detecting Nuclear Explosion and Their Applications to Earth Science

convener:Nurcan Meral Ozel(Comprehensive Nuclear-Test-Ban Treaty Organization), Hiroyuki Matsumoto(Japan Agency for Marine-Earth Science and Technology), Yosuke Naoi(Japan Atomic Energy Agency)

[MAG40-P01] Overview of the Japanese National Data Centre-1 (NDC-1)

*RYOHEI EMURA[1], Takayuki Otsu[1], Toyomi Sakamoto[1], Soshi Iwata[1], Takanari Fujii[1], Mami Nogami[1], Makiko Iwakuni[1], Masashi Motohashi[1] (1.Japan Weather Association)

[MAG40-P02] Challenging to utilize the infrasound technologies for civil and science application

*Masashi Motohashi[1], Nobuo Arai[2], Takayuki Otsu[1], Mami Nogami[1], Makiko Iwakuni[1], Ryohei Emura[1] (1.Japan Weather Association, 2.Disaster Mitigation Research Center, Nagoya Unicersity)

[MAG40-P03] CTBT IMS hydroacoustic signal detections from the Ioto volcanic island in the northwest Pacific Ocean

*Hiroyuki Matsumoto[1,2], Mario Zampolli[1], Georgios Haralabus[1], Jerry Stanley[1], James Mattila[1], Nurcan Meral Ozel[1] (1.Comprehensive Nuclear-Test-Ban Treaty Organization (CTBTO), 2.Japan Agency for Marine-Earth Science and Technology (JAMSTEC))

[MAG40-P04] Installation of a floating hydrophone system within the SOFAR channel

*Hiroko Sugioka[1], Masayuki Obayashi[2] (1.Kobe University, 2.JAMSTEC)

[MAG40-P05] Fin whale signals observed at S-net seismic stations

*Takeshi Nakamura[1], Ryoichi Iwase[2] (1.National Research Institute for Earth Science and Disaster Resilience, 2.Japan Agency for Marine-Earth Science and Technology)

[MAG40-P06] Implementation of integrated observation from seafloor through atmosphere – past, current, and future plans

*Keisuke Ariyoshi[1], Akira Nagano[1], Hiroyuki Matsumoto[1], Nurcan Meral Ozel[2] (1.Japan Agency for Marine-Earth Science and Technology, 2.Comprehensive Nuclear-Test-Ban Treaty Organization)

[E] Poster | P (Space and Planetary Sciences)：P-EM Solar-Terrestrial Sciences, Space Electromagnetism & Space Environment

Thu. May 30, 2019 3:30 PM - 5:00 PM JST | Thu. May 30, 2019 6:30 AM - 8:00 AM UTC | Poster Hall International Exhibition Hall8, Makuhari Messe_2

[P-EM15] Study of coupling processes in solar-terrestrial system

convener:Mamoru Yamamoto(Research Institute for Sustainable Humanosphere, Kyoto University), Yasunobu Ogawa(National Institute of Polar Research), Satonori Nozawa(Institute for Space-Earth Environment Research), Akimasa Yoshikawa(Department of Earth and Planetary Sciences, Kyushu University)

The Earth accepts vast input of energy and material from the Sun. The Earth's environment is maintained by the balance between their inputs and outputs. It is therefore important to study energy and mass transport on the Earth. This is an international session that discusses studies of the coupling processes in the Sun-Earth system based on the project "Study of coupling processes in solar-terrestrial system" that was approved by the Master Plan 2011/2014/2017 of Science Council of Japan. We continue proposing the project to the Master Plan 2020. The facilities and networks included are Equatorial MU Radar (EMU) in Indonesia to study the whole equatorial atmosphere, the EISCAT_3D radar system in northern Scandinavia to study detailed structures and elementary processes of the magnetosphere-ionosphere coupling in the polar region, and global networks of various ground-based instruments and observation data. We will show the current status of the project and discuss sciences by soliciting variety papers. This session is open to the world, and we strongly encourage submission of papers related to other facilities and projects, i.e., atmospheric or incoherent scatter radars, observation networks, satellites, and simulation or theoretical studies, etc.

[PEM15-P01] Study on adaptive clutter rejection system using external receiving antennas for the MU radar

*Hiroyuki Hashiguchi[1], Issei Terada[1], Mamoru Yamamoto[1] (1.Research Institute for Sustainable Humanosphere, Kyoto University)

[PEM15-P02] Detached cusp aurora for southward IMF

*Kohei Takasu[1], Satoshi Taguchi[1], Keisuke Hosokawa[2] (1.Department of Geophysics, Graduate School of Science, Kyoto University, 2.Department of Communication Engineering and Informatics, University of Electro-Communications)

[PEM15-P03] Motion of the inverted-V structure during an isolated substorm

*Morio Tanaka[1], Satoshi Taguchi[1], Kohei Takasu[1], Tomokazu Oigawa[1], Keisuke Hosokawa[2] (1.Department of Geophysics, Graduate school of science, Kyoto University, 2.Department of Communication Engineering and Informatics, University of Electro-Communications)

[PEM15-P04] Observation and modeling of Na layer response to energetic particle precipitation

*Takuo T. Tsuda[1], Kyogo Takizawa[1], Ryo Tozu[1], Takuya Kawahara[2], Yoshimasa Tanaka[3], Mitsumu K. Ejiri[3], Takanori Nishiyama[3], Takuji Nakamura[3] (1.The University of Electro-Communications, 2.Shinshu University, 3.National Institute of Polar Research)

[PEM15-P05] Lidar data analysis of the sodium atoms in the thermosphere observed at Tromsoe, Norway

*Takuya Kawahara[1], Satonori Nozawa[2], Norihito Saito[3], Takuo T. Tsuda[4], Toru Takahashi[5], Testuya Kawabata[2], Miki Nishimura[1], Yoshitaka Kobayashi[1] (1.Faculty of Engineering, Shinshu University, 2.ISEE, Nagoya University, 3.RIKEN, Center for Advanced Photonics, 4.The University of Electro-Communications, 5.National Institute of Polar Research)

[PEM15-P06] Spatial-temporal distribution of anomalous enhancement of ambipolar diffusion coefficient observed by meteor radars installed in the polar region

*Toru Takahashi[1], Masaki Tsutsumi[1,2], Yasunobu Ogawa[1,2,3], Satonori Nozawa[3], Chris Hall[4], Hiroshi Miyaoka[1,2] (1.National Institute of Polar Research, 2.SOKENDAI, 3.Institute for Space-Earth Environmental Research, 4.TGO, The Arctic University of Norway)

[PEM15-P07] Progress of ICSWSE and MAGDAS project in recent years

*Shuji Abe[1], Akimasa Yoshikawa[2,1], Teiji Uozumi[1], Akiko Fujimoto[3] (1.International Center for Space Weather Science and Education, Japan, 2.Department of Earth and Planetary Sciences, Kyushu University, 3.Kyushu Institute of Technology)

[PEM15-P08] Status of GNU Radio Beacon Receiver 2 (GRBR2) development

*Mamoru Yamamoto[1], Mayumi Matsunaga[2], Roland Tsunoda[3] (1.Research Institute for Sustainable Humanosphere, Kyoto University, 2.Tokyo University of Technology, 3.SRI International)

[PEM15-P09] Statistical comparison between plasma bubble day-to-day variability and neutral atmosphere by using GPS scintillation and GAIA model

*Mamoru Yamamoto[1], Keigo Kono[1] (1.Research Institute for Sustainable Humanosphere, Kyoto University)

[PEM15-P10] Redevelopment of the MU radar transceiver-module control system

*Mamoru Yamamoto[1], Koki Kurokawa[1], Hiroyuki Hashiguchi[1] (1.Research Institute for Sustainable Humanosphere, Kyoto University)

Study on adaptive clutter rejection system using external receiving antennas for the MU radar

*Hiroyuki Hashiguchi[1], Issei Terada[1], Mamoru Yamamoto[1]

1. Research Institute for Sustainable Humanosphere, Kyoto University

Strong clutter echoes from a hard target such as a mountain or building sometimes cause problems of observations with atmospheric radars. In order to reject or suppress ground clutter echoes, it is effective to use NC-DCMP (Norm Constrained- Directionally Constrained Minimum Power) method, which makes null toward the direction of the clutter, if we can receive signals independently from plural antennas [Nishimura et al., JTech., 2012]. It has been demonstrated that the NC-DCMP method is effective to real observation data with the MU (Middle and Upper atmosphere) radar [Hashiguchi et al., Radio Sci., 2018]. Although NC-DCMP method suppresses clutter echoes with almost maintaining the shape of main lobe to add pseudo-noise compared with the conventional DCMP method, the signal-to-noise ratio (S/N) of atmospheric echoes is somewhat degraded. We studied the clutter suppression method with little S/N degradation by using external antennas.

Four turnstile antennas are installed in the MU radar site. The signal from the antenna is sent to the MU radar observation room through the coaxial cable after amplified by the LNA with the limiter and BPF. It is further amplified by the LNA in the observation room, and then down-converted to intermediate frequency (5 MHz) signal to input to the multi-channel receiving system of the MU radar.

We compared the NC-DCMP method using the each received data of 25 channels, which is a conventional clutter suppression method, and the NC-DCMP method using the simple combination of 25 channels and 4 channels of external antennas. In the former case, the S/N of the atmospheric echoes is somewhat degraded, but in the latter case the main lobe shape is guaranteed by 25 channel simple synthesis, so the S/N degradation is not observed. In the latter case, the clutter suppression is sometimes insufficient. This cause is considered to be that the current positions of external antennas are biased to the north side. Antenna positions should be optimized in the future.

We can apply the achievement of this study to the Equatorial MU radar (EMU), which is proposed to be constructed at West Sumatera, Indonesia. The EMU system is the similar as the MU radar, but its antenna consists of 1045 Yagi antennas with 55 groups and it has 64 receiver channels.

Keywords: Atmospheric radar, Clutter rejection, NC-DCMP method, MU radar

©2019. Japan Geoscience Union. All Right Reserved.

Detached cusp aurora for southward IMF

*Kohei Takasu[1], Satoshi Taguchi[1], Keisuke Hosokawa[2]

1. Department of Geophysics, Graduate School of Science, Kyoto University, 2. Department of Communication Engineering and Informatics, University of Electro-Communications

A poleward-moving aurora is a typical phenomenon in the dayside cusp of the high-latitude ionosphere. This aurora usually originates near the equatorward boundary of the cusp, and diminishes near the poleward boundary of the persistent cusp auroral emissions. In this study we have examined faint poleward-moving auroras that are detached from the persistent cusp emissions by analyzing 630-nm aurora image data from an all-sky imager at Longyearbyen, Svalbard, and precipitating electron data from DMSP spacecraft. These auroras occur for southward IMF, and are located at latitudes higher than 80 MLAT. The intensities are very weak (less than 1 kilo Rayleigh). The result of the analysis shows that the speed of the auroral motion is 1 to 2 km/s, which is faster than typical convection speed in the dayside polar cap. We show the similarities and differences between the faint aurora and the typical poleward moving cusp aurora, and discuss how soft electron precipitation occurs in the region that is well separated from the cusp.

Keywords: Aurora, cusp, plasma convection, IMF

©2019. Japan Geoscience Union. All Right Reserved.

Motion of the inverted-V structure during an isolated substorm

*Morio Tanaka[1], Satoshi Taguchi[1], Kohei Takasu[1], Tomokazu Oigawa[1], Keisuke Hosokawa[2]

1. Department of Geophysics, Graduate school of science, Kyoto University, 2. Department of Communication Engineering and Informatics, University of Electro-Communications

The inverted-V is an energetic electron precipitation event, which can be seen as a V-shape structure in electron flux spectrograms, and causes intense auroral arcs. Previous studies have suggested that the inverted-V structure can move fast poleward or equatorward. However, we still do not understand what drives its motion. In this study we have investigated the detailed characteristics of an inverted-V structure moving poleward, which occurred during an isolated substorm, using simultaneous observations of auroras, precipitating electrons, and field-aligned currents. We analyzed aurora data (630-nm and 557.7-nm) from an all-sky imager at Longyearbyen, Svalbard, and precipitating electrons and magnetic field data from the DMSP spacecraft (F16, F17, F18, F19). One of the interesting characteristics of the poleward-moving inverted-V is the appearance of a downward field-aligned current equatorward of and adjacent to the inverted-V. We discuss how the region of the downward field-aligned current evolves in association with the motion and growth/decay of the inverted V structure, and possibility of a role of the downward field-aligned current for the latitudinal motion of the inverted V.

Keywords: Field-aligned current, aurora, inverted-V, isolated substorm

©2019. Japan Geoscience Union. All Right Reserved.

Observation and modeling of Na layer response to energetic particle precipitation

*Takuo T. Tsuda[1], Kyogo Takizawa[1], Ryo Tozu[1], Takuya Kawahara[2], Yoshimasa Tanaka[3], Mitsumu K. Ejiri[3], Takanori Nishiyama[3], Takuji Nakamura[3]

1. The University of Electro-Communications, 2. Shinshu University, 3. National Institute of Polar Research

Metallic layers, such as Na, Fe, Mg, K, and Ca layers, exist in the mesosphere and lower thermosphere (MLT). The height range of the MLT region corresponds to the ionospheric *D* and *E* regions, and in the polar region energetic particles precipitating from the magnetosphere can often penetrate into the *E* region and even into the *D* region. Therefore, the influence of energetic particles on the metallic layers is of interest regarding changes in atmospheric composition accompanied by auroral activity or geomagnetic activity.

In this study, we have performed a statistical investigation on relationship between Na density and cosmic noise absorption (CNA), which were obtained from 2000 to 2002 at Syowa Station, Antarctic (69.0ºS, 39.6ºE). From the investigation, we found the Na density decrease in accordance with the CNA increase, i.e., increase in the energetic particle precipitation. In the presentation, we will show these observational results, and discuss causality about the observed relationship based on numerical caculations using our Na chemistry model.

Keywords: Na layer, Energetic particle precipitation, Syowa Station, Na chemistry model

©2019. Japan Geoscience Union. All Right Reserved.

Lidar data analysis of the sodium atoms in the thermosphere observed at Tromsoe, Norway

*Takuya Kawahara[1], Satonori Nozawa[2], Norihito Saito[3], Takuo T. Tsuda[4], Toru Takahashi[5], Testuya Kawabata[2], Miki Nishimura[1], Yoshitaka Kobayashi[1]

1. Faculty of Engineering, Shinshu University, 2. ISEE, Nagoya University, 3. RIKEN, Center for Advanced Photonics, 4. The University of Electro-Communications, 5. National Institute of Polar Research

Distribution of low-density Na atoms in the thermosphere is interesting because of the capability of measuring neutral temperature and wind into the lower thermosphere up to 140 km. The thermospheric Na atoms significantly made the altitude range of Na lidar measurements expanded from the 80–105 km to 80–140 km, covering almost the entire E region (Liu et al., GRL, 2016).

The measurements of wind and temperature by a Na lidar in the northern mesosphere (80-105 km) at Tromsoe, Norway (69.6˚N, 19.2˚E) have been carried out in Polar winter season since 2010. However, thermospheric Na has not been seen in our data so far. This is because the automatic analysis program calculates the background signal level using the 140-150 km signals which possibly include a small amount of thermospheric Na signal. Deriving thermospheric Na is done by lowering the background signal level to emphasize thermospheric Na signals. The data at the new moon are selected which have a low background signal. Also, we calculated signal intensity from the Na atoms in the thermosphere based on our lidar parameters such as laser power, a telescope aperture area etc. by using the lidar equation. The results are summarized as follows. (1) Assuming that the Na density is 10 /cm^3, the signal from the Na atoms between 120 and 140 km is expected 300-400 photons, (2) The background signal observed is about 4,400 counts which means the noise level is about 220. So the signal intensity from the Na is nearly comparable to the noise level. (3) Thermospheric Na was not clearly seen in the re-calculated data. However, it depends on the smoothing technique to the original lidar data.

In this talk, we show the results derived by varying the binning time and discuss it.

Keywords: Na lidar, thermosphere, Tromsoe

©2019. Japan Geoscience Union. All Right Reserved.

Spatial-temporal distribution of anomalous enhancement of ambipolar diffusion coefficient observed by meteor radars installed in the polar region

*Toru Takahashi[1], Masaki Tsutsumi[1,2], Yasunobu Ogawa[1,2,3], Satonori Nozawa[3], Chris Hall[4], Hiroshi Miyaoka[1,2]

1. National Institute of Polar Research, 2. SOKENDAI, 3. Institute for Space-Earth Environmental Research, 4. TGO, The Arctic University of Norway

The meteor radar detected echoes of meteor tails as a tracer of neutral wind from 75 to 100 km altitudes (Hall et al., 2005). In addition, by using a decay time of the echo power, the meteor radar also estimated the ambipolar diffusion coefficient, which depends on the ion and electron temperature. The ambipolar diffusion coefficient was utilized to estimate the neutral temperature because the ion and electron temperature are generally in the thermal equilibrium with the neutral temperature. Recently, an anomalous enhancement of the ambipolar diffusion coefficient which could not be explained by the neutral temperature enhancement (hereafter called the anomalous enhancement) was observed by the meteor radar installed at Tromsoe, Norway (69.6 deg. N, 19.2 deg. E)
A previous study compared the anomalous enhancement with the ion velocity and the ion and electron temperature observed by EISCAT radar (Tsutsumi et al. 2017, Proceedings of the 30th Atmospheric Science Symposium, 2017). They reported that the anomalous enhancement tended to appear with the enhancement of ion velocity and electron temperature and frequently appeared at 16 UT. Furthermore, the anomalous enhancement was not seen during an event of the high energy particle precipitation on November 17, 2012 although one case study. Thus, the anomalous enhancement seems to be generated by the intense electric field and the high energy particle precipitation is not always necessary for its generation. As mentioned above, the previous study revealed a fundamental characteristics of the anomalous enhancement, however the generation mechanisms of the anomalous enhancement is still unclear. To clarify this, the comparison the spatial distribution of the anomalous enhancement with the convective electric field are needed. However, to date the latitudinal and local time occurrence of the anomalous enhancement was not revealed in the polar region.
Three meteor radars have been installed at Tromsoe, Bear island (74.5 deg. N, 19.0 deg. E), and Longyearbyen (78.2 deg. N, 16.2 deg. E). These meteor radars almost align on the same longitude line and can provide the spatial distribution of the anomalous enhancement. All meteor radars are a commercially produced VHF system (ENDR8-20) manufactured by ATRAD Pty Ltd. The antennas were produced by the Arctic University of Norway (Nozawa et al., 2012, JGR; Hall et al., 2002, GRL, Hall et al., 2006, JASTP). In this study, the spatial distribution and the occurrence rate of the anomalous enhancement was derived by these meteor radars.
Peaks of occurrence rate was seen at 20-22, 19-21, 16-19 MLT (~UT+3) at Tromsoe, Bear island, and Longyearbyen latitudes, respectively. This indicates that the anomalous enhancement appeared sequentially from high to low latitudes. In the morning sector, the peak of occurrence rate was only seen at 2-6 MLT above Bear island. In the case of high geomagnetic activity (Kp>3), the evening peaks of the occurrence rate shifted to an earlier time. On the other hand, clear peaks of the occurrence rate in the morning sector appeared at 3-5, 4-8, 7-10 MLT, respectively. Furthermore, the anomalous enhancement appeared with high possibility of 90% around 100 km south of Tromsoe. These characteristics which are seen during the time interval of high geomagnetic activity showed good agreement with the geomagnetic activity dependences of convective electric field.

©2019. Japan Geoscience Union. All Right Reserved.

We found another interesting characteristic in the geomagnetic dependence of the occurrence of the anomalous enhancement. The peak of occurrence rate in the evening sector was larger than it observed in the morning sector. This is considered to be related that auroral arcs appearing with intense electric field mainly observed in the evening sector. Thus, the generation of anomalous enhancement seems to relate both the convective electric field and the appearance of auroral arcs.
In this presentation, we will show the spatial distribution, MLT and geomagnetic activity dependence of the anomalous enhancement. We will also intend to present the comparison it with the electric filed observed by EISCAT and EISCAT Svalbard radars

Keywords: meteor radar, Tromsø, EISCAT radar

©2019. Japan Geoscience Union. All Right Reserved.

Progress of ICSWSE and MAGDAS project in recent years

*Shuji Abe[1], Akimasa Yoshikawa[2,1], Teiji Uozumi[1], Akiko Fujimoto[3]

1. International Center for Space Weather Science and Education, Japan, 2. Department of Earth and Planetary Sciences, Kyushu University, 3. Kyushu Institute of Technology

International Center for Space Weather Science and Education (ICSWSE), Kyushu University is the research institute for conducting research and education in space weather. Our magnetometer array named as "MAGDAS/CPMN (MAGnetic Data Acquisition System/Circum-pan Pacific Magnetometer Network)" (Principal Investigator: Dr. A. Yoshikawa) has over seventy fluxgate magnetometers, one induction magnetometer, and four FM-CW (Frequency Modulated Continuous Wave) radars around the world. One of our recent research topics is Equatorial Electrojet (EEJ). We calculate EE-index (Uozumi et al, 2008; Fujimoto et al., 2016) for space weather nowcast/forecast using realtime magnetometer data along the magnetic equator, and update it at each hour on the website (http://data.icswse.kyushu-u.ac.jp/eeindex/). To accelerate the understanding of EEJ structure, we constructed dense magnetometer array near magnetic equator at Peru and Malaysia in recent year. In addition, we finished to install new FM-CW radar at Sicaya, Peru. The instrument works well current now. We are providing our observational information and data including old project via our website (http://data.icswse.kyushu-u.ac.jp/). We also provide them via IUGONET (Inter-university Upper Atmosphere Observation NETwork) Type-A (http://search.iugonet.org/) which is one-stop web service system for researchers to search data, get the information of data, and plot data, and SPEDAS (Space Physics Environment Data Analysis System)/UDAS (iUgonet Data Analysis System). We will provide them via SuperMAG (http://supermag.jhuapl.edu/) in the near future. For accelerating the usage of MAGDAS and its science, we held a tutorial session in International Conference on Space Weather and Satellite Application 2018 at Malaysia, for handling MAGDAS and other data related our research field by using IUGONET system. We believe researchers use MAGDAS data on proper rule and develop their science. We will introduce other research activities in ICSWSE and MAGDAS project, for example, plasma bubble, geomagnetically induced current, and so on.

©2019. Japan Geoscience Union. All Right Reserved.

Status of GNU Radio Beacon Receiver 2 (GRBR2) development

*Mamoru Yamamoto[1], Mayumi Matsunaga[2], Roland Tsunoda[3]

1. Research Institute for Sustainable Humanosphere, Kyoto University, 2. Tokyo University of Technology, 3. SRI International

GNU Radio Beacon Receiver (GRBR) is the very successful digital receiver developed for dual-band (150/400MHz) beacon experiment. We were successfully conducted observations of total-electron content (TEC) of the ionosphere over Japan and in southeast Asia. However, many beacon satellites is now aging, and its number is decreasing. We now have a project to start new satellite-ground beacon experiment with new satellite constellations. One of them is TBEx (Tandem Beacon Explorer), a project by SRI International, to fly a constellation of two 3U cubesats with triband beacon transmitters. Another one is a project of FORMOSAT-7/COSMIC-2 by Taiwan/USA. Well-known mission of COSMIC-2 is GNSS occultation experiment, but the satellites carry triband beacon transmitters. All of these satellites will be placed into low-inclination orbits by the same launch vehicle in 2018, which will give us great opportunities to enhance studies of the low-latitude ionosphere. We develop a new digital receiver, GRBR2, for these new satellite beacon. GRBR2 is a four channel receiver at 150/400/965/1067MHz beacon signals from two satellite constellations. Now The reveiver system was finally fixed. Problem of the project of delay of the satellite launch. But it is now on schedule for launch by 2019 summer. We start deploying GRBR2 in southeast Asian countries. In this presentaiton, we will report GRBR2 system and its performance including results from test experiment in the field.

Keywords: Satellite beacon experiment, Digital receiver development, Total electron content

©2019. Japan Geoscience Union. All Right Reserved.

Statistical comparison between plasma bubble day-to-day variability and neutral atmosphere by using GPS scintillation and GAIA model

*Mamoru Yamamoto[1], Keigo Kono[1]

1. Research Institute for Sustainable Humanosphere, Kyoto University

Equational plasma bubble is one of the most intense irregularities in the ionosphere. The occurrence of the plasma bubble is considered related to weak changes of the underlying atmosphere which is called large-scale wavelike structure (LSWS). The LSWS is expected formed by penetration of the atmospheric wave into the ionosphere. But its real effect is not yet known in detail. The purpose of this research is to investigate the correlation between the neutral atmosphere and day-to-day variability of equatorial plasma bubbles mainly in the Southeast Asia region. We based on the study by Yamamoto et al (2018) that showed relationship between 40-km height temperature variation and S4 index over Kototabang, Indonesia. In this study we tried to extend the observation region and also tried to elucidate atmospheric waves that are related to the plasma bubble. For indicating activity of the plasma bubble, we used S4 index of GPS scintillation measured by ISEE, Nagoya Univ. at Kototabang, Indonesia. Atmospheric data were taken from GAIA database prepared by NICT. We analyzed data from 2003, 2004, 2012, and 2013 where the solar activity was high. Overall correlation between S4 index and the atmospheric temperature showed similar feature throughout these years. However, even when we tried to extract atmospheric wave components from the GAIA data, the correlation between the wave parameter to S4 index did not show large change. This means that the elucidation of the atmospheric wave component was not very successful so far. Further analyses are required.

Reference
Yamamoto, M., Y. Otsuka, H. Jin, Y. Miyoshi (2018) Relationship between day-to-day variability of equatorial plasma bubble activity from GPS scintillation and atmospheric properties from GAIA assimilation, Progress in Earth and Planetary Science, Vol. 5, page 26, doi: 10.1186/s40645-018-0184-7.

©2019. Japan Geoscience Union. All Right Reserved.

Redevelopment of the MU radar transceiver-module control system

*Mamoru Yamamoto[1], Koki Kurokawa[1], Hiroyuki Hashiguchi[1]

1. Research Institute for Sustainable Humanosphere, Kyoto University

The MU radar was installed in Shigaraki, Japan in 1984 as the world first atmospheric radar with active phased-array antenna system. The MU radar consists of 475 Yagi antennas in the circular field of about 100m diameter. By the electronic phase shift of each Yagi, the antenna beam is steered to one of pre-selected 2048 directions in the transmitting pulse-to-pulse basis. Success of the MU radar in the atmospheric/ionospheric research is well known, and its active phased-array configuration was followed by many other radar systems. The phase control of the MU radar is realized by the control of its transceiver-module (TR-module) that are equipped with each Yagi antenna. They are gathered into 25 groups of each 19 modules. One CPU (microcomputer board) is used for control of one group of modules. A weak point of the MU radar exists in this point because we are using the original 8085 CPU board that is connected to the host computer by 1200-baud (!) serial line. This control is very slow, and we could not meet demands for rapid change of observation parameters for long time. This time we tried to re-develop the new TR-module controller by using recent CPU board and electronic devices. In the presentation, we show hardware/software of the newly developed prototype of the MU radar TR-module controller.

Keywords: MU radar, control system, redevelopment

©2019. Japan Geoscience Union. All Right Reserved.

[E] Poster | P (Space and Planetary Sciences)：P-EM Solar-Terrestrial Sciences, Space Electromagnetism & Space Environment

Thu. May 30, 2019 5:15 PM - 6:30 PM JST | Thu. May 30, 2019 8:15 AM - 9:30 AM UTC | Poster Hall International Exhibition Hall8, Makuhari Messe_2

[P-EM15] Study of coupling processes in solar-terrestrial system

convener:Mamoru Yamamoto(Research Institute for Sustainable Humanosphere, Kyoto University), Yasunobu Ogawa(National Institute of Polar Research), Satonori Nozawa(Institute for Space-Earth Environment Research), Akimasa Yoshikawa(Department of Earth and Planetary Sciences, Kyushu University)

The Earth accepts vast input of energy and material from the Sun. The Earth's environment is maintained by the balance between their inputs and outputs. It is therefore important to study energy and mass transport on the Earth. This is an international session that discusses studies of the coupling processes in the Sun-Earth system based on the project "Study of coupling processes in solar-terrestrial system" that was approved by the Master Plan 2011/2014/2017 of Science Council of Japan. We continue proposing the project to the Master Plan 2020. The facilities and networks included are Equatorial MU Radar (EMU) in Indonesia to study the whole equatorial atmosphere, the EISCAT_3D radar system in northern Scandinavia to study detailed structures and elementary processes of the magnetosphere-ionosphere coupling in the polar region, and global networks of various ground-based instruments and observation data. We will show the current status of the project and discuss sciences by soliciting variety papers. This session is open to the world, and we strongly encourage submission of papers related to other facilities and projects, i.e., atmospheric or incoherent scatter radars, observation networks, satellites, and simulation or theoretical studies, etc.

[PEM15-P01] Study on adaptive clutter rejection system using external receiving antennas for the MU radar

*Hiroyuki Hashiguchi[1], Issei Terada[1], Mamoru Yamamoto[1] (1.Research Institute for Sustainable Humanosphere, Kyoto University)

[PEM15-P02] Detached cusp aurora for southward IMF

*Kohei Takasu[1], Satoshi Taguchi[1], Keisuke Hosokawa[2] (1.Department of Geophysics, Graduate School of Science, Kyoto University, 2.Department of Communication Engineering and Informatics, University of Electro-Communications)

[PEM15-P03] Motion of the inverted-V structure during an isolated substorm

*Morio Tanaka[1], Satoshi Taguchi[1], Kohei Takasu[1], Tomokazu Oigawa[1], Keisuke Hosokawa[2] (1.Department of Geophysics, Graduate school of science, Kyoto University, 2.Department of Communication Engineering and Informatics, University of Electro-Communications)

[PEM15-P04] Observation and modeling of Na layer response to energetic particle precipitation

*Takuo T. Tsuda[1], Kyogo Takizawa[1], Ryo Tozu[1], Takuya Kawahara[2], Yoshimasa Tanaka[3], Mitsumu K. Ejiri[3], Takanori Nishiyama[3], Takuji Nakamura[3] (1.The University of Electro-Communications, 2.Shinshu University, 3.National Institute of Polar Research)

[PEM15-P05] Lidar data analysis of the sodium atoms in the thermosphere observed at Tromsoe, Norway

*Takuya Kawahara[1], Satonori Nozawa[2], Norihito Saito[3], Takuo T. Tsuda[4], Toru Takahashi[5], Testuya Kawabata[2], Miki Nishimura[1], Yoshitaka Kobayashi[1] (1.Faculty of Engineering, Shinshu University, 2.ISEE, Nagoya University, 3.RIKEN, Center for Advanced Photonics, 4.The University of Electro-Communications, 5.National Institute of Polar Research)

[PEM15-P06] Spatial-temporal distribution of anomalous enhancement of ambipolar diffusion coefficient observed by meteor radars installed in the polar region

*Toru Takahashi[1], Masaki Tsutsumi[1,2], Yasunobu Ogawa[1,2,3], Satonori Nozawa[3], Chris Hall[4], Hiroshi Miyaoka[1,2] (1.National Institute of Polar Research, 2.SOKENDAI, 3.Institute for Space-Earth Environmental Research, 4.TGO, The Arctic University of Norway)

[PEM15-P07] Progress of ICSWSE and MAGDAS project in recent years

*Shuji Abe[1], Akimasa Yoshikawa[2,1], Teiji Uozumi[1], Akiko Fujimoto[3] (1.International Center for Space Weather Science and Education, Japan, 2.Department of Earth and Planetary Sciences, Kyushu University, 3.Kyushu Institute of Technology)

[PEM15-P08] Status of GNU Radio Beacon Receiver 2 (GRBR2) development

*Mamoru Yamamoto[1], Mayumi Matsunaga[2], Roland Tsunoda[3] (1.Research Institute for Sustainable Humanosphere, Kyoto University, 2.Tokyo University of Technology, 3.SRI International)

[PEM15-P09] Statistical comparison between plasma bubble day-to-day variability and neutral atmosphere by using GPS scintillation and GAIA model

*Mamoru Yamamoto[1], Keigo Kono[1] (1.Research Institute for Sustainable Humanosphere, Kyoto University)

[PEM15-P10] Redevelopment of the MU radar transceiver-module control system

*Mamoru Yamamoto[1], Koki Kurokawa[1], Hiroyuki Hashiguchi[1] (1.Research Institute for Sustainable Humanosphere, Kyoto University)

Study on adaptive clutter rejection system using external receiving antennas for the MU radar

*Hiroyuki Hashiguchi[1], Issei Terada[1], Mamoru Yamamoto[1]

1. Research Institute for Sustainable Humanosphere, Kyoto University

Strong clutter echoes from a hard target such as a mountain or building sometimes cause problems of observations with atmospheric radars. In order to reject or suppress ground clutter echoes, it is effective to use NC-DCMP (Norm Constrained- Directionally Constrained Minimum Power) method, which makes null toward the direction of the clutter, if we can receive signals independently from plural antennas [Nishimura et al., JTech., 2012]. It has been demonstrated that the NC-DCMP method is effective to real observation data with the MU (Middle and Upper atmosphere) radar [Hashiguchi et al., Radio Sci., 2018]. Although NC-DCMP method suppresses clutter echoes with almost maintaining the shape of main lobe to add pseudo-noise compared with the conventional DCMP method, the signal-to-noise ratio (S/N) of atmospheric echoes is somewhat degraded. We studied the clutter suppression method with little S/N degradation by using external antennas.

Four turnstile antennas are installed in the MU radar site. The signal from the antenna is sent to the MU radar observation room through the coaxial cable after amplified by the LNA with the limiter and BPF. It is further amplified by the LNA in the observation room, and then down-converted to intermediate frequency (5 MHz) signal to input to the multi-channel receiving system of the MU radar.

We compared the NC-DCMP method using the each received data of 25 channels, which is a conventional clutter suppression method, and the NC-DCMP method using the simple combination of 25 channels and 4 channels of external antennas. In the former case, the S/N of the atmospheric echoes is somewhat degraded, but in the latter case the main lobe shape is guaranteed by 25 channel simple synthesis, so the S/N degradation is not observed. In the latter case, the clutter suppression is sometimes insufficient. This cause is considered to be that the current positions of external antennas are biased to the north side. Antenna positions should be optimized in the future.

We can apply the achievement of this study to the Equatorial MU radar (EMU), which is proposed to be constructed at West Sumatera, Indonesia. The EMU system is the similar as the MU radar, but its antenna consists of 1045 Yagi antennas with 55 groups and it has 64 receiver channels.

Keywords: Atmospheric radar, Clutter rejection, NC-DCMP method, MU radar

©2019. Japan Geoscience Union. All Right Reserved.

Detached cusp aurora for southward IMF

*Kohei Takasu[1], Satoshi Taguchi[1], Keisuke Hosokawa[2]

1. Department of Geophysics, Graduate School of Science, Kyoto University, 2. Department of Communication Engineering and Informatics, University of Electro-Communications

A poleward-moving aurora is a typical phenomenon in the dayside cusp of the high-latitude ionosphere. This aurora usually originates near the equatorward boundary of the cusp, and diminishes near the poleward boundary of the persistent cusp auroral emissions. In this study we have examined faint poleward-moving auroras that are detached from the persistent cusp emissions by analyzing 630-nm aurora image data from an all-sky imager at Longyearbyen, Svalbard, and precipitating electron data from DMSP spacecraft. These auroras occur for southward IMF, and are located at latitudes higher than 80 MLAT. The intensities are very weak (less than 1 kilo Rayleigh). The result of the analysis shows that the speed of the auroral motion is 1 to 2 km/s, which is faster than typical convection speed in the dayside polar cap. We show the similarities and differences between the faint aurora and the typical poleward moving cusp aurora, and discuss how soft electron precipitation occurs in the region that is well separated from the cusp.

Keywords: Aurora, cusp, plasma convection, IMF

©2019. Japan Geoscience Union. All Right Reserved.

Motion of the inverted-V structure during an isolated substorm

*Morio Tanaka[1], Satoshi Taguchi[1], Kohei Takasu[1], Tomokazu Oigawa[1], Keisuke Hosokawa[2]

1. Department of Geophysics, Graduate school of science, Kyoto University, 2. Department of Communication Engineering and Informatics, University of Electro-Communications

The inverted-V is an energetic electron precipitation event, which can be seen as a V-shape structure in electron flux spectrograms, and causes intense auroral arcs. Previous studies have suggested that the inverted-V structure can move fast poleward or equatorward. However, we still do not understand what drives its motion. In this study we have investigated the detailed characteristics of an inverted-V structure moving poleward, which occurred during an isolated substorm, using simultaneous observations of auroras, precipitating electrons, and field-aligned currents. We analyzed aurora data (630-nm and 557.7-nm) from an all-sky imager at Longyearbyen, Svalbard, and precipitating electrons and magnetic field data from the DMSP spacecraft (F16, F17, F18, F19). One of the interesting characteristics of the poleward-moving inverted-V is the appearance of a downward field-aligned current equatorward of and adjacent to the inverted-V. We discuss how the region of the downward field-aligned current evolves in association with the motion and growth/decay of the inverted V structure, and possibility of a role of the downward field-aligned current for the latitudinal motion of the inverted V.

Keywords: Field-aligned current, aurora, inverted-V, isolated substorm

©2019. Japan Geoscience Union. All Right Reserved.

Observation and modeling of Na layer response to energetic particle precipitation

*Takuo T. Tsuda[1], Kyogo Takizawa[1], Ryo Tozu[1], Takuya Kawahara[2], Yoshimasa Tanaka[3], Mitsumu K. Ejiri[3], Takanori Nishiyama[3], Takuji Nakamura[3]

1. The University of Electro-Communications, 2. Shinshu University, 3. National Institute of Polar Research

Metallic layers, such as Na, Fe, Mg, K, and Ca layers, exist in the mesosphere and lower thermosphere (MLT). The height range of the MLT region corresponds to the ionospheric *D* and *E* regions, and in the polar region energetic particles precipitating from the magnetosphere can often penetrate into the *E* region and even into the *D* region. Therefore, the influence of energetic particles on the metallic layers is of interest regarding changes in atmospheric composition accompanied by auroral activity or geomagnetic activity.

In this study, we have performed a statistical investigation on relationship between Na density and cosmic noise absorption (CNA), which were obtained from 2000 to 2002 at Syowa Station, Antarctic (69.0ºS, 39.6ºE). From the investigation, we found the Na density decrease in accordance with the CNA increase, i.e., increase in the energetic particle precipitation. In the presentation, we will show these observational results, and discuss causality about the observed relationship based on numerical caculations using our Na chemistry model.

Keywords: Na layer, Energetic particle precipitation, Syowa Station, Na chemistry model

©2019. Japan Geoscience Union. All Right Reserved.

Lidar data analysis of the sodium atoms in the thermosphere observed at Tromsoe, Norway

*Takuya Kawahara[1], Satonori Nozawa[2], Norihito Saito[3], Takuo T. Tsuda[4], Toru Takahashi[5], Testuya Kawabata[2], Miki Nishimura[1], Yoshitaka Kobayashi[1]

1. Faculty of Engineering, Shinshu University, 2. ISEE, Nagoya University, 3. RIKEN, Center for Advanced Photonics, 4. The University of Electro-Communications, 5. National Institute of Polar Research

Distribution of low-density Na atoms in the thermosphere is interesting because of the capability of measuring neutral temperature and wind into the lower thermosphere up to 140 km. The thermospheric Na atoms significantly made the altitude range of Na lidar measurements expanded from the 80–105 km to 80–140 km, covering almost the entire E region (Liu et al., GRL, 2016).

The measurements of wind and temperature by a Na lidar in the northern mesosphere (80-105 km) at Tromsoe, Norway (69.6˚N, 19.2˚E) have been carried out in Polar winter season since 2010. However, thermospheric Na has not been seen in our data so far. This is because the automatic analysis program calculates the background signal level using the 140-150 km signals which possibly include a small amount of thermospheric Na signal. Deriving thermospheric Na is done by lowering the background signal level to emphasize thermospheric Na signals. The data at the new moon are selected which have a low background signal. Also, we calculated signal intensity from the Na atoms in the thermosphere based on our lidar parameters such as laser power, a telescope aperture area etc. by using the lidar equation. The results are summarized as follows. (1) Assuming that the Na density is 10 /cm^3, the signal from the Na atoms between 120 and 140 km is expected 300-400 photons, (2) The background signal observed is about 4,400 counts which means the noise level is about 220. So the signal intensity from the Na is nearly comparable to the noise level. (3) Thermospheric Na was not clearly seen in the re-calculated data. However, it depends on the smoothing technique to the original lidar data.

In this talk, we show the results derived by varying the binning time and discuss it.

Keywords: Na lidar, thermosphere, Tromsoe

©2019. Japan Geoscience Union. All Right Reserved.

Spatial-temporal distribution of anomalous enhancement of ambipolar diffusion coefficient observed by meteor radars installed in the polar region

*Toru Takahashi[1], Masaki Tsutsumi[1,2], Yasunobu Ogawa[1,2,3], Satonori Nozawa[3], Chris Hall[4], Hiroshi Miyaoka[1,2]

1. National Institute of Polar Research, 2. SOKENDAI, 3. Institute for Space-Earth Environmental Research, 4. TGO, The Arctic University of Norway

The meteor radar detected echoes of meteor tails as a tracer of neutral wind from 75 to 100 km altitudes (Hall et al., 2005). In addition, by using a decay time of the echo power, the meteor radar also estimated the ambipolar diffusion coefficient, which depends on the ion and electron temperature. The ambipolar diffusion coefficient was utilized to estimate the neutral temperature because the ion and electron temperature are generally in the thermal equilibrium with the neutral temperature. Recently, an anomalous enhancement of the ambipolar diffusion coefficient which could not be explained by the neutral temperature enhancement (hereafter called the anomalous enhancement) was observed by the meteor radar installed at Tromsoe, Norway (69.6 deg. N, 19.2 deg. E)
A previous study compared the anomalous enhancement with the ion velocity and the ion and electron temperature observed by EISCAT radar (Tsutsumi et al. 2017, Proceedings of the 30th Atmospheric Science Symposium, 2017). They reported that the anomalous enhancement tended to appear with the enhancement of ion velocity and electron temperature and frequently appeared at 16 UT. Furthermore, the anomalous enhancement was not seen during an event of the high energy particle precipitation on November 17, 2012 although one case study. Thus, the anomalous enhancement seems to be generated by the intense electric field and the high energy particle precipitation is not always necessary for its generation. As mentioned above, the previous study revealed a fundamental characteristics of the anomalous enhancement, however the generation mechanisms of the anomalous enhancement is still unclear. To clarify this, the comparison the spatial distribution of the anomalous enhancement with the convective electric field are needed. However, to date the latitudinal and local time occurrence of the anomalous enhancement was not revealed in the polar region.
Three meteor radars have been installed at Tromsoe, Bear island (74.5 deg. N, 19.0 deg. E), and Longyearbyen (78.2 deg. N, 16.2 deg. E). These meteor radars almost align on the same longitude line and can provide the spatial distribution of the anomalous enhancement. All meteor radars are a commercially produced VHF system (ENDR8-20) manufactured by ATRAD Pty Ltd. The antennas were produced by the Arctic University of Norway (Nozawa et al., 2012, JGR; Hall et al., 2002, GRL, Hall et al., 2006, JASTP). In this study, the spatial distribution and the occurrence rate of the anomalous enhancement was derived by these meteor radars.
Peaks of occurrence rate was seen at 20-22, 19-21, 16-19 MLT (~UT+3) at Tromsoe, Bear island, and Longyearbyen latitudes, respectively. This indicates that the anomalous enhancement appeared sequentially from high to low latitudes. In the morning sector, the peak of occurrence rate was only seen at 2-6 MLT above Bear island. In the case of high geomagnetic activity (Kp>3), the evening peaks of the occurrence rate shifted to an earlier time. On the other hand, clear peaks of the occurrence rate in the morning sector appeared at 3-5, 4-8, 7-10 MLT, respectively. Furthermore, the anomalous enhancement appeared with high possibility of 90% around 100 km south of Tromsoe. These characteristics which are seen during the time interval of high geomagnetic activity showed good agreement with the geomagnetic activity dependences of convective electric field.

©2019. Japan Geoscience Union. All Right Reserved.

We found another interesting characteristic in the geomagnetic dependence of the occurrence of the anomalous enhancement. The peak of occurrence rate in the evening sector was larger than it observed in the morning sector. This is considered to be related that auroral arcs appearing with intense electric field mainly observed in the evening sector. Thus, the generation of anomalous enhancement seems to relate both the convective electric field and the appearance of auroral arcs.
In this presentation, we will show the spatial distribution, MLT and geomagnetic activity dependence of the anomalous enhancement. We will also intend to present the comparison it with the electric filed observed by EISCAT and EISCAT Svalbard radars

Keywords: meteor radar, Tromsø, EISCAT radar

©2019. Japan Geoscience Union. All Right Reserved.

Progress of ICSWSE and MAGDAS project in recent years

*Shuji Abe[1], Akimasa Yoshikawa[2,1], Teiji Uozumi[1], Akiko Fujimoto[3]

1. International Center for Space Weather Science and Education, Japan, 2. Department of Earth and Planetary Sciences, Kyushu University, 3. Kyushu Institute of Technology

International Center for Space Weather Science and Education (ICSWSE), Kyushu University is the research institute for conducting research and education in space weather. Our magnetometer array named as "MAGDAS/CPMN (MAGnetic Data Acquisition System/Circum-pan Pacific Magnetometer Network)" (Principal Investigator: Dr. A. Yoshikawa) has over seventy fluxgate magnetometers, one induction magnetometer, and four FM-CW (Frequency Modulated Continuous Wave) radars around the world. One of our recent research topics is Equatorial Electrojet (EEJ). We calculate EE-index (Uozumi et al, 2008; Fujimoto et al., 2016) for space weather nowcast/forecast using realtime magnetometer data along the magnetic equator, and update it at each hour on the website (http://data.icswse.kyushu-u.ac.jp/eeindex/). To accelerate the understanding of EEJ structure, we constructed dense magnetometer array near magnetic equator at Peru and Malaysia in recent year. In addition, we finished to install new FM-CW radar at Sicaya, Peru. The instrument works well current now. We are providing our observational information and data including old project via our website (http://data.icswse.kyushu-u.ac.jp/). We also provide them via IUGONET (Inter-university Upper Atmosphere Observation NETwork) Type-A (http://search.iugonet.org/) which is one-stop web service system for researchers to search data, get the information of data, and plot data, and SPEDAS (Space Physics Environment Data Analysis System)/UDAS (iUgonet Data Analysis System). We will provide them via SuperMAG (http://supermag.jhuapl.edu/) in the near future. For accelerating the usage of MAGDAS and its science, we held a tutorial session in International Conference on Space Weather and Satellite Application 2018 at Malaysia, for handling MAGDAS and other data related our research field by using IUGONET system. We believe researchers use MAGDAS data on proper rule and develop their science. We will introduce other research activities in ICSWSE and MAGDAS project, for example, plasma bubble, geomagnetically induced current, and so on.

©2019. Japan Geoscience Union. All Right Reserved.

Status of GNU Radio Beacon Receiver 2 (GRBR2) development

*Mamoru Yamamoto[1], Mayumi Matsunaga[2], Roland Tsunoda[3]

1. Research Institute for Sustainable Humanosphere, Kyoto University, 2. Tokyo University of Technology, 3. SRI International

GNU Radio Beacon Receiver (GRBR) is the very successful digital receiver developed for dual-band (150/400MHz) beacon experiment. We were successfully conducted observations of total-electron content (TEC) of the ionosphere over Japan and in southeast Asia. However, many beacon satellites is now aging, and its number is decreasing. We now have a project to start new satellite-ground beacon experiment with new satellite constellations. One of them is TBEx (Tandem Beacon Explorer), a project by SRI International, to fly a constellation of two 3U cubesats with triband beacon transmitters. Another one is a project of FORMOSAT-7/COSMIC-2 by Taiwan/USA. Well-known mission of COSMIC-2 is GNSS occultation experiment, but the satellites carry triband beacon transmitters. All of these satellites will be placed into low-inclination orbits by the same launch vehicle in 2018, which will give us great opportunities to enhance studies of the low-latitude ionosphere. We develop a new digital receiver, GRBR2, for these new satellite beacon. GRBR2 is a four channel receiver at 150/400/965/1067MHz beacon signals from two satellite constellations. Now The reveiver system was finally fixed. Problem of the project of delay of the satellite launch. But it is now on schedule for launch by 2019 summer. We start deploying GRBR2 in southeast Asian countries. In this presentaiton, we will report GRBR2 system and its performance including results from test experiment in the field.

Keywords: Satellite beacon experiment, Digital receiver development, Total electron content

©2019. Japan Geoscience Union. All Right Reserved.

Statistical comparison between plasma bubble day-to-day variability and neutral atmosphere by using GPS scintillation and GAIA model

*Mamoru Yamamoto[1], Keigo Kono[1]

1. Research Institute for Sustainable Humanosphere, Kyoto University

Equational plasma bubble is one of the most intense irregularities in the ionosphere. The occurrence of the plasma bubble is considered related to weak changes of the underlying atmosphere which is called large-scale wavelike structure (LSWS). The LSWS is expected formed by penetration of the atmospheric wave into the ionosphere. But its real effect is not yet known in detail. The purpose of this research is to investigate the correlation between the neutral atmosphere and day-to-day variability of equatorial plasma bubbles mainly in the Southeast Asia region. We based on the study by Yamamoto et al (2018) that showed relationship between 40-km height temperature variation and S4 index over Kototabang, Indonesia. In this study we tried to extend the observation region and also tried to elucidate atmospheric waves that are related to the plasma bubble. For indicating activity of the plasma bubble, we used S4 index of GPS scintillation measured by ISEE, Nagoya Univ. at Kototabang, Indonesia. Atmospheric data were taken from GAIA database prepared by NICT. We analyzed data from 2003, 2004, 2012, and 2013 where the solar activity was high. Overall correlation between S4 index and the atmospheric temperature showed similar feature throughout these years. However, even when we tried to extract atmospheric wave components from the GAIA data, the correlation between the wave parameter to S4 index did not show large change. This means that the elucidation of the atmospheric wave component was not very successful so far. Further analyses are required.

Reference
Yamamoto, M., Y. Otsuka, H. Jin, Y. Miyoshi (2018) Relationship between day-to-day variability of equatorial plasma bubble activity from GPS scintillation and atmospheric properties from GAIA assimilation, Progress in Earth and Planetary Science, Vol. 5, page 26, doi: 10.1186/s40645-018-0184-7.

©2019. Japan Geoscience Union. All Right Reserved.

Redevelopment of the MU radar transceiver-module control system

*Mamoru Yamamoto[1], Koki Kurokawa[1], Hiroyuki Hashiguchi[1]

1. Research Institute for Sustainable Humanosphere, Kyoto University

The MU radar was installed in Shigaraki, Japan in 1984 as the world first atmospheric radar with active phased-array antenna system. The MU radar consists of 475 Yagi antennas in the circular field of about 100m diameter. By the electronic phase shift of each Yagi, the antenna beam is steered to one of pre-selected 2048 directions in the transmitting pulse-to-pulse basis. Success of the MU radar in the atmospheric/ionospheric research is well known, and its active phased-array configuration was followed by many other radar systems. The phase control of the MU radar is realized by the control of its transceiver-module (TR-module) that are equipped with each Yagi antenna. They are gathered into 25 groups of each 19 modules. One CPU (microcomputer board) is used for control of one group of modules. A weak point of the MU radar exists in this point because we are using the original 8085 CPU board that is connected to the host computer by 1200-baud (!) serial line. This control is very slow, and we could not meet demands for rapid change of observation parameters for long time. This time we tried to re-develop the new TR-module controller by using recent CPU board and electronic devices. In the presentation, we show hardware/software of the newly developed prototype of the MU radar TR-module controller.

Keywords: MU radar, control system, redevelopment

©2019. Japan Geoscience Union. All Right Reserved.

[E] Poster | A (Atmospheric and Hydrospheric Sciences)：A-AS Atmospheric Sciences, Meteorology & Atmospheric Environment

Thu. May 30, 2019 1:45 PM - 3:15 PM JST | Thu. May 30, 2019 4:45 AM - 6:15 AM UTC | Poster Hall International Exhibition Hall8, Makuhari Messe_1

[A-AS02] Advances in Tropical Cyclone Research: Past, Present, and Future

convener:Sachie Kanada(Nagoya University), Akiyoshi Wada(Department of Typhoon and Severe Weather Research, Meteorological Research Institute), Kosuke Ito(University of the Ryukyus), Yoshiaki Miyamoto(Faculty of Environment and Information Studies, Keio University)

Tropical cyclones (TC) sometimes cause destructive disasters in many countries by torrential rainfall, strong wind, storm surge, and high surf. In 2008, the western Japan suffered a record-breaking heavy rainfall related to Typhoon Prapirooon (2018) in July. Furthermore, two Category 4 typhoons, typhoons Jebi (2018) and Trami (2018), made landfalls on the western Japan in September and caused devastating disasters over the Japanese Islands. In the Northern Atlantic, Hurricane Florence caused catastrophic damage in the eastern side of U.S. Recent studies reported a northward shift of the location where a TC achieved the peak intensity and also reported increases in the frequency of rapidly intensifying storms. Thus, understanding the TC processes related to translation, intensity change and precipitation in the changing climate, and to provide more accurate forecasts and long-term projections are essential for the earth and planetary science.
Advances in innovative observations such as meteorological aircraft, weather satellite, supercomputer systems such as the Earth Simulator and K-computer, and introduction of new methods such as the deep-learning, have led to novel development of numerical weather forecasting and understanding of the phenomena related to TCs in the past, present and future climates. In this session, we welcome papers on various aspects of TC studies. We hope that the session will provide a new direction for future TC researches.

[AAS02-P01] Numerical study on lightning frequency in a tropical cyclone

*Yousuke Sato[1,3], Yoshiaki Miyamoto[2,3], Tomita Hirofumi[3] (1.Department of Applied Energy, Nagoya University, 2.Faculty of Environment and Information Studies, Keio University, 3.RIKEN Center for Computational Science)

[AAS02-P02] **Sensitivity of Numerical Simulation of Typhoon Nepartak (2016) to Cloud Condensation Nuclei Concentration**

*Yu-De Wu[1], Jian-Liang Wang[1] (1.Dept. of Environmental Informational and Engineering, Chung Cheng Institute of Technology, National Defense University, Taiwan)

[AAS02-P03] Moisture Budget Analysis for Hurricane Precipitation on Texas

*Satoshi Iizuka[1], Naoki Sakai[1] (1.National Research Institute for Earth Science and Disaster Resilience)

[AAS02-P04] Remote response of a developing tropical cyclone over the western North Pacific to large-scale vapor transport from the Kuroshio in boreal fall

*Keita Fujiwara[1], Ryuichi Kawamura[2], Tetsuya Kawano[2] (1.Graduate School of Science, Kyushu University, 2.Faculty of Science, Kyushu University)

[AAS02-P05] Asymmetrically Intensifying Processes of a Category 4 Super Typhoon Lan (2017) during High Vertical Wind Shear

*Sachie Kanada[1], Akiyoshi Wada[2], Kazuhisa Tsuboki[1] (1.Nagoya University, 2.Meteorological Research Institute)

[AAS02-P06] Roles of preexisting oceanic condition and ocean coupling processes in the intensity prediction during the mature phase of Typhoon Trami (2018)

*Akiyoshi Wada[1] (1.Typhoon Research Department Meteorological Research Institute)

[AAS02-P07] Development and assessment of the probabilistic storm surge forecast system in Taiwan: Case Study of Typhoon Maria in 2018

*Chun-Wei Lin[1], Tso-Ren Wu[1], Yu-Lin Tsai[1], Shu-Chun Chuang[1], Chi-Hao Chu[2], Chuen-Teyr Terng[2] (1.Graduate Institute of Hydrological and Oceanic Sciences, National Central University, Chungli, Taiwan, 2.Marine Meteorology Center, Central Weather Bureau, Taipei, Taiwan)

[AAS02-P08] Basic Data Construction for a Typhoon Disaster Prevention Model : Analysis and Changes by El Nino and La Nina year

*HANA NA[1], Woo-Sik Jung[1] (1.Department of Atmospheric Environment Information Engineering, Atmospheric Environment Information Research Center, Inje University, Gimhae 50834, Korea)

[AAS02-P09] Basic Data Construction for a Typhoon Disaster Prevention Model : Analysis According to the Typhoon Path Type

*HANA NA[1], Woo-Sik JUNG[1] (1.Department of Atmospheric Environment Information Engineering, Atmospheric Environment Information Research Center, Inje University, Gimhae 50834, Korea)

[AAS02-P10] Basic Data Construction for a Typhoon Disaster Prevention Model : Monthly Characteristics of Typhoon Rusa, Maemi, Kompasu, and Bolaven

*HANA NA[1], Woo-Sik Jung[1] (1.Department of Atmospheric Environment Information Engineering, Atmospheric Environment Information Research Center, Inje University, Gimhae 50834, Korea)

[AAS02-P11] The mechanism of typhoon generated in the earth that rotates in the space where the solar wind blows

*Shinji Karasawa[1] (1.Miyagi National College of Technology Professor emeritus)

Numerical study on lightning frequency in a tropical cyclone

*Yousuke Sato[1,3], Yoshiaki Miyamoto[2,3], Tomita Hirofumi[3]

1. Department of Applied Energy, Nagoya University, 2. Faculty of Environment and Information Studies, Keio University, 3. RIKEN Center for Computational Science

This study investigates frequency of lightning in each stage of lifecycle of tropical cyclone (TC) using the next generation weather and climate library called Scalable Computing for Advanced Library and Environment (SCALE; Sato et al. 2015, Nishizawa et al. 2015). Lightning component was developed and implemented into SCALE in this study. An idealized experiment based on an experimental setup of Miyamoto and Takemi (2013) was conducted by SCALE coupled with lightning component. The results of the simulation indicate that the lightning frequency is maximum before rapid intensification (RI) of TC, which supports the report of Price et al. (2009) derived from satellite observation. The frequency of lightning decreases after RI and it keeps small until the TC reaches steady state. Our analyses elucidate that the dependency of the lightning frequency upon the developing stage of TC is originated from the type of convection dominating at each growth stage. Before the RI, the convection generated by consuming convective available potential energy (CAPE) transport hydrometeors upward, and the charge split and the lightning frequently occur. During the steady state, the hydrometeors are mainly transported by the fast rotating flow in the simulated TC, which resulted in the weak charge split and small frequency of lightning.

Keywords: Tropical cyclone, Lightning

©2019. Japan Geoscience Union. All Right Reserved.

Sensitivity of Numerical Simulation of Typhoon Nepartak (2016) to Cloud Condensation Nuclei Concentration

*Yu-De Wu[1], Jian-Liang Wang[1]

1. Dept. of Environmental Informational and Engineering, Chung Cheng Institute of Technology, National Defense University, Taiwan

The study is carried out using the WRF model and the Cloud Condensation Nuclei, CCN, in the WDM6 microphysics scheme has been modified to test its impacts on typhoon simulations. The simulated track, intensity, and rainfall distribution of Typhoon Nepartak (2016) over Pacific Ocean are compared among numerical experiments of different initial concentration of CCN (wdm6_ctr, wdm6_10, and wdm6_50, where wdm6_10 and wdm6_50 represent that CCN are respectively 10 and 50 times of the value used in wdm6_ctr).

The simulated tracks in three runs are similar, but the intensity and the maximum dBz increase both in wdm6_10 and wdm6_50, but it takes more time for wdm6_50 to intensify. The comparison of mixing ratios of five water species shows that the cloud droplets mixing ratios increase as CCN is increased. The mixing ratios of rain, cloud ice, snow and graupel are enhanced more rapidly in wdm6_10 compared with wdm6_50. The same situation happens in the divergence field and upward motions. It is suggested that the increase of CCN will result in stronger typhoon, but the intensification will be slowed down with too much CCN.

Keywords: Cloud Condensation Nuclei, Typhoon Nepartak, Microphysics Scheme

©2019. Japan Geoscience Union. All Right Reserved.

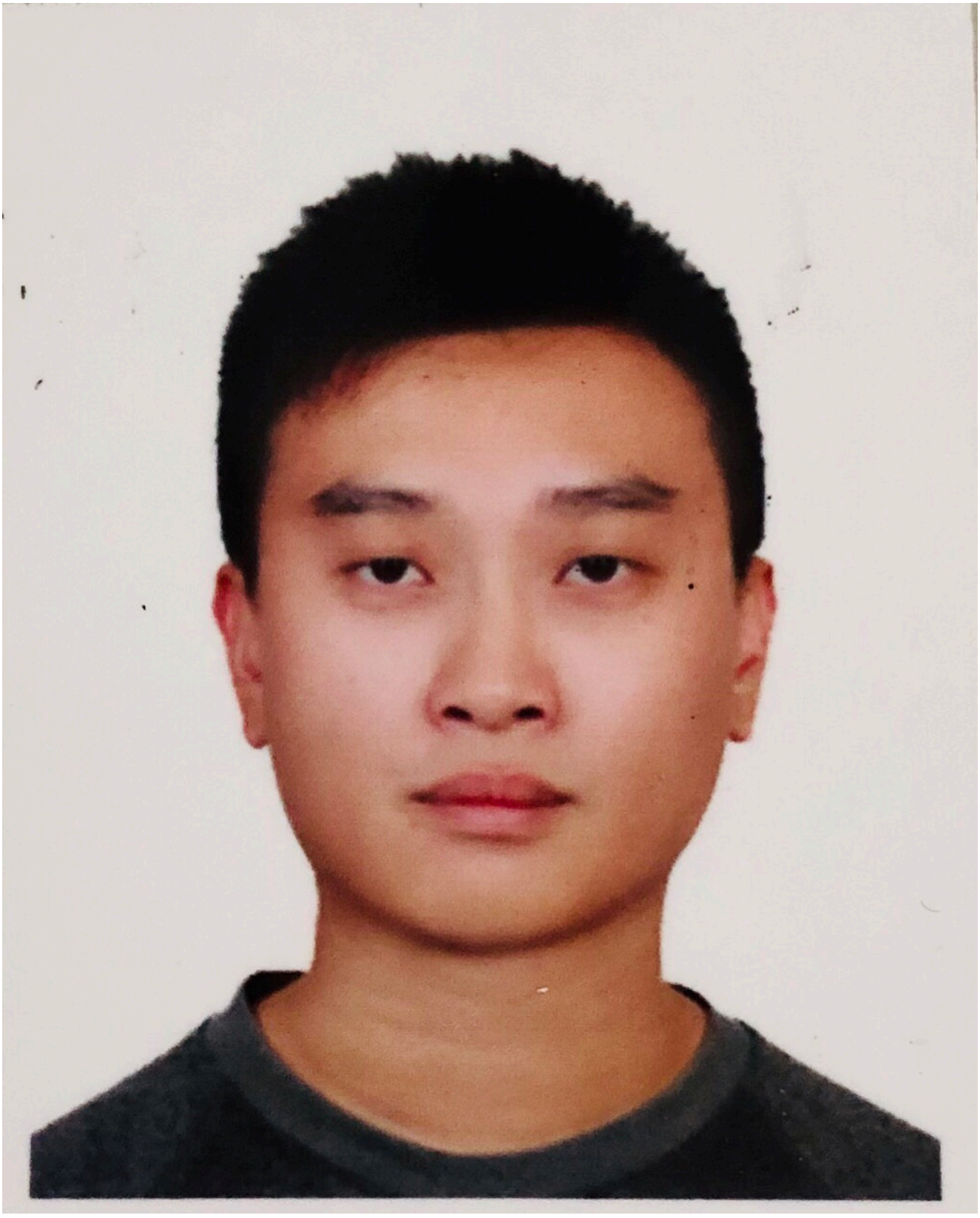

©2019. Japan Geoscience Union. All Right Reserved.

Moisture Budget Analysis for Hurricane Precipitation on Texas

*Satoshi Iizuka[1], Naoki Sakai[1]

1. National Research Institute for Earth Science and Disaster Resilience

In August 2017, Hurricane Harvey brought the unprecedented amount of rainfall and catastrophic flooding on the Houston metropolitan area, as it stagnated near the coast of Texas for several days after its decline to a tropical storm intensity. The present study compares the moisture budget for rainfall associated with Harvey with those of past hurricanes making landfall on Texas. It seems that the high pressure over the west coast region of the US, along with the meandering of the subtropical jet starting from the periphery of Hawaii and toward the south in Texas, stagnated Hurricane Harvey around the coast of Texas for several days. The meandering of the subtropical jet toward the south in Texas also caused the largest convergence of moisture advected from the Gulf of Mexico efficiently over Texas, although the accompanied high pressure was not extraordinary event. Therefore, it is suggested that surrounding meteorological conditions can greatly affect rainfall related to tropical cyclones.

Keywords: Hurricane Harvey, Precipitation, Moisture Budget

©2019. Japan Geoscience Union. All Right Reserved.

Remote response of a developing tropical cyclone over the western North Pacific to large-scale vapor transport from the Kuroshio in boreal fall

*Keita Fujiwara[1], Ryuichi Kawamura[2], Tetsuya Kawano[2]

1. Graduate School of Science, Kyushu University, 2. Faculty of Science, Kyushu University

A remote linkage between the development of tropical cyclone (TC) over the western North Pacific and moisture transport from the Kuroshio Current due to environmental flow toward TC was examined by using regional cloud resolving model and Lagrangian diagnostics. In this study, we specially highlighted a prototypical TC (Typhoon Chaba 2010), which developed and migrated northward over the Philippines Sea in boreal fall, and conducted sensitivity experiments that modified surface turbulent latent heat flux (LHF) over the Kuroshio. The large-scale environment was characterized by a combination of two synoptic systems, eastward-migrating anticyclone from the Asian continent and TC approaching Japan, bringing low-level northeasterly flows over the Kuroshio through an enhanced meridional pressure gradient in that region. Trajectory analyses suggested that air parcels along the northeasterlies modified by receiving abundant water vapor from the underlying Kuroshio may contribute to latent heating within Chaba’s inner core region as a remote effect, leading to TC development.

When LHF was removed or reduced over the Kuroshio under the dominance of the northwesterly flow, TC intensity attenuated during its developing stage even though TC was fairly far away from the Kuroshio. Since no or little modification of dry air parcels occurred in the atmospheric boundary layer over the Kuroshio, contribution of those parcels to latent heat release around Chaba’s eyewall become small. Furthermore, dry air penetration into TC’s inner core region may act as an inhibitor of convection within that region, resulting in deceleration of the TC development. These findings were consistent with another TC (Typhoon Toakge 2004) with a similar synoptic environment, increasing reliability of remote impact of moisture import from the Kuroshio on TC development.

Keywords: tropical cyclone, moisture transport, Kuroshio Current

©2019. Japan Geoscience Union. All Right Reserved.

Asymmetrically Intensifying Processes of a Category 4 Super Typhoon Lan (2017) during High Vertical Wind Shear

*Sachie Kanada[1], Akiyoshi Wada[2], Kazuhisa Tsuboki[1]

1. Nagoya University, 2. Meteorological Research Institute

On 21 October 2017, Typhoon Lan developed to a Category 4 super typhoon with the minimum central pressure (MCP) of 915 hPa at 25.6 degrees north latitude and maintained the peak intensity until the storm arrived at 29.9˚N under a strong environmental vertical wind shear (VWS) of 14 m s^{-1}. To understand the intensification processes of an intense typhoon with such high VWS, numerical simulations on Typhoon Lan were conducted using a high-resolution three-dimensional atmosphere regional model, the Cloud Resolving Storm Simulator (CReSS; Tsuboki and Sakakibara, 2002). Two sensitivity experiments, 1dO and FO, were conducted with different SST representations. In the 1dO experiment, a simple thermal diffusion model was used to express temperature changes due to ocean vertical mixing. The FO experiment with a time-fixed SST did not consider the evolution of SST. Both experiments used the same initial and boundary conditions and model specifications for the atmosphere, started at 0000 UTC 18 October 2017, and had an integration time of 5 days. The computational domain was 2˚N–37.8˚N and 115˚E–145˚E. The number of horizontal grids in the computational domain was 752×896 with the horizontal grid size of 0.04 longitude by 0.04 latitude.

The typhoon simulated in the 1dO experiment successfully achieved the MCP of 910 hPa at 29.5˚N, exhibiting strong asymmetric precipitation pattern as observed by the satellites. The intensification processes were accompanied by rapid developments of the strong winds and warm core in the low-levels. The strong northeast VWS forced to tilt the storm axis to downshear side (northeast) and, in the downshear quadrants, tall, intense and upstanding eyewall updrafts (CBs) formed from the low-level convergence of the storm travelling northeastward with a relatively fast translation speed of 10 m s^{-1}. Meanwhile, dry subsidence from the upper-levels intensified the low-level warm core in the upshear side of the eye. Despite the inner-core convection and precipitation exhibited strong asymmetric structures, the axisymmetricity of the storm circulation was maintained in the mid-to-low levels and abundant water vapor enclosed in the eye allowed to develop CBs around the radius of the maximum wind speeds. Although the FO storm overestimated the MCP of 879hPa, the similar asymmetric patterns in precipitation and convection were also found in the FO storm. The results indicated that the storm structures of typhoon Lan would be less sensitive to the SST-cooling effect.

Keywords: Typhoon, numerical model

©2019. Japan Geoscience Union. All Right Reserved.

Roles of preexisting oceanic condition and ocean coupling processes in the intensity prediction during the mature phase of Typhoon Trami (2018)

*Akiyoshi Wada[1]

1. Typhoon Research Department Meteorological Research Institute

Typhoon Trami (2018) is one of the typhoons that made landfall in Japan. According to the Regional Specialized Meteorological Center (RSMC) Tokyo best track analysis, the central pressure reached 915 hPa at 18 UTC on 24 September around 20˚N and then rapidly increased by 950 hPa in 18 hours. After the rapid increases in the central pressure, intensity forecasts announced further intensification to 935 hPa, but the typhoon could not intensify again. In order to clarify the impact of the cold eddies over the ocean on this forecast error, we conducted numerical simulations with different oceanic initial conditions (daily data from 19 to 25 September were used so that the number of ensemble members is seven) using a 2 km-mesh nonhydrostatic atmosphere model coupled with ocean surface wave and multilayer ocean models with the Japan Meteorological Agency (JMA) global objective analysis with horizontal resolution of 20 km and the JMA North Pacific Ocean analysis with horizontal resolution of 0.5˚. In addition, a sensitivity numerical experiment was conducted with the oceanic initial condition on 23 September merged with an artificial cold vortex centered at 21˚N, 129˚E of which both a mixed layer and thermocline was 50 m shallower than the control experiment. Moreover, a simulation with a 2 km-mesh nonhydrostatic atmosphere model was performed with the oceanic initial condition on 23 September. The initial time and integration period are 00 UTC on 23 September and 180 hours with the time interval of 3 seconds.

The results of simulated tracks were reasonable compared with the RSMC best track analysis, while the rapid decrease in the central pressure could not be simulated due to a large difference in central pressure at the initial time so that the simulated minimum central pressure was higher than the best track central pressure. From the analysis with the ratio of a difference to the standard deviation obtained from the ensemble experiments, the impact of different oceanic initial conditions on central pressure was different from that on the maximum wind speed particularly from 25 to 27 September when the typhoon passed near the cold eddy. The impact of ocean coupling on simulated central pressure and maximum wind speed was considerably greater than that of the artificial cold eddy and that of different oceanic initial conditions. The impact of the artificial cold eddy was a few times greater than that of different oceanic initial conditions around 26 September. The result indicates that more detailed observation and more accurate analysis regarding the cold eddy over the ocean will contribute to the improvement of typhoon intensity predictions.

Keywords: tropical cyclone, atmosphere-wave-ocean coupled model, intensity forecast, preexisting cold eddy

©2019. Japan Geoscience Union. All Right Reserved.

Development and assessment of the probabilistic storm surge forecast system in Taiwan: Case Study of Typhoon Maria in 2018

*Chun-Wei Lin[1], Tso-Ren Wu[1], Yu-Lin Tsai[1], Shu-Chun Chuang[1], Chi-Hao Chu[2], Chuen-Teyr Terng[2]

1. Graduate Institute of Hydrological and Oceanic Sciences, National Central University, Chungli, Taiwan, 2. Marine Meteorology Center, Central Weather Bureau, Taipei, Taiwan

From the forecast and the analyzed typhoon tracks in Taiwan, it is found that if the forecast track errors are greater than 100 km, roughly a quarter of the length of Taiwan, significant variability of storm surge elevation can be seen.
In order to consider the uncertainty of the atmospheric forecast, this study aims to develop the probabilistic storm surge forecast system. The coastal storm surge model applied in this study is COMCOT-SS (COrnell Multi-Grid COupled Tsunami Model –Storm Surge), which is the kernel of the operating deterministic storm surge forecast system in CWB, Taiwan. It solves nonlinear shallow water equations in the nested-grid scheme. Two ensemble methods are adopted in this study, one is Deterministic Track Error Distribution Method, D-TED Method. The other one is the Ensemble Track Analysis Method, ETA Method. D-TED Method is generated from the deterministic forecast, while the ETA Method obtains typhoon tracks and parameters from the CWB WEPS (CWB WRF Ensemble Prediction System).
From the case study of typhoon Maria in 2018, it shows that as the typhoon approaching Taiwan, the coverage of the tracks from ETA Method would be more convergence comparing to the tracks from D-TED Method, and it provides a more concentrated surge elevation distribution.

Keywords: storm surge, ensemble forecast, COMCOT-SS

©2019. Japan Geoscience Union. All Right Reserved.

Basic Data Construction for a Typhoon Disaster Prevention Model : Analysis and Changes by El Nino and La Nina year

*HANA NA[1], Woo-Sik Jung[1]

1. Department of Atmospheric Environment Information Engineering, Atmospheric Environment Information Research Center, Inje University, Gimhae 50834, Korea

Among the typhoons that affected the Korean Peninsula for approximately 110 years from 1904, when weather observation began until 2018, all of the top five typhoons in terms of the maximum wind speed and property damage record occurred after 2000. This implies that the intensity of typhoons is becoming stronger and the damage is more severe compared to the past. Moreover, typhoons are significantly affected by the sea temperature. The El Nino and La Nina phenomena, in which significant changes in the sea temperature occur, may significantly affect the occurrence and intensity of typhoons affecting the Korean Peninsula. Therefore, this study aims to analyze changes by year, and the years of El Nino and La Nina occurrences by estimating the maximum wind speed that can be generated during typhoon period based on the typhoons that affected the Korean Peninsula. This study was conducted for the period between 2002 and 2015. As a result of analyzing the maximum wind speed of the typhoons that affected the Korean Peninsula by year, high 3-second gusts tended to occur in the Gyeongsang-do area including the southeast coast of the Korean Peninsula from 2002 to 2006. Subsequently, the strong wind area of the 3-second gusts expanded, and high 3-second gusts occurred in the Seoul metropolitan area. Moreover, as a result of investigating the 3-second gust characteristics for the years of El Nino and La Nina occurrences, a higher maximum wind speed was observed from the typhoons that affected the Korean Peninsula in the years of El Nino occurrence.

This research was supported by Basic Science Research Program through the National Research Foundation of Korea(NRF) funded by the Ministry of Education(2017R1D1A3B03036152)

Keywords: Typhoon Disaster Prevention Model, 3-Second gust, El Nino, La Nina

©2019. Japan Geoscience Union. All Right Reserved.

Basic Data Construction for a Typhoon Disaster Prevention Model : Analysis and Changes by El Nino and La Nina year

Hana Na, Woo-Sik Jung

Among the typhoons that affected the Korean Peninsula for approximately 110 years from 1904, when weather observation began until 2018, all of the top five typhoons in terms of the maximum wind speed and property damage record occurred after 2000. This implies that the intensity of typhoons is becoming stronger and the damage is more severe compared to the past. Moreover, typhoons are significantly affected by the sea temperature. The El Nino and La Nina phenomena, in which significant changes in the sea temperature occur, may significantly affect the occurrence and intensity of typhoons affecting the Korean Peninsula. Therefore, this study aims to analyze changes by year, and the years of El Nino and La Nina occurrences by estimating the maximum wind speed that can be generated during typhoon period based on the typhoons that affected the Korean Peninsula. This study was conducted for the period between 2002 and 2015. As a result of analyzing the maximum wind speed of the typhoons that affected the Korean Peninsula by year, high 3-second gusts tended to occur in the Gyeongsang-do area including the southeast coast of the Korean Peninsula from 2002 to 2006. Subsequently, the strong wind area of the 3-second gusts expanded, and high 3-second gusts occurred in the Seoul metropolitan area. Moreover, as a result of investigating the 3-second gust characteristics for the years of El Nino and La Nina occurrences, a higher maximum wind speed was observed from the typhoons that affected the Korean Peninsula in the years of El Nino occurrence.

This research was supported by Basic Science Research Program through the National Research Foundation of Korea(NRF) funded by the Ministry of Education(2017R1D1A3B03036152)

Key words : Typhoon Disaster Prevention Model, WRF, 3-Second gust, El Nino, La Nina

©2019. Japan Geoscience Union. All Right Reserved.

Basic Data Construction for a Typhoon Disaster Prevention Model : Analysis According to the Typhoon Path Type

*HANA NA[1], Woo-Sik JUNG[1]

1. Department of Atmospheric Environment Information Engineering, Atmospheric Environment Information Research Center, Inje University, Gimhae 50834, Korea

In this study, a typhoon disaster prevention model was used to estimate the maximum wind speed during typhoon period by path type from all typhoons that affected the Korean Peninsula from 2002 to 2015. For the typhoon information and upper wind information used as input data, the results of the WRF numerical model, which utilized the Best Track data of the RSMC Tokyo Typhoon Center and the RDAPS data of the Korea Meteorological Administration, were applied. From analyzing the path type impact frequency using all typhoons that affected the Korean Peninsula during the study period (2002–2015), Type 7 that affected the Korean Peninsula through Japan was the most frequent, followed by Type 2 that directly landed on the Korean Peninsula through the southern coast. From analyzing the monthly path types of the typhoons that affected the Korean Peninsula, Type 2 that affected the Korean Peninsula by landing on the southern coast and Type 7 that affected the Korean Peninsula through Japan were the most frequent for the recently increasing September typhoons. The analysis of the maximum wind speed of the 3-second gust that may occur during typhoon period by path type revealed that Type 2 that affected the Korean Peninsula by landing on the southern coast exhibited the highest 3-second gust. As a result of examining the distribution of Type 2, high 3-second gusts occurred throughout the Korean Peninsula, including the southeast coast. As for the path of Type 2 that directly affected the Korean Peninsula by landing on the southern coast, the occurrence frequency was the second highest during the entire study period and the value of the 3-second gust, which was the maximum wind speed that may occur during typhoon period, was the highest.

This research was supported by Basic Science Research Program through the National Research Foundation of Korea(NRF) funded by the Ministry of Education(2017R1D1A3B03036152)

Keywords: Typhoon Path, 3-Second gust, Typhoon Disaster Prevention Model

©2019. Japan Geoscience Union. All Right Reserved.

Basic Data Construction for a Typhoon Disaster Prevention Model : Analysis According to the Typhoon Path Type

Hana Na, Woo-Sik Jung

In this study, a typhoon disaster prevention model was used to estimate the maximum wind speed during typhoon period by path type from all typhoons that affected the Korean Peninsula from 2002 to 2015. For the typhoon information and upper wind information used as input data, the results of the WRF numerical model, which utilized the Best Track data of the RSMC Tokyo Typhoon Center and the RDAPS data of the Korea Meteorological Administration, were applied. From analyzing the path type impact frequency using all typhoons that affected the Korean Peninsula during the study period (2002–2015), Type 7 that affected the Korean Peninsula through Japan was the most frequent, followed by Type 2 that directly landed on the Korean Peninsula through the southern coast. From analyzing the monthly path types of the typhoons that affected the Korean Peninsula, Type 2 that affected the Korean Peninsula by landing on the southern coast and Type 7 that affected the Korean Peninsula through Japan were the most frequent for the recently increasing September typhoons. The analysis of the maximum wind speed of the 3-second gust that may occur during typhoon period by path type revealed that Type 2 that affected the Korean Peninsula by landing on the southern coast exhibited the highest 3-second gust. As a result of examining the distribution of Type 2, high 3-second gusts occurred throughout the Korean Peninsula, including the southeast coast. As for the path of Type 2 that directly affected the Korean Peninsula by landing on the southern coast, the occurrence frequency was the second highest during the entire study period and the value of the 3-second gust, which was the maximum wind speed that may occur during typhoon period, was the highest.

This research was supported by Basic Science Research Program through the National Research Foundation of Korea(NRF) funded by the Ministry of Education(2017R1D1A3B03036152)

Keywords : Typhoon Disaster Prevention Model, WRF, Typhoon Track, 3-Second gust

©2019. Japan Geoscience Union. All Right Reserved.

Basic Data Construction for a Typhoon Disaster Prevention Model : Monthly Characteristics of Typhoon Rusa, Maemi, Kompasu, and Bolaven

*HANA NA[1], Woo-Sik Jung[1]

1. Department of Atmospheric Environment Information Engineering, Atmospheric Environment Information Research Center, Inje University, Gimhae 50834, Korea

According to a typhoon report that summarized the typhoons that had affected the Korean Peninsula for approximately 100 years since the start of weather observation in the Korean Peninsula, the number of typhoons that affected the Korean Peninsula was the highest in August, followed by July, and September. A study that analyzed the period between 1953 and 2003 revealed that the number of typhoons that affected the Korean Peninsula was 62 in August, 49 in July, and 45 in September. As shown, previous studies that analyzed the typhoons that affected the Korean Peninsula by month were primarily focused on the impact frequency. This study aims to estimate the monthly impact frequency of the typhoons that affected the Korean Peninsula as well as the maximum wind speed that accompanied the typhoons. It also aims to construct the basic data of a typhoon disaster prevention model by estimating the maximum wind speed during typhoon period using Typhoon Rusa that resulted in the highest property damage, Typhoon Maemi that recorded the maximum wind speed, Typhoon Kompasu that significantly affected the Seoul metropolitan area, and Typhoon Bolaven that recently recorded severe damages. A typhoon disaster prevention model was used to estimate the maximum wind speed of the 3-second gust that may occur, and the 700 hPa wind speed estimated through WRF(Weather Research and Forecasting) numerical simulation was used as input data.

Unlike the target period reported in the white paper on typhoons (1904–2010), this study analyzed the monthly impact frequency of the typhoons that affected the Korean Peninsula from 2002 and 2015. The result indicated that the impact frequency was the highest in August, followed by July and September. This result was the same as that of the typhoon report. An analysis by year revealed that typhoon period increased in September. The 3-second gust was found to be the highest in September, followed by August and July. When this result was analyzed in relation to the recently increasing autumn typhoons (September and October), the 3-second gust result was the highest in September, indicating disaster prevention must be emphasized. By additionally analyzing the maximum wind speed distributions of Typhoon Rusa, Maemi, Kompasu, and Bolaven, the area with the maximum wind speed varied depending on the typhoon path, and the 3-second gust was higher than 44 m/s based on the typhoon intensity classification and accounted for approximately10%.

This research was supported by Basic Science Research Program through the National Research Foundation of Korea(NRF) funded by the Ministry of Education(2017R1D1A3B03036152)

Keywords: Typhoon Disaster Prevention Model, WRF, 3-Second gust

©2019. Japan Geoscience Union. All Right Reserved.

Basic Data Construction for a Typhoon Disaster Prevention Model : Monthly Characteristics of Typhoon Rusa, Maemi, Kompasu, and Bolaven

Hana Na, Woo-Sik Jung

According to a typhoon report that summarized the typhoons that had affected the Korean Peninsula for approximately 100 years since the start of weather observation in the Korean Peninsula, the number of typhoons that affected the Korean Peninsula was the highest in August, followed by July, and September. A study that analyzed the period between 1953 and 2003 revealed that the number of typhoons that affected the Korean Peninsula was 62 in August, 49 in July, and 45 in September. As shown, previous studies that analyzed the typhoons that affected the Korean Peninsula by month were primarily focused on the impact frequency. This study aims to estimate the monthly impact frequency of the typhoons that affected the Korean Peninsula as well as the maximum wind speed that accompanied the typhoons. It also aims to construct the basic data of a typhoon disaster prevention model by estimating the maximum wind speed during typhoon period using Typhoon Rusa that resulted in the highest property damage, Typhoon Maemi that recorded the maximum wind speed, Typhoon Kompasu that significantly affected the Seoul metropolitan area, and Typhoon Bolaven that recently recorded severe damages. A typhoon disaster prevention model was used to estimate the maximum wind speed of the 3-second gust that may occur, and the 700 hPa wind speed estimated through WRF(Weather Research and Forecasting) numerical simulation was used as input data.

Unlike the target period reported in the white paper on typhoons (1904–2010), this study analyzed the monthly impact frequency of the typhoons that affected the Korean Peninsula from 2002 and 2015. The result indicated that the impact frequency was the highest in August, followed by July and September. This result was the same as that of the typhoon report. An analysis by year revealed that typhoon period increased in September. The 3-second gust was found to be the highest in September, followed by August and July. When this result was analyzed in relation to the recently increasing autumn typhoons (September and October), the 3-second gust result was the highest in September, indicating disaster prevention must be emphasized. By additionally analyzing the maximum wind speed distributions of Typhoon Rusa, Maemi, Kompasu, and Bolaven, the area with the maximum wind speed varied depending on the typhoon path, and the 3-second gust was higher than 44 m/s based on the typhoon intensity classification and accounted for approximately10%.

This research was supported by Basic Science Research Program through the National Research Foundation of Korea(NRF) funded by the Ministry of Education(2017R1D1A3B03036152)

Keywords : Typhoon Disaster Prevention Model, WRF, 3-Second gust, RUSA, MAEMI, KOMPASU, BOLAVEN

©2019. Japan Geoscience Union. All Right Reserved.

The mechanism of typhoon generated in the earth that rotates in the space where the solar wind blows

*Shinji Karasawa[1]

1. Miyagi National College of Technology Professor emeritus

The atmosphere in the upper tropical cyclone (TC) rotates the clock-wise direction by the trade winds and westerlies. The rotation speed near the center increases, because the angular momentum of the atmospheric molecule is transported. The eye of the typhoon is appeared at the place where the centrifugal force of the rotation on the flow exceeds compared with the difference of the pressure. The atmosphere including the vapor of water in the cumulonimbus are mixed with the cold air flow swirling in the clockwise direction at the eye of typhoon, where the water vapors become to the rain, and the cumulonimbus rotates in anticlockwise direction.
The solar wind includes rotational momentum and the rotational momentum of the solar wind generates the trade winds. On the other hand, the westerlies are caused by the solar wind that rotates the tail of Earth's magnetosphere on the opposite side of the Sun in anticlockwise rotation, and it gives the driving force of the westerlies. Ref. S. Karasawa.
https://www.youtube.com/watch?v=bzCup63G8z8&feature=youtu.be

Keywords: tropical cyclone, westerlies, trade winds, solar wind, Earth’ s rotation, Sun’ s rotation

©2019. Japan Geoscience Union. All Right Reserved.

[E] Poster | A (Atmospheric and Hydrospheric Sciences)：A-AS Atmospheric Sciences, Meteorology & Atmospheric Environment

Thu. May 30, 2019 5:15 PM - 6:30 PM JST | Thu. May 30, 2019 8:15 AM - 9:30 AM UTC | Poster Hall International Exhibition Hall8, Makuhari Messe_5

[A-AS02] Advances in Tropical Cyclone Research: Past, Present, and Future

convener:Sachie Kanada(Nagoya University), Akiyoshi Wada(Department of Typhoon and Severe Weather Research, Meteorological Research Institute), Kosuke Ito(University of the Ryukyus), Yoshiaki Miyamoto(Faculty of Environment and Information Studies, Keio University)

Tropical cyclones (TC) sometimes cause destructive disasters in many countries by torrential rainfall, strong wind, storm surge, and high surf. In 2008, the western Japan suffered a record-breaking heavy rainfall related to Typhoon Prapirooon (2018) in July. Furthermore, two Category 4 typhoons, typhoons Jebi (2018) and Trami (2018), made landfalls on the western Japan in September and caused devastating disasters over the Japanese Islands. In the Northern Atlantic, Hurricane Florence caused catastrophic damage in the eastern side of U.S. Recent studies reported a northward shift of the location where a TC achieved the peak intensity and also reported increases in the frequency of rapidly intensifying storms. Thus, understanding the TC processes related to translation, intensity change and precipitation in the changing climate, and to provide more accurate forecasts and long-term projections are essential for the earth and planetary science.
Advances in innovative observations such as meteorological aircraft, weather satellite, supercomputer systems such as the Earth Simulator and K-computer, and introduction of new methods such as the deep-learning, have led to novel development of numerical weather forecasting and understanding of the phenomena related to TCs in the past, present and future climates. In this session, we welcome papers on various aspects of TC studies. We hope that the session will provide a new direction for future TC researches.

[AAS02-P01] Numerical study on lightning frequency in a tropical cyclone

*Yousuke Sato[1,3], Yoshiaki Miyamoto[2,3], Tomita Hirofumi[3] (1.Department of Applied Energy, Nagoya University, 2.Faculty of Environment and Information Studies, Keio University, 3.RIKEN Center for Computational Science)

[AAS02-P02] **Sensitivity of Numerical Simulation of Typhoon Nepartak (2016) to Cloud Condensation Nuclei Concentration**

*Yu-De Wu[1], Jian-Liang Wang[1] (1.Dept. of Environmental Informational and Engineering, Chung Cheng Institute of Technology, National Defense University, Taiwan)

[AAS02-P03] Moisture Budget Analysis for Hurricane Precipitation on Texas

*Satoshi Iizuka[1], Naoki Sakai[1] (1.National Research Institute for Earth Science and Disaster Resilience)

[AAS02-P04] Remote response of a developing tropical cyclone over the western North Pacific to large-scale vapor transport from the Kuroshio in boreal fall

*Keita Fujiwara[1], Ryuichi Kawamura[2], Tetsuya Kawano[2] (1.Graduate School of Science, Kyushu University, 2.Faculty of Science, Kyushu University)

[AAS02-P05] Asymmetrically Intensifying Processes of a Category 4 Super Typhoon Lan (2017) during High Vertical Wind Shear

*Sachie Kanada[1], Akiyoshi Wada[2], Kazuhisa Tsuboki[1] (1.Nagoya University, 2.Meteorological Research Institute)

[AAS02-P06] Roles of preexisting oceanic condition and ocean coupling processes in the intensity prediction during the mature phase of Typhoon Trami (2018)

*Akiyoshi Wada[1] (1.Typhoon Research Department Meteorological Research Institute)

[AAS02-P07] Development and assessment of the probabilistic storm surge forecast system in Taiwan: Case Study of Typhoon Maria in 2018

*Chun-Wei Lin[1], Tso-Ren Wu[1], Yu-Lin Tsai[1], Shu-Chun Chuang[1], Chi-Hao Chu[2], Chuen-Teyr Terng[2] (1.Graduate Institute of Hydrological and Oceanic Sciences, National Central University, Chungli, Taiwan, 2.Marine Meteorology Center, Central Weather Bureau, Taipei, Taiwan)

[AAS02-P08] Basic Data Construction for a Typhoon Disaster Prevention Model : Analysis and Changes by El Nino and La Nina year

*HANA NA[1], Woo-Sik Jung[1] (1.Department of Atmospheric Environment Information Engineering, Atmospheric Environment Information Research Center, Inje University, Gimhae 50834, Korea)

[AAS02-P09] Basic Data Construction for a Typhoon Disaster Prevention Model : Analysis According to the Typhoon Path Type

*HANA NA[1], Woo-Sik JUNG[1] (1.Department of Atmospheric Environment Information Engineering, Atmospheric Environment Information Research Center, Inje University, Gimhae 50834, Korea)

[AAS02-P10] Basic Data Construction for a Typhoon Disaster Prevention Model : Monthly Characteristics of Typhoon Rusa, Maemi, Kompasu, and Bolaven

*HANA NA[1], Woo-Sik Jung[1] (1.Department of Atmospheric Environment Information Engineering, Atmospheric Environment Information Research Center, Inje University, Gimhae 50834, Korea)

[AAS02-P11] The mechanism of typhoon generated in the earth that rotates in the space where the solar wind blows

*Shinji Karasawa[1] (1.Miyagi National College of Technology Professor emeritus)

Numerical study on lightning frequency in a tropical cyclone

*Yousuke Sato[1,3], Yoshiaki Miyamoto[2,3], Tomita Hirofumi[3]

1. Department of Applied Energy, Nagoya University, 2. Faculty of Environment and Information Studies, Keio University, 3. RIKEN Center for Computational Science

This study investigates frequency of lightning in each stage of lifecycle of tropical cyclone (TC) using the next generation weather and climate library called Scalable Computing for Advanced Library and Environment (SCALE; Sato et al. 2015, Nishizawa et al. 2015). Lightning component was developed and implemented into SCALE in this study. An idealized experiment based on an experimental setup of Miyamoto and Takemi (2013) was conducted by SCALE coupled with lightning component. The results of the simulation indicate that the lightning frequency is maximum before rapid intensification (RI) of TC, which supports the report of Price et al. (2009) derived from satellite observation. The frequency of lightning decreases after RI and it keeps small until the TC reaches steady state. Our analyses elucidate that the dependency of the lightning frequency upon the developing stage of TC is originated from the type of convection dominating at each growth stage. Before the RI, the convection generated by consuming convective available potential energy (CAPE) transport hydrometeors upward, and the charge split and the lightning frequently occur. During the steady state, the hydrometeors are mainly transported by the fast rotating flow in the simulated TC, which resulted in the weak charge split and small frequency of lightning.

Keywords: Tropical cyclone, Lightning

©2019. Japan Geoscience Union. All Right Reserved.

Sensitivity of Numerical Simulation of Typhoon Nepartak (2016) to Cloud Condensation Nuclei Concentration

*Yu-De Wu[1], Jian-Liang Wang[1]

1. Dept. of Environmental Informational and Engineering, Chung Cheng Institute of Technology, National Defense University, Taiwan

The study is carried out using the WRF model and the Cloud Condensation Nuclei, CCN, in the WDM6 microphysics scheme has been modified to test its impacts on typhoon simulations. The simulated track, intensity, and rainfall distribution of Typhoon Nepartak (2016) over Pacific Ocean are compared among numerical experiments of different initial concentration of CCN (wdm6_ctr, wdm6_10, and wdm6_50, where wdm6_10 and wdm6_50 represent that CCN are respectively 10 and 50 times of the value used in wdm6_ctr).

The simulated tracks in three runs are similar, but the intensity and the maximum dBz increase both in wdm6_10 and wdm6_50, but it takes more time for wdm6_50 to intensify. The comparison of mixing ratios of five water species shows that the cloud droplets mixing ratios increase as CCN is increased. The mixing ratios of rain, cloud ice, snow and graupel are enhanced more rapidly in wdm6_10 compared with wdm6_50. The same situation happens in the divergence field and upward motions. It is suggested that the increase of CCN will result in stronger typhoon, but the intensification will be slowed down with too much CCN.

Keywords: Cloud Condensation Nuclei, Typhoon Nepartak, Microphysics Scheme

©2019. Japan Geoscience Union. All Right Reserved.

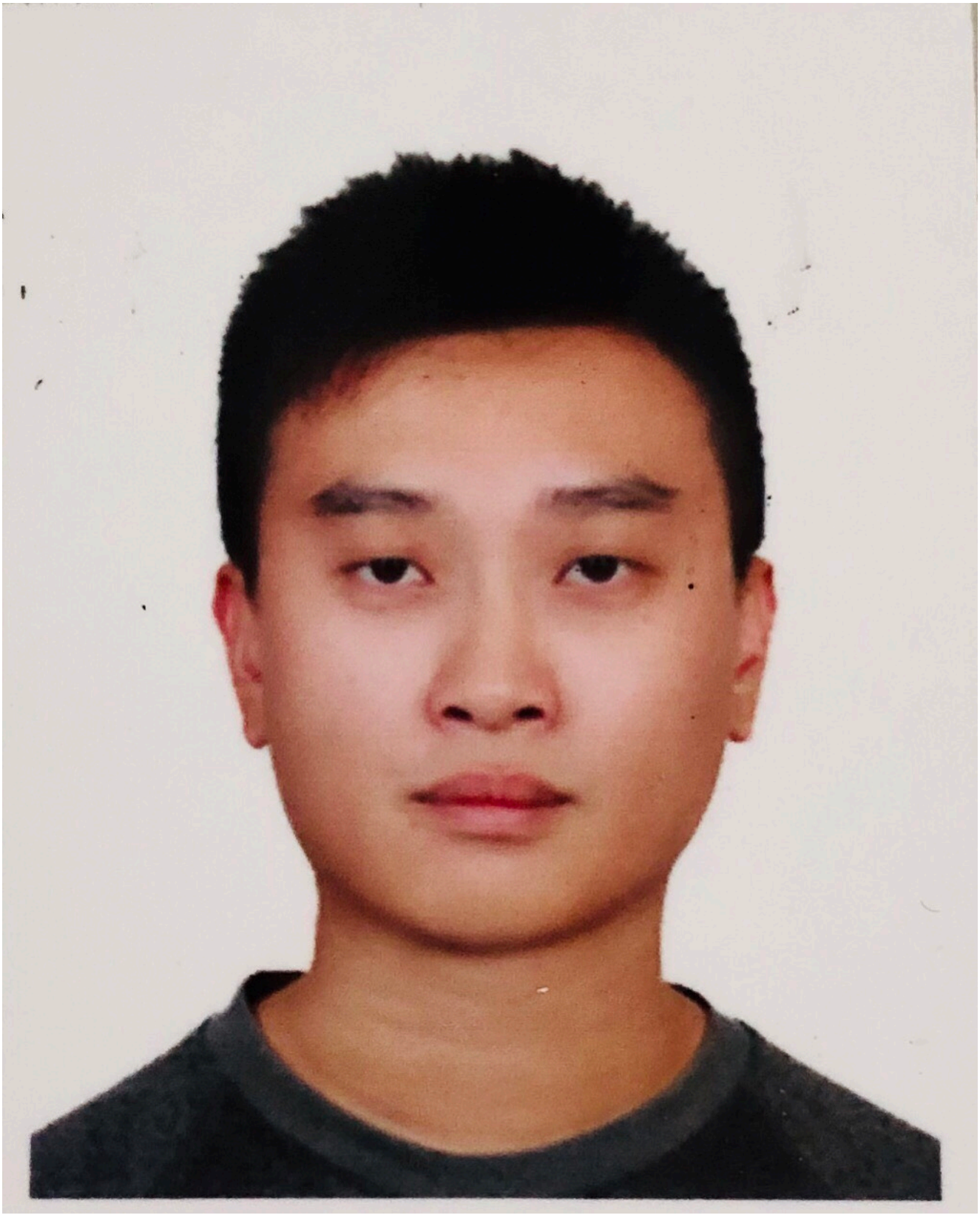

©2019. Japan Geoscience Union. All Right Reserved.

Moisture Budget Analysis for Hurricane Precipitation on Texas

*Satoshi Iizuka[1], Naoki Sakai[1]

1. National Research Institute for Earth Science and Disaster Resilience

In August 2017, Hurricane Harvey brought the unprecedented amount of rainfall and catastrophic flooding on the Houston metropolitan area, as it stagnated near the coast of Texas for several days after its decline to a tropical storm intensity. The present study compares the moisture budget for rainfall associated with Harvey with those of past hurricanes making landfall on Texas. It seems that the high pressure over the west coast region of the US, along with the meandering of the subtropical jet starting from the periphery of Hawaii and toward the south in Texas, stagnated Hurricane Harvey around the coast of Texas for several days. The meandering of the subtropical jet toward the south in Texas also caused the largest convergence of moisture advected from the Gulf of Mexico efficiently over Texas, although the accompanied high pressure was not extraordinary event. Therefore, it is suggested that surrounding meteorological conditions can greatly affect rainfall related to tropical cyclones.

Keywords: Hurricane Harvey, Precipitation, Moisture Budget

©2019. Japan Geoscience Union. All Right Reserved.

Remote response of a developing tropical cyclone over the western North Pacific to large-scale vapor transport from the Kuroshio in boreal fall

*Keita Fujiwara[1], Ryuichi Kawamura[2], Tetsuya Kawano[2]

1. Graduate School of Science, Kyushu University, 2. Faculty of Science, Kyushu University

A remote linkage between the development of tropical cyclone (TC) over the western North Pacific and moisture transport from the Kuroshio Current due to environmental flow toward TC was examined by using regional cloud resolving model and Lagrangian diagnostics. In this study, we specially highlighted a prototypical TC (Typhoon Chaba 2010), which developed and migrated northward over the Philippines Sea in boreal fall, and conducted sensitivity experiments that modified surface turbulent latent heat flux (LHF) over the Kuroshio. The large-scale environment was characterized by a combination of two synoptic systems, eastward-migrating anticyclone from the Asian continent and TC approaching Japan, bringing low-level northeasterly flows over the Kuroshio through an enhanced meridional pressure gradient in that region. Trajectory analyses suggested that air parcels along the northeasterlies modified by receiving abundant water vapor from the underlying Kuroshio may contribute to latent heating within Chaba’s inner core region as a remote effect, leading to TC development.

When LHF was removed or reduced over the Kuroshio under the dominance of the northwesterly flow, TC intensity attenuated during its developing stage even though TC was fairly far away from the Kuroshio. Since no or little modification of dry air parcels occurred in the atmospheric boundary layer over the Kuroshio, contribution of those parcels to latent heat release around Chaba’s eyewall become small. Furthermore, dry air penetration into TC’s inner core region may act as an inhibitor of convection within that region, resulting in deceleration of the TC development. These findings were consistent with another TC (Typhoon Toakge 2004) with a similar synoptic environment, increasing reliability of remote impact of moisture import from the Kuroshio on TC development.

Keywords: tropical cyclone, moisture transport, Kuroshio Current

©2019. Japan Geoscience Union. All Right Reserved.

Asymmetrically Intensifying Processes of a Category 4 Super Typhoon Lan (2017) during High Vertical Wind Shear

*Sachie Kanada[1], Akiyoshi Wada[2], Kazuhisa Tsuboki[1]

1. Nagoya University, 2. Meteorological Research Institute

On 21 October 2017, Typhoon Lan developed to a Category 4 super typhoon with the minimum central pressure (MCP) of 915 hPa at 25.6 degrees north latitude and maintained the peak intensity until the storm arrived at 29.9˚N under a strong environmental vertical wind shear (VWS) of 14 m s^{-1}. To understand the intensification processes of an intense typhoon with such high VWS, numerical simulations on Typhoon Lan were conducted using a high-resolution three-dimensional atmosphere regional model, the Cloud Resolving Storm Simulator (CReSS; Tsuboki and Sakakibara, 2002). Two sensitivity experiments, 1dO and FO, were conducted with different SST representations. In the 1dO experiment, a simple thermal diffusion model was used to express temperature changes due to ocean vertical mixing. The FO experiment with a time-fixed SST did not consider the evolution of SST. Both experiments used the same initial and boundary conditions and model specifications for the atmosphere, started at 0000 UTC 18 October 2017, and had an integration time of 5 days. The computational domain was 2˚N–37.8˚N and 115˚E–145˚E. The number of horizontal grids in the computational domain was 752×896 with the horizontal grid size of 0.04 longitude by 0.04 latitude.

The typhoon simulated in the 1dO experiment successfully achieved the MCP of 910 hPa at 29.5˚N, exhibiting strong asymmetric precipitation pattern as observed by the satellites. The intensification processes were accompanied by rapid developments of the strong winds and warm core in the low-levels. The strong northeast VWS forced to tilt the storm axis to downshear side (northeast) and, in the downshear quadrants, tall, intense and upstanding eyewall updrafts (CBs) formed from the low-level convergence of the storm travelling northeastward with a relatively fast translation speed of 10 m s^{-1}. Meanwhile, dry subsidence from the upper-levels intensified the low-level warm core in the upshear side of the eye. Despite the inner-core convection and precipitation exhibited strong asymmetric structures, the axisymmetricity of the storm circulation was maintained in the mid-to-low levels and abundant water vapor enclosed in the eye allowed to develop CBs around the radius of the maximum wind speeds. Although the FO storm overestimated the MCP of 879hPa, the similar asymmetric patterns in precipitation and convection were also found in the FO storm. The results indicated that the storm structures of typhoon Lan would be less sensitive to the SST-cooling effect.

Keywords: Typhoon, numerical model

©2019. Japan Geoscience Union. All Right Reserved.

Roles of preexisting oceanic condition and ocean coupling processes in the intensity prediction during the mature phase of Typhoon Trami (2018)

*Akiyoshi Wada[1]

1. Typhoon Research Department Meteorological Research Institute

Typhoon Trami (2018) is one of the typhoons that made landfall in Japan. According to the Regional Specialized Meteorological Center (RSMC) Tokyo best track analysis, the central pressure reached 915 hPa at 18 UTC on 24 September around 20˚N and then rapidly increased by 950 hPa in 18 hours. After the rapid increases in the central pressure, intensity forecasts announced further intensification to 935 hPa, but the typhoon could not intensify again. In order to clarify the impact of the cold eddies over the ocean on this forecast error, we conducted numerical simulations with different oceanic initial conditions (daily data from 19 to 25 September were used so that the number of ensemble members is seven) using a 2 km-mesh nonhydrostatic atmosphere model coupled with ocean surface wave and multilayer ocean models with the Japan Meteorological Agency (JMA) global objective analysis with horizontal resolution of 20 km and the JMA North Pacific Ocean analysis with horizontal resolution of 0.5˚. In addition, a sensitivity numerical experiment was conducted with the oceanic initial condition on 23 September merged with an artificial cold vortex centered at 21˚N, 129˚E of which both a mixed layer and thermocline was 50 m shallower than the control experiment. Moreover, a simulation with a 2 km-mesh nonhydrostatic atmosphere model was performed with the oceanic initial condition on 23 September. The initial time and integration period are 00 UTC on 23 September and 180 hours with the time interval of 3 seconds.

The results of simulated tracks were reasonable compared with the RSMC best track analysis, while the rapid decrease in the central pressure could not be simulated due to a large difference in central pressure at the initial time so that the simulated minimum central pressure was higher than the best track central pressure. From the analysis with the ratio of a difference to the standard deviation obtained from the ensemble experiments, the impact of different oceanic initial conditions on central pressure was different from that on the maximum wind speed particularly from 25 to 27 September when the typhoon passed near the cold eddy. The impact of ocean coupling on simulated central pressure and maximum wind speed was considerably greater than that of the artificial cold eddy and that of different oceanic initial conditions. The impact of the artificial cold eddy was a few times greater than that of different oceanic initial conditions around 26 September. The result indicates that more detailed observation and more accurate analysis regarding the cold eddy over the ocean will contribute to the improvement of typhoon intensity predictions.

Keywords: tropical cyclone, atmosphere-wave-ocean coupled model, intensity forecast, preexisting cold eddy

©2019. Japan Geoscience Union. All Right Reserved.

Development and assessment of the probabilistic storm surge forecast system in Taiwan: Case Study of Typhoon Maria in 2018

*Chun-Wei Lin[1], Tso-Ren Wu[1], Yu-Lin Tsai[1], Shu-Chun Chuang[1], Chi-Hao Chu[2], Chuen-Teyr Terng[2]

1. Graduate Institute of Hydrological and Oceanic Sciences, National Central University, Chungli, Taiwan, 2. Marine Meteorology Center, Central Weather Bureau, Taipei, Taiwan

From the forecast and the analyzed typhoon tracks in Taiwan, it is found that if the forecast track errors are greater than 100 km, roughly a quarter of the length of Taiwan, significant variability of storm surge elevation can be seen.
In order to consider the uncertainty of the atmospheric forecast, this study aims to develop the probabilistic storm surge forecast system. The coastal storm surge model applied in this study is COMCOT-SS (COrnell Multi-Grid COupled Tsunami Model –Storm Surge), which is the kernel of the operating deterministic storm surge forecast system in CWB, Taiwan. It solves nonlinear shallow water equations in the nested-grid scheme. Two ensemble methods are adopted in this study, one is Deterministic Track Error Distribution Method, D-TED Method. The other one is the Ensemble Track Analysis Method, ETA Method. D-TED Method is generated from the deterministic forecast, while the ETA Method obtains typhoon tracks and parameters from the CWB WEPS (CWB WRF Ensemble Prediction System).
From the case study of typhoon Maria in 2018, it shows that as the typhoon approaching Taiwan, the coverage of the tracks from ETA Method would be more convergence comparing to the tracks from D-TED Method, and it provides a more concentrated surge elevation distribution.

Keywords: storm surge, ensemble forecast, COMCOT-SS

©2019. Japan Geoscience Union. All Right Reserved.

Basic Data Construction for a Typhoon Disaster Prevention Model : Analysis and Changes by El Nino and La Nina year

*HANA NA[1], Woo-Sik Jung[1]

1. Department of Atmospheric Environment Information Engineering, Atmospheric Environment Information Research Center, Inje University, Gimhae 50834, Korea

Among the typhoons that affected the Korean Peninsula for approximately 110 years from 1904, when weather observation began until 2018, all of the top five typhoons in terms of the maximum wind speed and property damage record occurred after 2000. This implies that the intensity of typhoons is becoming stronger and the damage is more severe compared to the past. Moreover, typhoons are significantly affected by the sea temperature. The El Nino and La Nina phenomena, in which significant changes in the sea temperature occur, may significantly affect the occurrence and intensity of typhoons affecting the Korean Peninsula. Therefore, this study aims to analyze changes by year, and the years of El Nino and La Nina occurrences by estimating the maximum wind speed that can be generated during typhoon period based on the typhoons that affected the Korean Peninsula. This study was conducted for the period between 2002 and 2015. As a result of analyzing the maximum wind speed of the typhoons that affected the Korean Peninsula by year, high 3-second gusts tended to occur in the Gyeongsang-do area including the southeast coast of the Korean Peninsula from 2002 to 2006. Subsequently, the strong wind area of the 3-second gusts expanded, and high 3-second gusts occurred in the Seoul metropolitan area. Moreover, as a result of investigating the 3-second gust characteristics for the years of El Nino and La Nina occurrences, a higher maximum wind speed was observed from the typhoons that affected the Korean Peninsula in the years of El Nino occurrence.

This research was supported by Basic Science Research Program through the National Research Foundation of Korea(NRF) funded by the Ministry of Education(2017R1D1A3B03036152)

Keywords: Typhoon Disaster Prevention Model, 3-Second gust, El Nino, La Nina

©2019. Japan Geoscience Union. All Right Reserved.

Basic Data Construction for a Typhoon Disaster Prevention Model : Analysis and Changes by El Nino and La Nina year

Hana Na, Woo-Sik Jung

Among the typhoons that affected the Korean Peninsula for approximately 110 years from 1904, when weather observation began until 2018, all of the top five typhoons in terms of the maximum wind speed and property damage record occurred after 2000. This implies that the intensity of typhoons is becoming stronger and the damage is more severe compared to the past. Moreover, typhoons are significantly affected by the sea temperature. The El Nino and La Nina phenomena, in which significant changes in the sea temperature occur, may significantly affect the occurrence and intensity of typhoons affecting the Korean Peninsula. Therefore, this study aims to analyze changes by year, and the years of El Nino and La Nina occurrences by estimating the maximum wind speed that can be generated during typhoon period based on the typhoons that affected the Korean Peninsula. This study was conducted for the period between 2002 and 2015. As a result of analyzing the maximum wind speed of the typhoons that affected the Korean Peninsula by year, high 3-second gusts tended to occur in the Gyeongsang-do area including the southeast coast of the Korean Peninsula from 2002 to 2006. Subsequently, the strong wind area of the 3-second gusts expanded, and high 3-second gusts occurred in the Seoul metropolitan area. Moreover, as a result of investigating the 3-second gust characteristics for the years of El Nino and La Nina occurrences, a higher maximum wind speed was observed from the typhoons that affected the Korean Peninsula in the years of El Nino occurrence.

This research was supported by Basic Science Research Program through the National Research Foundation of Korea(NRF) funded by the Ministry of Education(2017R1D1A3B03036152)

Key words : Typhoon Disaster Prevention Model, WRF, 3-Second gust, El Nino, La Nina

©2019. Japan Geoscience Union. All Right Reserved.

Basic Data Construction for a Typhoon Disaster Prevention Model : Analysis According to the Typhoon Path Type

*HANA NA[1], Woo-Sik JUNG[1]

1. Department of Atmospheric Environment Information Engineering, Atmospheric Environment Information Research Center, Inje University, Gimhae 50834, Korea

In this study, a typhoon disaster prevention model was used to estimate the maximum wind speed during typhoon period by path type from all typhoons that affected the Korean Peninsula from 2002 to 2015. For the typhoon information and upper wind information used as input data, the results of the WRF numerical model, which utilized the Best Track data of the RSMC Tokyo Typhoon Center and the RDAPS data of the Korea Meteorological Administration, were applied. From analyzing the path type impact frequency using all typhoons that affected the Korean Peninsula during the study period (2002–2015), Type 7 that affected the Korean Peninsula through Japan was the most frequent, followed by Type 2 that directly landed on the Korean Peninsula through the southern coast. From analyzing the monthly path types of the typhoons that affected the Korean Peninsula, Type 2 that affected the Korean Peninsula by landing on the southern coast and Type 7 that affected the Korean Peninsula through Japan were the most frequent for the recently increasing September typhoons. The analysis of the maximum wind speed of the 3-second gust that may occur during typhoon period by path type revealed that Type 2 that affected the Korean Peninsula by landing on the southern coast exhibited the highest 3-second gust. As a result of examining the distribution of Type 2, high 3-second gusts occurred throughout the Korean Peninsula, including the southeast coast. As for the path of Type 2 that directly affected the Korean Peninsula by landing on the southern coast, the occurrence frequency was the second highest during the entire study period and the value of the 3-second gust, which was the maximum wind speed that may occur during typhoon period, was the highest.

This research was supported by Basic Science Research Program through the National Research Foundation of Korea(NRF) funded by the Ministry of Education(2017R1D1A3B03036152)

Keywords: Typhoon Path, 3-Second gust, Typhoon Disaster Prevention Model

©2019. Japan Geoscience Union. All Right Reserved.

Basic Data Construction for a Typhoon Disaster Prevention Model : Analysis According to the Typhoon Path Type

Hana Na, Woo-Sik Jung

In this study, a typhoon disaster prevention model was used to estimate the maximum wind speed during typhoon period by path type from all typhoons that affected the Korean Peninsula from 2002 to 2015. For the typhoon information and upper wind information used as input data, the results of the WRF numerical model, which utilized the Best Track data of the RSMC Tokyo Typhoon Center and the RDAPS data of the Korea Meteorological Administration, were applied. From analyzing the path type impact frequency using all typhoons that affected the Korean Peninsula during the study period (2002–2015), Type 7 that affected the Korean Peninsula through Japan was the most frequent, followed by Type 2 that directly landed on the Korean Peninsula through the southern coast. From analyzing the monthly path types of the typhoons that affected the Korean Peninsula, Type 2 that affected the Korean Peninsula by landing on the southern coast and Type 7 that affected the Korean Peninsula through Japan were the most frequent for the recently increasing September typhoons. The analysis of the maximum wind speed of the 3-second gust that may occur during typhoon period by path type revealed that Type 2 that affected the Korean Peninsula by landing on the southern coast exhibited the highest 3-second gust. As a result of examining the distribution of Type 2, high 3-second gusts occurred throughout the Korean Peninsula, including the southeast coast. As for the path of Type 2 that directly affected the Korean Peninsula by landing on the southern coast, the occurrence frequency was the second highest during the entire study period and the value of the 3-second gust, which was the maximum wind speed that may occur during typhoon period, was the highest.

This research was supported by Basic Science Research Program through the National Research Foundation of Korea(NRF) funded by the Ministry of Education(2017R1D1A3B03036152)

Keywords : Typhoon Disaster Prevention Model, WRF, Typhoon Track, 3-Second gust

©2019. Japan Geoscience Union. All Right Reserved.

Basic Data Construction for a Typhoon Disaster Prevention Model : Monthly Characteristics of Typhoon Rusa, Maemi, Kompasu, and Bolaven

*HANA NA[1], Woo-Sik Jung[1]

1. Department of Atmospheric Environment Information Engineering, Atmospheric Environment Information Research Center, Inje University, Gimhae 50834, Korea

According to a typhoon report that summarized the typhoons that had affected the Korean Peninsula for approximately 100 years since the start of weather observation in the Korean Peninsula, the number of typhoons that affected the Korean Peninsula was the highest in August, followed by July, and September. A study that analyzed the period between 1953 and 2003 revealed that the number of typhoons that affected the Korean Peninsula was 62 in August, 49 in July, and 45 in September. As shown, previous studies that analyzed the typhoons that affected the Korean Peninsula by month were primarily focused on the impact frequency. This study aims to estimate the monthly impact frequency of the typhoons that affected the Korean Peninsula as well as the maximum wind speed that accompanied the typhoons. It also aims to construct the basic data of a typhoon disaster prevention model by estimating the maximum wind speed during typhoon period using Typhoon Rusa that resulted in the highest property damage, Typhoon Maemi that recorded the maximum wind speed, Typhoon Kompasu that significantly affected the Seoul metropolitan area, and Typhoon Bolaven that recently recorded severe damages. A typhoon disaster prevention model was used to estimate the maximum wind speed of the 3-second gust that may occur, and the 700 hPa wind speed estimated through WRF(Weather Research and Forecasting) numerical simulation was used as input data.

Unlike the target period reported in the white paper on typhoons (1904–2010), this study analyzed the monthly impact frequency of the typhoons that affected the Korean Peninsula from 2002 and 2015. The result indicated that the impact frequency was the highest in August, followed by July and September. This result was the same as that of the typhoon report. An analysis by year revealed that typhoon period increased in September. The 3-second gust was found to be the highest in September, followed by August and July. When this result was analyzed in relation to the recently increasing autumn typhoons (September and October), the 3-second gust result was the highest in September, indicating disaster prevention must be emphasized. By additionally analyzing the maximum wind speed distributions of Typhoon Rusa, Maemi, Kompasu, and Bolaven, the area with the maximum wind speed varied depending on the typhoon path, and the 3-second gust was higher than 44 m/s based on the typhoon intensity classification and accounted for approximately10%.

This research was supported by Basic Science Research Program through the National Research Foundation of Korea(NRF) funded by the Ministry of Education(2017R1D1A3B03036152)

Keywords: Typhoon Disaster Prevention Model, WRF, 3-Second gust

©2019. Japan Geoscience Union. All Right Reserved.

Basic Data Construction for a Typhoon Disaster Prevention Model : Monthly Characteristics of Typhoon Rusa, Maemi, Kompasu, and Bolaven

Hana Na, Woo-Sik Jung

According to a typhoon report that summarized the typhoons that had affected the Korean Peninsula for approximately 100 years since the start of weather observation in the Korean Peninsula, the number of typhoons that affected the Korean Peninsula was the highest in August, followed by July, and September. A study that analyzed the period between 1953 and 2003 revealed that the number of typhoons that affected the Korean Peninsula was 62 in August, 49 in July, and 45 in September. As shown, previous studies that analyzed the typhoons that affected the Korean Peninsula by month were primarily focused on the impact frequency. This study aims to estimate the monthly impact frequency of the typhoons that affected the Korean Peninsula as well as the maximum wind speed that accompanied the typhoons. It also aims to construct the basic data of a typhoon disaster prevention model by estimating the maximum wind speed during typhoon period using Typhoon Rusa that resulted in the highest property damage, Typhoon Maemi that recorded the maximum wind speed, Typhoon Kompasu that significantly affected the Seoul metropolitan area, and Typhoon Bolaven that recently recorded severe damages. A typhoon disaster prevention model was used to estimate the maximum wind speed of the 3-second gust that may occur, and the 700 hPa wind speed estimated through WRF(Weather Research and Forecasting) numerical simulation was used as input data.

Unlike the target period reported in the white paper on typhoons (1904–2010), this study analyzed the monthly impact frequency of the typhoons that affected the Korean Peninsula from 2002 and 2015. The result indicated that the impact frequency was the highest in August, followed by July and September. This result was the same as that of the typhoon report. An analysis by year revealed that typhoon period increased in September. The 3-second gust was found to be the highest in September, followed by August and July. When this result was analyzed in relation to the recently increasing autumn typhoons (September and October), the 3-second gust result was the highest in September, indicating disaster prevention must be emphasized. By additionally analyzing the maximum wind speed distributions of Typhoon Rusa, Maemi, Kompasu, and Bolaven, the area with the maximum wind speed varied depending on the typhoon path, and the 3-second gust was higher than 44 m/s based on the typhoon intensity classification and accounted for approximately10%.

This research was supported by Basic Science Research Program through the National Research Foundation of Korea(NRF) funded by the Ministry of Education(2017R1D1A3B03036152)

Keywords : Typhoon Disaster Prevention Model, WRF, 3-Second gust, RUSA, MAEMI, KOMPASU, BOLAVEN

©2019. Japan Geoscience Union. All Right Reserved.

The mechanism of typhoon generated in the earth that rotates in the space where the solar wind blows

*Shinji Karasawa[1]

1. Miyagi National College of Technology Professor emeritus

The atmosphere in the upper tropical cyclone (TC) rotates the clock-wise direction by the trade winds and westerlies. The rotation speed near the center increases, because the angular momentum of the atmospheric molecule is transported. The eye of the typhoon is appeared at the place where the centrifugal force of the rotation on the flow exceeds compared with the difference of the pressure. The atmosphere including the vapor of water in the cumulonimbus are mixed with the cold air flow swirling in the clockwise direction at the eye of typhoon, where the water vapors become to the rain, and the cumulonimbus rotates in anticlockwise direction.
The solar wind includes rotational momentum and the rotational momentum of the solar wind generates the trade winds. On the other hand, the westerlies are caused by the solar wind that rotates the tail of Earth's magnetosphere on the opposite side of the Sun in anticlockwise rotation, and it gives the driving force of the westerlies. Ref. S. Karasawa.
https://www.youtube.com/watch?v=bzCup63G8z8&feature=youtu.be

Keywords: tropical cyclone, westerlies, trade winds, solar wind, Earth’ s rotation, Sun’ s rotation

©2019. Japan Geoscience Union. All Right Reserved.

[E] Poster | A (Atmospheric and Hydrospheric Sciences)：A-OS Ocean Sciences & Ocean Environment

Thu. May 30, 2019 10:45 AM - 12:15 PM JST | Thu. May 30, 2019 1:45 AM - 3:15 AM UTC | Poster Hall International Exhibition Hall8, Makuhari Messe_2

[A-OS07] Climate variability and predictability on subseasonal to decadal timescales

convener:Takashi Mochizuki(Japan Agency for Marine-Earth Science and Technology), V Ramaswamy(NOAA GFDL), Doug Smith(Met Office), Yushi Morioka(Japan Agency for Marine-Earth Science and Technology)

Climate variability poses growing threats to human lives and socio-economic activities through changes in frequency and intensity of abnormal weather such as cold/heat waves and floods/droughts. This involves several climate phenomena with a wide range of timescales from subseasonal to decadal variations (e.g. MJO, IOD, ENSO, PDV, AMV). Many efforts have been made for understanding and predicting climate variations on each timescale, but there remain large uncertainties in simulation and prediction of subseasonal to decadal climate variations. This highlights lack of understanding of weather and climate interaction across different spatial and temporal timescales (e.g. tropical cyclones and ENSO) as well as multiple physical processes underlying climate variations (e.g. troposphere-stratosphere coupling, air-sea-ice interaction). This session aims to share current knowledge of subseasonal to decadal climate variability and predictability in order to identify the unresolved issues for better understanding and accurate prediction. This session invites all the abstracts related to the observational, theoretical, process-level and modelling research on subseasonal to decadal climate variability and predictability.

[AOS07-P01] Changes in North American and European Heatwave Characteristics

*Szandra A. Peter[1], Ben Kirtman[1] (1.Rosenstiel School of Marine and Atmospheric Science)

[AOS07-P02] **The effects of the "New Climate" Warming on Western Mediterranean: Situation of the Recent Extreme Events**

*Mohammed-Said KARROUK[1] (1.Hassan II University of Casablanca)

[AOS07-P03] **Month-to-month Difference of the Western Pacific Subtropical High Simulated by CMIP5 Models**

*Xiao Dong[1], Renping Lin[1] (1.Institute of Atmospheric Physics)

[AOS07-P04] Potential regulation on the climatic effect of Tibetan Plateau heating by tropical air–sea coupling

*Ziqian Wang[1], Anmin Duan[2], Song Yang[1] (1.School of Atmospheric Sciences, Sun Yat-sen University, 2.Institute of Atmospheric Physics, Chinese Academy of Sciences)

[AOS07-P05] Intraseasonal variation of the South Asian high and its role in connecting the Indian and East Asian summer monsoons

*Wei Wei[1] (1.Sun Yat-sen University)

[AOS07-P06] Mean Surface Air Temperatures in Japan - Regional Classification and Interranual Variability

*Pascal Oettli[1], Masami Nonaka[1], Swadhin Behera[1] (1.Japan Agency for Marine-Earth Science and Technology)

[AOS07-P07] Inter-Annual Variability of the Indonesian Rainfall and Air-Sea Interaction over the Indian-Pacific Ocean Associated with Regime Shift

*Murni Ngestu Nurutami[1], Tadahiro Hayasaka[1] (1.Center for Atmospheric and Oceanic Studies, Graduate School of Science, Tohoku University)

[AOS07-P08] Exploring synoptic-scale drivers of interannual rainfall variability over Africa

*Piotr Wolski[1], Chris Jack[1], Waarith Abrahams[1], Stefaan Conradie[1] (1.University of Cape Town)

[AOS07-P09] **Effect of El Niño on the response ratio of Hadley circulation to different SST meridional structures**

*Juan Feng[1] (1.Beijing Normal University)

[AOS07-P10] **Novel data-driven approach for ENSO prediction**

*Dmitri Kondrashov[1], Evgeniy Loskutov[2], Andrei Gavrilov[2], Dmitry Mukhin[2], Alexander Feigin[2] (1.University of California, Los Angeles, United States, 2.Institute of Applied Physics of the Russian Academy of Sciences, Nizhny Novgorod, Russian Federation)

[AOS07-P11] Experimental seasonal climate prediction using CFES: Comparison with the SINTEX-F systems

*Nobumasa Komori[1], Bunmei Taguchi[2], Akira Kuwano-Yoshida[3,1], Takeshi Doi[1], Masami Nonaka[1] (1.Japan Agency for Marine-Earth Science and Technology, 2.Research Center for Advanced Science and Technology, The University of Tokyo, 3.Disaster Prevention Research Institute, Kyoto University)

[AOS07-P12] Exploring the SST error growth during ENSO developing phase by using BCC_CSM1.1(m)

*Ben Tian[1], Hongli Ren[1] (1.National Climate Center, China Meteorological Administration)

[AOS07-P13] Role of sea-ice initialization in climate predictability over the Weddell Sea

*Yushi Morioka[1], Takeshi Doi[1], Doroteaciro Iovino[2], Simona Masina[2], Swadhin Behera[1] (1.Japan Agency for Marine-Earth Science and Technology (JAMSTEC), 2.Centro Euro-Mediterraneo sui Cambiamenti Climatici (CMCC))

[AOS07-P14] Observed and hindcasted subdecadal variability of the tropical Pacific climate

*Takashi Mochizuki[1], Masahiro Watanabe[2] (1.Japan Agency for Marine-Earth Science and Technology, 2.Atmosphere-Ocean Research Institute, The University of Tokyo)

Changes in North American and European Heatwave Characteristics

*Szandra A. Peter[1], Ben Kirtman[1]

1. Rosenstiel School of Marine and Atmospheric Science

Heat waves are a serious threat to ecosystems, society and the economies of the world. By calculating specific threshold values from daily maximum 2 m temperatures of the NCEP/NCAR reanalysis data (Kalnay et al. 1996), the frequency of heat waves during summer months (JJA) in Europe and the US is determined for the period of 1982 to 2017. The differences between the first and the second half of the 36-year period are discussed, and the results are compared to the North American Multi-Model Ensemble (NMME) forecast with specific focus on recent heat waves in the Pacific Northwest of North America and Central Europe. The connection between heat waves and known climate variability (i.e., the NAO, PNA) is analyzed. We strive to assess the importance of natural variability, such as the NAO, in the frequency of heat waves by comparing the first and last half of the studied 36-year period. We also examine how well the NMME retrospective and real-time forecasts capture heat waves (and cold spells), and the sources of predictability (i.e., sea surface temperature anomalies, land surface conditions), and how the predictability connects to the various modes of climate variability.

©2019. Japan Geoscience Union. All Right Reserved.

The effects of the "New Climate" Warming on Western Mediterranean: Situation of the Recent Extreme Events

*Mohammed-Said KARROUK[1]

1. Hassan II University of Casablanca

Since the nineties of the last century, climatological research following a great scientific advance in the field of prediction, not the variability and evolution of the different climatic parameters was beginning to be clearer!

But today, since the beginning of 2005, certainly due to oceanic thermal cumulations, and the shift of climatic zones towards poles in selective forms (more intense on the oceans present on the continents); Climatic events do not evolve according to the usual and expected rhythms: atmospheric circulation, precipitation, temperatures, seasonal phenomena, etc. These conditions are a spatiotemporal evolution and distribution, which characterize the new "global climate", by the new atmospheric regime imposing the Meridian Atmospheric Circulation (MAC), alternating the conditions of Freshness (humidity) and Heat (drought) along the year.

In this new situation, Western Mediterranean, located in the climate transition zone, is fully affected by the "New Climate". Usually, the atmospheric response to major climatic events (ENSO) in this region such as "El Niño" was characterized by the establishment of the NAO positive index, stability and drought, due to dominance Zonal Atmospheric Circulation in winter. On the other hand, in the "La Niña" episode, the negative index of the NAO and the predominant Meridian Atmospheric Circulation and precipitation became abundant.

Since the beginning of this century, qualified meteorological events of "exceptional !" causing floods have continued to occur in Western Mediterranean, with increasing recurrence, prompting us to wonder about the "new" mode of hydro-thermal function of the climate system that induces torrential rains, as well as its effect on environments and societies.

Thanks to spatial observation and monitoring of meteorological conditions over the last 15 years, these types of alternating Heat / Cold conditions have become predictable, enabling decision-makers today to prepare adequately for the management of related risks to the "New Climate" warmed.

Keywords: "New Climate" Warmed, New Atmospheric Circulation, Meridian Atmospheric Circulation (MAC) , Western Mediterranean, Heat / Cold, Drought / Flood

©2019. Japan Geoscience Union. All Right Reserved.

Month-to-month Difference of the Western Pacific Subtropical High Simulated by CMIP5 Models

*Xiao Dong[1], Renping Lin[1]

1. Institute of Atmospheric Physics

The western Pacific subtropical high (WPSH) is an important circulation system of the East Asian summer monsoon (EASM). Most previous studies have focused on the variability of summer mean WPSH. Note that the WPSH also experiences subseasonal variation from early to late summer. In this study we examined the month-to-month shift of the WPSH in boreal summer, that is, from June to July and from July to August, simulated by CMIP5 Atmospheric General Circulation Models (AGCMs) and coupled models. Results show that climatologically AGCMs can reproduce the northward shift of the WPSH better than eastward retreat from July to August. Compared with AGCMs, coupled models can improve the month-to-month shift simulation to some extent, indicating that the air-sea coupling processes are also important in subseasonal timescale.

Keywords: western Pacific subtropical high, CMIP5 simulation, month to month variation

©2019. Japan Geoscience Union. All Right Reserved.

Potential regulation on the climatic effect of Tibetan Plateau heating by tropical air–sea coupling

*Ziqian Wang[1], Anmin Duan[2], Song Yang[1]

1. School of Atmospheric Sciences, Sun Yat-sen University, 2. Institute of Atmospheric Physics, Chinese Academy of Sciences

Based on the conventional weather research and forecasting (WRF) model and the air–sea coupled mode WRF-OMLM, we investigate the potential regulation on the climatic effect of Tibetan Plateau (TP) heating by the air–sea coupling over the tropical Indian Ocean and western Pacific. Results indicate that the TP heating significantly enhances the southwesterly monsoon circulation over the northern Indian Ocean and the South Asia subcontinent. The intensified southwesterly wind cools the sea surface mainly through the wind-evaporation-SST (sea surface temperature) feedback. Cold SST anomaly then weakens monsoon convective activity, especially that over the Bay of Bengal, and less water vapor is thus transported into the TP along its southern slope from the tropical oceans. As a result, summer precipitation decreases over the TP, which further weakens the TP local heat source. Finally, the changed TP heating continues to influence the summer monsoon precipitation and atmospheric circulation. To a certain extent, the air–sea coupling over the adjacent oceans may weaken the effect of TP heating on the mean climate in summer. It is also implied that considerations of air–sea interaction are necessary in future simulation studies of the TP heating effect.

Keywords: Air–sea coupling, Tibetan Plateau, Thermal forcing, Regional model

©2019. Japan Geoscience Union. All Right Reserved.

Intraseasonal variation of the South Asian high and its role in connecting the Indian and East Asian summer monsoons

*Wei Wei[1]

1. Sun Yat-sen University

The South Asian high (SAH) is the most intense and persistent upper-level circulation system in the Asian monsoon region during boreal summer. It plays a crucial role in the onset and variation of the Asian summer monsoon. Ample evidence shows that the monsoon onset and activities are closely related to the intraseasonal oscillation (ISO). Previous studies have found that the ISO in the East Asian summer monsoon (EASM) is impacted by the northward or northwestward propagation of the ISO in the South China Sea and the western North Pacific, and the northeastward propagation of the ISO in the tropical Indian Ocean. However, seldom research mentioned the effect of the ISO in the SAH. Our previous studies have shown that the SAH plays an important role in connecting the Indian summer monsoon (ISM) and the EASM on the interannual time scale. However, the effect of the SAH on the connection of the ISM and the EASM on the intraseasonal time scale is still not clear. Actually, the ISO in the SAH is significant in its zonal variation. In this study, we firstly figured out the intraseasonal variation feature of the SAH. And then, we explored the upper-level signal which will lead to the onset, advance and retreat of the EASM. Considering significant ISO in the ISM, we investigated the ISO feature in the ISM and its effect on the ISO in the SAH. Finally, we addressed a new physical process that the ISO in the ISM will impact the ISO in the SAH, and further influence the advance and retreat of the EASM on the intraseasonal time scale. We try to learn about the intraseasonal variation of the EASM in a new view, and propose a new way to improve the short-term climate prediction and the extended-range weather forecast.

©2019. Japan Geoscience Union. All Right Reserved.

Mean Surface Air Temperatures in Japan - Regional Classification and Interranual Variability

*Pascal Oettli[1], Masami Nonaka[1], Swadhin Behera[1]

1. Japan Agency for Marine-Earth Science and Technology

Back to the year 1886, several divisions of the climate of Japan into homogeneous climatic regions have been proposed, following different approaches of the question. This includes the Köppen climate classification (Fukui in 1933; Sekiguchi in 1949), the new Thornthwaite climate classification (Isozaki in 1933; Fukui in 1957) or the similarities of weather conditions. The latter is performed either throughout the year (Nakagawa in 1899; Sekiguchi in 1959; Yoshino in 1980) or during specific seasons (Iwakiri in 1967; Murata and Yoshino in 1988), sometimes with the help of statistical techniques, such as principal component analysis and the cluster analysis (Mikami in 1975; Koizumi and Kato in 2012.)

Using a type of artificial neural network called Self-Organizing Map, or SOM, we propose another division of the climate of Japan, solely based on the mean areal surface air temperature anomalies. SOM has been successfully employed in climate studies for more than a decade and has showed its ability to extract simple features from high-dimensional data. Here, SOM is applied to group 762 AMeDAS stations, taken throughout Japan for the last 30 years, into homogeneous clusters (=regions). Clustering is performed seasonally, with a focus on boreal winter (December to February) and boreal summer (June to August). As a result, eight regions are defined and associated time series of temperature anomalies (=indices) are computed.

Subsequently, possible source(s) of the interannual variability of mean surface air temperature anomalies are explored, for a better understanding of the regional differences. For this, correlation coefficients between indices previously defined and different climatic variable anomaly fields (sea-surface temperatures, outgoing longwave radiation, geopotential height...) are calculated. Hopefully, this work would also lead to a better seasonal forecast, taking into account the specificity of each region in regard to their link to the large-scale variability.

Keywords: Japan, Air temperature, Classification, Interannual variability

©2019. Japan Geoscience Union. All Right Reserved.

Inter-Annual Variability of the Indonesian Rainfall and Air-Sea Interaction over the Indian-Pacific Ocean Associated with Regime Shift

*Murni Ngestu Nurutami[1], Tadahiro Hayasaka[1]

1. Center for Atmospheric and Oceanic Studies, Graduate School of Science, Tohoku University

The inter-annual and inter-decadal variability of the Indonesian rainfall are investigated in association with the interannual climate modes over Indian-Pacific Oceans and the inter-decadal modulation on inter-annual climate variability impact. Rainfall data of the Climate Research Unit (CRU) from 1901 to 2016 and the Global Precipitation Climatology Project (GPCP) from 1979 to 2016 for June –November (JJASON) are used. The empirical orthogonal function (EOF) is used to identify the dominant spatial and temporal variability patterns of rainfall and the standard and partial correlation techniques are used to compare and to quantify the linear relationship between two or more time-series datasets. Based on the first principle component (PC1) of both CRU and GPCP data, the results show that canonical El Niño Southern-Oscillation (canonical ENSO), ENSO Modoki, and Indian Ocean Dipole (IOD) are the major climate modes influencing the inter-annual variability of the Indonesian rainfall, and the Inter-decadal Pacific Oscillation (IPO) is the major decadal phenomenon which affects the decadal variability of Indonesian rainfall. All of the inter-annual climate modes and IPO have negative correlation with the Indonesian rainfall, but the spatial distributions of Indonesian rainfall change associated with each phenomenon are different. During 1970 to 2016, three phases of IPO have been identified which are strongly related to Indonesian rainfall with the correlation coefficient of -0.75. The three phases are a negative phase in 1970-1978, a positive phase in 1979-1997, and another negative phase in 1998-2015. Mostly, these climate modes occur simultaneously, and the impacts of them on rainfall are combined. The driest condition of rainfall occurs when El Niño coincides with positive IOD during positive IPO, and the wettest condition occurs when La Niña –La Niña Modoki coincides with negative IOD during negative IPO over the whole region of Indonesia. The IPO plays a role in modulating the impact of these inter-annual climate modes on their frequencies and magnitudes to Indonesian rainfall from 1970s until present. The responses of the Indonesian rainfall to each inter-annual climate mode modulated by IPO are different as based on their time series correlation coefficient. The negative correlation between canonical ENSO and Indonesian rainfall weakens during negative IPO from early 2000s and intensifies during positive IPO. On the other hand, the negative correlation between ENSO Modoki and Indonesian rainfall and between IOD and Indonesian rainfall increases during negative phase of IPO from late 1990s, and the negative correlation between ENSO Modoki and Indonesian rainfall weakens during positive IPO. Recently, the frequency of ENSO Modoki and IOD and their impacts on Indonesian rainfall increase.

Keywords: Indonesian rainfall variability, El Niño Southern-Oscillation (ENSO), ENSO Modoki, Interannual Variability, Decadal Variability, Interdecadal Pacific Oscillation

©2019. Japan Geoscience Union. All Right Reserved.

Exploring synoptic-scale drivers of interannual rainfall variability over Africa

*Piotr Wolski[1], Chris Jack[1], Waarith Abrahams[1], Stefaan Conradie[1]

1. University of Cape Town

Variability in local climate is a result of an interplay of multi-scale drivers –processes and feedbacks - intertwined within dependency or conditioning chain across spatial scales: from global to synoptic to meso- to local. Resolving these drivers and dependencies can be framed through the following questions: where does a deterministic signal at a particular time scale arise, how does it propagate through space and scales, and how can we maximize our ability to capture it? Here, we report on an exploratory study focusing on the synoptic-scale forcing underlying rainfall variability at the interannual time scale over Africa. In that, we systematically map, over the continent, variables and spatial scales which provide the strongest explanatory power of interannual rainfall variability. In addition, we constrast the explanatory power of mean state of synoptic fields with that of their variance, and of frequency of individual (daily) states. The analyses utilize multiple regression and CCA performed on mean de-orthogonalized fields of q,t,u,v,z at various pressure levels, with daily states of synoptic variables classified using self-organizing maps (SOM). The results are interpreted from the process perspective in terms of their agreement with the current understanding of the role of process chains affecting rainfall over various regions of the contient, and in terms of their implications to statistical downscaling of climate projections and seasonal forecasts.

Keywords: rainfall variability, statistical climatology, Africa, self organizing maps

©2019. Japan Geoscience Union. All Right Reserved.

Effect of El Niño on the response ratio of Hadley circulation to different SST meridional structures

*Juan Feng[1]

1. Beijing Normal University

The role of El Niño in influencing the response ratio of the Hadley circulation (HC) to different tropical sea surface temperature (SST) meridional structures is investigated over the period 1979–2016. The explained variance of the equatorially asymmetric principal mode of HC variability is enhanced during El Niño events that are characterized by equatorially symmetric El Niño SST anomalies. The reason for the enhanced explained variance is examined. It is shown that the response ratio of the HC to different SST meridional structures is greatly enhanced in El Niño events; this is because the SST over the Indo-Pacific warm pool (IPWP) shows inhomogeneous warming in El Niño events, with greater values in the southern IPWP. The asymmetric warming over the IPWP is opposite to the climatological meridional structure of the SST over the IPWP, which intensifies the equatorially symmetric variation of SST, and contributes to the enhanced response ratio of the HC to SST. This point is further verified by the suppression of this enhanced response ratio in El Niño events of the HC to SST when the effects of SST over the IPWP are removed, implying the different warming amplitude within the IPWP during the El Niño events contributes to the enhanced response ratio. The response in La Niña events is also explored, indicating a difference between El Niño and La Niña events. These results may help explain the corresponding variations of the HC during the El Niño events, and highlight the different influences of the El Niño and La Niña events on the response of the HC to SST.

Keywords: Hadley circulation, sea surface temperature, Indo-Pacific warm pool, El Niño

©2019. Japan Geoscience Union. All Right Reserved.

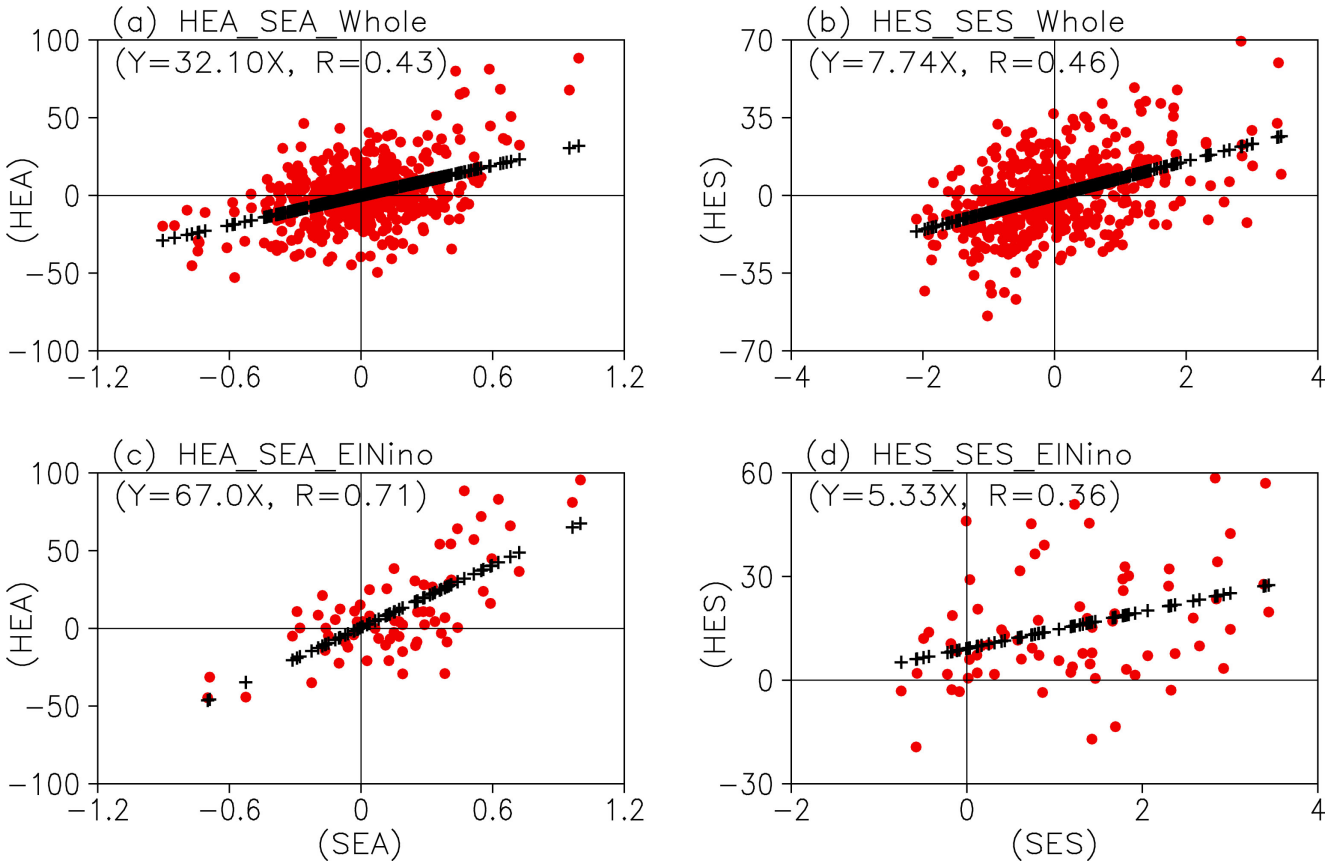

©2019. Japan Geoscience Union. All Right Reserved.

Novel data-driven approach for ENSO prediction

*Dmitri Kondrashov[1], Evgeniy Loskutov[2], Andrei Gavrilov[2], Dmitry Mukhin[2], Alexander Feigin[2]

1. University of California, Los Angeles, United States, 2. Institute of Applied Physics of the Russian Academy of Sciences, Nizhny Novgorod, Russian Federation

We have developed novel data-driven technique for ENSO prediction that combines two existing approaches: linear dynamical mode (LDM) decomposition of spatially distributed data, and multilevel empirical model reduction (EMR) stochastic modeling approach. The nonlinear EMR model that utilizes dynamical variables obtained by empirical orthogonal function (EOF) decomposition of tropical Pacific SST’ s (Kondrashov et al. 2005), had already achieved a very competitive skill in International Research Institute for Climate and Society (IRI) ENSO real-time multi-model plume (Barnston et al. 2012). On the other hand, Gavrilov et al. (2018) have shown that LDM decomposition provides better modes for ENSO forecast than EOFs.

In the presented results we have used LDM modes as dynamical variables at the main level of multilevel linear EMR model. The model was trained on monthly 1960 -- 2014 sea surface temperatures (30S to 30N, 2x2 deg). The results of comparing skill of the retrospective predictions of the SST-based ENSO indices obtained by EMR model with LDM and EOF modes, will be discussed.

1. Kondrashov, D., Kravtsov, S., Robertson, A. W., & Ghil, M. (2005). A Hierarchy of Data-Based ENSO Models. Journal of Climate, 18(21), 4425–4444. doi:10.1175/JCLI3567.1

2. Gavrilov, A., Seleznev, A., Mukhin, D., Loskutov, E., Feigin, A., & Kurths, J. (2018). Linear dynamical modes as new variables for data-driven ENSO forecast. Climate Dynamics, 1–18. http://doi.org/10.1007/s00382-018-4255-7.

3. Barnston, A. G., M. K. Tippett, M. L. Heureux, S. Li, and D. G. DeWitt, 2012: Skill of real-time seasonal ENSO model predictions during 2002–2011 —is our capability improving? *Bulletin of the American Meteorological Society*, **93 (5)**, 631–651, doi:10.1175/BAMS-D-11-00111.1.

Keywords: ENSO, stochastic modeling, prediction

©2019. Japan Geoscience Union. All Right Reserved.

Experimental seasonal climate prediction using CFES: Comparison with the SINTEX-F systems

*Nobumasa Komori[1], Bunmei Taguchi[2], Akira Kuwano-Yoshida[3,1], Takeshi Doi[1], Masami Nonaka[1]

1. Japan Agency for Marine-Earth Science and Technology, 2. Research Center for Advanced Science and Technology, The University of Tokyo, 3. Disaster Prevention Research Institute, Kyoto University

An experimental seasonal climate prediction system has been developed based on the Coupled atmosphere-ocean general circulation model for the Earth Simulator (CFES). Following the well-established systems based on the SINTEX-F model, initial conditions for seasonal climate prediction are constructed by strongly nudging sea surface temperature (SST) to observed one.

At this stage, 12-member ensemble 6-month predictions from the 1st day of March, June, September, and December have been conducted from 1983 through 2018, after 32-years of coupled spin-up integration with SST-nudging to the observed climatology. The experimental system exhibits skill in predicting variability of seasonal-mean 2-m air temperature over the tropical Pacific, and contributes to the improvement of multi-model ensemble prediction with the SINTEX-F systems.

Keywords: experimental seasonal climate prediction, global coupled atmosphere-ocean GCM, atmosphere-ocean interaction, multi-model ensemble

©2019. Japan Geoscience Union. All Right Reserved.

Exploring the SST error growth during ENSO developing phase by using BCC_CSM1.1(m)

*Ben Tian[1], Hongli Ren[1]

1. National Climate Center, China Meteorological Administration

Here we assess the ENSO prediction errors as a function of lead time using the seasonal hindcast of the Beijing Climate Center System Model, BCC_CSM1.1(m). The ensemble mean forecasts seems to be more challenging during the developing years of ENSO, compared with those made towards the decay phase. The composites of SST prediction errors are significantly negative and cover a large area in central-eastern tropical Pacific, thus limiting the model in forecasting the onset and intensity of El Niño. The large-scale errors, at their early stage, are generated gradually by negative anomalies in the subsurface temperature of the central-western equatorial Pacific, a process similar to El Niño decay and then transition to La Nina growth phase. Our results support others' work of "sensitive areas" for ENSO predictions, and emphasize the essential accuracy of initial fields and their early evolution, providing information for further improving the forecasting skill of ENSO.

Keywords: El Nino prediction, error evolution, sea surface temperature

©2019. Japan Geoscience Union. All Right Reserved.

Role of sea-ice initialization in climate predictability over the Weddell Sea

*Yushi Morioka[1], Takeshi Doi[1], Doroteaciro Iovino[2], Simona Masina[2], Swadhin Behera[1]

1. Japan Agency for Marine-Earth Science and Technology (JAMSTEC), 2. Centro Euro-Mediterraneo sui Cambiamenti Climatici (CMCC)

Potential impact of sea-ice initialization on the interannual climate predictability over the Weddell Sea is investigated using a coupled general circulation model. Climate variability in the Weddell Sea is generally believed to have association with remote forcing such as El Niño-Southern Oscillation and the Southern Annual Mode. However, sea-ice variability in the Weddell Sea has been recently suggested to play additional roles in modulating local atmospheric variability through changes in surface air temperature and near-surface baroclinicity. When both the model’s sea-surface temperature (SST) and sea-ice concentration (SIC) are initialized with observations using nudging schemes, reforecast experiments from September 1st show improvements in predicting the observed SIC anomalies in the Weddell Sea up to four months ahead, compared to the other experiments with only SST initialization. During austral spring (Oct-Dec) of lower-than-normal sea-ice years in the Weddell Sea, reforecast experiments with the SST and SIC initializations reasonably predict high surface air temperature anomalies in the Weddell Sea and high sea-level pressure anomalies over the Atlantic sector of the Southern Ocean. These results suggest that accurate initialization of sea-ice conditions during austral winter is necessary for skillful prediction of climate variability over the Weddell Sea during austral spring.

Keywords: Air-sea-ice interaction, Climate predictability, Weddell Sea

©2019. Japan Geoscience Union. All Right Reserved.

Observed and hindcasted subdecadal variability of the tropical Pacific climate

*Takashi Mochizuki[1], Masahiro Watanabe[2]

1. Japan Agency for Marine-Earth Science and Technology, 2. Atmosphere-Ocean Research Institute, The University of Tokyo

The tropical Pacific is highly responsible for controlling the tendencies of global climate. Here, we have found a subdecadal (i.e., 3-year-running means) variation that has been distinctively observed in the 2000s over the tropical Pacific. The warm water that originated from the positive ocean-heat-content (OHC) anomaly over the western Pacific in 2000 slowly extended eastward and stayed at the central equatorial Pacific between 2002-2005, rather than reaching the eastern edge. At the same time, an accompanying anti-cyclonic surface wind anomaly was observed in the off-equatorial North Pacific. This dynamical response of the upper ocean may have contributed to the subsequent warming in the western Pacific. In the preceding decades, in contrast, the observed OHC has usually represented a periodic fluctuation in the tropical Pacific, characterized by anomalous heat input/output in the meridional direction and slow eastward adjustment in the equatorial ocean thermocline. This subdecadal variation in the 2000s is quite distinct from our decadal hindcasts with initialization in Coupled Model Intercomparison Project Phase 5. The model predominantly simulates periodic-type fluctuations in any decade, and the resultant low predictability of the subdecadal variation in the 2000s can work to modulate the predictive skills at a lead time of several years.

Keywords: subdecadal variability, climate prediction, predictability, tropical Pacific

©2019. Japan Geoscience Union. All Right Reserved.

[E] Poster | A (Atmospheric and Hydrospheric Sciences)：A-OS Ocean Sciences & Ocean Environment

Thu. May 30, 2019 5:15 PM - 6:30 PM JST | Thu. May 30, 2019 8:15 AM - 9:30 AM UTC | Poster Hall International Exhibition Hall8, Makuhari Messe_7

[A-OS07] Climate variability and predictability on subseasonal to decadal timescales

convener:Takashi Mochizuki(Japan Agency for Marine-Earth Science and Technology), V Ramaswamy(NOAA GFDL), Doug Smith(Met Office), Yushi Morioka(Japan Agency for Marine-Earth Science and Technology)

Climate variability poses growing threats to human lives and socio-economic activities through changes in frequency and intensity of abnormal weather such as cold/heat waves and floods/droughts. This involves several climate phenomena with a wide range of timescales from subseasonal to decadal variations (e.g. MJO, IOD, ENSO, PDV, AMV). Many efforts have been made for understanding and predicting climate variations on each timescale, but there remain large uncertainties in simulation and prediction of subseasonal to decadal climate variations. This highlights lack of understanding of weather and climate interaction across different spatial and temporal timescales (e.g. tropical cyclones and ENSO) as well as multiple physical processes underlying climate variations (e.g. troposphere-stratosphere coupling, air-sea-ice interaction). This session aims to share current knowledge of subseasonal to decadal climate variability and predictability in order to identify the unresolved issues for better understanding and accurate prediction. This session invites all the abstracts related to the observational, theoretical, process-level and modelling research on subseasonal to decadal climate variability and predictability.

[AOS07-P01] Changes in North American and European Heatwave Characteristics

*Szandra A. Peter[1], Ben Kirtman[1] (1.Rosenstiel School of Marine and Atmospheric Science)

[AOS07-P02] **The effects of the "New Climate" Warming on Western Mediterranean: Situation of the Recent Extreme Events**

*Mohammed-Said KARROUK[1] (1.Hassan II University of Casablanca)

[AOS07-P03] **Month-to-month Difference of the Western Pacific Subtropical High Simulated by CMIP5 Models**

*Xiao Dong[1], Renping Lin[1] (1.Institute of Atmospheric Physics)

[AOS07-P04] Potential regulation on the climatic effect of Tibetan Plateau heating by tropical air–sea coupling

*Ziqian Wang[1], Anmin Duan[2], Song Yang[1] (1.School of Atmospheric Sciences, Sun Yat-sen University, 2.Institute of Atmospheric Physics, Chinese Academy of Sciences)

[AOS07-P05] Intraseasonal variation of the South Asian high and its role in connecting the Indian and East Asian summer monsoons

*Wei Wei[1] (1.Sun Yat-sen University)

[AOS07-P06] Mean Surface Air Temperatures in Japan - Regional Classification and Interranual Variability

*Pascal Oettli[1], Masami Nonaka[1], Swadhin Behera[1] (1.Japan Agency for Marine-Earth Science and Technology)

[AOS07-P07] Inter-Annual Variability of the Indonesian Rainfall and Air-Sea Interaction over the Indian-Pacific Ocean Associated with Regime Shift

*Murni Ngestu Nurutami[1], Tadahiro Hayasaka[1] (1.Center for Atmospheric and Oceanic Studies, Graduate School of Science, Tohoku University)

[AOS07-P08] Exploring synoptic-scale drivers of interannual rainfall variability over Africa

*Piotr Wolski[1], Chris Jack[1], Waarith Abrahams[1], Stefaan Conradie[1] (1.University of Cape Town)

[AOS07-P09] **Effect of El Niño on the response ratio of Hadley circulation to different SST meridional structures**

*Juan Feng[1] (1.Beijing Normal University)

[AOS07-P10] **Novel data-driven approach for ENSO prediction**

*Dmitri Kondrashov[1], Evgeniy Loskutov[2], Andrei Gavrilov[2], Dmitry Mukhin[2], Alexander Feigin[2] (1.University of California, Los Angeles, United States, 2.Institute of Applied Physics of the Russian Academy of Sciences, Nizhny Novgorod, Russian Federation)

[AOS07-P11] Experimental seasonal climate prediction using CFES: Comparison with the SINTEX-F systems

*Nobumasa Komori[1], Bunmei Taguchi[2], Akira Kuwano-Yoshida[3,1], Takeshi Doi[1], Masami Nonaka[1] (1.Japan Agency for Marine-Earth Science and Technology, 2.Research Center for Advanced Science and Technology, The University of Tokyo, 3.Disaster Prevention Research Institute, Kyoto University)

[AOS07-P12] Exploring the SST error growth during ENSO developing phase by using BCC_CSM1.1(m)

*Ben Tian[1], Hongli Ren[1] (1.National Climate Center, China Meteorological Administration)

[AOS07-P13] Role of sea-ice initialization in climate predictability over the Weddell Sea

*Yushi Morioka[1], Takeshi Doi[1], Doroteaciro Iovino[2], Simona Masina[2], Swadhin Behera[1] (1.Japan Agency for Marine-Earth Science and Technology (JAMSTEC), 2.Centro Euro-Mediterraneo sui Cambiamenti Climatici (CMCC))

[AOS07-P14] Observed and hindcasted subdecadal variability of the tropical Pacific climate

*Takashi Mochizuki[1], Masahiro Watanabe[2] (1.Japan Agency for Marine-Earth Science and Technology, 2.Atmosphere-Ocean Research Institute, The University of Tokyo)

Changes in North American and European Heatwave Characteristics

*Szandra A. Peter[1], Ben Kirtman[1]

1. Rosenstiel School of Marine and Atmospheric Science

Heat waves are a serious threat to ecosystems, society and the economies of the world. By calculating specific threshold values from daily maximum 2 m temperatures of the NCEP/NCAR reanalysis data (Kalnay et al. 1996), the frequency of heat waves during summer months (JJA) in Europe and the US is determined for the period of 1982 to 2017. The differences between the first and the second half of the 36-year period are discussed, and the results are compared to the North American Multi-Model Ensemble (NMME) forecast with specific focus on recent heat waves in the Pacific Northwest of North America and Central Europe. The connection between heat waves and known climate variability (i.e., the NAO, PNA) is analyzed. We strive to assess the importance of natural variability, such as the NAO, in the frequency of heat waves by comparing the first and last half of the studied 36-year period. We also examine how well the NMME retrospective and real-time forecasts capture heat waves (and cold spells), and the sources of predictability (i.e., sea surface temperature anomalies, land surface conditions), and how the predictability connects to the various modes of climate variability.

©2019. Japan Geoscience Union. All Right Reserved.

The effects of the "New Climate" Warming on Western Mediterranean: Situation of the Recent Extreme Events

*Mohammed-Said KARROUK[1]

1. Hassan II University of Casablanca

Since the nineties of the last century, climatological research following a great scientific advance in the field of prediction, not the variability and evolution of the different climatic parameters was beginning to be clearer!

But today, since the beginning of 2005, certainly due to oceanic thermal cumulations, and the shift of climatic zones towards poles in selective forms (more intense on the oceans present on the continents); Climatic events do not evolve according to the usual and expected rhythms: atmospheric circulation, precipitation, temperatures, seasonal phenomena, etc. These conditions are a spatiotemporal evolution and distribution, which characterize the new "global climate", by the new atmospheric regime imposing the Meridian Atmospheric Circulation (MAC), alternating the conditions of Freshness (humidity) and Heat (drought) along the year.

In this new situation, Western Mediterranean, located in the climate transition zone, is fully affected by the "New Climate". Usually, the atmospheric response to major climatic events (ENSO) in this region such as "El Niño" was characterized by the establishment of the NAO positive index, stability and drought, due to dominance Zonal Atmospheric Circulation in winter. On the other hand, in the "La Niña" episode, the negative index of the NAO and the predominant Meridian Atmospheric Circulation and precipitation became abundant.

Since the beginning of this century, qualified meteorological events of "exceptional !" causing floods have continued to occur in Western Mediterranean, with increasing recurrence, prompting us to wonder about the "new" mode of hydro-thermal function of the climate system that induces torrential rains, as well as its effect on environments and societies.

Thanks to spatial observation and monitoring of meteorological conditions over the last 15 years, these types of alternating Heat / Cold conditions have become predictable, enabling decision-makers today to prepare adequately for the management of related risks to the "New Climate" warmed.

Keywords: "New Climate" Warmed, New Atmospheric Circulation, Meridian Atmospheric Circulation (MAC) , Western Mediterranean, Heat / Cold, Drought / Flood

©2019. Japan Geoscience Union. All Right Reserved.

Month-to-month Difference of the Western Pacific Subtropical High Simulated by CMIP5 Models

*Xiao Dong[1], Renping Lin[1]

1. Institute of Atmospheric Physics

The western Pacific subtropical high (WPSH) is an important circulation system of the East Asian summer monsoon (EASM). Most previous studies have focused on the variability of summer mean WPSH. Note that the WPSH also experiences subseasonal variation from early to late summer. In this study we examined the month-to-month shift of the WPSH in boreal summer, that is, from June to July and from July to August, simulated by CMIP5 Atmospheric General Circulation Models (AGCMs) and coupled models. Results show that climatologically AGCMs can reproduce the northward shift of the WPSH better than eastward retreat from July to August. Compared with AGCMs, coupled models can improve the month-to-month shift simulation to some extent, indicating that the air-sea coupling processes are also important in subseasonal timescale.

Keywords: western Pacific subtropical high, CMIP5 simulation, month to month variation

©2019. Japan Geoscience Union. All Right Reserved.

Potential regulation on the climatic effect of Tibetan Plateau heating by tropical air–sea coupling

*Ziqian Wang[1], Anmin Duan[2], Song Yang[1]

1. School of Atmospheric Sciences, Sun Yat-sen University, 2. Institute of Atmospheric Physics, Chinese Academy of Sciences

Based on the conventional weather research and forecasting (WRF) model and the air–sea coupled mode WRF-OMLM, we investigate the potential regulation on the climatic effect of Tibetan Plateau (TP) heating by the air–sea coupling over the tropical Indian Ocean and western Pacific. Results indicate that the TP heating significantly enhances the southwesterly monsoon circulation over the northern Indian Ocean and the South Asia subcontinent. The intensified southwesterly wind cools the sea surface mainly through the wind-evaporation-SST (sea surface temperature) feedback. Cold SST anomaly then weakens monsoon convective activity, especially that over the Bay of Bengal, and less water vapor is thus transported into the TP along its southern slope from the tropical oceans. As a result, summer precipitation decreases over the TP, which further weakens the TP local heat source. Finally, the changed TP heating continues to influence the summer monsoon precipitation and atmospheric circulation. To a certain extent, the air–sea coupling over the adjacent oceans may weaken the effect of TP heating on the mean climate in summer. It is also implied that considerations of air–sea interaction are necessary in future simulation studies of the TP heating effect.

Keywords: Air–sea coupling, Tibetan Plateau, Thermal forcing, Regional model

©2019. Japan Geoscience Union. All Right Reserved.

Intraseasonal variation of the South Asian high and its role in connecting the Indian and East Asian summer monsoons

*Wei Wei[1]

1. Sun Yat-sen University

The South Asian high (SAH) is the most intense and persistent upper-level circulation system in the Asian monsoon region during boreal summer. It plays a crucial role in the onset and variation of the Asian summer monsoon. Ample evidence shows that the monsoon onset and activities are closely related to the intraseasonal oscillation (ISO). Previous studies have found that the ISO in the East Asian summer monsoon (EASM) is impacted by the northward or northwestward propagation of the ISO in the South China Sea and the western North Pacific, and the northeastward propagation of the ISO in the tropical Indian Ocean. However, seldom research mentioned the effect of the ISO in the SAH. Our previous studies have shown that the SAH plays an important role in connecting the Indian summer monsoon (ISM) and the EASM on the interannual time scale. However, the effect of the SAH on the connection of the ISM and the EASM on the intraseasonal time scale is still not clear. Actually, the ISO in the SAH is significant in its zonal variation. In this study, we firstly figured out the intraseasonal variation feature of the SAH. And then, we explored the upper-level signal which will lead to the onset, advance and retreat of the EASM. Considering significant ISO in the ISM, we investigated the ISO feature in the ISM and its effect on the ISO in the SAH. Finally, we addressed a new physical process that the ISO in the ISM will impact the ISO in the SAH, and further influence the advance and retreat of the EASM on the intraseasonal time scale. We try to learn about the intraseasonal variation of the EASM in a new view, and propose a new way to improve the short-term climate prediction and the extended-range weather forecast.

©2019. Japan Geoscience Union. All Right Reserved.

Mean Surface Air Temperatures in Japan - Regional Classification and Interranual Variability

*Pascal Oettli[1], Masami Nonaka[1], Swadhin Behera[1]

1. Japan Agency for Marine-Earth Science and Technology

Back to the year 1886, several divisions of the climate of Japan into homogeneous climatic regions have been proposed, following different approaches of the question. This includes the Köppen climate classification (Fukui in 1933; Sekiguchi in 1949), the new Thornthwaite climate classification (Isozaki in 1933; Fukui in 1957) or the similarities of weather conditions. The latter is performed either throughout the year (Nakagawa in 1899; Sekiguchi in 1959; Yoshino in 1980) or during specific seasons (Iwakiri in 1967; Murata and Yoshino in 1988), sometimes with the help of statistical techniques, such as principal component analysis and the cluster analysis (Mikami in 1975; Koizumi and Kato in 2012.)

Using a type of artificial neural network called Self-Organizing Map, or SOM, we propose another division of the climate of Japan, solely based on the mean areal surface air temperature anomalies. SOM has been successfully employed in climate studies for more than a decade and has showed its ability to extract simple features from high-dimensional data. Here, SOM is applied to group 762 AMeDAS stations, taken throughout Japan for the last 30 years, into homogeneous clusters (=regions). Clustering is performed seasonally, with a focus on boreal winter (December to February) and boreal summer (June to August). As a result, eight regions are defined and associated time series of temperature anomalies (=indices) are computed.

Subsequently, possible source(s) of the interannual variability of mean surface air temperature anomalies are explored, for a better understanding of the regional differences. For this, correlation coefficients between indices previously defined and different climatic variable anomaly fields (sea-surface temperatures, outgoing longwave radiation, geopotential height...) are calculated. Hopefully, this work would also lead to a better seasonal forecast, taking into account the specificity of each region in regard to their link to the large-scale variability.

Keywords: Japan, Air temperature, Classification, Interannual variability

©2019. Japan Geoscience Union. All Right Reserved.

Inter-Annual Variability of the Indonesian Rainfall and Air-Sea Interaction over the Indian-Pacific Ocean Associated with Regime Shift

*Murni Ngestu Nurutami[1], Tadahiro Hayasaka[1]

1. Center for Atmospheric and Oceanic Studies, Graduate School of Science, Tohoku University

The inter-annual and inter-decadal variability of the Indonesian rainfall are investigated in association with the interannual climate modes over Indian-Pacific Oceans and the inter-decadal modulation on inter-annual climate variability impact. Rainfall data of the Climate Research Unit (CRU) from 1901 to 2016 and the Global Precipitation Climatology Project (GPCP) from 1979 to 2016 for June –November (JJASON) are used. The empirical orthogonal function (EOF) is used to identify the dominant spatial and temporal variability patterns of rainfall and the standard and partial correlation techniques are used to compare and to quantify the linear relationship between two or more time-series datasets. Based on the first principle component (PC1) of both CRU and GPCP data, the results show that canonical El Niño Southern-Oscillation (canonical ENSO), ENSO Modoki, and Indian Ocean Dipole (IOD) are the major climate modes influencing the inter-annual variability of the Indonesian rainfall, and the Inter-decadal Pacific Oscillation (IPO) is the major decadal phenomenon which affects the decadal variability of Indonesian rainfall. All of the inter-annual climate modes and IPO have negative correlation with the Indonesian rainfall, but the spatial distributions of Indonesian rainfall change associated with each phenomenon are different. During 1970 to 2016, three phases of IPO have been identified which are strongly related to Indonesian rainfall with the correlation coefficient of -0.75. The three phases are a negative phase in 1970-1978, a positive phase in 1979-1997, and another negative phase in 1998-2015. Mostly, these climate modes occur simultaneously, and the impacts of them on rainfall are combined. The driest condition of rainfall occurs when El Niño coincides with positive IOD during positive IPO, and the wettest condition occurs when La Niña –La Niña Modoki coincides with negative IOD during negative IPO over the whole region of Indonesia. The IPO plays a role in modulating the impact of these inter-annual climate modes on their frequencies and magnitudes to Indonesian rainfall from 1970s until present. The responses of the Indonesian rainfall to each inter-annual climate mode modulated by IPO are different as based on their time series correlation coefficient. The negative correlation between canonical ENSO and Indonesian rainfall weakens during negative IPO from early 2000s and intensifies during positive IPO. On the other hand, the negative correlation between ENSO Modoki and Indonesian rainfall and between IOD and Indonesian rainfall increases during negative phase of IPO from late 1990s, and the negative correlation between ENSO Modoki and Indonesian rainfall weakens during positive IPO. Recently, the frequency of ENSO Modoki and IOD and their impacts on Indonesian rainfall increase.

Keywords: Indonesian rainfall variability, El Niño Southern-Oscillation (ENSO), ENSO Modoki, Interannual Variability, Decadal Variability, Interdecadal Pacific Oscillation

©2019. Japan Geoscience Union. All Right Reserved.

Exploring synoptic-scale drivers of interannual rainfall variability over Africa

*Piotr Wolski[1], Chris Jack[1], Waarith Abrahams[1], Stefaan Conradie[1]

1. University of Cape Town

Variability in local climate is a result of an interplay of multi-scale drivers –processes and feedbacks - intertwined within dependency or conditioning chain across spatial scales: from global to synoptic to meso- to local. Resolving these drivers and dependencies can be framed through the following questions: where does a deterministic signal at a particular time scale arise, how does it propagate through space and scales, and how can we maximize our ability to capture it? Here, we report on an exploratory study focusing on the synoptic-scale forcing underlying rainfall variability at the interannual time scale over Africa. In that, we systematically map, over the continent, variables and spatial scales which provide the strongest explanatory power of interannual rainfall variability. In addition, we constrast the explanatory power of mean state of synoptic fields with that of their variance, and of frequency of individual (daily) states. The analyses utilize multiple regression and CCA performed on mean de-orthogonalized fields of q,t,u,v,z at various pressure levels, with daily states of synoptic variables classified using self-organizing maps (SOM). The results are interpreted from the process perspective in terms of their agreement with the current understanding of the role of process chains affecting rainfall over various regions of the contient, and in terms of their implications to statistical downscaling of climate projections and seasonal forecasts.

Keywords: rainfall variability, statistical climatology, Africa, self organizing maps

©2019. Japan Geoscience Union. All Right Reserved.

Effect of El Niño on the response ratio of Hadley circulation to different SST meridional structures

*Juan Feng[1]

1. Beijing Normal University

The role of El Niño in influencing the response ratio of the Hadley circulation (HC) to different tropical sea surface temperature (SST) meridional structures is investigated over the period 1979–2016. The explained variance of the equatorially asymmetric principal mode of HC variability is enhanced during El Niño events that are characterized by equatorially symmetric El Niño SST anomalies. The reason for the enhanced explained variance is examined. It is shown that the response ratio of the HC to different SST meridional structures is greatly enhanced in El Niño events; this is because the SST over the Indo-Pacific warm pool (IPWP) shows inhomogeneous warming in El Niño events, with greater values in the southern IPWP. The asymmetric warming over the IPWP is opposite to the climatological meridional structure of the SST over the IPWP, which intensifies the equatorially symmetric variation of SST, and contributes to the enhanced response ratio of the HC to SST. This point is further verified by the suppression of this enhanced response ratio in El Niño events of the HC to SST when the effects of SST over the IPWP are removed, implying the different warming amplitude within the IPWP during the El Niño events contributes to the enhanced response ratio. The response in La Niña events is also explored, indicating a difference between El Niño and La Niña events. These results may help explain the corresponding variations of the HC during the El Niño events, and highlight the different influences of the El Niño and La Niña events on the response of the HC to SST.

Keywords: Hadley circulation, sea surface temperature, Indo-Pacific warm pool, El Niño

©2019. Japan Geoscience Union. All Right Reserved.

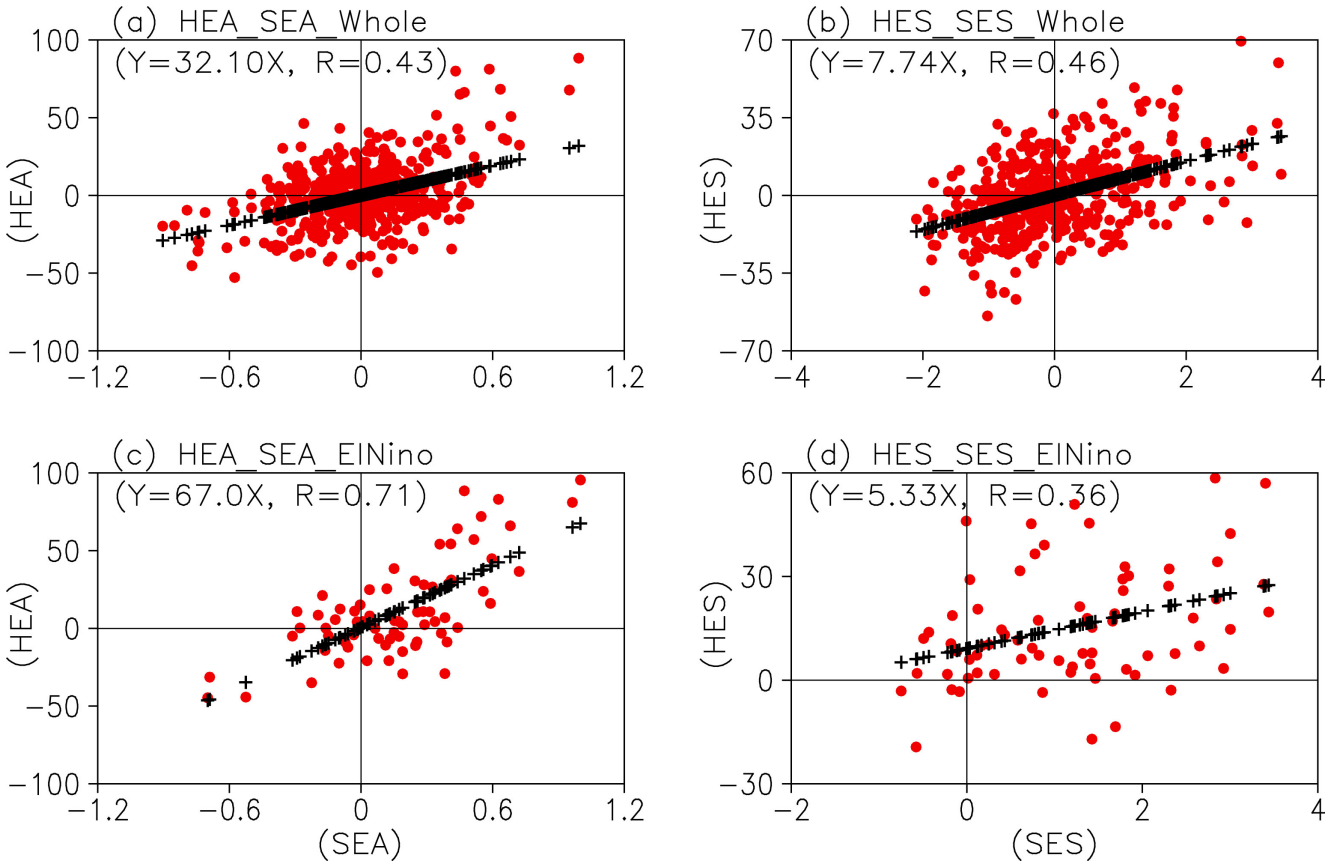

©2019. Japan Geoscience Union. All Right Reserved.

Novel data-driven approach for ENSO prediction

*Dmitri Kondrashov[1], Evgeniy Loskutov[2], Andrei Gavrilov[2], Dmitry Mukhin[2], Alexander Feigin[2]

1. University of California, Los Angeles, United States, 2. Institute of Applied Physics of the Russian Academy of Sciences, Nizhny Novgorod, Russian Federation

We have developed novel data-driven technique for ENSO prediction that combines two existing approaches: linear dynamical mode (LDM) decomposition of spatially distributed data, and multilevel empirical model reduction (EMR) stochastic modeling approach. The nonlinear EMR model that utilizes dynamical variables obtained by empirical orthogonal function (EOF) decomposition of tropical Pacific SST’ s (Kondrashov et al. 2005), had already achieved a very competitive skill in International Research Institute for Climate and Society (IRI) ENSO real-time multi-model plume (Barnston et al. 2012). On the other hand, Gavrilov et al. (2018) have shown that LDM decomposition provides better modes for ENSO forecast than EOFs.

In the presented results we have used LDM modes as dynamical variables at the main level of multilevel linear EMR model. The model was trained on monthly 1960 -- 2014 sea surface temperatures (30S to 30N, 2x2 deg). The results of comparing skill of the retrospective predictions of the SST-based ENSO indices obtained by EMR model with LDM and EOF modes, will be discussed.

1. Kondrashov, D., Kravtsov, S., Robertson, A. W., & Ghil, M. (2005). A Hierarchy of Data-Based ENSO Models. Journal of Climate, 18(21), 4425–4444. doi:10.1175/JCLI3567.1

2. Gavrilov, A., Seleznev, A., Mukhin, D., Loskutov, E., Feigin, A., & Kurths, J. (2018). Linear dynamical modes as new variables for data-driven ENSO forecast. Climate Dynamics, 1–18. http://doi.org/10.1007/s00382-018-4255-7.

3. Barnston, A. G., M. K. Tippett, M. L. Heureux, S. Li, and D. G. DeWitt, 2012: Skill of real-time seasonal ENSO model predictions during 2002–2011 —is our capability improving? *Bulletin of the American Meteorological Society*, **93 (5)**, 631–651, doi:10.1175/BAMS-D-11-00111.1.

Keywords: ENSO, stochastic modeling, prediction

©2019. Japan Geoscience Union. All Right Reserved.

Experimental seasonal climate prediction using CFES: Comparison with the SINTEX-F systems

*Nobumasa Komori[1], Bunmei Taguchi[2], Akira Kuwano-Yoshida[3,1], Takeshi Doi[1], Masami Nonaka[1]

1. Japan Agency for Marine-Earth Science and Technology, 2. Research Center for Advanced Science and Technology, The University of Tokyo, 3. Disaster Prevention Research Institute, Kyoto University

An experimental seasonal climate prediction system has been developed based on the Coupled atmosphere-ocean general circulation model for the Earth Simulator (CFES). Following the well-established systems based on the SINTEX-F model, initial conditions for seasonal climate prediction are constructed by strongly nudging sea surface temperature (SST) to observed one.

At this stage, 12-member ensemble 6-month predictions from the 1st day of March, June, September, and December have been conducted from 1983 through 2018, after 32-years of coupled spin-up integration with SST-nudging to the observed climatology. The experimental system exhibits skill in predicting variability of seasonal-mean 2-m air temperature over the tropical Pacific, and contributes to the improvement of multi-model ensemble prediction with the SINTEX-F systems.

Keywords: experimental seasonal climate prediction, global coupled atmosphere-ocean GCM, atmosphere-ocean interaction, multi-model ensemble

©2019. Japan Geoscience Union. All Right Reserved.

Exploring the SST error growth during ENSO developing phase by using BCC_CSM1.1(m)

*Ben Tian[1], Hongli Ren[1]

1. National Climate Center, China Meteorological Administration

Here we assess the ENSO prediction errors as a function of lead time using the seasonal hindcast of the Beijing Climate Center System Model, BCC_CSM1.1(m). The ensemble mean forecasts seems to be more challenging during the developing years of ENSO, compared with those made towards the decay phase. The composites of SST prediction errors are significantly negative and cover a large area in central-eastern tropical Pacific, thus limiting the model in forecasting the onset and intensity of El Niño. The large-scale errors, at their early stage, are generated gradually by negative anomalies in the subsurface temperature of the central-western equatorial Pacific, a process similar to El Niño decay and then transition to La Nina growth phase. Our results support others' work of "sensitive areas" for ENSO predictions, and emphasize the essential accuracy of initial fields and their early evolution, providing information for further improving the forecasting skill of ENSO.

Keywords: El Nino prediction, error evolution, sea surface temperature

©2019. Japan Geoscience Union. All Right Reserved.

Role of sea-ice initialization in climate predictability over the Weddell Sea

*Yushi Morioka[1], Takeshi Doi[1], Doroteaciro Iovino[2], Simona Masina[2], Swadhin Behera[1]

1. Japan Agency for Marine-Earth Science and Technology (JAMSTEC), 2. Centro Euro-Mediterraneo sui Cambiamenti Climatici (CMCC)

Potential impact of sea-ice initialization on the interannual climate predictability over the Weddell Sea is investigated using a coupled general circulation model. Climate variability in the Weddell Sea is generally believed to have association with remote forcing such as El Niño-Southern Oscillation and the Southern Annual Mode. However, sea-ice variability in the Weddell Sea has been recently suggested to play additional roles in modulating local atmospheric variability through changes in surface air temperature and near-surface baroclinicity. When both the model’s sea-surface temperature (SST) and sea-ice concentration (SIC) are initialized with observations using nudging schemes, reforecast experiments from September 1st show improvements in predicting the observed SIC anomalies in the Weddell Sea up to four months ahead, compared to the other experiments with only SST initialization. During austral spring (Oct-Dec) of lower-than-normal sea-ice years in the Weddell Sea, reforecast experiments with the SST and SIC initializations reasonably predict high surface air temperature anomalies in the Weddell Sea and high sea-level pressure anomalies over the Atlantic sector of the Southern Ocean. These results suggest that accurate initialization of sea-ice conditions during austral winter is necessary for skillful prediction of climate variability over the Weddell Sea during austral spring.

Keywords: Air-sea-ice interaction, Climate predictability, Weddell Sea

©2019. Japan Geoscience Union. All Right Reserved.

Observed and hindcasted subdecadal variability of the tropical Pacific climate

*Takashi Mochizuki[1], Masahiro Watanabe[2]

1. Japan Agency for Marine-Earth Science and Technology, 2. Atmosphere-Ocean Research Institute, The University of Tokyo

The tropical Pacific is highly responsible for controlling the tendencies of global climate. Here, we have found a subdecadal (i.e., 3-year-running means) variation that has been distinctively observed in the 2000s over the tropical Pacific. The warm water that originated from the positive ocean-heat-content (OHC) anomaly over the western Pacific in 2000 slowly extended eastward and stayed at the central equatorial Pacific between 2002-2005, rather than reaching the eastern edge. At the same time, an accompanying anti-cyclonic surface wind anomaly was observed in the off-equatorial North Pacific. This dynamical response of the upper ocean may have contributed to the subsequent warming in the western Pacific. In the preceding decades, in contrast, the observed OHC has usually represented a periodic fluctuation in the tropical Pacific, characterized by anomalous heat input/output in the meridional direction and slow eastward adjustment in the equatorial ocean thermocline. This subdecadal variation in the 2000s is quite distinct from our decadal hindcasts with initialization in Coupled Model Intercomparison Project Phase 5. The model predominantly simulates periodic-type fluctuations in any decade, and the resultant low predictability of the subdecadal variation in the 2000s can work to modulate the predictive skills at a lead time of several years.

Keywords: subdecadal variability, climate prediction, predictability, tropical Pacific

©2019. Japan Geoscience Union. All Right Reserved.

[E] Poster | A (Atmospheric and Hydrospheric Sciences)：A-OS Ocean Sciences & Ocean Environment

Thu. May 30, 2019 3:30 PM - 5:00 PM JST | Thu. May 30, 2019 6:30 AM - 8:00 AM UTC | Poster Hall International Exhibition Hall8, Makuhari Messe_4

[A-OS10] Atlantic climate variability, and its global impacts and predictability

convener:Ingo Richter(JAMSTEC Japan Agency for Marine-Earth Science and Technology), Hiroki Tokinaga(Research Institute for Applied Mechanics, Kyushu University), Noel S Keenlyside(Geophysical Institute Bergen), Carlos R Mechoso(University of California Los Angeles)

The Atlantic Ocean is subject to pronounced climate variations that occur on a wide range of time scales, including interannual variability in the equatorial and subtropical regions, and Atlantic multi-decadal variability (AMV), which has been linked with the Atlantic meridional overturning circulation (AMOC). These are connected to other climate variations across the globe. The AMV, e.g., has long been known to have global impacts, such as changes in the Indian, Asian and South American summer monsoons, and changes in the Pacific associated with the "global hiatus". Interannual variability in the equatorial and subtropical Atlantic has also been shown to influence global climate, including over Asia, while the freshening of the North Atlantic by melting of the Greenland ice cap is expected to influence all ocean basins via atmospheric bridges. Likewise, misrepresentation of the Atlantic can have global ramifications in climate models. Misrepresentation of the AMOC, e.g., has been associated with model biases in the entire Northern Hemisphere.

This session seeks observational, modeling, and theoretical studies on the mechanisms that determine the Atlantic mean climate and variability, as well as the predictability and global impacts of such variability. We also seek studies that evaluate climate model performance in the region. Topics include atmosphere-ocean-cloud interactions in the tropical Atlantic and their remote impacts; relationships between tropical and mid/high latitude variability; air-sea interaction along the Gulf Stream and its influence on cyclones and storm track evolution; variability in the Benguela upwelling region; influence of Agulhas leakage on the South Atlantic; coupled climate models biases in the region and their impacts; AMOC and long-term climate change.

[AOS10-P01] The strengthening of Amazonian precipitation during the wet season driven by tropical sea surface temperature forcing

*Xinyue Wang[1], Xichen Li[1], Jiang Zhu[1], Clemente A S Tanajura[2] (1.Institute of Atmospheric Physics, Chinese Academy of Sciences, 2.Institute of Physics, Federal University of Bahia, Salvador, Brazil)

[AOS10-P02] Linear inverse modeling of the tropical Atlantic

*Ingo Richter[1], Ping Chang[2] (1.JAMSTEC Japan Agency for Marine-Earth Science and Technology, 2.Texas A&M University)

[AOS10-P03] Relationships Among Inter-model Spread and Biases in Tropical Atlantic Sea Surface Temperatures

Elsa - Mohino Harris[1], *Belen Rodriguez-Fonseca[1,2], Teresa - Losada[1], Irene - Polo[1], Roberto - Mechoso[3] (1.Department of Physics of the Earth and Astrophysics, Universidad Complutense de Madrid, 28040, Madrid, Spain. , 2.Institute of Geosciences IGEO,UCM-CSIC, 28040, Madrid, Spain., 3.Department of Atmospheric and Oceanic Sciences, UCLA, Los Angeles, USA)

[AOS10-P04] Revisiting the CMIP5 Thermocline in the Equatorial Pacific and Atlantic Oceans

Antonio - Castaño[1,2], Elsa - Mohino[1], *Belen Rodriguez-Fonseca[1,2], Teresa - Losada[1] (1.Department of Physics of the Earth and Astrophysics, Universidad Complutense de Madrid, 28040, Madrid, Spain., 2.Institute of Geosciences, IGEO, UCM-CSIC 28040, Madrid, Spain.)

[AOS10-P05] Lagged Effects of North Atlantic SST Anomalies on Weather in Remote Areas

*Natalia Gnatiuk[1], Timo Vihma[2], Leonid Bobylev[1] (1.Nansen International Environmental and Remote Sensing Centre, 2.Finnish Meteorological Institute)

[AOS10-P06] SST anomalies in the northern tropical Atlantic as a negative feedback to ENSO development

*Ingo Richter[1], Hiroki Tokinaga[2], Yu Kosaka[3], Takeshi Doi[1] (1.JAMSTEC Japan Agency for Marine-Earth Science and Technology, 2.Kyoto University, 3.University of Tokyo)

The strengthening of Amazonian precipitation during the wet season driven by tropical sea surface temperature forcing

*Xinyue Wang[1], Xichen Li[1], Jiang Zhu[1], Clemente A S Tanajura[2]

1. Institute of Atmospheric Physics, Chinese Academy of Sciences, 2. Institute of Physics, Federal University of Bahia, Salvador, Brazil

Amazonian rainfall plays a critical role in the global climate system and the hydrological cycle. It is thus important to quantify changes in the Amazonian rainfall and clarify its mechanism. Previous studies indicate that the interannual variability of Amazonian precipitation could be largely attributed to variabilities in the South American monsoon system and the El Niño Southern Oscillation. However, the trend of the wet season tropical Amazonian precipitation during recent decades is not very well investigated. In this study, by combining both satellite and in situ observations, it is revealed that tropical Amazonian precipitation has significantly increased by~180 to 600 mm (in different datasets) in the wet season during the satellite era from 1979 to 2015. We then use a state-of-the-art atmospheric model to simulate the impact of the tropical sea surface temperatures (SSTs) on the precipitation changes. Results show that the multidecadal warming of the tropical Atlantic has contributed more than half of this precipitation change over the past three decades, while the east Pacific cooling plays a secondary role. We finally combine the simulation results and the reanalysis data to investigate the mechanisms of this process, i.e. the SST variability dramatically increases the convergence of the moisture transport over the Amazon region. The precipitation changes over the Amazon region largely impact on the local hydrological cycle and the ecosystem, and have important impacts on the global climate system by mediating the teleconnection between the Pacific and the Atlantic oceans. Our results show that the long-term change in the wet season Amazonian precipitation is important and deserves further investigation and discussion.

Keywords: convective precipitation, Amazon, tropical Atlantic, moisture convergence

©2019. Japan Geoscience Union. All Right Reserved.

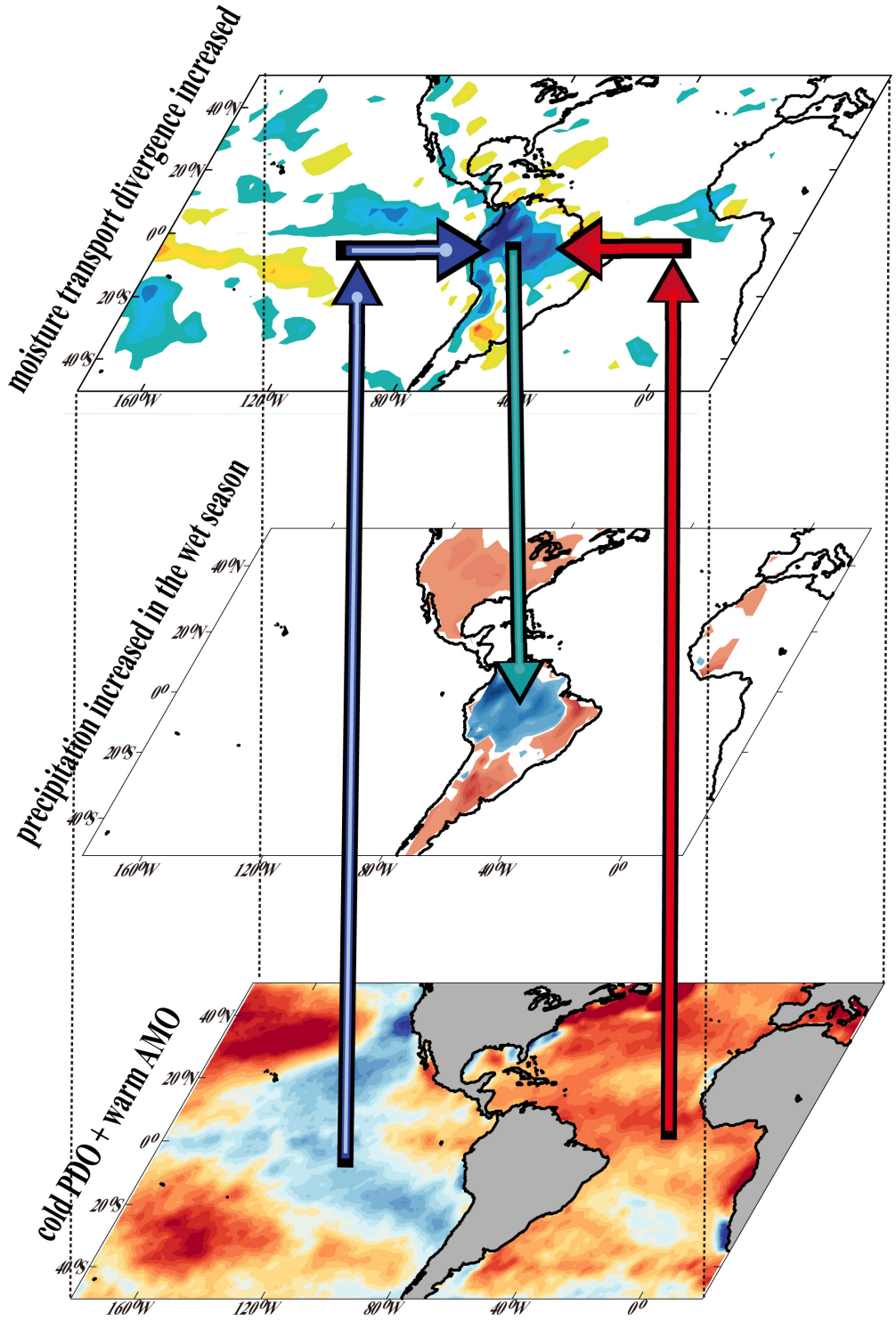

©2019. Japan Geoscience Union. All Right Reserved.

Linear inverse modeling of the tropical Atlantic

*Ingo Richter[1], Ping Chang[2]

1. JAMSTEC Japan Agency for Marine-Earth Science and Technology, 2. Texas A&M University

The tropical Atlantic features variability at interannual and decadal time scales that is known to have a strong influence on the surrounding continents and possibly other ocean basins. Current prediction systems, however, struggle to skillfully predict sea-surface temperature (SST), let alone its impact on rainfall over the adjacent continents. It is often assumed that this poor prediction skill is due to the severe SST biases and misrepresented variability patterns that most models feature in the region but this has recently been called into question.

In the present study, we construct a simple statistical model of the tropical Atlantic to 1) investigate the influence of model biases on prediction skill, and 2) establish a benchmark to evaluate dynamical model against. Using 35 fully coupled ocean-atmosphere GCMs from the pre-industrial control experiment (piControl) of the Coupled Model Intercomparison Project Phase 5 (CMIP5) we construct a linear inverse model (LIM) for each GCM based on tropical SSTs only. The LIM thus constructed is then used to predict SSTs for the period 2000-2017 from the NCEP/NCAR reanalysis. These predictions are compared to those from a LIM constructed using the NCEP/NCAR reference for the period 1948-1999 as training data. Since each of the model LIMs is constructed from more or less unrealistic variability patterns one would expect to see a clear impact on prediction skill.

The results, however, indicate that prediction skill in the tropical Atlantic is relatively insensitive to the tropical variability patterns of each model. Only some cases see a marked deterioration of prediction skill relative to the reference model. The LIM performs well in the subtropical north and south Atlantic. In the equatorial Atlantic, on the other hand, skill is rather poor at 3 months lead time, though clearly above persistence. Our analysis suggests that in many CMIP5 models misrepresentation of variability should not be a major stumbling block toward skillful prediction. This indicates that the current lack of prediction skill in the region is due to other factors, such as model initialization or inherent predictability limits due to noise.
Comparing several dynamical hindcast experiments with the LIM constructed from observations, we find that the LIM generally has superior prediction skill over most parts of the tropical Atlantic.

Keywords: linear inverse modeling, tropical Atlantic, seasonal prediction

©2019. Japan Geoscience Union. All Right Reserved.

Relationships Among Inter-model Spread and Biases in Tropical Atlantic Sea Surface Temperatures

Elsa - Mohino Harris[1], *Belen Rodriguez-Fonseca[1,2], Teresa - Losada[1], Irene - Polo[1], Roberto - Mechoso[3]

1. Department of Physics of the Earth and Astrophysics, Universidad Complutense de Madrid, 28040, Madrid, Spain. , 2. Institute of Geosciences IGEO,UCM-CSIC, 28040, Madrid, Spain., 3. Department of Atmospheric and Oceanic Sciences, UCLA, Los Angeles, USA

State-of-the-art general circulation models show important systematic errors in their simulation of sea surface temperatures (SST), especially in the Tropical Atlantic. In this work the spread in the simulation of climatological SST in the Tropical Atlantic by 24 CMIP5 models is examined, and its relationship with the mean systematic biases in the region is explored. The modes of inter-model variability are estimated by applying Principal Component (PC) analysis to the SSTs in the region 70ºW-20ºE, 20ºS-20ºN. The inter-model variability is approximately explained by the first three modes. The first mode is related to warmer SSTs in the basin, shows worldwide connections with same-signed loads over most of the tropics and is connected with lower low cloud cover over the eastern parts of the subtropical oceans. The second mode is restricted to the Atlantic, where it shows negative and positive loads to the north and south of the equator, respectively, and is connected to a too weak Atlantic Meridional Overturning Circulation (AMOC). The third mode is related to the double Intertropical Convergence Zone bias in the Pacific and to an interhemispheric asymmetry in the net radiation at the top of the atmosphere. According to the results, the most important of these contributors for SST biases spread in the Tropical Atlantic is the second mode, with models having stronger biases simulating weaker AMOCs.

Keywords: GCM bias, CMIP5, tropical Atlantic, intermodel spread

©2019. Japan Geoscience Union. All Right Reserved.

Revisiting the CMIP5 Thermocline in the Equatorial Pacific and Atlantic Oceans

Antonio - Castaño[1,2], Elsa - Mohino[1], *Belen Rodriguez-Fonseca[1,2], Teresa - Losada[1]

1. Department of Physics of the Earth and Astrophysics, Universidad Complutense de Madrid, 28040, Madrid, Spain., 2. Institute of Geosciences, IGEO, UCM-CSIC 28040, Madrid, Spain.

The thermocline is defined as the ocean layer for which the vertical thermal gradient is maximum. In the equatorial ocean, observations led to the use of the 20˚C isotherm depth (z20) as an estimate of the thermocline. This work compares z20 against the physical thermocline in the Equatorial Atlantic and Pacific Oceans, using SODA reanalysis and CMIP5 Pre-Industrial Control simulations. Our results show that in models z20 is systematically deeper and flatter than the thermocline and does not respond correctly to surface wind stress variations. It is also shown that the annual cycle of z20 is much weaker than that of the physical thermocline. This happens in both equatorial basins and indicates that z20 does not react to the same mechanisms as the thermocline. Possible consequences in the assessment of air-sea coupling in current GCMs and bias reduction strategies are also suggested, as well as possible effects in the representation of upwelling systems in the tropical region.

Keywords: CMIP5, defining thermocline, tropical atlantic, air-sea interactions

©2019. Japan Geoscience Union. All Right Reserved.

Lagged Effects of North Atlantic SST Anomalies on Weather in Remote Areas

*Natalia Gnatiuk[1], Timo Vihma[2], Leonid Bobylev[1]

1. Nansen International Environmental and Remote Sensing Centre, 2. Finnish Meteorological Institute

Polar climate has experienced dramatic changes during observed global warming. These changes in turn have, as hypothesised, strong influences on the mid-latitude weather. Many proposed linkages focus on the effects of changes in sea ice, sea surface temperature or terrestrial snow pack on the air temperature in selected mid-latitude areas. Our hypothesis is that from the point of view of the atmosphere, it does not matter whether the thermal forcing from the surface originates from sea ice melt, terrestrial snow melt, or changes in SST. Most important is to quantify how the atmosphere responds to anomalies in surface temperature, and how the local/regional responses may affect weather patterns in remote areas. By analysing these responses systematically in global scale, we can identify the regions and seasons where/when the response is strongest. Comparing these regions/seasons to observed changes in sea ice, terrestrial snow, and open ocean SST, we will obtain information on the relative importance of forcing from these three factors. For this purpose, we studied the relationships between anomalies in the surface temperature (Ts) in the Northern Hemisphere (on grid 1.5^{o}-1.5^{o}) and 2-m air temperature (T2m) in selected 13 study regions in Europe, Greenland, and parts of Asia and North Africa for the period 1979-2018 based on the ERA-Interim reanalysis. Applying also detrended data, we eliminated spurious correlations resulting from similar trends in the two variables.

We detected significant correlations between the surface temperature over the Labrador Sea, Canadian archipelago and North Atlantic and 2-m air temperature in different study regions for inter-seasonal spring - summer (MAM-JJA) and autumn - winter (SON-DJF) relationships. Among the strongest correlations between the spring Ts and summer T2m were the positive correlations found between Ts in the North Atlantic and T2m in Scandinavia, Ts in the Labrador Sea and T2m in Northeast Europe, and Ts in Norther Sahara and T2m in Urals. As well, among the strongest correlations between the autumn Ts and winter T2m were the positive correlations found between Ts in the North Atlantic and the Labrador Sea and T2m in Scandinavia and Northwest Africa; and the negative correlations found between Ts in the Labrador Sea and the North Atlantic and T2m in Scandinavia, Northeast Europe, Urals, Black Sea region and Northcentral Asia.

In order to identify thermal forcing factors and to assess their relative importance, we analysed the multiyear averages and anomalies of sea-ice concentration, snow cover and surface heat fluxes. According to the results, in all identified cases, changes in SST mostly were an influencing factor.

Another big challenge was to understand the physical mechanisms responsible for the obtained statistical results. For this purpose, we analysed surface pressure, geopotential heights, wind components, air-mass trajectories, incoming solar radiation, cloud cover, and total precipitation for sub-sets of 10 coldest and 10 warmest seasons in the period 1979-2018. There is a detectable effect on anomalies in the atmospheric pressure field and wind components in these regions.

The research is granted by the “ERA.Net RUS Plus” Initiative, ID 166 and national RFBR project No. 18-55-76004; and partly by RSF grant №. 17-17-01151.

©2019. Japan Geoscience Union. All Right Reserved.

Keywords: Sea surface temperature anomalies, Teleconnections, Mid-latitude weather, North Atlantic

©2019. Japan Geoscience Union. All Right Reserved.

SST anomalies in the northern tropical Atlantic as a negative feedback to ENSO development

*Ingo Richter[1], Hiroki Tokinaga[2], Yu Kosaka[3], Takeshi Doi[1]

1. JAMSTEC Japan Agency for Marine-Earth Science and Technology, 2. Kyoto University, 3. University of Tokyo

It has been known for some time that SST anomalies in the equatorial Pacific induce same-signed anomalies in the northern tropical Atlantic (NTA) through changes in the Atlantic trade winds. More recently, it has been suggested that the NTA, in turn, can influence the equatorial Pacific through changes in the surface zonal winds over the western part of the basin. The sign of these wind anomalies, however, would act to force equatorial Pacific SST anomalies that are opposite to those in the NTA. The present study takes a closer look at this apparent conundrum by conducting GCM experiments with prescribed SSTs for the period 1982-2014. In the control experiment, observed SSTs are prescribed globally, while in two sensitivity experiments SST anomalies are removed from either the tropical Atlantic or the tropical Pacific. For the control experiment, analysis suggests that NTA warming is accompanied by SST warming and westerly wind anomalies in the equatorial Pacific. When tropical Pacific SST anomalies are removed, on the other hand, NTA warming coincides with easterly anomalies. Moreover, when SST anomalies are removed from the tropical Atlantic, wind variability over the western equatorial Pacific is enhanced. These results suggest that SST anomalies in the NTA, which are strongly influenced by the tropical Pacific, act as a negative feedback to ENSO development. This interbasin link may be further complicated by other influences on the NTA, such as local air-sea coupling and the North Atlantic Oscillation.

Keywords: tropical Atlantic, ENSO, teleconnections

©2019. Japan Geoscience Union. All Right Reserved.

[E] Poster | A (Atmospheric and Hydrospheric Sciences)：A-OS Ocean Sciences & Ocean Environment

Thu. May 30, 2019 5:15 PM - 6:30 PM JST | Thu. May 30, 2019 8:15 AM - 9:30 AM UTC | Poster Hall International Exhibition Hall8, Makuhari Messe_8

[A-OS10] Atlantic climate variability, and its global impacts and predictability

convener:Ingo Richter(JAMSTEC Japan Agency for Marine-Earth Science and Technology), Hiroki Tokinaga(Research Institute for Applied Mechanics, Kyushu University), Noel S Keenlyside(Geophysical Institute Bergen), Carlos R Mechoso(University of California Los Angeles)

The Atlantic Ocean is subject to pronounced climate variations that occur on a wide range of time scales, including interannual variability in the equatorial and subtropical regions, and Atlantic multi-decadal variability (AMV), which has been linked with the Atlantic meridional overturning circulation (AMOC). These are connected to other climate variations across the globe. The AMV, e.g., has long been known to have global impacts, such as changes in the Indian, Asian and South American summer monsoons, and changes in the Pacific associated with the "global hiatus". Interannual variability in the equatorial and subtropical Atlantic has also been shown to influence global climate, including over Asia, while the freshening of the North Atlantic by melting of the Greenland ice cap is expected to influence all ocean basins via atmospheric bridges. Likewise, misrepresentation of the Atlantic can have global ramifications in climate models. Misrepresentation of the AMOC, e.g., has been associated with model biases in the entire Northern Hemisphere.

This session seeks observational, modeling, and theoretical studies on the mechanisms that determine the Atlantic mean climate and variability, as well as the predictability and global impacts of such variability. We also seek studies that evaluate climate model performance in the region. Topics include atmosphere-ocean-cloud interactions in the tropical Atlantic and their remote impacts; relationships between tropical and mid/high latitude variability; air-sea interaction along the Gulf Stream and its influence on cyclones and storm track evolution; variability in the Benguela upwelling region; influence of Agulhas leakage on the South Atlantic; coupled climate models biases in the region and their impacts; AMOC and long-term climate change.

[AOS10-P01] The strengthening of Amazonian precipitation during the wet season driven by tropical sea surface temperature forcing

*Xinyue Wang[1], Xichen Li[1], Jiang Zhu[1], Clemente A S Tanajura[2] (1.Institute of Atmospheric Physics, Chinese Academy of Sciences, 2.Institute of Physics, Federal University of Bahia, Salvador, Brazil)

[AOS10-P02] Linear inverse modeling of the tropical Atlantic

*Ingo Richter[1], Ping Chang[2] (1.JAMSTEC Japan Agency for Marine-Earth Science and Technology, 2.Texas A&M University)

[AOS10-P03] Relationships Among Inter-model Spread and Biases in Tropical Atlantic Sea Surface Temperatures

Elsa - Mohino Harris[1], *Belen Rodriguez-Fonseca[1,2], Teresa - Losada[1], Irene - Polo[1], Roberto - Mechoso[3] (1.Department of Physics of the Earth and Astrophysics, Universidad Complutense de Madrid, 28040, Madrid, Spain. , 2.Institute of Geosciences IGEO,UCM-CSIC, 28040, Madrid, Spain., 3.Department of Atmospheric and Oceanic Sciences, UCLA, Los Angeles, USA)

[AOS10-P04] Revisiting the CMIP5 Thermocline in the Equatorial Pacific and Atlantic Oceans

Antonio - Castaño[1,2], Elsa - Mohino[1], *Belen Rodriguez-Fonseca[1,2], Teresa - Losada[1] (1.Department of Physics of the Earth and Astrophysics, Universidad Complutense de Madrid, 28040, Madrid, Spain., 2.Institute of Geosciences, IGEO, UCM-CSIC 28040, Madrid, Spain.)

[AOS10-P05] Lagged Effects of North Atlantic SST Anomalies on Weather in Remote Areas

*Natalia Gnatiuk[1], Timo Vihma[2], Leonid Bobylev[1] (1.Nansen International Environmental and Remote Sensing Centre, 2.Finnish Meteorological Institute)

[AOS10-P06] SST anomalies in the northern tropical Atlantic as a negative feedback to ENSO development

*Ingo Richter[1], Hiroki Tokinaga[2], Yu Kosaka[3], Takeshi Doi[1] (1.JAMSTEC Japan Agency for Marine-Earth Science and Technology, 2.Kyoto University, 3.University of Tokyo)

The strengthening of Amazonian precipitation during the wet season driven by tropical sea surface temperature forcing

*Xinyue Wang[1], Xichen Li[1], Jiang Zhu[1], Clemente A S Tanajura[2]

1. Institute of Atmospheric Physics, Chinese Academy of Sciences, 2. Institute of Physics, Federal University of Bahia, Salvador, Brazil

Amazonian rainfall plays a critical role in the global climate system and the hydrological cycle. It is thus important to quantify changes in the Amazonian rainfall and clarify its mechanism. Previous studies indicate that the interannual variability of Amazonian precipitation could be largely attributed to variabilities in the South American monsoon system and the El Niño Southern Oscillation. However, the trend of the wet season tropical Amazonian precipitation during recent decades is not very well investigated. In this study, by combining both satellite and in situ observations, it is revealed that tropical Amazonian precipitation has significantly increased by~180 to 600 mm (in different datasets) in the wet season during the satellite era from 1979 to 2015. We then use a state-of-the-art atmospheric model to simulate the impact of the tropical sea surface temperatures (SSTs) on the precipitation changes. Results show that the multidecadal warming of the tropical Atlantic has contributed more than half of this precipitation change over the past three decades, while the east Pacific cooling plays a secondary role. We finally combine the simulation results and the reanalysis data to investigate the mechanisms of this process, i.e. the SST variability dramatically increases the convergence of the moisture transport over the Amazon region. The precipitation changes over the Amazon region largely impact on the local hydrological cycle and the ecosystem, and have important impacts on the global climate system by mediating the teleconnection between the Pacific and the Atlantic oceans. Our results show that the long-term change in the wet season Amazonian precipitation is important and deserves further investigation and discussion.

Keywords: convective precipitation, Amazon, tropical Atlantic, moisture convergence

©2019. Japan Geoscience Union. All Right Reserved.

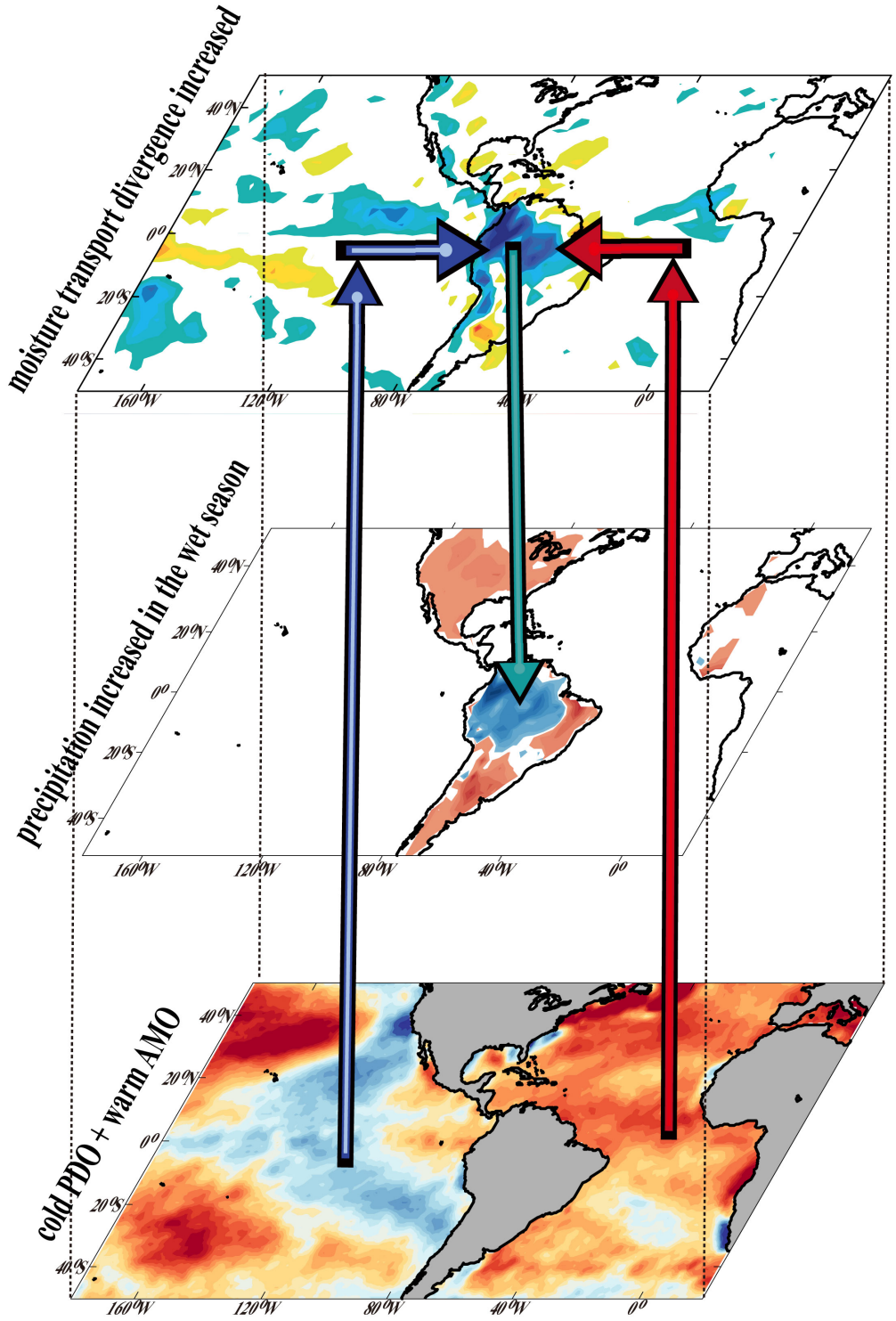

©2019. Japan Geoscience Union. All Right Reserved.

Linear inverse modeling of the tropical Atlantic

*Ingo Richter[1], Ping Chang[2]

1. JAMSTEC Japan Agency for Marine-Earth Science and Technology, 2. Texas A&M University

The tropical Atlantic features variability at interannual and decadal time scales that is known to have a strong influence on the surrounding continents and possibly other ocean basins. Current prediction systems, however, struggle to skillfully predict sea-surface temperature (SST), let alone its impact on rainfall over the adjacent continents. It is often assumed that this poor prediction skill is due to the severe SST biases and misrepresented variability patterns that most models feature in the region but this has recently been called into question.

In the present study, we construct a simple statistical model of the tropical Atlantic to 1) investigate the influence of model biases on prediction skill, and 2) establish a benchmark to evaluate dynamical model against. Using 35 fully coupled ocean-atmosphere GCMs from the pre-industrial control experiment (piControl) of the Coupled Model Intercomparison Project Phase 5 (CMIP5) we construct a linear inverse model (LIM) for each GCM based on tropical SSTs only. The LIM thus constructed is then used to predict SSTs for the period 2000-2017 from the NCEP/NCAR reanalysis. These predictions are compared to those from a LIM constructed using the NCEP/NCAR reference for the period 1948-1999 as training data. Since each of the model LIMs is constructed from more or less unrealistic variability patterns one would expect to see a clear impact on prediction skill.

The results, however, indicate that prediction skill in the tropical Atlantic is relatively insensitive to the tropical variability patterns of each model. Only some cases see a marked deterioration of prediction skill relative to the reference model. The LIM performs well in the subtropical north and south Atlantic. In the equatorial Atlantic, on the other hand, skill is rather poor at 3 months lead time, though clearly above persistence. Our analysis suggests that in many CMIP5 models misrepresentation of variability should not be a major stumbling block toward skillful prediction. This indicates that the current lack of prediction skill in the region is due to other factors, such as model initialization or inherent predictability limits due to noise.
Comparing several dynamical hindcast experiments with the LIM constructed from observations, we find that the LIM generally has superior prediction skill over most parts of the tropical Atlantic.

Keywords: linear inverse modeling, tropical Atlantic, seasonal prediction

©2019. Japan Geoscience Union. All Right Reserved.

Relationships Among Inter-model Spread and Biases in Tropical Atlantic Sea Surface Temperatures

Elsa - Mohino Harris[1], *Belen Rodriguez-Fonseca[1,2], Teresa - Losada[1], Irene - Polo[1], Roberto - Mechoso[3]

1. Department of Physics of the Earth and Astrophysics, Universidad Complutense de Madrid, 28040, Madrid, Spain. , 2. Institute of Geosciences IGEO,UCM-CSIC, 28040, Madrid, Spain., 3. Department of Atmospheric and Oceanic Sciences, UCLA, Los Angeles, USA

State-of-the-art general circulation models show important systematic errors in their simulation of sea surface temperatures (SST), especially in the Tropical Atlantic. In this work the spread in the simulation of climatological SST in the Tropical Atlantic by 24 CMIP5 models is examined, and its relationship with the mean systematic biases in the region is explored. The modes of inter-model variability are estimated by applying Principal Component (PC) analysis to the SSTs in the region 70ºW-20ºE, 20ºS-20ºN. The inter-model variability is approximately explained by the first three modes. The first mode is related to warmer SSTs in the basin, shows worldwide connections with same-signed loads over most of the tropics and is connected with lower low cloud cover over the eastern parts of the subtropical oceans. The second mode is restricted to the Atlantic, where it shows negative and positive loads to the north and south of the equator, respectively, and is connected to a too weak Atlantic Meridional Overturning Circulation (AMOC). The third mode is related to the double Intertropical Convergence Zone bias in the Pacific and to an interhemispheric asymmetry in the net radiation at the top of the atmosphere. According to the results, the most important of these contributors for SST biases spread in the Tropical Atlantic is the second mode, with models having stronger biases simulating weaker AMOCs.

Keywords: GCM bias, CMIP5, tropical Atlantic, intermodel spread

©2019. Japan Geoscience Union. All Right Reserved.

Revisiting the CMIP5 Thermocline in the Equatorial Pacific and Atlantic Oceans

Antonio - Castaño[1,2], Elsa - Mohino[1], *Belen Rodriguez-Fonseca[1,2], Teresa - Losada[1]

1. Department of Physics of the Earth and Astrophysics, Universidad Complutense de Madrid, 28040, Madrid, Spain., 2. Institute of Geosciences, IGEO, UCM-CSIC 28040, Madrid, Spain.

The thermocline is defined as the ocean layer for which the vertical thermal gradient is maximum. In the equatorial ocean, observations led to the use of the 20˚C isotherm depth (z20) as an estimate of the thermocline. This work compares z20 against the physical thermocline in the Equatorial Atlantic and Pacific Oceans, using SODA reanalysis and CMIP5 Pre-Industrial Control simulations. Our results show that in models z20 is systematically deeper and flatter than the thermocline and does not respond correctly to surface wind stress variations. It is also shown that the annual cycle of z20 is much weaker than that of the physical thermocline. This happens in both equatorial basins and indicates that z20 does not react to the same mechanisms as the thermocline. Possible consequences in the assessment of air-sea coupling in current GCMs and bias reduction strategies are also suggested, as well as possible effects in the representation of upwelling systems in the tropical region.

Keywords: CMIP5, defining thermocline, tropical atlantic, air-sea interactions

©2019. Japan Geoscience Union. All Right Reserved.

Lagged Effects of North Atlantic SST Anomalies on Weather in Remote Areas

*Natalia Gnatiuk[1], Timo Vihma[2], Leonid Bobylev[1]

1. Nansen International Environmental and Remote Sensing Centre, 2. Finnish Meteorological Institute

Polar climate has experienced dramatic changes during observed global warming. These changes in turn have, as hypothesised, strong influences on the mid-latitude weather. Many proposed linkages focus on the effects of changes in sea ice, sea surface temperature or terrestrial snow pack on the air temperature in selected mid-latitude areas. Our hypothesis is that from the point of view of the atmosphere, it does not matter whether the thermal forcing from the surface originates from sea ice melt, terrestrial snow melt, or changes in SST. Most important is to quantify how the atmosphere responds to anomalies in surface temperature, and how the local/regional responses may affect weather patterns in remote areas. By analysing these responses systematically in global scale, we can identify the regions and seasons where/when the response is strongest. Comparing these regions/seasons to observed changes in sea ice, terrestrial snow, and open ocean SST, we will obtain information on the relative importance of forcing from these three factors. For this purpose, we studied the relationships between anomalies in the surface temperature (Ts) in the Northern Hemisphere (on grid 1.5^{o}-1.5^{o}) and 2-m air temperature (T2m) in selected 13 study regions in Europe, Greenland, and parts of Asia and North Africa for the period 1979-2018 based on the ERA-Interim reanalysis. Applying also detrended data, we eliminated spurious correlations resulting from similar trends in the two variables.

We detected significant correlations between the surface temperature over the Labrador Sea, Canadian archipelago and North Atlantic and 2-m air temperature in different study regions for inter-seasonal spring - summer (MAM-JJA) and autumn - winter (SON-DJF) relationships. Among the strongest correlations between the spring Ts and summer T2m were the positive correlations found between Ts in the North Atlantic and T2m in Scandinavia, Ts in the Labrador Sea and T2m in Northeast Europe, and Ts in Norther Sahara and T2m in Urals. As well, among the strongest correlations between the autumn Ts and winter T2m were the positive correlations found between Ts in the North Atlantic and the Labrador Sea and T2m in Scandinavia and Northwest Africa; and the negative correlations found between Ts in the Labrador Sea and the North Atlantic and T2m in Scandinavia, Northeast Europe, Urals, Black Sea region and Northcentral Asia.

In order to identify thermal forcing factors and to assess their relative importance, we analysed the multiyear averages and anomalies of sea-ice concentration, snow cover and surface heat fluxes. According to the results, in all identified cases, changes in SST mostly were an influencing factor.

Another big challenge was to understand the physical mechanisms responsible for the obtained statistical results. For this purpose, we analysed surface pressure, geopotential heights, wind components, air-mass trajectories, incoming solar radiation, cloud cover, and total precipitation for sub-sets of 10 coldest and 10 warmest seasons in the period 1979-2018. There is a detectable effect on anomalies in the atmospheric pressure field and wind components in these regions.

The research is granted by the “ERA.Net RUS Plus” Initiative, ID 166 and national RFBR project No. 18-55-76004; and partly by RSF grant №. 17-17-01151.

©2019. Japan Geoscience Union. All Right Reserved.

Keywords: Sea surface temperature anomalies, Teleconnections, Mid-latitude weather, North Atlantic

©2019. Japan Geoscience Union. All Right Reserved.

SST anomalies in the northern tropical Atlantic as a negative feedback to ENSO development

*Ingo Richter[1], Hiroki Tokinaga[2], Yu Kosaka[3], Takeshi Doi[1]

1. JAMSTEC Japan Agency for Marine-Earth Science and Technology, 2. Kyoto University, 3. University of Tokyo

It has been known for some time that SST anomalies in the equatorial Pacific induce same-signed anomalies in the northern tropical Atlantic (NTA) through changes in the Atlantic trade winds. More recently, it has been suggested that the NTA, in turn, can influence the equatorial Pacific through changes in the surface zonal winds over the western part of the basin. The sign of these wind anomalies, however, would act to force equatorial Pacific SST anomalies that are opposite to those in the NTA. The present study takes a closer look at this apparent conundrum by conducting GCM experiments with prescribed SSTs for the period 1982-2014. In the control experiment, observed SSTs are prescribed globally, while in two sensitivity experiments SST anomalies are removed from either the tropical Atlantic or the tropical Pacific. For the control experiment, analysis suggests that NTA warming is accompanied by SST warming and westerly wind anomalies in the equatorial Pacific. When tropical Pacific SST anomalies are removed, on the other hand, NTA warming coincides with easterly anomalies. Moreover, when SST anomalies are removed from the tropical Atlantic, wind variability over the western equatorial Pacific is enhanced. These results suggest that SST anomalies in the NTA, which are strongly influenced by the tropical Pacific, act as a negative feedback to ENSO development. This interbasin link may be further complicated by other influences on the NTA, such as local air-sea coupling and the North Atlantic Oscillation.

Keywords: tropical Atlantic, ENSO, teleconnections

©2019. Japan Geoscience Union. All Right Reserved.

[E] Poster | A (Atmospheric and Hydrospheric Sciences)：A-HW Hydrology & Water Environment

Thu. May 30, 2019 3:30 PM - 5:00 PM JST | Thu. May 30, 2019 6:30 AM - 8:00 AM UTC | Poster Hall International Exhibition Hall8, Makuhari Messe_5

[A-HW22] Materials transport and nutrient cycles in watersheds; from headwaters to coastal seas

convener:Masahiro Kobayashi(Forestry and Forest Products Research Institute), Seiko Yoshikawa(Institute for Agro-environmental Sciences, National Agriculture and Food Research Organization), Jun Yasumoto(University of the Ryukyus, Faculty of Agriculuture), Adina Paytan(University of California Santa Cruz)

This session aims to synthetize watershed sciences in order to understand dynamical processes of materials transport and nutrient cycles in watersheds from headwaters to coastal seas. The session will be integrating a variety of research disciplines including limnology, ground water hydrology, coastal oceanography, meteorology, pedology, sedimentology, forestry, agriculture, fishery, ecology, social science and more. This session calls for ideas on new methods for the watershed sciences, such as tracer and molecular technique, hydrological modeling, paleontological approaches, laboratory and field experiments, social-scientific evaluation of ecosystem services and social-ecological systems, and so on, in order to elucidate physical, chemical and biological mechanisms for shedding light on natural phenomena and their changes over time in complex and dynamic watershed systems under human and climate impacts. Through this session, we would like to facilitate interdisciplinary collaboration among participants to create new knowledge on watershed sciences.

[AHW22-P01] Phosphate Enrichment Hampers Development of Juvenile Acropora digitifera Coral by Inhibiting Skeleton Formation

Mariko Iijima[1], *Yasumoto Ko[1], Jun Yasumoto[2], Mina Hirose[3], Mitsuru Jimbo[1], Shugo Watabe[1] (1.Kitasato University School of Marine Biosciences, 2.Faculty of Agriculture, University of the Ryukyus, 3.Tropical Technology Plus)

[AHW22-P02] Modeling chlorophyll-a concentration using remote sensing in shallow water systems: Comparison of sensors

*Assefa M Melesse[1], Tara Blakey[1], Mohammad Haji Gholizadeh[1], Mohd Manzar Abbas[1] (1.Florida International University)

[AHW22-P03] Dynamics in groundwater flow system with seasonal water table variation in a coastal and island

*Yusuke Tomozawa[1], Shin-ichi Onodera[1], Mitsuyo Saito[2] (1.Graduate School of Integrated Arts and Sciences Hiroshima University, 2.Graduate School of Environmental and Life Science, Okayama University)

[AHW22-P04] The Tracing of Groundwater Contamination Sources in Indonesian Coastal Alluvial Groundwater using $\delta^{34}S$ and $\delta^{15}N$ Isotopes

*Anna Fadliah Rusydi[1,4], Mitsuyo Saito[2], Seiichiro Ioka[3], Shin-ichi Onodera[1] (1.Graduate School of Integrated Arts and Sciences, Hiroshima University, Japan, 2.Graduate School of Environmental and Life Sciences, Okayama University, Japan, 3.Research Institute for Sustainable Energy, Hirosaki University, Japan, 4.Research Center for Geotechnology, Indonesian Institute of Sciences, Indonesia)

[AHW22-P05] Spatio-temporal dynamics of orthophosphate with implications for limitation of phytoplankton growth in north basin of Lake Biwa, Japan

*Xin Liu[1], Rong Yi[1], Masahiro Maruo[1], Syuhei Ban[1] (1.The University of Shiga Prefecture)

[AHW22-P06] Microbial phase analysis in aquifer of Ryukyu Limestone Zone using next generation sequencer

*Umi Murao[1], Jun Yasumoto[1], Yasumoto Ko[3], Mina Hirose[2], Nanami Mizusawa[3], Ryo Iguchi[4], Bam H.N. Razafindrabe[5], Syugo Watabe[3] (1.University of the Ryukyus, Faculty of Agriculuture Department of Regional Agricultural Engineering, 2.Tropical Tecnology Plus, 3.Kitasato University School of Marine Biosciences, 4.National Institute of Advanced Industrial Science and Technology, 5.University of the Ryukyus, Faculty of Agriculuture Department of Subtropical Agro-Environmental Sciences)

[AHW22-P07] Evaluation for temporal variation in groundwater inflow to the lagoons connected to Lake Biwa by radon (^{222}Rn) tracer analysis

*Mitsuyo Saito[1], Shin-ichi Onodera[2], Yusuke Tomozawa[2], Kunyang Wang[2], Syuhei Ban[3], Noboru Okuda[4] (1.Graduate School of Environmental and Life Science, Okayama University, 2.Graduate School of Integrated Arts and Sciences, Hiroshima University, 3.School of Environmental Sciences, The University of Shiga Prefecture, 4.Research Institute for Humanity and Nature)

[AHW22-P08] Br/Cl ratio characteristics of groundwater in coastal areas in Indonesia

*Seiichiro Ioka[1], Shin-ichi Onodera[2], Mitsuyo Saito[3], Anna Fadliah Rusydi[2,4] (1.Institute of Regional Innovation, Hirosaki University, Japan, 2.Graduate School of Integrated Arts and Sciences, Hiroshima University, Japan, 3.Graduate School of Environmental and Life Sciences, Okayama University, Japan, 4.Research Center for Geotechnology, Indonesian Institute of Sciences, Indonesia)

[AHW22-P09] Estimation of groundwater recharge and phosphorus transport under different precipitation conditions in a suburban catchment, using SWAT model

*Kunyang Wang[1,2], Shin-ichi Onodera[1], Mitsuyo Saito[3], Noboru Okuda[4], Takuya Okubo[5] (1.Graduate School of Integrated Arts and Science, Hiroshima University, 2.Capital Normal University, 3.Okayama University, 4.Research Institute for Humanity and Nature, 5.University of the Shiga Prefecture)

[AHW22-P10] Losses of phosphorus with soil erosion and nitrate with groundwater recharge in an agricultural catchment, subtropical small island

*Shin-ichi Onodera[1], Mitsuyo Saito[2], Yang Cao[1], Anna Fadliah Rusydi[1], Hide Omae[3], Yoshiko Iizumi[4], Yusuke Tomozawa[1] (1.Graduate School of Integrated and Arts Sciences, Hiroshima University, 2.Graduate School of Environmental and Life Science, Okayama University, 3.JIRCAS TARF, 4.JIRCAS HQ)

[AHW22-P11] Phosphate solubilizing bacteria as an indicator of sediment phosphorus in freshwater lakes

*Sreekumari Kurissery[1], Katelynn Crawford[1], Nandakumar Kanavillil[1] (1.Lakehead University, Canada)

[AHW22-P12] A Study on the dynamics of various phosphate forms in soil and groundwater in Ryukyu limestone regions

*Masashi Nozaki[1], Jun Yasumoto[2], Yasumoto Ko[3], Hirose Mina[4], Iijima Mariko[3], Ryuichi Shinjo[5], Bam H.N. Razafindrabe[6] (1.University of The Ryukyus, Graduate School of Agriculture,, 2.University of the Ryukyus, Faculty of Agriculture, Department of Regional Agricultural Engineering, 3.Kitasato University School of Marine Biosciences, 4.Tropical Technology Plus, 5.Department of Physics and Earth Sciences, University of the Ryukyus, 6.University of the Ryukyus, Faculty of Agriculture, Department of Subtropical Agro-Environmental Sciences)

[AHW22-P13] Impacts of highly concentrated turbid water on the groundwater in the Tedori River alluvial fan, Japan

*Yoichi Fujihara[1], Shunsuke Chono[1], Keiji Takase[1], Eiji Ichion[1] (1.Department of Environmental Science, Ishikawa Prefectural University)

[AHW22-P14] Altitude effect of water stable isotopic ratio of ravine water and its contribution to groundwater in alluvial plains - Comparison in east and west side catchments of Lake Biwa –

*Yusuke Tomozawa[1], Kunyang Wang[1], Mitsuyo Saito[2], Syuhei Ban[3], Noboru Okuda[4], Shin-ichi Onodera[1] (1.Graduate School of Integrated Arts and Sciences Hiroshima University, 2.Graduate School of

Environmental and Life Science, Okayama University, 3.School of Environmental Science, The University of Shiga Prefecture, 4.Research Institute for Humanity and Nature)

[AHW22-P15] Calculation of TN and TP concentration coefficients of river water for each land use by a simple watershed model.

*Seiko Yoshikawa[1], Donglai Ma[1,4], Tadamasa Saito[1,5], Kenji Matsumori[2], Yuko Itoh[3], Masahiro Kobayashi[3] (1.Institute for Agro-environmental Sciences, National Agriculture and Food Research Organization, 2.Western Region Agricultural Research Center, National Agriculture and Food Research Organization, 3.Forestry and Forest Products Research Institute, 4.Graduate school,Tsukuba University, 5.Faculty of Agriculture, Ibaraki University)

[AHW22-P16] **Possibility of nutrients transportation from littoral slope for enhancement of phytoplankton growth in north basin of Lake Biwa**

*Syuhei Ban[1], Rong YI[1], Xin Liu[1], Masahiro Maruo[1], Miki Sudo[1], Naoshige Goto[1], Jun Murase[2] (1.The University of Shiga Prefecture, 2.Nagoya University)

[AHW22-P17] SWAT model analysis for confirming the effects of crop growth on the suspended sediment concentration from a settling basin catchment on Ishigaki island

*Yang Cao[1], Shin-ichi Onodera[1], Mitsuyo Saito[2], Hide Omae[3], Yoshiko Iizumi[3] (1.Graduate School of Integrate Arts and Sciences, Hiroshima University, 2.Graduate School of Environmental and life Science, Okayama University, 3.Tropical Agriculture Research Front (TARF), Japan International Research Center for Agricultural Sciences (JIRCAS))

[AHW22-P18] Estimating the runoff of water, sediment, and nutrient using SWAT model in Kikuchi-river watershed, Kumamoto, and the influence of the forest

*Soichiro Fujii[1], Masahiko Kanamori[1], Yuko Nagano[1], Maki Kinoshita[2], Yuta Shimizu[3], Shin-ichi Onodera[4] (1.Japan Forest Technology Association, 2.PASCO Corporation, 3.Western Region Agricultural Research Center, National Agriculture and Food Research Organization, 4.Graduate School of Integrated and Arts Sciences, Hiroshima University)

[AHW22-P19] Atmospheric depositions on forest ecosystems in areas along the Sea of Japan

*Yuko Itoh[1], Keiji Takase[2], Yoichi Fujihara[2], Toru Okamoto[1] (1.Forestry and Forest Products Research Institute, Japan, 2.Ishikawa Prefectural University)

[AHW22-P20] Continuous and simultaneous flux measurement of N_2O and CO_2 from agricultural soil using a portable multi-turn time-of-flight mass spectrometer

*Noriko Nakayama[1], Yusuke Iwai[1], Yo Toma[2], Hiroshi Furutani[1], Ryusuke Hatano[3], Michisato Toyoda[1] (1.Osaka University, 2.Ehime University, 3.Hokkaido University)

[AHW22-P21] Effects of introduction of cyclic irrigation system on mass balances of SS and T-P in Lake Inbanuma, Chiba, Japan

*Tomijiro Kubota[1] (1.National Agriculture and Food Research Organization, Institute for Rural Engineering)

Phosphate Enrichment Hampers Development of Juvenile Acropora digitifera Coral by Inhibiting Skeleton Formation

Mariko Iijima[1], *Yasumoto Ko[1], Jun Yasumoto[2], Mina Hirose[3], Mitsuru Jimbo[1], Shugo Watabe[1]

1. Kitasato University School of Marine Biosciences, 2. Faculty of Agriculture, University of the Ryukyus, 3. Tropical Technology Plus

Coral reef degradation resulting from various types of local stress on corals such as excessive nutrient enrichment in and gravel inflow into coastal waters is of an increasing global concern. Because tropical and subtropical seawaters are generally poor in nutrients and thus oligotrophic, these stresses are thought to result in the decline of environments favorable to coral growth. Inorganic phosphates have been especially considered to possibly inhibit the formation of coral skeleton. Despite many studies available on the effects of nutrients on corals, a clear consensus for how nutrients exert deteriorative effects on the corals has not been established satisfactorily. Recently, we found that biogenic polyamines react with carbon dioxide (CO_2) and accelerate an aragonite formation of calcium carbonate ($CaCO_3$) in seawater. In this study, we examined the effects of phosphates and nitrates on *in vitro* aragonite formation of $CaCO_3$ by using biogenic polyamines and *in vivo* aragonite formation of juvenile coral *Acropora digitifera* skeletons, showing that phosphates clearly inhibited both *in vitro* and *in vivo* $CaCO_3$ formations at similar concentrations. In contrast, nitrates inhibited neither *in vitro* aragonite formation of $CaCO_3$ nor *in vivo* aragonite formation of juvenile coral skeletons. These findings indicate that phosphates have a detrimental effect on bioinorganic coral calcification. Furthermore, the findings that phosphate enrichment inhibits coral skeleton formation led us to conclude that enriched phosphate is adsorbed on juvenile coral skeleton surface and inhibits inorganically normal development of juvenile coral skeleton.

Keywords: phosphate, calcification

©2019. Japan Geoscience Union. All Right Reserved.

Modeling chlorophyll-a concentration using remote sensing in shallow water systems: Comparison of sensors

*Assefa M Melesse[1], Tara Blakey[1], Mohammad Haji Gholizadeh[1], Mohd Manzar Abbas[1]

1. Florida International University

The level of productivity in the upland and coastal water bodies is highly linked to land processes (land use, water management, water and nutrient fluxes). Understanding the linkage between these processes and the level of algal blooms in the water bodies is crucial for improving water quality. A comparative study was conducted using remote sensing data from three different sensors (SeaWIFS, MoDIS and Landsat) to evaluate the capability of reflectance data from these sensors for estimation of chl-a concentrations in three water bodies in the USA (Lake Okeechobee, Florida Bay and Chesapeake Bay). Observed chl-a data were gathered and compared with simulation results. The analysis found that all of the sensors have performed well in deeper water bodies than in shallow sections due to the bottom reflectance from non-algal blooms. For shallow water bodies, selection of the proper bands and band combinations, identification of the non-algal bloom reflectance and the corresponding algorithms can improve the simulation. Seasonality as well as spatial variability (using cross-sections) were evaluated and the results showed that chl-a values were highly variable for the selected summer months. Indicative of the effect of land surface fluxes of nutrients, chl-a values were higher closer to coastal areas in the Florida bay and Chesapeake Bay. The chl-a in the freshwater lake of Okeechobee was simulated using Landsat 8 data and the results found were very good. Comparison of the SeaWIFS and MoDIS chl-a value to that of the measured concentrations in the deeper section of Florida Bay and Chesapeake Bay, respectively showed very good agreement.

Keywords: Chl-a, SeaWIFS, Water qulity modeling, South Florida, Remote sensing

©2019. Japan Geoscience Union. All Right Reserved.

Dynamics in groundwater flow system with seasonal water table variation in a coastal and island

*Yusuke Tomozawa[1], Shin-ichi Onodera[1], Mitsuyo Saito[2]

1. Graduate School of Integrated Arts and Sciences Hiroshima University, 2. Graduate School of Environmental and Life Science, Okayama University

In islands, freshwater water resources are valuable as living and agricultural use, and dug wells water and reservoirs had been utilized for more than 100 years. In order to use such water resources sustainably, it is important to evaluate groundwater flow as well as water budget.

In this research, we examined to confirm the seasonal variation in water stable isotopic ratios in observation boreholes at the coastal lowland in Ikuchi Island Hiroshima prefecture. Moreover, considering that the target area is coastal, Cl^- concentration was analyzed to evaluate the influence of salt fresh water boundary.

The experimental site is located on Ikuchi Island in Hiroshima prefecture. The highest altitude is 456 m. The basement rock is mainly composed of granite. Annual average precipitation is 1058.8 mm. Observation boreholes are located at the coastal lowland in the southeastern part of the island. The upper site (Site U) with the altitude of 5.1 m asl has 3 boreholes with the depths of 2 m, 15 m, 30 m, the lower site (Site D) with 2.5 m asl has 8 with the depth of 1 m, 2 m, 3 m, 10 m, 15 m, 20 m, 30 m, 40 m, respectively. The water sampling was carried out from monthly to half year interval since 2015. Every samples were analyzed for water isotopic ratios by PICARO and anion component by ion chromatography. Especially samples in January in 2019 were analyzed for CFCs and SF6.

Based on the previous study (Saito and Onodera, 2007), the distinct altitude effect of isotopic ratio in precipitation has been confirmed. Due to spatial and temporal variations in isotopic ratios, recharge process to groundwater was suggested as follows, 1) recharge on site to shallow groundwater (2-3m deep) at D ($\delta^{18}O$: -7.8 to - 7.4 ‰), 2) river water contribution to the shallow groundwater (2-15m) at U ($\delta^{18}O$: - 8.3 to - 7.5 ‰), 3) recharge in the mountain slope with the altitude of about 360 m to deep groundwater (30m) at U ($\delta^{18}O$: - 8.4 to - 8.1 ‰), 4) recharge at 400 m on near the mountain top to deep groundwater (10-30 m) at D($\delta^{18}O$: - 8.7 to - 8.4 ‰), 5) recharge of precipitation with lower isotope than in present to deeper groundwater (40 m) at D ($\delta^{18}O$: -8.9 to - 8.8 ‰)

The deepest groundwater (40m) at D had lower isotopic ratios with higher Cl^- concentration (250 to 584 mg / L) during a lower water table in the winter. This indicated the seawater –fresh water boundary rose with water table according to Gyben-Hrzberg concept. These phenomena also suggest to cause the rise of deeper and older groundwater flow line. Consequently, we suggest the lower isotopic ratio in deeper groundwater indicates the immobile water which were recharged in the glacial period. Based on other tracers (CFC, SF 6), we will discuss more.

Keywords: stable isotope, groundwater, coastal

©2019. Japan Geoscience Union. All Right Reserved.

The Tracing of Groundwater Contamination Sources in Indonesian Coastal Alluvial Groundwater using $\delta^{34}S$ and $\delta^{15}N$ Isotopes

*Anna Fadliah Rusydi[1,4], Mitsuyo Saito[2], Seiichiro Ioka[3], Shin-ichi Onodera[1]

1. Graduate School of Integrated Arts and Sciences, Hiroshima University, Japan, 2. Graduate School of Environmental and Life Sciences, Okayama University, Japan, 3. Research Institute for Sustainable Energy, Hirosaki University, Japan, 4. Research Center for Geotechnology, Indonesian Institute of Sciences, Indonesia

The coastal area is one of the Indonesian Government priorities as an archipelago country. The groundwater in the area is one of the most reliable clean water resources, therefore it is crucial to understanding the vulnerability of this resource. Our research area was located at Indramayu, a developing rural coastal area in Indonesia, where, the environment was relatively pristine. This research aimed was to identify the effect of natural condition and human activity to groundwater quality by using stable isotope $\delta^{34}S$ and $\delta^{15}N$.

Totally, there were 20 samples taken from groundwater (18) and river (2). The nitrate and sulfate were detected in a total of 5 and 19 samples, respectively. The isotopes composition for isotope nitrate were -11.2 ‰–+22.22‰ for $\delta^{15}N\text{-}NO_3$ and -3.4 ‰–+17.1‰ for $\delta^{18}O\text{-}NO_3$. Moreover, the values of $\delta^{34}S\text{-}SO_4$ and $\delta^{18}O\text{- }SO_4$ were varied from -4.2 ‰–+28.4‰ and +7.3 ‰–+18.8 ‰, respectively. The isotopic signatures of nitrate suggested that the used of inorganic fertilizer and animal manure give the impact to both groundwater and river. Similarly, the isotopic signatures of sulfur were showing that those detected sulfate in the groundwater were mostly coming from fertilizer. Moreover, the soil was mineralized by organic sulfate as well. At one point, located in the fishery area, the groundwater was indicated the seawater contamination. It was shown by the heavy composition of sulfur isotope (28.4‰ for $\delta^{34}S$ and 18.8‰ for $\delta^{18}O$). Lastly, our results showed those combined isotopes of $\delta^{34}S$ and $\delta^{15}N$ along with land-use evaluation could explain the possible sources of groundwater in coastal area at very early urbanization stage.

Keywords: Sulfur Isotope, Nitrate Isotope, Coastal Groundwater, Indramayu

©2019. Japan Geoscience Union. All Right Reserved.

Spatio-temporal dynamics of orthophosphate with implications for limitation of phytoplankton growth in north basin of Lake Biwa, Japan

*Xin Liu[1], Rong Yi[1], Masahiro Maruo[1], Syuhei Ban[1]

1. The University of Shiga Prefecture

Orthophosphate (PO_4-P) is the main chemical form of phosphorus (P) for phytoplankton growth, often considered as a limiting nutrient for primary production in freshwater ecosystems. However, few information on accurate measurements for PO_4-P concentrations in epilimnion of meso- and oligotrophic lakes due to lower than the detection limit (60 nM) of soluble reactive P using traditional spectrophotometrical method. In the present study, we measured PO_4-P concentrations using ion chromatography with a detection limit of 5 nM, and determined truly vertical distribution of PO_4-P throughout the year with other abiotic and biotic environmental factors in north basin of Lake Biwa, to accurately understand biogeochemical processes of P in this mesotrophic lake.

Field investigations were conducted monthly from April to December 2018 at station K4 (35º19'9.6"N, 136º11'2.7"E; 50 m deep). Phosphate enrichment experiments were also made at each sampling occasion to clarify P limitation for phytoplankton growth. Lake water including phytoplankton assemblage collected from epilimnion (0–20 m) was enriched with 1 μM of PO_4-P (+P) and incubated together with untreated one (control) for 2 days under ambient light and temperature conditions. To evaluate the effect of potentially nutrient-rich bottom water, the filtered bottom water was mixed with untreated epilimnion water including phytoplankton at 1:1 (+B) was incubated at the same conditions as the +P treatment. Phytoplankton growth rate (g) was calculated with equation of $g=\ln(C_t/C_0)/2$, where C_0 and C_t are chlorophyll *a* (chl. *a*) concentrations at start and end of the experiment, respectively.

Water temperature increased in the epilimnion from May, and strict thermocline was developed from June to September. Chl. *a* concentrations increased from June to July in 10–20 m, and from October to November in 0–20 m. PO_4-P concentrations were always low, <20 nM, in the epilimnion from April to June. The concentrations below 30 m increased up to 140 nM in May, but decreased after that until July. In August and September, the concentrations increased up to 30–40 nM even in the epilimnion probably due to disturbance by typhoon. The concentrations below 30 m increased with depth, and the highest values were frequently observed near the bottom, up to 220 nM. On average throughout the water column, PO_4-P concentrations were 24–48 nM from April to June, then slightly increased up to 73 nM until September, being constant, 50–63 nM until December.

Total P, total dissolved P, dissolved organic P and particulate P exhibited similar spatio-temporal distributions, but different pattern from those of PO_4-P. NH_4-N increased in 10–20 m from May to July, whereas the NO_3-N increased in the hypolimnion as season progressed. Sestonic C:N:P ratios suggested a terrible P deficiency in July and October when phytoplankton biomass increased.

Phosphate enrichment experiments showed that phytoplankton in the epilimnion was mostly limited with P for its growth. Phytoplankton g in control varied −0.05-0.08 d^{-1}, being always lower than those in +P (−0.04-0.44 d^{-1}) and/or +B (−0.04-0.49 d^{-1}) treatments except for November and December. In November, no growth was found even in +P treatment. This might be caused by nitrogen limitation because of <6 μM of NO_3-N in the epilimnion. The g of control was similar as that of +P and +B (ca. 0.1 d^{-1}) in December, indicating that P deficiency for phytoplankton growth was relaxed until December by vertical convection.

©2019. Japan Geoscience Union. All Right Reserved.

We firstly determined completely vertical distributions of PO_4-P in north basin of Lake Biwa from spring to winter, and detected 20–40 nM of PO_4-P in the epilimnion. Phosphate enrichment experiments showed that 20 nM of PO_4-P might be critical concentration for phytoplankton growth in the lake. No phytoplankton growth even in +P treatment in November implied that nitrogen limitation for phytoplankton growth will be possible in Autumn. Further study for clarify this will be needed.

Keywords: Orthophosphate dynamics, Phosphorus limitation, Phytoplankton growth rate, Ion chromatography, Biogeochemical processes, Freshwater ecosystem

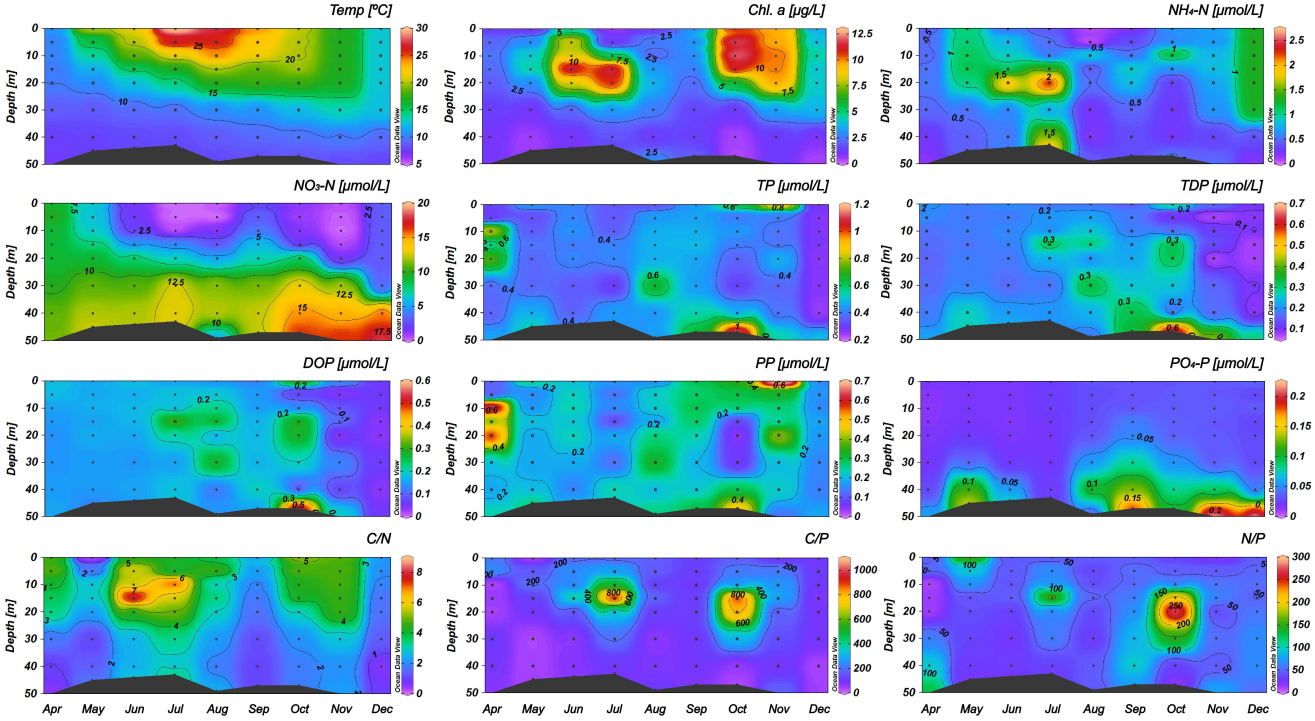

©2019. Japan Geoscience Union. All Right Reserved.

Microbial phase analysis in aquifer of Ryukyu Limestone Zone using next generation sequencer

*Umi Murao[1], Jun Yasumoto[1], Yasumoto Ko[3], Mina Hirose[2], Nanami Mizusawa[3], Ryo Iguchi[4], Bam H.N. Razafindrabe[5], Syugo Watabe[3]

1. University of the Ryukyus, Faculty of Agriculuture Department of Regional Agricultural Engineering, 2. Tropical Tecnology Plus, 3. Kitasato University School of Marine Biosciences, 4. National Institute of Advanced Industrial Science and Technology, 5. University of the Ryukyus, Faculty of Agriculuture Department of Subtropical Agro-Environmental Sciences

Clean water and sanitation (Sustainable development Goals (6)) is one of the world's important issues. People use groundwater in many areas as a water source, but various cases of contamination by agricultural activities and substances derived from human and animal excrements have been reported.

On the other hand, genetic analysis techniques using molecular biological methods have been applied to the analysis of microbial phase in the water environment.

In recent years, the method using the latest analysis equipment of next generation Sequencer is established, mainly for microorganisms. In addition, new monitoring indices such as environmental DNA have been developed. It is thought that the microbial phase in groundwater varies depending on the influence of various environmental factors and human activity, but the actual condition is not clear.

The next generation Sequencer is a very powerful tool used to grasp the microbial phase in groundwater. It is thought that the microbial phase can be an important indicator in water resource management of basins in the future.

The purpose of this study is to investigate the microbial species and their coexistence in groundwater in the Ryukyu Limestone area using the next generation sequencer.

Keywords: groundwater, microbial community analysis, genetic analysis

©2019. Japan Geoscience Union. All Right Reserved.

Evaluation for temporal variation in groundwater inflow to the lagoons connected to Lake Biwa by radon (^{222}Rn) tracer analysis

*Mitsuyo Saito[1], Shin-ichi Onodera[2], Yusuke Tomozawa[2], Kunyang Wang[2], Syuhei Ban[3], Noboru Okuda[4]

1. Graduate School of Environmental and Life Science, Okayama University, 2. Graduate School of Integrated Arts and Sciences, Hiroshima University, 3. School of Environmental Sciences, The University of Shiga Prefecture, 4. Research Institute for Humanity and Nature

Primary production in freshwater lakes and reservoirs are usually controlled by phosphorus (P). Lacustrine groundwater discharge (LGD), direct discharge of subsurface water to lake, is regarded as a potential nutrient paths, including phosphorus from a catchment to lake water environment. There are more than 20 lagoons around Lake Biwa which were originally a part of the lake. These lagoons are regarded to have important functions as settling ponds of inflowing loads from the catchments to Lake Biwa, refuges for shallow water ecosystems and so on. Because these lagoons are connected to Lake Biwa, evaluation of nutrient budget is important for the nutrient cycle in the lake. Some researchers have pointed out the presence of LGD in littoral area of Lake Biwa. However, it has not been evaluated for the lagoons around the lake. In the present research, we aimed to evaluate the temporal variation in groundwater inflow to a lagoon connected to Lake Biwa by radon (^{222}Rn) tracer analysis.

The field campaigns were conducted in December 2017, August and October 2018 for the lagoons (Noda-Numa and Hasu-Ike) located on northeastern shore of Lake Biwa. The volume of inflow and outflow, water temperature, electric conductivity, chlorophyll-a and radon (^{222}Rn) concentration were measured in the lagoon. ^{222}Rn is a radioactive element of uranium (^{238}U) series with 3.8 day of half-life. ^{222}Rn is a useful tracer of groundwater discharge because it generally enriched in groundwater than surface water. To examine the temporal variation in groundwater inflow, the time-series ^{222}Rn concentration in water was obtained. Water samples were collected at the inlet, outlet and near the center of the lagoons and natural springs and groundwater wells around the lagoons. Water and ^{222}Rn balance suggest that groundwater inflow is larger in Noda-Numa than Hasu-Ike. The catchment topography may influence on this difference. ^{222}Rn balance-based residence time of lagoon water was estimated 10-20 days in Noda-Numa, and 4-5 days in Hasu-Ike, were similar with that based on water balance. These results suggest the groundwater inflow is a potential phosphorus path to Noda-Numa.

Keywords: Groundwater inflow, Connected lagoons, Lake Biwa, Radon (222Rn)

©2019. Japan Geoscience Union. All Right Reserved.

Br/Cl ratio characteristics of groundwater in coastal areas in Indonesia

*Seiichiro Ioka[1], Shin-ichi Onodera[2], Mitsuyo Saito[3], Anna Fadliah Rusydi[2,4]

1. Institute of Regional Innovation, Hirosaki University, Japan, 2. Graduate School of Integrated Arts and Sciences, Hiroshima University, Japan, 3. Graduate School of Environmental and Life Sciences, Okayama University, Japan, 4. Research Center for Geotechnology, Indonesian Institute of Sciences, Indonesia

The urban development in Indonesia’ s coastal areas has led to an increase of groundwater demand, which then has resulted in groundwater salinization. In this study, we analyze bromide and Br/Cl ratio characteristics, as index of groundwater salinization, in three cities of Indonesian coastal areas, namely: Indramayu, Mataram, and Semarang. Each research site is at different stage of urbanization. Indramayu is in very early stage of urbanization, followed by Mataram as a developing tourism area, and the last one Semarang as a heavy urbanization city. The results show that concentrations of bromide in groundwater are ranged from 0.05 to 38 mg/L in Indramayu, 0.01 to 0.8 mg/L in Mataram, and 0.02 to 8.0 mg/L in Semarang. Furthermore, the occurrence of Br is described in terms of the Br/Cl weight ratio, which allows for small changes in bromide concentrations to be assessed in terms of salinity. Median values of Br/Cl weight ratio in the groundwater of Indramayu, Mataram, and Semarang were approximately 0.0035, 0.0027, and 0.0025, respectively, while the ratio in seawater is generally around 0.0035. The relationship between Br/Cl weight ratio and chloride concentration indicate the groundwater in Indramayu is undergoing salinization due to seawater intrusion compared to the other two areas, meanwhile the groundwater in Semarang is experiencing chloride contamination due to anthropogenic activities based on the study by Andreasen and Fleck (1997).

Keywords: Indonesia, groundwater, Br/Cl ratio, coastal area

©2019. Japan Geoscience Union. All Right Reserved.

Estimation of groundwater recharge and phosphorus transport under different precipitation conditions in a suburban catchment, using SWAT model

*Kunyang Wang[1,2], Shin-ichi Onodera[1], Mitsuyo Saito[3], Noboru Okuda[4], Takuya Okubo[5]

1. Graduate School of Integrated Arts and Science, Hiroshima University, 2. Capital Normal University, 3. Okayama University, 4. Research Institute for Humanity and Nature, 5. University of the Shiga Prefecture

The quantification of the groundwater recharge and phosphorus transport in water is one of the most important indicators of the water cycle in lakes because these processes are related to the transport of large nutrient loads. The Yasu River is one of the important water sources of the Biwa Lake. In this paper, Geographic Information System technology is used to analyze and predict the land use change in the Yasu River Basin. The water balance was simulated using the Soil and Water Assessment Tool. Simulations of different years in different precipitation seasons were carried out. The correlation coefficient and the Nash Sutcliffe coefficient are higher than the reference values. The sensitivity analysis of the parameters reveals the different degrees of sensitivity of the parameters in different water seasons, CN2 always has a high sensitivity during all kinds of water season. The total groundwater recharge and discharge are 180 million m^3 and 179 million m^3 in the normal precipitation season, respectively. The trends differ in the dry and wet seasons. In the dry season of 2007, the groundwater recharge was below 140 million m^3, while it exceeded 240 million m^3 in the rainy season in 2003. In addition, the process of phosphorus loss in the basin and release into Lake Biwa are explained from the perspective of space and time. This is closely related to the spatial distribution of the main channel and the time distribution of precipitation. The total amount of nonpoint source pollution of phosphorus in three years is equivalent to 4.08 kg/ha of paddy fields in the watershed. The spatial distribution of phosphorus loss is related to the stream flow, it is mainly concentrated in the area with paddy fields and urban. The time distribution is related to the distribution of the precipitation. With increasing precipitation, the nonpoint source pollution of phosphorus slightly increases. This is due to the driving effect of precipitation on the phosphorus transfer and erosion of soil.

Keywords: Phosphorus transport, Groundwater recharge, Different precipitation conditions, SWAT model

©2019. Japan Geoscience Union. All Right Reserved.

Losses of phosphorus with soil erosion and nitrate with groundwater recharge in an agricultural catchment, subtropical small island

*Shin-ichi Onodera[1], Mitsuyo Saito[2], Yang Cao[1], Anna Fadliah Rusydi[1], Hide Omae[3], Yoshiko Iizumi[4], Yusuke Tomozawa[1]

1. Graduate School of Integrated and Arts Sciences, Hiroshima University, 2. Graduate School of Environmental and Life Science, Okayama University, 3. JIRCAS TARF, 4. JIRCAS HQ

In tropical and subtropical region, the rainfall intensity is strong and soil erosion in an agricultural land is one of big environmental issues. Especially, the impact of large sediment discharge on the coral reef is serious around small islands, such as Okinawa and Philippines. In case of Okinawa Prefecture, to reduce the sediment discharge and conserve corals, many sediment trap ponds are constructed in a downstream area of agricultural lands. However, sediment deposition rate, variation of trap effect, and component of sediment in a pond have not been confirmed.

To estimate of erosion rate and deposition process of a small pond in an agricultural catchment of a subtropical small island, we examine to observe the sediment deposition in a small pond and monitor water level and chlorophyll a in a pond and runoff and turbidity of an inflow stream in a small catchment with the area of 300m2 in Ishigaki Island, Okinawa Prefecture, Subtropical region. Our monitoring was started from February 2017 after removing all sediment in a pond in January, and up to April 2018. Observation of sediment deposition was conducted with collecting the samples at 5 sites in June 2017 and January 2018. Inflow and outflow water samples were collected every one month.
The sediment deposition was extremely large from January to May 2017, the average erosion rate in all catchment area was estimated to be 6mm. On the other hand, the sediment deposition was nothing from June 2017 to January 2018. Based on the monitoring of stream runoff and turbidity, one big storm event in April with strong intensity mainly contributes to sediment discharge and overflow of the pond occurred. On the other hand, the later period had also big events. This difference is suggested to be the difference of land cover by crops and availability of sediment trap in this pond. In addition, the sediment component mainly was composed of surface soft layer, subsurface sandy layer, and bottom gravel layer. The average thickness was 2cm in surface layer, 100cm in mid sandy layer, and 10cm in gravel layer, respectively. Especially, the surface soft layer had high nutrient content. The dissolved nutrient of inflow stream water and pond water were high concentration. But the 10% of nutrient in the inflow decreased in pond. This means the plankton was produced, using this nutrient and that was deposited later. The soft layer is suggested to be effect of organic fertilizer, it is expected to apply to agricultural lands.

Keywords: Phosphorus, groundwater, nitrate

©2019. Japan Geoscience Union. All Right Reserved.

Phosphate solubilizing bacteria as an indicator of sediment phosphorus in freshwater lakes

*Sreekumari Kurissery[1], Katelynn Crawford[1], Nandakumar Kanavillil[1]

1. Lakehead University, Canada

It has been well documented that phosphorus pollution is one of the most significant factors impeding the overall health of freshwater lakes. Various measures are being taken to reduce phosphorus input into the lakes by anthropogenic activities and thus to maintain a healthy ecosystem. However, it is well known that bioavailable phosphorus tends to bind with substances such as ferric iron and calcium present in the water, become insoluble, and settles into the sediments. The presentstudy has been carried out to understand the relationship between the sediment phosphorus concentration and density of phosphate solubilizing bacteria (PSB) in two lakes in Ontario, Canada, namely, Lake Simcoe and Sparrow Lake. In September 2017, 20cm sediment cores were collected from the nearshore sites of these two lakes to determine the presence of PSB in relation to the sediment phosphorus concentration. PSB could potentially release phosphorus back into the water column through a process called internal phosphorus loading from the inorganic phosphates in the sediment when the right conditions are present. PSB were isolated from the sediment cores at 5 cm intervals by plating on to Pikovskaya’ s agar. Five grams of sediment was used to analyze total reactive phosphorus in the sediment. In Lake Simcoe, PSB ranged from $3x10^1$ to $1.1x10^1$ cfu/g, and the amount of total reactive phosphorus ranged from 0.19 to 0.46 mg/g. In Sparrow Lake, PSB ranged from $4x10^0$ to $3x10^1$ cfu/g and the amount of total reactive phosphorus ranged from 0.21 to 0.39 mg/g. A linear regression was completed to determine the relationship between total reactive phosphorus and PSB for each core. The results showed a negative relationship between these two tested parameters (Lake Simcoe: r^2=0.23, $y = -35.34x + 30.811$ p=0.5206, and Sparrow Lake: r^2 =0.87, $y = -155.9x + 62.322$, p=0.067). While PSB density decreased with core depth, the concentration of reactive phosphorus increased. This indicates that the density of PSB in lake sediment may indicate the concentration of total reactive phosphorus and thus the internal phosphorus loading. More study is recommended to confirm the results.

Keywords: Phosphate Solubilizing Bacteria, Freshwater Lakes , Sediment Phosphorus , Canada

©2019. Japan Geoscience Union. All Right Reserved.

A Study on the dynamics of various phosphate forms in soil and groundwater in Ryukyu limestone regions

*Masashi Nozaki[1], Jun Yasumoto[2], Yasumoto Ko[3], Hirose Mina[4], Iijima Mariko[3], Ryuichi Shinjo[5], Bam H.N. Razafindrabe[6]

1. University of The Ryukyus, Graduate School of Agriculture,, 2. University of the Ryukyus, Faculty of Agriculture, Department of Regional Agricultural Engineering, 3. Kitasato University School of Marine Biosciences, 4. Tropical Technology Plus, 5. Department of Physics and Earth Sciences, University of the Ryukyus, 6. University of the Ryukyus, Faculty of Agriculture, Department of Subtropical Agro-Environmental Sciences

Phosphorus in water environment exists in various forms and size, such as dissolved, particulate, organic and inorganic forms. However, there are many unclear points in Phosphorus in groundwater. In this study, we tried to understand the dynamics of various phosphate forms in soil and groundwater in Ryukyu limestone regions by combining Inductively Coupled Plasma Atomic Emission Spectrometry (ICP-AES) and ^{31}P Nuclear Magnetic Resonance (^{31}P-NMR), in addition to Colorimetric (molybdenum blue method). From August 2017 to August 2018, we took groundwater samples in southern part of Okinawa, Japan, with Ryukyu limestone distribution on a monthly basis. We measured pH, electronic conductivity (EC), Oxidation-Reduction Potential (ORP), dissolved oxygen (DO) and alkalinity (HCO_3^-) on site, and analyzed major dissolved ion (Cl^-, HCO_3^-, NO_2^-, NO_3^-, SO_4^{2-}, Na^+, K^+, Mg^{2+}, Ca^{2+}), suspended solid (SS) and phosphorus concentration. Phosphorus concentration analyzed 3 different method to molybdenum blue method (Col-P), ICP-AES (ICP-P) and Total P (T-P). Phosphate form analysis used ^{31}P-NMR.
We compared Col-P and ICP-P in order to understand dissolved phosphorus spatial distribution. The results show that ICP-P is 1.06~49.24 times larger than Col-P. It is inferred that ICP-P is also measuring fine particulate phosphorus and organic phosphorus. As a result, several forms of phosphate without orthophosphate were found in groundwater. Particulate phosphorus was determined by subtracting ICP-P from T-P. A positive correlation (r= 0.78) was found between P-P and SS. According to these results, it is thought that PP adsorbs various forms of phosphate including orthophosphate. We analyzed the correlation between dissolved phosphorus (Col-P, ICP-P) and all measured value in order to understand the characteristics of seasonal variation to dissolved phosphorus. There was a negative correlation between Col-P to water temperature. When focusing on seasonal variation of Col-P, we found that Col-P concentration decreases when water temperature increases. Moreover, Col-P concentration increases as water temperature increases. Through the analysis of various forms of phosphate in soil and SS by using ^{31}P-NMR, along with orthophosphate, pyrophosphate, pyrophosphate ester, orthophosphate monoester were also detected. It is thus suggested that the phosphate of polymeric or organic forms other than orthophosphate are from plant origin, as a result of microbial activities and microorganism decomposition.

Keywords: Phosphorus, 31P-NMR, Groundwater

©2019. Japan Geoscience Union. All Right Reserved.

Impacts of highly concentrated turbid water on the groundwater in the Tedori River alluvial fan, Japan

*Yoichi Fujihara[1], Shunsuke Chono[1], Keiji Takase[1], Eiji Ichion[1]

1. Department of Environmental Science, Ishikawa Prefectural University

The Tedori River alluvial fan in the Ishikawa prefecture is a representative alluvial fan in the Hokuriku region in Japan. The river water is taken by a headworks located at the top of the alluvial fan and is used for irrigation in paddy fields with a total area of about 7,500 ha. Seepages from the riverbed and percolations from the paddy area are the main sources of groundwater in the Tedori River alluvial fan. In 2015, large-scale landslides in the upper reaches of the Tedori River caused a long period of high turbidity in the river. Highly concentrated turbid water with an average concentration of 585 mg/L (a maximum of 4,012 mg/L) has been discharged continuously into the river since May, 2015. This turbidity has caused concerns about the recharge functions of groundwater in the alluvial fan.

In this study, the measurements of paddy percolations and riverbed seepages, before and after the occurrence of high turbidity, were used to examine the influence of these phenomena on groundwater recharge functions in the alluvial fan. We measured water requirement rates in the paddy area in the Tedori River alluvial fan. The measurements were conducted before and after the midsummer-drainage period at >100 paddy fields. We also measured the river discharges in the cross-sections of the river throughout the alluvial fan. The number of cross-sections was 16 and we estimated the riverbed seepages by calculating the discharge differences between the cross-sections.

The results revealed that the amount of paddy percolation decreased significantly due to the turbidity of the river water. The average percolation in the paddy area was found to be 12.4 mm/day in 2014 and 7.9 mm/day in 2016 before the midsummer-drainage period. Moreover, the average percolation in the paddy was found to be 19.6 mm/day in 2014 and 13.7 mm/day in 2016 after the midsummer-drainage period. The volume of the riverbed seepage was observed to have reduced and the seepage section were also observed to have shortened. The observed seepages from the river bed were 4.72 m3/s in 2009 and 3.33 m3/s in 2016 for the irrigation period, whereas for the non-irrigation period, these values were 5.92 m3/s in 2009 and 1.25 m3/s in 2016. Furthermore, the seepage section was found to shorten from 14.2 km to 8.0 km, due to the high turbidity of the water.

Finally, we estimated the amount of groundwater recharge based on these measurements, which revealed that the groundwater recharge from paddy percolation decreased by 270 mm/year (36%), and the recharge from riverbed decreased by 591 mm/year (61%). The total groundwater recharge decreased by 861 mm/year (36%), a value that corresponded to the groundwater level measurements. From these results, we can conclude that the effects of highly concentrated turbid water on the groundwater are quite serious in the Tedori River alluvial fan.

Keywords: groundwater, paddy percolation, riverbed seepage

©2019. Japan Geoscience Union. All Right Reserved.

Altitude effect of water stable isotopic ratio of ravine water and its contribution to groundwater in alluvial plains - Comparison in east and west side catchments of Lake Biwa –

*Yusuke Tomozawa[1], Kunyang Wang[1], Mitsuyo Saito[2], Syuhei Ban[3], Noboru Okuda[4], Shin-ichi Onodera[1]

1. Graduate School of Integrated Arts and Sciences Hiroshima University, 2. Graduate School of Environmental and Life Science, Okayama University, 3. School of Environmental Science, The University of Shiga Prefecture, 4. Research Institute for Humanity and Nature

The stable isotope ratio of hydrogen and oxygen in water is one of useful tracers for hydrological cycle and processes in the catchment scale as well as global. The typical characteristics are spatial or geographical distribution trend such as “altitude effect” or “inland effect”, which are lower in the higher altitude or more inland. Based on these trend, the groundwater recharge area had been estimated. However, the merger of these effects and additional effect such as the seasonal variation of isotopic ratio in precipitation or vapor causes various trend.
In this study, we examined to confirm the altitude effect of water stable isotope ratio and estimate recharge altitude to groundwater in alluvial plains, with comparing in the east and west side catchments of Lake Biwa .
Sampling of spring water in the Serikawa upstream area on the east side of Lake Biwa was conducted in July 2017, December 2017, August 2018. Sampling of ravine water in the Adogawa / Ukawa upstream area on the west side of Lake Biwa was conducted in August 2018. Water samples of spring in the head water and groundwater in the alluvial plain were collected at 11 and 2 sites in the east and at 13 and 2 in the west with measuring EC, pH and DO, respectively. The water stable isotopic ratios were analyzed by PICARO.
Stable isotopic ratios in groundwater were lower than surface water in both east and west. Altitude effects of spring water in the head water were recognizable. This means the surface water in the alluvial plain was mainly contributed from Lake Biwa, whereas groundwater was from the head water. The altitude effect of oxygen stable isotopic ratio was 0.15 - 0.13 ‰/ 100 m on the east side and 0.15 ‰/ 100 m on the west side (only in the upper stream of the Ado River). In addition, the d value of isotopic ratio in the precipitation was 23‰ in the upper Adokawa in August 2018, 18 ‰in Ugawa, and 20 ‰in Serikawa.
We also estimated groundwater recharge elevation and water contribution rate in the upstream region based on these.

Keywords: stable isotope, altitude effect, groundwater recharge

©2019. Japan Geoscience Union. All Right Reserved.

Calculation of TN and TP concentration coefficients of river water for each land use by a simple watershed model.

*Seiko Yoshikawa[1], Donglai Ma[1,4], Tadamasa Saito[1,5], Kenji Matsumori[2], Yuko Itoh[3], Masahiro Kobayashi[3]

1. Institute for Agro-environmental Sciences, National Agriculture and Food Research Organization, 2. Western Region Agricultural Research Center, National Agriculture and Food Research Organization, 3. Forestry and Forest Products Research Institute, 4. Graduate school,Tsukuba University, 5. Faculty of Agriculture, Ibaraki University

Water quality deterioration of rivers caused by leakage of fertilizer components such as nitrogen and phosphorus from paddy and upland fields is a environmental problem. Also, runoff of fertilizer components are expected to increase with the accelerated water and sediment runoff by intensification and localization of rainfall caused by climate change. Although it is difficult to predict the place and extent of heavy-rainfall-related disasters, we firstly grasp the average concentrations of nitrogen and phosphorus and predict increase and decrease in those concentrations when the way of rain changes. Nitrogen and phosphorus runoff is depend on land use and land cover, conservative measures, topography, climate condition mainly rainfall etc.. Among them, the land use and land cover is expected to be a main factor in normal climate conditions. In order to contribute to the prediction of heavy-rain related disasters in the future, coefficients that indicate the total nitrogen (TN) and total phosphorus (TP) load intensity to rivers of each land use for the river watersheds across the country are calculated using a simple watershed land use model. Watersheds whose lower ends are observation points of water quality, and whose land use ratios were determined by GIS technique using published database of DEM (GSI, 10B) and LULC mesh data (JAXA , ALOS AVNIR-2). The TN and TP concentration coefficients of paddy, upland, forest, and urban were calculated by applying the below multiple regression equation using the land use ratios and published TN and TP data(Ministry of Environment).

$c = a_1 x_1 + a_2 x_2 + a_3 x_3 + a_4 x_4$

C: TN or TP concentration (mg L^{-1}) a_i : TN or TP concentration coefficient for land use *I,* x_i : ratio of land use *I,* Land use: 1;paddy, 2;upland fields, 3;forest, 4;urban

TN concentration coefficient across Japan is 1.67 (from lower limit 95% value 1.34 to upper limit 95% value 2.01), 4.08 (from 3.64 to 4.51), 0.76 (from 0.67 to 0.90), 3.57 (from 3.38 to 3.76) for paddy fields, upland fields, forests and urban areas respectively (n=3256). The TP concentration coefficient is 0.146 (lower limit 95% value 0.119 to upper limit 95% value 0.172), 0.172 (0.138 to 0.206), 0.044 (0.033 to 0.055), 0.267 (0.253 to 0.282) for paddy fields, upland fields, forests and urban areas respectively (n=3256,). Prefectural TN and TP concentration coefficients for paddy and upland fields related only loosely to prefectural surplus N and surplus P. On the other hand, prefectural TN and TP concentration coefficients for forests and urban related to prefectural population densities by logarithmic functions with determination coefficients R^2 from 0.45 to 0.48.

Keywords: watershed land-use model, TN, TP, concentration coefficient

©2019. Japan Geoscience Union. All Right Reserved.

Possibility of nutrients transportation from littoral slope for enhancement of phytoplankton growth in north basin of Lake Biwa

*Syuhei Ban[1], Rong YI[1], Xin Liu[1], Masahiro Maruo[1], Miki Sudo[1], Naoshige Goto[1], Jun Murase[2]

1. The University of Shiga Prefecture, 2. Nagoya University

Nutrient loading from non-point source in a lake ecosystem has not been well recognized yet. In Lake Biwa, total phosphorus (TP) does not decline to the level before eutrophication period, 1960s to 1970s, despite of decreasing the loading from point sources surrounding the lake after that. One of the reasons for no well lowering TP in the lake is attributed to agricultural runoff, in which suspended materials including phosphorus would be deposited to the littoral bottom. In our previous study, subsurface maximum of ammonium as a proxy of dissolved materials from anaerobic interstitial waters in the littoral bottom sediments was found along a transect from littoral to pelagic regions, implying horizontal transportation of nutrients from littoral sediments. There were no such evidences of soluble reactive phosphorus (SRP) yet due to always below the detection limit in the pelagic waters. Recently, we developed modified protocol using an ion chromatography for measuring orthophosphate concentration at nano-molar levels. In this presentation, we’ d like to provide several evidences for horizontal transportation of dissolved nutrients including orthophosphate along a transect from littoral to pelagic sites in north basin of Lake Biwa.

Total of the 6 times transect surveys for determining vertical profiles of nutrients, methane and herbicides were made in 2010-2011. Additional two transect surveys for determining those of nutrients including orthophosphate were made in 16 May and 25 July of 2018. During the 2010-2011 campaigns, *in situ* phytoplankton primary production was measured during the stagnation period using light intensity and chlorophyll *a*concentration monitored by sensors attached to a mooring buoy situated at an offshore station in north basin of Lake Biwa and an equation of photosynthesis - light intensity (P-I) curve.

In 2010-2011 campaigns, we detected sub-surface maximum layer, 20-30 m, of ammonium and methane as a proxy of dissolved materials transported from interstitial water in the sediment of littoral slope. Herbicides, which were used in rice paddy during the rice planting and proxy of materials transported from terrestrial environments surrounding the lake, were also detected in 20-30 m even at the offshore regions in the lake. Primary production monitoring suggested that phytoplankton production depended on some environmental variables other than solar irradiance, e.g. nutrients, until summer months. These results suggested that nutrients for enhancing algal growth might be horizontally transported from sediment in the littoral slope, and that the source of the nutrients might be provided from the drainage of rice paddy.

In 2018 campaigns, sub-surface maximum of ammonium was clearly found along a transect from littoral to pelagic sites in both May and July, but no such sub-surface maximum of orthophosphate was found. Several reasons for failure to find sub-surface maximum of orthophosphate might be proposed. Phosphate would be used by both phytoplankton and bacteria, while ammonium would be used by phytoplankton alone in the euphotic layer. In phosphate limited environment, such as pelagic areas in north basin of Lake Biwa, sub-surface maximum could not be easily detected due to rapid absorption by both phytoplankton and bacteria. Or, a transportation of nutrients from the littoral sloop would sporadically occur, and then we simply missed to detect it. This is on-going research project, and then further studies will be conducted to clarify this issue.

©2019. Japan Geoscience Union. All Right Reserved.

Keywords: Horizontal nutrient transportation, non-point source loading, agricultural runoff, Lake Biwa

©2019. Japan Geoscience Union. All Right Reserved.

SWAT model analysis for confirming the effects of crop growth on the suspended sediment concentration from a settling basin catchment on Ishigaki island

*Yang Cao[1], Shin-ichi Onodera[1], Mitsuyo Saito[2], Hide Omae[3], Yoshiko Iizumi[3]

1. Graduate School of Integrate Arts and Sciences, Hiroshima University, 2. Graduate School of Environmental and life Science, Okayama University, 3. Tropical Agriculture Research Front (TARF), Japan International Research Center for Agricultural Sciences (JIRCAS)

Crop growth has a significant effect on soil erosion in small watersheds. Exploring the characteristics and occurrences of soil erosion in small watersheds assists in our understanding of the water and material cycles in agricultural areas. The small catchment on the tropical island of Ishigaki, Japan, was chosen as the research area. The effects of sugarcane growth at different stages on the suspended sediment concentration in the basin from January 2017 to July 2018 were analyzed based on the Soil and Water Assessment Tool (SWAT) model. This study will explore the possible driving factors of these phenomena. The results show that the suspended sediment concentration in the basin reached its highest value on a rainy day near the sugarcane planting period because of the soil relaxation caused by tillage and cultivation. At the end of the sugarcane growth period, the sediment concentration was not at a high level when the rainfall reached 150 mm, because of the effective protection of the soil by sugarcane. The simulated sediment concentration of precipitation per mm showed that the simulated sediment concentration was at its highest during the crop planting period, followed by the period of bare land, and at the lowest during the crop growth period.

Keywords: SWAT model, Small catchment, Sugarcane, Sediment, Ishigaki

©2019. Japan Geoscience Union. All Right Reserved.

Estimating the runoff of water, sediment, and nutrient using SWAT model in Kikuchi-river watershed, Kumamoto, and the influence of the forest

*Soichiro Fujii[1], Masahiko Kanamori[1], Yuko Nagano[1], Maki Kinoshita[2], Yuta Shimizu[3], Shin-ichi Onodera[4]

1. Japan Forest Technology Association, 2. PASCO Corporation, 3. Western Region Agricultural Research Center, National Agriculture and Food Research Organization, 4. Graduate School of Integrated and Arts Sciences, Hiroshima University

Recently, enclosed sea area such as Ariake-sea have severe nutrient enrichment problem and is decreasing the produce of fishery industry. Such enclosed sea area is commonly affected by river water quality discharged from the land area. Therefore, estimating the load of sediment and nutrient from its land area is important. However, most of researches estimating discharge from land area is conducted by simple method using primary load factor. These method only can provide the estimates in annual scale regardless of the land use. On the other hand, the positive effect of forest to water quality in the river, so-called green dam, is paid attention recently, and supposed to play important roll on improvement to sea environment. However, the effect of forest to water quality is not explained enough, and few research has conducted in watershed scale. In this study, we aim to simulate water, sediment, and nutrient runoff in order to provide more detail information about discharge from land area, and to estimate the influence of the forest to water quality. We use Soil and Water Assessment Tool (SWAT) and chose Kikuchi-river as a model watershed, which has the third largest watershed area among the rivers drain into Ariake-sea.

We set Komoda observatory as the most downstream point of Kikuchi-river and the model watershed is the upstream side from there. More than half of this watershed is covered by forest. We collected land use data, soil data, climate data and 30m mesh digital elevation model (DEM) data of this watershed in order to establish the model. In order to calibrate and validate the model performance, observed data of daily stream flow from 2008 to 2016, and sampling data of sediment and nutrient were collected. Moreover, we measured the amount of sediment, phosphorus and nitrogen during flood situation in 2016 and 2017. The parameters in the model were modified according to the result of calibration, and the performance of the model was evaluated from three indices such as Nash-Sutcliffe index.

The model performance was evaluated as more than satisfactory for all materials: water, sediment, phosphorus and nitrogen. Therefore, this model can simulate daily runoff from 2008 to 2017. The runoff rate of sediment and most of nutrient from forest was less than 30% of the annual average in whole watershed, although water discharge was the same level to the rate of forest area, which indicates the function of forest to provide low concentrate water of sediment and nutrient to the river. In conclusion, modelling the runoff from land area using SWAT model has potential to provide detail information about land area discharge and estimate the influence of forest to river water quality.

Keywords: SWAT model, Runoff estimation

©2019. Japan Geoscience Union. All Right Reserved.

Atmospheric depositions on forest ecosystems in areas along the Sea of Japan

*Yuko Itoh[1], Keiji Takase[2], Yoichi Fujihara[2], Toru Okamoto[1]

1. Forestry and Forest Products Research Institute, Japan, 2. Ishikawa Prefectural University

In recent years, concerns about the effects of excess-nitrogen usage by human activities on terrestrial environment, including forest ecosystems, have been increasing at a global scale. The phenomenon of high-nitrate efflux from several forest watersheds has already been reported in the surroundings of metropolitan areas in Japan. Furthermore, concerns regarding the effects of transboundary air pollution on areas along the Sea of Japan with expanding economic activities have been increasing in Asian countries. However, on-site monitoring throughout the year is difficult in most of these areas because of heavy snow, especially in the mountainous area. Therefore, the behaviors of elements within forest ecosystems throughout a year have primarily not yet been elucidated in this district. This study was conducted to determine the influxes and effluxes of elements in this heavy snowy region and to understand the contribution of transboundary air pollution to the quantity of atmospheric deposition. We also carried out rainfall and stream water investigations from the headwater area to the lower stream area in the Tedori River Basin and an inland mountainous area to understand the geographical distribution of the actual conditions of elements' influxes and effluxes in this region. We started monitoring the major and minor elements in a small forested watershed in the middle part of the Tedori River Basin, Ishikawa prefecture, Japan, in 2013. In this study site, we observed a large amount of precipitation throughout the year. Regarding the annual snowfall amount, there were extensive variations among the years. Seasonal fluctuations were observed in the influx of atmospheric deposition; in particular, the distribution of most of the elements increased during winter. The annual deposition average of inorganic nitrogen (NH_4-N + NO_3-N) in this site was 15.8 kg ha^{-1}. The contribution of winter season deposition to the annual inputs was high. The influx of nitrogen by bulk precipitation during winter season was 2.3 times that of summer, and that of sulfur sulfate was 3.7 times. The nitrogen influx quantity was similar to or more than that reported in nitrogen-saturated forested areas of the Kanto district. Therefore, similar to that in the Kanto district, higher nitrogen deposition loads from the atmosphere could also be influenced on the effect of nitrogen dynamics and the increase in nitrogen efflux at these forest watersheds. However, the efflux concentrations of most of the dissolved elements in stream water did not show clear seasonal fluctuations. Stream water nitrate concentration was stable and low. In addition to the seasonal fluctuation of nitrogen and sulfur, the ratios among some trace elements, which are anthropogenic substances (Pb, V, As, etc.), and sea salts and yellow sand could be useful indicators to elucidate the contribution of transboundary air pollution to these regions. We compared the element inputs associated with precipitation during the non-snowy season (July–November) at six locations in the Tedori River Basin and one location in the inland area. The inorganic nitrogen and sulfuric acid sulfur influxes were the largest at the middle reaches of the Tedori River Basin. The inflow amount of inorganic nitrogen and sulfuric acid sulfur at two points in the mountainous area was approximately half or less than that at the middle region and was approximately the same as the inflow amount at the inland mountainous area. Furthermore, we investigated stream water, spring water, and ground water samples from the headwater area to the lower stream area in the Tedori River Basin. The nitrate concentrations in all the samples ranged from 0.00 to 2.93 mgL^{-1} (median value: 0.69 mgL^{-1}). In contrast, the nitrate concentrations of stream water in the Tsukuba experimental forest watershed, which has been reported as a nitrogen-saturated forested area of the Kanto district, were much higher (average value: 7.56 mgL^{-1}) than those in the Tedori River Basin. Compared with the influx, the efflux concentrations of nitrate in the water

©2019. Japan Geoscience Union. All Right Reserved.

samples were generally very low around this basin. Therefore, higher nitrogen depositions have not yet distinctly influenced the nitrate concentrations of stream water in this area. To elucidate the influence of transboundary air pollutant influx on the entire Tedori River Basin, it is necessary to evaluate the inflow amount during the snowy season in the mountainous area. Therefore, it is important to establish a method that can be used to observe the influx and efflux of elements throughout the year even in mountainous areas with heavy snow.

©2019. Japan Geoscience Union. All Right Reserved.

Continuous and simultaneous flux measurement of N_2O and CO_2 from agricultural soil using a portable multi-turn time-of-flight mass spectrometer

*Noriko Nakayama[1], Yusuke Iwai[1], Yo Toma[2], Hiroshi Furutani[1], Ryusuke Hatano[3], Michisato Toyoda[1]

1. Osaka University, 2. Ehime University, 3. Hokkaido University

Agricultural soil is one of the important sources/sinks of greenhouse gases such as N_2O, CO_2, and CH_4. The formation and consumption of such greenhouse gases in agricultural soils are dependent on not only the chemical and biological properties of the soil, but also their variations. Hence continuous monitoring of such greenhouse gases as tracer gases are quite useful to track chemical and biological processes and variations of soil properties.

In this paper, we describe a new field-deployable gas flux measurement system for the continuous monitoring of multiple agricultural soil gases (N_2O, CO_2, and CH_4) using a high resolution multi-turn time-of-flight mass spectrometer (MULTUM) combined with an automated flux chamber system. The new system measured the soil gases every 2.5 min with the precisions of ~6% for N_2O, CH_4, and 2% or better for CO_2 and O_2 at atmospheric concentrations with one relative standard deviation (RSD) for n = 10.

To demonstrate the utility of the continuous multi-gas flux measurement system, we conducted a field study at the Ehime University farm (Ehime, Japan) from September 3rd to 8th, 2018. In the field study, an automated flux chamber was placed in the agricultural field and the soil gas concentrations in the chamber were continuously monitored by the MULTUM system. Soil temperature/moisture sensor were also monitored at the depth of 7.5 cm underground in addition to a weather information (wind speed, precipitation, solar radiation). The continuous measurement had been continued with operators almost unattended except for a daily system check.

For one flux measurement (20 min), eight gas samples were taken every 2.5 min with the flux chamber closed. Gas flux of N_2O and CO_2 had been carried out by applying linear regression to the eight gas measurements. We found that a significant correlation of N_2O flux with soil electrical conductivity and water content, although no significant correlation of CO_2 flux to soil electrical conductivity was observed. Significant and rapid decreases in N_2O and CO_2 flux during rainfall events were also observed. Our preliminary result shows that high time-resolution flux data obtained by MULTUM system is quite useful for tracking the variation in soil properties and biological processes and their activity in soil environment.

Keywords: on-site mass spectorometry, MULTUM, soil-to-atmospher gas flux

©2019. Japan Geoscience Union. All Right Reserved.

Effects of introduction of cyclic irrigation system on mass balances of SS and T-P in Lake Inbanuma, Chiba, Japan

*Tomijiro Kubota[1]

1. National Agriculture and Food Research Organization, Institute for Rural Engineering

Introduction

The introduction of cyclic irrigation has been advanced since 2010 in the Lake Inbanuma as part of the update project of the irrigation facilities. In the present study, mass balances of SS and T-P were examined before and after the introduction of the cyclic irrigation.

Materials and methods

The irrigation block where the cyclic irrigation began in 2015 was selected as the investigation site, and the investigation was executed to the irrigation period in 2014 and 2015. The hydrological and water quality investigation was executed at ① division works of irrigation canal and ② drainage pumping station. Water samples were taken at the two points and the TOC, SS, TN, NO3-N, NO2-N, NH4-N, TP, and PO4-P were analyzed in the regular investigation executed about once a month. Besides regular investigation, water samples were taken once a day (8:00AM or noon) by the automatic water sampler and SS and T-P were analysed. The turbidity and water level were measured every ten minutes by using data loggers at same sites. The turbidity data were converted into the concentration of SS and TP by using the regression curve. The quantity of water intaken from the lake and drainage to the lake were obtained from the records of the facility manager.

Result and discussion

The inflow and outflow loads and the balance were calculated before and after the introduction of the cyclic irrigation. In 2014, before the start of cyclic irrigation, both the outflow loads of SS and T-P were small to compare with those inflow loads. The amount of accumulation of SS and T-P were about 1.3t and 2kg respectively when having no rainfall in the irrigation block. On the other hand, the outflow of SS and T-P were about 3.5t/day and 20kg/day respectively in rainy days. If 2015 year is compared to 2014, it had increased in T-P though the load of irrigation water each day at no rainfall periods and it had not been change in SS though an accurate comparison is difficult according to the missing value. However, after the cyclic irrigation had been started, the amount of the outflow loads had decreased greatly like 35% in SS and 38% in T-P. The balance of the outflow loads during the irrigation periods of 2014 were -470kg/day in SS, which meant the purification type, while +2.6kg/day in T-P. as a result, it was found that the introduction of cyclic irrigation system had worked for water purification in SS and T-P effectively.

Keywords: cyclic irrigation system, water pollution, suspended solid, total phosphorus

©2019. Japan Geoscience Union. All Right Reserved.

[E] Poster | A (Atmospheric and Hydrospheric Sciences)：A-HW Hydrology & Water Environment

Thu. May 30, 2019 5:15 PM - 6:30 PM JST | Thu. May 30, 2019 8:15 AM - 9:30 AM UTC | Poster Hall International Exhibition Hall8, Makuhari Messe_9

[A-HW22] Materials transport and nutrient cycles in watersheds; from headwaters to coastal seas

convener:Masahiro Kobayashi(Forestry and Forest Products Research Institute), Seiko Yoshikawa(Institute for Agro-environmental Sciences, National Agriculture and Food Research Organization), Jun Yasumoto(University of the Ryukyus, Faculty of Agriculuture), Adina Paytan(University of California Santa Cruz)

This session aims to synthetize watershed sciences in order to understand dynamical processes of materials transport and nutrient cycles in watersheds from headwaters to coastal seas. The session will be integrating a variety of research disciplines including limnology, ground water hydrology, coastal oceanography, meteorology, pedology, sedimentology, forestry, agriculture, fishery, ecology, social science and more. This session calls for ideas on new methods for the watershed sciences, such as tracer and molecular technique, hydrological modeling, paleontological approaches, laboratory and field experiments, social-scientific evaluation of ecosystem services and social-ecological systems, and so on, in order to elucidate physical, chemical and biological mechanisms for shedding light on natural phenomena and their changes over time in complex and dynamic watershed systems under human and climate impacts. Through this session, we would like to facilitate interdisciplinary collaboration among participants to create new knowledge on watershed sciences.

[AHW22-P01] Phosphate Enrichment Hampers Development of Juvenile Acropora digitifera Coral by Inhibiting Skeleton Formation

Mariko Iijima[1], *Yasumoto Ko[1], Jun Yasumoto[2], Mina Hirose[3], Mitsuru Jimbo[1], Shugo Watabe[1] (1.Kitasato University School of Marine Biosciences, 2.Faculty of Agriculture, University of the Ryukyus, 3.Tropical Technology Plus)

[AHW22-P02] Modeling chlorophyll-a concentration using remote sensing in shallow water systems: Comparison of sensors

*Assefa M Melesse[1], Tara Blakey[1], Mohammad Haji Gholizadeh[1], Mohd Manzar Abbas[1] (1.Florida International University)

[AHW22-P03] Dynamics in groundwater flow system with seasonal water table variation in a coastal and island

*Yusuke Tomozawa[1], Shin-ichi Onodera[1], Mitsuyo Saito[2] (1.Graduate School of Integrated Arts and Sciences Hiroshima University, 2.Graduate School of Environmental and Life Science, Okayama University)

[AHW22-P04] The Tracing of Groundwater Contamination Sources in Indonesian Coastal Alluvial Groundwater using $\delta^{34}S$ and $\delta^{15}N$ Isotopes

*Anna Fadliah Rusydi[1,4], Mitsuyo Saito[2], Seiichiro Ioka[3], Shin-ichi Onodera[1] (1.Graduate School of Integrated Arts and Sciences, Hiroshima University, Japan, 2.Graduate School of Environmental and Life Sciences, Okayama University, Japan, 3.Research Institute for Sustainable Energy, Hirosaki University, Japan, 4.Research Center for Geotechnology, Indonesian Institute of Sciences, Indonesia)

[AHW22-P05] Spatio-temporal dynamics of orthophosphate with implications for limitation of phytoplankton growth in north basin of Lake Biwa, Japan

*Xin Liu[1], Rong Yi[1], Masahiro Maruo[1], Syuhei Ban[1] (1.The University of Shiga Prefecture)

[AHW22-P06] Microbial phase analysis in aquifer of Ryukyu Limestone Zone using next generation sequencer

*Umi Murao[1], Jun Yasumoto[1], Yasumoto Ko[3], Mina Hirose[2], Nanami Mizusawa[3], Ryo Iguchi[4], Bam H.N. Razafindrabe[5], Syugo Watabe[3] (1.University of the Ryukyus, Faculty of Agriculuture Department of Regional Agricultural Engineering, 2.Tropical Tecnology Plus, 3.Kitasato University School of Marine Biosciences, 4.National Institute of Advanced Industrial Science and Technology, 5.University of the Ryukyus, Faculty of Agriculuture Department of Subtropical Agro-Environmental Sciences)

[AHW22-P07] Evaluation for temporal variation in groundwater inflow to the lagoons connected to Lake Biwa by radon (^{222}Rn) tracer analysis

*Mitsuyo Saito[1], Shin-ichi Onodera[2], Yusuke Tomozawa[2], Kunyang Wang[2], Syuhei Ban[3], Noboru Okuda[4] (1.Graduate School of Environmental and Life Science, Okayama University, 2.Graduate School of Integrated Arts and Sciences, Hiroshima University, 3.School of Environmental Sciences, The University of Shiga Prefecture, 4.Research Institute for Humanity and Nature)

[AHW22-P08] Br/Cl ratio characteristics of groundwater in coastal areas in Indonesia

*Seiichiro Ioka[1], Shin-ichi Onodera[2], Mitsuyo Saito[3], Anna Fadliah Rusydi[2,4] (1.Institute of Regional Innovation, Hirosaki University, Japan, 2.Graduate School of Integrated Arts and Sciences, Hiroshima University, Japan, 3.Graduate School of Environmental and Life Sciences, Okayama University, Japan, 4.Research Center for Geotechnology, Indonesian Institute of Sciences, Indonesia)

[AHW22-P09] Estimation of groundwater recharge and phosphorus transport under different precipitation conditions in a suburban catchment, using SWAT model

*Kunyang Wang[1,2], Shin-ichi Onodera[1], Mitsuyo Saito[3], Noboru Okuda[4], Takuya Okubo[5] (1.Graduate School of Integrated Arts and Science, Hiroshima University, 2.Capital Normal University, 3.Okayama University, 4.Research Institute for Humanity and Nature, 5.University of the Shiga Prefecture)

[AHW22-P10] Losses of phosphorus with soil erosion and nitrate with groundwater recharge in an agricultural catchment, subtropical small island

*Shin-ichi Onodera[1], Mitsuyo Saito[2], Yang Cao[1], Anna Fadliah Rusydi[1], Hide Omae[3], Yoshiko Iizumi[4], Yusuke Tomozawa[1] (1.Graduate School of Integrated and Arts Sciences, Hiroshima University, 2.Graduate School of Environmental and Life Science, Okayama University, 3.JIRCAS TARF, 4.JIRCAS HQ)

[AHW22-P11] Phosphate solubilizing bacteria as an indicator of sediment phosphorus in freshwater lakes

*Sreekumari Kurissery[1], Katelynn Crawford[1], Nandakumar Kanavillil[1] (1.Lakehead University, Canada)

[AHW22-P12] A Study on the dynamics of various phosphate forms in soil and groundwater in Ryukyu limestone regions

*Masashi Nozaki[1], Jun Yasumoto[2], Yasumoto Ko[3], Hirose Mina[4], Iijima Mariko[3], Ryuichi Shinjo[5], Bam H.N. Razafindrabe[6] (1.University of The Ryukyus, Graduate School of Agriculture,, 2.University of the Ryukyus, Faculty of Agriculture, Department of Regional Agricultural Engineering, 3.Kitasato University School of Marine Biosciences, 4.Tropical Technology Plus, 5.Department of Physics and Earth Sciences, University of the Ryukyus, 6.University of the Ryukyus, Faculty of Agriculture, Department of Subtropical Agro-Environmental Sciences)

[AHW22-P13] Impacts of highly concentrated turbid water on the groundwater in the Tedori River alluvial fan, Japan

*Yoichi Fujihara[1], Shunsuke Chono[1], Keiji Takase[1], Eiji Ichion[1] (1.Department of Environmental Science, Ishikawa Prefectural University)

[AHW22-P14] Altitude effect of water stable isotopic ratio of ravine water and its contribution to groundwater in alluvial plains - Comparison in east and west side catchments of Lake Biwa –

*Yusuke Tomozawa[1], Kunyang Wang[1], Mitsuyo Saito[2], Syuhei Ban[3], Noboru Okuda[4], Shin-ichi Onodera[1] (1.Graduate School of Integrated Arts and Sciences Hiroshima University, 2.Graduate School of

Environmental and Life Science, Okayama University, 3.School of Environmental Science, The University of Shiga Prefecture, 4.Research Institute for Humanity and Nature)

[AHW22-P15] Calculation of TN and TP concentration coefficients of river water for each land use by a simple watershed model.

*Seiko Yoshikawa[1], Donglai Ma[1,4], Tadamasa Saito[1,5], Kenji Matsumori[2], Yuko Itoh[3], Masahiro Kobayashi[3] (1.Institute for Agro-environmental Sciences, National Agriculture and Food Research Organization, 2.Western Region Agricultural Research Center, National Agriculture and Food Research Organization, 3.Forestry and Forest Products Research Institute, 4.Graduate school,Tsukuba University, 5.Faculty of Agriculture, Ibaraki University)

[AHW22-P16] **Possibility of nutrients transportation from littoral slope for enhancement of phytoplankton growth in north basin of Lake Biwa**

*Syuhei Ban[1], Rong YI[1], Xin Liu[1], Masahiro Maruo[1], Miki Sudo[1], Naoshige Goto[1], Jun Murase[2] (1.The University of Shiga Prefecture, 2.Nagoya University)

[AHW22-P17] SWAT model analysis for confirming the effects of crop growth on the suspended sediment concentration from a settling basin catchment on Ishigaki island

*Yang Cao[1], Shin-ichi Onodera[1], Mitsuyo Saito[2], Hide Omae[3], Yoshiko Iizumi[3] (1.Graduate School of Integrate Arts and Sciences, Hiroshima University, 2.Graduate School of Environmental and life Science, Okayama University, 3.Tropical Agriculture Research Front (TARF), Japan International Research Center for Agricultural Sciences (JIRCAS))

[AHW22-P18] Estimating the runoff of water, sediment, and nutrient using SWAT model in Kikuchi-river watershed, Kumamoto, and the influence of the forest

*Soichiro Fujii[1], Masahiko Kanamori[1], Yuko Nagano[1], Maki Kinoshita[2], Yuta Shimizu[3], Shin-ichi Onodera[4] (1.Japan Forest Technology Association, 2.PASCO Corporation, 3.Western Region Agricultural Research Center, National Agriculture and Food Research Organization, 4.Graduate School of Integrated and Arts Sciences, Hiroshima University)

[AHW22-P19] Atmospheric depositions on forest ecosystems in areas along the Sea of Japan

*Yuko Itoh[1], Keiji Takase[2], Yoichi Fujihara[2], Toru Okamoto[1] (1.Forestry and Forest Products Research Institute, Japan, 2.Ishikawa Prefectural University)

[AHW22-P20] Continuous and simultaneous flux measurement of N_2O and CO_2 from agricultural soil using a portable multi-turn time-of-flight mass spectrometer

*Noriko Nakayama[1], Yusuke Iwai[1], Yo Toma[2], Hiroshi Furutani[1], Ryusuke Hatano[3], Michisato Toyoda[1] (1.Osaka University, 2.Ehime University, 3.Hokkaido University)

[AHW22-P21] Effects of introduction of cyclic irrigation system on mass balances of SS and T-P in Lake Inbanuma, Chiba, Japan

*Tomijiro Kubota[1] (1.National Agriculture and Food Research Organization, Institute for Rural Engineering)

Phosphate Enrichment Hampers Development of Juvenile Acropora digitifera Coral by Inhibiting Skeleton Formation

Mariko Iijima[1], *Yasumoto Ko[1], Jun Yasumoto[2], Mina Hirose[3], Mitsuru Jimbo[1], Shugo Watabe[1]

1. Kitasato University School of Marine Biosciences, 2. Faculty of Agriculture, University of the Ryukyus, 3. Tropical Technology Plus

Coral reef degradation resulting from various types of local stress on corals such as excessive nutrient enrichment in and gravel inflow into coastal waters is of an increasing global concern. Because tropical and subtropical seawaters are generally poor in nutrients and thus oligotrophic, these stresses are thought to result in the decline of environments favorable to coral growth. Inorganic phosphates have been especially considered to possibly inhibit the formation of coral skeleton. Despite many studies available on the effects of nutrients on corals, a clear consensus for how nutrients exert deteriorative effects on the corals has not been established satisfactorily. Recently, we found that biogenic polyamines react with carbon dioxide (CO_2) and accelerate an aragonite formation of calcium carbonate ($CaCO_3$) in seawater. In this study, we examined the effects of phosphates and nitrates on *in vitro* aragonite formation of $CaCO_3$ by using biogenic polyamines and *in vivo* aragonite formation of juvenile coral *Acropora digitifera* skeletons, showing that phosphates clearly inhibited both *in vitro* and *in vivo* $CaCO_3$ formations at similar concentrations. In contrast, nitrates inhibited neither *in vitro* aragonite formation of $CaCO_3$ nor *in vivo* aragonite formation of juvenile coral skeletons. These findings indicate that phosphates have a detrimental effect on bioinorganic coral calcification. Furthermore, the findings that phosphate enrichment inhibits coral skeleton formation led us to conclude that enriched phosphate is adsorbed on juvenile coral skeleton surface and inhibits inorganically normal development of juvenile coral skeleton.

Keywords: phosphate, calcification

©2019. Japan Geoscience Union. All Right Reserved.

Modeling chlorophyll-a concentration using remote sensing in shallow water systems: Comparison of sensors

*Assefa M Melesse[1], Tara Blakey[1], Mohammad Haji Gholizadeh[1], Mohd Manzar Abbas[1]

1. Florida International University

The level of productivity in the upland and coastal water bodies is highly linked to land processes (land use, water management, water and nutrient fluxes). Understanding the linkage between these processes and the level of algal blooms in the water bodies is crucial for improving water quality. A comparative study was conducted using remote sensing data from three different sensors (SeaWIFS, MoDIS and Landsat) to evaluate the capability of reflectance data from these sensors for estimation of chl-a concentrations in three water bodies in the USA (Lake Okeechobee, Florida Bay and Chesapeake Bay). Observed chl-a data were gathered and compared with simulation results. The analysis found that all of the sensors have performed well in deeper water bodies than in shallow sections due to the bottom reflectance from non-algal blooms. For shallow water bodies, selection of the proper bands and band combinations, identification of the non-algal bloom reflectance and the corresponding algorithms can improve the simulation. Seasonality as well as spatial variability (using cross-sections) were evaluated and the results showed that chl-a values were highly variable for the selected summer months. Indicative of the effect of land surface fluxes of nutrients, chl-a values were higher closer to coastal areas in the Florida bay and Chesapeake Bay. The chl-a in the freshwater lake of Okeechobee was simulated using Landsat 8 data and the results found were very good. Comparison of the SeaWIFS and MoDIS chl-a value to that of the measured concentrations in the deeper section of Florida Bay and Chesapeake Bay, respectively showed very good agreement.

Keywords: Chl-a, SeaWIFS, Water qulity modeling, South Florida, Remote sensing

©2019. Japan Geoscience Union. All Right Reserved.

Dynamics in groundwater flow system with seasonal water table variation in a coastal and island

*Yusuke Tomozawa[1], Shin-ichi Onodera[1], Mitsuyo Saito[2]

1. Graduate School of Integrated Arts and Sciences Hiroshima University, 2. Graduate School of Environmental and Life Science, Okayama University

In islands, freshwater water resources are valuable as living and agricultural use, and dug wells water and reservoirs had been utilized for more than 100 years. In order to use such water resources sustainably, it is important to evaluate groundwater flow as well as water budget.

In this research, we examined to confirm the seasonal variation in water stable isotopic ratios in observation boreholes at the coastal lowland in Ikuchi Island Hiroshima prefecture. Moreover, considering that the target area is coastal, Cl^- concentration was analyzed to evaluate the influence of salt fresh water boundary.

The experimental site is located on Ikuchi Island in Hiroshima prefecture. The highest altitude is 456 m. The basement rock is mainly composed of granite. Annual average precipitation is 1058.8 mm. Observation boreholes are located at the coastal lowland in the southeastern part of the island. The upper site (Site U) with the altitude of 5.1 m asl has 3 boreholes with the depths of 2 m, 15 m, 30 m, the lower site (Site D) with 2.5 m asl has 8 with the depth of 1 m, 2 m, 3 m, 10 m, 15 m, 20 m, 30 m, 40 m, respectively. The water sampling was carried out from monthly to half year interval since 2015. Every samples were analyzed for water isotopic ratios by PICARO and anion component by ion chromatography. Especially samples in January in 2019 were analyzed for CFCs and SF6.

Based on the previous study (Saito and Onodera, 2007), the distinct altitude effect of isotopic ratio in precipitation has been confirmed. Due to spatial and temporal variations in isotopic ratios, recharge process to groundwater was suggested as follows, 1) recharge on site to shallow groundwater (2-3m deep) at D ($\delta^{18}O$: -7.8 to - 7.4 ‰), 2) river water contribution to the shallow groundwater (2-15m) at U ($\delta^{18}O$: - 8.3 to - 7.5 ‰), 3) recharge in the mountain slope with the altitude of about 360 m to deep groundwater (30m) at U ($\delta^{18}O$: - 8.4 to - 8.1 ‰), 4) recharge at 400 m on near the mountain top to deep groundwater (10-30 m) at D($\delta^{18}O$: - 8.7 to - 8.4 ‰), 5) recharge of precipitation with lower isotope than in present to deeper groundwater (40 m) at D ($\delta^{18}O$: -8.9 to - 8.8 ‰)

The deepest groundwater (40m) at D had lower isotopic ratios with higher Cl^- concentration (250 to 584 mg / L) during a lower water table in the winter. This indicated the seawater –fresh water boundary rose with water table according to Gyben-Hrzberg concept. These phenomena also suggest to cause the rise of deeper and older groundwater flow line. Consequently, we suggest the lower isotopic ratio in deeper groundwater indicates the immobile water which were recharged in the glacial period. Based on other tracers (CFC, SF 6), we will discuss more.

Keywords: stable isotope, groundwater, coastal

©2019. Japan Geoscience Union. All Right Reserved.

The Tracing of Groundwater Contamination Sources in Indonesian Coastal Alluvial Groundwater using $\delta^{34}S$ and $\delta^{15}N$ Isotopes

*Anna Fadliah Rusydi[1,4], Mitsuyo Saito[2], Seiichiro Ioka[3], Shin-ichi Onodera[1]

1. Graduate School of Integrated Arts and Sciences, Hiroshima University, Japan, 2. Graduate School of Environmental and Life Sciences, Okayama University, Japan, 3. Research Institute for Sustainable Energy, Hirosaki University, Japan, 4. Research Center for Geotechnology, Indonesian Institute of Sciences, Indonesia

The coastal area is one of the Indonesian Government priorities as an archipelago country. The groundwater in the area is one of the most reliable clean water resources, therefore it is crucial to understanding the vulnerability of this resource. Our research area was located at Indramayu, a developing rural coastal area in Indonesia, where, the environment was relatively pristine. This research aimed was to identify the effect of natural condition and human activity to groundwater quality by using stable isotope $\delta^{34}S$ and $\delta^{15}N$.

Totally, there were 20 samples taken from groundwater (18) and river (2). The nitrate and sulfate were detected in a total of 5 and 19 samples, respectively. The isotopes composition for isotope nitrate were -11.2 ‰–+22.22‰ for $\delta^{15}N\text{-}NO_3$ and -3.4 ‰–+17.1‰ for $\delta^{18}O\text{-}NO_3$. Moreover, the values of $\delta^{34}S\text{-}SO_4$ and $\delta^{18}O\text{- }SO_4$ were varied from -4.2 ‰–+28.4‰ and +7.3 ‰–+18.8 ‰, respectively. The isotopic signatures of nitrate suggested that the used of inorganic fertilizer and animal manure give the impact to both groundwater and river. Similarly, the isotopic signatures of sulfur were showing that those detected sulfate in the groundwater were mostly coming from fertilizer. Moreover, the soil was mineralized by organic sulfate as well. At one point, located in the fishery area, the groundwater was indicated the seawater contamination. It was shown by the heavy composition of sulfur isotope (28.4‰ for $\delta^{34}S$ and 18.8‰ for $\delta^{18}O$). Lastly, our results showed those combined isotopes of $\delta^{34}S$ and $\delta^{15}N$ along with land-use evaluation could explain the possible sources of groundwater in coastal area at very early urbanization stage.

Keywords: Sulfur Isotope, Nitrate Isotope, Coastal Groundwater, Indramayu

©2019. Japan Geoscience Union. All Right Reserved.

Spatio-temporal dynamics of orthophosphate with implications for limitation of phytoplankton growth in north basin of Lake Biwa, Japan

*Xin Liu[1], Rong Yi[1], Masahiro Maruo[1], Syuhei Ban[1]

1. The University of Shiga Prefecture

Orthophosphate (PO_4-P) is the main chemical form of phosphorus (P) for phytoplankton growth, often considered as a limiting nutrient for primary production in freshwater ecosystems. However, few information on accurate measurements for PO_4-P concentrations in epilimnion of meso- and oligotrophic lakes due to lower than the detection limit (60 nM) of soluble reactive P using traditional spectrophotometrical method. In the present study, we measured PO_4-P concentrations using ion chromatography with a detection limit of 5 nM, and determined truly vertical distribution of PO_4-P throughout the year with other abiotic and biotic environmental factors in north basin of Lake Biwa, to accurately understand biogeochemical processes of P in this mesotrophic lake.

Field investigations were conducted monthly from April to December 2018 at station K4 (35º19'9.6"N, 136º11'2.7"E; 50 m deep). Phosphate enrichment experiments were also made at each sampling occasion to clarify P limitation for phytoplankton growth. Lake water including phytoplankton assemblage collected from epilimnion (0–20 m) was enriched with 1 μM of PO_4-P (+P) and incubated together with untreated one (control) for 2 days under ambient light and temperature conditions. To evaluate the effect of potentially nutrient-rich bottom water, the filtered bottom water was mixed with untreated epilimnion water including phytoplankton at 1:1 (+B) was incubated at the same conditions as the +P treatment. Phytoplankton growth rate (g) was calculated with equation of $g=\ln(C_t/C_0)/2$, where C_0 and C_t are chlorophyll *a* (chl. *a*) concentrations at start and end of the experiment, respectively.

Water temperature increased in the epilimnion from May, and strict thermocline was developed from June to September. Chl. *a* concentrations increased from June to July in 10–20 m, and from October to November in 0–20 m. PO_4-P concentrations were always low, <20 nM, in the epilimnion from April to June. The concentrations below 30 m increased up to 140 nM in May, but decreased after that until July. In August and September, the concentrations increased up to 30–40 nM even in the epilimnion probably due to disturbance by typhoon. The concentrations below 30 m increased with depth, and the highest values were frequently observed near the bottom, up to 220 nM. On average throughout the water column, PO_4-P concentrations were 24–48 nM from April to June, then slightly increased up to 73 nM until September, being constant, 50–63 nM until December.

Total P, total dissolved P, dissolved organic P and particulate P exhibited similar spatio-temporal distributions, but different pattern from those of PO_4-P. NH_4-N increased in 10–20 m from May to July, whereas the NO_3-N increased in the hypolimnion as season progressed. Sestonic C:N:P ratios suggested a terrible P deficiency in July and October when phytoplankton biomass increased.

Phosphate enrichment experiments showed that phytoplankton in the epilimnion was mostly limited with P for its growth. Phytoplankton g in control varied −0.05-0.08 d^{-1}, being always lower than those in +P (−0.04-0.44 d^{-1}) and/or +B (−0.04-0.49 d^{-1}) treatments except for November and December. In November, no growth was found even in +P treatment. This might be caused by nitrogen limitation because of <6 μM of NO_3-N in the epilimnion. The g of control was similar as that of +P and +B (ca. 0.1 d^{-1}) in December, indicating that P deficiency for phytoplankton growth was relaxed until December by vertical convection.

©2019. Japan Geoscience Union. All Right Reserved.

We firstly determined completely vertical distributions of PO_4-P in north basin of Lake Biwa from spring to winter, and detected 20–40 nM of PO_4-P in the epilimnion. Phosphate enrichment experiments showed that 20 nM of PO_4-P might be critical concentration for phytoplankton growth in the lake. No phytoplankton growth even in +P treatment in November implied that nitrogen limitation for phytoplankton growth will be possible in Autumn. Further study for clarify this will be needed.

Keywords: Orthophosphate dynamics, Phosphorus limitation, Phytoplankton growth rate, Ion chromatography, Biogeochemical processes, Freshwater ecosystem

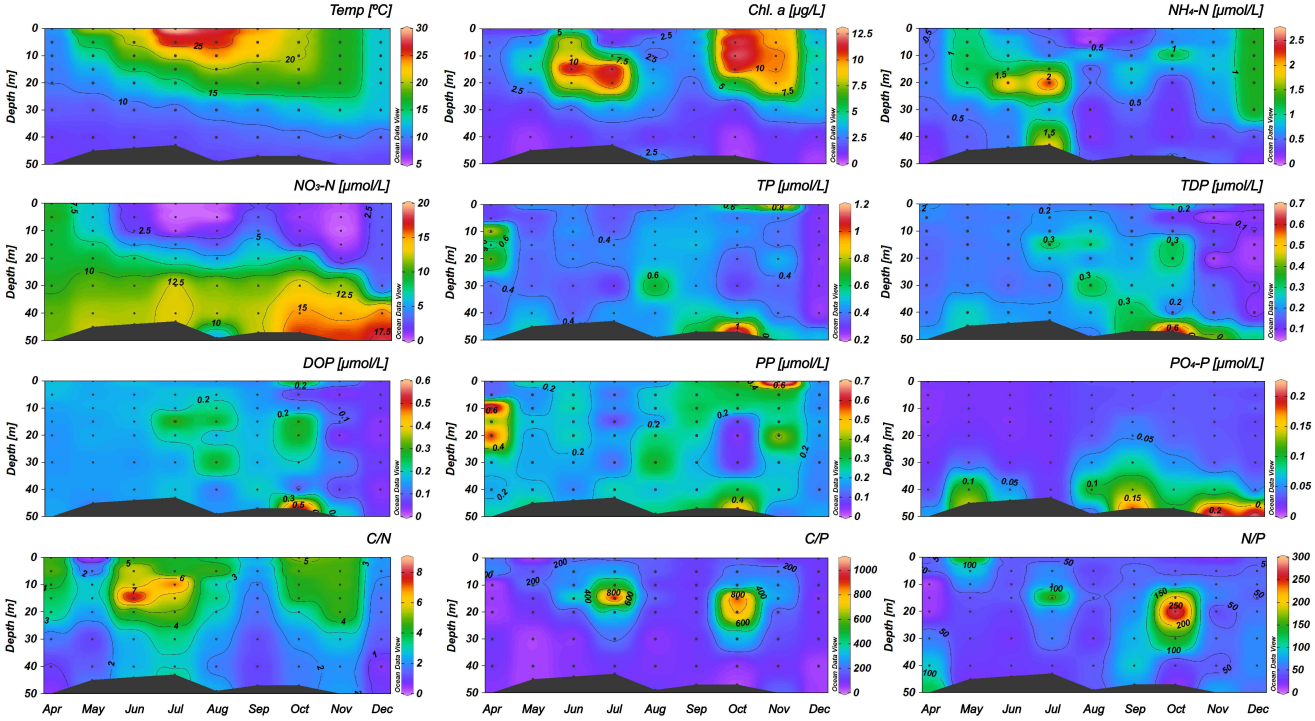

©2019. Japan Geoscience Union. All Right Reserved.

Microbial phase analysis in aquifer of Ryukyu Limestone Zone using next generation sequencer

*Umi Murao[1], Jun Yasumoto[1], Yasumoto Ko[3], Mina Hirose[2], Nanami Mizusawa[3], Ryo Iguchi[4], Bam H.N. Razafindrabe[5], Syugo Watabe[3]

1. University of the Ryukyus, Faculty of Agriculuture Department of Regional Agricultural Engineering, 2. Tropical Tecnology Plus, 3. Kitasato University School of Marine Biosciences, 4. National Institute of Advanced Industrial Science and Technology, 5. University of the Ryukyus, Faculty of Agriculuture Department of Subtropical Agro-Environmental Sciences

Clean water and sanitation (Sustainable development Goals (6)) is one of the world's important issues. People use groundwater in many areas as a water source, but various cases of contamination by agricultural activities and substances derived from human and animal excrements have been reported.

On the other hand, genetic analysis techniques using molecular biological methods have been applied to the analysis of microbial phase in the water environment.

In recent years, the method using the latest analysis equipment of next generation Sequencer is established, mainly for microorganisms. In addition, new monitoring indices such as environmental DNA have been developed. It is thought that the microbial phase in groundwater varies depending on the influence of various environmental factors and human activity, but the actual condition is not clear.

The next generation Sequencer is a very powerful tool used to grasp the microbial phase in groundwater. It is thought that the microbial phase can be an important indicator in water resource management of basins in the future.

The purpose of this study is to investigate the microbial species and their coexistence in groundwater in the Ryukyu Limestone area using the next generation sequencer.

Keywords: groundwater, microbial community analysis, genetic analysis

©2019. Japan Geoscience Union. All Right Reserved.

Evaluation for temporal variation in groundwater inflow to the lagoons connected to Lake Biwa by radon (^{222}Rn) tracer analysis

*Mitsuyo Saito[1], Shin-ichi Onodera[2], Yusuke Tomozawa[2], Kunyang Wang[2], Syuhei Ban[3], Noboru Okuda[4]

1. Graduate School of Environmental and Life Science, Okayama University, 2. Graduate School of Integrated Arts and Sciences, Hiroshima University, 3. School of Environmental Sciences, The University of Shiga Prefecture, 4. Research Institute for Humanity and Nature

Primary production in freshwater lakes and reservoirs are usually controlled by phosphorus (P). Lacustrine groundwater discharge (LGD), direct discharge of subsurface water to lake, is regarded as a potential nutrient paths, including phosphorus from a catchment to lake water environment. There are more than 20 lagoons around Lake Biwa which were originally a part of the lake. These lagoons are regarded to have important functions as settling ponds of inflowing loads from the catchments to Lake Biwa, refuges for shallow water ecosystems and so on. Because these lagoons are connected to Lake Biwa, evaluation of nutrient budget is important for the nutrient cycle in the lake. Some researchers have pointed out the presence of LGD in littoral area of Lake Biwa. However, it has not been evaluated for the lagoons around the lake. In the present research, we aimed to evaluate the temporal variation in groundwater inflow to a lagoon connected to Lake Biwa by radon (^{222}Rn) tracer analysis.

The field campaigns were conducted in December 2017, August and October 2018 for the lagoons (Noda-Numa and Hasu-Ike) located on northeastern shore of Lake Biwa. The volume of inflow and outflow, water temperature, electric conductivity, chlorophyll-a and radon (^{222}Rn) concentration were measured in the lagoon. ^{222}Rn is a radioactive element of uranium (^{238}U) series with 3.8 day of half-life. ^{222}Rn is a useful tracer of groundwater discharge because it generally enriched in groundwater than surface water. To examine the temporal variation in groundwater inflow, the time-series ^{222}Rn concentration in water was obtained. Water samples were collected at the inlet, outlet and near the center of the lagoons and natural springs and groundwater wells around the lagoons. Water and ^{222}Rn balance suggest that groundwater inflow is larger in Noda-Numa than Hasu-Ike. The catchment topography may influence on this difference. ^{222}Rn balance-based residence time of lagoon water was estimated 10-20 days in Noda-Numa, and 4-5 days in Hasu-Ike, were similar with that based on water balance. These results suggest the groundwater inflow is a potential phosphorus path to Noda-Numa.

Keywords: Groundwater inflow, Connected lagoons, Lake Biwa, Radon (222Rn)

©2019. Japan Geoscience Union. All Right Reserved.

Br/Cl ratio characteristics of groundwater in coastal areas in Indonesia

*Seiichiro Ioka[1], Shin-ichi Onodera[2], Mitsuyo Saito[3], Anna Fadliah Rusydi[2,4]

1. Institute of Regional Innovation, Hirosaki University, Japan, 2. Graduate School of Integrated Arts and Sciences, Hiroshima University, Japan, 3. Graduate School of Environmental and Life Sciences, Okayama University, Japan, 4. Research Center for Geotechnology, Indonesian Institute of Sciences, Indonesia

The urban development in Indonesia’ s coastal areas has led to an increase of groundwater demand, which then has resulted in groundwater salinization. In this study, we analyze bromide and Br/Cl ratio characteristics, as index of groundwater salinization, in three cities of Indonesian coastal areas, namely: Indramayu, Mataram, and Semarang. Each research site is at different stage of urbanization. Indramayu is in very early stage of urbanization, followed by Mataram as a developing tourism area, and the last one Semarang as a heavy urbanization city. The results show that concentrations of bromide in groundwater are ranged from 0.05 to 38 mg/L in Indramayu, 0.01 to 0.8 mg/L in Mataram, and 0.02 to 8.0 mg/L in Semarang. Furthermore, the occurrence of Br is described in terms of the Br/Cl weight ratio, which allows for small changes in bromide concentrations to be assessed in terms of salinity. Median values of Br/Cl weight ratio in the groundwater of Indramayu, Mataram, and Semarang were approximately 0.0035, 0.0027, and 0.0025, respectively, while the ratio in seawater is generally around 0.0035. The relationship between Br/Cl weight ratio and chloride concentration indicate the groundwater in Indramayu is undergoing salinization due to seawater intrusion compared to the other two areas, meanwhile the groundwater in Semarang is experiencing chloride contamination due to anthropogenic activities based on the study by Andreasen and Fleck (1997).

Keywords: Indonesia, groundwater, Br/Cl ratio, coastal area

©2019. Japan Geoscience Union. All Right Reserved.

Estimation of groundwater recharge and phosphorus transport under different precipitation conditions in a suburban catchment, using SWAT model

*Kunyang Wang[1,2], Shin-ichi Onodera[1], Mitsuyo Saito[3], Noboru Okuda[4], Takuya Okubo[5]

1. Graduate School of Integrated Arts and Science, Hiroshima University, 2. Capital Normal University, 3. Okayama University, 4. Research Institute for Humanity and Nature, 5. University of the Shiga Prefecture

The quantification of the groundwater recharge and phosphorus transport in water is one of the most important indicators of the water cycle in lakes because these processes are related to the transport of large nutrient loads. The Yasu River is one of the important water sources of the Biwa Lake. In this paper, Geographic Information System technology is used to analyze and predict the land use change in the Yasu River Basin. The water balance was simulated using the Soil and Water Assessment Tool. Simulations of different years in different precipitation seasons were carried out. The correlation coefficient and the Nash Sutcliffe coefficient are higher than the reference values. The sensitivity analysis of the parameters reveals the different degrees of sensitivity of the parameters in different water seasons, CN2 always has a high sensitivity during all kinds of water season. The total groundwater recharge and discharge are 180 million m^3 and 179 million m^3 in the normal precipitation season, respectively. The trends differ in the dry and wet seasons. In the dry season of 2007, the groundwater recharge was below 140 million m^3, while it exceeded 240 million m^3 in the rainy season in 2003. In addition, the process of phosphorus loss in the basin and release into Lake Biwa are explained from the perspective of space and time. This is closely related to the spatial distribution of the main channel and the time distribution of precipitation. The total amount of nonpoint source pollution of phosphorus in three years is equivalent to 4.08 kg/ha of paddy fields in the watershed. The spatial distribution of phosphorus loss is related to the stream flow, it is mainly concentrated in the area with paddy fields and urban. The time distribution is related to the distribution of the precipitation. With increasing precipitation, the nonpoint source pollution of phosphorus slightly increases. This is due to the driving effect of precipitation on the phosphorus transfer and erosion of soil.

Keywords: Phosphorus transport, Groundwater recharge, Different precipitation conditions, SWAT model

©2019. Japan Geoscience Union. All Right Reserved.

Losses of phosphorus with soil erosion and nitrate with groundwater recharge in an agricultural catchment, subtropical small island

*Shin-ichi Onodera[1], Mitsuyo Saito[2], Yang Cao[1], Anna Fadliah Rusydi[1], Hide Omae[3], Yoshiko Iizumi[4], Yusuke Tomozawa[1]

1. Graduate School of Integrated and Arts Sciences, Hiroshima University, 2. Graduate School of Environmental and Life Science, Okayama University, 3. JIRCAS TARF, 4. JIRCAS HQ

In tropical and subtropical region, the rainfall intensity is strong and soil erosion in an agricultural land is one of big environmental issues. Especially, the impact of large sediment discharge on the coral reef is serious around small islands, such as Okinawa and Philippines. In case of Okinawa Prefecture, to reduce the sediment discharge and conserve corals, many sediment trap ponds are constructed in a downstream area of agricultural lands. However, sediment deposition rate, variation of trap effect, and component of sediment in a pond have not been confirmed.

To estimate of erosion rate and deposition process of a small pond in an agricultural catchment of a subtropical small island, we examine to observe the sediment deposition in a small pond and monitor water level and chlorophyll a in a pond and runoff and turbidity of an inflow stream in a small catchment with the area of 300m2 in Ishigaki Island, Okinawa Prefecture, Subtropical region. Our monitoring was started from February 2017 after removing all sediment in a pond in January, and up to April 2018. Observation of sediment deposition was conducted with collecting the samples at 5 sites in June 2017 and January 2018. Inflow and outflow water samples were collected every one month.
The sediment deposition was extremely large from January to May 2017, the average erosion rate in all catchment area was estimated to be 6mm. On the other hand, the sediment deposition was nothing from June 2017 to January 2018. Based on the monitoring of stream runoff and turbidity, one big storm event in April with strong intensity mainly contributes to sediment discharge and overflow of the pond occurred. On the other hand, the later period had also big events. This difference is suggested to be the difference of land cover by crops and availability of sediment trap in this pond. In addition, the sediment component mainly was composed of surface soft layer, subsurface sandy layer, and bottom gravel layer. The average thickness was 2cm in surface layer, 100cm in mid sandy layer, and 10cm in gravel layer, respectively. Especially, the surface soft layer had high nutrient content. The dissolved nutrient of inflow stream water and pond water were high concentration. But the 10% of nutrient in the inflow decreased in pond. This means the plankton was produced, using this nutrient and that was deposited later. The soft layer is suggested to be effect of organic fertilizer, it is expected to apply to agricultural lands.

Keywords: Phosphorus, groundwater, nitrate

©2019. Japan Geoscience Union. All Right Reserved.

Phosphate solubilizing bacteria as an indicator of sediment phosphorus in freshwater lakes

*Sreekumari Kurissery[1], Katelynn Crawford[1], Nandakumar Kanavillil[1]

1. Lakehead University, Canada

It has been well documented that phosphorus pollution is one of the most significant factors impeding the overall health of freshwater lakes. Various measures are being taken to reduce phosphorus input into the lakes by anthropogenic activities and thus to maintain a healthy ecosystem. However, it is well known that bioavailable phosphorus tends to bind with substances such as ferric iron and calcium present in the water, become insoluble, and settles into the sediments. The presentstudy has been carried out to understand the relationship between the sediment phosphorus concentration and density of phosphate solubilizing bacteria (PSB) in two lakes in Ontario, Canada, namely, Lake Simcoe and Sparrow Lake. In September 2017, 20cm sediment cores were collected from the nearshore sites of these two lakes to determine the presence of PSB in relation to the sediment phosphorus concentration. PSB could potentially release phosphorus back into the water column through a process called internal phosphorus loading from the inorganic phosphates in the sediment when the right conditions are present. PSB were isolated from the sediment cores at 5 cm intervals by plating on to Pikovskaya’ s agar. Five grams of sediment was used to analyze total reactive phosphorus in the sediment. In Lake Simcoe, PSB ranged from $3x10^1$ to $1.1x10^1$ cfu/g, and the amount of total reactive phosphorus ranged from 0.19 to 0.46 mg/g. In Sparrow Lake, PSB ranged from $4x10^0$ to $3x10^1$ cfu/g and the amount of total reactive phosphorus ranged from 0.21 to 0.39 mg/g. A linear regression was completed to determine the relationship between total reactive phosphorus and PSB for each core. The results showed a negative relationship between these two tested parameters (Lake Simcoe: r^2=0.23, $y = -35.34x + 30.811$ p=0.5206, and Sparrow Lake: r^2 =0.87, $y = -155.9x + 62.322$, p=0.067). While PSB density decreased with core depth, the concentration of reactive phosphorus increased. This indicates that the density of PSB in lake sediment may indicate the concentration of total reactive phosphorus and thus the internal phosphorus loading. More study is recommended to confirm the results.

Keywords: Phosphate Solubilizing Bacteria, Freshwater Lakes , Sediment Phosphorus , Canada

©2019. Japan Geoscience Union. All Right Reserved.

A Study on the dynamics of various phosphate forms in soil and groundwater in Ryukyu limestone regions

*Masashi Nozaki[1], Jun Yasumoto[2], Yasumoto Ko[3], Hirose Mina[4], Iijima Mariko[3], Ryuichi Shinjo[5], Bam H.N. Razafindrabe[6]

1. University of The Ryukyus, Graduate School of Agriculture,, 2. University of the Ryukyus, Faculty of Agriculture, Department of Regional Agricultural Engineering, 3. Kitasato University School of Marine Biosciences, 4. Tropical Technology Plus, 5. Department of Physics and Earth Sciences, University of the Ryukyus, 6. University of the Ryukyus, Faculty of Agriculture, Department of Subtropical Agro-Environmental Sciences

Phosphorus in water environment exists in various forms and size, such as dissolved, particulate, organic and inorganic forms. However, there are many unclear points in Phosphorus in groundwater. In this study, we tried to understand the dynamics of various phosphate forms in soil and groundwater in Ryukyu limestone regions by combining Inductively Coupled Plasma Atomic Emission Spectrometry (ICP-AES) and ^{31}P Nuclear Magnetic Resonance (^{31}P-NMR), in addition to Colorimetric (molybdenum blue method). From August 2017 to August 2018, we took groundwater samples in southern part of Okinawa, Japan, with Ryukyu limestone distribution on a monthly basis. We measured pH, electronic conductivity (EC), Oxidation-Reduction Potential (ORP), dissolved oxygen (DO) and alkalinity (HCO_3^-) on site, and analyzed major dissolved ion (Cl^-, HCO_3^-, NO_2^-, NO_3^-, SO_4^{2-}, Na^+, K^+, Mg^{2+}, Ca^{2+}), suspended solid (SS) and phosphorus concentration. Phosphorus concentration analyzed 3 different method to molybdenum blue method (Col-P), ICP-AES (ICP-P) and Total P (T-P). Phosphate form analysis used ^{31}P-NMR.
We compared Col-P and ICP-P in order to understand dissolved phosphorus spatial distribution. The results show that ICP-P is 1.06~49.24 times larger than Col-P. It is inferred that ICP-P is also measuring fine particulate phosphorus and organic phosphorus. As a result, several forms of phosphate without orthophosphate were found in groundwater. Particulate phosphorus was determined by subtracting ICP-P from T-P. A positive correlation (r= 0.78) was found between P-P and SS. According to these results, it is thought that PP adsorbs various forms of phosphate including orthophosphate. We analyzed the correlation between dissolved phosphorus (Col-P, ICP-P) and all measured value in order to understand the characteristics of seasonal variation to dissolved phosphorus. There was a negative correlation between Col-P to water temperature. When focusing on seasonal variation of Col-P, we found that Col-P concentration decreases when water temperature increases. Moreover, Col-P concentration increases as water temperature increases. Through the analysis of various forms of phosphate in soil and SS by using ^{31}P-NMR, along with orthophosphate, pyrophosphate, pyrophosphate ester, orthophosphate monoester were also detected. It is thus suggested that the phosphate of polymeric or organic forms other than orthophosphate are from plant origin, as a result of microbial activities and microorganism decomposition.

Keywords: Phosphorus, 31P-NMR, Groundwater

©2019. Japan Geoscience Union. All Right Reserved.

Impacts of highly concentrated turbid water on the groundwater in the Tedori River alluvial fan, Japan

*Yoichi Fujihara[1], Shunsuke Chono[1], Keiji Takase[1], Eiji Ichion[1]

1. Department of Environmental Science, Ishikawa Prefectural University

The Tedori River alluvial fan in the Ishikawa prefecture is a representative alluvial fan in the Hokuriku region in Japan. The river water is taken by a headworks located at the top of the alluvial fan and is used for irrigation in paddy fields with a total area of about 7,500 ha. Seepages from the riverbed and percolations from the paddy area are the main sources of groundwater in the Tedori River alluvial fan. In 2015, large-scale landslides in the upper reaches of the Tedori River caused a long period of high turbidity in the river. Highly concentrated turbid water with an average concentration of 585 mg/L (a maximum of 4,012 mg/L) has been discharged continuously into the river since May, 2015. This turbidity has caused concerns about the recharge functions of groundwater in the alluvial fan.

In this study, the measurements of paddy percolations and riverbed seepages, before and after the occurrence of high turbidity, were used to examine the influence of these phenomena on groundwater recharge functions in the alluvial fan. We measured water requirement rates in the paddy area in the Tedori River alluvial fan. The measurements were conducted before and after the midsummer-drainage period at >100 paddy fields. We also measured the river discharges in the cross-sections of the river throughout the alluvial fan. The number of cross-sections was 16 and we estimated the riverbed seepages by calculating the discharge differences between the cross-sections.

The results revealed that the amount of paddy percolation decreased significantly due to the turbidity of the river water. The average percolation in the paddy area was found to be 12.4 mm/day in 2014 and 7.9 mm/day in 2016 before the midsummer-drainage period. Moreover, the average percolation in the paddy was found to be 19.6 mm/day in 2014 and 13.7 mm/day in 2016 after the midsummer-drainage period. The volume of the riverbed seepage was observed to have reduced and the seepage section were also observed to have shortened. The observed seepages from the river bed were 4.72 m3/s in 2009 and 3.33 m3/s in 2016 for the irrigation period, whereas for the non-irrigation period, these values were 5.92 m3/s in 2009 and 1.25 m3/s in 2016. Furthermore, the seepage section was found to shorten from 14.2 km to 8.0 km, due to the high turbidity of the water.

Finally, we estimated the amount of groundwater recharge based on these measurements, which revealed that the groundwater recharge from paddy percolation decreased by 270 mm/year (36%), and the recharge from riverbed decreased by 591 mm/year (61%). The total groundwater recharge decreased by 861 mm/year (36%), a value that corresponded to the groundwater level measurements. From these results, we can conclude that the effects of highly concentrated turbid water on the groundwater are quite serious in the Tedori River alluvial fan.

Keywords: groundwater, paddy percolation, riverbed seepage

©2019. Japan Geoscience Union. All Right Reserved.

Altitude effect of water stable isotopic ratio of ravine water and its contribution to groundwater in alluvial plains - Comparison in east and west side catchments of Lake Biwa –

*Yusuke Tomozawa[1], Kunyang Wang[1], Mitsuyo Saito[2], Syuhei Ban[3], Noboru Okuda[4], Shin-ichi Onodera[1]

1. Graduate School of Integrated Arts and Sciences Hiroshima University, 2. Graduate School of Environmental and Life Science, Okayama University, 3. School of Environmental Science, The University of Shiga Prefecture, 4. Research Institute for Humanity and Nature

The stable isotope ratio of hydrogen and oxygen in water is one of useful tracers for hydrological cycle and processes in the catchment scale as well as global. The typical characteristics are spatial or geographical distribution trend such as “altitude effect” or “inland effect”, which are lower in the higher altitude or more inland. Based on these trend, the groundwater recharge area had been estimated. However, the merger of these effects and additional effect such as the seasonal variation of isotopic ratio in precipitation or vapor causes various trend.
In this study, we examined to confirm the altitude effect of water stable isotope ratio and estimate recharge altitude to groundwater in alluvial plains, with comparing in the east and west side catchments of Lake Biwa .
Sampling of spring water in the Serikawa upstream area on the east side of Lake Biwa was conducted in July 2017, December 2017, August 2018. Sampling of ravine water in the Adogawa / Ukawa upstream area on the west side of Lake Biwa was conducted in August 2018. Water samples of spring in the head water and groundwater in the alluvial plain were collected at 11 and 2 sites in the east and at 13 and 2 in the west with measuring EC, pH and DO, respectively. The water stable isotopic ratios were analyzed by PICARO.
Stable isotopic ratios in groundwater were lower than surface water in both east and west. Altitude effects of spring water in the head water were recognizable. This means the surface water in the alluvial plain was mainly contributed from Lake Biwa, whereas groundwater was from the head water. The altitude effect of oxygen stable isotopic ratio was 0.15 - 0.13 ‰/ 100 m on the east side and 0.15 ‰/ 100 m on the west side (only in the upper stream of the Ado River). In addition, the d value of isotopic ratio in the precipitation was 23‰ in the upper Adokawa in August 2018, 18 ‰in Ugawa, and 20 ‰in Serikawa.
We also estimated groundwater recharge elevation and water contribution rate in the upstream region based on these.

Keywords: stable isotope, altitude effect, groundwater recharge

©2019. Japan Geoscience Union. All Right Reserved.

Calculation of TN and TP concentration coefficients of river water for each land use by a simple watershed model.

*Seiko Yoshikawa[1], Donglai Ma[1,4], Tadamasa Saito[1,5], Kenji Matsumori[2], Yuko Itoh[3], Masahiro Kobayashi[3]

1. Institute for Agro-environmental Sciences, National Agriculture and Food Research Organization, 2. Western Region Agricultural Research Center, National Agriculture and Food Research Organization, 3. Forestry and Forest Products Research Institute, 4. Graduate school,Tsukuba University, 5. Faculty of Agriculture, Ibaraki University

Water quality deterioration of rivers caused by leakage of fertilizer components such as nitrogen and phosphorus from paddy and upland fields is a environmental problem. Also, runoff of fertilizer components are expected to increase with the accelerated water and sediment runoff by intensification and localization of rainfall caused by climate change. Although it is difficult to predict the place and extent of heavy-rainfall-related disasters, we firstly grasp the average concentrations of nitrogen and phosphorus and predict increase and decrease in those concentrations when the way of rain changes. Nitrogen and phosphorus runoff is depend on land use and land cover, conservative measures, topography, climate condition mainly rainfall etc.. Among them, the land use and land cover is expected to be a main factor in normal climate conditions. In order to contribute to the prediction of heavy-rain related disasters in the future, coefficients that indicate the total nitrogen (TN) and total phosphorus (TP) load intensity to rivers of each land use for the river watersheds across the country are calculated using a simple watershed land use model. Watersheds whose lower ends are observation points of water quality, and whose land use ratios were determined by GIS technique using published database of DEM (GSI, 10B) and LULC mesh data (JAXA , ALOS AVNIR-2). The TN and TP concentration coefficients of paddy, upland, forest, and urban were calculated by applying the below multiple regression equation using the land use ratios and published TN and TP data(Ministry of Environment).

$c = a_1 x_1 + a_2 x_2 + a_3 x_3 + a_4 x_4$

C: TN or TP concentration (mg L^{-1}) a_i : TN or TP concentration coefficient for land use *I,* x_i : ratio of land use *I,* Land use: 1;paddy, 2;upland fields, 3;forest, 4;urban

TN concentration coefficient across Japan is 1.67 (from lower limit 95% value 1.34 to upper limit 95% value 2.01), 4.08 (from 3.64 to 4.51), 0.76 (from 0.67 to 0.90), 3.57 (from 3.38 to 3.76) for paddy fields, upland fields, forests and urban areas respectively (n=3256). The TP concentration coefficient is 0.146 (lower limit 95% value 0.119 to upper limit 95% value 0.172), 0.172 (0.138 to 0.206), 0.044 (0.033 to 0.055), 0.267 (0.253 to 0.282) for paddy fields, upland fields, forests and urban areas respectively (n=3256,). Prefectural TN and TP concentration coefficients for paddy and upland fields related only loosely to prefectural surplus N and surplus P. On the other hand, prefectural TN and TP concentration coefficients for forests and urban related to prefectural population densities by logarithmic functions with determination coefficients R^2 from 0.45 to 0.48.

Keywords: watershed land-use model, TN, TP, concentration coefficient

©2019. Japan Geoscience Union. All Right Reserved.

Possibility of nutrients transportation from littoral slope for enhancement of phytoplankton growth in north basin of Lake Biwa

*Syuhei Ban[1], Rong YI[1], Xin Liu[1], Masahiro Maruo[1], Miki Sudo[1], Naoshige Goto[1], Jun Murase[2]

1. The University of Shiga Prefecture, 2. Nagoya University

Nutrient loading from non-point source in a lake ecosystem has not been well recognized yet. In Lake Biwa, total phosphorus (TP) does not decline to the level before eutrophication period, 1960s to 1970s, despite of decreasing the loading from point sources surrounding the lake after that. One of the reasons for no well lowering TP in the lake is attributed to agricultural runoff, in which suspended materials including phosphorus would be deposited to the littoral bottom. In our previous study, subsurface maximum of ammonium as a proxy of dissolved materials from anaerobic interstitial waters in the littoral bottom sediments was found along a transect from littoral to pelagic regions, implying horizontal transportation of nutrients from littoral sediments. There were no such evidences of soluble reactive phosphorus (SRP) yet due to always below the detection limit in the pelagic waters. Recently, we developed modified protocol using an ion chromatography for measuring orthophosphate concentration at nano-molar levels. In this presentation, we’ d like to provide several evidences for horizontal transportation of dissolved nutrients including orthophosphate along a transect from littoral to pelagic sites in north basin of Lake Biwa.

Total of the 6 times transect surveys for determining vertical profiles of nutrients, methane and herbicides were made in 2010-2011. Additional two transect surveys for determining those of nutrients including orthophosphate were made in 16 May and 25 July of 2018. During the 2010-2011 campaigns, *in situ* phytoplankton primary production was measured during the stagnation period using light intensity and chlorophyll *a*concentration monitored by sensors attached to a mooring buoy situated at an offshore station in north basin of Lake Biwa and an equation of photosynthesis - light intensity (P-I) curve.

In 2010-2011 campaigns, we detected sub-surface maximum layer, 20-30 m, of ammonium and methane as a proxy of dissolved materials transported from interstitial water in the sediment of littoral slope. Herbicides, which were used in rice paddy during the rice planting and proxy of materials transported from terrestrial environments surrounding the lake, were also detected in 20-30 m even at the offshore regions in the lake. Primary production monitoring suggested that phytoplankton production depended on some environmental variables other than solar irradiance, e.g. nutrients, until summer months. These results suggested that nutrients for enhancing algal growth might be horizontally transported from sediment in the littoral slope, and that the source of the nutrients might be provided from the drainage of rice paddy.

In 2018 campaigns, sub-surface maximum of ammonium was clearly found along a transect from littoral to pelagic sites in both May and July, but no such sub-surface maximum of orthophosphate was found. Several reasons for failure to find sub-surface maximum of orthophosphate might be proposed. Phosphate would be used by both phytoplankton and bacteria, while ammonium would be used by phytoplankton alone in the euphotic layer. In phosphate limited environment, such as pelagic areas in north basin of Lake Biwa, sub-surface maximum could not be easily detected due to rapid absorption by both phytoplankton and bacteria. Or, a transportation of nutrients from the littoral sloop would sporadically occur, and then we simply missed to detect it. This is on-going research project, and then further studies will be conducted to clarify this issue.

©2019. Japan Geoscience Union. All Right Reserved.

Keywords: Horizontal nutrient transportation, non-point source loading, agricultural runoff, Lake Biwa

©2019. Japan Geoscience Union. All Right Reserved.

SWAT model analysis for confirming the effects of crop growth on the suspended sediment concentration from a settling basin catchment on Ishigaki island

*Yang Cao[1], Shin-ichi Onodera[1], Mitsuyo Saito[2], Hide Omae[3], Yoshiko Iizumi[3]

1. Graduate School of Integrate Arts and Sciences, Hiroshima University, 2. Graduate School of Environmental and life Science, Okayama University, 3. Tropical Agriculture Research Front (TARF), Japan International Research Center for Agricultural Sciences (JIRCAS)

Crop growth has a significant effect on soil erosion in small watersheds. Exploring the characteristics and occurrences of soil erosion in small watersheds assists in our understanding of the water and material cycles in agricultural areas. The small catchment on the tropical island of Ishigaki, Japan, was chosen as the research area. The effects of sugarcane growth at different stages on the suspended sediment concentration in the basin from January 2017 to July 2018 were analyzed based on the Soil and Water Assessment Tool (SWAT) model. This study will explore the possible driving factors of these phenomena. The results show that the suspended sediment concentration in the basin reached its highest value on a rainy day near the sugarcane planting period because of the soil relaxation caused by tillage and cultivation. At the end of the sugarcane growth period, the sediment concentration was not at a high level when the rainfall reached 150 mm, because of the effective protection of the soil by sugarcane. The simulated sediment concentration of precipitation per mm showed that the simulated sediment concentration was at its highest during the crop planting period, followed by the period of bare land, and at the lowest during the crop growth period.

Keywords: SWAT model, Small catchment, Sugarcane, Sediment, Ishigaki

©2019. Japan Geoscience Union. All Right Reserved.

Estimating the runoff of water, sediment, and nutrient using SWAT model in Kikuchi-river watershed, Kumamoto, and the influence of the forest

*Soichiro Fujii[1], Masahiko Kanamori[1], Yuko Nagano[1], Maki Kinoshita[2], Yuta Shimizu[3], Shin-ichi Onodera[4]

1. Japan Forest Technology Association, 2. PASCO Corporation, 3. Western Region Agricultural Research Center, National Agriculture and Food Research Organization, 4. Graduate School of Integrated and Arts Sciences, Hiroshima University

Recently, enclosed sea area such as Ariake-sea have severe nutrient enrichment problem and is decreasing the produce of fishery industry. Such enclosed sea area is commonly affected by river water quality discharged from the land area. Therefore, estimating the load of sediment and nutrient from its land area is important. However, most of researches estimating discharge from land area is conducted by simple method using primary load factor. These method only can provide the estimates in annual scale regardless of the land use. On the other hand, the positive effect of forest to water quality in the river, so-called green dam, is paid attention recently, and supposed to play important roll on improvement to sea environment. However, the effect of forest to water quality is not explained enough, and few research has conducted in watershed scale. In this study, we aim to simulate water, sediment, and nutrient runoff in order to provide more detail information about discharge from land area, and to estimate the influence of the forest to water quality. We use Soil and Water Assessment Tool (SWAT) and chose Kikuchi-river as a model watershed, which has the third largest watershed area among the rivers drain into Ariake-sea.

We set Komoda observatory as the most downstream point of Kikuchi-river and the model watershed is the upstream side from there. More than half of this watershed is covered by forest. We collected land use data, soil data, climate data and 30m mesh digital elevation model (DEM) data of this watershed in order to establish the model. In order to calibrate and validate the model performance, observed data of daily stream flow from 2008 to 2016, and sampling data of sediment and nutrient were collected. Moreover, we measured the amount of sediment, phosphorus and nitrogen during flood situation in 2016 and 2017. The parameters in the model were modified according to the result of calibration, and the performance of the model was evaluated from three indices such as Nash-Sutcliffe index.

The model performance was evaluated as more than satisfactory for all materials: water, sediment, phosphorus and nitrogen. Therefore, this model can simulate daily runoff from 2008 to 2017. The runoff rate of sediment and most of nutrient from forest was less than 30% of the annual average in whole watershed, although water discharge was the same level to the rate of forest area, which indicates the function of forest to provide low concentrate water of sediment and nutrient to the river. In conclusion, modelling the runoff from land area using SWAT model has potential to provide detail information about land area discharge and estimate the influence of forest to river water quality.

Keywords: SWAT model, Runoff estimation

©2019. Japan Geoscience Union. All Right Reserved.

Atmospheric depositions on forest ecosystems in areas along the Sea of Japan

*Yuko Itoh[1], Keiji Takase[2], Yoichi Fujihara[2], Toru Okamoto[1]

1. Forestry and Forest Products Research Institute, Japan, 2. Ishikawa Prefectural University

In recent years, concerns about the effects of excess-nitrogen usage by human activities on terrestrial environment, including forest ecosystems, have been increasing at a global scale. The phenomenon of high-nitrate efflux from several forest watersheds has already been reported in the surroundings of metropolitan areas in Japan. Furthermore, concerns regarding the effects of transboundary air pollution on areas along the Sea of Japan with expanding economic activities have been increasing in Asian countries. However, on-site monitoring throughout the year is difficult in most of these areas because of heavy snow, especially in the mountainous area. Therefore, the behaviors of elements within forest ecosystems throughout a year have primarily not yet been elucidated in this district. This study was conducted to determine the influxes and effluxes of elements in this heavy snowy region and to understand the contribution of transboundary air pollution to the quantity of atmospheric deposition. We also carried out rainfall and stream water investigations from the headwater area to the lower stream area in the Tedori River Basin and an inland mountainous area to understand the geographical distribution of the actual conditions of elements' influxes and effluxes in this region. We started monitoring the major and minor elements in a small forested watershed in the middle part of the Tedori River Basin, Ishikawa prefecture, Japan, in 2013. In this study site, we observed a large amount of precipitation throughout the year. Regarding the annual snowfall amount, there were extensive variations among the years. Seasonal fluctuations were observed in the influx of atmospheric deposition; in particular, the distribution of most of the elements increased during winter. The annual deposition average of inorganic nitrogen (NH_4-N + NO_3-N) in this site was 15.8 kg ha^{-1}. The contribution of winter season deposition to the annual inputs was high. The influx of nitrogen by bulk precipitation during winter season was 2.3 times that of summer, and that of sulfur sulfate was 3.7 times. The nitrogen influx quantity was similar to or more than that reported in nitrogen-saturated forested areas of the Kanto district. Therefore, similar to that in the Kanto district, higher nitrogen deposition loads from the atmosphere could also be influenced on the effect of nitrogen dynamics and the increase in nitrogen efflux at these forest watersheds. However, the efflux concentrations of most of the dissolved elements in stream water did not show clear seasonal fluctuations. Stream water nitrate concentration was stable and low. In addition to the seasonal fluctuation of nitrogen and sulfur, the ratios among some trace elements, which are anthropogenic substances (Pb, V, As, etc.), and sea salts and yellow sand could be useful indicators to elucidate the contribution of transboundary air pollution to these regions. We compared the element inputs associated with precipitation during the non-snowy season (July–November) at six locations in the Tedori River Basin and one location in the inland area. The inorganic nitrogen and sulfuric acid sulfur influxes were the largest at the middle reaches of the Tedori River Basin. The inflow amount of inorganic nitrogen and sulfuric acid sulfur at two points in the mountainous area was approximately half or less than that at the middle region and was approximately the same as the inflow amount at the inland mountainous area. Furthermore, we investigated stream water, spring water, and ground water samples from the headwater area to the lower stream area in the Tedori River Basin. The nitrate concentrations in all the samples ranged from 0.00 to 2.93 mgL^{-1} (median value: 0.69 mgL^{-1}). In contrast, the nitrate concentrations of stream water in the Tsukuba experimental forest watershed, which has been reported as a nitrogen-saturated forested area of the Kanto district, were much higher (average value: 7.56 mgL^{-1}) than those in the Tedori River Basin. Compared with the influx, the efflux concentrations of nitrate in the water

©2019. Japan Geoscience Union. All Right Reserved.

samples were generally very low around this basin. Therefore, higher nitrogen depositions have not yet distinctly influenced the nitrate concentrations of stream water in this area. To elucidate the influence of transboundary air pollutant influx on the entire Tedori River Basin, it is necessary to evaluate the inflow amount during the snowy season in the mountainous area. Therefore, it is important to establish a method that can be used to observe the influx and efflux of elements throughout the year even in mountainous areas with heavy snow.

©2019. Japan Geoscience Union. All Right Reserved.

Continuous and simultaneous flux measurement of N_2O and CO_2 from agricultural soil using a portable multi-turn time-of-flight mass spectrometer

*Noriko Nakayama[1], Yusuke Iwai[1], Yo Toma[2], Hiroshi Furutani[1], Ryusuke Hatano[3], Michisato Toyoda[1]

1. Osaka University, 2. Ehime University, 3. Hokkaido University

Agricultural soil is one of the important sources/sinks of greenhouse gases such as N_2O, CO_2, and CH_4. The formation and consumption of such greenhouse gases in agricultural soils are dependent on not only the chemical and biological properties of the soil, but also their variations. Hence continuous monitoring of such greenhouse gases as tracer gases are quite useful to track chemical and biological processes and variations of soil properties.

In this paper, we describe a new field-deployable gas flux measurement system for the continuous monitoring of multiple agricultural soil gases (N_2O, CO_2, and CH_4) using a high resolution multi-turn time-of-flight mass spectrometer (MULTUM) combined with an automated flux chamber system. The new system measured the soil gases every 2.5 min with the precisions of ~6% for N_2O, CH_4, and 2% or better for CO_2 and O_2 at atmospheric concentrations with one relative standard deviation (RSD) for n = 10.

To demonstrate the utility of the continuous multi-gas flux measurement system, we conducted a field study at the Ehime University farm (Ehime, Japan) from September 3rd to 8th, 2018. In the field study, an automated flux chamber was placed in the agricultural field and the soil gas concentrations in the chamber were continuously monitored by the MULTUM system. Soil temperature/moisture sensor were also monitored at the depth of 7.5 cm underground in addition to a weather information (wind speed, precipitation, solar radiation). The continuous measurement had been continued with operators almost unattended except for a daily system check.

For one flux measurement (20 min), eight gas samples were taken every 2.5 min with the flux chamber closed. Gas flux of N_2O and CO_2 had been carried out by applying linear regression to the eight gas measurements. We found that a significant correlation of N_2O flux with soil electrical conductivity and water content, although no significant correlation of CO_2 flux to soil electrical conductivity was observed. Significant and rapid decreases in N_2O and CO_2 flux during rainfall events were also observed. Our preliminary result shows that high time-resolution flux data obtained by MULTUM system is quite useful for tracking the variation in soil properties and biological processes and their activity in soil environment.

Keywords: on-site mass spectorometry, MULTUM, soil-to-atmospher gas flux

©2019. Japan Geoscience Union. All Right Reserved.

Effects of introduction of cyclic irrigation system on mass balances of SS and T-P in Lake Inbanuma, Chiba, Japan

*Tomijiro Kubota[1]

1. National Agriculture and Food Research Organization, Institute for Rural Engineering

Introduction

The introduction of cyclic irrigation has been advanced since 2010 in the Lake Inbanuma as part of the update project of the irrigation facilities. In the present study, mass balances of SS and T-P were examined before and after the introduction of the cyclic irrigation.

Materials and methods

The irrigation block where the cyclic irrigation began in 2015 was selected as the investigation site, and the investigation was executed to the irrigation period in 2014 and 2015. The hydrological and water quality investigation was executed at ① division works of irrigation canal and ② drainage pumping station. Water samples were taken at the two points and the TOC, SS, TN, NO3-N, NO2-N, NH4-N, TP, and PO4-P were analyzed in the regular investigation executed about once a month. Besides regular investigation, water samples were taken once a day (8:00AM or noon) by the automatic water sampler and SS and T-P were analysed. The turbidity and water level were measured every ten minutes by using data loggers at same sites. The turbidity data were converted into the concentration of SS and TP by using the regression curve. The quantity of water intaken from the lake and drainage to the lake were obtained from the records of the facility manager.

Result and discussion

The inflow and outflow loads and the balance were calculated before and after the introduction of the cyclic irrigation. In 2014, before the start of cyclic irrigation, both the outflow loads of SS and T-P were small to compare with those inflow loads. The amount of accumulation of SS and T-P were about 1.3t and 2kg respectively when having no rainfall in the irrigation block. On the other hand, the outflow of SS and T-P were about 3.5t/day and 20kg/day respectively in rainy days. If 2015 year is compared to 2014, it had increased in T-P though the load of irrigation water each day at no rainfall periods and it had not been change in SS though an accurate comparison is difficult according to the missing value. However, after the cyclic irrigation had been started, the amount of the outflow loads had decreased greatly like 35% in SS and 38% in T-P. The balance of the outflow loads during the irrigation periods of 2014 were -470kg/day in SS, which meant the purification type, while +2.6kg/day in T-P. as a result, it was found that the introduction of cyclic irrigation system had worked for water purification in SS and T-P effectively.

Keywords: cyclic irrigation system, water pollution, suspended solid, total phosphorus

©2019. Japan Geoscience Union. All Right Reserved.

[E] Poster | A (Atmospheric and Hydrospheric Sciences)：A-CG Complex & General

Thu. May 30, 2019 1:45 PM - 3:15 PM JST | Thu. May 30, 2019 4:45 AM - 6:15 AM UTC | Poster Hall International Exhibition Hall8, Makuhari Messe_3

[A-CG34] Satellite Earth Environment Observation

convener:Riko Oki(Japan Aerospace Exploration Agency), Yoshiaki HONDA(Center for Environmental Remote Sensing, Chiba University), Yukari Takayabu(Atmosphere and Ocean Research Institute, the University of Tokyo), Tsuneo Matsunaga(Center for Global Environmental Research and Satellite Observation Center, National Institute for Environmental Studies)

In recent years, we cannot avoid facing issues on global environmental changes that occur in various spatiotemporal scales. The earth environmental observation data by satellites became the necessary basic data to tackle and solve those issues. Due to the recent advancement in the observation sensor technique and the data processing technique, the satellite observation has been showing rapid progress, and the time is changing from examining the accuracy of the observation sensor data to the advancement of the data application, leading to broaden potential users. In these days application became synergetic, so we comprehensively pick
up this topic in the Atmospheric and Hydrospheric Sciences Session of this Union Meeting that enables to comprise the atmospheric, oceanic and land sciences; by combining the intelligence and the knowledge of the party, we propose a session that aims to prompt further studies towards the issues on earth environmental change, the advancement in the data application and future plans of Earth Observation missions.

[ACG34-P01] Impact of usage of multiple-satellite sensors on accuracy of daily-mean sea surface wind data

*Ayumi Koizumi[1], Masahisa Kubota[2], Kunio Kutsuwada[3], Hiroyuki Tomita[4], Tsutomu Hihara[5] (1.Tokai University, 2.Tokai University, Institute of Ocean Research and Development, 3.School of Marine Science and Technology, Tokai University, 4.Institute for Space-Earth Environmental, Nagoya University, 5.Japan Agency for Marine-Erth Science and Technology)

[ACG34-P02] Temperature and Size Variability of Warm Pools in the Global Oceans

*ChunYi Lin[1] (1.National Museum of Marine Science & Technology)

[ACG34-P03] Sea surface temperature from SGLI aboard the GCOM-C satellite of JAXA

*Yukio Kurihara[1], Kazunori Ogata[2], Hiroshi Murakami[2], Misako Kachi[2] (1.Tripli-I Co., Ltd., 2.JAXA EORC)

[ACG34-P04] Concept of small satellite UV/visible imaging spectrometer optimized for tropospheric NO_2 measurements in air quality monitoring

*Tamaki Fujinawa[1,5], Katsuyuki Noguchi[2], Akihiko Kuze[3], Andreas Richter[4], John P. Burrows[4], Andreas C. Meier[4], Tomohiro Sato[1], Takeshi Kuroda[1], Naohiro Yoshida[5], YASUKO KASAI[1,5] (1.National Institute of Information and Communications Technology, 2.Nara Women's University, 3.Japan Aerospace Exploration Agency, 4.University of Bremen, 5.Tokyo Institute of Technology)

[ACG34-P05] EarthCARE L2 algorithms for cloud and precipitation

*Kaori Sato[1], Hajime Okamoto[1], Hiroshi Ishimoto[2] (1.Research Institute for Applied Mechanics, Kyushu University, 2.Meteorological Research Institute)

[ACG34-P06] Analysis of the Surface Echo Characteristics Derived from GPM/DPR Wide Swath Observation Experiment

*Kosuke Yamamoto[1], Kinji Furukawa[1], Nobuhiro Takahashi[2], Takuji Kubota[1] (1.Japan Aerospace Exploration Agency, 2.Nagoya University)

[ACG34-P07] The Recent Results from the Global Precipitation Measurement (GPM) mission in Japan

*Riko Oki[1], Takuji Kubota[1], Kinji Furukawa[1], Yuki Kaneko[1], Moeka Yamaji[1], Kosuke Yamamoto[1], Toshio Iguchi[2], Yukari Takayabu[3] (1.Japan Aerospace Exploration Agency, 2.NICT, 3.the University of Tokyo)

[ACG34-P08] **Verification of Global Satellite Mapping of precipitation (GSMaP) for providing its error information**

*Moeka Yamaji[1], Takuji Kubota[1] (1.Earth Observation Research Center, Japan Aerospace Exploration Agency)

[ACG34-P09] Detection of the mixed phase top using the measured dual-frequency ratio of reflectivity with GPM/DPR

*Yuki Kaneko[1], Toshio Iguchi[2] (1.Japan Aerospace Exploration Agency, 2.National Institute of Information and Communications Technology)

[ACG34-P10] **Comparison between high frequency satellite rainfall estimation and APHRODITE-2 ground rain gauge observation**

*Hitoshi Hirose[1], Koichi Toyoshima[1], Atsushi Higuchi[1], Akiyo Yatagai[2], Natsuko Yasutomi[3] (1.Center for Environmental Remote Sensing, Chiba University, 2.Hirosaki University, 3.Disaster Prevention Research Institute, Kyoto University)

[ACG34-P11] Development of the high resolution GSMaP by the Himawari-8

*Tomoaki Mega[1], Tomoo Ushio[1] (1.Tokyo Metropolitan University)

[ACG34-P12] Preliminary results of on-orbit estimation for polarization sensitivity of GCOM-C/SGLI

*Risa Miyazaki[1], Hiroshi Murakami[1], Masahiro Hori[1] (1.Japan Aerospace Exploration Agency)

[ACG34-P13] Analysis of SGLI validation datas based on the effects of the growth and ground types for the AGB development

*Ryota Ishibashi[1], Koji KAJIWARA[1], Yoshiaki HONDA[1] (1.Center for environmental remote sensing, Chiba University)

[ACG34-P14] Remote sensing of aerosol optical properties and water-leaving radiance based on the optimal estimation approach

*Chong Shi[1], Teruyuki Nakajima[1], Makiko Hashimoto[1], Hideaki Takenaka[1] (1.Japan Aerospace Exploration Agency)

[ACG34-P15] Aerosol retrieval and PM2.5 from space using GOSAT/TANSO-CAI

*Makiko Hashimoto[1], Hideaki Takenaka[1], Teruyuki Nakajima[1], Akiko Higurashi[2] (1.Japan Aerospace Explortion Agency, 2.NIES)

[ACG34-P16] **Establishing a high resolution road fugitive dust emission inventory in Kaifeng City, China**

*Yiming Xu[1], Shili Liu[1], Xinyue Cao[1], Xianbao Shen[1], Zhiliang Yao[1] (1.Department of Environmental Science and Engineering, Beijing Technology and Business University)

[ACG34-P17] A Relationship between Diurnal Change Patterns of Land Surface Temperature and Spatial Configuration of the Osaka Metropolitan Area Captured by Himawari-8

*Yuhei Yamamoto[1], Hirohiko Ishikawa[1] (1.Disaster Prevention Research Institute, Kyoto University)

Impact of usage of multiple-satellite sensors on accuracy of daily-mean sea surface wind data

*Ayumi Koizumi[1], Masahisa Kubota[2], Kunio Kutsuwada[3], Hiroyuki Tomita[4], Tsutomu Hihara[5]

1. Tokai University, 2. Tokai University, Institute of Ocean Research and Development, 3. School of Marine Science and Technology, Tokai University, 4. Institute for Space-Earth Environmental, Nagoya University, 5. Japan Agency for Marine-Erth Science and Technology

Most satellites observing sea surface winds have sun-synchronous orbits and provide observation data at the same place two times per a day. We can expect that daily-mean values estimated from these data have some errors when diurnal changes in wind field cannot be neglected. For this problem, use of multiple satellites is helpful. Since the number of sensors used to construct daily-mean data is different among the years, it is expected that the accuracy of a daily-mean value changes from year to year.

The purpose of this study is to describe time variation of accuracy in daily-mean wind data in the Japanese Ocean Flux Data Sets with Use of Remote Sensing Observation (J-OFURO)-3 and to investigate its causes by comparing with in-situ measurement data by moored buoys and calculating three statistical values.

Results reveal that the statistical values are improved with year. To examine the relationship between the yearly statistics and the yearly number of satellite sensors, we plotted a scatter diagram between the number of satellites and three statistical values in each year. We found that the correlations between them are very high. We also focused on a time interval of the satellite wind observation, namely maximum missing time within a day. The result showed that the correlation between three statistical values and maximum missing time intervals is high. Since the relation between these two factors is not independent, we analyzed by considering both factors together. First, we chose five buoys with various standard deviations for a daily-mean value. Next, we picked up data from buoy's hourly data using random numbers, and calculated the daily mean value using the random data, and then determined the number of observations and the maximum missing time interval each day. Assuming the daily mean value calculated from 24 hourly data as a true value, the RMSE between this true value and the daily mean created from random data was calculated. From the result of this analysis, it was found that the value of Root Mean Square Error(RMSE) depends on the maximum missing time interval rather than the number of observations. Furthermore, when RMSE was normalized by standard deviation, the same figures were obtained for all buoys. This result implies that the RMSE of the daily mean value of the buoy station can be estimated if the magnitude of diurnal variation is known by giving the number of satellites used for observation and the maximum missing time interval, Moreover, by applying this result, we think that it is possible to show the optimal number of sensors and observation time for target accuracy. This result gives very breakthrough information to the design of the satellite observation system for sea surface wind.

Keywords: Multiple-satellite sensors, Sea surface wind

©2019. Japan Geoscience Union. All Right Reserved.

Temperature and Size Variability of Warm Pools in the Global Oceans

*ChunYi Lin[1]

1. National Museum of Marine Science & Technology

Using advance satellite-derived Sea surface height anomaly, sea surface temperature (SST) data, and heat flux data, we investigate the thermal variability, temperature and size variability of warm pools in the global oceans, the Pacific, the Atlantic, and the Indian Ocean, respectively. Because of the high density and specific heat of seawater, water can store and transport large amounts of heat. High SST has particular influence on global climate system. Furthermore previous studies focused on the global warming or area warming, in this investigation we present results of warm pool SST binned into 1 ˚C interval. Detecting temperature and size variability of warm pools in the global oceans, it suggests that the high SST area (SST ≧ 28˚C) has faster increasing rate than surrounding area (SST 20˚C - 27˚C) in the global oceans, the Pacific, the Atlantic, and the Indian Ocean, respectively. To understand the role of surface heat flux in the tropical SST fluctuation, we analyze the mixed layer heat balance equation. Upper ocean heat budget between the heat advection and heat diffusion term are compared and heat diffusion processes may be a mechanism for transporting excessive amount of heat that the warm pool through enhancing the SST gradient around the edge of the warm pool. In order to find out dominant period components and the relationship of energy-frequency distribution without influenced induced by nonlinear and nonstationary signals, the Hilbert-Huang Transform applied by ensemble empirical mode decomposition is employed. The ensemble empirical mode decomposition analysis indicates that the interannual component has strong influence on the variability of the warm core pool in the Pacific, presumably because of the presence of El Niño phenomenon, while the annual cycle dominates the variability in the Indian and the Atlantic Ocean.

Keywords: warm pool, SST, heat flux

©2019. Japan Geoscience Union. All Right Reserved.

Sea surface temperature from SGLI aboard the GCOM-C satellite of JAXA

*Yukio Kurihara[1], Kazunori Ogata[2], Hiroshi Murakami[2], Misako Kachi[2]

1. Tripli-I Co., Ltd., 2. JAXA EORC

The Global Change Observation Mission-Climate (GCOM-C) satellite, which is one of two satellites for the GCOM mission of the Japan Aerospace and Exploration Agency (JAXA), was launched on 23 December 2017. The Second Generation Global Imager (SGLI) is the optical sensor aboard GCOM-C which consists of two components: the Visible and Near-infrared Radiometer (VNR) and the Infrared Scanner (IRS). SGLI has switchable spatial resolution from 250 m x 250 m to 1 km x 1 km. The resolution of 250 m x 250 m is expected to reveal complicated structure of geophysical parameters. Sea surface temperature (SST), which is one of the important parameters in the geophysical field, is also determinable by using split window data of SGLI. SGLI SST is retrieved by utilization of newly developed cloud masking method and a modified SST method originally developed for Himawari-8. Considering combined utilization of satellite SSTs, the methods developed for SGLI SST will be applied back to Himawari-8 data as well as the data from the Visible Infrared Imaging Radiometer Suite (VIIRS) aboard the Suomi National Polar-orbiting Partnership (Suomi NPP) satellite. SGLI SST is validated by comparison with buoy data. The comparison result shows RMSD of ~0.4 K, good agreement between SGLI SSTs and buoy data. Triple comparison with Himawari-8 and VIIRS SSTs is being started. Operational retrieval of SGLI SST started at the end of 2018. The products are available at the G-Portal site of JAXA and the JAXA Satellite Monitoring and Environmental Studies (JASMES) site of the Earth Observation Center (EORC) of JAXA.

©2019. Japan Geoscience Union. All Right Reserved.

Concept of small satellite UV/visible imaging spectrometer optimized for tropospheric NO_2 measurements in air quality monitoring

*Tamaki Fujinawa[1,5], Katsuyuki Noguchi[2], Akihiko Kuze[3], Andreas Richter[4], John P. Burrows[4], Andreas C. Meier[4], Tomohiro Sato[1], Takeshi Kuroda[1], Naohiro Yoshida[5], YASUKO KASAI[1,5]

1. National Institute of Information and Communications Technology, 2. Nara Women's University, 3. Japan Aerospace Exploration Agency, 4. University of Bremen, 5. Tokyo Institute of Technology

Satellite observations at nadir can potentially facilitate a better understanding of the emissions and distribution of tropospheric nitrogen dioxide, NO_2. The identification of emissions requires adequate spatiotemporal resolution measurements of the total column amounts of NO_2. The spatial resolution of previous and current observations is insufficient for the identification of NO_2 hot-spots. Switching to a spatial resolution of ~1 km x ~1 km can improve the identification of local sources of NO_2 and their emissions. To investigate the feasibility of observations with such a high spatial resolution, we simulated radiance spectra for different cases under varying parameters, such as area, season, satellite altitude, and surface reflectance by using the radiative transfer model SCIATRAN. We subsequently retrieved NO_2 slant column densities (SCDs) using the differential optical absorption spectroscopy (DOAS) technique with several fit windows. For test cases associated with polluted conditions, we found that the conceptual nadir-observing instrument on a satellite at an altitude of ~300 km involved the lowest retrieval errors for signal-to-noise ratios of around 1000 with accuracy better than the required 5% for tropospheric NO_2 SCD and that the fit window of 425--497 nm met the scientific requirements for both surface reflectance cases.

Keywords: Nitrogen dioxide, Earth observation, Radiative transfer model, Remote sensing

©2019. Japan Geoscience Union. All Right Reserved.

EarthCARE L2 algorithms for cloud and precipitation

*Kaori Sato[1], Hajime Okamoto[1], Hiroshi Ishimoto[2]

1. Research Institute for Applied Mechanics, Kyushu University, 2. Meteorological Research Institute

The EarthCARE (Earth Clouds, Aerosols and Radiation Explorer, JAXA-ESA) mission will carry the first 94GHz Doppler Cloud Profiling Radar (CPR) with a high spectral resolution atmospheric lidar (ATLID) at 355nm. Recent progresses in EarthCARE L2 cloud/precipitation algorithms for the treatment of multiple scattering and cloud particle nonsphericity are presented.

Keywords: spaceborne active sensor, cloud

©2019. Japan Geoscience Union. All Right Reserved.

Analysis of the Surface Echo Characteristics Derived from GPM/DPR Wide Swath Observation Experiment

*Kosuke Yamamoto[1], Kinji Furukawa[1], Nobuhiro Takahashi[2], Takuji Kubota[1]

1. Japan Aerospace Exploration Agency, 2. Nagoya University

The observation from spaceborne precipitation radar has been contributed to better understanding of earth climate system. Global Precipitation Measurement (GPM) core satellite Dual-frequency Precipitation Radar (DPR) provides us 3-dimentional information of precipitation by the scan width of about 250 km, but there have been arguments that to bring systematic impact on the weather monitoring through global rainfall map such as GSMaP, wider swath observation by precipitation radar is necessary.

Based on those requirements, the scan pattern of GPM/DPR was experimentally changed for 1 day from 13UTC on September 26th. In this experiment, the scan angle was changed to observe from nadir to about +34˚ assuming future spaceborne precipitation radar with wider swath width, while in the normal observation DPR scans ±17˚. The height and strength of the mainlobe clutter with larger incident angle were assessed statistically to examine the possibility of the rainfall retrieval with wide swath observation by DPR.

In order to examine mainlobe clutter height, it is inevitable to reduce sidelobe and grating lobe effect. In this study, clutter-free observation data is extracted based on following procedures; 1) extract bins above mainlobe clutter; 2) extract bins under non-precipitation condition from 1); 3) extract bins that satisfy |received power −averaged noise power| < 2 sigma of the noise power from 2). Note that this procedure was applied only for KuPR observation since sidelobe and grating lobe clutter is not prominent in KaPR.

The result for KuPR observation shows that the mainlobe clutter top height at the larger incident angle over ocean is somehow suppressed at around 4 km while over land it increases almost linearly up to around 5 km due to the strong surface scattering. The same tendency is found on the KaPR observation, but it has lower clutter top height of around 2.5 km and 3.5 km, over ocean and land respectively. Suppression is clearer over ocean thanks to the specular reflection. The results also indicate that relatively intense rainfall can be retrieved while shallow rainfall with weak echo power may not be acceptable for retrieval because it should be masked by the surface clutter.

Keywords: precipitation radar, radar clutter, GPM core satellite

©2019. Japan Geoscience Union. All Right Reserved.

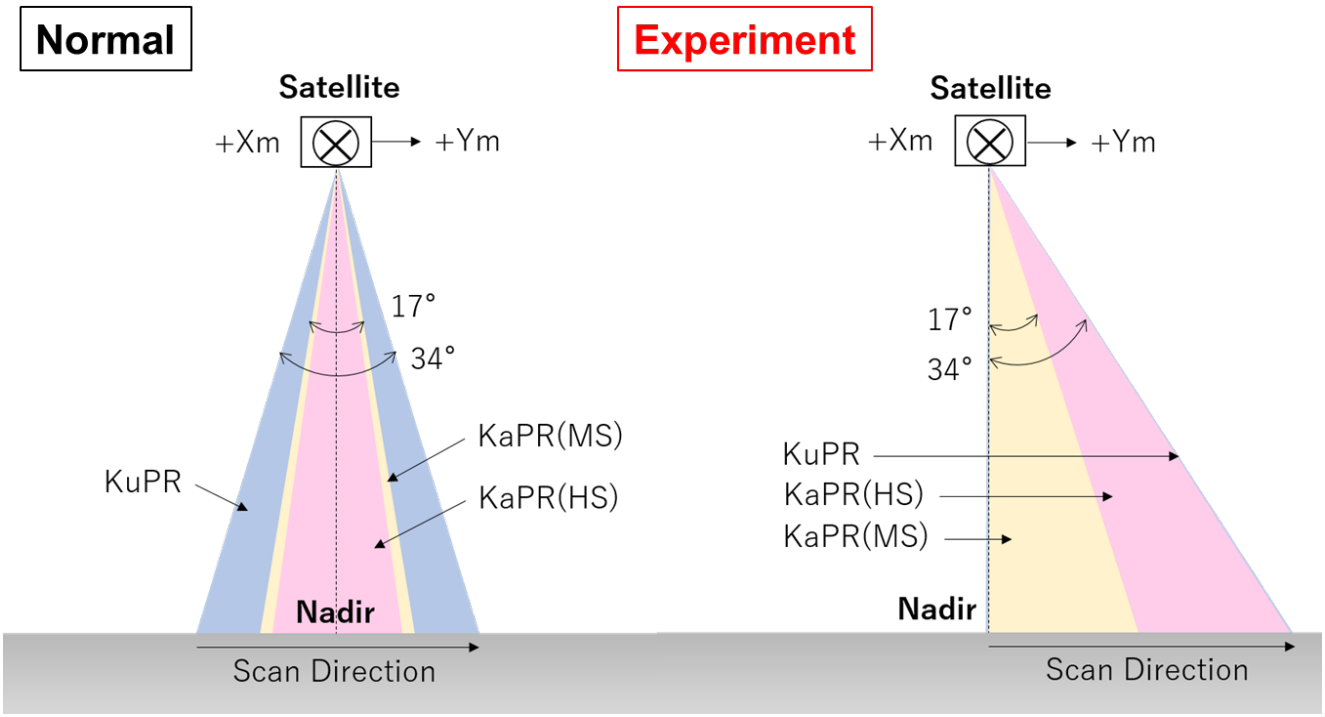

©2019. Japan Geoscience Union. All Right Reserved.

The Recent Results from the Global Precipitation Measurement (GPM) mission in Japan

*Riko Oki[1], Takuji Kubota[1], Kinji Furukawa[1], Yuki Kaneko[1], Moeka Yamaji[1], Kosuke Yamamoto[1], Toshio Iguchi[2], Yukari Takayabu[3]

1. Japan Aerospace Exploration Agency, 2. NICT, 3. the University of Tokyo

The Global Precipitation Measurement (GPM) mission is an international cooperate satellite project to achieve highly accurate and highly frequent global precipitation observations. The GPM mission consists of the GPM Core satellite jointly developed by the U.S. and Japan and Constellation Satellites that carry microwave radiometers and provided by the GPM partner agencies. The GPM Core satellite carries the Dual-frequency Precipitation Radar (DPR) by the Japan Aerospace Exploration Agency (JAXA) and the National Institute of Information and Communications Technology (NICT) and the GPM Microwave Imager (GMI) provided by National Aeronautics and Space Administration (NASA). The GPM Core satellite was launched in February 2014 and achieved its prime mission period planned for 3 years in 2017.

It has been continuing its observation as the extended mission phase after that.

JAXA develops the DPR Level 1 algorithm and the NASA-JAXA Joint Algorithm Team develops the DPR Level 2 and DPR-GMI combined Level 2 algorithms. The DPR, the DPR-GMI combined algorithms and the latent heating algorithm were updated, and those products were released in October 2018 as Version 0.6. Using dual frequency information of DPR, the latest Level 2 products include information such as precipitation phase at surface, heavy ice precipitation and so on. Also, the calibration factors of TRMM/PR were re-examined to have consistency between DPR/Ku. The same GPM Ku-band radar L2 algorithm now applies to the TRMM/PR, so that the long radar precipitation data exceeding more than 20 years are now available. From May 2018 in the extended mission period, the scan pattern of the Ka-band radar has been changed to realize matched beam observation in full swath. The new algorithm applying to the changed scan pattern is now under development.

JAXA also develops the Global Satellite Mapping of Precipitation (GSMaP), that is hourly and 0.1-degree horizontal resolution global rainfall map. It is available through the “JAXA Global Rainfall Watch” website (https://sharaku.eorc.jaxa.jp/GSMaP/index.htm). GSMaP product family includes different data latency products and rain gauge calibrated products and so on. The GSMaP near-real-time version (GSMaP_NRT) product provides global rainfall map in 4-hour after observation, and an improved version of GSMaP near-real-time gauge-adjusted (GSMaP_Gauge_NRT) product has been released since Dec. 2018.

The GSMaP real-time product called GSMaP_NOW now product is providing data at the earliest timing. It has been realized using the geostationary satellite Himawari-8 operated by the Japan Meteorological Agency (JMA) since November 2015. Since Nov. 2018 the domain of GSMaP_NOW has been extended to the region of the geostationary satellite Meteosat operated by the European Organization for the Exploitation of Meteorological Satellites (EUMETSAT) in November 2018. JAXA is further developing the GSMaP_NOW to provide global real-time rainfall product.

Keywords: GPM, Satellite Remote Sensing, Precipitation

©2019. Japan Geoscience Union. All Right Reserved.

©2019. Japan Geoscience Union. All Right Reserved.

Verification of Global Satellite Mapping of precipitation (GSMaP) for providing its error information

*Moeka Yamaji[1], Takuji Kubota[1]

1. Earth Observation Research Center, Japan Aerospace Exploration Agency

Precipitation is one of the most essential parameters in the Earth system. Due to address water issues like water shortage or floods, JAXA has developed and provided Global Satellite Mapping of Precipitation (GSMaP), which is hourly global precipitation dataset. It is under the Global Precipitation Measurement (GPM) mission and contributes.
GSMaP allows us to capture the hourly horizontal distribution of precipitation with good latency after observation. The spatial resolution is 0.1 x 0.1 degrees latitude/longitude. It has been used for various kinds of utilization purposes.
In terms of accuracy, GSMaP algorithms were updated in several times, and GSMaP has been getting more accurate day by day, however, it is known that the inhomogeneous of accuracy is existed depending on algorithm characteristics. It has been needed to provide information about the uncertainty and accuracy of GSMaP by users.
In this study, verification result of GSMaP near-realtime product version 6 (GSMaP_NRT) is reported. The radar/raingauge analysed precipitation data by Japan Meteorological Agency, which is an hourly rainfall analysis generated from ground-based precipitation radars corrected by automated rain gauges, are used as the reference data. Since the purpose of this study is for providing generalized error information, root mean square errors (RMSE) is statistically calculated for each precipitation level and each reliability flag during May-June-July-August-September-October in 2015-2018. Some initial results showed that the RMSE qualitatively represented the error for each precipitation level and reliability flag. The RMSE ratio to the average precipitation rate got larger as the precipitation rate became smaller while it became stable around 60 –80 % when precipitation rate was more than 10 mm/h. We report the validation results in detail, such as land/ocean difference or sampling dependence, and focus on the effectiveness of it.

Keywords: precipitation, GPM, GSMaP, validation

©2019. Japan Geoscience Union. All Right Reserved.

Detection of the mixed phase top using the measured dual-frequency ratio of reflectivity with GPM/DPR

*Yuki Kaneko[1], Toshio Iguchi[2]

1. Japan Aerospace Exploration Agency, 2. National Institute of Information and Communications Technology

The core observatory of the Global Precipitation Measurement (GPM) mission was launched in 2014 and has been observing rain and snow between 65˚S and 65˚N by the Dual Frequency Precipitation Radar (DPR) and the GPM Microwave Imager (GMI). The DPR provides three-dimensional structure of storms derived from reflected energy from precipitation particles. Precipitation echoes at the two frequencies of the DPR, Ka-band (25GHz) and Ku-band (14GHz), make it possible to infer the mean size and physical property of precipitation particles. The swath width of Ka-band scanning was 125 kilometers centered at nadir and was nested within the Ku-band’ s wider scan width of 254 kilometers. On May 21 2018, the Ka-band scan pattern was changed to match with the Ku-band’ s. Dual frequency radar reflectivity factors are available for full swath of 254 kilometers now.

The classification (CSF) module in the standard DPR level2 algorithm detects a bright band (BB) and classifies precipitation into three types, stratiform, convective, and other. Rain types affect the retrievals of rain amount and latent heating in the DPR algorithm. Accurate classification is also important in the Global Satellite Mapping of Precipitation (GSMaP) algorithm because it affects the rain profile database used in the rain retrieval with microwave radiometers. The BB detectability by the standard CSF algorithm is lower at and near the swath edges than near nadir because only Ku-band data was available in the outer swath before and because slant incidence of radar beams smears the vertical profiles.

As the Ka-band scan pattern has changed to cover the full swath, we can apply a dual-frequency method to detect a BB now. We have developed a method that uses the dual frequency ratio (DFR) to detect the mixed phase top. It looks at the slope of DFR as a function of range to identify the transition height from ice to water. DFR itself is estimated from measured DFR (DFRm) with attenuation correction. Preliminary experiments show that the developed method can detect the BB in stratiform rain over the swath almost uniformly. This method also has a potential to identify the transition height even in some convective cases. In this research we evaluate the performance of the algorithm by comparing the altitude of BB and the transition height with those estimated by using X-band multi-parameter radar (XRAIN) data.

Keywords: GPM, Melting Layer, Precipitation Radar

©2019. Japan Geoscience Union. All Right Reserved.

Comparison between high frequency satellite rainfall estimation and APHRODITE-2 ground rain gauge observation

*Hitoshi Hirose[1], Koichi Toyoshima[1], Atsushi Higuchi[1], Akiyo Yatagai[2], Natsuko Yasutomi[3]

1. Center for Environmental Remote Sensing, Chiba University, 2. Hirosaki University, 3. Disaster Prevention Research Institute, Kyoto University

APHRODITE project collects daily precipitation observation data from ground rain gauges in each country, and then performs appropriate quality control and converts it into gridded data. APHRODITE holds long-term data from the 1960s to the present and focuses on analyzes such as changes in characteristics of extreme rainfall due to long-term climate change. However, ground-based daily rain observations has a problem which end of the day (EOD) in each country is different from each other. To estimate the EOD in each country, we developed a Rain Potential Map (RPM) which is a product that can estimate global rain probability using geostationary meteorological satellites (GEO) (Hirose et al., 2016, JMSJ). In this study, we used the RPM, GSMaP and CMORPH which are global satellite rain estimation data based on microwave satellite and GEO observations.

Since the above satellite rainfall observation data can estimate global precipitation every hour, it is possible to create daily average data in which the average section is shifted by one hour. By correlating the satellite daily precipitation observation time series with the APHRODITE daily precipitation observation time series, the EOD value in each country was estimated from the time when the correlation coefficient is largest. We confirmed that the reliability of this method is high by a verification analysis in the field where true value of EOD is already known. Moreover, we made pseudo hourly rain time series of APHRODITE by inserting APHDOITE daily rain time series to satellite hourly rain time series. By this method, we will try to make a new APHRODITE data that is corrected for the EOD difference between each country.

Keywords: Precipitaition, Satellite, APHRODITE

©2019. Japan Geoscience Union. All Right Reserved.

Development of the high resolution GSMaP by the Himawari-8

*Tomoaki Mega[1], Tomoo Ushio[1]

1. Tokyo Metropolitan University

There is a new generation infrared (IR) imager on new-generation gestationary weather-satellite such as the Himawari-8 and the Geostationary Operational Environmental Satellite-R series. The imagers observe multi-channel passive imaging radiometer. The imagers observe wave a full disk with several km in about ten minutes. In Near-future, the IR imager observation should cover the globe.

Global precipitation information is an important tool for water management or earth science. Spaceborne sensors is one of the most convenient tools of global observation. The sensors cover global and provide uniform quality data. Precipitation estimation use microwave radiometer in low earth orbit (LOE). A microwave radiometer has high spatial resolution. However, one drawback of the microwave radiometer in LOE is narrow observation area. Whole earth observation by a microwave radiometer on a LOE satellite need some days. Therefore, global precipitation map is made from combined satellite data. However, combined data of microwave radiometer on LOE don’ t cover global in one hour. One of the global precipitation map is the Global satellite mapping of Precipitation (GSMaP). Precipitation estimation of the GSMaP made from microwave radiometer data. The GSMaP Moving Vector with Kalmanfilter (MVK) and Near real time compensate precipitation of no observation area by IR information. Spatial and temporal resolution of the GSMaP MVK achives 0.1 degree and one hour. This study shows downscale technique for GSMaP precipitation map by High-spatial and temporal resolution IR data of the Himawari-8. IR datasets of Himawari-8 are available every 2.5 minutes in the Japan region. In the presentation, we will also show validation the high resolution GSMaP and ground-radar network in Japan.

Keywords: Precipitation, GSMaP, Microwave Radiometer, Infrared Radiometer, Algorithm

©2019. Japan Geoscience Union. All Right Reserved.

Preliminary results of on-orbit estimation for polarization sensitivity of GCOM-C/SGLI

*Risa Miyazaki[1], Hiroshi Murakami[1], Masahiro Hori[1]

1. Japan Aerospace Exploration Agency

The GCOM-C has been launched successfully on 23th Dec. 2017 from the Tanegashima Space Center by H-IIA vehicle No.37. After the initial calibration/validation phase of one year after launch, all SGLI standard products have been released from JAXA’s data providing service (G-Portal) from Dec. 20, 2018.

In generally, the radiance reflected by the sea surface and the atmosphere is strongly polarized. When observing a large polarized light, the output radiance vary from the actual radiance because of the polarization sensitivity characteristic of the optical sensor. Especially for ocean color products, it is important to evaluate the effect of polarization sensitivity because it is necessary to extract the weak water-leaving reflectance (<10% of the whole) by the accurate atmospheric correction.
The polarization sensitivity of GCOM-C/SGLI of each NP (Non-Polarization) band has been measured in the pre-launch ground test. The ground test results of polarization sensitivity were shown to be <3.5% on average in the pixel direction in all bands. In this study, we evaluate whether the polarization sensitivity estimated from on-orbit observation data is consistent with the pre-launch test results. In this work, we report on the RED bands (VN07, VN08) and the NIR bands (VN10, VN11) of SGLI.
Polarization sensitivity on-orbit was evaluated based on Gordon and Zhang (1997) and Meister et al. (2005). We use the observation data by SGLI/PL (Polarization) band to estimate the real stokes vector components at the top of atmosphere (TOA). In order to obtain the polarization sensitivity with respect to directly observed radiance at TOA, L1B before inter-pixel sensitivity correction and before inter-telescope sensitivity correction was self-made from L1A data.
We analyzed the observation data of 12 path that PL band is observed nadir direction. The characteristics of the instrument for polarization sensitivity (polarization factor) were estimated by the least squares method. On the east side of the observation image, the error is large because of Sun-Glint. Although the variation in the pixel direction was still large, the estimated polarization factors (3 to 5 %) were consisted with the prelaunch ground test (~ 3.5%). However, sensitivity patterns in the pixel direction could not be identified, so we will continue to improve the evaluation in the future.

Keywords: GCOM-C, SGLI, Polarization sensitivity

©2019. Japan Geoscience Union. All Right Reserved.

Analysis of SGLI validation datas based on the effects of the growth and ground types for the AGB development

*Ryota Ishibashi[1], Koji KAJIWARA[1], Yoshiaki HONDA[1]

1. Center for environmental remote sensing, Chiba University

The effects of the earth of the time variant system should be difficult to detect the influence of the growth types and also the effects of the growth field’s variations. The research may occur the SGLI’s RSRF datas of the calculated AGB data accuracy analysis that observed between every kinds of the growth and also the ground types. The significance area of the SGLI observed, each of detected datas accuracy have to be considered. We show observation ways for the ground truth of the reflectance, LAI and fAPAR. The first case we use is a case of vegetation at the grassland. And then, based of reflectance values, we compare the other type as the Mixed coniferous forest example. The influence of an effect of the type of growth may occur the reflectance of the distributed area. We will detect these effects of the growth type. The influence at the observed area be necessarily to be verified.

The research topic includes the ground truth observation for the accuracy verification of a SGLI data obtained. For development of ground truth, the way to obtain datas were important. This paper explains how to examine growth (such as a second growth forest and other) and the slope factor of the second growth forest area and also the reflectance of each forest types. Then, this paper make ground truth observation scheme for the high accuracy AGB referenced data development at ground cover area. We explain the method of examine the error detection way including observation devices and also the problem of the research topic to be examined. Results may occur an example case of such kinds of the sloped forest and the kinds of the plane. The results shows a typical difference between the sloped and the plane, and then the results may occur the possibility that comparison of standard deviation may be an effective way to detect the volume of the forest type between every ground truth.

The case of we use as the sloped fields, reflectance of each wavelength were low and then the near 400 to 700 nm area will be higher than other wavelength (ANOVA values of results: $p < 0.001$). And then, we can see the effects of slope should be detected at total values of the reflectance. The reflectance of a wavelength were obtained that aimed to detect the verification of the slope and the growth type’s reflectance. When the mixed coniferous forest, static observation develop same reflectance values but the effect of the sloped factor occur the high value of the standard deviations. Then, our method applied to the method of the SGLI’s data calculation scheme, and then the growth factor of the area be affects the influence of the from 400 to 700 nm wavelength and also the factor of slope region be affects the wavelength of reflectance. SGLI data analysis, the factor of these parameters were used to remake the size of RSRF data from 250 m to 1000 m resolution. The future, we investigate more and then, the mask area of high value difference around the nearest 16 pixels be considered. Datas were significant at some pixels, such as a steep sloped, growth types, or error detected area. Data development of RSRF, the reflectance of each cells are detected as the values of the every ground types by the standard deviation.

Keywords: SGLI's data verifications, Reflectance maps, Statistical ANOVA analysis

©2019. Japan Geoscience Union. All Right Reserved.

Factor analysis of variable results (Three-way ANOVA)

Sloped factors: Mean values of the SD of each (dynamic/semi-static)
Canopy factors: Difference of each SD of the every SD
Growth typed factors: Difference of each Mean and SD

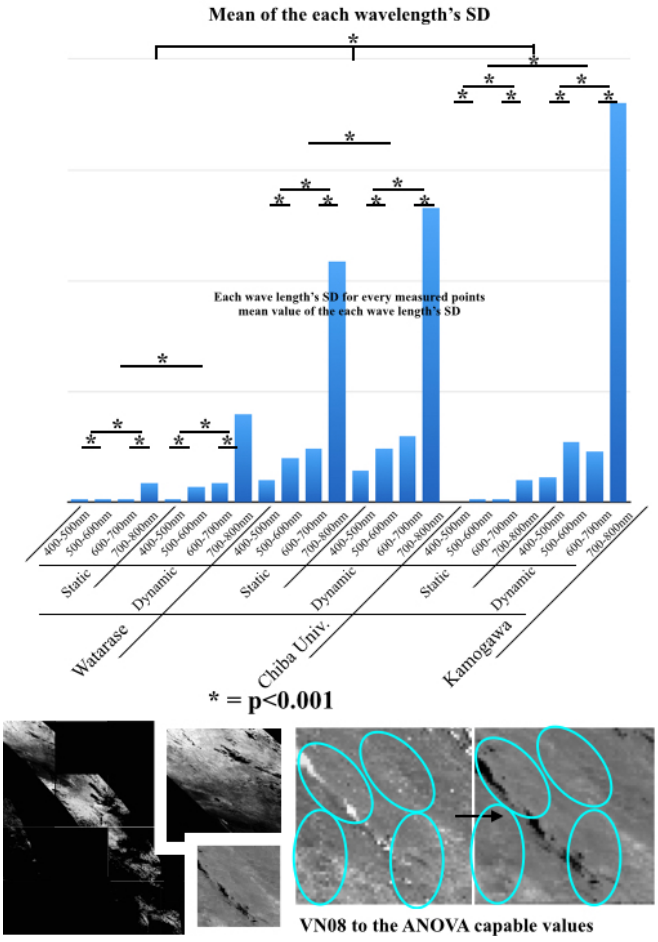

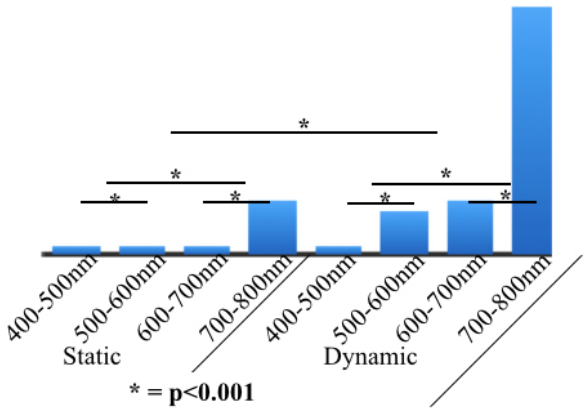

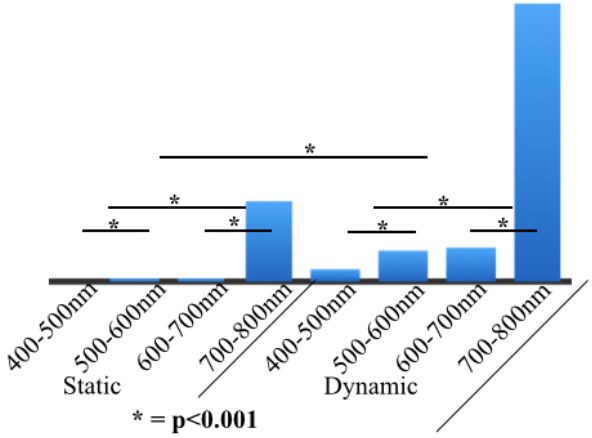

©2019. Japan Geoscience Union. All Right Reserved.

Remote sensing of aerosol optical properties and water-leaving radiance based on the optimal estimation approach

*Chong Shi[1], Teruyuki Nakajima[1], Makiko Hashimoto[1], Hideaki Takenaka[1]

1. Japan Aerospace Exploration Agency

A flexible inversion algorithm is proposed for jointly retrieving aerosol optical properties and water-leaving radiance from multispectral instrument over the ocean. A combined multi-wavelength and multi-pixel constraint approach is used to estimate aerosol and hydrosol over clear and turbid waters, based on the forward simulation from a coupled atmospher-ocean radiative transfer model. This sort of simultaneous inversion helps to correct the biases induced by the neglect of water-leaving radiance in the traditional aerosol retrieval algorithms, in addition, it can provide more aerosol information than the standard ocean color approach. To investigate the availability of current scheme, we conduct the retrieval in the process of MODIS, GOSAT/CAI and GCOM-C/SGLI instruments.

©2019. Japan Geoscience Union. All Right Reserved.

Aerosol retrieval and PM2.5 from space using GOSAT/TANSO-CAI

*Makiko Hashimoto[1], Hideaki Takenaka[1], Teruyuki Nakajima[1], Akiko Higurashi[2]

1. Japan Aerospace Explortion Agency, 2. NIES

Aerosol in the atmosphere has a great impact not only for the Earth’ s radiation budget and changing the Earth’ s climate, but also on human health. Especially, the fine particle, which is often called PM2.5, has drawn attention as a cause of health damage.

The urban area is a source of anthropogenic aerosol, which is mostly composed of small particles, and the particles are transported to other regions. Satellite remote sensing provides effective means to monitor the atmospheric aerosols in wide area including urban areas.

Accurate retrieval of fine mode aerosol optical thickness (AOT) is necessary to calculate an equivalent value of PM2.5 from space. Therefore, an aerosol retrieval algorithm for satellite remote sensing of urban areas to improve the retrieval accuracy of aerosol properties, which is called MWPM (Multiple wavelengths and pixels method) (Hashimoto and Nakajima, 2017), was developed. The method simultaneously retrieves fine and coarse mode AOT and single scattering albedo by using several wavelengths and spatial difference of surface reflectance. The method is useful for aerosol retrieval over spatially inhomogeneous surface like an urban area.

The algorithm was applied to GOSAT (Greenhouse Gases Observing Satellite) / TANSO-CAI (Cloud and Aerosol Imager, CAI) data. The GOSAT launched ten years ago (on January 23th, 2009) is a satellite to monitor greenhouse gases (GHG) such as carbon dioxide and methane with TANSO-FTS (Fourier Transform Spectrometer, FTS). The CAI is a supplementarysensor of the FTS, detecting cloud and deriving aerosol optical properties.

PM2.5 using retrieved fine mode AOT by MWPM in East Asian region from 2009 was calculated. The poster presents a retrieval result of PM2.5 over the East Asian region from space in several years and discusses the seasonal and annual variations.
Monitoring of aerosol properties such as AOT, PM2.5 and soot mixing ratio over land is added to the mission of GOSAT-2 that was launched on Otober 29th 2018. As a near-future plan, the algorithm will be applied to GOSAT-2/TANSO-CAI-2 data to generate standard PM2.5 data products.

Keywords: Remote sensing , Aerosol

©2019. Japan Geoscience Union. All Right Reserved.

Establishing a high resolution road fugitive dust emission inventory in Kaifeng City, China

*Yiming Xu[1], Shili Liu[1], Xinyue Cao[1], Xianbao Shen[1], Zhiliang Yao[1]

1. Department of Environmental Science and Engineering, Beijing Technology and Business University

Due to the rapid urbanization and industrialization in many Chinese cities, ambient particulate matter pollution such as road fugitive dust pollution becomes a serious environmental problem. However, the emission of road fugitive dust is relatively difficult to quantify as it is of high uncertainty and spatial heterogeneity. The research aims to build a high resolution road fugitive dust emission inventory which is transferrable and applicable to other cities in China. High spatial resolution images were utilized to digitalize whole road network of Kaifeng City, Henan Province, China. Vehicle flows of the whole road network were estimated by incorporating the whole road network, field measured data and GPS data on an hourly, daily, weekly, monthly and yearly basis at city level. By fusing the road network information, vehicle flow, road dust load, average vehicle weight, a high resolution road fugitive dust emission inventory was established. The results showed that the total emissions of PM_{10}, $PM_{2.5}$ and Total Suspended Particulate from road fugitive dust at commuter time and downtown were much higher compared with other time and location in Kaifeng City. The framework of this road fugitive dust emission inventory can be applied to other cities, and it can provide data support and guide fugitive dust management in China.

Keywords: Road Fugitive Dust, High Resolution Remote Sensing, Satellite Data, Air Pollutant Emission Inventory

©2019. Japan Geoscience Union. All Right Reserved.

A Relationship between Diurnal Change Patterns of Land Surface Temperature and Spatial Configuration of the Osaka Metropolitan Area Captured by Himawari-8

*Yuhei Yamamoto[1], Hirohiko Ishikawa[1]

1. Disaster Prevention Research Institute, Kyoto University

Land surface temperature (LST) is a physical quantity that greatly contributes to the formation of an urban thermal environment. Therefore, understanding the spatiotemporal characteristics of LST is necessary for constructing a sustainable urban environment. The spatial distribution relationship between the instantaneous LST and urban land use has been investigated using polar-orbiting satellite/airborne sensors. This study explored how the urban spatial configuration and meteorological field affect the temporal changes of LST by using Japanese geostationary satellite (Himawari-8) sensor.
The study area is the Osaka metropolitan area in Japan and target days are three days that were clear-sky throughout the day in summer (August 12, 2016, July 19, 2018, and August 4, 2018). We used 100 m-mesh urban land use data and ground-based meteorological observation data to examine the urban spatial configuration and meteorological fields, respectively. The temporal changes of LST are the amplitude and phase mainly forming the diurnal change of LST. These two temporal changes were extracted by applying principal component analysis to the diurnal changes of LST represented by the 10-minute LST dataset retrieved from Himawari-8 data.
Our results showed that the spatial variations in the amplitude and phase corresponded to the penetration time and duration of the sea breeze and the thermal inertia of surface materials. Besides, it was found that the LST change during daytime was larger in the high-density low-building areas than in the low-density low-building areas. This result suggests that the increase in building density increases the LST change during the daytime. These findings lead to a deeper understanding of an urban hot environment and are helpful for urban planning to mitigate the deterioration of a hot environment.

Keywords: Land Surface Temperature, Himawari-8, Urban Heat Island

©2019. Japan Geoscience Union. All Right Reserved.

[E] Poster | A (Atmospheric and Hydrospheric Sciences)：A-CG Complex & General

Thu. May 30, 2019 5:15 PM - 6:30 PM JST | Thu. May 30, 2019 8:15 AM - 9:30 AM UTC | Poster Hall International Exhibition Hall8, Makuhari Messe_12

[A-CG34] Satellite Earth Environment Observation

convener:Riko Oki(Japan Aerospace Exploration Agency), Yoshiaki HONDA(Center for Environmental Remote Sensing, Chiba University), Yukari Takayabu(Atmosphere and Ocean Research Institute, the University of Tokyo), Tsuneo Matsunaga(Center for Global Environmental Research and Satellite Observation Center, National Institute for Environmental Studies)

In recent years, we cannot avoid facing issues on global environmental changes that occur in various spatiotemporal scales. The earth environmental observation data by satellites became the necessary basic data to tackle and solve those issues. Due to the recent advancement in the observation sensor technique and the data processing technique, the satellite observation has been showing rapid progress, and the time is changing from examining the accuracy of the observation sensor data to the advancement of the data application, leading to broaden potential users. In these days application became synergetic, so we comprehensively pick
up this topic in the Atmospheric and Hydrospheric Sciences Session of this Union Meeting that enables to comprise the atmospheric, oceanic and land sciences; by combining the intelligence and the knowledge of the party, we propose a session that aims to prompt further studies towards the issues on earth environmental change, the advancement in the data application and future plans of Earth Observation missions.

[ACG34-P01] Impact of usage of multiple-satellite sensors on accuracy of daily-mean sea surface wind data

*Ayumi Koizumi[1], Masahisa Kubota[2], Kunio Kutsuwada[3], Hiroyuki Tomita[4], Tsutomu Hihara[5] (1.Tokai University, 2.Tokai University, Institute of Ocean Research and Development, 3.School of Marine Science and Technology, Tokai University, 4.Institute for Space-Earth Environmental, Nagoya University, 5.Japan Agency for Marine-Erth Science and Technology)

[ACG34-P02] Temperature and Size Variability of Warm Pools in the Global Oceans

*ChunYi Lin[1] (1.National Museum of Marine Science & Technology)

[ACG34-P03] Sea surface temperature from SGLI aboard the GCOM-C satellite of JAXA

*Yukio Kurihara[1], Kazunori Ogata[2], Hiroshi Murakami[2], Misako Kachi[2] (1.Tripli-I Co., Ltd., 2.JAXA EORC)

[ACG34-P04] Concept of small satellite UV/visible imaging spectrometer optimized for tropospheric NO_2 measurements in air quality monitoring

*Tamaki Fujinawa[1,5], Katsuyuki Noguchi[2], Akihiko Kuze[3], Andreas Richter[4], John P. Burrows[4], Andreas C. Meier[4], Tomohiro Sato[1], Takeshi Kuroda[1], Naohiro Yoshida[5], YASUKO KASAI[1,5] (1.National Institute of Information and Communications Technology, 2.Nara Women's University, 3.Japan Aerospace Exploration Agency, 4.University of Bremen, 5.Tokyo Institute of Technology)

[ACG34-P05] EarthCARE L2 algorithms for cloud and precipitation

*Kaori Sato[1], Hajime Okamoto[1], Hiroshi Ishimoto[2] (1.Research Institute for Applied Mechanics, Kyushu University, 2.Meteorological Research Institute)

[ACG34-P06] Analysis of the Surface Echo Characteristics Derived from GPM/DPR Wide Swath Observation Experiment

*Kosuke Yamamoto[1], Kinji Furukawa[1], Nobuhiro Takahashi[2], Takuji Kubota[1] (1.Japan Aerospace Exploration Agency, 2.Nagoya University)

[ACG34-P07] The Recent Results from the Global Precipitation Measurement (GPM) mission in Japan

*Riko Oki[1], Takuji Kubota[1], Kinji Furukawa[1], Yuki Kaneko[1], Moeka Yamaji[1], Kosuke Yamamoto[1], Toshio Iguchi[2], Yukari Takayabu[3] (1.Japan Aerospace Exploration Agency, 2.NICT, 3.the University of Tokyo)

[ACG34-P08] **Verification of Global Satellite Mapping of precipitation (GSMaP) for providing its error information**

*Moeka Yamaji[1], Takuji Kubota[1] (1.Earth Observation Research Center, Japan Aerospace Exploration Agency)

[ACG34-P09] Detection of the mixed phase top using the measured dual-frequency ratio of reflectivity with GPM/DPR

*Yuki Kaneko[1], Toshio Iguchi[2] (1.Japan Aerospace Exploration Agency, 2.National Institute of Information and Communications Technology)

[ACG34-P10] **Comparison between high frequency satellite rainfall estimation and APHRODITE-2 ground rain gauge observation**

*Hitoshi Hirose[1], Koichi Toyoshima[1], Atsushi Higuchi[1], Akiyo Yatagai[2], Natsuko Yasutomi[3] (1.Center for Environmental Remote Sensing, Chiba University, 2.Hirosaki University, 3.Disaster Prevention Research Institute, Kyoto University)

[ACG34-P11] Development of the high resolution GSMaP by the Himawari-8

*Tomoaki Mega[1], Tomoo Ushio[1] (1.Tokyo Metropolitan University)

[ACG34-P12] Preliminary results of on-orbit estimation for polarization sensitivity of GCOM-C/SGLI

*Risa Miyazaki[1], Hiroshi Murakami[1], Masahiro Hori[1] (1.Japan Aerospace Exploration Agency)

[ACG34-P13] Analysis of SGLI validation datas based on the effects of the growth and ground types for the AGB development

*Ryota Ishibashi[1], Koji KAJIWARA[1], Yoshiaki HONDA[1] (1.Center for environmental remote sensing, Chiba University)

[ACG34-P14] Remote sensing of aerosol optical properties and water-leaving radiance based on the optimal estimation approach

*Chong Shi[1], Teruyuki Nakajima[1], Makiko Hashimoto[1], Hideaki Takenaka[1] (1.Japan Aerospace Exploration Agency)

[ACG34-P15] Aerosol retrieval and PM2.5 from space using GOSAT/TANSO-CAI

*Makiko Hashimoto[1], Hideaki Takenaka[1], Teruyuki Nakajima[1], Akiko Higurashi[2] (1.Japan Aerospace Explortion Agency, 2.NIES)

[ACG34-P16] **Establishing a high resolution road fugitive dust emission inventory in Kaifeng City, China**

*Yiming Xu[1], Shili Liu[1], Xinyue Cao[1], Xianbao Shen[1], Zhiliang Yao[1] (1.Department of Environmental Science and Engineering, Beijing Technology and Business University)

[ACG34-P17] A Relationship between Diurnal Change Patterns of Land Surface Temperature and Spatial Configuration of the Osaka Metropolitan Area Captured by Himawari-8

*Yuhei Yamamoto[1], Hirohiko Ishikawa[1] (1.Disaster Prevention Research Institute, Kyoto University)

Impact of usage of multiple-satellite sensors on accuracy of daily-mean sea surface wind data

*Ayumi Koizumi[1], Masahisa Kubota[2], Kunio Kutsuwada[3], Hiroyuki Tomita[4], Tsutomu Hihara[5]

1. Tokai University, 2. Tokai University, Institute of Ocean Research and Development, 3. School of Marine Science and Technology, Tokai University, 4. Institute for Space-Earth Environmental, Nagoya University, 5. Japan Agency for Marine-Erth Science and Technology

Most satellites observing sea surface winds have sun-synchronous orbits and provide observation data at the same place two times per a day. We can expect that daily-mean values estimated from these data have some errors when diurnal changes in wind field cannot be neglected. For this problem, use of multiple satellites is helpful. Since the number of sensors used to construct daily-mean data is different among the years, it is expected that the accuracy of a daily-mean value changes from year to year.

The purpose of this study is to describe time variation of accuracy in daily-mean wind data in the Japanese Ocean Flux Data Sets with Use of Remote Sensing Observation (J-OFURO)-3 and to investigate its causes by comparing with in-situ measurement data by moored buoys and calculating three statistical values.

Results reveal that the statistical values are improved with year. To examine the relationship between the yearly statistics and the yearly number of satellite sensors, we plotted a scatter diagram between the number of satellites and three statistical values in each year. We found that the correlations between them are very high. We also focused on a time interval of the satellite wind observation, namely maximum missing time within a day. The result showed that the correlation between three statistical values and maximum missing time intervals is high. Since the relation between these two factors is not independent, we analyzed by considering both factors together. First, we chose five buoys with various standard deviations for a daily-mean value. Next, we picked up data from buoy's hourly data using random numbers, and calculated the daily mean value using the random data, and then determined the number of observations and the maximum missing time interval each day. Assuming the daily mean value calculated from 24 hourly data as a true value, the RMSE between this true value and the daily mean created from random data was calculated. From the result of this analysis, it was found that the value of Root Mean Square Error(RMSE) depends on the maximum missing time interval rather than the number of observations. Furthermore, when RMSE was normalized by standard deviation, the same figures were obtained for all buoys. This result implies that the RMSE of the daily mean value of the buoy station can be estimated if the magnitude of diurnal variation is known by giving the number of satellites used for observation and the maximum missing time interval, Moreover, by applying this result, we think that it is possible to show the optimal number of sensors and observation time for target accuracy. This result gives very breakthrough information to the design of the satellite observation system for sea surface wind.

Keywords: Multiple-satellite sensors, Sea surface wind

©2019. Japan Geoscience Union. All Right Reserved.

Temperature and Size Variability of Warm Pools in the Global Oceans

*ChunYi Lin[1]

1. National Museum of Marine Science & Technology

Using advance satellite-derived Sea surface height anomaly, sea surface temperature (SST) data, and heat flux data, we investigate the thermal variability, temperature and size variability of warm pools in the global oceans, the Pacific, the Atlantic, and the Indian Ocean, respectively. Because of the high density and specific heat of seawater, water can store and transport large amounts of heat. High SST has particular influence on global climate system. Furthermore previous studies focused on the global warming or area warming, in this investigation we present results of warm pool SST binned into 1 ˚C interval. Detecting temperature and size variability of warm pools in the global oceans, it suggests that the high SST area (SST ≧ 28˚C) has faster increasing rate than surrounding area (SST 20˚C - 27˚C) in the global oceans, the Pacific, the Atlantic, and the Indian Ocean, respectively. To understand the role of surface heat flux in the tropical SST fluctuation, we analyze the mixed layer heat balance equation. Upper ocean heat budget between the heat advection and heat diffusion term are compared and heat diffusion processes may be a mechanism for transporting excessive amount of heat that the warm pool through enhancing the SST gradient around the edge of the warm pool. In order to find out dominant period components and the relationship of energy-frequency distribution without influenced induced by nonlinear and nonstationary signals, the Hilbert-Huang Transform applied by ensemble empirical mode decomposition is employed. The ensemble empirical mode decomposition analysis indicates that the interannual component has strong influence on the variability of the warm core pool in the Pacific, presumably because of the presence of El Niño phenomenon, while the annual cycle dominates the variability in the Indian and the Atlantic Ocean.

Keywords: warm pool, SST, heat flux

©2019. Japan Geoscience Union. All Right Reserved.

Sea surface temperature from SGLI aboard the GCOM-C satellite of JAXA

*Yukio Kurihara[1], Kazunori Ogata[2], Hiroshi Murakami[2], Misako Kachi[2]

1. Tripli-I Co., Ltd., 2. JAXA EORC

The Global Change Observation Mission-Climate (GCOM-C) satellite, which is one of two satellites for the GCOM mission of the Japan Aerospace and Exploration Agency (JAXA), was launched on 23 December 2017. The Second Generation Global Imager (SGLI) is the optical sensor aboard GCOM-C which consists of two components: the Visible and Near-infrared Radiometer (VNR) and the Infrared Scanner (IRS). SGLI has switchable spatial resolution from 250 m x 250 m to 1 km x 1 km. The resolution of 250 m x 250 m is expected to reveal complicated structure of geophysical parameters. Sea surface temperature (SST), which is one of the important parameters in the geophysical field, is also determinable by using split window data of SGLI. SGLI SST is retrieved by utilization of newly developed cloud masking method and a modified SST method originally developed for Himawari-8. Considering combined utilization of satellite SSTs, the methods developed for SGLI SST will be applied back to Himawari-8 data as well as the data from the Visible Infrared Imaging Radiometer Suite (VIIRS) aboard the Suomi National Polar-orbiting Partnership (Suomi NPP) satellite. SGLI SST is validated by comparison with buoy data. The comparison result shows RMSD of ~0.4 K, good agreement between SGLI SSTs and buoy data. Triple comparison with Himawari-8 and VIIRS SSTs is being started. Operational retrieval of SGLI SST started at the end of 2018. The products are available at the G-Portal site of JAXA and the JAXA Satellite Monitoring and Environmental Studies (JASMES) site of the Earth Observation Center (EORC) of JAXA.

©2019. Japan Geoscience Union. All Right Reserved.

Concept of small satellite UV/visible imaging spectrometer optimized for tropospheric NO_2 measurements in air quality monitoring

*Tamaki Fujinawa[1,5], Katsuyuki Noguchi[2], Akihiko Kuze[3], Andreas Richter[4], John P. Burrows[4], Andreas C. Meier[4], Tomohiro Sato[1], Takeshi Kuroda[1], Naohiro Yoshida[5], YASUKO KASAI[1,5]

1. National Institute of Information and Communications Technology, 2. Nara Women's University, 3. Japan Aerospace Exploration Agency, 4. University of Bremen, 5. Tokyo Institute of Technology

Satellite observations at nadir can potentially facilitate a better understanding of the emissions and distribution of tropospheric nitrogen dioxide, NO_2. The identification of emissions requires adequate spatiotemporal resolution measurements of the total column amounts of NO_2. The spatial resolution of previous and current observations is insufficient for the identification of NO_2 hot-spots. Switching to a spatial resolution of ~1 km x ~1 km can improve the identification of local sources of NO_2 and their emissions. To investigate the feasibility of observations with such a high spatial resolution, we simulated radiance spectra for different cases under varying parameters, such as area, season, satellite altitude, and surface reflectance by using the radiative transfer model SCIATRAN. We subsequently retrieved NO_2 slant column densities (SCDs) using the differential optical absorption spectroscopy (DOAS) technique with several fit windows. For test cases associated with polluted conditions, we found that the conceptual nadir-observing instrument on a satellite at an altitude of ~300 km involved the lowest retrieval errors for signal-to-noise ratios of around 1000 with accuracy better than the required 5% for tropospheric NO_2 SCD and that the fit window of 425--497 nm met the scientific requirements for both surface reflectance cases.

Keywords: Nitrogen dioxide, Earth observation, Radiative transfer model, Remote sensing

©2019. Japan Geoscience Union. All Right Reserved.

EarthCARE L2 algorithms for cloud and precipitation

*Kaori Sato[1], Hajime Okamoto[1], Hiroshi Ishimoto[2]

1. Research Institute for Applied Mechanics, Kyushu University, 2. Meteorological Research Institute

The EarthCARE (Earth Clouds, Aerosols and Radiation Explorer, JAXA-ESA) mission will carry the first 94GHz Doppler Cloud Profiling Radar (CPR) with a high spectral resolution atmospheric lidar (ATLID) at 355nm. Recent progresses in EarthCARE L2 cloud/precipitation algorithms for the treatment of multiple scattering and cloud particle nonsphericity are presented.

Keywords: spaceborne active sensor, cloud

©2019. Japan Geoscience Union. All Right Reserved.

Analysis of the Surface Echo Characteristics Derived from GPM/DPR Wide Swath Observation Experiment

*Kosuke Yamamoto[1], Kinji Furukawa[1], Nobuhiro Takahashi[2], Takuji Kubota[1]

1. Japan Aerospace Exploration Agency, 2. Nagoya University

The observation from spaceborne precipitation radar has been contributed to better understanding of earth climate system. Global Precipitation Measurement (GPM) core satellite Dual-frequency Precipitation Radar (DPR) provides us 3-dimentional information of precipitation by the scan width of about 250 km, but there have been arguments that to bring systematic impact on the weather monitoring through global rainfall map such as GSMaP, wider swath observation by precipitation radar is necessary.

Based on those requirements, the scan pattern of GPM/DPR was experimentally changed for 1 day from 13UTC on September 26th. In this experiment, the scan angle was changed to observe from nadir to about +34˚ assuming future spaceborne precipitation radar with wider swath width, while in the normal observation DPR scans ±17˚. The height and strength of the mainlobe clutter with larger incident angle were assessed statistically to examine the possibility of the rainfall retrieval with wide swath observation by DPR.

In order to examine mainlobe clutter height, it is inevitable to reduce sidelobe and grating lobe effect. In this study, clutter-free observation data is extracted based on following procedures; 1) extract bins above mainlobe clutter; 2) extract bins under non-precipitation condition from 1); 3) extract bins that satisfy |received power −averaged noise power| < 2 sigma of the noise power from 2). Note that this procedure was applied only for KuPR observation since sidelobe and grating lobe clutter is not prominent in KaPR.

The result for KuPR observation shows that the mainlobe clutter top height at the larger incident angle over ocean is somehow suppressed at around 4 km while over land it increases almost linearly up to around 5 km due to the strong surface scattering. The same tendency is found on the KaPR observation, but it has lower clutter top height of around 2.5 km and 3.5 km, over ocean and land respectively. Suppression is clearer over ocean thanks to the specular reflection. The results also indicate that relatively intense rainfall can be retrieved while shallow rainfall with weak echo power may not be acceptable for retrieval because it should be masked by the surface clutter.

Keywords: precipitation radar, radar clutter, GPM core satellite

©2019. Japan Geoscience Union. All Right Reserved.

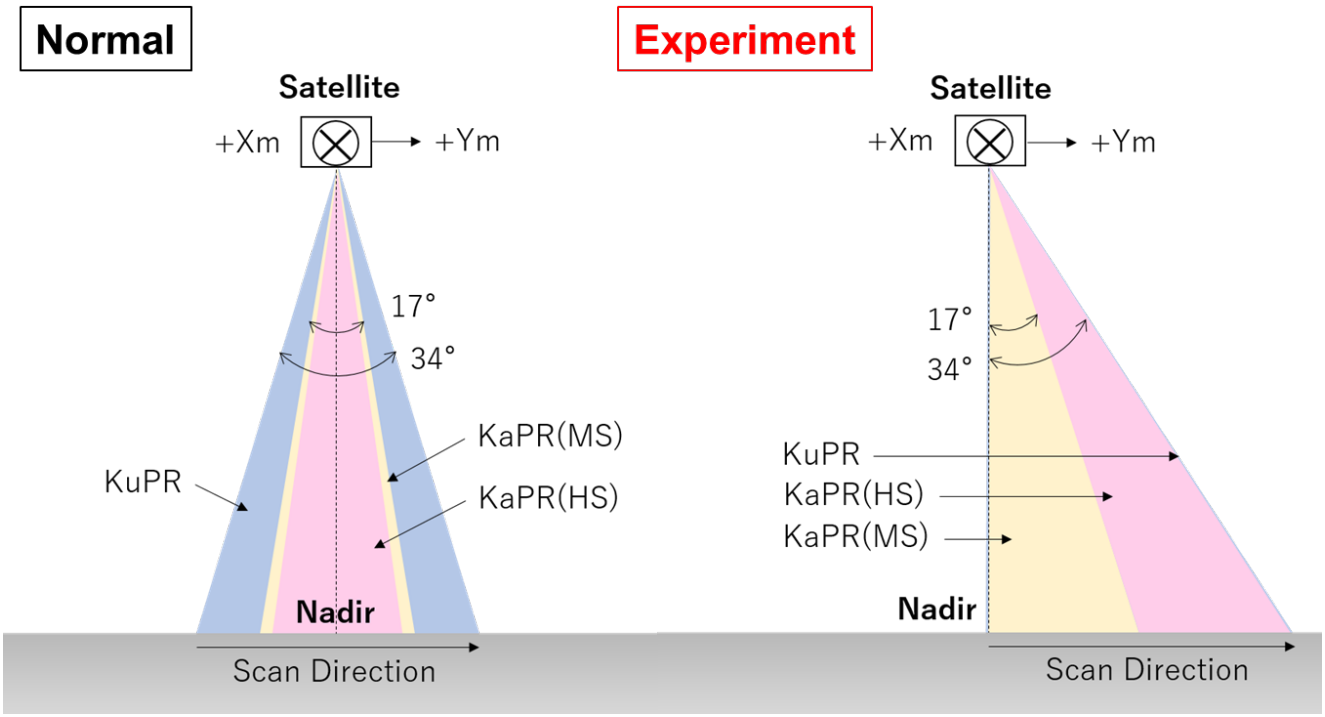

©2019. Japan Geoscience Union. All Right Reserved.

The Recent Results from the Global Precipitation Measurement (GPM) mission in Japan

*Riko Oki[1], Takuji Kubota[1], Kinji Furukawa[1], Yuki Kaneko[1], Moeka Yamaji[1], Kosuke Yamamoto[1], Toshio Iguchi[2], Yukari Takayabu[3]

1. Japan Aerospace Exploration Agency, 2. NICT, 3. the University of Tokyo

The Global Precipitation Measurement (GPM) mission is an international cooperate satellite project to achieve highly accurate and highly frequent global precipitation observations. The GPM mission consists of the GPM Core satellite jointly developed by the U.S. and Japan and Constellation Satellites that carry microwave radiometers and provided by the GPM partner agencies. The GPM Core satellite carries the Dual-frequency Precipitation Radar (DPR) by the Japan Aerospace Exploration Agency (JAXA) and the National Institute of Information and Communications Technology (NICT) and the GPM Microwave Imager (GMI) provided by National Aeronautics and Space Administration (NASA). The GPM Core satellite was launched in February 2014 and achieved its prime mission period planned for 3 years in 2017.

It has been continuing its observation as the extended mission phase after that.

JAXA develops the DPR Level 1 algorithm and the NASA-JAXA Joint Algorithm Team develops the DPR Level 2 and DPR-GMI combined Level 2 algorithms. The DPR, the DPR-GMI combined algorithms and the latent heating algorithm were updated, and those products were released in October 2018 as Version 0.6. Using dual frequency information of DPR, the latest Level 2 products include information such as precipitation phase at surface, heavy ice precipitation and so on. Also, the calibration factors of TRMM/PR were re-examined to have consistency between DPR/Ku. The same GPM Ku-band radar L2 algorithm now applies to the TRMM/PR, so that the long radar precipitation data exceeding more than 20 years are now available. From May 2018 in the extended mission period, the scan pattern of the Ka-band radar has been changed to realize matched beam observation in full swath. The new algorithm applying to the changed scan pattern is now under development.

JAXA also develops the Global Satellite Mapping of Precipitation (GSMaP), that is hourly and 0.1-degree horizontal resolution global rainfall map. It is available through the “JAXA Global Rainfall Watch” website (https://sharaku.eorc.jaxa.jp/GSMaP/index.htm). GSMaP product family includes different data latency products and rain gauge calibrated products and so on. The GSMaP near-real-time version (GSMaP_NRT) product provides global rainfall map in 4-hour after observation, and an improved version of GSMaP near-real-time gauge-adjusted (GSMaP_Gauge_NRT) product has been released since Dec. 2018.

The GSMaP real-time product called GSMaP_NOW now product is providing data at the earliest timing. It has been realized using the geostationary satellite Himawari-8 operated by the Japan Meteorological Agency (JMA) since November 2015. Since Nov. 2018 the domain of GSMaP_NOW has been extended to the region of the geostationary satellite Meteosat operated by the European Organization for the Exploitation of Meteorological Satellites (EUMETSAT) in November 2018. JAXA is further developing the GSMaP_NOW to provide global real-time rainfall product.

Keywords: GPM, Satellite Remote Sensing, Precipitation

©2019. Japan Geoscience Union. All Right Reserved.

©2019. Japan Geoscience Union. All Right Reserved.

Verification of Global Satellite Mapping of precipitation (GSMaP) for providing its error information

*Moeka Yamaji[1], Takuji Kubota[1]

1. Earth Observation Research Center, Japan Aerospace Exploration Agency

Precipitation is one of the most essential parameters in the Earth system. Due to address water issues like water shortage or floods, JAXA has developed and provided Global Satellite Mapping of Precipitation (GSMaP), which is hourly global precipitation dataset. It is under the Global Precipitation Measurement (GPM) mission and contributes.
GSMaP allows us to capture the hourly horizontal distribution of precipitation with good latency after observation. The spatial resolution is 0.1 x 0.1 degrees latitude/longitude. It has been used for various kinds of utilization purposes.
In terms of accuracy, GSMaP algorithms were updated in several times, and GSMaP has been getting more accurate day by day, however, it is known that the inhomogeneous of accuracy is existed depending on algorithm characteristics. It has been needed to provide information about the uncertainty and accuracy of GSMaP by users.
In this study, verification result of GSMaP near-realtime product version 6 (GSMaP_NRT) is reported. The radar/raingauge analysed precipitation data by Japan Meteorological Agency, which is an hourly rainfall analysis generated from ground-based precipitation radars corrected by automated rain gauges, are used as the reference data. Since the purpose of this study is for providing generalized error information, root mean square errors (RMSE) is statistically calculated for each precipitation level and each reliability flag during May-June-July-August-September-October in 2015-2018. Some initial results showed that the RMSE qualitatively represented the error for each precipitation level and reliability flag. The RMSE ratio to the average precipitation rate got larger as the precipitation rate became smaller while it became stable around 60 –80 % when precipitation rate was more than 10 mm/h. We report the validation results in detail, such as land/ocean difference or sampling dependence, and focus on the effectiveness of it.

Keywords: precipitation, GPM, GSMaP, validation

©2019. Japan Geoscience Union. All Right Reserved.

Detection of the mixed phase top using the measured dual-frequency ratio of reflectivity with GPM/DPR

*Yuki Kaneko[1], Toshio Iguchi[2]

1. Japan Aerospace Exploration Agency, 2. National Institute of Information and Communications Technology

The core observatory of the Global Precipitation Measurement (GPM) mission was launched in 2014 and has been observing rain and snow between 65˚S and 65˚N by the Dual Frequency Precipitation Radar (DPR) and the GPM Microwave Imager (GMI). The DPR provides three-dimensional structure of storms derived from reflected energy from precipitation particles. Precipitation echoes at the two frequencies of the DPR, Ka-band (25GHz) and Ku-band (14GHz), make it possible to infer the mean size and physical property of precipitation particles. The swath width of Ka-band scanning was 125 kilometers centered at nadir and was nested within the Ku-band’ s wider scan width of 254 kilometers. On May 21 2018, the Ka-band scan pattern was changed to match with the Ku-band’ s. Dual frequency radar reflectivity factors are available for full swath of 254 kilometers now.

The classification (CSF) module in the standard DPR level2 algorithm detects a bright band (BB) and classifies precipitation into three types, stratiform, convective, and other. Rain types affect the retrievals of rain amount and latent heating in the DPR algorithm. Accurate classification is also important in the Global Satellite Mapping of Precipitation (GSMaP) algorithm because it affects the rain profile database used in the rain retrieval with microwave radiometers. The BB detectability by the standard CSF algorithm is lower at and near the swath edges than near nadir because only Ku-band data was available in the outer swath before and because slant incidence of radar beams smears the vertical profiles.

As the Ka-band scan pattern has changed to cover the full swath, we can apply a dual-frequency method to detect a BB now. We have developed a method that uses the dual frequency ratio (DFR) to detect the mixed phase top. It looks at the slope of DFR as a function of range to identify the transition height from ice to water. DFR itself is estimated from measured DFR (DFRm) with attenuation correction. Preliminary experiments show that the developed method can detect the BB in stratiform rain over the swath almost uniformly. This method also has a potential to identify the transition height even in some convective cases. In this research we evaluate the performance of the algorithm by comparing the altitude of BB and the transition height with those estimated by using X-band multi-parameter radar (XRAIN) data.

Keywords: GPM, Melting Layer, Precipitation Radar

©2019. Japan Geoscience Union. All Right Reserved.

Comparison between high frequency satellite rainfall estimation and APHRODITE-2 ground rain gauge observation

*Hitoshi Hirose[1], Koichi Toyoshima[1], Atsushi Higuchi[1], Akiyo Yatagai[2], Natsuko Yasutomi[3]

1. Center for Environmental Remote Sensing, Chiba University, 2. Hirosaki University, 3. Disaster Prevention Research Institute, Kyoto University

APHRODITE project collects daily precipitation observation data from ground rain gauges in each country, and then performs appropriate quality control and converts it into gridded data. APHRODITE holds long-term data from the 1960s to the present and focuses on analyzes such as changes in characteristics of extreme rainfall due to long-term climate change. However, ground-based daily rain observations has a problem which end of the day (EOD) in each country is different from each other. To estimate the EOD in each country, we developed a Rain Potential Map (RPM) which is a product that can estimate global rain probability using geostationary meteorological satellites (GEO) (Hirose et al., 2016, JMSJ). In this study, we used the RPM, GSMaP and CMORPH which are global satellite rain estimation data based on microwave satellite and GEO observations.

Since the above satellite rainfall observation data can estimate global precipitation every hour, it is possible to create daily average data in which the average section is shifted by one hour. By correlating the satellite daily precipitation observation time series with the APHRODITE daily precipitation observation time series, the EOD value in each country was estimated from the time when the correlation coefficient is largest. We confirmed that the reliability of this method is high by a verification analysis in the field where true value of EOD is already known. Moreover, we made pseudo hourly rain time series of APHRODITE by inserting APHDOITE daily rain time series to satellite hourly rain time series. By this method, we will try to make a new APHRODITE data that is corrected for the EOD difference between each country.

Keywords: Precipitaition, Satellite, APHRODITE

©2019. Japan Geoscience Union. All Right Reserved.

Development of the high resolution GSMaP by the Himawari-8

*Tomoaki Mega[1], Tomoo Ushio[1]

1. Tokyo Metropolitan University

There is a new generation infrared (IR) imager on new-generation gestationary weather-satellite such as the Himawari-8 and the Geostationary Operational Environmental Satellite-R series. The imagers observe multi-channel passive imaging radiometer. The imagers observe wave a full disk with several km in about ten minutes. In Near-future, the IR imager observation should cover the globe.

Global precipitation information is an important tool for water management or earth science. Spaceborne sensors is one of the most convenient tools of global observation. The sensors cover global and provide uniform quality data. Precipitation estimation use microwave radiometer in low earth orbit (LOE). A microwave radiometer has high spatial resolution. However, one drawback of the microwave radiometer in LOE is narrow observation area. Whole earth observation by a microwave radiometer on a LOE satellite need some days. Therefore, global precipitation map is made from combined satellite data. However, combined data of microwave radiometer on LOE don’ t cover global in one hour. One of the global precipitation map is the Global satellite mapping of Precipitation (GSMaP). Precipitation estimation of the GSMaP made from microwave radiometer data. The GSMaP Moving Vector with Kalmanfilter (MVK) and Near real time compensate precipitation of no observation area by IR information. Spatial and temporal resolution of the GSMaP MVK achives 0.1 degree and one hour. This study shows downscale technique for GSMaP precipitation map by High-spatial and temporal resolution IR data of the Himawari-8. IR datasets of Himawari-8 are available every 2.5 minutes in the Japan region. In the presentation, we will also show validation the high resolution GSMaP and ground-radar network in Japan.

Keywords: Precipitation, GSMaP, Microwave Radiometer, Infrared Radiometer, Algorithm

©2019. Japan Geoscience Union. All Right Reserved.

Preliminary results of on-orbit estimation for polarization sensitivity of GCOM-C/SGLI

*Risa Miyazaki[1], Hiroshi Murakami[1], Masahiro Hori[1]

1. Japan Aerospace Exploration Agency

The GCOM-C has been launched successfully on 23th Dec. 2017 from the Tanegashima Space Center by H-IIA vehicle No.37. After the initial calibration/validation phase of one year after launch, all SGLI standard products have been released from JAXA’s data providing service (G-Portal) from Dec. 20, 2018.

In generally, the radiance reflected by the sea surface and the atmosphere is strongly polarized. When observing a large polarized light, the output radiance vary from the actual radiance because of the polarization sensitivity characteristic of the optical sensor. Especially for ocean color products, it is important to evaluate the effect of polarization sensitivity because it is necessary to extract the weak water-leaving reflectance (<10% of the whole) by the accurate atmospheric correction.
The polarization sensitivity of GCOM-C/SGLI of each NP (Non-Polarization) band has been measured in the pre-launch ground test. The ground test results of polarization sensitivity were shown to be <3.5% on average in the pixel direction in all bands. In this study, we evaluate whether the polarization sensitivity estimated from on-orbit observation data is consistent with the pre-launch test results. In this work, we report on the RED bands (VN07, VN08) and the NIR bands (VN10, VN11) of SGLI.
Polarization sensitivity on-orbit was evaluated based on Gordon and Zhang (1997) and Meister et al. (2005). We use the observation data by SGLI/PL (Polarization) band to estimate the real stokes vector components at the top of atmosphere (TOA). In order to obtain the polarization sensitivity with respect to directly observed radiance at TOA, L1B before inter-pixel sensitivity correction and before inter-telescope sensitivity correction was self-made from L1A data.
We analyzed the observation data of 12 path that PL band is observed nadir direction. The characteristics of the instrument for polarization sensitivity (polarization factor) were estimated by the least squares method. On the east side of the observation image, the error is large because of Sun-Glint. Although the variation in the pixel direction was still large, the estimated polarization factors (3 to 5 %) were consisted with the prelaunch ground test (~ 3.5%). However, sensitivity patterns in the pixel direction could not be identified, so we will continue to improve the evaluation in the future.

Keywords: GCOM-C, SGLI, Polarization sensitivity

©2019. Japan Geoscience Union. All Right Reserved.

Analysis of SGLI validation datas based on the effects of the growth and ground types for the AGB development

*Ryota Ishibashi[1], Koji KAJIWARA[1], Yoshiaki HONDA[1]

1. Center for environmental remote sensing, Chiba University

The effects of the earth of the time variant system should be difficult to detect the influence of the growth types and also the effects of the growth field’s variations. The research may occur the SGLI’s RSRF datas of the calculated AGB data accuracy analysis that observed between every kinds of the growth and also the ground types. The significance area of the SGLI observed, each of detected datas accuracy have to be considered. We show observation ways for the ground truth of the reflectance, LAI and fAPAR. The first case we use is a case of vegetation at the grassland. And then, based of reflectance values, we compare the other type as the Mixed coniferous forest example. The influence of an effect of the type of growth may occur the reflectance of the distributed area. We will detect these effects of the growth type. The influence at the observed area be necessarily to be verified.

The research topic includes the ground truth observation for the accuracy verification of a SGLI data obtained. For development of ground truth, the way to obtain datas were important. This paper explains how to examine growth (such as a second growth forest and other) and the slope factor of the second growth forest area and also the reflectance of each forest types. Then, this paper make ground truth observation scheme for the high accuracy AGB referenced data development at ground cover area. We explain the method of examine the error detection way including observation devices and also the problem of the research topic to be examined. Results may occur an example case of such kinds of the sloped forest and the kinds of the plane. The results shows a typical difference between the sloped and the plane, and then the results may occur the possibility that comparison of standard deviation may be an effective way to detect the volume of the forest type between every ground truth.

The case of we use as the sloped fields, reflectance of each wavelength were low and then the near 400 to 700 nm area will be higher than other wavelength (ANOVA values of results: $p < 0.001$). And then, we can see the effects of slope should be detected at total values of the reflectance. The reflectance of a wavelength were obtained that aimed to detect the verification of the slope and the growth type’s reflectance. When the mixed coniferous forest, static observation develop same reflectance values but the effect of the sloped factor occur the high value of the standard deviations. Then, our method applied to the method of the SGLI’s data calculation scheme, and then the growth factor of the area be affects the influence of the from 400 to 700 nm wavelength and also the factor of slope region be affects the wavelength of reflectance. SGLI data analysis, the factor of these parameters were used to remake the size of RSRF data from 250 m to 1000 m resolution. The future, we investigate more and then, the mask area of high value difference around the nearest 16 pixels be considered. Datas were significant at some pixels, such as a steep sloped, growth types, or error detected area. Data development of RSRF, the reflectance of each cells are detected as the values of the every ground types by the standard deviation.

Keywords: SGLI's data verifications, Reflectance maps, Statistical ANOVA analysis

©2019. Japan Geoscience Union. All Right Reserved.

Factor analysis of variable results (Three-way ANOVA)

Sloped factors: Mean values of the SD of each (dynamic/semi-static)
Canopy factors: Difference of each SD of the every SD
Growth typed factors: Difference of each Mean and SD

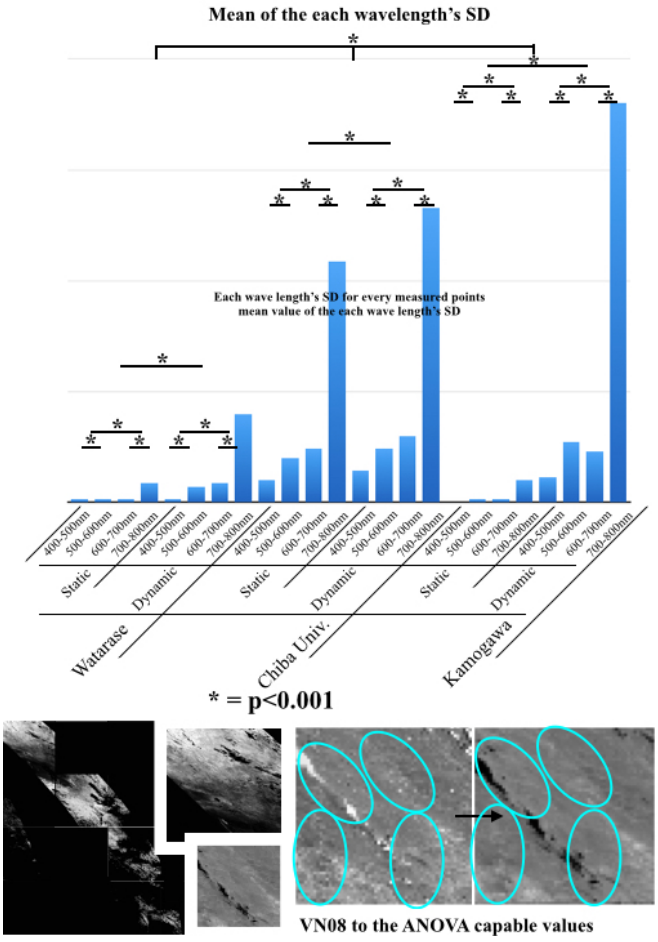

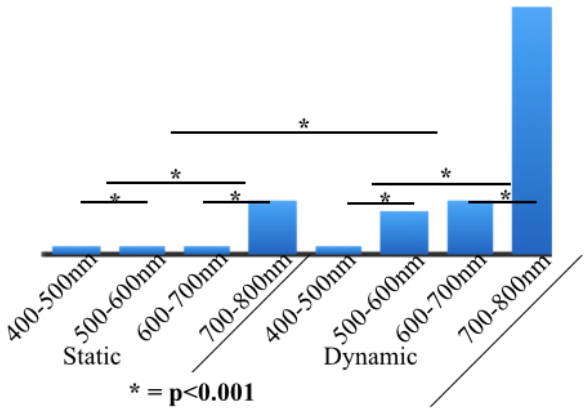

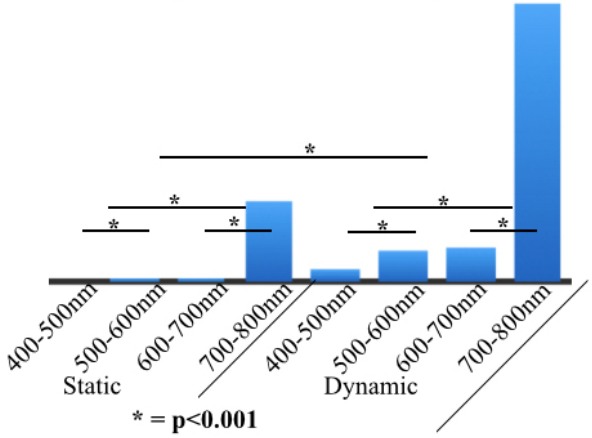

©2019. Japan Geoscience Union. All Right Reserved.

Remote sensing of aerosol optical properties and water-leaving radiance based on the optimal estimation approach

*Chong Shi[1], Teruyuki Nakajima[1], Makiko Hashimoto[1], Hideaki Takenaka[1]

1. Japan Aerospace Exploration Agency

A flexible inversion algorithm is proposed for jointly retrieving aerosol optical properties and water-leaving radiance from multispectral instrument over the ocean. A combined multi-wavelength and multi-pixel constraint approach is used to estimate aerosol and hydrosol over clear and turbid waters, based on the forward simulation from a coupled atmospher-ocean radiative transfer model. This sort of simultaneous inversion helps to correct the biases induced by the neglect of water-leaving radiance in the traditional aerosol retrieval algorithms, in addition, it can provide more aerosol information than the standard ocean color approach. To investigate the availability of current scheme, we conduct the retrieval in the process of MODIS, GOSAT/CAI and GCOM-C/SGLI instruments.

©2019. Japan Geoscience Union. All Right Reserved.

Aerosol retrieval and PM2.5 from space using GOSAT/TANSO-CAI

*Makiko Hashimoto[1], Hideaki Takenaka[1], Teruyuki Nakajima[1], Akiko Higurashi[2]

1. Japan Aerospace Explortion Agency, 2. NIES

Aerosol in the atmosphere has a great impact not only for the Earth’ s radiation budget and changing the Earth’ s climate, but also on human health. Especially, the fine particle, which is often called PM2.5, has drawn attention as a cause of health damage.

The urban area is a source of anthropogenic aerosol, which is mostly composed of small particles, and the particles are transported to other regions. Satellite remote sensing provides effective means to monitor the atmospheric aerosols in wide area including urban areas.

Accurate retrieval of fine mode aerosol optical thickness (AOT) is necessary to calculate an equivalent value of PM2.5 from space. Therefore, an aerosol retrieval algorithm for satellite remote sensing of urban areas to improve the retrieval accuracy of aerosol properties, which is called MWPM (Multiple wavelengths and pixels method) (Hashimoto and Nakajima, 2017), was developed. The method simultaneously retrieves fine and coarse mode AOT and single scattering albedo by using several wavelengths and spatial difference of surface reflectance. The method is useful for aerosol retrieval over spatially inhomogeneous surface like an urban area.

The algorithm was applied to GOSAT (Greenhouse Gases Observing Satellite) / TANSO-CAI (Cloud and Aerosol Imager, CAI) data. The GOSAT launched ten years ago (on January 23th, 2009) is a satellite to monitor greenhouse gases (GHG) such as carbon dioxide and methane with TANSO-FTS (Fourier Transform Spectrometer, FTS). The CAI is a supplementarysensor of the FTS, detecting cloud and deriving aerosol optical properties.

PM2.5 using retrieved fine mode AOT by MWPM in East Asian region from 2009 was calculated. The poster presents a retrieval result of PM2.5 over the East Asian region from space in several years and discusses the seasonal and annual variations.
Monitoring of aerosol properties such as AOT, PM2.5 and soot mixing ratio over land is added to the mission of GOSAT-2 that was launched on Otober 29th 2018. As a near-future plan, the algorithm will be applied to GOSAT-2/TANSO-CAI-2 data to generate standard PM2.5 data products.

Keywords: Remote sensing , Aerosol

©2019. Japan Geoscience Union. All Right Reserved.

Establishing a high resolution road fugitive dust emission inventory in Kaifeng City, China

*Yiming Xu[1], Shili Liu[1], Xinyue Cao[1], Xianbao Shen[1], Zhiliang Yao[1]

1. Department of Environmental Science and Engineering, Beijing Technology and Business University

Due to the rapid urbanization and industrialization in many Chinese cities, ambient particulate matter pollution such as road fugitive dust pollution becomes a serious environmental problem. However, the emission of road fugitive dust is relatively difficult to quantify as it is of high uncertainty and spatial heterogeneity. The research aims to build a high resolution road fugitive dust emission inventory which is transferrable and applicable to other cities in China. High spatial resolution images were utilized to digitalize whole road network of Kaifeng City, Henan Province, China. Vehicle flows of the whole road network were estimated by incorporating the whole road network, field measured data and GPS data on an hourly, daily, weekly, monthly and yearly basis at city level. By fusing the road network information, vehicle flow, road dust load, average vehicle weight, a high resolution road fugitive dust emission inventory was established. The results showed that the total emissions of PM_{10}, $PM_{2.5}$ and Total Suspended Particulate from road fugitive dust at commuter time and downtown were much higher compared with other time and location in Kaifeng City. The framework of this road fugitive dust emission inventory can be applied to other cities, and it can provide data support and guide fugitive dust management in China.

Keywords: Road Fugitive Dust, High Resolution Remote Sensing, Satellite Data, Air Pollutant Emission Inventory

©2019. Japan Geoscience Union. All Right Reserved.

A Relationship between Diurnal Change Patterns of Land Surface Temperature and Spatial Configuration of the Osaka Metropolitan Area Captured by Himawari-8

*Yuhei Yamamoto[1], Hirohiko Ishikawa[1]

1. Disaster Prevention Research Institute, Kyoto University

Land surface temperature (LST) is a physical quantity that greatly contributes to the formation of an urban thermal environment. Therefore, understanding the spatiotemporal characteristics of LST is necessary for constructing a sustainable urban environment. The spatial distribution relationship between the instantaneous LST and urban land use has been investigated using polar-orbiting satellite/airborne sensors. This study explored how the urban spatial configuration and meteorological field affect the temporal changes of LST by using Japanese geostationary satellite (Himawari-8) sensor.
The study area is the Osaka metropolitan area in Japan and target days are three days that were clear-sky throughout the day in summer (August 12, 2016, July 19, 2018, and August 4, 2018). We used 100 m-mesh urban land use data and ground-based meteorological observation data to examine the urban spatial configuration and meteorological fields, respectively. The temporal changes of LST are the amplitude and phase mainly forming the diurnal change of LST. These two temporal changes were extracted by applying principal component analysis to the diurnal changes of LST represented by the 10-minute LST dataset retrieved from Himawari-8 data.
Our results showed that the spatial variations in the amplitude and phase corresponded to the penetration time and duration of the sea breeze and the thermal inertia of surface materials. Besides, it was found that the LST change during daytime was larger in the high-density low-building areas than in the low-density low-building areas. This result suggests that the increase in building density increases the LST change during the daytime. These findings lead to a deeper understanding of an urban hot environment and are helpful for urban planning to mitigate the deterioration of a hot environment.

Keywords: Land Surface Temperature, Himawari-8, Urban Heat Island

©2019. Japan Geoscience Union. All Right Reserved.

[E] Poster | H (Human Geosciences)：H-TT Technology & Techniques

Thu. May 30, 2019 10:45 AM - 12:15 PM JST | Thu. May 30, 2019 1:45 AM - 3:15 AM UTC | Poster Hall International Exhibition Hall8, Makuhari Messe_3

[H-TT19] Geographic Information Systems and Cartography

convener:Takashi Oguchi(Center for Spatial Information Science, The University of Tokyo), Yuji Murayama(Graduate School of Life and Environmental Sciences), Yoshiki Wakabayashi(Graduate School of Urban Environmental Sciences, Tokyo Metropolitan University)

This session discusses various methods which acquire, store, analyze and visualize geospatial data, and presents the outcomes of empirical studies using GIS or mapping methods. The session also deals with applications of digital data, and GIS, and mapping to various fields of earth and planetary science and human society. All presentations and discussion of this session are made in English.

[HTT19-P01] Monitoring and Simulating Land Use/Cover Changes and its Impact on Land Surface Temperature in Sapporo City, Japan

*RUCI WANG[1], YUJI MURAYAMA[1] (1.University of Tsukuba)

[HTT19-P02] Spatiotemporal Variations of Land Cover/Use and Sustainable Urban Heat Island (UHI) Mitigation Strategies: A Case Study of Chinese Bay Megacities

★Invited Papers

*Fei LIU[1], Yuji MURAYAMA[1] (1. University of Tsukuba)

[HTT19-P03] A LST Study of the Seoul Metropolitan City, South Korea, Based on Landsat Data (1996 – 2017)

*Prabath Priyankara[1,3], Manjula Ranagalage[1,4], DMSLB Dissanayake[1,4], Takehiro Morimoto[1,2], Yuji Murayama[1,2] (1.Graduate School of Life and Environmental Sciences, University of Tsukuba, Japan, 2.Faculty of Life and Environmental Sciences, University of Tsukuba, Japan, 3.Faculty of Agriculture, University of Ruhuna, Sri Lanka, 4.Faculty of Social Sciences and Humanities, Rajarata University of Sri Lanka, Sri Lanka)

[HTT19-P04] Improvement of GIS exercise classes using the GIS open educational resources based on questionnaire surveys

★Invited Papers

*Hiroyuki Yamauchi[1], Takashi Oguchi[1], Yuichi S. Hayakawa[2,1], Kotaro Iizuka[1] (1.Center for Spatial Information Science, The University of Tokyo, 2.Environmental Geography, Faculty of Environmental Earth Science, Hokkaido University)

[HTT19-P05] The Development of COP for Tzu Chi Disaster Prevention System by Using QGIS-Taking 2018 Hualien Earthquake as an Example

*kuan-wen tseng[1], Ming-Ta Tsai[1], Yun-Ching Wang[1], Ming-Chih Wang[1], Chien-Hsien Liu[1] (1.03-3809093)

[HTT19-P06] Comparative study on shape and distribution of landslides caused by the 2012 Northern Kyushu heavy rainfall and the 2016 Kumamoto earthquake in the Aso region, Kumamoto, Japan

*Yasutaka Haneda[1], Takashi Oguchi[2], Kotaro Iizuka[2], Hitoshi SAITO[3,2], Yuichi S. Hayakawa[4,2], Shoichiro Uchiyama[5] (1.Graduate School of Frontier Science, The University of Tokyo, 2.Center for Spatial Information Science, The University of Tokyo, 3.College of Economics, Kanto Gakuin University, 4.Faculty of Environmental Earth Science, Hokkaido University, 5.National Research Institute for Earth Science and Disaster Resilience)

[HTT19-P07] Using GIS and remote sensing to assess relationships between landslides and land cover changes in the Sanbagawa and Mikabu Belts, Shikoku, Japan

*Roxanne Lai[1], Takashi Oguchi[1] (1.University of Tokyo)

[HTT19-P08] **Analysis of Morphometric Parameters for Mountains Ranges and Landslides due to the July 2018 Heavy Rain in Western Japan Using GIS Data**

*Toshikazu Fukuba[1], Takashi Oguchi[2] (1.Department of Earth and Planetary Environmental Science, The University of Tokyo, 2.Center for Spatial Information Science, The University of Tokyo)

[HTT19-P09] Analyzing short-term topographic change in coastal sand dunes using UAS-SfM photogrammetry: A case study in Northern Kujukuri, Japan

*Seulgi Lee[1], Yasutaka Nakata[2], Kotaro Iizuka[3], Takashi Oguchi[3] (1.Graduate School of Frontier Sciences, The University of Tokyo, 2.Forest Research Department, Forestry Research Institute, Hokkaido Research Organization, 3.Center for Spatial Information Science, The University of Tokyo)

[HTT19-P10] **Responses of suspended sediment yield to precipitation, topography and dam control in the Yellow River Basin, China**

*Ruiqi Zhang[1], Takashi Oguchi[2] (1. Department of Natural Environmental Studies, Graduate School of Frontier Sciences, The University of Tokyo, 2.Center for Spatial Information Science, The University of Tokyo)

Monitoring and Simulating Land Use/Cover Changes and its Impact on Land Surface Temperature in Sapporo City, Japan

*RUCI WANG[1], YUJI MURAYAMA[1]

1. University of Tsukuba

In recent years, urban heat island phenomenon (UHI) which prevails in many cities worldwide has caused broad public concern. UHI phenomenon impairs healthy urban development and causes excessive energy consumption, climatic and environmental deterioration. Land use/cover changes are one of the most crucial variables influencing on UHI. Therefore, monitoring and simulating land use/cover changes and analyzing its effects on LST are essential for healthy urban development. This study aims to capture the impact of land use/cover on LST and simulate the LST under various land use/cover scenarios in Sapporo city, Japan. At first, we monitored the land use/cover changes from 1985 to 2015 and detect the change of LST concerning land use/cover distribution. Then, we predicted the future conditions of LST based on various land use/cover scenarios. The results show that the LST differs according to land use/cover types, and the proportion of land use/cover types is the most significant factor affecting LST. The findings also indicate that the built-up area and paddy field have the highest average LST, while the green space and water area help cool the city. In the future, the green area such as urban green parks and grassland should be planned in the city to mitigate the UHI phenomenon. It reveals the spatial characterization of LST which provides significant insights for government and city planners.

Keywords: Geographical information science, Urban heat island, Land surface temperature, Land use/cover change, Sapporo city

©2019. Japan Geoscience Union. All Right Reserved.

Spatiotemporal Variations of Land Cover/Use and Sustainable Urban Heat Island (UHI) Mitigation Strategies: A Case Study of Chinese Bay Megacities

*Fei LIU[1], Yuji MURAYAMA[1]

1. University of Tsukuba

Rapid urbanization significantly affects the urban thermal environment in the context of global climate change. The assessment of surface urban heat island (SUHI) and development of mitigation strategies in megacities have become frontier issues on human health and urban sustainability. In this study, taking of the three Chinese bay megacities, we attempt to 1) disclose the relationship between land surface temperature (LST) and land cover using remote sensing quantified analysis, 2) to clarify the mechanism and characteristics of SUHI formation based on bi-temporal patterns and variations of land cover, and 3) to sustainably regulate and optimize the urban environment and further create urban planning and policies for relieving urban thermal effect. The study target is Guangzhou metropolitan area (GMA), Hangzhou metropolitan area (HMA) and Shanghai Metropolitan area (SMA) in China. The result of this study indicated remarkably different characteristics, arrangement, and variations among different bay thermal environments. Overall, spatial layouts and changes in the thermal environment of these three megacities were substantially identical with their land cover pattern and tendency. Although land covers significantly influenced the LST as a whole, the different areas had different magnitudes of SUHI coming from different land cover compositions and differentials. The results would provide a valuable reference to disentangle spatiotemporal variation of the bay urban thermal environments, and the urbanization-induced land covers temperature dynamics. This study would contribute to the development of future SUHI mitigation solutions.

Keywords: Land Cover/Use , Urban Heat Island (UHI), Mitigation Strategies

©2019. Japan Geoscience Union. All Right Reserved.

A LST Study of the Seoul Metropolitan City, South Korea, Based on Landsat Data (1996 –2017)

*Prabath Priyankara[1,3], Manjula Ranagalage[1,4], DMSLB Dissanayake[1,4], Takehiro Morimoto[1,2], Yuji Murayama[1,2]

1. Graduate School of Life and Environmental Sciences, University of Tsukuba, Japan, 2. Faculty of Life and Environmental Sciences, University of Tsukuba, Japan, 3. Faculty of Agriculture, University of Ruhuna, Sri Lanka, 4. Faculty of Social Sciences and Humanities, Rajarata University of Sri Lanka, Sri Lanka

Rapid urban growth often replaced urban vegetation with impervious surfaces which leads to increase land surface temperature (LST) periodically and tends to form urban heat islands (UHI). This is a serious issue of urbanized cities and the increase of LST badly affects the well-being of the life and environments of the cities. The Seoul Metropolitan City (SMC), South Korea, is one of the developed and rapidly urbanizing metropolitan city in Asia. The aim of this study was to examine the spatiotemporal variations of LST in the SMC and surroundings in the context of the UHI using Landsat data. The study examined the relationship of LST with the normalized difference vegetation index (NDVI) and the normalized difference built-up index (NDBI) at three time periods 1996, 2006, and 2017. Also, the study was investigated the environmentally critical areas based on LST and NDVI by modeling environmental criticality index (ECI). According to the results of the study, there is a negative correlation between LST with NDVI and positive correlation of LST with NDBI across all three time periods. In SMC, most of the environmentally critical areas are located in the central business district (CBD), near the harbor, and along the main transportation network. According to the results of the study, it is recommended that the identified environmentally critical areas to be considered in the urban planning of the city. Green spaces of the city will help to improve the life and environmental well-being of the SMC.

Keywords: Urban Heat Island, Land Surface Temperature, NDVI, NDBI, Environmental Criticality Index, Seoul Metropolitan City

©2019. Japan Geoscience Union. All Right Reserved.

Improvement of GIS exercise classes using the GIS open educational resources based on questionnaire surveys

*Hiroyuki Yamauchi[1], Takashi Oguchi[1], Yuichi S. Hayakawa[2,1], Kotaro Iizuka[1]

1. Center for Spatial Information Science, The University of Tokyo, 2. Environmental Geography, Faculty of Environmental Earth Science, Hokkaido University

Free and open source GIS software has been utilized for GIS education all over the world. However, as far as we recognize, GIS education in many Japanese universities underutilize such software packages. Therefore, we developed GIS exercise materials explaining spatial data analyses using free and open-source GIS. We have been providing these materials for higher education and designated them as the GIS Open Educational Resources. We used the materials in a university exercise class, which was held as an intensive course for three days at The University of Tokyo. During the exercise, we have conducted questionnaire surveys to clarify the three criteria: difficulty, understanding and satisfactory levels of the students. The results showed that the students felt difficulty in some situations such as the utilization of GIS for the first time and complex operations using different types of data. The contents of the exercise syllabus and materials were improved based on the feedback. We conducted another GIS exercise class at the university to verify the utility of improvements. In this presentation, we show the improvements in the exercise syllabus and the comparison of educational effects on students before and after the improvements.

Keywords: GIS education, exercise, Open Educational Resources, Free and open-source GIS

©2019. Japan Geoscience Union. All Right Reserved.

The Development of COP for Tzu Chi Disaster Prevention System by Using QGIS-Taking 2018 Hualien Earthquake as an Example

*kuan-wen tseng[1], Ming-Ta Tsai[1], Yun-Ching Wang[1], Ming-Chih Wang[1], Chien-Hsien Liu[1]

1. 03-3809093

The Hualien earthquake occurred at 23:50 and 41.6 seconds on February 6, 2018. The epicenter was located in the coastal area of Hualien County. The earthquake scale was 6.2 and the Seismic source depth was 6.3 kilometers. The earthquake disaster along the Milun fault was mainly concentrated in Hualien City, and collapsed the first and second floors of the “Tongshuai” building. The “Yunmen Cuidi” Building showed a 45-degree tilt. The lower floors of the residential community building "Baijin Shuangxing" and “Wuzhu Wusu” at Guosheng Sixth Street were destroyed. This study mainly uses the powerful geospatial analysis capabilities of Geographic Information System (GIS) to provide Tzu Chi's plans for disaster mitigation. The projects include: (1) humanitarian cares; (2) visiting and reporting of damage situations around main disaster areas and (3) “Reassuring Homes Visits” in order to provide assistance to Tzu Chi people for operations of disaster mitigation.

Keywords: Millun fault, geographic information system, spatial analysis, Tzu Chi Foundation

©2019. Japan Geoscience Union. All Right Reserved.

Comparative study on shape and distribution of landslides caused by the 2012 Northern Kyushu heavy rainfall and the 2016 Kumamoto earthquake in the Aso region, Kumamoto, Japan

*Yasutaka Haneda[1], Takashi Oguchi[2], Kotaro Iizuka[2], Hitoshi SAITO[3,2], Yuichi S. Hayakawa[4,2], Shoichiro Uchiyama[5]

1. Graduate School of Frontier Science, The University of Tokyo, 2. Center for Spatial Information Science, The University of Tokyo, 3. College of Economics, Kanto Gakuin University, 4. Faculty of Environmental Earth Science, Hokkaido University, 5. National Research Institute for Earth Science and Disaster Resilience

The 2016 Kumamoto earthquake triggered many landslides in the Aso region, southwestern Japan. Previous studies have revealed the processes of some large representative landslides in the western Aso region, but they have not comprehensively dealt with lots of small landslides. Other studies have discussed landslide distribution and relationships with that of the heavy rainfall events in July 2012 in the northern part of the Central Cones of the Aso volcano. However, they have not been investigated the western part of the Aso region which has various topographical and geological characteristics. Therefore, this study compares the formation and distribution of landslides caused by the heavy rainfall and earthquake events in both the central and western part of the Aso region.

The study areas are the western part of the Aso region and the Sensuikyo region at the northern part of the Central Cones (Fig. 1). The western part was divided into three sites: site P (caldera walls and the outer rim), Q (western part of Central Cones), and R (river terrace and talus) based on geomorphological and geological characteristics. The Sensuikyo region is referred to as site S. This study utilized multi-temporal datasets derived from airborne lidar and photogrammetry using UAV photographs: (i) before the heavy rainfall, (ii) between the heavy rainfall and the earthquake, and (iii) after the earthquake. By using digital elevation data and a sediment transportation map, elevation lowering spots caused by the landslides were identified. Then terrain information and the indexes of shape and spatial distribution were analyzed at the elevation lowering spots.

From the analysis, it was found that the heavy rainfall induced 374 landslides and the earthquake triggered 440 landslides. Landslides affected by the two different events were recognized in sites P and S. In site S, the indexes of spatial distribution showed that the earthquake caused the displacement of regolith remained on the upper convex part of the slope. In site P, the shape indexes indicated that the former event led to removal of topsoil, whereas the latter event induced the failure of lava and pyroclastic rocks. In site Q, failed slopes are not as steep as locations where landslides occurred due to past heavy rainfall events, and remained thick unconsolidated topsoil is composed of volcanic ash. It slipped deeply in 2016 due to strong seismic shaking strengthened by topographic site effects on the convex part of the slope. In site R, landslide shapes and comparison with those in site P suggest that collapsed soil directly fell into rivers without erosion of topsoil.

This study has revealed that the distribution of landslides due to the earthquake is related to that by the heavy rainfall in the Sensuikyo region. On the other hand, in the western part of the Aso region, differences in shape and distribution are found between landslides caused by the two events. Moreover, there are differences in the formation of earthquake-induced landslides among the different study sites.

©2019. Japan Geoscience Union. All Right Reserved.

Keywords: The 2016 Kumamoto Earthquake, July 2012 Northern Kyushu Heavy rainfall, landslides

©2019. Japan Geoscience Union. All Right Reserved.

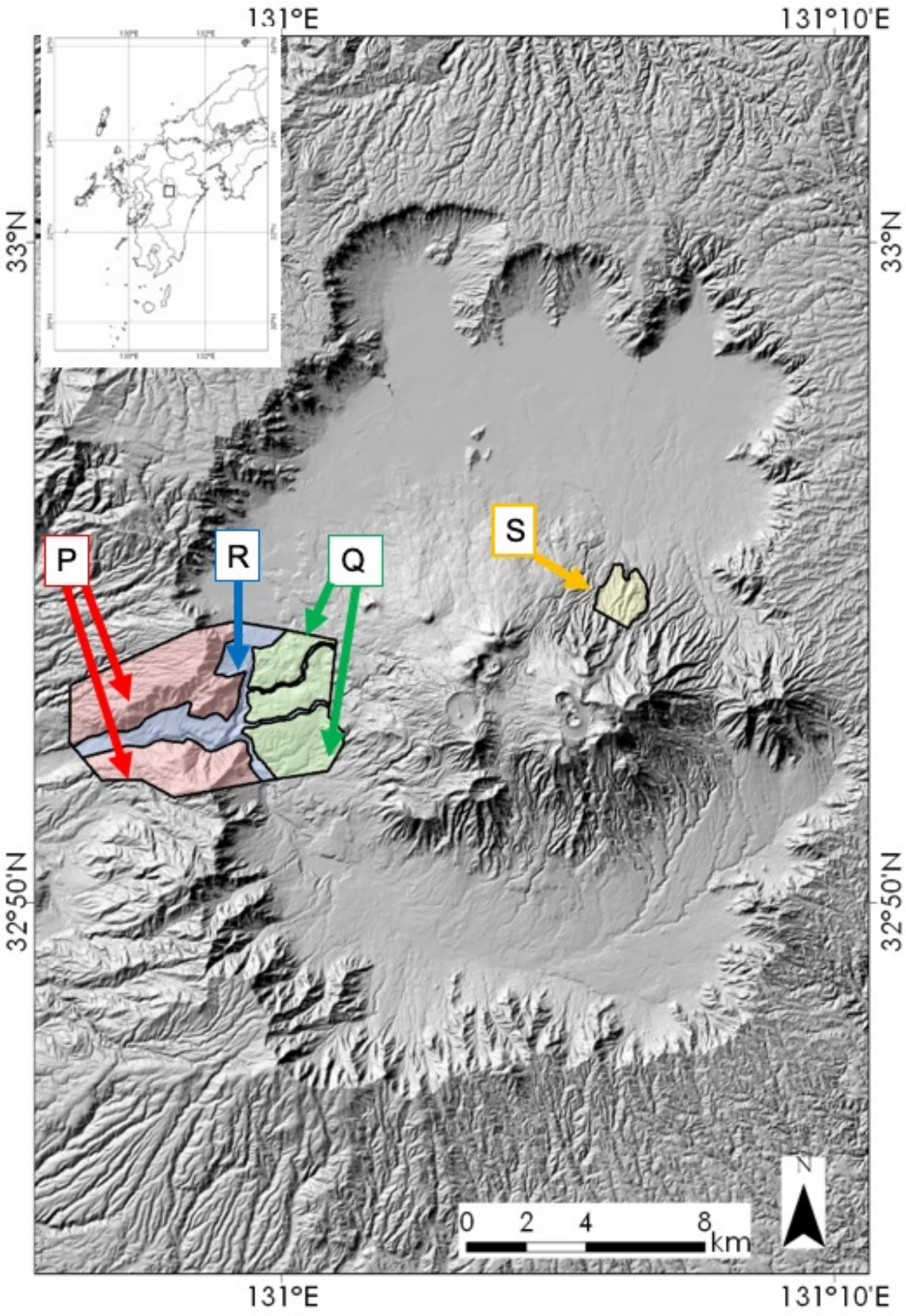

©2019. Japan Geoscience Union. All Right Reserved.

Using GIS and remote sensing to assess relationships between landslides and land cover changes in the Sanbagawa and Mikabu Belts, Shikoku, Japan

*Roxanne Lai[1], Takashi Oguchi[1]

1. University of Tokyo

The Sanbagawa and Mikabu Belts are metamorphic belts that run across Southwest Japan, and are home to numerous large crystalline schist landslides, including the widely-studied slow but continuously moving Zentoku landslide. Villages and communities have been built on these landslide areas due to historical and cultural factors, as well as the fertility of the soil. With changing human needs and social trends, however, changing land uses is becoming an increasingly important issue. In Japan, movement of the population from rural to urban areas have resulted in much land and agricultural land abandonment. As vegetation cover changes after land abandonment, this temporal and spatial effect may have important effects on geomorphic processes such as landslide susceptibility and landslide kinematics.

Here we track long-term land cover changes over vegetated landslide areas of the Sanbagawa and Mikabu Belts of Shikoku Island, Japan, and conduct spatio-temporal analyses to assess relationships between landslides and land cover changes. Given changing land uses, including land abandonment in these landslide areas over time, we use long-term high-resolution land cover vegetation datasets to examine first the long-term land use changes, and then use statistical methods to explore their relationships with landslide susceptibility and kinematics. Mapping of spatial data and their analysis using GIS constitute a core part of the research. The results suggest interconnections between land use changes and land movement.

Keywords: Landslides, Shikoku, GIS , Remote Sensing

©2019. Japan Geoscience Union. All Right Reserved.

Analysis of Morphometric Parameters for Mountains Ranges and Landslides due to the July 2018 Heavy Rain in Western Japan Using GIS Data

*Toshikazu Fukuba[1], Takashi Oguchi[2]

1. Department of Earth and Planetary Environmental Science, The University of Tokyo, 2. Center for Spatial Information Science, The University of Tokyo

Morphometric parameters for mountains ranges have been analyzed in many studies. These studies in recent years used Digital Elevation Models (DEMs) to calculate values of morphometric parameters within mountains and provided consideration on landform evolution. In addition, morphometric parameters calculated by DEMs have been used for producing landslide hazard maps. This study investigates geomorphometric parameters within the Chugoku and Shikoku Mountains, Japan, and the relationships among the parameters. In addition, landslides caused by the July 2018 heavy rain in western Japan is also investigated and the relationships between the landforms of the mountains and the landslides are discussed. Altitude, slope angle, slope aspect and slope curvature are chosen for morphometric parameters to be investigated.

Morphometric parameters for the Chugoku and in Shikoku Mountains computed using DEMs and GIS have some characteristics common to the Japanese Alps. For example, for wide altitudinal zones, slope angle tends to be constant around 30 to 40 degrees even if altitude changes. However, the values of the constant slope angle are not the same, which may be due to geological differences or the difference in the formation age of mountains. Although the frequency distribution of slope aspect is similar to the Chugoku and Shikoku Mountains, anisotropy of slope aspect is different between the two mountains. This may be caused by differences in the formation age, formation mechanism, or geology of the mountains.

Analysis of landslides caused by the July 2018 heavy rain in Hiroshima using landslide data and DEMs revealed that landslides mostly occurred around 300 m in altitude, at 15 to 30 degrees in slope angle, and on concave slopes. Although the characteristics slope angles higher than 30 degrees point to frequent slope failures at high and steep mountain slopes in the Chugoku and Shikoku Mountains, landslides corresponding to one rainfall event do not necessarily follow this, because they depend on the distribution of rainfall during the event. Therefore, possibility of landslides in low and gentle mountains close to populated areas needs to be considered seriously for mitigating landslide disasters.

Keywords: GIS, Mountain landform, Landslide, Morphometric parameters

©2019. Japan Geoscience Union. All Right Reserved.

Analyzing short-term topographic change in coastal sand dunes using UAS-SfM photogrammetry: A case study in Northern Kujukuri, Japan

*Seulgi Lee[1], Yasutaka Nakata[2], Kotaro Iizuka[3], Takashi Oguchi[3]

1. Graduate School of Frontier Sciences, The University of Tokyo, 2. Forest Research Department, Forestry Research Institute, Hokkaido Research Organization, 3. Center for Spatial Information Science, The University of Tokyo

Collection of spatial data is critical for the identification of coastlines and coastal zones and related studies in coastal geomorphology. It is particularly important to obtain high-resolution elevation data in order to observe topographical changes of coastal sand dunes with frequent dynamic movements during a short period of time. Unmanned Aerial System (UAS) photogrammetry combined with Structure from Motion (SfM) offers an effective solution to the acquisition of such data. Kujukuri, facing the Pacific Ocean in Chiba Prefecture, Japan, is a region with a long coastal zone of about 60 km. Although the development of this area since the 1960s has destroyed many natural landscapes, they are relatively preserved in Northern Kujukuri. This study focuses on short-term topographic changes in coastal sand dunes there and discusses the effects of vegetation and wind.
UAV-SfM surveys were conducted seven times from September 2016 to December 2018, and the obtained topographic data were analyzed using GIS software (ArcGIS Pro) to evaluate changes in terrain conditions by season and year. We also analyzed the wind direction data provided by the Japan Meteorological Agency. Vegetation data were obtained from the field surveys and the green-red vegetation index extracted from the UAS images. The following three characteristics were identified: 1) Short-term topographic changes tend to be influenced by specific events such as storm events, and therefore terrain conditions in the same season may be different from year to year. 2) General wind conditions represented by the meteorological data corresponding to the overall change of sand dune topography, especially at seasonal or longer scales. 3) Formation of small sand dunes is affected by vegetation distribution. This study has suggested factors affecting short-term topographic changes of coastal sand dunes based on frequent data acquisition in the field and geospatial technologies.

Keywords: GIS, Coastal sand dunes, UAV, SfM

©2019. Japan Geoscience Union. All Right Reserved.

Responses of suspended sediment yield to precipitation, topography and dam control in the Yellow River Basin, China

*Ruiqi Zhang[1], Takashi Oguchi[2]

1. Department of Natural Environmental Studies, Graduate School of Frontier Sciences, The University of Tokyo, 2. Center for Spatial Information Science, The University of Tokyo

Soil erosion has long been a serious problem in the Yellow River Basin in China. The high sediment load carried by the Yellow River results in deposition along its path, raising the riverbed and increasing the flood risk in the lower reaches. To mitigate this situation, large-scale soil conservation measures have been put into practice such as the construction of dams to effectively trap fluvial sediments. Previous studies on this topic focused on the interannual fluctuation of sediment yield caused by dams and reservoirs. However, few studies focused on their effects on the seasonal variation of sediment yield. In 2002, the Yellow River Conservancy Committee began to implement the water-sediment regulation (WSR) scheme to regulate the river water, which further strengthen the impact of dam control on the seasonality of sediment yield. Therefore, this research aims to integrate natural contributing factors such as topography and precipitation with the WSR-based dam control to analyze the seasonal and spatial variations of sediment yield in the Yellow River, for the years 2008 to 2012. Data of daily suspended sediment concentration, water discharge, and precipitation were downloaded from the Chinese Data Sharing Infrastructure of Earth System Science, and the ASTER GLOBAL DEMs with a resolution of 1 arc-second were downloaded from the U.S. Geological Survey web site. ArcGIS and R software packages are used to analyze the obtained data. Inspection of data quality revealed that consecutive sediment yield and precipitation data for 97 watersheds are usable.

Data analysis indicated the following four basic hydrological characteristics of the watersheds. 1) Water discharge within each watershed is not stable both interannually and seasonally, because it has been affected by the implementation of dam regulation as well as low discharge conditions mostly in spring and winter especially in some small watersheds. 2) The variation of sediment yield in some natural watersheds reflects change in precipitation, leading to sediment yield peaks in summer. 3) In other watersheds, the variation of sediment yield tends to be independent of precipitation. Instead, some artificial conservation measures such as dam control effectively intercept sediments from the upstream area. 4) The correlation between suspended sediment yield and water discharge varies among watersheds, and the correlation coefficient can be used as a parameter representing hydrological characteristics. The DEMs have been also analyzed to relate hydrology and climate with geomorphology. The obtained results may help the policy makers better understand the erosion situations in the Yellow River Basin and regulate the soil conservation measures.

Keywords: Suspended sediment yield, the Yellow River basin, seasonality, precipitation, topography, dam control

©2019. Japan Geoscience Union. All Right Reserved.

[E] Poster | H (Human Geosciences)：H-TT Technology & Techniques

Thu. May 30, 2019 5:15 PM - 6:30 PM JST | Thu. May 30, 2019 8:15 AM - 9:30 AM UTC | Poster Hall International Exhibition Hall8, Makuhari Messe_16

[H-TT19] Geographic Information Systems and Cartography

convener:Takashi Oguchi(Center for Spatial Information Science, The University of Tokyo), Yuji Murayama(Graduate School of Life and Environmental Sciences), Yoshiki Wakabayashi(Graduate School of Urban Environmental Sciences, Tokyo Metropolitan University)

This session discusses various methods which acquire, store, analyze and visualize geospatial data, and presents the outcomes of empirical studies using GIS or mapping methods. The session also deals with applications of digital data, and GIS, and mapping to various fields of earth and planetary science and human society. All presentations and discussion of this session are made in English.

[HTT19-P01] Monitoring and Simulating Land Use/Cover Changes and its Impact on Land Surface Temperature in Sapporo City, Japan

*RUCI WANG[1], YUJI MURAYAMA[1] (1.University of Tsukuba)

[HTT19-P02] Spatiotemporal Variations of Land Cover/Use and Sustainable Urban Heat Island (UHI) Mitigation Strategies: A Case Study of Chinese Bay Megacities

★Invited Papers

*Fei LIU[1], Yuji MURAYAMA[1] (1. University of Tsukuba)

[HTT19-P03] A LST Study of the Seoul Metropolitan City, South Korea, Based on Landsat Data (1996 – 2017)

*Prabath Priyankara[1,3], Manjula Ranagalage[1,4], DMSLB Dissanayake[1,4], Takehiro Morimoto[1,2], Yuji Murayama[1,2] (1.Graduate School of Life and Environmental Sciences, University of Tsukuba, Japan, 2.Faculty of Life and Environmental Sciences, University of Tsukuba, Japan, 3.Faculty of Agriculture, University of Ruhuna, Sri Lanka, 4.Faculty of Social Sciences and Humanities, Rajarata University of Sri Lanka, Sri Lanka)

[HTT19-P04] Improvement of GIS exercise classes using the GIS open educational resources based on questionnaire surveys

★Invited Papers

*Hiroyuki Yamauchi[1], Takashi Oguchi[1], Yuichi S. Hayakawa[2,1], Kotaro Iizuka[1] (1.Center for Spatial Information Science, The University of Tokyo, 2.Environmental Geography, Faculty of Environmental Earth Science, Hokkaido University)

[HTT19-P05] The Development of COP for Tzu Chi Disaster Prevention System by Using QGIS-Taking 2018 Hualien Earthquake as an Example

*kuan-wen tseng[1], Ming-Ta Tsai[1], Yun-Ching Wang[1], Ming-Chih Wang[1], Chien-Hsien Liu[1] (1.03-3809093)

[HTT19-P06] Comparative study on shape and distribution of landslides caused by the 2012 Northern Kyushu heavy rainfall and the 2016 Kumamoto earthquake in the Aso region, Kumamoto, Japan

*Yasutaka Haneda[1], Takashi Oguchi[2], Kotaro Iizuka[2], Hitoshi SAITO[3,2], Yuichi S. Hayakawa[4,2], Shoichiro Uchiyama[5] (1.Graduate School of Frontier Science, The University of Tokyo, 2.Center for Spatial Information Science, The University of Tokyo, 3.College of Economics, Kanto Gakuin University, 4.Faculty of Environmental Earth Science, Hokkaido University, 5.National Research Institute for Earth Science and Disaster Resilience)

[HTT19-P07] Using GIS and remote sensing to assess relationships between landslides and land cover changes in the Sanbagawa and Mikabu Belts, Shikoku, Japan

*Roxanne Lai[1], Takashi Oguchi[1] (1.University of Tokyo)

[HTT19-P08] **Analysis of Morphometric Parameters for Mountains Ranges and Landslides due to the July 2018 Heavy Rain in Western Japan Using GIS Data**

*Toshikazu Fukuba[1], Takashi Oguchi[2] (1.Department of Earth and Planetary Environmental Science, The University of Tokyo, 2.Center for Spatial Information Science, The University of Tokyo)

[HTT19-P09] Analyzing short-term topographic change in coastal sand dunes using UAS-SfM photogrammetry: A case study in Northern Kujukuri, Japan

*Seulgi Lee[1], Yasutaka Nakata[2], Kotaro Iizuka[3], Takashi Oguchi[3] (1.Graduate School of Frontier Sciences, The University of Tokyo, 2.Forest Research Department, Forestry Research Institute, Hokkaido Research Organization, 3.Center for Spatial Information Science, The University of Tokyo)

[HTT19-P10] **Responses of suspended sediment yield to precipitation, topography and dam control in the Yellow River Basin, China**

*Ruiqi Zhang[1], Takashi Oguchi[2] (1. Department of Natural Environmental Studies, Graduate School of Frontier Sciences, The University of Tokyo, 2.Center for Spatial Information Science, The University of Tokyo)

Monitoring and Simulating Land Use/Cover Changes and its Impact on Land Surface Temperature in Sapporo City, Japan

*RUCI WANG[1], YUJI MURAYAMA[1]

1. University of Tsukuba

In recent years, urban heat island phenomenon (UHI) which prevails in many cities worldwide has caused broad public concern. UHI phenomenon impairs healthy urban development and causes excessive energy consumption, climatic and environmental deterioration. Land use/cover changes are one of the most crucial variables influencing on UHI. Therefore, monitoring and simulating land use/cover changes and analyzing its effects on LST are essential for healthy urban development. This study aims to capture the impact of land use/cover on LST and simulate the LST under various land use/cover scenarios in Sapporo city, Japan. At first, we monitored the land use/cover changes from 1985 to 2015 and detect the change of LST concerning land use/cover distribution. Then, we predicted the future conditions of LST based on various land use/cover scenarios. The results show that the LST differs according to land use/cover types, and the proportion of land use/cover types is the most significant factor affecting LST. The findings also indicate that the built-up area and paddy field have the highest average LST, while the green space and water area help cool the city. In the future, the green area such as urban green parks and grassland should be planned in the city to mitigate the UHI phenomenon. It reveals the spatial characterization of LST which provides significant insights for government and city planners.

Keywords: Geographical information science, Urban heat island, Land surface temperature, Land use/cover change, Sapporo city

©2019. Japan Geoscience Union. All Right Reserved.

Spatiotemporal Variations of Land Cover/Use and Sustainable Urban Heat Island (UHI) Mitigation Strategies: A Case Study of Chinese Bay Megacities

*Fei LIU[1], Yuji MURAYAMA[1]

1. University of Tsukuba

Rapid urbanization significantly affects the urban thermal environment in the context of global climate change. The assessment of surface urban heat island (SUHI) and development of mitigation strategies in megacities have become frontier issues on human health and urban sustainability. In this study, taking of the three Chinese bay megacities, we attempt to 1) disclose the relationship between land surface temperature (LST) and land cover using remote sensing quantified analysis, 2) to clarify the mechanism and characteristics of SUHI formation based on bi-temporal patterns and variations of land cover, and 3) to sustainably regulate and optimize the urban environment and further create urban planning and policies for relieving urban thermal effect. The study target is Guangzhou metropolitan area (GMA), Hangzhou metropolitan area (HMA) and Shanghai Metropolitan area (SMA) in China. The result of this study indicated remarkably different characteristics, arrangement, and variations among different bay thermal environments. Overall, spatial layouts and changes in the thermal environment of these three megacities were substantially identical with their land cover pattern and tendency. Although land covers significantly influenced the LST as a whole, the different areas had different magnitudes of SUHI coming from different land cover compositions and differentials. The results would provide a valuable reference to disentangle spatiotemporal variation of the bay urban thermal environments, and the urbanization-induced land covers temperature dynamics. This study would contribute to the development of future SUHI mitigation solutions.

Keywords: Land Cover/Use , Urban Heat Island (UHI), Mitigation Strategies

©2019. Japan Geoscience Union. All Right Reserved.

A LST Study of the Seoul Metropolitan City, South Korea, Based on Landsat Data (1996 –2017)

*Prabath Priyankara[1,3], Manjula Ranagalage[1,4], DMSLB Dissanayake[1,4], Takehiro Morimoto[1,2], Yuji Murayama[1,2]

1. Graduate School of Life and Environmental Sciences, University of Tsukuba, Japan, 2. Faculty of Life and Environmental Sciences, University of Tsukuba, Japan, 3. Faculty of Agriculture, University of Ruhuna, Sri Lanka, 4. Faculty of Social Sciences and Humanities, Rajarata University of Sri Lanka, Sri Lanka

Rapid urban growth often replaced urban vegetation with impervious surfaces which leads to increase land surface temperature (LST) periodically and tends to form urban heat islands (UHI). This is a serious issue of urbanized cities and the increase of LST badly affects the well-being of the life and environments of the cities. The Seoul Metropolitan City (SMC), South Korea, is one of the developed and rapidly urbanizing metropolitan city in Asia. The aim of this study was to examine the spatiotemporal variations of LST in the SMC and surroundings in the context of the UHI using Landsat data. The study examined the relationship of LST with the normalized difference vegetation index (NDVI) and the normalized difference built-up index (NDBI) at three time periods 1996, 2006, and 2017. Also, the study was investigated the environmentally critical areas based on LST and NDVI by modeling environmental criticality index (ECI). According to the results of the study, there is a negative correlation between LST with NDVI and positive correlation of LST with NDBI across all three time periods. In SMC, most of the environmentally critical areas are located in the central business district (CBD), near the harbor, and along the main transportation network. According to the results of the study, it is recommended that the identified environmentally critical areas to be considered in the urban planning of the city. Green spaces of the city will help to improve the life and environmental well-being of the SMC.

Keywords: Urban Heat Island, Land Surface Temperature, NDVI, NDBI, Environmental Criticality Index, Seoul Metropolitan City

©2019. Japan Geoscience Union. All Right Reserved.

Improvement of GIS exercise classes using the GIS open educational resources based on questionnaire surveys

*Hiroyuki Yamauchi[1], Takashi Oguchi[1], Yuichi S. Hayakawa[2,1], Kotaro Iizuka[1]

1. Center for Spatial Information Science, The University of Tokyo, 2. Environmental Geography, Faculty of Environmental Earth Science, Hokkaido University

Free and open source GIS software has been utilized for GIS education all over the world. However, as far as we recognize, GIS education in many Japanese universities underutilize such software packages. Therefore, we developed GIS exercise materials explaining spatial data analyses using free and open-source GIS. We have been providing these materials for higher education and designated them as the GIS Open Educational Resources. We used the materials in a university exercise class, which was held as an intensive course for three days at The University of Tokyo. During the exercise, we have conducted questionnaire surveys to clarify the three criteria: difficulty, understanding and satisfactory levels of the students. The results showed that the students felt difficulty in some situations such as the utilization of GIS for the first time and complex operations using different types of data. The contents of the exercise syllabus and materials were improved based on the feedback. We conducted another GIS exercise class at the university to verify the utility of improvements. In this presentation, we show the improvements in the exercise syllabus and the comparison of educational effects on students before and after the improvements.

Keywords: GIS education, exercise, Open Educational Resources, Free and open-source GIS

©2019. Japan Geoscience Union. All Right Reserved.

The Development of COP for Tzu Chi Disaster Prevention System by Using QGIS-Taking 2018 Hualien Earthquake as an Example

*kuan-wen tseng[1], Ming-Ta Tsai[1], Yun-Ching Wang[1], Ming-Chih Wang[1], Chien-Hsien Liu[1]

1. 03-3809093

The Hualien earthquake occurred at 23:50 and 41.6 seconds on February 6, 2018. The epicenter was located in the coastal area of Hualien County. The earthquake scale was 6.2 and the Seismic source depth was 6.3 kilometers. The earthquake disaster along the Milun fault was mainly concentrated in Hualien City, and collapsed the first and second floors of the “Tongshuai” building. The “Yunmen Cuidi” Building showed a 45-degree tilt. The lower floors of the residential community building "Baijin Shuangxing" and “Wuzhu Wusu” at Guosheng Sixth Street were destroyed. This study mainly uses the powerful geospatial analysis capabilities of Geographic Information System (GIS) to provide Tzu Chi's plans for disaster mitigation. The projects include: (1) humanitarian cares; (2) visiting and reporting of damage situations around main disaster areas and (3) “Reassuring Homes Visits” in order to provide assistance to Tzu Chi people for operations of disaster mitigation.

Keywords: Millun fault, geographic information system, spatial analysis, Tzu Chi Foundation

©2019. Japan Geoscience Union. All Right Reserved.

Comparative study on shape and distribution of landslides caused by the 2012 Northern Kyushu heavy rainfall and the 2016 Kumamoto earthquake in the Aso region, Kumamoto, Japan

*Yasutaka Haneda[1], Takashi Oguchi[2], Kotaro Iizuka[2], Hitoshi SAITO[3,2], Yuichi S. Hayakawa[4,2], Shoichiro Uchiyama[5]

1. Graduate School of Frontier Science, The University of Tokyo, 2. Center for Spatial Information Science, The University of Tokyo, 3. College of Economics, Kanto Gakuin University, 4. Faculty of Environmental Earth Science, Hokkaido University, 5. National Research Institute for Earth Science and Disaster Resilience

The 2016 Kumamoto earthquake triggered many landslides in the Aso region, southwestern Japan. Previous studies have revealed the processes of some large representative landslides in the western Aso region, but they have not comprehensively dealt with lots of small landslides. Other studies have discussed landslide distribution and relationships with that of the heavy rainfall events in July 2012 in the northern part of the Central Cones of the Aso volcano. However, they have not been investigated the western part of the Aso region which has various topographical and geological characteristics. Therefore, this study compares the formation and distribution of landslides caused by the heavy rainfall and earthquake events in both the central and western part of the Aso region.

The study areas are the western part of the Aso region and the Sensuikyo region at the northern part of the Central Cones (Fig. 1). The western part was divided into three sites: site P (caldera walls and the outer rim), Q (western part of Central Cones), and R (river terrace and talus) based on geomorphological and geological characteristics. The Sensuikyo region is referred to as site S. This study utilized multi-temporal datasets derived from airborne lidar and photogrammetry using UAV photographs: (i) before the heavy rainfall, (ii) between the heavy rainfall and the earthquake, and (iii) after the earthquake. By using digital elevation data and a sediment transportation map, elevation lowering spots caused by the landslides were identified. Then terrain information and the indexes of shape and spatial distribution were analyzed at the elevation lowering spots.

From the analysis, it was found that the heavy rainfall induced 374 landslides and the earthquake triggered 440 landslides. Landslides affected by the two different events were recognized in sites P and S. In site S, the indexes of spatial distribution showed that the earthquake caused the displacement of regolith remained on the upper convex part of the slope. In site P, the shape indexes indicated that the former event led to removal of topsoil, whereas the latter event induced the failure of lava and pyroclastic rocks. In site Q, failed slopes are not as steep as locations where landslides occurred due to past heavy rainfall events, and remained thick unconsolidated topsoil is composed of volcanic ash. It slipped deeply in 2016 due to strong seismic shaking strengthened by topographic site effects on the convex part of the slope. In site R, landslide shapes and comparison with those in site P suggest that collapsed soil directly fell into rivers without erosion of topsoil.

This study has revealed that the distribution of landslides due to the earthquake is related to that by the heavy rainfall in the Sensuikyo region. On the other hand, in the western part of the Aso region, differences in shape and distribution are found between landslides caused by the two events. Moreover, there are differences in the formation of earthquake-induced landslides among the different study sites.

©2019. Japan Geoscience Union. All Right Reserved.

Keywords: The 2016 Kumamoto Earthquake, July 2012 Northern Kyushu Heavy rainfall, landslides

©2019. Japan Geoscience Union. All Right Reserved.

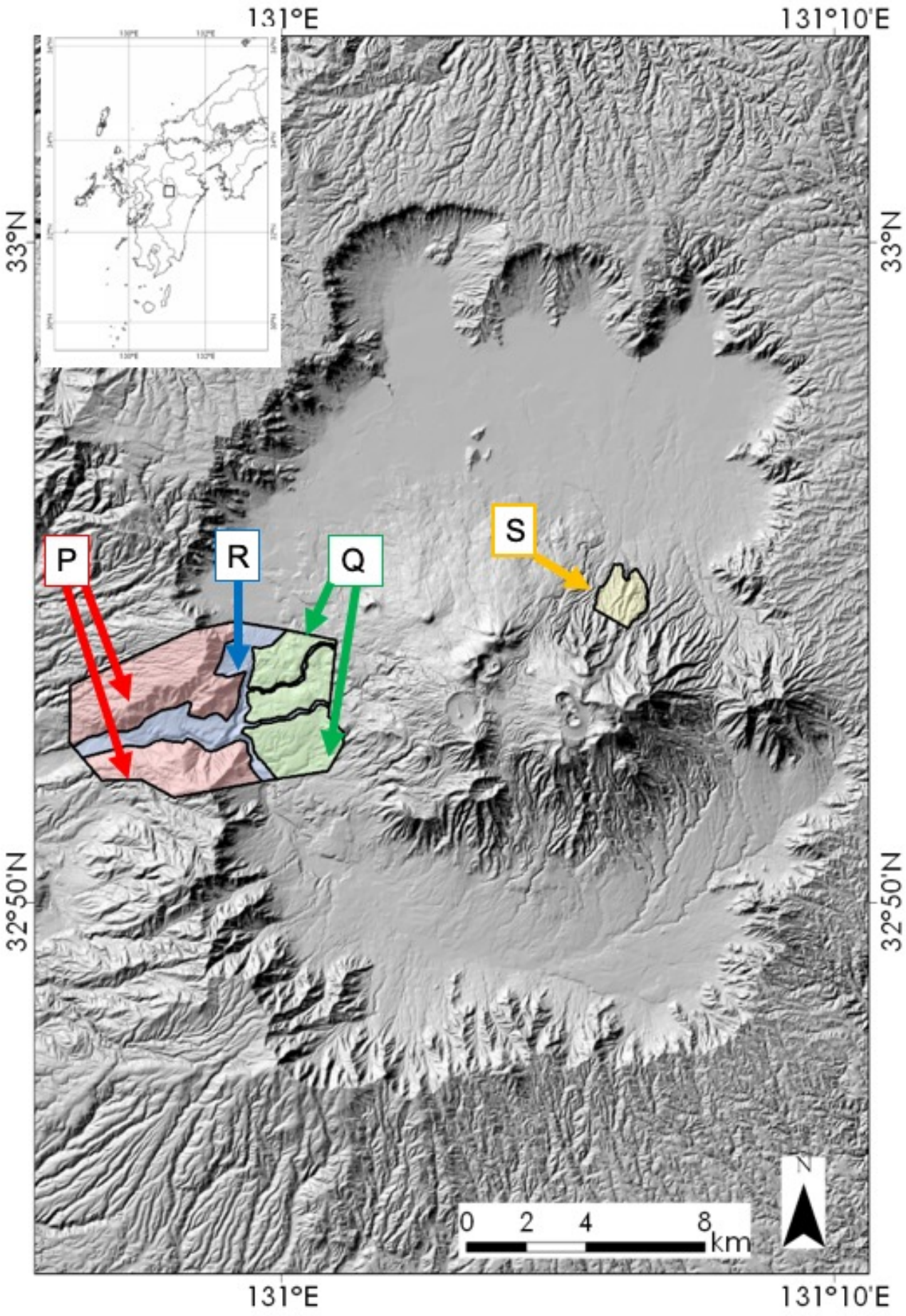

©2019. Japan Geoscience Union. All Right Reserved.

Using GIS and remote sensing to assess relationships between landslides and land cover changes in the Sanbagawa and Mikabu Belts, Shikoku, Japan

*Roxanne Lai[1], Takashi Oguchi[1]

1. University of Tokyo

The Sanbagawa and Mikabu Belts are metamorphic belts that run across Southwest Japan, and are home to numerous large crystalline schist landslides, including the widely-studied slow but continuously moving Zentoku landslide. Villages and communities have been built on these landslide areas due to historical and cultural factors, as well as the fertility of the soil. With changing human needs and social trends, however, changing land uses is becoming an increasingly important issue. In Japan, movement of the population from rural to urban areas have resulted in much land and agricultural land abandonment. As vegetation cover changes after land abandonment, this temporal and spatial effect may have important effects on geomorphic processes such as landslide susceptibility and landslide kinematics.

Here we track long-term land cover changes over vegetated landslide areas of the Sanbagawa and Mikabu Belts of Shikoku Island, Japan, and conduct spatio-temporal analyses to assess relationships between landslides and land cover changes. Given changing land uses, including land abandonment in these landslide areas over time, we use long-term high-resolution land cover vegetation datasets to examine first the long-term land use changes, and then use statistical methods to explore their relationships with landslide susceptibility and kinematics. Mapping of spatial data and their analysis using GIS constitute a core part of the research. The results suggest interconnections between land use changes and land movement.

Keywords: Landslides, Shikoku, GIS , Remote Sensing

©2019. Japan Geoscience Union. All Right Reserved.

Analysis of Morphometric Parameters for Mountains Ranges and Landslides due to the July 2018 Heavy Rain in Western Japan Using GIS Data

*Toshikazu Fukuba[1], Takashi Oguchi[2]

1. Department of Earth and Planetary Environmental Science, The University of Tokyo, 2. Center for Spatial Information Science, The University of Tokyo

Morphometric parameters for mountains ranges have been analyzed in many studies. These studies in recent years used Digital Elevation Models (DEMs) to calculate values of morphometric parameters within mountains and provided consideration on landform evolution. In addition, morphometric parameters calculated by DEMs have been used for producing landslide hazard maps. This study investigates geomorphometric parameters within the Chugoku and Shikoku Mountains, Japan, and the relationships among the parameters. In addition, landslides caused by the July 2018 heavy rain in western Japan is also investigated and the relationships between the landforms of the mountains and the landslides are discussed. Altitude, slope angle, slope aspect and slope curvature are chosen for morphometric parameters to be investigated.

Morphometric parameters for the Chugoku and in Shikoku Mountains computed using DEMs and GIS have some characteristics common to the Japanese Alps. For example, for wide altitudinal zones, slope angle tends to be constant around 30 to 40 degrees even if altitude changes. However, the values of the constant slope angle are not the same, which may be due to geological differences or the difference in the formation age of mountains. Although the frequency distribution of slope aspect is similar to the Chugoku and Shikoku Mountains, anisotropy of slope aspect is different between the two mountains. This may be caused by differences in the formation age, formation mechanism, or geology of the mountains.

Analysis of landslides caused by the July 2018 heavy rain in Hiroshima using landslide data and DEMs revealed that landslides mostly occurred around 300 m in altitude, at 15 to 30 degrees in slope angle, and on concave slopes. Although the characteristics slope angles higher than 30 degrees point to frequent slope failures at high and steep mountain slopes in the Chugoku and Shikoku Mountains, landslides corresponding to one rainfall event do not necessarily follow this, because they depend on the distribution of rainfall during the event. Therefore, possibility of landslides in low and gentle mountains close to populated areas needs to be considered seriously for mitigating landslide disasters.

Keywords: GIS, Mountain landform, Landslide, Morphometric parameters

©2019. Japan Geoscience Union. All Right Reserved.

Analyzing short-term topographic change in coastal sand dunes using UAS-SfM photogrammetry: A case study in Northern Kujukuri, Japan

*Seulgi Lee[1], Yasutaka Nakata[2], Kotaro Iizuka[3], Takashi Oguchi[3]

1. Graduate School of Frontier Sciences, The University of Tokyo, 2. Forest Research Department, Forestry Research Institute, Hokkaido Research Organization, 3. Center for Spatial Information Science, The University of Tokyo

Collection of spatial data is critical for the identification of coastlines and coastal zones and related studies in coastal geomorphology. It is particularly important to obtain high-resolution elevation data in order to observe topographical changes of coastal sand dunes with frequent dynamic movements during a short period of time. Unmanned Aerial System (UAS) photogrammetry combined with Structure from Motion (SfM) offers an effective solution to the acquisition of such data. Kujukuri, facing the Pacific Ocean in Chiba Prefecture, Japan, is a region with a long coastal zone of about 60 km. Although the development of this area since the 1960s has destroyed many natural landscapes, they are relatively preserved in Northern Kujukuri. This study focuses on short-term topographic changes in coastal sand dunes there and discusses the effects of vegetation and wind.
UAV-SfM surveys were conducted seven times from September 2016 to December 2018, and the obtained topographic data were analyzed using GIS software (ArcGIS Pro) to evaluate changes in terrain conditions by season and year. We also analyzed the wind direction data provided by the Japan Meteorological Agency. Vegetation data were obtained from the field surveys and the green-red vegetation index extracted from the UAS images. The following three characteristics were identified: 1) Short-term topographic changes tend to be influenced by specific events such as storm events, and therefore terrain conditions in the same season may be different from year to year. 2) General wind conditions represented by the meteorological data corresponding to the overall change of sand dune topography, especially at seasonal or longer scales. 3) Formation of small sand dunes is affected by vegetation distribution. This study has suggested factors affecting short-term topographic changes of coastal sand dunes based on frequent data acquisition in the field and geospatial technologies.

Keywords: GIS, Coastal sand dunes, UAV, SfM

©2019. Japan Geoscience Union. All Right Reserved.

Responses of suspended sediment yield to precipitation, topography and dam control in the Yellow River Basin, China

*Ruiqi Zhang[1], Takashi Oguchi[2]

1. Department of Natural Environmental Studies, Graduate School of Frontier Sciences, The University of Tokyo, 2. Center for Spatial Information Science, The University of Tokyo

Soil erosion has long been a serious problem in the Yellow River Basin in China. The high sediment load carried by the Yellow River results in deposition along its path, raising the riverbed and increasing the flood risk in the lower reaches. To mitigate this situation, large-scale soil conservation measures have been put into practice such as the construction of dams to effectively trap fluvial sediments. Previous studies on this topic focused on the interannual fluctuation of sediment yield caused by dams and reservoirs. However, few studies focused on their effects on the seasonal variation of sediment yield. In 2002, the Yellow River Conservancy Committee began to implement the water-sediment regulation (WSR) scheme to regulate the river water, which further strengthen the impact of dam control on the seasonality of sediment yield. Therefore, this research aims to integrate natural contributing factors such as topography and precipitation with the WSR-based dam control to analyze the seasonal and spatial variations of sediment yield in the Yellow River, for the years 2008 to 2012. Data of daily suspended sediment concentration, water discharge, and precipitation were downloaded from the Chinese Data Sharing Infrastructure of Earth System Science, and the ASTER GLOBAL DEMs with a resolution of 1 arc-second were downloaded from the U.S. Geological Survey web site. ArcGIS and R software packages are used to analyze the obtained data. Inspection of data quality revealed that consecutive sediment yield and precipitation data for 97 watersheds are usable.

Data analysis indicated the following four basic hydrological characteristics of the watersheds. 1) Water discharge within each watershed is not stable both interannually and seasonally, because it has been affected by the implementation of dam regulation as well as low discharge conditions mostly in spring and winter especially in some small watersheds. 2) The variation of sediment yield in some natural watersheds reflects change in precipitation, leading to sediment yield peaks in summer. 3) In other watersheds, the variation of sediment yield tends to be independent of precipitation. Instead, some artificial conservation measures such as dam control effectively intercept sediments from the upstream area. 4) The correlation between suspended sediment yield and water discharge varies among watersheds, and the correlation coefficient can be used as a parameter representing hydrological characteristics. The DEMs have been also analyzed to relate hydrology and climate with geomorphology. The obtained results may help the policy makers better understand the erosion situations in the Yellow River Basin and regulate the soil conservation measures.

Keywords: Suspended sediment yield, the Yellow River basin, seasonality, precipitation, topography, dam control

©2019. Japan Geoscience Union. All Right Reserved.

[E] Poster | S (Solid Earth Sciences)：S-IT Science of the Earth's Interior & Techtonophysics

Thu. May 30, 2019 3:30 PM - 5:00 PM JST | Thu. May 30, 2019 6:30 AM - 8:00 AM UTC | Poster Hall International Exhibition Hall8, Makuhari Messe_10

[S-IT25] Planetary cores: Structure, formation, and evolution

convener:Hidenori Terasaki(Graduate School of Science, Osaka University), Eiji Ohtani(Department of Earth and Planetary Materials Science, Graduate School of Science, Tohoku University), William F McDonough(University of Maryland College Park), George Helffrich(Earth-Life Science Institute, Tokyo Institute of Technology)

There are fundamental links between the formation and evolution of planets and their satellites to that of their cores. Defining the physical and chemical properties of the cores of these terrestrial bodies are fundamental for understanding their internal structures and thermal profile. Recent advances in experimental and theoretical studies provide new insights and applications to the Earth's cores and other terrestrial bodies. Near-future exploration missions will obtain data on the internal structure of terrestrial planets (e.g., Mars and Mercury) and planet-satellite systems. We anticipate presentations on recent advances on the physical and chemical properties of cores and discussions regarding the latest views of their formation and evolution. We welcome contributions from mineral/rock physics, geophysics, geochemistry, geodynamics, and planetary science.

[SIT25-P01] Stratification of the Earth’s core by SiO_2 crystallisation

*George Helffrich[1], Satoshi Kaneshima[2], Kei Hirose[1,3] (1.Earth-Life Science Institute, Tokyo Institute of Technology, 2.Earth and Planetary Sciences, Kyushu University, 3.Earth and Planetary Sciences Department, University of Tokyo)

[SIT25-P02] Relation between sound velocity and density for liquid iron alloys under Earth’s core pressures by laser-shock compression

*Tatsuhiro Sakaiya[1], Tadashi Kondo[1], Hidenori Terasaki[1], Keisuke Shigemori[2], Yoichiro Hironaka[2] (1.Graduate School of Science, Osaka University, 2.Institute of Laser Engineering, Osaka University)

[SIT25-P03] Geochemical estimates of Earth's core heat content at the end of accretion

*Vincent Clesi[1], Renaud Deguen[1] (1.Laboratoire de Geologie de Lyon - Terre, Planètes, Environnement, Université Claude Bernard Lyon 1, CNRS, ENS-Lyon, 69622 Villeurbanne, France.)

[SIT25-P04] The effect of temperature on density of solid metals

*Asaka Kamiya[1], Hidenori Terasaki[1], Tadashi Kondo[1] (1.Osaka University)

[SIT25-P05] Phase relations in the Fe-Ni-Si system at high pressures and high temperatures

*Daijo Ikuta[1], Eiji Ohtani[1], Saori Kawaguchi[2], Naohisa Hirao[2], Yasuo Ohishi[2] (1.Department of Earth Science, Tohoku University, 2.JASRI)

Stratification of the Earth's core by SiO_2 crystallisation

*George Helffrich[1], Satoshi Kaneshima[2], Kei Hirose[1,3]

1. Earth-Life Science Institute, Tokyo Institute of Technology, 2. Earth and Planetary Sciences, Kyushu University, 3. Earth and Planetary Sciences Department, University of Tokyo

Based on various studies reporting seismic wavespeed deviations from PREM in the outermost outer core, the core appears to be stratified. Compositional layering, where liquids of different densities overlie one another is one stratification possibility. This mechanism, however, inhibits vertical flows in the liquid near the surface of the core implied by models of secular variation of the Earth's magnetic field. To avoid this limitation, we propose a mechanism by which the layering arises in an analogous way to atmospheric cloud formation. If liquid metal containing dissolved Si+O reaches a saturation level in the outermost outer core, SiO_2 will crystallize and rise to the core-mantle boundary (CMB), causing density changes in the liquid by release of latent heat and changing composition. We present an physical model for this process and show that it explains the observed outer core wavespeed variations better than previous parameterizations. For a CMB temperature of 3800 K and a core light element content of 5 wt% Si+O, SiO_2 begins crystallizing 260 km below the CMB through an interval about 160 km thick, yet core liquid can flow freely through the crystallization interval, facilitating magnetic field changes on decadal to century time scales.

©2019. Japan Geoscience Union. All Right Reserved.

Relation between sound velocity and density for liquid iron alloys under Earth's core pressures by laser-shock compression

*Tatsuhiro Sakaiya[1], Tadashi Kondo[1], Hidenori Terasaki[1], Keisuke Shigemori[2], Yoichiro Hironaka[2]

1. Graduate School of Science, Osaka University, 2. Institute of Laser Engineering, Osaka University

Sound velocity at Earth's core conditions are one of the most important physical properties in Earth science because it can be directly compared with the seismological Earth model (PREM: Preliminary Reference Earth Model) [1]. The composition of solid inner core is estimated from the comparison of the model [1] and the extrapolation of sound velocities as a function of density of iron and iron alloys obtained by the static compression experiment [2, 3]. Birch's law, a linear sound velocity–density relation [4], is used to extrapolate sound velocities to densities in the core condition. On the other hand, the composition of liquid outer core is estimated from the partitioning and solubility data in the inner core boundary condition for the composition of solid core. There has been some works for the sound velocity of iron and iron alloys on the Earth's core condition by dynamic techniques using explosive [5], gas gun [5-11], and laser [12-14]. In this study, we measure the sound velocity and density of liquid iron alloys by shock-compression method using high-power laser.
We conducted shock-compression experiments using a High Intensity Plasma Experimental Research (HIPER) system at the GEKKO-XII laser irradiation facility [15] at the Institute of Laser Engineering, Osaka University. The samples were Fe-Ni alloys, pure nickel, Fe-Si alloys, pure silicon, and pyrrhotite. The sound velocities and densities of shock-compressed iron alloys using the high-power laser were measured by x-ray radiography [12-14] at pressures up to 1000 GPa.
Part of this work was performed under the joint research project of the Institute of Laser Engineering, Osaka University and supported by JSPS KAKENHI Grant Number JP16K05541.

References
[1] A. M. Dziewonski and D. L. Anderson, Phys. Earth Planet. Inter. 25, 297-356 (1981).
[2] J. Badro et al., Earth Planet. Sci. Lett. 254, 233-238 (2007).
[3] G. Fiquet et al., Phys. Earth Planet. Inter. 172, 125-129 (2009).
[4] F. Birch, Geophys. J. R. Astron. Soc. 4, 295-311 (1961).
[5] J. M. Brown and R. G. McQueen, J. Geophys. Res. 91, 7485-7494 (1986).
[6] J. H. Nguyen and N. C. Holmes, Nature 427, 339-342 (2004).
[7] J. W. Shaner et al., Shock Waves in Condensed Matter, 135-138 (1988).
[8] H. Huang et al., J. Geophys. Res. 116, B04201 (2010).
[9] H. Huang et al., Nature 479, 513-516 (2011).
[10] Y. Zhang et al., Sci. Rep. 6, 22473 (2016).
[11] H. Huang et al., J. Geophys. Res. 123, 4730 (2018).
[12] K. Shigemori et al., Eur. Phys. J. D 44, 301-305 (2007).
[13] K. Shigemori et al., Rev. Sci. Instrum. 83, 10E529 (2012).
[14] T. Sakaiya et al., Earth Planet. Sci. Lett. 392, 80-85 (2014).
[15] C. Yamanaka et al., Nucl. Fusion 27, 19-30 (1987).

Keywords: sound velocity, shock compression, iron alloy, Earth's core, Birch's law

©2019. Japan Geoscience Union. All Right Reserved.

Geochemical estimates of Earth's core heat content at the end of accretion

*Vincent Clesi[1], Renaud Deguen[1]

1. Laboratoire de Geologie de Lyon - Terre, Planètes, Environnement, Université Claude Bernard Lyon 1, CNRS, ENS-Lyon, 69622 Villeurbanne, France.

The composition of Earth's mantle, when compared to experimentally determined partitioning coefficients, can be used to constrain the conditions of equilibration - pressure *P*, temperature *T*, and oxygen fugacity fO_2 - of the metal and silicates during core-mantle differentiation.
This places constraints on the thermal state of the planet during its accretion, and it is tempting to try to use these data to estimate the heat content of the core at the end of accretion.
To do so, we develop an analytical model of the thermal evolution of the metal phase during its descent through the solid mantle toward the growing core, taking into account compression heating, viscous dissipation heating, and heat exchange with the surrounding silicates. For each impact, the model takes as initial condition the pressure and temperature at the base of the magma ocean, and gives the temperature of the metal when it reaches the core. The growth of the planet results in additional pressure increase and compression heating of the core.
The thermal model is coupled to a Monte-Carlo inversion of the metal/silicates equilibration conditions (P, T, fO_2) in the course of accretion from the abundance of Ni, Co, V and Cr in the mantle, and provides an estimate of the core heat content at the end of accretion for each geochemically successful accretion.
The core heat content depends on the mean degree of metal-silicates equilibration, on the mode of metal/silicates separation in the mantle (diapirism, percolation, or dyking), but also very significantly on the shape of the equilibration conditions curve (equilibration *P* and *T* vs. fraction of Earth accreted).
We find that many accretion histories which are successful in reproducing the mantle composition yield a core that is colder than its current state.
Imposing that the temperature of the core at the end of accretion is higher than its current values therefore provides strong constraints on the accretion history.
In particular, we find that the core heat content depends significantly on the last stages of accretion

Keywords: Core formation, Model

©2019. Japan Geoscience Union. All Right Reserved.

The effect of temperature on density of solid metals

*Asaka Kamiya[1], Hidenori Terasaki[1], Tadashi Kondo[1]

1. Osaka University

It is reported that sound velocities of several solid metals show drastic non-linear reduction at near the melting temperature. This is called premelting effect. Nadal and Le Poac (2013) reported that the sound velocity (P-wave and S-wave velocities) of solid tin (Sn) decreased drastically just before melting (T/T_m ~0.99) at ambient pressure. They suggested that this decrease is due to reduction of elastic moduli (bulk and shear moduli). To understand the premelting effect more accurately, density data of tin near the melting temperature is also required in addition to sound velocity data. However, the precise density behavior of tin around the melting temperature is still missing. In this study, we measured the density of solid metals (tin and nickel) at ambient pressure and studied the effect of temperature on the density near melting temperature. The densities of solid metals were measured from optical image of the sample in the high-temperature furnace up to 673 K for Sn and 1873 K for fcc-Ni. The densities in this study were measured with error of 0.07 % for Sn and 0.4 % for Ni. Density of Sn decreases linearly with increasing temperature up to 490 K and reduced drastically above 490 K (at T/T_m~0.97). This drastic decrease in density of Sn is likely to relate to the premelting effect suggested from sound velocity measurement. In contrast, density of Ni decreases almost linearly with increasing temperature up to melting point and no drastic density change was observed in solid state.

Keywords: premelting effect, Tin, Ni, density, high temperature, electric furnace

©2019. Japan Geoscience Union. All Right Reserved.

Phase relations in the Fe-Ni-Si system at high pressures and high temperatures

*Daijo Ikuta[1], Eiji Ohtani[1], Saori Kawaguchi[2], Naohisa Hirao[2], Yasuo Ohishi[2]

1. Department of Earth Science, Tohoku University, 2. JASRI

The Earth's core has supposed to be constituted by iron-nickel alloys with some light elements. Silicon is one of the most convincing candidates among the light elements. Therefore, the study of high pressure and high temperature properties and behaviors for the Fi-Ni-Si system is important in understanding and constraining to the properties of the Earth's core. In this study, high pressure and high temperature properties for three different contents of Fe-Ni-Si alloys were investigated by using laser heated diamond anvil cells and in situ X-ray diffraction with synchrotron radiation. We determined the phase relations of $Fe_{(0.94-x)}Ni_{0.06}Si_x$ (x = 0.10, 0.17, 0.26) up to 166 GPa and 2800 K, respectively. According to previous Fe-Si system studies, $Fe_{0.83}Si_{0.17}$ alloys transform from hcp to hcp+B2 and fcc+hcp+B2 phases with increasing temperature in isobaric conditions. We observed the change in temperature increase and positive slope of these boundaries due to the nickel containing effect and the difference in silicon content. We report the details of phase relations in the Fe-Ni-Si system and discuss with the differences from the Fe-Si system.

Keywords: Fe-Ni-Si system, phase relation, high pressure

©2019. Japan Geoscience Union. All Right Reserved.

[E] Poster | S (Solid Earth Sciences)：S-IT Science of the Earth's Interior & Techtonophysics

Thu. May 30, 2019 5:15 PM - 6:30 PM JST | Thu. May 30, 2019 8:15 AM - 9:30 AM UTC | Poster Hall International Exhibition Hall8, Makuhari Messe_21

[S-IT25] Planetary cores: Structure, formation, and evolution

convener:Hidenori Terasaki(Graduate School of Science, Osaka University), Eiji Ohtani(Department of Earth and Planetary Materials Science, Graduate School of Science, Tohoku University), William F McDonough(University of Maryland College Park), George Helffrich(Earth-Life Science Institute, Tokyo Institute of Technology)

There are fundamental links between the formation and evolution of planets and their satellites to that of their cores. Defining the physical and chemical properties of the cores of these terrestrial bodies are fundamental for understanding their internal structures and thermal profile. Recent advances in experimental and theoretical studies provide new insights and applications to the Earth's cores and other terrestrial bodies. Near-future exploration missions will obtain data on the internal structure of terrestrial planets (e.g., Mars and Mercury) and planet-satellite systems. We anticipate presentations on recent advances on the physical and chemical properties of cores and discussions regarding the latest views of their formation and evolution. We welcome contributions from mineral/rock physics, geophysics, geochemistry, geodynamics, and planetary science.

[SIT25-P01] Stratification of the Earth’s core by SiO_2 crystallisation

*George Helffrich[1], Satoshi Kaneshima[2], Kei Hirose[1,3] (1.Earth-Life Science Institute, Tokyo Institute of Technology, 2.Earth and Planetary Sciences, Kyushu University, 3.Earth and Planetary Sciences Department, University of Tokyo)

[SIT25-P02] Relation between sound velocity and density for liquid iron alloys under Earth’s core pressures by laser-shock compression

*Tatsuhiro Sakaiya[1], Tadashi Kondo[1], Hidenori Terasaki[1], Keisuke Shigemori[2], Yoichiro Hironaka[2] (1.Graduate School of Science, Osaka University, 2.Institute of Laser Engineering, Osaka University)

[SIT25-P03] Geochemical estimates of Earth's core heat content at the end of accretion

*Vincent Clesi[1], Renaud Deguen[1] (1.Laboratoire de Geologie de Lyon - Terre, Planètes, Environnement, Université Claude Bernard Lyon 1, CNRS, ENS-Lyon, 69622 Villeurbanne, France.)

[SIT25-P04] The effect of temperature on density of solid metals

*Asaka Kamiya[1], Hidenori Terasaki[1], Tadashi Kondo[1] (1.Osaka University)

[SIT25-P05] Phase relations in the Fe-Ni-Si system at high pressures and high temperatures

*Daijo Ikuta[1], Eiji Ohtani[1], Saori Kawaguchi[2], Naohisa Hirao[2], Yasuo Ohishi[2] (1.Department of Earth Science, Tohoku University, 2.JASRI)

Stratification of the Earth's core by SiO_2 crystallisation

*George Helffrich[1], Satoshi Kaneshima[2], Kei Hirose[1,3]

1. Earth-Life Science Institute, Tokyo Institute of Technology, 2. Earth and Planetary Sciences, Kyushu University, 3. Earth and Planetary Sciences Department, University of Tokyo

Based on various studies reporting seismic wavespeed deviations from PREM in the outermost outer core, the core appears to be stratified. Compositional layering, where liquids of different densities overlie one another is one stratification possibility. This mechanism, however, inhibits vertical flows in the liquid near the surface of the core implied by models of secular variation of the Earth's magnetic field. To avoid this limitation, we propose a mechanism by which the layering arises in an analogous way to atmospheric cloud formation. If liquid metal containing dissolved Si+O reaches a saturation level in the outermost outer core, SiO_2 will crystallize and rise to the core-mantle boundary (CMB), causing density changes in the liquid by release of latent heat and changing composition. We present an physical model for this process and show that it explains the observed outer core wavespeed variations better than previous parameterizations. For a CMB temperature of 3800 K and a core light element content of 5 wt% Si+O, SiO_2 begins crystallizing 260 km below the CMB through an interval about 160 km thick, yet core liquid can flow freely through the crystallization interval, facilitating magnetic field changes on decadal to century time scales.

©2019. Japan Geoscience Union. All Right Reserved.

Relation between sound velocity and density for liquid iron alloys under Earth's core pressures by laser-shock compression

*Tatsuhiro Sakaiya[1], Tadashi Kondo[1], Hidenori Terasaki[1], Keisuke Shigemori[2], Yoichiro Hironaka[2]

1. Graduate School of Science, Osaka University, 2. Institute of Laser Engineering, Osaka University

Sound velocity at Earth's core conditions are one of the most important physical properties in Earth science because it can be directly compared with the seismological Earth model (PREM: Preliminary Reference Earth Model) [1]. The composition of solid inner core is estimated from the comparison of the model [1] and the extrapolation of sound velocities as a function of density of iron and iron alloys obtained by the static compression experiment [2, 3]. Birch's law, a linear sound velocity–density relation [4], is used to extrapolate sound velocities to densities in the core condition. On the other hand, the composition of liquid outer core is estimated from the partitioning and solubility data in the inner core boundary condition for the composition of solid core. There has been some works for the sound velocity of iron and iron alloys on the Earth's core condition by dynamic techniques using explosive [5], gas gun [5-11], and laser [12-14]. In this study, we measure the sound velocity and density of liquid iron alloys by shock-compression method using high-power laser.
We conducted shock-compression experiments using a High Intensity Plasma Experimental Research (HIPER) system at the GEKKO-XII laser irradiation facility [15] at the Institute of Laser Engineering, Osaka University. The samples were Fe-Ni alloys, pure nickel, Fe-Si alloys, pure silicon, and pyrrhotite. The sound velocities and densities of shock-compressed iron alloys using the high-power laser were measured by x-ray radiography [12-14] at pressures up to 1000 GPa.
Part of this work was performed under the joint research project of the Institute of Laser Engineering, Osaka University and supported by JSPS KAKENHI Grant Number JP16K05541.

References
[1] A. M. Dziewonski and D. L. Anderson, Phys. Earth Planet. Inter. 25, 297-356 (1981).
[2] J. Badro et al., Earth Planet. Sci. Lett. 254, 233-238 (2007).
[3] G. Fiquet et al., Phys. Earth Planet. Inter. 172, 125-129 (2009).
[4] F. Birch, Geophys. J. R. Astron. Soc. 4, 295-311 (1961).
[5] J. M. Brown and R. G. McQueen, J. Geophys. Res. 91, 7485-7494 (1986).
[6] J. H. Nguyen and N. C. Holmes, Nature 427, 339-342 (2004).
[7] J. W. Shaner et al., Shock Waves in Condensed Matter, 135-138 (1988).
[8] H. Huang et al., J. Geophys. Res. 116, B04201 (2010).
[9] H. Huang et al., Nature 479, 513-516 (2011).
[10] Y. Zhang et al., Sci. Rep. 6, 22473 (2016).
[11] H. Huang et al., J. Geophys. Res. 123, 4730 (2018).
[12] K. Shigemori et al., Eur. Phys. J. D 44, 301-305 (2007).
[13] K. Shigemori et al., Rev. Sci. Instrum. 83, 10E529 (2012).
[14] T. Sakaiya et al., Earth Planet. Sci. Lett. 392, 80-85 (2014).
[15] C. Yamanaka et al., Nucl. Fusion 27, 19-30 (1987).

Keywords: sound velocity, shock compression, iron alloy, Earth's core, Birch's law

©2019. Japan Geoscience Union. All Right Reserved.

Geochemical estimates of Earth's core heat content at the end of accretion

*Vincent Clesi[1], Renaud Deguen[1]

1. Laboratoire de Geologie de Lyon - Terre, Planètes, Environnement, Université Claude Bernard Lyon 1, CNRS, ENS-Lyon, 69622 Villeurbanne, France.

The composition of Earth's mantle, when compared to experimentally determined partitioning coefficients, can be used to constrain the conditions of equilibration - pressure *P*, temperature *T*, and oxygen fugacity fO_2 - of the metal and silicates during core-mantle differentiation.
This places constraints on the thermal state of the planet during its accretion, and it is tempting to try to use these data to estimate the heat content of the core at the end of accretion.
To do so, we develop an analytical model of the thermal evolution of the metal phase during its descent through the solid mantle toward the growing core, taking into account compression heating, viscous dissipation heating, and heat exchange with the surrounding silicates. For each impact, the model takes as initial condition the pressure and temperature at the base of the magma ocean, and gives the temperature of the metal when it reaches the core. The growth of the planet results in additional pressure increase and compression heating of the core.
The thermal model is coupled to a Monte-Carlo inversion of the metal/silicates equilibration conditions (P, T, fO_2) in the course of accretion from the abundance of Ni, Co, V and Cr in the mantle, and provides an estimate of the core heat content at the end of accretion for each geochemically successful accretion.
The core heat content depends on the mean degree of metal-silicates equilibration, on the mode of metal/silicates separation in the mantle (diapirism, percolation, or dyking), but also very significantly on the shape of the equilibration conditions curve (equilibration *P* and *T* vs. fraction of Earth accreted).
We find that many accretion histories which are successful in reproducing the mantle composition yield a core that is colder than its current state.
Imposing that the temperature of the core at the end of accretion is higher than its current values therefore provides strong constraints on the accretion history.
In particular, we find that the core heat content depends significantly on the last stages of accretion

Keywords: Core formation, Model

©2019. Japan Geoscience Union. All Right Reserved.

The effect of temperature on density of solid metals

*Asaka Kamiya[1], Hidenori Terasaki[1], Tadashi Kondo[1]

1. Osaka University

It is reported that sound velocities of several solid metals show drastic non-linear reduction at near the melting temperature. This is called premelting effect. Nadal and Le Poac (2013) reported that the sound velocity (P-wave and S-wave velocities) of solid tin (Sn) decreased drastically just before melting (T/T_m ~0.99) at ambient pressure. They suggested that this decrease is due to reduction of elastic moduli (bulk and shear moduli). To understand the premelting effect more accurately, density data of tin near the melting temperature is also required in addition to sound velocity data. However, the precise density behavior of tin around the melting temperature is still missing. In this study, we measured the density of solid metals (tin and nickel) at ambient pressure and studied the effect of temperature on the density near melting temperature. The densities of solid metals were measured from optical image of the sample in the high-temperature furnace up to 673 K for Sn and 1873 K for fcc-Ni. The densities in this study were measured with error of 0.07 % for Sn and 0.4 % for Ni. Density of Sn decreases linearly with increasing temperature up to 490 K and reduced drastically above 490 K (at T/T_m~0.97). This drastic decrease in density of Sn is likely to relate to the premelting effect suggested from sound velocity measurement. In contrast, density of Ni decreases almost linearly with increasing temperature up to melting point and no drastic density change was observed in solid state.

Keywords: premelting effect, Tin, Ni, density, high temperature, electric furnace

©2019. Japan Geoscience Union. All Right Reserved.

Phase relations in the Fe-Ni-Si system at high pressures and high temperatures

*Daijo Ikuta[1], Eiji Ohtani[1], Saori Kawaguchi[2], Naohisa Hirao[2], Yasuo Ohishi[2]

1. Department of Earth Science, Tohoku University, 2. JASRI

The Earth's core has supposed to be constituted by iron-nickel alloys with some light elements. Silicon is one of the most convincing candidates among the light elements. Therefore, the study of high pressure and high temperature properties and behaviors for the Fi-Ni-Si system is important in understanding and constraining to the properties of the Earth's core. In this study, high pressure and high temperature properties for three different contents of Fe-Ni-Si alloys were investigated by using laser heated diamond anvil cells and in situ X-ray diffraction with synchrotron radiation. We determined the phase relations of $Fe_{(0.94-x)}Ni_{0.06}Si_x$ (x = 0.10, 0.17, 0.26) up to 166 GPa and 2800 K, respectively. According to previous Fe-Si system studies, $Fe_{0.83}Si_{0.17}$ alloys transform from hcp to hcp+B2 and fcc+hcp+B2 phases with increasing temperature in isobaric conditions. We observed the change in temperature increase and positive slope of these boundaries due to the nickel containing effect and the difference in silicon content. We report the details of phase relations in the Fe-Ni-Si system and discuss with the differences from the Fe-Si system.

Keywords: Fe-Ni-Si system, phase relation, high pressure

©2019. Japan Geoscience Union. All Right Reserved.

[E] Poster | S (Solid Earth Sciences)：S-VC Volcanology

Thu. May 30, 2019 3:30 PM - 5:00 PM JST | Thu. May 30, 2019 6:30 AM - 8:00 AM UTC | Poster Hall International Exhibition Hall8, Makuhari Messe_12

[S-VC34] Connecting magma dynamics in vent-conduit system with surface expression of volcanic eruption

convener:Takahiro Miwa(National research institute for earth science and disaster prevention), Nobuo Geshi(Geological Survey of Japan, The National Institute of Advanced Industrial Science and Technology)

Magma dynamics within a shallow conduit system control the diversity of behavior of volcanic eruptions. Recent advancements in geophysical, airborne and ground-based observation techniques provide quantitative data about the dynamic behavior of volcanic eruptions. New analytical methods of the macro and microtextures of eruptive products also open new insights on detailed dynamics of magmas within conduit. The aim of this session is the integration of these new techniques to approach the dynamics of magma ascending from a shallow part of conduit to vent. This session seeks submissions that explore magma dynamics controlling the behaviors of volcanic eruption by integrated investigation of 1) degassing, outgassing, crystallization, and fragmentation of ascending magma, 2) emission and recycling of eruptive product, and 3) morphological characterization of the vent-conduit system. We encourage contributions based on textural-petrological analyses of eruptive product, experimental study reproducing magma in the conduit, geophysical observation on surface expression of volcanic eruption, and related numerical modeling.

[SVC34-P01] A new formulation of viscosity-included bubble nucleation rate in ascending magmas and re-estimation of bubble number density (2)

*Mizuki Nishiwaki[1], Atsushi Toramaru[2] (1.Department of Earth and Planetary Sciences, Graduate School of Sciences, Kyushu University, 2.Department of Earth and Planetary Sciences, Faculty of Sciences, Kyushu University)

[SVC34-P02] Kinetic delay of crystal growth controls plagioclase-basaltic melt apparent disequilibrium

*Ryoya Oida[1], Hidemi Ishibashi[1], ATSUSHI YASUDA[2], Natsumi Hokanishi[2] (1.Faculty of Science, Shizuoka University, 2.Earthquake Research Institute, University of Tokyo)

[SVC34-P03] **Eruptive trends and dynamics of remote volcanoes detected form space-based thermal data and SO_2 emissions: a comparative analysis of Stromboli, Batu Tara and Tinakula volcanoes**

*Corrado CIGOLINI[1], Marco Laiolo[1], Francesco Massimetti[1,2], Maurizio Ripepe[2], Diego Coppola[1] (1.Department of Earth Sciences, University of Torino, Italy, 2.Department of Earth Sciences, University of Firenze, Italy)

[SVC34-P04] The source depth of Strombolian explosions: a multiparametric approach and comparison

*Jacopo Taddeucci[1], Miguel Angel Alatorre-Ibarguengoitia[2], Valeria Cigala[3], Elisabetta Del Bello[1], Damien Gaudin[4], Ulrich Kueppers[4], Tullio Ricci[1], Valentino Salvatore[5], Piergiorgio Scarlato[1] (1.Istituto Nazionale di Geofisica e Vulcanologia, Rome, Italy, 2.Centro de Investigación en Gestión de Riesgo y Cambio Climático, Universidad de Ciencias y Artes de Chiapas, Tuxtla Gutiérrez, Mexico, 3.Department of Geosciences, Università degli Studi di Padova, Padua, Italy, 4.Department of Earth and Environmental Sciences. Ludwig-Maximilians-Universität (LMU). Munich, Germany, 5.Dipartimento di Scienze della Terra, Sapienza Università di Roma, Rome, Italy)

[SVC34-P05] Magmatic aggregate of basaltic ash particles

*Takahiro Miwa[1], Nobuo Geshi[2] (1.National research institute for earth science and disaster prevention, 2.National Institute of Advanced Industrial Science and Technology)

[SVC34-P06] Melt inclusion study on the eruption process of Izu-Omuroyama monogenetic volcano, Japan

Risako Hatada[1], *Hidemi Ishibashi[1], Yusuke Suzuki[2], ATSUSHI YASUDA[3], Natsumi Hokanishi[3] (1.Faculty of Science, Shizuoka University, 2.Izu Peninsula Geopark, 3.Earthquake Research Institute, University of Tokyo)

[SVC34-P07] Time-series variation in the textures of ejecta of the An'ei eruption, Izu-Oshima

*Yuya Ikenaga[1], Fukashi Maeno[1], ATSUSHI YASUDA[1] (1.Earthquake Research Institute, The University of Tokyo)

[SVC34-P08] The textural analysis of pumice from the Plinian eruption of Taupo volcano: implications for tube pumice

*Masatoshi Ohashi[1], Mie Ichihara[2], Fukashi Maeno[2], Ben Kennedy[3], Darren Gravley[3] (1.Department of Earth and Planetary Science, Graduate School of Science, The University of Tokyo, 2.Earthquake Research Institute, The University of Tokyo, 3.Department of Geological Sciences, The University of Canterbury)

A new formulation of viscosity-included bubble nucleation rate in ascending magmas and re-estimation of bubble number density (2)

*Mizuki Nishiwaki[1], Atsushi Toramaru[2]

1. Department of Earth and Planetary Sciences, Graduate School of Sciences, Kyushu University, 2. Department of Earth and Planetary Sciences, Faculty of Sciences, Kyushu University

To evaluate the effect of melt viscosity on bubble nucleation, we newly formulate homogeneous nucleation rate of water bubbles to explicitly include melt viscosity. The viscosity appears in the pre-exponential factor of the nucleation rate in terms of the Péclet number: the ratio of bubble growth timescale by molecular diffusion and viscous relaxation timescale. The pre-exponential factor linearly decreases with increasing viscosity (or decreasing Péclet number) under a given supersaturation. We numerically solve the evolution of bubble nucleation and growth processes in ascending magmas by using the new formula of nucleation rate and a precise approximation of moment equations of bubble size distribution function. In high viscosity or high decompression rate region, the effect of melt viscosity reduces bubble number density by several orders of magnitude compared with the previous study. Because of the lack of experimental data in this high-viscous regime, the reality of this regime will be verified by future experiments.

Keywords: bubble nucleation, bubble growth, BND (Bubble Number Density), BSD (Bubble Size Distribution), Péclet number

©2019. Japan Geoscience Union. All Right Reserved.

Kinetic delay of crystal growth controls plagioclase-basaltic melt apparent disequilibrium

*Ryoya Oida[1], Hidemi Ishibashi[1], ATSUSHI YASUDA[2], Natsumi Hokanishi[2]

1. Faculty of Science, Shizuoka University, 2. Earthquake Research Institute, University of Tokyo

Plagioclase-melt compositional relations sensitively depend on temperature, T, and water content, X_W, of melt. Therefore, the relations are formulated as functions of T and X_W and used as geothermohygrometer (e.g., Putirka, 2008). Plagioclase-melt equilibrium is postulated for applying the thermohygrometer models. However, validity of the assumption is unobvious for microlite crystallization driven by degassing and/or cooling during eruption. Can we apply the thermohygrometers to the plagioclase-melt pairs formed by dynamic crystallization? To examine the issue, the cooling crystallization experiments of the high-Al basaltic melt were carried out and textural and chemical analyses were performed the run samples.

We used the high-Al basalt lava from Waianae, Hawaii Oahu as the starting material for the cooling crystallization experiments. This experiment was conducted using the 1atm fO_2-controlled furnace at University of Hawaii at Manoa. After 3 hours pre-heating at 1180℃, ~30K higher than the liquidus, the samples were cooled at cooling rates, R_c, of 0.1, 0.3, 1, 3, and 10K/min, and then quenched in water at four target temperatures, T_q, of 1150, 1120, 1090, and 1060℃. We used FE-EPMA (JEOL-JXA-8530FPlus) and EPMA (JEOL8800R) at Earthquake Research Institute, University of Tokyo, for textural and chemical analyses of the run samples.

As R_c and/or T_q increase, the abundance and size of plagioclase crystals decrease. As R_c increases, the shape of plagioclase changes from euhedral to dendritic. The R_c-dependent shape change is more obvious at lower T_q. Pyroxene crystallization was suppressed in the run samples coolied at higher R_c. In addition, melt boundary layers are observed around pyroxene in the samples cooled at 0.3-1K/min, quenched at 1090℃ and cooled at 0.3-3K/min, quenched at 1060℃, and around plagioclase in the samples cooled at >3K/min, quenched at <1120℃. Lower diffusivity of Al_2O_3 compared to those of FeO and MgO is responsible for lower threshold cooling rate of melt boundary layer formation around pyroxene.

The maximum An# [=100Ca/(Ca + Na)] of plagioclase was almost the same among all run samples. We applied both plagioclase liquidus and plagioclase-melt An-partitioning thermometers of Putirka (2008) to the pairs of plagioclase rim-boundary layer melt (BLM) and plagioclase rim-far field melt (FFM) to estimate temperatures recorded in their phase compositions. At T_q=1150℃, the estimated temperatures well represent T_q for both BLM and FFM. However, at lower T_q, both of the thermometers estimate temperatures higher than T_q; difference between estimated temperature and T_q, ΔT, increases as decreasing T_q. The two thermometers estimate similar temperatures for each sample, and the differences between the two estimated temperatures do not depend on R_c. These results suggest that the plagioclase-melt partition coefficient of An component does not depend on the R_c. Therefore, the increase of ΔT at lower T_q is not due to the R_c-dependence of the partition coefficient. It is attributed to the kinetic delay of the crystal growth at lower temperature. On the other hand, the coincidence between calculated temperatures and T_q at 1150℃ suggests that kinetic delay of plagioclase crystal growth is small at near liquidus temperature.

©2019. Japan Geoscience Union. All Right Reserved.

Present results show that plagioclase-melt thermometers can be applied regardless of the R_c at higher temperatures, while magmatic temperature tends to be overestimated due to kinetic delay of crystal growth at lower temperature.

Keywords: plagioclase, crystallization, kinetics, basalt, geothermometry

©2019. Japan Geoscience Union. All Right Reserved.

Eruptive trends and dynamics of remote volcanoes detected form space-based thermal data and SO_2 emissions: a comparative analysis of Stromboli, Batu Tara and Tinakula volcanoes

*Corrado CIGOLINI[1], Marco Laiolo[1], Francesco Massimetti[1,2], Maurizio Ripepe[2], Diego Coppola[1]

1. Department of Earth Sciences, University of Torino, Italy, 2. Department of Earth Sciences, University of Firenze, Italy

South-Eastern Pacific has a large number of unmonitored volcanoes that may potentially produce large-scale eruptive events capable to affect highly-populated areas. Therefore, forecasting changes in volcanic activity in the light of historical time-series is a rather intriguing challenge for the space-based earth observations.
Batu Tara (Indonesia) and Tinakula (Solomon Island) are two poorly known volcanic islands with morphologies and reported short-term activities rather similar to the ones observed at Stromboli volcano (Italy). However, thanks to over a decade-long satellite data we are able to effectively compare the activity occurring at Stromboli (a unique natural laboratory and “open-vent” system) with those taking place at the above volcanoes.
We process and analyse the radiant flux (thermal activity) coupled with SO_2 emissions (degassing activity) at these three volcanoes for over a decade. The combined analysis of Volcanic Radiant Power (from MODIS data) and SO_2 burden (from OMI data) reveals different long-term eruptive trends, and contrasting ratio of gas vs. thermal emissions. In fact, the persistent open-vent explosive activity of Stromboli volcano is interrupted by flank effusions that periodically drain the degassed magma stored at shallow levels. On the other hand, the long-lasting exponential decay of both thermal and gas emissions observed at Batu Tara is consistent with the eruption of an “undegassed magma” from a deep, and likely a “closed” magma chamber. Finally, Tinakula volcano exhibits multiple year-long eruptive phases, characterised by evolving gas vs. thermal ratio correlated with an increasing eruptive intensity: thus suggesting the involvement of a volatile-zoned magma chamber with periodic phases of gas/magma accumulations.
Our results suggest that the combined analysis of satellite thermal/gas data is a useful tool for better understanding long-term volcanic dynamics and interpreting volcanic processes occurring at a shorter time-scale. We also stress that large satellite datasets on active volcanoes, available from different platforms, greatly enhance the opportunity to efficiently monitor remote volcanic targets in the attempt to mitigate volcanic risk.

Keywords: Remote volcanoes, satellite datasets, Volcanic Radiative Power, SO2 emissions, volcanic risk

©2019. Japan Geoscience Union. All Right Reserved.

The source depth of Strombolian explosions: a multiparametric approach and comparison

*Jacopo Taddeucci[1], Miguel Angel Alatorre-Ibarguengoitia[2], Valeria Cigala[3], Elisabetta Del Bello[1], Damien Gaudin[4], Ulrich Kueppers[4], Tullio Ricci[1], Valentino Salvatore[5], Piergiorgio Scarlato[1]

1. Istituto Nazionale di Geofisica e Vulcanologia, Rome, Italy, 2. Centro de Investigación en Gestión de Riesgo y Cambio Climático, Universidad de Ciencias y Artes de Chiapas, Tuxtla Gutiérrez, Mexico, 3. Department of Geosciences, Università degli Studi di Padova, Padua, Italy, 4. Department of Earth and Environmental Sciences. Ludwig-Maximilians-Universität (LMU). Munich, Germany, 5. Dipartimento di Scienze della Terra, Sapienza Università di Roma, Rome, Italy

The source depth of an individual explosion during Strombolian-style explosive volcanic activity can be defined as the depth of the region within the volcanic conduit where magma fragmentation occurs and the acceleration of pyroclasts by the expanding gas continuum begins. Source depth is thought to exert a first-order control on the final ejection dynamics of the pyroclasts and the ensuing eruptive styles and hazards. As such, different methods to estimate source depth have been developed in the past.

Here, we used three independent methods to estimate the source depth of some Strombolian explosions from Stromboli and Etna volcanoes (Italy). The first method uses the back-tracking of the trajectories of pyroclasts leaving the vent to infer their minimum release depth. It is a purely geometric method relying on the assumption that pyroclasts follow linear trajectories after fragmentation. The second method uses the time delay between the appearance of pyroclasts at the vent and the arrival of acoustic waves at a recording station at a known distance from the vent. This method relies on several assumptions, including (i) the sound velocity inside the conduit, (ii) the co-location of source depth of pyroclasts and acoustic waves, and (iii) a constant velocity of pyroclasts in the conduit, following the initial acceleration. The third method uses the velocity of pyroclasts progressively exiting the vent. This velocity decays following a non-linear trend which is function of the source depth, as illustrated by previous experimental and theoretical studies. As for the second method, also this last one assumes a constant velocity of pyroclasts rising in the conduit.

For the Etna case, the three methods provide consistent results and a shallow (<20 m) source depth of the explosions. For the Stromboli case, the first and third methods provide shallow (around 6 and 15 m, respectively) source depths while the second method provides depths of around 60 m. The incompatibility of such large depths with the first two methods, and given the relative assumptions, we believe that in the Stromboli case the co-location of the particles and acoustic source is probably the least strong assumption. These results suggest that caution should be used in assessing source depth from a single methodology, and that more investigations are required on the source of acoustic signals from the explosions and on the motion (specifically the acceleration and deceleration) of pyroclasts ascending along the conduit.

Keywords: strombolian, explosion, depth

©2019. Japan Geoscience Union. All Right Reserved.

Magmatic aggregate of basaltic ash particles

*Takahiro Miwa[1], Nobuo Geshi[2]

1. National research institute for earth science and disaster prevention, 2. National Institute of Advanced Industrial Science and Technology

Dynamics of volcanic cloud and jet at the vent is largely controled by a grain size of pyroclast. The grain size is considered to be determined by primary fragmentation of magma, and subsequent breakup of pyroclasts due to therir collsions in upper conduit (Dufek et al. 2012). However, whether the breakup occurs or not depend on viscoelastic responce of magma (Dingwell and Webb, 1989).
In this study, we report aggregate of ash particles which is formed in magmatic temperature. We observed basaltic ash samples from Stromboli volcano, Italy, and Aso volcano, Japan. The “magmatic aggretate” shows texture that numerous small guest particles (< 200 μm) adhere or stick on a host particle (> 1 mm). All the host particles are catergorized to sideromelane having fluidal morphology. The guest particles are on fluidal surface of the host particle, and show fluidal and dense morphology. These characteristics found in the magmatic aggregate can be explaned by collision and aggretation of ash particles in high temperature condition. Here we model formation of the magmatic aggregates as passing of two frying particles bearing viscoelastic nature, by using viscosity of magma estimated (10^4-10^5 Pa s). When the relative velocity of the two particles falls the critical value, the two particles behave as viscous material, coalsece each other, and then form the magmatic aggregate. The result of calculation demonstrates that the critical relative velocity is approximately 10^{-2} m/s, and implies the magmatic aggregation is difficult to occur for silisic magma with highly viscosity. Thus we conclude that the collision can increase average grain size of pyroclast in basaltic system.

Keywords: Eruptive dynamics, Interaction of ash particles, Viscoelastic response of magma

©2019. Japan Geoscience Union. All Right Reserved.

Melt inclusion study on the eruption process of Izu-Omuroyama monogenetic volcano, Japan

Risako Hatada[1], *Hidemi Ishibashi[1], Yusuke Suzuki[2], ATSUSHI YASUDA[3], Natsumi Hokanishi[3]

1. Faculty of Science, Shizuoka University, 2. Izu Peninsula Geopark, 3. Earthquake Research Institute, University of Tokyo

Izu-Omuroyama is one of monogenetic volcanoes in Izu-Tobu volcanic field, which is the largest pyroclastic cone formed by ~4ka eruption with ~450 million tons of tephra and lava (Koyano et al., 1996). Because a monogenetic volcano such as Omuroyama is built by the first eruption of a newly-formed magma plumbing system, phenocrysts and melt inclusions (MIs) in its volcanic products may record information about the initial process of formation of the magma plumbing system. In this study, textural and chemical analyses were performed for phenocrysts and MIs in Strombolian scoria of the Omuroyama eruption to clarify the eruption process of the monogenetic volcano.

According to Koyano et al. (1996), Omuroyama eruption started from sub-plinian phase (stage-A), followed by weak ash-eruption phase (stage-B), and then shifted to the main phase of Strombolian eruption (stage-C). Omuroyama pyroclastic cone was built during the stage-C. In this study, we performed textural and chemical analyses for phenocrysts and MIs in the fall scoria erupted during the stage-C, by using FE-EPMA and EPMA at ERI, Univ. Tokyo, Japan.

The scoria contain ~3.3 vol.% of olivine and ~5.4 vol.% of plagioclase as phenocrysts, and their groundmass include olivine and plagioclase microphenocsyts (MPs) of several tens-100 microns sizes embedded in almost glassy or microlite-rich matrix. Olivine phenocrysts are homogeneous (Fo~74-83 with concentration at 83-84) in each grain except for normal zoned rim. Olivine MPs has compositions similar to Fo-poor phenocrysts. Most of plagioclase phenocrysts show reverse zoning with cores of An~30-60 and rims of An~84 and dusty zones are often found. Plagioclase MPs have compositions identical to those of phenocryst rims. Olivine- and plagioclase-hosted MIs have SiO_2 contents of ~52-60 wt.% and 57-78 wt.%, respectively. Compositions of both olivine- and plagioclase-hosted MIs with SiO_2~57-60 wt.% are identical with glass in microlite-poor groundmass, indicating that the melt was saturated with olivine and plagioclase. Based on the olivine-plagioclase-melt compositional relation, temperature and H_2O content conditions of the melt is estimated to be ~1080ºC and ~2 wt.% (H2O-saturated depth of ~2km), respectively. Majority of MIs in plagioclase phenocrysts are rhyolitic with SiO2~70-74wt.%. FeO content of host plagioclase crystals are consistent with those in equilibrium with the MIs. H_2O contents of the MIs are estimated by melt-plagioclase hygrometer to be ~6.2-9.2 wt.% (H_2O-saturated depth of ~8-14km), under assumption of temperature of 800-850 ºC. In addition, olivine-hosted MIs with $SiO_2 < 57$ wt.% are enriched in SO_3 (~0.3-0.5 wt.%), indicating their origin deeper than those of more evolved MIs ($SO_3 < 0.1$ wt.%).

Present results suggest that (1) deep-derived, olivine-bearing mafc melt ascent, captured plagioclase phenocrysts and rhyolitic melt and mixed with them at 11km depth, and crystallized MPs at 2km depth before the eruption, and (2) rhyolitic melt existed at ~11km depth beneath the volcanic field at ca. 800 years before the first eruption of rhyolitic magma at Kawagodaira volcano.

Keywords: melt inclusion, monogenetic volcano, rhyolite, Izu-Omuroyama, plagioclase

©2019. Japan Geoscience Union. All Right Reserved.

©2019. Japan Geoscience Union. All Right Reserved.

Time-series variation in the textures of ejecta of the An'ei eruption, Izu-Oshima

*Yuya Ikenaga[1], Fukashi Maeno[1], ATSUSHI YASUDA[1]

1. Earthquake Research Institute, The University of Tokyo

In Izu-Oshima, a large-scale eruption called the An’ ei eruption began in 1777. This eruption lasted for 15 years, and scoria and lava flows were strongly ejected before ash eruption period (Nakamura, 1964; Isshiki, 1984; Koyama and Hayakawa, 1996, Tsukui et al, 2009). As for scoria eruption, the transition of the intensity of eruption was unveiled (Ikenaga et al., 2018). Scoria eruption in the initial stage (Unit A) was somewhat weak and scoria is poor in plagioclase phenocrysts (Pl). After the small-scale scoria eruption (Unit B, rich in Pl), the climax stage (Unit C) occurred. Scoria in Unit C is richest in Pl and eruption column height of this unit is inferred to be approximately 10km. The change in the textures of scoriae among these 3 units, however, has not been investigated yet. It becomes clear in this study that there are differences in the textures of scoriae.

The scoria of Unit A (A-scoria) is rich in microlites and the groundmass glass has low transparency. The surface of bubbles is rough and many bubbles are connected each other. On the other hand, the scoria of Unit C (C-scoria) has almost no microlites and the glass is transparent. The shape of bubbles is spherical or ellipsoid, and the surface of bubbles is smooth. The connectivity of bubbles is low. The characteristics of the scoria of Unit B (B-scoria) are intermediate between those of A- and C-scoria. Considering the transition in the intensity of eruption, magma ascent rate of Unit A is expected to have been low than that of Unit C, and the crystallization of microlites and connection of bubbles in Unit A were probably caused because of low decompression rate.

The compositions of Pl, groundmass glass and melt inclusions in Pl of scoriae were measured using EPMA, and there are no difference in these compositions among 3 units. It is inferred from this result that the change in the intensity of 3 units was not caused by injection of undifferentiated magma into magma chamber, but caused by other processes, such as decompression of magma chamber after the eruption of Unit A. It is a future issue to reveal the cause of the change in intensity.

Keywords: Izu-Oshima, Transition in texture, Composition of eruption products

©2019. Japan Geoscience Union. All Right Reserved.

The textural analysis of pumice from the Plinian eruption of Taupo volcano: implications for tube pumice

*Masatoshi Ohashi[1], Mie Ichihara[2], Fukashi Maeno[2], Ben Kennedy[3], Darren Gravley[3]

1. Department of Earth and Planetary Science, Graduate School of Science, The University of Tokyo, 2. Earthquake Research Institute, The University of Tokyo, 3. Department of Geological Sciences, The University of Canterbury

Tube pumice is characterized by aligned highly elongated bubbles and is a common product of explosive silicic eruptions. This bubble texture is thought to reflect shear deformations during flow in a conduit (Marti et al., 1999). Therefore, quantitative measurements of tube pumice texture can inform conduit flow models. Recent development in X-ray tomography allows us to measure bubble shapes in 3D pumice accurately (e.g., Dingwell et al., 2016). In addition to the microscopic structures of individual pumices, the abundance of tube and non-tube pumices in the stratigraphy is important in inferring temporal and spatial variations in a conduit flow. This study aims at quantifying micro-structural and stratigraphic features of pumice from the 1.8 ka eruption of Taupo volcano, New Zealand.

The 1.8 ka eruption is the most recent large eruptive event from Taupo volcano. It is characterized by various eruptive styles, including three phreatomagmatic fall deposits (units 1, 3, 4), Hatepe plinian fall deposit (unit 2), Taupo plinian fall deposit (unit 5), and Taupo ignimbrite (unit 6) (Houghton et al., 2010). Since those deposits show chemically uniform pumices and melt inclusions, the great diversity of bubble textures in pumices may reflect purely physical processes in the eruption. We collected samples from the units of the two plinian eruptions (units 2 and 5) and the ignimbrite (unit 6), and measured bubble textures and vesicularities. Among those units, we focused on unit 5 to investigate the transition from plinian fall to ignimbrite. For this purpose, a detailed sampling of unit 5 was conducted at an outcrop about 25 km away from the vent, where the unit consists of a fine lower part (40 cm) and a coarse upper part (180 cm). We sampled clasts from the bottom to top of the unit 5 layer at 20cm interval. The bubble textures of more than 1000 pumice samples were measured by a digital microscope (VHX-1000, Keyence) with variable illumination function. The illumination was optimized to make good luminance contrast between the flat surface and bubbles for image analysis.

The image analysis shows that bubbles in unit 5 are more elongated than those in unit 2 and less elongated than those in unit 6. The average values of bubble elongation in unit 2 and 6 are proportional to those of vesicularity. In contrast, bubble elongation and vesicularity are uniform within unit 5. The component analysis over unit 5 shows that the weight percentage of lithics is also uniform except in the lowest part. The relatively high lithic content in the lowest part suggests vent widened or shifted location at the beginning of the Taupo plinian event.

Previous studies in other volcanoes suggest that bubbles in the pre-ignimbrite phase become more elongated toward the flow stage (Taddeucci and Wohletz 2001, Polacci et al., 2003). The increased amount of tube pumice is thought to reflect a gradual transition from fallout to ignimbrite, and it was interpreted as a result of increased erosive activity near the conduit wall, or a greater conduit area available for shearing (Polacci et al., 2003). In contrast, no such variation of bubble texture is observed in Taupo plinian event (unit 5), which implies that a steady conduit flow was sustained during the pre-ignimbrite fallout eruption. The ignimbrite (unit 6) might not simply be the result of a collapsing plinian eruption column. It is also possible that the topmost part of unit 5 had been eroded by and/or mixed with the pyroclastic flow that deposited the subsequent ignimbrite (unit 6).

©2019. Japan Geoscience Union. All Right Reserved.

Keywords: bubble texture, tube pumice, Taupo

©2019. Japan Geoscience Union. All Right Reserved.

[E] Poster | S (Solid Earth Sciences)：S-VC Volcanology

Thu. May 30, 2019 5:15 PM - 6:30 PM JST | Thu. May 30, 2019 8:15 AM - 9:30 AM UTC | Poster Hall International Exhibition Hall8, Makuhari Messe_23

[S-VC34] Connecting magma dynamics in vent-conduit system with surface expression of volcanic eruption

convener:Takahiro Miwa(National research institute for earth science and disaster prevention), Nobuo Geshi(Geological Survey of Japan, The National Institute of Advanced Industrial Science and Technology)

Magma dynamics within a shallow conduit system control the diversity of behavior of volcanic eruptions. Recent advancements in geophysical, airborne and ground-based observation techniques provide quantitative data about the dynamic behavior of volcanic eruptions. New analytical methods of the macro and microtextures of eruptive products also open new insights on detailed dynamics of magmas within conduit. The aim of this session is the integration of these new techniques to approach the dynamics of magma ascending from a shallow part of conduit to vent. This session seeks submissions that explore magma dynamics controlling the behaviors of volcanic eruption by integrated investigation of 1) degassing, outgassing, crystallization, and fragmentation of ascending magma, 2) emission and recycling of eruptive product, and 3) morphological characterization of the vent-conduit system. We encourage contributions based on textural-petrological analyses of eruptive product, experimental study reproducing magma in the conduit, geophysical observation on surface expression of volcanic eruption, and related numerical modeling.

[SVC34-P01] A new formulation of viscosity-included bubble nucleation rate in ascending magmas and re-estimation of bubble number density (2)

*Mizuki Nishiwaki[1], Atsushi Toramaru[2] (1.Department of Earth and Planetary Sciences, Graduate School of Sciences, Kyushu University, 2.Department of Earth and Planetary Sciences, Faculty of Sciences, Kyushu University)

[SVC34-P02] Kinetic delay of crystal growth controls plagioclase-basaltic melt apparent disequilibrium

*Ryoya Oida[1], Hidemi Ishibashi[1], ATSUSHI YASUDA[2], Natsumi Hokanishi[2] (1.Faculty of Science, Shizuoka University, 2.Earthquake Research Institute, University of Tokyo)

[SVC34-P03] Eruptive trends and dynamics of remote volcanoes detected form space-based thermal data and SO_2 emissions: a comparative analysis of Stromboli, Batu Tara and Tinakula volcanoes

*Corrado CIGOLINI[1], Marco Laiolo[1], Francesco Massimetti[1,2], Maurizio Ripepe[2], Diego Coppola[1] (1.Department of Earth Sciences, University of Torino, Italy, 2.Department of Earth Sciences, University of Firenze, Italy)

[SVC34-P04] The source depth of Strombolian explosions: a multiparametric approach and comparison

*Jacopo Taddeucci[1], Miguel Angel Alatorre-Ibarguengoitia[2], Valeria Cigala[3], Elisabetta Del Bello[1], Damien Gaudin[4], Ulrich Kueppers[4], Tullio Ricci[1], Valentino Salvatore[5], Piergiorgio Scarlato[1] (1.Istituto Nazionale di Geofisica e Vulcanologia, Rome, Italy, 2.Centro de Investigación en Gestión de Riesgo y Cambio Climático, Universidad de Ciencias y Artes de Chiapas, Tuxtla Gutiérrez, Mexico, 3.Department of Geosciences, Università degli Studi di Padova, Padua, Italy, 4.Department of Earth and Environmental Sciences. Ludwig-Maximilians-Universität (LMU). Munich, Germany, 5.Dipartimento di Scienze della Terra, Sapienza Università di Roma, Rome, Italy)

[SVC34-P05] Magmatic aggregate of basaltic ash particles

*Takahiro Miwa[1], Nobuo Geshi[2] (1.National research institute for earth science and disaster prevention, 2.National Institute of Advanced Industrial Science and Technology)

[SVC34-P06] Melt inclusion study on the eruption process of Izu-Omuroyama monogenetic volcano, Japan

Risako Hatada[1], *Hidemi Ishibashi[1], Yusuke Suzuki[2], ATSUSHI YASUDA[3], Natsumi Hokanishi[3] (1.Faculty of Science, Shizuoka University, 2.Izu Peninsula Geopark, 3.Earthquake Research Institute, University of Tokyo)

[SVC34-P07] Time-series variation in the textures of ejecta of the An'ei eruption, Izu-Oshima

*Yuya Ikenaga[1], Fukashi Maeno[1], ATSUSHI YASUDA[1] (1.Earthquake Research Institute, The University of Tokyo)

[SVC34-P08] The textural analysis of pumice from the Plinian eruption of Taupo volcano: implications for tube pumice

*Masatoshi Ohashi[1], Mie Ichihara[2], Fukashi Maeno[2], Ben Kennedy[3], Darren Gravley[3] (1.Department of Earth and Planetary Science, Graduate School of Science, The University of Tokyo, 2.Earthquake Research Institute, The University of Tokyo, 3.Department of Geological Sciences, The University of Canterbury)

A new formulation of viscosity-included bubble nucleation rate in ascending magmas and re-estimation of bubble number density (2)

*Mizuki Nishiwaki[1], Atsushi Toramaru[2]

1. Department of Earth and Planetary Sciences, Graduate School of Sciences, Kyushu University, 2. Department of Earth and Planetary Sciences, Faculty of Sciences, Kyushu University

To evaluate the effect of melt viscosity on bubble nucleation, we newly formulate homogeneous nucleation rate of water bubbles to explicitly include melt viscosity. The viscosity appears in the pre-exponential factor of the nucleation rate in terms of the Péclet number: the ratio of bubble growth timescale by molecular diffusion and viscous relaxation timescale. The pre-exponential factor linearly decreases with increasing viscosity (or decreasing Péclet number) under a given supersaturation. We numerically solve the evolution of bubble nucleation and growth processes in ascending magmas by using the new formula of nucleation rate and a precise approximation of moment equations of bubble size distribution function. In high viscosity or high decompression rate region, the effect of melt viscosity reduces bubble number density by several orders of magnitude compared with the previous study. Because of the lack of experimental data in this high-viscous regime, the reality of this regime will be verified by future experiments.

Keywords: bubble nucleation, bubble growth, BND (Bubble Number Density), BSD (Bubble Size Distribution), Péclet number

©2019. Japan Geoscience Union. All Right Reserved.

Kinetic delay of crystal growth controls plagioclase-basaltic melt apparent disequilibrium

*Ryoya Oida[1], Hidemi Ishibashi[1], ATSUSHI YASUDA[2], Natsumi Hokanishi[2]

1. Faculty of Science, Shizuoka University, 2. Earthquake Research Institute, University of Tokyo

Plagioclase-melt compositional relations sensitively depend on temperature, T, and water content, X_W, of melt. Therefore, the relations are formulated as functions of T and X_W and used as geothermohygrometer (e.g., Putirka, 2008). Plagioclase-melt equilibrium is postulated for applying the thermohygrometer models. However, validity of the assumption is unobvious for microlite crystallization driven by degassing and/or cooling during eruption. Can we apply the thermohygrometers to the plagioclase-melt pairs formed by dynamic crystallization? To examine the issue, the cooling crystallization experiments of the high-Al basaltic melt were carried out and textural and chemical analyses were performed the run samples.

We used the high-Al basalt lava from Waianae, Hawaii Oahu as the starting material for the cooling crystallization experiments. This experiment was conducted using the 1atm fO_2-controlled furnace at University of Hawaii at Manoa. After 3 hours pre-heating at 1180℃, ~30K higher than the liquidus, the samples were cooled at cooling rates, R_c, of 0.1, 0.3, 1, 3, and 10K/min, and then quenched in water at four target temperatures, T_q, of 1150, 1120, 1090, and 1060℃. We used FE-EPMA (JEOL-JXA-8530FPlus) and EPMA (JEOL8800R) at Earthquake Research Institute, University of Tokyo, for textural and chemical analyses of the run samples.

As R_c and/or T_q increase, the abundance and size of plagioclase crystals decrease. As R_c increases, the shape of plagioclase changes from euhedral to dendritic. The R_c-dependent shape change is more obvious at lower T_q. Pyroxene crystallization was suppressed in the run samples coolied at higher R_c. In addition, melt boundary layers are observed around pyroxene in the samples cooled at 0.3-1K/min, quenched at 1090℃ and cooled at 0.3-3K/min, quenched at 1060℃, and around plagioclase in the samples cooled at >3K/min, quenched at <1120℃. Lower diffusivity of Al_2O_3 compared to those of FeO and MgO is responsible for lower threshold cooling rate of melt boundary layer formation around pyroxene.

The maximum An# [=100Ca/(Ca + Na)] of plagioclase was almost the same among all run samples. We applied both plagioclase liquidus and plagioclase-melt An-partitioning thermometers of Putirka (2008) to the pairs of plagioclase rim-boundary layer melt (BLM) and plagioclase rim-far field melt (FFM) to estimate temperatures recorded in their phase compositions. At T_q=1150℃, the estimated temperatures well represent T_q for both BLM and FFM. However, at lower T_q, both of the thermometers estimate temperatures higher than T_q; difference between estimated temperature and T_q, ΔT, increases as decreasing T_q. The two thermometers estimate similar temperatures for each sample, and the differences between the two estimated temperatures do not depend on R_c. These results suggest that the plagioclase-melt partition coefficient of An component does not depend on the R_c. Therefore, the increase of ΔT at lower T_q is not due to the R_c-dependence of the partition coefficient. It is attributed to the kinetic delay of the crystal growth at lower temperature. On the other hand, the coincidence between calculated temperatures and T_q at 1150℃ suggests that kinetic delay of plagioclase crystal growth is small at near liquidus temperature.

©2019. Japan Geoscience Union. All Right Reserved.

Present results show that plagioclase-melt thermometers can be applied regardless of the R_c at higher temperatures, while magmatic temperature tends to be overestimated due to kinetic delay of crystal growth at lower temperature.

Keywords: plagioclase, crystallization, kinetics, basalt, geothermometry

©2019. Japan Geoscience Union. All Right Reserved.

Eruptive trends and dynamics of remote volcanoes detected form space-based thermal data and SO_2 emissions: a comparative analysis of Stromboli, Batu Tara and Tinakula volcanoes

*Corrado CIGOLINI[1], Marco Laiolo[1], Francesco Massimetti[1,2], Maurizio Ripepe[2], Diego Coppola[1]

1. Department of Earth Sciences, University of Torino, Italy, 2. Department of Earth Sciences, University of Firenze, Italy

South-Eastern Pacific has a large number of unmonitored volcanoes that may potentially produce large-scale eruptive events capable to affect highly-populated areas. Therefore, forecasting changes in volcanic activity in the light of historical time-series is a rather intriguing challenge for the space-based earth observations.
Batu Tara (Indonesia) and Tinakula (Solomon Island) are two poorly known volcanic islands with morphologies and reported short-term activities rather similar to the ones observed at Stromboli volcano (Italy). However, thanks to over a decade-long satellite data we are able to effectively compare the activity occurring at Stromboli (a unique natural laboratory and “open-vent” system) with those taking place at the above volcanoes.
We process and analyse the radiant flux (thermal activity) coupled with SO_2 emissions (degassing activity) at these three volcanoes for over a decade. The combined analysis of Volcanic Radiant Power (from MODIS data) and SO_2 burden (from OMI data) reveals different long-term eruptive trends, and contrasting ratio of gas vs. thermal emissions. In fact, the persistent open-vent explosive activity of Stromboli volcano is interrupted by flank effusions that periodically drain the degassed magma stored at shallow levels. On the other hand, the long-lasting exponential decay of both thermal and gas emissions observed at Batu Tara is consistent with the eruption of an “undegassed magma” from a deep, and likely a “closed” magma chamber. Finally, Tinakula volcano exhibits multiple year-long eruptive phases, characterised by evolving gas vs. thermal ratio correlated with an increasing eruptive intensity: thus suggesting the involvement of a volatile-zoned magma chamber with periodic phases of gas/magma accumulations.
Our results suggest that the combined analysis of satellite thermal/gas data is a useful tool for better understanding long-term volcanic dynamics and interpreting volcanic processes occurring at a shorter time-scale. We also stress that large satellite datasets on active volcanoes, available from different platforms, greatly enhance the opportunity to efficiently monitor remote volcanic targets in the attempt to mitigate volcanic risk.

Keywords: Remote volcanoes, satellite datasets, Volcanic Radiative Power, SO2 emissions, volcanic risk

©2019. Japan Geoscience Union. All Right Reserved.

The source depth of Strombolian explosions: a multiparametric approach and comparison

*Jacopo Taddeucci[1], Miguel Angel Alatorre-Ibarguengoitia[2], Valeria Cigala[3], Elisabetta Del Bello[1], Damien Gaudin[4], Ulrich Kueppers[4], Tullio Ricci[1], Valentino Salvatore[5], Piergiorgio Scarlato[1]

1. Istituto Nazionale di Geofisica e Vulcanologia, Rome, Italy, 2. Centro de Investigación en Gestión de Riesgo y Cambio Climático, Universidad de Ciencias y Artes de Chiapas, Tuxtla Gutiérrez, Mexico, 3. Department of Geosciences, Università degli Studi di Padova, Padua, Italy, 4. Department of Earth and Environmental Sciences. Ludwig-Maximilians-Universität (LMU). Munich, Germany, 5. Dipartimento di Scienze della Terra, Sapienza Università di Roma, Rome, Italy

The source depth of an individual explosion during Strombolian-style explosive volcanic activity can be defined as the depth of the region within the volcanic conduit where magma fragmentation occurs and the acceleration of pyroclasts by the expanding gas continuum begins. Source depth is thought to exert a first-order control on the final ejection dynamics of the pyroclasts and the ensuing eruptive styles and hazards. As such, different methods to estimate source depth have been developed in the past.

Here, we used three independent methods to estimate the source depth of some Strombolian explosions from Stromboli and Etna volcanoes (Italy). The first method uses the back-tracking of the trajectories of pyroclasts leaving the vent to infer their minimum release depth. It is a purely geometric method relying on the assumption that pyroclasts follow linear trajectories after fragmentation. The second method uses the time delay between the appearance of pyroclasts at the vent and the arrival of acoustic waves at a recording station at a known distance from the vent. This method relies on several assumptions, including (i) the sound velocity inside the conduit, (ii) the co-location of source depth of pyroclasts and acoustic waves, and (iii) a constant velocity of pyroclasts in the conduit, following the initial acceleration. The third method uses the velocity of pyroclasts progressively exiting the vent. This velocity decays following a non-linear trend which is function of the source depth, as illustrated by previous experimental and theoretical studies. As for the second method, also this last one assumes a constant velocity of pyroclasts rising in the conduit.

For the Etna case, the three methods provide consistent results and a shallow (<20 m) source depth of the explosions. For the Stromboli case, the first and third methods provide shallow (around 6 and 15 m, respectively) source depths while the second method provides depths of around 60 m. The incompatibility of such large depths with the first two methods, and given the relative assumptions, we believe that in the Stromboli case the co-location of the particles and acoustic source is probably the least strong assumption. These results suggest that caution should be used in assessing source depth from a single methodology, and that more investigations are required on the source of acoustic signals from the explosions and on the motion (specifically the acceleration and deceleration) of pyroclasts ascending along the conduit.

Keywords: strombolian, explosion, depth

©2019. Japan Geoscience Union. All Right Reserved.

Magmatic aggregate of basaltic ash particles

*Takahiro Miwa[1], Nobuo Geshi[2]

1. National research institute for earth science and disaster prevention, 2. National Institute of Advanced Industrial Science and Technology

Dynamics of volcanic cloud and jet at the vent is largely controled by a grain size of pyroclast. The grain size is considered to be determined by primary fragmentation of magma, and subsequent breakup of pyroclasts due to therir collsions in upper conduit (Dufek et al. 2012). However, whether the breakup occurs or not depend on viscoelastic responce of magma (Dingwell and Webb, 1989).
In this study, we report aggregate of ash particles which is formed in magmatic temperature. We observed basaltic ash samples from Stromboli volcano, Italy, and Aso volcano, Japan. The “magmatic aggretate” shows texture that numerous small guest particles (< 200 μm) adhere or stick on a host particle (> 1 mm). All the host particles are catergorized to sideromelane having fluidal morphology. The guest particles are on fluidal surface of the host particle, and show fluidal and dense morphology. These characteristics found in the magmatic aggregate can be explaned by collision and aggretation of ash particles in high temperature condition. Here we model formation of the magmatic aggregates as passing of two frying particles bearing viscoelastic nature, by using viscosity of magma estimated (10^4-10^5 Pa s). When the relative velocity of the two particles falls the critical value, the two particles behave as viscous material, coalsece each other, and then form the magmatic aggregate. The result of calculation demonstrates that the critical relative velocity is approximately 10^{-2} m/s, and implies the magmatic aggregation is difficult to occur for silisic magma with highly viscosity. Thus we conclude that the collision can increase average grain size of pyroclast in basaltic system.

Keywords: Eruptive dynamics, Interaction of ash particles, Viscoelastic response of magma

©2019. Japan Geoscience Union. All Right Reserved.

Melt inclusion study on the eruption process of Izu-Omuroyama monogenetic volcano, Japan

Risako Hatada[1], *Hidemi Ishibashi[1], Yusuke Suzuki[2], ATSUSHI YASUDA[3], Natsumi Hokanishi[3]

1. Faculty of Science, Shizuoka University, 2. Izu Peninsula Geopark, 3. Earthquake Research Institute, University of Tokyo

Izu-Omuroyama is one of monogenetic volcanoes in Izu-Tobu volcanic field, which is the largest pyroclastic cone formed by ~4ka eruption with ~450 million tons of tephra and lava (Koyano et al., 1996). Because a monogenetic volcano such as Omuroyama is built by the first eruption of a newly-formed magma plumbing system, phenocrysts and melt inclusions (MIs) in its volcanic products may record information about the initial process of formation of the magma plumbing system. In this study, textural and chemical analyses were performed for phenocrysts and MIs in Strombolian scoria of the Omuroyama eruption to clarify the eruption process of the monogenetic volcano.

According to Koyano et al. (1996), Omuroyama eruption started from sub-plinian phase (stage-A), followed by weak ash-eruption phase (stage-B), and then shifted to the main phase of Strombolian eruption (stage-C). Omuroyama pyroclastic cone was built during the stage-C. In this study, we performed textural and chemical analyses for phenocrysts and MIs in the fall scoria erupted during the stage-C, by using FE-EPMA and EPMA at ERI, Univ. Tokyo, Japan.

The scoria contain ~3.3 vol.% of olivine and ~5.4 vol.% of plagioclase as phenocrysts, and their groundmass include olivine and plagioclase microphenocsyts (MPs) of several tens-100 microns sizes embedded in almost glassy or microlite-rich matrix. Olivine phenocrysts are homogeneous (Fo~74-83 with concentration at 83-84) in each grain except for normal zoned rim. Olivine MPs has compositions similar to Fo-poor phenocrysts. Most of plagioclase phenocrysts show reverse zoning with cores of An~30-60 and rims of An~84 and dusty zones are often found. Plagioclase MPs have compositions identical to those of phenocryst rims. Olivine- and plagioclase-hosted MIs have SiO_2 contents of ~52-60 wt.% and 57-78 wt.%, respectively. Compositions of both olivine- and plagioclase-hosted MIs with SiO_2~57-60 wt.% are identical with glass in microlite-poor groundmass, indicating that the melt was saturated with olivine and plagioclase. Based on the olivine-plagioclase-melt compositional relation, temperature and H_2O content conditions of the melt is estimated to be ~1080ºC and ~2 wt.% (H2O-saturated depth of ~2km), respectively. Majority of MIs in plagioclase phenocrysts are rhyolitic with SiO2~70-74wt.%. FeO content of host plagioclase crystals are consistent with those in equilibrium with the MIs. H_2O contents of the MIs are estimated by melt-plagioclase hygrometer to be ~6.2-9.2 wt.% (H_2O-saturated depth of ~8-14km), under assumption of temperature of 800-850 ºC. In addition, olivine-hosted MIs with $SiO_2 < 57$ wt.% are enriched in SO_3 (~0.3-0.5 wt.%), indicating their origin deeper than those of more evolved MIs ($SO_3 < 0.1$ wt.%).

Present results suggest that (1) deep-derived, olivine-bearing mafc melt ascent, captured plagioclase phenocrysts and rhyolitic melt and mixed with them at 11km depth, and crystallized MPs at 2km depth before the eruption, and (2) rhyolitic melt existed at ~11km depth beneath the volcanic field at ca. 800 years before the first eruption of rhyolitic magma at Kawagodaira volcano.

Keywords: melt inclusion, monogenetic volcano, rhyolite, Izu-Omuroyama, plagioclase

©2019. Japan Geoscience Union. All Right Reserved.

©2019. Japan Geoscience Union. All Right Reserved.

Time-series variation in the textures of ejecta of the An'ei eruption, Izu-Oshima

*Yuya Ikenaga[1], Fukashi Maeno[1], ATSUSHI YASUDA[1]

1. Earthquake Research Institute, The University of Tokyo

In Izu-Oshima, a large-scale eruption called the An’ ei eruption began in 1777. This eruption lasted for 15 years, and scoria and lava flows were strongly ejected before ash eruption period (Nakamura, 1964; Isshiki, 1984; Koyama and Hayakawa, 1996, Tsukui et al, 2009). As for scoria eruption, the transition of the intensity of eruption was unveiled (Ikenaga et al., 2018). Scoria eruption in the initial stage (Unit A) was somewhat weak and scoria is poor in plagioclase phenocrysts (Pl). After the small-scale scoria eruption (Unit B, rich in Pl), the climax stage (Unit C) occurred. Scoria in Unit C is richest in Pl and eruption column height of this unit is inferred to be approximately 10km. The change in the textures of scoriae among these 3 units, however, has not been investigated yet. It becomes clear in this study that there are differences in the textures of scoriae.

The scoria of Unit A (A-scoria) is rich in microlites and the groundmass glass has low transparency. The surface of bubbles is rough and many bubbles are connected each other. On the other hand, the scoria of Unit C (C-scoria) has almost no microlites and the glass is transparent. The shape of bubbles is spherical or ellipsoid, and the surface of bubbles is smooth. The connectivity of bubbles is low. The characteristics of the scoria of Unit B (B-scoria) are intermediate between those of A- and C-scoria. Considering the transition in the intensity of eruption, magma ascent rate of Unit A is expected to have been low than that of Unit C, and the crystallization of microlites and connection of bubbles in Unit A were probably caused because of low decompression rate.

The compositions of Pl, groundmass glass and melt inclusions in Pl of scoriae were measured using EPMA, and there are no difference in these compositions among 3 units. It is inferred from this result that the change in the intensity of 3 units was not caused by injection of undifferentiated magma into magma chamber, but caused by other processes, such as decompression of magma chamber after the eruption of Unit A. It is a future issue to reveal the cause of the change in intensity.

Keywords: Izu-Oshima, Transition in texture, Composition of eruption products

©2019. Japan Geoscience Union. All Right Reserved.

The textural analysis of pumice from the Plinian eruption of Taupo volcano: implications for tube pumice

*Masatoshi Ohashi[1], Mie Ichihara[2], Fukashi Maeno[2], Ben Kennedy[3], Darren Gravley[3]

1. Department of Earth and Planetary Science, Graduate School of Science, The University of Tokyo, 2. Earthquake Research Institute, The University of Tokyo, 3. Department of Geological Sciences, The University of Canterbury

Tube pumice is characterized by aligned highly elongated bubbles and is a common product of explosive silicic eruptions. This bubble texture is thought to reflect shear deformations during flow in a conduit (Marti et al., 1999). Therefore, quantitative measurements of tube pumice texture can inform conduit flow models. Recent development in X-ray tomography allows us to measure bubble shapes in 3D pumice accurately (e.g., Dingwell et al., 2016). In addition to the microscopic structures of individual pumices, the abundance of tube and non-tube pumices in the stratigraphy is important in inferring temporal and spatial variations in a conduit flow. This study aims at quantifying micro-structural and stratigraphic features of pumice from the 1.8 ka eruption of Taupo volcano, New Zealand.

The 1.8 ka eruption is the most recent large eruptive event from Taupo volcano. It is characterized by various eruptive styles, including three phreatomagmatic fall deposits (units 1, 3, 4), Hatepe plinian fall deposit (unit 2), Taupo plinian fall deposit (unit 5), and Taupo ignimbrite (unit 6) (Houghton et al., 2010). Since those deposits show chemically uniform pumices and melt inclusions, the great diversity of bubble textures in pumices may reflect purely physical processes in the eruption. We collected samples from the units of the two plinian eruptions (units 2 and 5) and the ignimbrite (unit 6), and measured bubble textures and vesicularities. Among those units, we focused on unit 5 to investigate the transition from plinian fall to ignimbrite. For this purpose, a detailed sampling of unit 5 was conducted at an outcrop about 25 km away from the vent, where the unit consists of a fine lower part (40 cm) and a coarse upper part (180 cm). We sampled clasts from the bottom to top of the unit 5 layer at 20cm interval. The bubble textures of more than 1000 pumice samples were measured by a digital microscope (VHX-1000, Keyence) with variable illumination function. The illumination was optimized to make good luminance contrast between the flat surface and bubbles for image analysis.

The image analysis shows that bubbles in unit 5 are more elongated than those in unit 2 and less elongated than those in unit 6. The average values of bubble elongation in unit 2 and 6 are proportional to those of vesicularity. In contrast, bubble elongation and vesicularity are uniform within unit 5. The component analysis over unit 5 shows that the weight percentage of lithics is also uniform except in the lowest part. The relatively high lithic content in the lowest part suggests vent widened or shifted location at the beginning of the Taupo plinian event.

Previous studies in other volcanoes suggest that bubbles in the pre-ignimbrite phase become more elongated toward the flow stage (Taddeucci and Wohletz 2001, Polacci et al., 2003). The increased amount of tube pumice is thought to reflect a gradual transition from fallout to ignimbrite, and it was interpreted as a result of increased erosive activity near the conduit wall, or a greater conduit area available for shearing (Polacci et al., 2003). In contrast, no such variation of bubble texture is observed in Taupo plinian event (unit 5), which implies that a steady conduit flow was sustained during the pre-ignimbrite fallout eruption. The ignimbrite (unit 6) might not simply be the result of a collapsing plinian eruption column. It is also possible that the topmost part of unit 5 had been eroded by and/or mixed with the pyroclastic flow that deposited the subsequent ignimbrite (unit 6).

©2019. Japan Geoscience Union. All Right Reserved.

Keywords: bubble texture, tube pumice, Taupo

©2019. Japan Geoscience Union. All Right Reserved.

[E] Poster | S (Solid Earth Sciences)：S-CG Complex & General

Thu. May 30, 2019 3:30 PM - 5:00 PM JST | Thu. May 30, 2019 6:30 AM - 8:00 AM UTC | Poster Hall International Exhibition Hall8, Makuhari Messe_14

[S-CG50] Intraslab and intraplate earthquakes

convener:Saeko Kita(International Institute of Seismology and Earthquake Engineering, BRI), Tomohiro Ohuchi(Geodynamics Research Center, Ehime University), Marcel Thielmann(Bavarian Geoinstitute, University of Bayreuth), Ryo Okuwaki(Research Institute of Earthquake and Volcano Geology, Geological Survey of Japan, National Institute of Advanced Industrial Science and Technology)

The purpose of this session is to share recent advances of geo-scientifical studies for intraslab and shallow-depth intraplate earthquakes. We seek to formulate future directions of the interdisciplinary study of the occurrence of intermediate-depth and deep earthquakes from the viewpoint of seismology, geodynamics and mineral physics. We welcome presentations from a wide variety of scientific disciplines, including seismology, seismotectonics, geodynamics, mineral and rock physics, other geophysics, geology, and numerical modeling.

[SCG50-P01] Changes in seismicity rate, stress orientations, and b-values before and after ETS events in the Philippine sea plate under Kii Peninsula

*Saeko Kita[1], Heidi Houston[2], Sachiko Tanaka[3], Youichi Asano[3], Takuo Shibutani[4], Naoki Suda[5] (1.Building Research Institute, 2.USC, 3.NIED, 4.DPRI, Kyoto University, 5.Hiroshima University)

[SCG50-P02] **Inhomogeneous conduit across slab controlled by intraslab stress heterogeneity in the Nankai subduction zone**

*Makoto Otsubo[1], Ayumu Miyakawa[2], Ikuo Katayama[3], Keishi Okazaki[4] (1.Geological Survey of Japan, Research Institute of Earthquake and Volcano Geology, 2.Geological Survey of Japan, Research Institute of Geology and Geoinformation, 3.Hiroshima University, 4.JAMSTEC)

[SCG50-P03] New insights into the mechanism of deep-focus earthquakes

*Ayako Tsuchiyama[1], Junichi Nakajima[1] (1.Tokyo Institute of Technology)

[SCG50-P04] Faulting in deforming harzburgite under wet conditions

*Tomohiro Ohuchi[1], Xinglin Lei[2], Yuji Higo[3], Yoshinori Tange[3], Takeshi Sakai[1] (1.Geodynamics Research Center, Ehime University, 2.National Institute of Advanced Industrial Science and Technology, 3.Japan Synchrotron Radiation Research Institute)

[SCG50-P05] Semi-brittle behavior of olivine single crystals under the conditions of Earth's mantle transition zone

Yoshihisa Naruse[1], *Tomohiro Ohuchi[1] (1.Geodynamics Research Center, Ehime University)

[SCG50-P06] High-pressure deformation experiments on peridotite gouges under hydrothermal conditions, using a deformation-DIA apparatus

*Maki Semba[1], Ken-ichi Hirauchi[1], Tomohiro Ohuchi[2], Katsuyoshi Michibayashi[3] (1.Department of Geosciences, Faculty of Science, Shizuoka University, 2.Geodynamics Research Center, Ehime University, 3.Department of Earth and Planetary Sciences, Nagoya university)

[SCG50-P07] Stable fault slip in antigorite-olivine aggregates at high pressures

Mai Ikehara[1], *Tomoaki Kubo[1], Takuya Iwasato[2], Yuji Higo[3], Masahiro Imamura[1], Yoshinori Tange[3] (1.Kyushu University, 2.Shin-Nippon Nondestructive Inspection Co., Ltd., 3.JASRI)

[SCG50-P08] Rheology and frictional instability of lawsonite in high pressure deformation experiments

*Rei Shiraishi[1], Jun Muto[1], Akihiro Tsunoda[2], Sando Sawa[1], Akio Suzuki[1] (1.Department of Earth Science, Graduate School of Science, Tohoku University, 2.Earthquake Research Institute, University of Tokyo)

[SCG50-P09] Grain Size Dependency of Olivine-Spinel Phase Transformational Mechanism Responsible for Deep-focus Earthquakes

*Sando Sawa[1], Jun Muto[1], Nobuyoshi Miyajima[2], Hiroyuki Nagahama[1] (1.Department of Earth Science, Tohoku University, 2.Bayerisches Geoinstitut, University of Bayreuth)

[SCG50-P10] **Seismicity and mineral destabilizations in the subducting mantle up to 6 GPa, 200 km depth**

*Thomas P. Ferrand[1] (1.Earthquake Research Institute)

[SCG50-P11] Receiver function imaging of subducting Pacific plate and mantle wedge under Japanese islands using denser network of stations

*HyeJeong Kim[1], Hitoshi Kawakatsu[1], Takeshi Akuhara[1], Masanao Shinohara[1] (1.Earthquake Research Institute, The University of Tokyo)

[SCG50-P12] Strong S-wave attenuation in the mantle wedge beneath the NE Japan and interpretations of high-frequency wave propagation path of intraslab earthquakes

*Takahiro Shiina[1,2], Kei Katsumata[2], Kiyoshi Yomogida[3], Aitaro Kato[1] (1.Earthquake Research Institute, The University of Tokyo, 2.Institute of Seismology and Volcanology, Graduate School of Science, Hokkaido University, 3.Graduate School of Science, Hokkaido University)

Changes in seismicity rate, stress orientations, and b-values before and after ETS events in the Philippine sea plate under Kii Peninsula

*Saeko Kita[1], Heidi Houston[2], Sachiko Tanaka[3], Youichi Asano[3], Takuo Shibutani[4], Naoki Suda[5]

1. Building Research Institute, 2. USC, 3. NIED, 4. DPRI, Kyoto University, 5. Hiroshima University

The slip on the plate interface has the potential to affect the stress field and seismicity within the subducting slab. Several studies have examined the interaction of slow slip phenomena with intraslab earthquakes [Nankai and Tokai regions, Han et al. 2014; Mexico, Radiguet et al. 2018, 2018 JpGU meeting; New Zealand, 2018, Warren-Smith, 2018 AGU meeting]. Kita et al. [2018, SSJ meeting] reported the stress change in the whole slab associated with ETS times based on stress tensor inversion results. However, we find a clear double seismic zone under Kii Peninsula, as also noted in a previous study [e.g. Miyoshi and Ishibashi, 2004]. Therefore, we here examine seismicity rate variations, stress changes, and b-value variations of seismicity separately for the upper plane events and oceanic mantle ones relative to ETS timings beneath the Kii Peninsula. We use the JMA earthquake catalog, the NIED tremor catalog, the upper surface of the Philippine sea plate estimated by Shibutani and Hirahara [2016], P-wave polarity data by NIED, and a stress tensor inversion code [Vavrycuk, 2014].

We determined the timings of ~30 large ETS beneath the Kii Peninsula from 2001 to 2017, and categorized slab seismicity relative to the occurrence times of nearby the ETS (i.e., 60 days before or after). We then combined or stacked the slab seismicity based on these relative occurrence times. The rate of seismicity both in the upper plane events and in the oceanic mantle ones after the ETS timings clearly decreased, compared to the rate before the ETS timings. The peaks of b-values of seismicity both in the upper plane events and oceanic mantle ones were found to occur 1.5 months before ETS. A change in stress orientations before and after the ETS was seen in the oceanic mantle, and a relatively small change was seen for the upper plane events. The stress change in the upper plane events appears to be larger in the region updip of the ETS zone. The results of our study suggest that the aseismic slip on the plate boundary may affect the stress field and the occurrence of seismicity within the subducting slab beneath the Kii Peninsula. Fluid migration from the oceanic slab into the ETS zone on the plate boundary could be related to the interaction of slow slip phenomena with intraslab earthquakes.

Keywords: Intraslab earthquake, ETS, stress change, b-value, time change, Kii peninsula

©2019. Japan Geoscience Union. All Right Reserved.

Inhomogeneous conduit across slab controlled by intraslab stress heterogeneity in the Nankai subduction zone

*Makoto Otsubo[1], Ayumu Miyakawa[2], Ikuo Katayama[3], Keishi Okazaki[4]

1. Geological Survey of Japan, Research Institute of Earthquake and Volcano Geology, 2. Geological Survey of Japan, Research Institute of Geology and Geoinformation, 3. Hiroshima University, 4. JAMSTEC

Non volcanic deep low-frequency tremors and slow slip events occur simultaneously in the transition zone from locked to continuously creeping fault at the down dip portion of the Nankai Trough subduction zone, southwestern Japan. The occurrence of these slow earthquakes is attributed to the effect of high pore pressures on the plate boundaries. The Nankai Trough subduction zone has a discontinuous band of occurrence of these slow earthquakes along the trench. Here we show that spatial variation of intraslab stress can control fluid migration through the subducted Philippine Sea slab to the plate boundary. The tri-axial normal faulting stress detected by the stress tensor inversion by using focal mechanisms in the slab controls anisotropies of permeability trending NNW–SSE sub-horizontal orientation from the subducted Philippine Sea slab to the plate boundary. The inhomogeneous condition controlled by the spatial stress heterogeneities in the subducted Philippine Sea slab represents the intraslab fluid pathway. The hypothesis is consistent with spatial heterogeneity of slow earthquake activities and $^{3}He/^{4}He$ ratio distributions.

Keywords: Fluid, Nankai Trough, Slab, Slow earthquake, Stress

©2019. Japan Geoscience Union. All Right Reserved.

New insights into the mechanism of deep-focus earthquakes

*Ayako Tsuchiyama[1], Junichi Nakajima[1]

1. Tokyo Institute of Technology

Generally, deep-focus earthquakes were generated in subducting slabs and occurred along some specific regions such as Izu-Bonin zone and Tonga-Fiji zone. We have not identified their occurrence mechanisms, even though some plausible hypotheses, dehydration embrittlement, thermal and shear plastic instability, and transformational faulting, were proposed. In this study, we try to obtain new constraints that deepen the understanding of deep-focus earthquakes through waveform analysis of earthquakes in the Izu-Bonin subduction zone.

First, we picked up 460 quakes at a depth range of 300-400 km in 2003-2015 beneath Tokai area from the catalog data provided by Japan Meteorological Agency, and relocated them with double-difference earthquake relocation algorithm (hypoDD; Waldhauser and Ellsworth, 2000). Second, we computed their coherence values between all available pairs of earthquakes with cross-spectrum analysis. Then, we were successful to identify a few earthquake clusters that had a very high coherence value over 0.9 in a long time window of 40 s including P and S waves. Moreover, we relocated these earthquakes with hypoDD again by using precisely-determined differential travel-time data derived from waveform data. As a result, we could find that earthquakes in each cluster occurred on single fault plane with complementary rapture areas.

Additionally, we implemented moment tensor inversion (Gephart and Forsyth, 1984) and estimated the stress field around the region where we discovered a few clusters showing waveform similarities. Moreover, we computed the amount of stress drop of the similar earthquakes with spectrum analysis of seismic wave. Through these waveform analyses, we interpreted that the mechanism of these similar deep-focus earthquakes could be explained by combining two possible mechanisms; dehydration embrittlement that regulates the rupture initiation and thermal and shear plastic instability that controls the rupture propagation along a pre-existing fault.

Keywords: deep-focus earthquakes, intraslab earthquakes

©2019. Japan Geoscience Union. All Right Reserved.

Faulting in deforming harzburgite under wet conditions

*Tomohiro Ohuchi[1], Xinglin Lei[2], Yuji Higo[3], Yoshinori Tange[3], Takeshi Sakai[1]

1. Geodynamics Research Center, Ehime University, 2. National Institute of Advanced Industrial Science and Technology, 3. Japan Synchrotron Radiation Research Institute

The subduction zone produces a major fraction of the Earth's seismic activity. The mechanisms of intermediate-depth (> 40 km depth) and deep-focus (> 300 km) earthquakes are fundamentally different from those of shallow (< 40 km) earthquakes. This is because the frictional strength of silicate rocks exceeds the upper limit of the stress level in the upper mantle (< 300 MPa: Obata and Karato, 1995) at pressures higher than 1 GPa (~30 km depth). Therefore, the cause of intraslab seismicity at intermediate depths has been attributed to dehydration of serpentinite (e.g., Peakock, 2001) because the water released during dehydration reaction of serpentinite reduces the effective confining pressure. The dehydration embrittlement model is now widely accepted, because the location of the double seismic zone in the subducting Pacific slab corresponds to the main dehydration field in the pressure-temperature diagram of the hydrous peridotite (Omori et al., 2002).

To evaluate the effect of water on semi-brittle behavior of harzburgite, we conducted in-situ uniaxial deformation experiments on as-is/water-saturated harzburgite at pressures 1.2-3.0 GPa and temperatures 770-1250 K with a constant displacement rate using a deformation-DIA apparatus. Pressure, stress, and strain were measured in situ by using x-ray diffraction patterns and radiographs. Acoustic emissions (AEs) were also recorded continuously on six sensors, and three-dimensional AE source location were determined.

Formation of throughgoing faults was observed even when differential stress is much lower than the confining pressure (i.e., > 0.3 times of confining pressure) in water-saturated harzburgite. This is contrast to the case of water-saturated dunite (Ohuchi et al., 2018), in which fracture strength exceeds the confining pressure (i.e., Goetze's criterion). Creep strength of water-saturated harzburgite was lower than that of as-is harzburgite (~0.5-1 GPa at each temperature). Weakening of the harzburgite by the aqueous fluid resulted in the reduction in the number of AE events and decrease in fault slip rate (< 3.6E-4 s^{-1} at a stress of < 1.05 GPa). Stress/pressure drop around the timing of a faulting was limited at strains of 1E-4 s^{-1}. The aseismic faulting observed in the water-saturated harzburgite implies that silent slip events around the subduction interface is due to semi-brittle flow of water-saturated harzburgite (i.e., a dehydration product of antigorite).

Keywords: harzburgite, water, semi-brittle flow

©2019. Japan Geoscience Union. All Right Reserved.

Semi-brittle behavior of olivine single crystals under the conditions of Earth’s mantle transition zone

Yoshihisa Naruse[1], *Tomohiro Ohuchi[1]

1. Geodynamics Research Center, Ehime University

The origin of deep-focus earthquakes, which occur at depths of 300-700km in the subducting slabs, fundamentally differs from that of other earthquakes and has been attributed to the pressure-induced phase transition in olivine. Previous studies on Mg_2GeO_4 olivine have shown that grain size reduction induced by the phase transition in olivine causes shear localization (e.g., Burnley et al., 1991; Schubnel et al., 2013). Schubnel et al. (2013) reported intense acoustic emissions around the timing of a faulting which would be induced by shear localization in polycrystalline Mg_2GeO_4 olivine. In order to understand the relationship between fracturing and the phase transition in olivine, we conducted deformation experiments on single crystals of San Carlos olivine (Fo_{91}) at pressure of 10-15 GPa and temperatures of 1000-1100 degC using a deformation-DIA apparatus. Single crystal of olivine was chosen to exclude the effect of grain boundaries on nucleation of high-pressure phases of olivine (i.e., wadsleyite and ringwoodite).

Array of microcrack parallel to either (100), (010) or (110) plane was developed at an ~50 degree to the direction of uniaxial compression. Rotation of olivine axes associating the formation of subgrain boundaries was observed around the microcrack arrays, showing that plastic deformation of the olivine single crystal inevitably associated formation of the microcracks. In most samples, microcracks coalesced and then a few throughgoing fractures were developed. Particles of wadsleyite /ringwoodite having a diameter of a few micrometer or less were preferentially nucleated on the microcrack surfaces. Ultrafine-grained domains, which consist of the wadsleyite /ringwoodite particles, were formed along the throughgoing fractures. Development of a banded ultrafine-grained domain was also observed along a throughgoing fracture, implying that shear localization could occur as a result of semi-brittle flow of olivine and a transition from dislocation creep to grain-size-sensitive creep in subducting slabs at depths > 410 km.

Keywords: olivine, phase transition, semi-brittle flow, microcrack, deep-focus earthquake

©2019. Japan Geoscience Union. All Right Reserved.

High-pressure deformation experiments on peridotite gouges under hydrothermal conditions, using a deformation-DIA apparatus

*Maki Semba[1], Ken-ichi Hirauchi[1], Tomohiro Ohuchi[2], Katsuyoshi Michibayashi[3]

1. Department of Geosciences, Faculty of Science, Shizuoka University, 2. Geodynamics Research Center, Ehime University, 3. Department of Earth and Planetary Sciences, Nagoya university

In subducting oceanic plates, the focal depth of intraslab earthquakes is deeper (>40 km) than that of interplate earthquakes. Since the normal stress on faults (e.g., outer-rise faults) hosting the intraslab earthquakes is too high to generate brittle shear failure, there may be some mechanisms to weaken effective fault strength. In addition, the hypocenter distribution of intraslab earthquakes forms double-planed structure of the deep seismic zone, and the location of the lower plane is in accord with the stability limit of serpentine (antigorite), suggesting shear deformation of antigorite-bearing peridotite gouges in the presence of hydrothermal water. Here, in order to understand the influence of hydrous minerals on the fault strength, we performed deformation experiments on simulated peridotite gouges with compositions of dunite (100% olivine) and harzburgite (70% olivine/30% orthopyroxene) under hydrothermal conditions, using a deformation-DIA apparatus. The experiments were conducted at a temperature of 580˚C, a confining pressure of 2.5 GPa, and shear strain rates of 2.70 $\times 10^{-5}$ to 1.03 $\times 10^{-4}$ s^{-1}. In the deformed peridotite gouges, localized shear zones such as R_1 and B shears were observed, and these shears were accompanied with newly formed hydrous phases (serpentine or talc). Olivine grains have a crystal preferred orientation characterized by a slip system of [001] (010). These results indicate that semi-brittle flow is a major deformation mechanism of the peridotite gouges. Considering low coefficients of friction of serpentine and talc, we can suggest that the infiltration of seawater along outer-rise fault planes and subsequent hydrothermal alteration result in effective shear strengths low enough to produce intraslab earthquakes.

Keywords: deformation-DIA apparatus, peridotite, serpentinization, frictional strength

©2019. Japan Geoscience Union. All Right Reserved.

Stable fault slip in antigorite-olivine aggregates at high pressures

Mai Ikehara[1], *Tomoaki Kubo[1], Takuya Iwasato[2], Yuji Higo[3], Masahiro Imamura[1], Yoshinori Tange[3]

1. Kyushu University, 2. Shin-Nippon Nondestructive Inspection Co., Ltd., 3. JASRI

Intermediate-depth earthquakes are observed to occur within subducting oceanic plates at depths of about 60-300 km where most materials exhibit plastic deformation rather than brittle failure, owing to high pressures and temperatures. Dehydration embrittlement of hydrous minerals, particularly antigorite serpentine, is one of the most popular hypotheses for explaining shear instability under such conditions (e.g., Raleigh and Paterson, 1965). Recent high-pressure deformation experiments, monitoring Acoustic Emission (AE) activities upon syndeformational antigorite dehydration, showed that dehydration embrittlement was not observed on single-phase antigorite (Gasc et al., 2017), whereas dehydration related faulting was formed on antigorite-olivine aggregates with strong AEs (Ferrand et al., 2017). However, most of the previous high-pressure studies have been conducted in axial compression at relatively low pressures (< 3.5 GPa), insufficient to consider intermediate-depth earthquakes. Therefore, in this study, we conducted high-pressure shear deformation experiments on two-phase aggregates of antigorite and olivine, considering partially serpentinized peridotites, in order to investigate possible shear localization and shear instability up to 7 GPa.

Deformation experiments were conducted at 5-7 GPa, 350-700 ℃ using Deformation-DIA apparatuses at SPring-8 (BL04B1). Monochromatic X-rays (50-60 keV) were used to measure dehydration kinetics, shear strain and stress with recording AEs. We used three kinds of starting materials; natural cored antigorite from Kawarakoba in Nagasaki prefecture, forsterite polycrystal, and two-phase sintered mixtures of antigorite and San Carlos olivine (antigorite 10, 30, 50 vol %). The samples were cut into disks having thickness of 300 μm and used for a shear deformation study by being assembled between two 45˚-cut alumina pistons. In shear deformation experiments, the starting disk was compressed to 5 or 7 GPa at room temperature, annealed at 350 or 400 ℃ for 1 h, and then deformed with an anvil displacement rate of 200 μm/h. In some experiments, we increased temperature during shear deformation with a ramping rate of 0.1 ℃/sec to induce dehydration reaction. Microstructures of the recovered samples were examined by an optical microscope and a scanning electron microscope (SEM).

From X-ray radiography images, we observed shear localization in all two-phase samples deformed within the antigorite stability field at 5 GPa. The locallization occurred when homogeneous shear strain γ reached 0.4-0.9 (strain rate 1.3-2.2 $\times 10^{-4}$/s), and then most strains were partitioned to the fault zone with the slip velocity of 4.6-9.1 $\times 10^{-2}$ μm/s. Because no AEs were detected from the sample region, the localized deformation is thought to occur by stable sliding. SEM observations revealed that a thin shear deformation zone was formed along the fault, where the plastic deformation of both antigorite and olivine was significant. Striation and nanograins were observed on the fault plane, suggesting the formation of nanogouge. In contrast, homogeneous deformation was developed during antigorite dehydration with temperature ramping, even in the sample showing shear localization in the antigorite stability field. Under higher pressure condition 7 GPa, shear localization did not occur in all samples regardless of temperature. These results suggest that, although AE activities were detected with the dehydration in the antigorite-olivine aggregates up to 3.5 GPa in the previous study, further increase of pressure inhibits shear instability and shear localization. Thus, other dehydration reactions and/or instability mechanisms are required to explain intermediate-depth earthquakes deeper than ~100 km.

©2019. Japan Geoscience Union. All Right Reserved.

©2019. Japan Geoscience Union. All Right Reserved.

Rheology and frictional instability of lawsonite in high pressure deformation experiments

*Rei Shiraishi[1], Jun Muto[1], Akihiro Tsunoda[2], Sando Sawa[1], Akio Suzuki[1]

1. Department of Earth Science, Graduate School of Science, Tohoku University, 2. Earthquake Research Institute, University of Tokyo

The cause of intermediate-depth earthquakes (50-300 km) in subducting slabs have been proposed to be the dehydration embrittlement (e.g., Raleigh and Paterson, 1965), because there are many kinds of hydrous minerals in a subducting slab and hypocenter distribution coincides with the dehydration boundary determined by high pressure experiments (e.g., Hacker et al., 2003). Many experimental studies on antigorite have been conducted, but a few previous works about dehydration embrittlement of lawsonite-bearing rocks experimentally. Lawsonite, $CaAl_2Si_2O_7(OH)_2H_2O$, is a hydrous mineral which contains 11 wt% water in its structure as both water molecules and a hydroxy group (Cmodi and Zanazzi, 1996). Lawsonite is one of the candidate for dehydration embrittlement in cold subducting slabs, however previous works have apparently contradictory results. Okazaki and Hirth (2016) showed that lawsonite dehydration induced unstable fault slip based on deformation experiments of pure lawsonite using Griggs-type deformation apparatus at 1 GPa. On the other hand, Incel et al. (2017) also investigated deformation properties of lawsonite and glaucophane mixture at 1.5 to 3.0 GPa using deformation-DIA apparatus. They insisted that there is no evidence for a straightforward relation to the dehydration of lawsonite and the brittle failure of samples. So, we have conducted the deformation experiments of lawsonite under the cold slab conditions in order to clarify the deformation property of lawsonite and understand the relationship between dehydration and brittle failure.

Experiments were carried out using Deformation-Cubic Anvil Press (D-CAP) installed at KEK PF AR-NE7A beamline. Pure lawsonite powder (98%) was used as starting materials. Deformation experiments were carried out at a pressure of 6 GPa and temperatures of 300 - 800 ˚C. The temperature was increased at the same time as deformation started. The temperature ramping rate over the strain rate was set the ranges for the real subducting slab, which ranges from 10^2 to 10^4 ˚C (Chernak and Hirth, 2011; Okazaki and Hirth, 2016). During deformation stages, strain, stress and transformation rate were measured for in-situ using a monochromatic X-ray beam with an energy of 60 keV.

Four experiments showed rapid stress drop during temperature ramping before lawsonite dehydration starts. We observed microstructure of recovered samples, there are many through going faults and microcracks but no dehydration products. Our results indicate that brittle process and frictional sliding occur without dehydration of lawsonite. This suggests that the intermediate-depth earthquakes can be caused by the deformation itself of lawsonite without the dehydration of lawsonite.

Keywords: intermediate-depth earthquakes, dehydration embrittlement, Lawsonite

©2019. Japan Geoscience Union. All Right Reserved.

Grain Size Dependency of Olivine-Spinel Phase Transformational Mechanism Responsible for Deep-focus Earthquakes

*Sando Sawa[1], Jun Muto[1], Nobuyoshi Miyajima[2], Hiroyuki Nagahama[1]

1. Department of Earth Science, Tohoku University, 2. Bayerisches Geoinstitut, University of Bayreuth

Deep-focus earthquakes occur at the depth from 440 km to 660 km in the subducting slab. The mechanism responsible for the earthquakes is thought to be different from that of shallow earthquakes, so that previous studies have reported the various mechanisms. By the geophysical observations and deformation experiments, the phase transformational faulting mechanism is presumed as the precursor of deep-focus earthquakes (e.g., Zhan et al., 2014). The phase transformational faulting mechanism is that metastable olivine in the slab undergoes the phase transformation to fine-grained spinel and faulting occurs with strain localization into the fine-grained spinel. This shear instability depends on grain size. Furthermore, the grain size may restrict the pressure- and temperature-conditions where the shear instability occurs, that is, the region of slab where deep-focus earthquakes occur. However, previous studies have conducted deformation experiments with finer grain size than expected in the slab (e.g., Burnley et al., 1991). Hence, the results from the laboratory experiments cannot directly apply to the geophysical observation. In this study, to reveal the grain size dependency on the phase transformational faulting, we conducted the deformation experiments of germanate olivine (about 3 μm), which is an analogue material of silicate olivine, finer-grained than that in previous studies (30 μm). We used a Griggs-type solid-confining media deformation apparatus. The confining pressure, temperature and strain rate are 1.2 GPa, 400~900 ℃ and 2.0×10^{-4} s^{-1}, respectively. Even though deformation experiments were conducted under wider temperature conditions than previous studies, we did not observe any shear instability event with apparent stress drops. Also, Raman spectroscopy clarified that the germanate olivine underwent the transformation to spinel at temperatures higher than 500 ℃. Shear instability does not occur because the difference in grain sizes between olivine and nucleated spinel in this study was smaller than those in previous studies. Also, the transformation temperature in this study was much lower than those in previous study (T > 1000 ℃ in Burnley et al., 1991). Considering the rate equation of the transformation (Chan, 1956), small grain size promotes the transformation, but these fast rates of the transformation cannot be explained only by the effect of the grain size. Therefore, the presence of water such as absorbed water in a starting material can also contribute to promote the transformation. Hence, both small initial grain size and a little amount of water promote the transformation even at lower temperature. These results indicate that the phase transformational faulting mechanism has strong grain size dependency. In summary, the pressure- and temperature-conditions where the faulting occurs depends on the grain size of olivine and amount of water. Because the grain size in the slab is larger than that in the experiments, by extrapolating from these results, we may restrict the region of slab where deep-focus earthquakes occur.

This work was supported by the JSPS Japanese-German Graduate Externship.

[Reference]
Burnley et al. (1991), JGR, vol 96, 425-443.
Chan (1956), Acta Metallurgica, vol 4, 449-459.
Zhan et al. (2014), EPSL, vol 385, 89-96.

©2019. Japan Geoscience Union. All Right Reserved.

Keywords: Deep-focus earthquakes, Griggs type piston-cylinder apparatus, phase transformation

©2019. Japan Geoscience Union. All Right Reserved.

Seismicity and mineral destabilizations in the subducting mantle up to 6 GPa, 200 km depth

*Thomas P. Ferrand[1]

1. Earthquake Research Institute

In the subducting oceanic lithosphere, a significant part of the seismicity is triggered in the mantle, especially along the upper and lower Wadati-Benioff planes. Several studies have investigated the potential involvement of dehydration reactions in the triggering mechanism of mantle earthquakes. Recent experimental results reveal that, under subduction conditions, mechanical instabilities nucleate in strong stable mineral aggregates during the destabilization of minor amounts of antigorite, i.e. the high-temperature serpentine, through a stress transfer, without any fluid overpressure. Here I confront these laboratory results to seismological observations. On one hand, most of the natural hydrous magnesium silicates seem to be known, with experimentally-deduced stability limits up to 7 GPa, at least, available as relatively accurate estimates. On the other hand, recent achievements in thermal structure of subduction zones combined with precise hypocentre relocation give access to pressure and temperature conditions at earthquakes hypocentres. A series of P-T diagrams summarizes the stability limit of minerals that may be part of natural peridotite with variable compositions at pressures from 0.5 to 6 GPa and temperatures from 200 to 950˚C, and compares it with seismicity. Both hydrous and anhydrous phases are considered. A myriad of minor metamorphic reactions could participate in a transformation-driven stress transfer, even if the stability limits of serpentine minerals seem to correlate with most of the observed seismicity.

Keywords: earthquakes, intraslab, DDST, dehydration, transformation, subduction

©2019. Japan Geoscience Union. All Right Reserved.

Receiver function imaging of subducting Pacific plate and mantle wedge under Japanese islands using denser network of stations

*HyeJeong Kim[1], Hitoshi Kawakatsu[1], Takeshi Akuhara[1], Masanao Shinohara[1]

1. Earthquake Research Institute, The University of Tokyo

Receiver function imaging has been frequently used by different groups focusing on different depths of the Japanese subduction zone. The overlying crust (Shiomi and Park, 2008, Bianchi et al, 2015), the Pacific plate before (Kawakatsu et al., 2009) and after subduction (Kawakatsu and Watada, 2007; Wirth and Long, 2012), and the mantle transition zones (Kawakatsu and Yoshioka, 2011; Tauzin et al., 2018) were discussed using the NIED array stations (Hi-net and F-net). Recently, deployment of ocean bottom seismometers (OBSs) enabled studies of subduction zones closer to the trench (e.g., Akuhara and Mochizuki, 2015). Kawakatsu and Kim (2018, SSJ) have obtained a new version of receiver function imaging using 14-year long of Hi-net data. However, there are other land stations (e.g., J-array) that can improve the station coverage. Here, we collect data from available on-land stations deployed in north-eastern Japan to obtain a denser 2-D array of stations. Additionally, data from temporary OBS stations (Shinohara et al. 2012) are gathered to image the subducted Pacific plate in shallower depths than previously available. Continuous imaging from ocean to land will help to constrain transition of the hydrated oceanic crust along subduction that is expressed as a low velocity layer for better understanding of the hydration/dehydration processes during subduction, which might be related to the occurrence of subduction zone earthquakes.

Keywords: subduction zone, receiver function, ccp stacking

©2019. Japan Geoscience Union. All Right Reserved.

Strong S-wave attenuation in the mantle wedge beneath the NE Japan and interpretations of high-frequency wave propagation path of intraslab earthquakes

*Takahiro Shiina[1,2], Kei Katsumata[2], Kiyoshi Yomogida[3], Aitaro Kato[1]

1. Earthquake Research Institute, The University of Tokyo, 2. Institute of Seismology and Volcanology, Graduate School of Science, Hokkaido University, 3. Graduate School of Science, Hokkaido University

For intraslab earthquakes at intermediate-depths in NE Japan, especially at greater than about 100-km depths, it has been often recorded that high-frequency waveform higher than 8 Hz show a remarkable delay of arrival compared with S wave which predominates in a low-frequency band. The magnitude of the delay is little in the forearc region, whereas it increases up to about 40 s in the backarc region. In this study, we investigate the details in the propagation processes of the high-frequency later phase observed for the intraslab earthquakes at the intermediate-depths. To constrain the source location of the high-frequency later phase, we employ the source-scanning algorithm (SSA) [Kao and Shan, 2004] with realistic velocity and attenuation structures, assuming that the high-frequency later phase is generated by the single scattering process. Namely, we estimate a scattering point by using mean-square amplitudes which is synthesized from two horizontal components of the observed waveforms.
Results in frequency bands of 4-32 Hz show that scattering points are distributed beneath the forearc region. The scattering points can reproduce the observed delays of amplitude amplifications associating with the high-frequency later phases. Moreover, similar locations of the scattering points are imaged along the forearc region in the entire NE Japan. These results indicate that high-frequency later phase is a wave scattered at the forearc region and that short wave-length heterogeneity generally developed in the forearc region of NE Japan.
This interpretation well matches implications from previous studies [e.g., Yomogida et al., 2004; Hasemi and Horiuchi, 2010]. Additionally, the obtained distributions of scattering points which appear to surround the highly attenuating mantle wedge suggest that attenuation structure strongly controls propagation paths of seismic wave, in particular, a high-frequency wave. In other words, the identifications of high-frequency later phase may become easy because the amplitude of direct wave crossing the high-attenuation zone decreases. To confirm this consideration, we estimate *Qs* along the direct wave by using the coda-normalization method [e.g., Aki, 1980]. This estimation provides 2-3 times smaller path-averaged *Qs* in seismic records of which rays lay on the backarc and the volcanic front than that of which rays lay on the forearc region. These results support that spatial variation in *QS* produces heterogenous propagations of seismic waves emitted from intraslab earthquakes. It is thus required to take scattering and attenuation structures simultaneously into account to understand complex behaviors of high-frequency waves in a future study.

Keywords: S-wave attenuation, Intraslab earthquakes, High-frequency later phase, Scattered wave

©2019. Japan Geoscience Union. All Right Reserved.

[E] Poster | S (Solid Earth Sciences)：S-CG Complex & General

Thu. May 30, 2019 5:15 PM - 6:30 PM JST | Thu. May 30, 2019 8:15 AM - 9:30 AM UTC | Poster Hall International Exhibition Hall8, Makuhari Messe_26

[S-CG50] Intraslab and intraplate earthquakes

convener:Saeko Kita(International Institute of Seismology and Earthquake Engineering, BRI), Tomohiro Ohuchi(Geodynamics Research Center, Ehime University), Marcel Thielmann(Bavarian Geoinstitute, University of Bayreuth), Ryo Okuwaki(Research Institute of Earthquake and Volcano Geology, Geological Survey of Japan, National Institute of Advanced Industrial Science and Technology)

The purpose of this session is to share recent advances of geo-scientifical studies for intraslab and shallow-depth intraplate earthquakes. We seek to formulate future directions of the interdisciplinary study of the occurrence of intermediate-depth and deep earthquakes from the viewpoint of seismology, geodynamics and mineral physics. We welcome presentations from a wide variety of scientific disciplines, including seismology, seismotectonics, geodynamics, mineral and rock physics, other geophysics, geology, and numerical modeling.

[SCG50-P01] Changes in seismicity rate, stress orientations, and b-values before and after ETS events in the Philippine sea plate under Kii Peninsula

*Saeko Kita[1], Heidi Houston[2], Sachiko Tanaka[3], Youichi Asano[3], Takuo Shibutani[4], Naoki Suda[5] (1.Building Research Institute, 2.USC, 3.NIED, 4.DPRI, Kyoto University, 5.Hiroshima University)

[SCG50-P02] **Inhomogeneous conduit across slab controlled by intraslab stress heterogeneity in the Nankai subduction zone**

*Makoto Otsubo[1], Ayumu Miyakawa[2], Ikuo Katayama[3], Keishi Okazaki[4] (1.Geological Survey of Japan, Research Institute of Earthquake and Volcano Geology, 2.Geological Survey of Japan, Research Institute of Geology and Geoinformation, 3.Hiroshima University, 4.JAMSTEC)

[SCG50-P03] New insights into the mechanism of deep-focus earthquakes

*Ayako Tsuchiyama[1], Junichi Nakajima[1] (1.Tokyo Institute of Technology)

[SCG50-P04] Faulting in deforming harzburgite under wet conditions

*Tomohiro Ohuchi[1], Xinglin Lei[2], Yuji Higo[3], Yoshinori Tange[3], Takeshi Sakai[1] (1.Geodynamics Research Center, Ehime University, 2.National Institute of Advanced Industrial Science and Technology, 3.Japan Synchrotron Radiation Research Institute)

[SCG50-P05] Semi-brittle behavior of olivine single crystals under the conditions of Earth's mantle transition zone

Yoshihisa Naruse[1], *Tomohiro Ohuchi[1] (1.Geodynamics Research Center, Ehime University)

[SCG50-P06] High-pressure deformation experiments on peridotite gouges under hydrothermal conditions, using a deformation-DIA apparatus

*Maki Semba[1], Ken-ichi Hirauchi[1], Tomohiro Ohuchi[2], Katsuyoshi Michibayashi[3] (1.Department of Geosciences, Faculty of Science, Shizuoka University, 2.Geodynamics Research Center, Ehime University, 3.Department of Earth and Planetary Sciences, Nagoya university)

[SCG50-P07] Stable fault slip in antigorite-olivine aggregates at high pressures

Mai Ikehara[1], *Tomoaki Kubo[1], Takuya Iwasato[2], Yuji Higo[3], Masahiro Imamura[1], Yoshinori Tange[3] (1.Kyushu University, 2.Shin-Nippon Nondestructive Inspection Co., Ltd., 3.JASRI)

[SCG50-P08] Rheology and frictional instability of lawsonite in high pressure deformation experiments

*Rei Shiraishi[1], Jun Muto[1], Akihiro Tsunoda[2], Sando Sawa[1], Akio Suzuki[1] (1.Department of Earth Science, Graduate School of Science, Tohoku University, 2.Earthquake Research Institute, University of Tokyo)

[SCG50-P09] Grain Size Dependency of Olivine-Spinel Phase Transformational Mechanism Responsible for Deep-focus Earthquakes

*Sando Sawa[1], Jun Muto[1], Nobuyoshi Miyajima[2], Hiroyuki Nagahama[1] (1.Department of Earth Science, Tohoku University, 2.Bayerisches Geoinstitut, University of Bayreuth)

[SCG50-P10] **Seismicity and mineral destabilizations in the subducting mantle up to 6 GPa, 200 km depth**

*Thomas P. Ferrand[1] (1.Earthquake Research Institute)

[SCG50-P11] Receiver function imaging of subducting Pacific plate and mantle wedge under Japanese islands using denser network of stations

*HyeJeong Kim[1], Hitoshi Kawakatsu[1], Takeshi Akuhara[1], Masanao Shinohara[1] (1.Earthquake Research Institute, The University of Tokyo)

[SCG50-P12] Strong S-wave attenuation in the mantle wedge beneath the NE Japan and interpretations of high-frequency wave propagation path of intraslab earthquakes

*Takahiro Shiina[1,2], Kei Katsumata[2], Kiyoshi Yomogida[3], Aitaro Kato[1] (1.Earthquake Research Institute, The University of Tokyo, 2.Institute of Seismology and Volcanology, Graduate School of Science, Hokkaido University, 3.Graduate School of Science, Hokkaido University)

Changes in seismicity rate, stress orientations, and b-values before and after ETS events in the Philippine sea plate under Kii Peninsula

*Saeko Kita[1], Heidi Houston[2], Sachiko Tanaka[3], Youichi Asano[3], Takuo Shibutani[4], Naoki Suda[5]

1. Building Research Institute, 2. USC, 3. NIED, 4. DPRI, Kyoto University, 5. Hiroshima University

The slip on the plate interface has the potential to affect the stress field and seismicity within the subducting slab. Several studies have examined the interaction of slow slip phenomena with intraslab earthquakes [Nankai and Tokai regions, Han et al. 2014; Mexico, Radiguet et al. 2018, 2018 JpGU meeting; New Zealand, 2018, Warren-Smith, 2018 AGU meeting]. Kita et al. [2018, SSJ meeting] reported the stress change in the whole slab associated with ETS times based on stress tensor inversion results. However, we find a clear double seismic zone under Kii Peninsula, as also noted in a previous study [e.g. Miyoshi and Ishibashi, 2004]. Therefore, we here examine seismicity rate variations, stress changes, and b-value variations of seismicity separately for the upper plane events and oceanic mantle ones relative to ETS timings beneath the Kii Peninsula. We use the JMA earthquake catalog, the NIED tremor catalog, the upper surface of the Philippine sea plate estimated by Shibutani and Hirahara [2016], P-wave polarity data by NIED, and a stress tensor inversion code [Vavrycuk, 2014].

We determined the timings of ~30 large ETS beneath the Kii Peninsula from 2001 to 2017, and categorized slab seismicity relative to the occurrence times of nearby the ETS (i.e., 60 days before or after). We then combined or stacked the slab seismicity based on these relative occurrence times. The rate of seismicity both in the upper plane events and in the oceanic mantle ones after the ETS timings clearly decreased, compared to the rate before the ETS timings. The peaks of b-values of seismicity both in the upper plane events and oceanic mantle ones were found to occur 1.5 months before ETS. A change in stress orientations before and after the ETS was seen in the oceanic mantle, and a relatively small change was seen for the upper plane events. The stress change in the upper plane events appears to be larger in the region updip of the ETS zone. The results of our study suggest that the aseismic slip on the plate boundary may affect the stress field and the occurrence of seismicity within the subducting slab beneath the Kii Peninsula. Fluid migration from the oceanic slab into the ETS zone on the plate boundary could be related to the interaction of slow slip phenomena with intraslab earthquakes.

Keywords: Intraslab earthquake, ETS, stress change, b-value, time change, Kii peninsula

©2019. Japan Geoscience Union. All Right Reserved.

Inhomogeneous conduit across slab controlled by intraslab stress heterogeneity in the Nankai subduction zone

*Makoto Otsubo[1], Ayumu Miyakawa[2], Ikuo Katayama[3], Keishi Okazaki[4]

1. Geological Survey of Japan, Research Institute of Earthquake and Volcano Geology, 2. Geological Survey of Japan, Research Institute of Geology and Geoinformation, 3. Hiroshima University, 4. JAMSTEC

Non volcanic deep low-frequency tremors and slow slip events occur simultaneously in the transition zone from locked to continuously creeping fault at the down dip portion of the Nankai Trough subduction zone, southwestern Japan. The occurrence of these slow earthquakes is attributed to the effect of high pore pressures on the plate boundaries. The Nankai Trough subduction zone has a discontinuous band of occurrence of these slow earthquakes along the trench. Here we show that spatial variation of intraslab stress can control fluid migration through the subducted Philippine Sea slab to the plate boundary. The tri-axial normal faulting stress detected by the stress tensor inversion by using focal mechanisms in the slab controls anisotropies of permeability trending NNW–SSE sub-horizontal orientation from the subducted Philippine Sea slab to the plate boundary. The inhomogeneous condition controlled by the spatial stress heterogeneities in the subducted Philippine Sea slab represents the intraslab fluid pathway. The hypothesis is consistent with spatial heterogeneity of slow earthquake activities and $^{3}He/^{4}He$ ratio distributions.

Keywords: Fluid, Nankai Trough, Slab, Slow earthquake, Stress

©2019. Japan Geoscience Union. All Right Reserved.

New insights into the mechanism of deep-focus earthquakes

*Ayako Tsuchiyama[1], Junichi Nakajima[1]

1. Tokyo Institute of Technology

Generally, deep-focus earthquakes were generated in subducting slabs and occurred along some specific regions such as Izu-Bonin zone and Tonga-Fiji zone. We have not identified their occurrence mechanisms, even though some plausible hypotheses, dehydration embrittlement, thermal and shear plastic instability, and transformational faulting, were proposed. In this study, we try to obtain new constraints that deepen the understanding of deep-focus earthquakes through waveform analysis of earthquakes in the Izu-Bonin subduction zone.

First, we picked up 460 quakes at a depth range of 300-400 km in 2003-2015 beneath Tokai area from the catalog data provided by Japan Meteorological Agency, and relocated them with double-difference earthquake relocation algorithm (hypoDD; Waldhauser and Ellsworth, 2000). Second, we computed their coherence values between all available pairs of earthquakes with cross-spectrum analysis. Then, we were successful to identify a few earthquake clusters that had a very high coherence value over 0.9 in a long time window of 40 s including P and S waves. Moreover, we relocated these earthquakes with hypoDD again by using precisely-determined differential travel-time data derived from waveform data. As a result, we could find that earthquakes in each cluster occurred on single fault plane with complementary rapture areas.

Additionally, we implemented moment tensor inversion (Gephart and Forsyth, 1984) and estimated the stress field around the region where we discovered a few clusters showing waveform similarities. Moreover, we computed the amount of stress drop of the similar earthquakes with spectrum analysis of seismic wave. Through these waveform analyses, we interpreted that the mechanism of these similar deep-focus earthquakes could be explained by combining two possible mechanisms; dehydration embrittlement that regulates the rupture initiation and thermal and shear plastic instability that controls the rupture propagation along a pre-existing fault.

Keywords: deep-focus earthquakes, intraslab earthquakes

©2019. Japan Geoscience Union. All Right Reserved.

Faulting in deforming harzburgite under wet conditions

*Tomohiro Ohuchi[1], Xinglin Lei[2], Yuji Higo[3], Yoshinori Tange[3], Takeshi Sakai[1]

1. Geodynamics Research Center, Ehime University, 2. National Institute of Advanced Industrial Science and Technology, 3. Japan Synchrotron Radiation Research Institute

The subduction zone produces a major fraction of the Earth's seismic activity. The mechanisms of intermediate-depth (> 40 km depth) and deep-focus (> 300 km) earthquakes are fundamentally different from those of shallow (< 40 km) earthquakes. This is because the frictional strength of silicate rocks exceeds the upper limit of the stress level in the upper mantle (< 300 MPa: Obata and Karato, 1995) at pressures higher than 1 GPa (~30 km depth). Therefore, the cause of intraslab seismicity at intermediate depths has been attributed to dehydration of serpentinite (e.g., Peakock, 2001) because the water released during dehydration reaction of serpentinite reduces the effective confining pressure. The dehydration embrittlement model is now widely accepted, because the location of the double seismic zone in the subducting Pacific slab corresponds to the main dehydration field in the pressure-temperature diagram of the hydrous peridotite (Omori et al., 2002).

To evaluate the effect of water on semi-brittle behavior of harzburgite, we conducted in-situ uniaxial deformation experiments on as-is/water-saturated harzburgite at pressures 1.2-3.0 GPa and temperatures 770-1250 K with a constant displacement rate using a deformation-DIA apparatus. Pressure, stress, and strain were measured in situ by using x-ray diffraction patterns and radiographs. Acoustic emissions (AEs) were also recorded continuously on six sensors, and three-dimensional AE source location were determined.

Formation of throughgoing faults was observed even when differential stress is much lower than the confining pressure (i.e., > 0.3 times of confining pressure) in water-saturated harzburgite. This is contrast to the case of water-saturated dunite (Ohuchi et al., 2018), in which fracture strength exceeds the confining pressure (i.e., Goetze's criterion). Creep strength of water-saturated harzburgite was lower than that of as-is harzburgite (~0.5-1 GPa at each temperature). Weakening of the harzburgite by the aqueous fluid resulted in the reduction in the number of AE events and decrease in fault slip rate (< 3.6E-4 s^{-1} at a stress of < 1.05 GPa). Stress/pressure drop around the timing of a faulting was limited at strains of 1E-4 s^{-1}. The aseismic faulting observed in the water-saturated harzburgite implies that silent slip events around the subduction interface is due to semi-brittle flow of water-saturated harzburgite (i.e., a dehydration product of antigorite).

Keywords: harzburgite, water, semi-brittle flow

©2019. Japan Geoscience Union. All Right Reserved.

Semi-brittle behavior of olivine single crystals under the conditions of Earth’s mantle transition zone

Yoshihisa Naruse[1], *Tomohiro Ohuchi[1]

1. Geodynamics Research Center, Ehime University

The origin of deep-focus earthquakes, which occur at depths of 300-700km in the subducting slabs, fundamentally differs from that of other earthquakes and has been attributed to the pressure-induced phase transition in olivine. Previous studies on Mg_2GeO_4 olivine have shown that grain size reduction induced by the phase transition in olivine causes shear localization (e.g., Burnley et al., 1991; Schubnel et al., 2013). Schubnel et al. (2013) reported intense acoustic emissions around the timing of a faulting which would be induced by shear localization in polycrystalline Mg_2GeO_4 olivine. In order to understand the relationship between fracturing and the phase transition in olivine, we conducted deformation experiments on single crystals of San Carlos olivine (Fo_{91}) at pressure of 10-15 GPa and temperatures of 1000-1100 degC using a deformation-DIA apparatus. Single crystal of olivine was chosen to exclude the effect of grain boundaries on nucleation of high-pressure phases of olivine (i.e., wadsleyite and ringwoodite).

Array of microcrack parallel to either (100), (010) or (110) plane was developed at an ~50 degree to the direction of uniaxial compression. Rotation of olivine axes associating the formation of subgrain boundaries was observed around the microcrack arrays, showing that plastic deformation of the olivine single crystal inevitably associated formation of the microcracks. In most samples, microcracks coalesced and then a few throughgoing fractures were developed. Particles of wadsleyite /ringwoodite having a diameter of a few micrometer or less were preferentially nucleated on the microcrack surfaces. Ultrafine-grained domains, which consist of the wadsleyite /ringwoodite particles, were formed along the throughgoing fractures. Development of a banded ultrafine-grained domain was also observed along a throughgoing fracture, implying that shear localization could occur as a result of semi-brittle flow of olivine and a transition from dislocation creep to grain-size-sensitive creep in subducting slabs at depths > 410 km.

Keywords: olivine, phase transition, semi-brittle flow, microcrack, deep-focus earthquake

©2019. Japan Geoscience Union. All Right Reserved.

High-pressure deformation experiments on peridotite gouges under hydrothermal conditions, using a deformation-DIA apparatus

*Maki Semba[1], Ken-ichi Hirauchi[1], Tomohiro Ohuchi[2], Katsuyoshi Michibayashi[3]

1. Department of Geosciences, Faculty of Science, Shizuoka University, 2. Geodynamics Research Center, Ehime University, 3. Department of Earth and Planetary Sciences, Nagoya university

In subducting oceanic plates, the focal depth of intraslab earthquakes is deeper (>40 km) than that of interplate earthquakes. Since the normal stress on faults (e.g., outer-rise faults) hosting the intraslab earthquakes is too high to generate brittle shear failure, there may be some mechanisms to weaken effective fault strength. In addition, the hypocenter distribution of intraslab earthquakes forms double-planed structure of the deep seismic zone, and the location of the lower plane is in accord with the stability limit of serpentine (antigorite), suggesting shear deformation of antigorite-bearing peridotite gouges in the presence of hydrothermal water. Here, in order to understand the influence of hydrous minerals on the fault strength, we performed deformation experiments on simulated peridotite gouges with compositions of dunite (100% olivine) and harzburgite (70% olivine/30% orthopyroxene) under hydrothermal conditions, using a deformation-DIA apparatus. The experiments were conducted at a temperature of 580˚C, a confining pressure of 2.5 GPa, and shear strain rates of 2.70 $\times 10^{-5}$ to 1.03 $\times 10^{-4}$ s^{-1}. In the deformed peridotite gouges, localized shear zones such as R_1 and B shears were observed, and these shears were accompanied with newly formed hydrous phases (serpentine or talc). Olivine grains have a crystal preferred orientation characterized by a slip system of [001] (010). These results indicate that semi-brittle flow is a major deformation mechanism of the peridotite gouges. Considering low coefficients of friction of serpentine and talc, we can suggest that the infiltration of seawater along outer-rise fault planes and subsequent hydrothermal alteration result in effective shear strengths low enough to produce intraslab earthquakes.

Keywords: deformation-DIA apparatus, peridotite, serpentinization, frictional strength

©2019. Japan Geoscience Union. All Right Reserved.

Stable fault slip in antigorite-olivine aggregates at high pressures

Mai Ikehara[1], *Tomoaki Kubo[1], Takuya Iwasato[2], Yuji Higo[3], Masahiro Imamura[1], Yoshinori Tange[3]

1. Kyushu University, 2. Shin-Nippon Nondestructive Inspection Co., Ltd., 3. JASRI

Intermediate-depth earthquakes are observed to occur within subducting oceanic plates at depths of about 60-300 km where most materials exhibit plastic deformation rather than brittle failure, owing to high pressures and temperatures. Dehydration embrittlement of hydrous minerals, particularly antigorite serpentine, is one of the most popular hypotheses for explaining shear instability under such conditions (e.g., Raleigh and Paterson, 1965). Recent high-pressure deformation experiments, monitoring Acoustic Emission (AE) activities upon syndeformational antigorite dehydration, showed that dehydration embrittlement was not observed on single-phase antigorite (Gasc et al., 2017), whereas dehydration related faulting was formed on antigorite-olivine aggregates with strong AEs (Ferrand et al., 2017). However, most of the previous high-pressure studies have been conducted in axial compression at relatively low pressures (< 3.5 GPa), insufficient to consider intermediate-depth earthquakes. Therefore, in this study, we conducted high-pressure shear deformation experiments on two-phase aggregates of antigorite and olivine, considering partially serpentinized peridotites, in order to investigate possible shear localization and shear instability up to 7 GPa.

Deformation experiments were conducted at 5-7 GPa, 350-700 ℃ using Deformation-DIA apparatuses at SPring-8 (BL04B1). Monochromatic X-rays (50-60 keV) were used to measure dehydration kinetics, shear strain and stress with recording AEs. We used three kinds of starting materials; natural cored antigorite from Kawarakoba in Nagasaki prefecture, forsterite polycrystal, and two-phase sintered mixtures of antigorite and San Carlos olivine (antigorite 10, 30, 50 vol %). The samples were cut into disks having thickness of 300 μm and used for a shear deformation study by being assembled between two 45˚-cut alumina pistons. In shear deformation experiments, the starting disk was compressed to 5 or 7 GPa at room temperature, annealed at 350 or 400 ℃ for 1 h, and then deformed with an anvil displacement rate of 200 μm/h. In some experiments, we increased temperature during shear deformation with a ramping rate of 0.1 ℃/sec to induce dehydration reaction. Microstructures of the recovered samples were examined by an optical microscope and a scanning electron microscope (SEM).

From X-ray radiography images, we observed shear localization in all two-phase samples deformed within the antigorite stability field at 5 GPa. The locallization occurred when homogeneous shear strain γ reached 0.4-0.9 (strain rate 1.3-2.2 $\times 10^{-4}$/s), and then most strains were partitioned to the fault zone with the slip velocity of 4.6-9.1 $\times 10^{-2}$ μm/s. Because no AEs were detected from the sample region, the localized deformation is thought to occur by stable sliding. SEM observations revealed that a thin shear deformation zone was formed along the fault, where the plastic deformation of both antigorite and olivine was significant. Striation and nanograins were observed on the fault plane, suggesting the formation of nanogouge. In contrast, homogeneous deformation was developed during antigorite dehydration with temperature ramping, even in the sample showing shear localization in the antigorite stability field. Under higher pressure condition 7 GPa, shear localization did not occur in all samples regardless of temperature. These results suggest that, although AE activities were detected with the dehydration in the antigorite-olivine aggregates up to 3.5 GPa in the previous study, further increase of pressure inhibits shear instability and shear localization. Thus, other dehydration reactions and/or instability mechanisms are required to explain intermediate-depth earthquakes deeper than ~100 km.

©2019. Japan Geoscience Union. All Right Reserved.

©2019. Japan Geoscience Union. All Right Reserved.

Rheology and frictional instability of lawsonite in high pressure deformation experiments

*Rei Shiraishi[1], Jun Muto[1], Akihiro Tsunoda[2], Sando Sawa[1], Akio Suzuki[1]

1. Department of Earth Science, Graduate School of Science, Tohoku University, 2. Earthquake Research Institute, University of Tokyo

The cause of intermediate-depth earthquakes (50-300 km) in subducting slabs have been proposed to be the dehydration embrittlement (e.g., Raleigh and Paterson, 1965), because there are many kinds of hydrous minerals in a subducting slab and hypocenter distribution coincides with the dehydration boundary determined by high pressure experiments (e.g., Hacker et al., 2003). Many experimental studies on antigorite have been conducted, but a few previous works about dehydration embrittlement of lawsonite-bearing rocks experimentally. Lawsonite, $CaAl_2Si_2O_7(OH)_2H_2O$, is a hydrous mineral which contains 11 wt% water in its structure as both water molecules and a hydroxy group (Cmodi and Zanazzi, 1996). Lawsonite is one of the candidate for dehydration embrittlement in cold subducting slabs, however previous works have apparently contradictory results. Okazaki and Hirth (2016) showed that lawsonite dehydration induced unstable fault slip based on deformation experiments of pure lawsonite using Griggs-type deformation apparatus at 1 GPa. On the other hand, Incel et al. (2017) also investigated deformation properties of lawsonite and glaucophane mixture at 1.5 to 3.0 GPa using deformation-DIA apparatus. They insisted that there is no evidence for a straightforward relation to the dehydration of lawsonite and the brittle failure of samples. So, we have conducted the deformation experiments of lawsonite under the cold slab conditions in order to clarify the deformation property of lawsonite and understand the relationship between dehydration and brittle failure.

Experiments were carried out using Deformation-Cubic Anvil Press (D-CAP) installed at KEK PF AR-NE7A beamline. Pure lawsonite powder (98%) was used as starting materials. Deformation experiments were carried out at a pressure of 6 GPa and temperatures of 300 - 800 ˚C. The temperature was increased at the same time as deformation started. The temperature ramping rate over the strain rate was set the ranges for the real subducting slab, which ranges from 10^2 to 10^4 ˚C (Chernak and Hirth, 2011; Okazaki and Hirth, 2016). During deformation stages, strain, stress and transformation rate were measured for in-situ using a monochromatic X-ray beam with an energy of 60 keV.

Four experiments showed rapid stress drop during temperature ramping before lawsonite dehydration starts. We observed microstructure of recovered samples, there are many through going faults and microcracks but no dehydration products. Our results indicate that brittle process and frictional sliding occur without dehydration of lawsonite. This suggests that the intermediate-depth earthquakes can be caused by the deformation itself of lawsonite without the dehydration of lawsonite.

Keywords: intermediate-depth earthquakes, dehydration embrittlement, Lawsonite

©2019. Japan Geoscience Union. All Right Reserved.

Grain Size Dependency of Olivine-Spinel Phase Transformational Mechanism Responsible for Deep-focus Earthquakes

*Sando Sawa[1], Jun Muto[1], Nobuyoshi Miyajima[2], Hiroyuki Nagahama[1]

1. Department of Earth Science, Tohoku University, 2. Bayerisches Geoinstitut, University of Bayreuth

Deep-focus earthquakes occur at the depth from 440 km to 660 km in the subducting slab. The mechanism responsible for the earthquakes is thought to be different from that of shallow earthquakes, so that previous studies have reported the various mechanisms. By the geophysical observations and deformation experiments, the phase transformational faulting mechanism is presumed as the precursor of deep-focus earthquakes (e.g., Zhan et al., 2014). The phase transformational faulting mechanism is that metastable olivine in the slab undergoes the phase transformation to fine-grained spinel and faulting occurs with strain localization into the fine-grained spinel. This shear instability depends on grain size. Furthermore, the grain size may restrict the pressure- and temperature-conditions where the shear instability occurs, that is, the region of slab where deep-focus earthquakes occur. However, previous studies have conducted deformation experiments with finer grain size than expected in the slab (e.g., Burnley et al., 1991). Hence, the results from the laboratory experiments cannot directly apply to the geophysical observation. In this study, to reveal the grain size dependency on the phase transformational faulting, we conducted the deformation experiments of germanate olivine (about 3 μm), which is an analogue material of silicate olivine, finer-grained than that in previous studies (30 μm). We used a Griggs-type solid-confining media deformation apparatus. The confining pressure, temperature and strain rate are 1.2 GPa, 400~900 ℃ and 2.0×10^{-4} s^{-1}, respectively. Even though deformation experiments were conducted under wider temperature conditions than previous studies, we did not observe any shear instability event with apparent stress drops. Also, Raman spectroscopy clarified that the germanate olivine underwent the transformation to spinel at temperatures higher than 500 ℃. Shear instability does not occur because the difference in grain sizes between olivine and nucleated spinel in this study was smaller than those in previous studies. Also, the transformation temperature in this study was much lower than those in previous study (T > 1000 ℃ in Burnley et al., 1991). Considering the rate equation of the transformation (Chan, 1956), small grain size promotes the transformation, but these fast rates of the transformation cannot be explained only by the effect of the grain size. Therefore, the presence of water such as absorbed water in a starting material can also contribute to promote the transformation. Hence, both small initial grain size and a little amount of water promote the transformation even at lower temperature. These results indicate that the phase transformational faulting mechanism has strong grain size dependency. In summary, the pressure- and temperature-conditions where the faulting occurs depends on the grain size of olivine and amount of water. Because the grain size in the slab is larger than that in the experiments, by extrapolating from these results, we may restrict the region of slab where deep-focus earthquakes occur.

This work was supported by the JSPS Japanese-German Graduate Externship.

[Reference]
Burnley et al. (1991), JGR, vol 96, 425-443.
Chan (1956), Acta Metallurgica, vol 4, 449-459.
Zhan et al. (2014), EPSL, vol 385, 89-96.

©2019. Japan Geoscience Union. All Right Reserved.

Keywords: Deep-focus earthquakes, Griggs type piston-cylinder apparatus, phase transformation

©2019. Japan Geoscience Union. All Right Reserved.

Seismicity and mineral destabilizations in the subducting mantle up to 6 GPa, 200 km depth

*Thomas P. Ferrand[1]

1. Earthquake Research Institute

In the subducting oceanic lithosphere, a significant part of the seismicity is triggered in the mantle, especially along the upper and lower Wadati-Benioff planes. Several studies have investigated the potential involvement of dehydration reactions in the triggering mechanism of mantle earthquakes. Recent experimental results reveal that, under subduction conditions, mechanical instabilities nucleate in strong stable mineral aggregates during the destabilization of minor amounts of antigorite, i.e. the high-temperature serpentine, through a stress transfer, without any fluid overpressure. Here I confront these laboratory results to seismological observations. On one hand, most of the natural hydrous magnesium silicates seem to be known, with experimentally-deduced stability limits up to 7 GPa, at least, available as relatively accurate estimates. On the other hand, recent achievements in thermal structure of subduction zones combined with precise hypocentre relocation give access to pressure and temperature conditions at earthquakes hypocentres. A series of P-T diagrams summarizes the stability limit of minerals that may be part of natural peridotite with variable compositions at pressures from 0.5 to 6 GPa and temperatures from 200 to 950˚C, and compares it with seismicity. Both hydrous and anhydrous phases are considered. A myriad of minor metamorphic reactions could participate in a transformation-driven stress transfer, even if the stability limits of serpentine minerals seem to correlate with most of the observed seismicity.

Keywords: earthquakes, intraslab, DDST, dehydration, transformation, subduction

©2019. Japan Geoscience Union. All Right Reserved.

Receiver function imaging of subducting Pacific plate and mantle wedge under Japanese islands using denser network of stations

*HyeJeong Kim[1], Hitoshi Kawakatsu[1], Takeshi Akuhara[1], Masanao Shinohara[1]

1. Earthquake Research Institute, The University of Tokyo

Receiver function imaging has been frequently used by different groups focusing on different depths of the Japanese subduction zone. The overlying crust (Shiomi and Park, 2008, Bianchi et al, 2015), the Pacific plate before (Kawakatsu et al., 2009) and after subduction (Kawakatsu and Watada, 2007; Wirth and Long, 2012), and the mantle transition zones (Kawakatsu and Yoshioka, 2011; Tauzin et al., 2018) were discussed using the NIED array stations (Hi-net and F-net). Recently, deployment of ocean bottom seismometers (OBSs) enabled studies of subduction zones closer to the trench (e.g., Akuhara and Mochizuki, 2015). Kawakatsu and Kim (2018, SSJ) have obtained a new version of receiver function imaging using 14-year long of Hi-net data. However, there are other land stations (e.g., J-array) that can improve the station coverage. Here, we collect data from available on-land stations deployed in north-eastern Japan to obtain a denser 2-D array of stations. Additionally, data from temporary OBS stations (Shinohara et al. 2012) are gathered to image the subducted Pacific plate in shallower depths than previously available. Continuous imaging from ocean to land will help to constrain transition of the hydrated oceanic crust along subduction that is expressed as a low velocity layer for better understanding of the hydration/dehydration processes during subduction, which might be related to the occurrence of subduction zone earthquakes.

Keywords: subduction zone, receiver function, ccp stacking

©2019. Japan Geoscience Union. All Right Reserved.

Strong S-wave attenuation in the mantle wedge beneath the NE Japan and interpretations of high-frequency wave propagation path of intraslab earthquakes

*Takahiro Shiina[1,2], Kei Katsumata[2], Kiyoshi Yomogida[3], Aitaro Kato[1]

1. Earthquake Research Institute, The University of Tokyo, 2. Institute of Seismology and Volcanology, Graduate School of Science, Hokkaido University, 3. Graduate School of Science, Hokkaido University

For intraslab earthquakes at intermediate-depths in NE Japan, especially at greater than about 100-km depths, it has been often recorded that high-frequency waveform higher than 8 Hz show a remarkable delay of arrival compared with S wave which predominates in a low-frequency band. The magnitude of the delay is little in the forearc region, whereas it increases up to about 40 s in the backarc region. In this study, we investigate the details in the propagation processes of the high-frequency later phase observed for the intraslab earthquakes at the intermediate-depths. To constrain the source location of the high-frequency later phase, we employ the source-scanning algorithm (SSA) [Kao and Shan, 2004] with realistic velocity and attenuation structures, assuming that the high-frequency later phase is generated by the single scattering process. Namely, we estimate a scattering point by using mean-square amplitudes which is synthesized from two horizontal components of the observed waveforms.
Results in frequency bands of 4-32 Hz show that scattering points are distributed beneath the forearc region. The scattering points can reproduce the observed delays of amplitude amplifications associating with the high-frequency later phases. Moreover, similar locations of the scattering points are imaged along the forearc region in the entire NE Japan. These results indicate that high-frequency later phase is a wave scattered at the forearc region and that short wave-length heterogeneity generally developed in the forearc region of NE Japan.
This interpretation well matches implications from previous studies [e.g., Yomogida et al., 2004; Hasemi and Horiuchi, 2010]. Additionally, the obtained distributions of scattering points which appear to surround the highly attenuating mantle wedge suggest that attenuation structure strongly controls propagation paths of seismic wave, in particular, a high-frequency wave. In other words, the identifications of high-frequency later phase may become easy because the amplitude of direct wave crossing the high-attenuation zone decreases. To confirm this consideration, we estimate *Qs* along the direct wave by using the coda-normalization method [e.g., Aki, 1980]. This estimation provides 2-3 times smaller path-averaged *Qs* in seismic records of which rays lay on the backarc and the volcanic front than that of which rays lay on the forearc region. These results support that spatial variation in *QS* produces heterogenous propagations of seismic waves emitted from intraslab earthquakes. It is thus required to take scattering and attenuation structures simultaneously into account to understand complex behaviors of high-frequency waves in a future study.

Keywords: S-wave attenuation, Intraslab earthquakes, High-frequency later phase, Scattered wave

©2019. Japan Geoscience Union. All Right Reserved.

[E] Poster | S (Solid Earth Sciences)：S-CG Complex & General

Thu. May 30, 2019 10:45 AM - 12:15 PM JST | Thu. May 30, 2019 1:45 AM - 3:15 AM UTC | Poster Hall International Exhibition Hall8, Makuhari Messe_6

[S-CG51] Role of volatiles on Earth and planetary dynamics

convener:Takayuki Ishii(Bavarian Research Institute, University of Bayreuth), Eiji Ohtani(Department of Earth and Planetary Materials Science, Graduate School of Science, Tohoku University), Michihiko Nakamura(Division of Earth and Planetary Materials Science, Department of Earth Science, Graduate School of Science, Tohoku University), Bjorn Mysen(Geophysical Laboratory, Carnegie Inst. Washington)

This session addresses how volatile species affect dynamics of the
Earth and planets from natural observations, laboratory experiments, and
numerical modeling in the temperature, pressure, and oxygen activity
range from the early stage of the planet formation to the present. The
volatiles can be critical in zones of magma storage and ascent, mantle
upwelling and melting in the fluid-enriched subduction zones, in the
mantle transition zone, in the lower mantle, in the core-mantle boundary,
and in Earth and planetary cores. However, volatiles affect properties
and processes differently depending on their pressure, temperature, and
redox conditions, which vary in time and space.
 This session aims to address how volatiles control the dynamic
processes of the Earth and planets, governed by their geophysical and
geochemical properties. We welcome papers dealing with geological and
laboratory observations coupled with numerical modeling on the role of
volatiles. The topics include (1) Stability relations, chemical and
physical properties of crystalline, molten and fluid phases,
partitioning of volatiles among these phases, (2) Rheological and other
physical properties of minerals, and the effects of intergranular fluid
on the properties, (3) Volatiles and dehydration induced seismicity and
volcanism in various tectonic regions including subduction zones, and (4)
Effects of volatiles in numerical simulation of geo-tectonics, and (5)
Magma outgassing and its control of volcanic eruption dynamics.

[SCG51-P01] Permeability prediction of porous media with the finite difference Stokes solver LaMEM

*Philipp Eichheimer[1], Wakana Fujita[2], Marcel Thielmann[1], Anton Popov[3], Gregor Golabek[1], Boris Kaus[3], Maximilian Kottwitz[3] (1.Bayerisches Geoinstitut, University of Bayreuth, 2.Department of Earth Science, Tohoku University, Sendai, 3.Institute of Geosciences, Johannes Gutenberg University Mainz)

[SCG51-P02] Grain growth-induced fluid localization and permeability reduction

*Wakana Fujita[1], Michihiko Nakamura[1], Kentaro Uesugi[2] (1.Graduate School of Science, Tohoku University, 2.JASRI/SPring-8)

[SCG51-P03] Pargasite stability in the upper mantle at H_2O-undersaturated conditions

*Marija Putak Juricek[1], Hans Keppler[1] (1.BGI)

[SCG51-P04] **Constraining the water content at the top of the mantle transition zone with the elasticity of wadsleyite and olivine**

*Zhongqing Wu[1] (1.University of Science and Technology of China)

[SCG51-P05] ***Single crystal elasticity of Fe-bearing phase E by Brillouin spectroscopy***

*Niccolo Satta[1], Hauke Marquardt [2], Alexander Kurnosov[1], Tiziana Boffa Ballaran [1], Johannes Buchen[3], Catherine McCammon[1], Takaaki Kawazoe[4] (1.Bayerisches Geoinstitut, University of Bayreuth, 95440 Bayreuth, Germany, 2.Department of Earth Sciences, University of Oxford, South Parks Road, Oxford, UK., 3.Seismological Laboratory, California Institute of Technology, Pasadena, CA 91125, USA., 4.Department of Earth and Planetary Systems Science, Hiroshima University, Hiroshima 739-8526, Japan.)

[SCG51-P06] Discovery of two hexagonal phases in (Fe,Al)OOH under the P-T conditions of the deep lower mantle

*Lu Liu[1,2], Li Zhang[1], Hongsheng Yuan[1] (1.Center for High Pressure Science and Technology Advanced Research, 2.University of Science and Technology of China)

[SCG51-P07] **Effect of grid resolution on tectonic regimes in global-scale convection models**

*Enrico Marzotto[1], Marcel Thielmann[1], Gregor Golabek[1] (1.Bayerisches Geoinstitut)

[SCG51-P08] A 3-D crust and uppermost mantle electrical conductivity model of subduction zone beneath NE Japan

*Masahiro Ichiki[1,2], Toshiki Kaida[1], Yasuo Ogawa[3] (1.Graduate School of Science, Tohoku University, 2.International Research Institute of Disaster Science, 3.School of Science, Tokyo Institute of Technology)

[SCG51-P09] *The conditions of sublithospheric diamond formation constrained from ferric iron-rich exsolution from ferropericlase inclusions.*

*Caterina Melai[1], Daniel Frost[1], Tiziana Boffa Ballaran[1], Catherine McCammon[1] (1.Bayerisches Geoinstitute)

[SCG51-P10] **Probing the variation of the oxygen fugacity in diamond anvil cells using the Fe-Ir alloy as redox sensor**

*Serena Dominijanni[1], Catherine McCammon[1], Leonid Dubrovinsky[1], Dan Frost[1], Nobuyoshi Miyajima[1] (1.Bayerisches Geoinstitut)

[SCG51-P11] Goethite behavior at Earth's lower mantle conditions

*Egor Gennadievich Koemets[1], Maxim Bykov[1], George Aprilis[2], Timofey Fedotenko[2], Stella Chariton[1], Saiana Khandarkhaeva[1], Iuliia Koemets[1], Marcel Thielmann[1], Natalia Dubrovinsaia[2], Leonid Dubrovinsky[1] (1.BGI (Bayerisches Geoinstitut), Universität Bayreuth, Germany, 2.Material Physics and Technology at Extreme Conditions, Laboratory of Crystallography, Universität Bayreuth, Germany)

[SCG51-P12] The oxygen content of sulphides in the mantle and a geothermometer for diamond formation

*Sumith Abeykoon[1], Dan Frost[1], Vera Laurenz[1] (1.Bayerisches Geoinstitut, University of Bayreuth)

Permeability prediction of porous media with the finite difference Stokes solver LaMEM

*Philipp Eichheimer[1], Wakana Fujita[2], Marcel Thielmann[1], Anton Popov[3], Gregor Golabek[1], Boris Kaus[3], Maximilian Kottwitz[3]

1. Bayerisches Geoinstitut, University of Bayreuth, 2. Department of Earth Science, Tohoku University, Sendai, 3. Institute of Geosciences, Johannes Gutenberg University Mainz

The flow of fluids through porous media such as groundwater flow or magma migration is one of the most important processes in geological sciences. The property controlling the efficiency of the flow is the permeability of the rock, thus an accurate determination and prediction of its value is of crucial importance. For this reason, permeability of rocks has been measured across different scales. As laboratory measurements exhibit a range of limitations, the numerical prediction of permeability at conditions where laboratory experiments struggle has become an important method to complement laboratory approaches. At high resolutions, this prediction becomes computationally very expensive, which makes it crucial to develop methods that maximize accuracy. In this work we introduce the open-source finite difference solver LaMEM that can be used to numerically predict the permeability of porous media under laminar conditions. We employ a stencil rescaling method to increase accuracy due to a better description of the solid-fluid interface, thus reducing the computational cost. To validate the method, we perform a series of tests employing both analytical solutions for simplified geometries as well as results from other numerical approaches for more complicated geometries. Furthermore we compare our numerical results to laboratory measurements on glass bead samples with porosities ranging from 20% to 2.5%, showing good agreement.

Keywords: Permeability, Numerical modelling, Digital Rock Physics

©2019. Japan Geoscience Union. All Right Reserved.

Grain growth-induced fluid localization and permeability reduction

*Wakana Fujita[1], Michihiko Nakamura[1], Kentaro Uesugi[2]

1. Graduate School of Science, Tohoku University, 2. JASRI/SPring-8

Efficiency of segregation of geological fluids such as aqueous fluids and melts is an essential elementary process for volatile cycles in subduction zones. Permeability is an intrinsic rock property that controls flow rate of fluid. Various permeability models have been presented by numerical models of textually equilibrated rocks (e.g. 1, 2), laboratory measurements on synthetic rocks (e.g. 3) and estimation from cross-sectional area of synthetic rocks (4). However, there exist discrepancies among those models. Because permeability is very sensitive to microscopic geometry of pore fluid, those disagreements may arise from lack of understanding toward three-dimensional (3D) microstructure of fluid network.

Dihedral angle has been considered to be a critical parameter that controls fluid geometry and thus permeability. Beside, some previous studies shed light on the effect of grain growth on fluid distribution because it could induce pore fluid distortion and coalescence (5, 6). These studies suggest that in the actual systems where the microstructure of rocks evolve in dynamic processes, grain growth would be important along with the dihedral angle.

To investigate the effect of grain growth on the fluid distribution and permeability, we present 3D images of quartz–CHO fluid aggregates, containing nominal fluid fractions between 0.03 and 0.10. Samples were synthesized from a powdered mixture of Arkansus quartz and amorphous silica prepared by sol-gel method and hot-pressed in a piston–cylinder apparatus at 900˚C and 1.0 GPa for 192h. The fluid fractions and the dihedral angles were controlled using brucite added in the capsule bottom and oxalic acid dihydrate mixed with SiO_2 powder. 3D images were obtained using synchrotron X-ray microtomography at BL20XU experimental hutch2 of SPring-8. Regardless of dihedral angles (CO_2 content in fluids), both cross-sectional area and 3D images of samples showed grain-scale fluid localization which would be formed by pore fluid coalescence induced by grain growth. Computed permeabilities using numerical model, LaMEM (7) were almost consistent with laboratory measurements by (3) but more than one order of magnitude lower than a numerical model by (2). This would indicate that localized fluids extensively reduce permeability by reducing the diameter of fluid tubes along grain edges, which would suggest transport of water into Earth’ s deep interior by the subducting slab.

Reference:
1. von Bargen and Waff. 1986, J. Geophys. Res. 91, 9261–9276.
2. Rudge, J.F. 2018, Proc. R. Soc. Lond. A 474, 20170639.
3. Wark and Watson. 1998, Earth Planet. Sci. Lett. 164, 591–605.
4. Faul, U.H. 1997, J. Geophys. Res. 102, 10299–10311.
5. Walte et al. 2003, Geology 2003 31, 1009-1012.
6. Yoshino and Watson. 2005, Earth Planet. Sci. Lett. 235, 453–468.
7. Kaus et al. 2016, NIC Symposium 2016

Keywords: Permeability, Quartz, Grain growth, Dihedral angle, Fluid segregation

©2019. Japan Geoscience Union. All Right Reserved.

Pargasite stability in the upper mantle at H_2O-undersaturated conditions

*Marija Putak Juricek[1], Hans Keppler[1]

1. BGI

Amphibole is the most commonly occurring hydrous mineral in mantle xenoliths and the majority of upper mantle amphiboles have compositions close to pargasite end member. Previous experimental work has demonstrated that pargasite stability is sensitive to variations in bulk alkali and water content of the starting material. While it has been successfully shown that addition of more alkali leads to stabilization of pargasite to higher P and T, the effect of water on amphibole stability is not so straightforward.

At H_2O-saturated conditions, alkali elements partition strongly into aqueous fluid and become less available for crystallization of amphibole. As a result, amphibole seemingly becomes stable at higher P and T when less H_2O is added to the starting material. This observation led to the hypothesis that pargasite may be a ubiquitous phase in the upper mantle, which is believed to contain only several hundred ppm of H_2O. However, most of the previous studies determined pargasite stability at H_2 O-saturated conditions where solid phases coexist with an aqueous fluid during experiments. Since such environments are not representative of the nearly dry upper mantle, the purpose of this study is to investigate pargasite stability at H_2O-undersaturated conditions.

Because of the high specific surface area of powders, adsorption of atmospheric H_2O on fine grained starting materials prevents attaining H_2O-undersaturation by adding small amounts of water to the sample. Instead, H_2O-undersaturated conditions may be precisely controlled by diluting the water in the sample with another component. Under such conditions, solid phases are expected to coexist with a low water activity fluid throughout the experiment. As molecular nitrogen is mostly insoluble in upper mantle minerals, it can be used to adjust the water activity of the fluid to a desired low value.

All experiments were performed in a piston cylinder apparatus. The samples for H_2O-undersaturated experiments were prepared by adding silver azide (AgN_3) and brucite to a synthetic peridotite mixture. In several experiments water was added directly as $H_2O_{(l)}$. The amount of water was kept constant in all experiments (1 wt. percent) and the molar fraction of water in the N_2-H_2O fluid was adjusted to the desired value by weighing an appropriate amount of AgN_3, which decomposed to metallic silver and molecular nitrogen during heating. In H_2O-saturated experiments, no silver azide was added to the peridotite mixture. Experimental products were analyzed using JEOL JXA-8200 electron microprobe.

Preliminary results show that pargasite is not stable in equilibrium with fluids diluted to X_{H2O}=0.1 at pressures above 1 GPa. At H_2O-saturated conditions pargasite stability field can extend to pressures of 4 GPa and above 1100 ℃, depending on bulk alkali and water contents. Results from experiments at X_{H2O} =0.1 and X_{H2O}=1 suggest that pargasite can exist only in regions of the upper mantle which have been affected by high water activity fluids, such as areas in the vicinity of subduction zones. The ambient nominally anhydrous upper mantle, better represented by experiments at H_2O-undersaturated conditions, is not expected to contain pargasite.

Keywords: pargasite, stability, upper, mantle

©2019. Japan Geoscience Union. All Right Reserved.

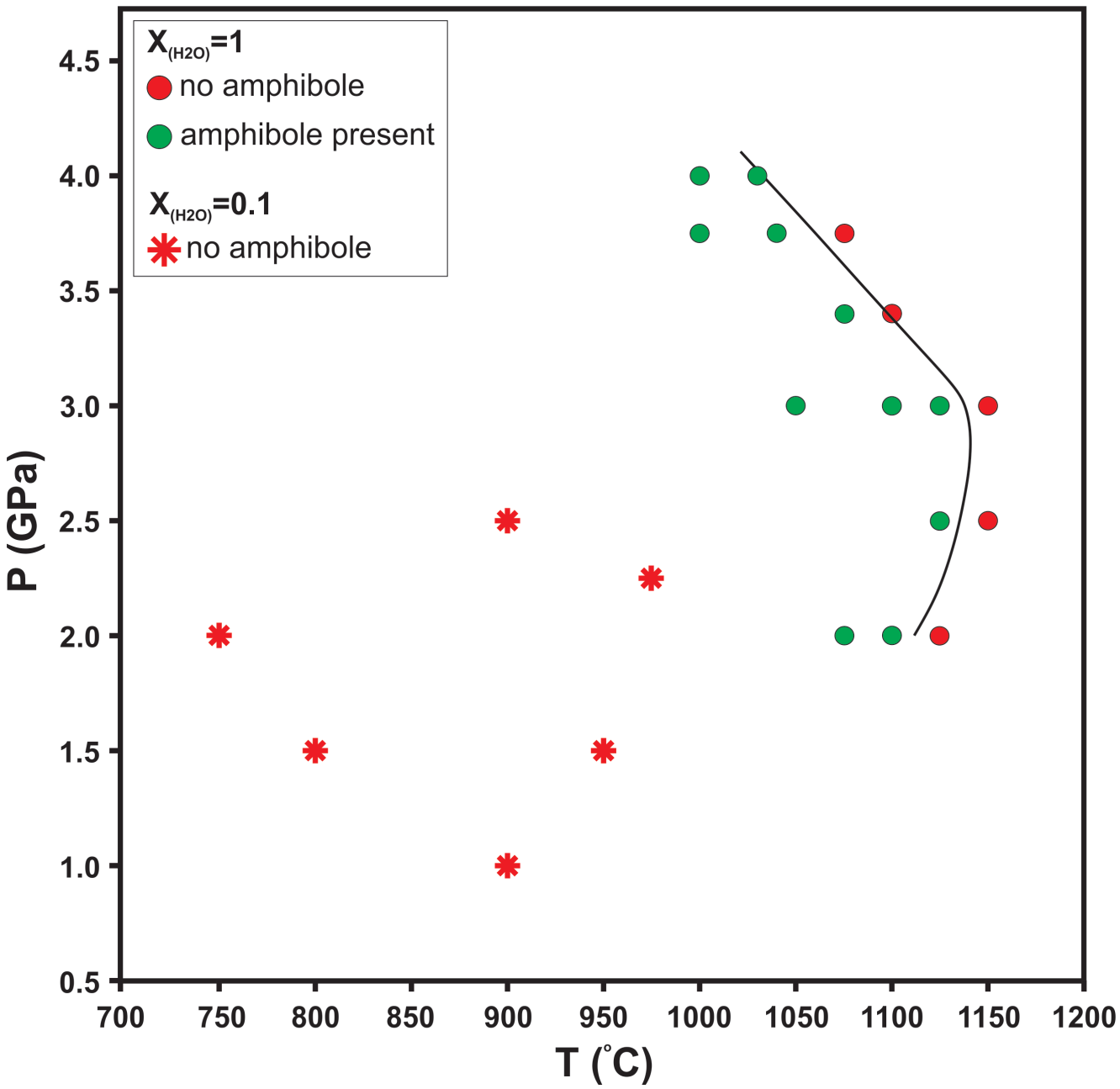

©2019. Japan Geoscience Union. All Right Reserved.

Constraining the water content at the top of the mantle transition zone with the elasticity of wadsleyite and olivine

*Zhongqing Wu[1]

1. University of Science and Technology of China

Zhongqing Wu[a,b,*], Wenzhong Wang[a,b], Michael J. Walter[c] ,Ye Peng[a,b], Simon Redfern[d],

[a] Laboratory of Seismology and Physics of Earth’ s Interior, School of Earth and Space Sciences, University of Science and Technology of China, Hefei, Anhui 230026, China

[b] Mengcheng National Geophysical Observatory, Anhui, China

[c]School of Earth Sciences, University of Bristol, Bristol BS8 1RJ, UK

[d]Department of Earth Science, University of Cambridge, Cambridge CB2 3EQ, UK

The water content in the mantle transition zone (MTZ) exerts a controlling influence on the dynamical and chemical evolution of Earth, but is poorly known. In principle the water content at the top of the transition zone can be inferred by comparing the velocity and density contrasts across the 410-km seismic discontinuity with predictions based on the phase transition of olivine to wadsleyite. The high-quality elastic data of at pressure and temperature (PT) conditions of the transition zone are crucial but are very challenge for experiments to obtain. Calculating these elastic data at high PT conditions in conventional method are also very expensive. Instead, these elastic data were calculated using the method of Wu and Wentzcovitch (2011), which reduces the computational workload to tenth of the conventional method. All calculations for two phases were conducted using the same computational details as far as possible, which guarantees that the velocity and density differences between two phases have very high precise. All these calculated elastic data agree well with the available experimental data. The iron and water effect on the elasticity are also well described.

With these high-quality elastic data covered the PT condition of the transition zone, we analyze the water and wadsleyite content at the top of the transition zone. We found that the water content of wadsleyite at the top of the transition zone can be well constrained when density and velocities jumps are considered together. For a pyrolitic mantle composition with ~60% olivine, our best fit is ~ 0.5 wt% water at the top of the transition zone. If the transition zone is dry, as suggested by some electrical conductivity models, the upper mantle may only contain ~ 50% olivine.

Wu, Z., Wentzcovitch, R.M., 2011. Quasiharmonic thermal elasticity of crystals: An analytical approach. Phys. Rev. B - Condens. Matter Mater. Phys. 83, 1–8. doi:10.1103/PhysRevB.83.184115

©2019. Japan Geoscience Union. All Right Reserved.

Single crystal elasticity of Fe-bearing phase E by Brillouin spectroscopy

*Niccolo Satta[1], Hauke Marquardt [2], Alexander Kurnosov[1], Tiziana Boffa Ballaran [1], Johannes Buchen[3], Catherine McCammon[1], Takaaki Kawazoe[4]

1. Bayerisches Geoinstitut, University of Bayreuth, 95440 Bayreuth, Germany, 2. Department of Earth Sciences, University of Oxford, South Parks Road, Oxford, UK., 3. Seismological Laboratory, California Institute of Technology, Pasadena, CA 91125, USA., 4. Department of Earth and Planetary Systems Science, Hiroshima University, Hiroshima 739-8526, Japan.

Earth’s deep water cycle plays a key role for the dynamic evolution of our planet and the development of habitable conditions. Surface water can be transported to Earth’s mantle by subduction of oceanic lithosphere. Experimental investigations have shown that water can be efficiently stored in Dense Hydrous Magnesium Silicates (DHMS) in cold subducting slabs. However, quantification of the incoming water budget based on the interpretation of seismological observations is hampered by a lack of elasticity measurements of DHMSs. Here, we report single-crystal elasticity measurements of Fe-bearing phase E, a DHMS that is stable at pressures and temperature of Earth’s mantle transition zone. A very low bulk modulus has been reported for phase E, suggesting that it might produce seismic velocity heterogeneities detectable by seismological investigations. However, the shear modulus of phase E has not been quantified.

We synthesized Fe-bearing phase E single crystals in a multi-anvil apparatus. Chemical composition as well as crystal structure have been determined using electron microprobe analysis, Mössbauer spectroscopy, and single-crystal X-ray diffraction. We derived the full elastic stiffness tensor by Brillouin spectroscopy on two single crystals of selected orientations. We found phase E to have both the lowest bulk modulus and shear modulus among the DHMSs at ambient conditions. Phase E shows very low compressional and shear velocities especially when compared to the other principal minerals likely present in subducting slabs after serpentine breakdown. Modelling of seismic velocities in dry and hydrated upper mantle and transition zone rocks suggests that the presence of even small amounts of phase E can appreciably lower seismic wave velocities. Phase E could be used as seismological indicator for water stored at depth in subducting scenarios. The elasticity of phase E under mantle conditions will be explored in future research.

Keywords: Brillouin scattering, Phase E, Seismic wave velocities

©2019. Japan Geoscience Union. All Right Reserved.

Discovery of two hexagonal phases in (Fe,Al)OOH under the P-T conditions of the deep lower mantle

*Lu Liu[1,2], Li Zhang[1], Hongsheng Yuan[1]

1. Center for High Pressure Science and Technology Advanced Research, 2. University of Science and Technology of China

Deep water can cause a series of complex seismological phenomena by changing the density and thermal stability of lower mantle components. δ-H solid solution phase (AlOOH-$MgSiO_2(OH)$) is stable at lower mantle conditions[1],because the crystallographic frameworks of the phase H is similar to that of the δ-AlOOH phase, with very strong hydrogen bonds[2,3]. δ-AlOOH and ε-FeOOH can also form solid solution[4] (δ - ε solution). It is reasonable to infer that δ - ε solid solution may have similar thermal stability as that of H- δ solution, considering their similar crystal structure[5]. In our experiments, we synthesized the δ - ε solution at 79GPa and 1600K in a laser-heated diamond anvil cell. As the temperature increases to 2100k, the orthorhombic δ - ε solution transformed into a hexagonal-structured phase. By combining powder X-ray diffraction techniques with multigrain indexation[6], we determined its hexagonal lattice with a=b=10.019Å and c=2.614Å. At 79GPa and 2400K, the hexagonal phase transforms into another hexagonal phase, with the lattice parameters of a=b=2.733Å and c=9.343Å. The discovery of these two new phases may provide new insights into the deep-water storage.

References
1.Ohira I, Ohtani E, Sakai T, et al. Stability of a hydrous δ-phase, AlOOH-$MgSiO_2(OH)_2$, and a mechanism for water transport into the base of lower mantle[J].Earth and Planetary Science Letters, 2014, 401: 12-17.
2.Ohtani, E., Amaike, Y., Kamada, S., Sakamaki, T. and Hirao, N. Stability of hydrous phase H $MgSiO_4H_2$ under lower mantle conditions. Geophys. Res. Lett. 41, -8287 (2014).
3.Nishi M,Kuwayama Y,Tsuchiya J,et al.The pyrite-type high-pressure form of FeOOH[J]. Nature,2017,54(7662):205-208.
4.T Kawazoe,I Ohira,T Ishii et al. Single crystal synthesis of δ-(Al,Fe)OOH American Mineralogist. Volume 102, pages 1953–1956, (2017)
5.Gleason A E,Quiroga C E,Suzuki A,et al.Symmetrization driven spin transition in ε-FeOOH at high pressure[J]. Earth and Planetary Science Letters, 2013, 379: 49-55.
6.Zhang L,Yuan H,Meng Y,et al.Discovery of a hexagonal ultradense hydrous phase in (Fe, Al) OOH[J]. Proceedings of the National Academy of Sciences,2018,115(12):2908-2911.

Keywords: High temperature and high pressure experiment, hydrous phase, diamond anvil cell

©2019. Japan Geoscience Union. All Right Reserved.

Effect of grid resolution on tectonic regimes in global-scale convection models

*Enrico Marzotto[1], Marcel Thielmann[1], Gregor Golabek[1]

1. Bayerisches Geoinstitut

Global-scale convection models using a visco-plastic rheology coupled with a temperature-dependent viscosity usually show different tectonic regimes: mobile, episodic or stagnant lid.

In the mobilelidregime, the lid is continuously subducting into the mantle (plate-like behavior). The episodic lid regime is characterized by the stability of the lid until sufficiently large lithospheric stresses break it, causing rapid resurfacing. Finally the stagnant lid regime is defined by an undeformable lid that does not participate in convection

In numerical simulations these three types of regimes can be obtained by varying some target parameters such as: temperature-dependency of viscosity and yield stress.

The yield stress in particular is a key parameter because it sets the stress necessary to cause plastic yielding, hence, in a visco-plastic rheology, the stress necessary to break the cold surface regions. A high yield stress will result in a stagnant lid. On the other hand, a low yield stress causes a weak lid that is constantly broken and sinks into the mantle.Despite the key importance of physical parameters, also numerical parameters have an effect on the tectonic regime, determining different outcomes justby changing the grid resolution.

Here we use the code StagYY (*Tackley, 2008*) in a 2D spherical annulus geometry (*Hernlund & Tackley, 2008*) to determine the resolution-dependent tectonic regime for different yield stresses in global-scale convection models. To assess the effect of grid resolution on lid behavior we use 16 different resolutions keeping all physical parameters unchanged. To make sure that steady state has been reached each simulation is run for 15 Gyrs. Tested resolutions vary from 128x32 to 1024x256 grid points. To understand this influence on the tectonic regime we study the resolution within the lid requiring an appropriate lid definition, based on the thermal and velocity field. Our results show that there is a correspondence between low radial resolution and mobile lid regime and that low aspect ratio cells (azimuthal to radial grid spacing) favor a plate-like behavior of the lid, while for large aspect ratios the mobile lid regime is persistent.

This work is the first part of a larger project, aiming to studyslab stagnation and hydration of the mantle transition zone (MTZ) using self-consistent global-scale mantle convection models, where subducting slabs carry water from the surface into the Earth’ s interior and potentially hydrate the MTZ. We expect that our previous work packages will help us to obtain realistic slab ponding in the MTZ, so we can study the hydration state of this region over time.

References:

Tackley, P. J. (2008). Modelling compressible mantle convection with large viscosity contrasts in a

©2019. Japan Geoscience Union. All Right Reserved.

three-dimensional spherical shell using the yin-yang grid. *Phys. Earth Planet. Int.* 171, 7-18.

Hernlund, J. W. and P. J. Tackley (2008). Modeling mantle convection in the spherical annulus. *Phys. Earth Planet. Int.* 171, 48-54

Keywords: Geodynamical Modelling, StagYY, Grid Resolution

©2019. Japan Geoscience Union. All Right Reserved.

A 3-D crust and uppermost mantle electrical conductivity model of subduction zone beneath NE Japan

*Masahiro Ichiki[1,2], Toshiki Kaida[1], Yasuo Ogawa[3]

1. Graduate School of Science, Tohoku University, 2. International Research Institute of Disaster Science, 3. School of Science, Tokyo Institute of Technology

The crustal fluids beneath NE Japan is originated from dehydration of subducting Pacific slab or from convection in the backarc mantle, as is shown by seismic tomography [e.g. Zhao, 2017]. We investigated the fluid transportation paths from upper mantle to crust of subduction zone using electrical conductivity exploration.

We expanded electromagnetic field observation sites (96 sites) to northern part of NE Japan and obtained magnetotelluric responses and geomagnetic transfer functions in the period range of 20 –30720 seconds (22 periods) by BIRRP code [Chave and Thomson, 2004]. We used WSINV3D [Siripunvaraporn and Egbert, 2009] to invert those responses into three dimensional electrical resistivity model.

The preliminary model gives normalized root mean square misfit 5.87. A prominent conductor appears in the crust to uppermost mantle and the conductor spreads towards backarc direction. In our previous model [Ichiki et al., 2015], we found the overturned shape conductor towards backarc direction in the mantle wedge beneath central part of NE Japan. This study has found it beneath northern part NE Japan as well.

Those imply the crustal fluid and/or melt is transported along the pathway that is the plate boundary beneath the volcanic front to the backarc crust. The fluid transportation can explain the presence of enigmatic backarc volcano in the NE Japan. In this presenation, we speculate and discuss evolution of this pathway in geological time on the basis of the chlonological data of igneous rocks [Yoshida et al., 2013].

Acknouwledgement: This study is financially supported by KAKEN-HI No.26109006.

Keywords: electrical conductivity, resistivity, magnetotelluric, subduction zone

©2019. Japan Geoscience Union. All Right Reserved.

The conditions of sublithospheric diamond formation constrained from ferric iron-rich exsolution from ferropericlase inclusions.

*Caterina Melai[1], Daniel Frost[1], Tiziana Boffa Ballaran[1], Catherine McCammon[1]

1. Bayerisches Geoinstitute

Ferropericlase is apparently one of the more common inclusions to be found in sub-lithospheric diamonds, which are considered to form in the convecting mantle. Although relatively rare, these inclusions have been examined in a number of studies in the hope of providing information on the formation conditions of such deep diamonds, which could potentially be in the transition zone or lower mantle. The wide range of oxide Fe/(Fe+Mg) ratios found has raised the idea that they may form through the oxidation of iron metal. During TEM investigations, however, evidence for the exsolution of Fe_2O_3-rich phases such as magnesioferrite have been found, which implies that a more complex scenario may be involved. Ferropericlase-magnesiowüstite diamond inclusions are most likely some of the deepest available samples from the mantle and they potentially provide the most direct evidence for deep mantle carbon transport processes. The ferric iron contents of such inclusions alone may not provide a direct estimate for the oxygen fugacity at which the inclusions were trapped, particularly if pressure has a strong effect on the fo_2 - Fe^{3+}/Fe_{tot} relationship. However, using experimental data it is possible to determine the oxygen fugacity at which the exsolution observed in the diamond inclusions occurred and coupled with the oxide Fe^{3+}/Fe_{tot} ratio this could be used to estimate the pressure of formation.

The ferropericlase- magnesioferrite system has been investigated by several studies at room pressure but the stability field of the two components has been shown to become more complicated at high pressure due to the formation of mixed valence oxides. We have combined experimental measurements with thermodynamic modelling in order to address two main questions: at which P, T, fO_2 conditions do Fe_2O_3 -rich phases exsolve from ferropericlase? And what is the maximum Fe^{3+}/Fe_{tot} ratio of ferropericlase. To answer these questions, multianvil experiments have been performed between 6 –25 GPa and 1200-1800˚C using a starting composition of $(Mg_{86}Fe_{14})O$ plus 20 % Fe_2O_3. Pt powder was added to the experiments to act as a redox sensor and minor amounts of Ni, Cr, Mn and Na were also added. Samples were then analyzed with the scanning electron microscope, electron microprobe, Mössbauer spectroscopy and X-ray diffraction. In the recovered experiments ferropericlase coexists with magnetite-magnesioferrite solid solution up to 10 GPa and $Mg_2Fe_2O_5$-Fe_4O_5 solid solution at higher pressures. In the calculation of the oxygen fugacity a ferropericlase model in the FeO-$Fe_{2/3}O$-MgO system was employed and exchange of Mg and Fe^{2+} in magnetite was accounted for. Oxygen fugacities at which the phases coexist can be calculated in the magnetite-magnesioferrite field using three different equilibria and a quite simple ferropericlase mixing model results in calculated oxygen fugacities that are within 0.1 log units of each other for all three equilibria. The results show that magnetite-magnesioferrite solid solution should not be in equilibrium with ferropericlase in the diamond stability field. Our results imply that the exsolution of Fe^{3+} rich phases observed in natural samples likely occurred at pressures corresponding to the transition zone or deeper.

©2019. Japan Geoscience Union. All Right Reserved.

Probing the variation of the oxygen fugacity in diamond anvil cells using the Fe-Ir alloy as redox sensor

*Serena Dominijanni[1], Catherine McCammon[1], Leonid Dubrovinsky[1], Dan Frost[1], Nobuyoshi Miyajima[1]

1. Bayerisches Geoinstitut

Understanding the oxygen fugacity (fO_2) in diamond anvil cells (DACs) is an important issue for many reasons, among them reconciling contradictory results that have been obtained for carbonate studies (Cerantola et al., 2017; Dorfman et al., 2018) that might be due to different redox conditions during the experiments. We therefore investigated the fO_2 conditions during DAC experiments using powder X-ray diffraction (beamlines ID15b and ID27) and energy-domain Synchrotron Mössbauer Source (SMS) spectroscopy (beamline ID18) at the European Synchrotron Radiation Facility (Grenoble, France). Double sided laser heating experiments (Aprilis et al., 2017) were carried out at high pressure and temperature using a mixture of synthetic ferropericlase ($Mg_{0.75}Fe_{0.25}$)O and pure iridium powder as a sliding redox sensor (Borisov and Palme, 2000; Swartzendruber, 1984; Taylor et al., 1992). The Fe content in the Fe-Ir alloy, together with the amount of FeO in ferropericlase, allows a calculation of fO_2 during the experiments (Stagno et al., 2011; Woodland and O'Neill, 1997). Preliminary results from powder X-ray diffraction data show that, after heating, an Fe-Ir metal alloy that can be indexed in the Fm-3m space group is formed by the reaction of pure Ir and Fe from ferropericlase according to the reaction:

(Mg,Fe)O + Ir --> (Mg,Fe)O + (Fe,Ir)

The compressibility of the Fe-Ir alloy and ferropericlase was measured up to ~ 60 GPa and SMS data were collected before and after heating. X-ray diffraction results coupled with energy-dispersive X-ray spectroscopy (EDS) measurements and a simple thermodynamic model indicate that the redox conditions during the DAC experiments were close to the iron-wüstite (IW) buffer, although some inhomogeneity was observed. Further chemical analyses and additional experiments are ongoing to understand the variation of oxygen fugacity in a DAC during laser heating.

Keywords: oxygen fugacity , redox sensor, diamond anvil cell

©2019. Japan Geoscience Union. All Right Reserved.

Goethite behavior at Earth's lower mantle conditions

*Egor Gennadievich Koemets[1], Maxim Bykov[1], George Aprilis[2], Timofey Fedotenko[2], Stella Chariton[1], Saiana Khandarkhaeva[1], Iuliia Koemets[1], Marcel Thielmann[1], Natalia Dubrovinsaia[2], Leonid Dubrovinsky[1]

1. BGI (Bayerisches Geoinstitut), Universität Bayreuth, Germany, 2. Material Physics and Technology at Extreme Conditions, Laboratory of Crystallography, Universität Bayreuth, Germany

Water and water-bearing species have a strong impact on numerous processes in Earth’ s interiors. Presence of water affects chemical and physical properties of mantle minerals, changes melting temperatures, sound velocities and viscosity of materials, and causing different global phenomena such as, for example, arc volcanism and plate tectonics. Thereby, the deep Earth’ s regions enriched with water are crucial for understanding our planet’ s geodynamics and geochemistry. Still, mechanisms of water circulation between geospheres remain poorly understood. Recent studies suggest that goethite present in Banded Iron Formations (BIFs) may transfer some quantities of water to the deep Earth interiors with subducting slabs. It was reported that goethite remains stable in the sinking slab until it reaches the base of a lower mantle. By the meaning of in situ powder XRD it was revealed that at pressures corresponding to the depths ~1500-1800 km and moderately high temperatures goethite undergoes a phase transition to form a novel stable pyrite-type phase FeO_2H_x with $0 \leqq x \leqq 1$ (named as Py-phase). Thus, goethite and its HP pyrite-type form became a candidate for water and/or hydrogen transfer and storage to the lower mantle and the core-mantle boundary. Using laser-heating in diamond anvil cells we performed a series of experiments on an investigation of goethite (as a starting material) stability at P-T conditions covering possible range in subducting slabs. By the meaning of sensitive in situ single-crystal XRD in DACs we registered decomposition of goethite and formation of known (such as ι-Fe_2O_3, η-Fe_2O_3, a high-pressure orthorhombic form of Fe_3O_4, Fe_5O_7) and novel iron-oxygen compounds. Results of structure solution and refinement established these compounds to be orthorhombic Fe_7O_{10} and hexagonal non-stoichiometric phase $Fe_{6.31}O_9$. Our results suggest that FeOOH cannot transport water into the deep of Earth’ s mantle.

Keywords: Goethite, Diamond anvil cell, High Pressure, Single-crystal XRD, Subducting slabs

©2019. Japan Geoscience Union. All Right Reserved.

The oxygen content of sulphides in the mantle and a geothermometer for diamond formation

*Sumith Abeykoon[1], Dan Frost[1], Vera Laurenz[1]

1. Bayerisches Geoinstitut, University of Bayreuth

Sulphides are ubiquitous accessory minerals in mantle rocks and form the most prevalent type of inclusion in diamonds. Diamond sulphide inclusions are trapped as sulphide melts that crystallise on cooling to form Fe-Ni monosulphide solid solution (MSS) and ultimately recrystallizes to assemblages containing pyrrhotite, $Fe_{(1-x)}S$ (x = 0 to 0.2), pentlandite, $(Fe,Ni)_9S_8$, and sometimes pyrite (FeS_2). Sulphide inclusions are also found in many xenoliths but those which are hosted by diamonds provide potentially the most pristine samples from the lithospheric mantle and deeper. Previous experiments indicate that oxygen partitions into sulphide melts and although sparse, some measurements of natural sulphide inclusions from mantle xenoliths indeed show measurable and in some cases relatively high oxygen concentrations. If the parameters that control sulphide oxygen concentration can be determined then they could be potentially used to understand conditions in the mantle and in particular in sublithospheric diamonds. The oxygen content of sulphides separating to the core during core formation could have also influenced the oxygen fugacity of the early mantle.
We have measured the oxygen contents of sulphide melts within experimentally produced mantle assemblages at high pressures and temperatures. A series of multi-anvil experiments were conducted to equilibrate a peridotite assemblage with molten sulphide (FeS) at pressures between 3 –11 GPa and temperatures of 1300 ˚C –1700 ˚C. The effects of pressure, temperature, oxygen fugacity and composition have been investigated. Oxygen fugacity was determined in some experiments by saturating the sulphide in Ir to produce a separate Ir-Fe metal alloy, for which the Fe content is a function of oxygen fugacity. The results show that sulphide melt oxygen contents can range up to 16 weight % FeO, at mantle conditions. Moreover, the content of oxygen in the sulphide is found to be not controlled by fO_2 or fS_2, which is in disagreement with previous experimental studies conducted at ambient pressure conditions. The experiments indicate that the oxygen concentration is mainly controlled by the FeO activity in coexisting silicates phases and the temperature, although further work is still required to calibrate effects of Ni and Cu. In order to fit the data and to account for the FeO dependence, we developed a thermodynamic model using an end-member equilibrium between olivine, pyroxene and FeO in the sulphide melt. The resulting relationship can be used as a geothermometer based on sulphide inclusion oxygen contents and could be particularly useful for determining diamond formation temperatures for sub lithospheric diamonds.

Keywords: Sulfide, Oxygen, Geothermometer

©2019. Japan Geoscience Union. All Right Reserved.

[E] Poster | S (Solid Earth Sciences)：S-CG Complex & General

Thu. May 30, 2019 5:15 PM - 6:30 PM JST | Thu. May 30, 2019 8:15 AM - 9:30 AM UTC | Poster Hall International Exhibition Hall8, Makuhari Messe_27

[S-CG51] Role of volatiles on Earth and planetary dynamics

convener:Takayuki Ishii(Bavarian Research Institute, University of Bayreuth), Eiji Ohtani(Department of Earth and Planetary Materials Science, Graduate School of Science, Tohoku University), Michihiko Nakamura(Division of Earth and Planetary Materials Science, Department of Earth Science, Graduate School of Science, Tohoku University), Bjorn Mysen(Geophysical Laboratory, Carnegie Inst. Washington)

This session addresses how volatile species affect dynamics of the
Earth and planets from natural observations, laboratory experiments, and
numerical modeling in the temperature, pressure, and oxygen activity
range from the early stage of the planet formation to the present. The
volatiles can be critical in zones of magma storage and ascent, mantle
upwelling and melting in the fluid-enriched subduction zones, in the
mantle transition zone, in the lower mantle, in the core-mantle boundary,
and in Earth and planetary cores. However, volatiles affect properties
and processes differently depending on their pressure, temperature, and
redox conditions, which vary in time and space.
 This session aims to address how volatiles control the dynamic
processes of the Earth and planets, governed by their geophysical and
geochemical properties. We welcome papers dealing with geological and
laboratory observations coupled with numerical modeling on the role of
volatiles. The topics include (1) Stability relations, chemical and
physical properties of crystalline, molten and fluid phases,
partitioning of volatiles among these phases, (2) Rheological and other
physical properties of minerals, and the effects of intergranular fluid
on the properties, (3) Volatiles and dehydration induced seismicity and
volcanism in various tectonic regions including subduction zones, and (4)
Effects of volatiles in numerical simulation of geo-tectonics, and (5)
Magma outgassing and its control of volcanic eruption dynamics.

[SCG51-P01] Permeability prediction of porous media with the finite difference Stokes solver LaMEM

*Philipp Eichheimer[1], Wakana Fujita[2], Marcel Thielmann[1], Anton Popov[3], Gregor Golabek[1], Boris Kaus[3], Maximilian Kottwitz[3] (1.Bayerisches Geoinstitut, University of Bayreuth, 2.Department of Earth Science, Tohoku University, Sendai, 3.Institute of Geosciences, Johannes Gutenberg University Mainz)

[SCG51-P02] Grain growth-induced fluid localization and permeability reduction

*Wakana Fujita[1], Michihiko Nakamura[1], Kentaro Uesugi[2] (1.Graduate School of Science, Tohoku University, 2.JASRI/SPring-8)

[SCG51-P03] Pargasite stability in the upper mantle at H_2O-undersaturated conditions

*Marija Putak Juricek[1], Hans Keppler[1] (1.BGI)

[SCG51-P04] **Constraining the water content at the top of the mantle transition zone with the elasticity of wadsleyite and olivine**

*Zhongqing Wu[1] (1.University of Science and Technology of China)

[SCG51-P05] ***Single crystal elasticity of Fe-bearing phase E by Brillouin spectroscopy***

*Niccolo Satta[1], Hauke Marquardt [2], Alexander Kurnosov[1], Tiziana Boffa Ballaran [1], Johannes Buchen[3], Catherine McCammon[1], Takaaki Kawazoe[4] (1.Bayerisches Geoinstitut, University of Bayreuth, 95440 Bayreuth, Germany, 2.Department of Earth Sciences, University of Oxford, South Parks Road, Oxford, UK., 3.Seismological Laboratory, California Institute of Technology, Pasadena, CA 91125, USA., 4.Department of Earth and Planetary Systems Science, Hiroshima University, Hiroshima 739-8526, Japan.)

[SCG51-P06] Discovery of two hexagonal phases in (Fe,Al)OOH under the P-T conditions of the deep lower mantle

*Lu Liu[1,2], Li Zhang[1], Hongsheng Yuan[1] (1.Center for High Pressure Science and Technology Advanced Research, 2.University of Science and Technology of China)

[SCG51-P07] **Effect of grid resolution on tectonic regimes in global-scale convection models**

*Enrico Marzotto[1], Marcel Thielmann[1], Gregor Golabek[1] (1.Bayerisches Geoinstitut)

[SCG51-P08] A 3-D crust and uppermost mantle electrical conductivity model of subduction zone beneath NE Japan

*Masahiro Ichiki[1,2], Toshiki Kaida[1], Yasuo Ogawa[3] (1.Graduate School of Science, Tohoku University, 2.International Research Institute of Disaster Science, 3.School of Science, Tokyo Institute of Technology)

[SCG51-P09] *The conditions of sublithospheric diamond formation constrained from ferric iron-rich exsolution from ferropericlase inclusions.*

*Caterina Melai[1], Daniel Frost[1], Tiziana Boffa Ballaran[1], Catherine McCammon[1] (1.Bayerisches Geoinstitute)

[SCG51-P10] **Probing the variation of the oxygen fugacity in diamond anvil cells using the Fe-Ir alloy as redox sensor**

*Serena Dominijanni[1], Catherine McCammon[1], Leonid Dubrovinsky[1], Dan Frost[1], Nobuyoshi Miyajima[1] (1.Bayerisches Geoinstitut)

[SCG51-P11] Goethite behavior at Earth's lower mantle conditions

*Egor Gennadievich Koemets[1], Maxim Bykov[1], George Aprilis[2], Timofey Fedotenko[2], Stella Chariton[1], Saiana Khandarkhaeva[1], Iuliia Koemets[1], Marcel Thielmann[1], Natalia Dubrovinsaia[2], Leonid Dubrovinsky[1] (1.BGI (Bayerisches Geoinstitut), Universität Bayreuth, Germany, 2.Material Physics and Technology at Extreme Conditions, Laboratory of Crystallography, Universität Bayreuth, Germany)

[SCG51-P12] The oxygen content of sulphides in the mantle and a geothermometer for diamond formation

*Sumith Abeykoon[1], Dan Frost[1], Vera Laurenz[1] (1.Bayerisches Geoinstitut, University of Bayreuth)

Permeability prediction of porous media with the finite difference Stokes solver LaMEM

*Philipp Eichheimer[1], Wakana Fujita[2], Marcel Thielmann[1], Anton Popov[3], Gregor Golabek[1], Boris Kaus[3], Maximilian Kottwitz[3]

1. Bayerisches Geoinstitut, University of Bayreuth, 2. Department of Earth Science, Tohoku University, Sendai, 3. Institute of Geosciences, Johannes Gutenberg University Mainz

The flow of fluids through porous media such as groundwater flow or magma migration is one of the most important processes in geological sciences. The property controlling the efficiency of the flow is the permeability of the rock, thus an accurate determination and prediction of its value is of crucial importance. For this reason, permeability of rocks has been measured across different scales. As laboratory measurements exhibit a range of limitations, the numerical prediction of permeability at conditions where laboratory experiments struggle has become an important method to complement laboratory approaches. At high resolutions, this prediction becomes computationally very expensive, which makes it crucial to develop methods that maximize accuracy. In this work we introduce the open-source finite difference solver LaMEM that can be used to numerically predict the permeability of porous media under laminar conditions. We employ a stencil rescaling method to increase accuracy due to a better description of the solid-fluid interface, thus reducing the computational cost. To validate the method, we perform a series of tests employing both analytical solutions for simplified geometries as well as results from other numerical approaches for more complicated geometries. Furthermore we compare our numerical results to laboratory measurements on glass bead samples with porosities ranging from 20% to 2.5%, showing good agreement.

Keywords: Permeability, Numerical modelling, Digital Rock Physics

©2019. Japan Geoscience Union. All Right Reserved.

Grain growth-induced fluid localization and permeability reduction

*Wakana Fujita[1], Michihiko Nakamura[1], Kentaro Uesugi[2]

1. Graduate School of Science, Tohoku University, 2. JASRI/SPring-8

Efficiency of segregation of geological fluids such as aqueous fluids and melts is an essential elementary process for volatile cycles in subduction zones. Permeability is an intrinsic rock property that controls flow rate of fluid. Various permeability models have been presented by numerical models of textually equilibrated rocks (e.g. 1, 2), laboratory measurements on synthetic rocks (e.g. 3) and estimation from cross-sectional area of synthetic rocks (4). However, there exist discrepancies among those models. Because permeability is very sensitive to microscopic geometry of pore fluid, those disagreements may arise from lack of understanding toward three-dimensional (3D) microstructure of fluid network.

Dihedral angle has been considered to be a critical parameter that controls fluid geometry and thus permeability. Beside, some previous studies shed light on the effect of grain growth on fluid distribution because it could induce pore fluid distortion and coalescence (5, 6). These studies suggest that in the actual systems where the microstructure of rocks evolve in dynamic processes, grain growth would be important along with the dihedral angle.

To investigate the effect of grain growth on the fluid distribution and permeability, we present 3D images of quartz–CHO fluid aggregates, containing nominal fluid fractions between 0.03 and 0.10. Samples were synthesized from a powdered mixture of Arkansus quartz and amorphous silica prepared by sol-gel method and hot-pressed in a piston–cylinder apparatus at 900˚C and 1.0 GPa for 192h. The fluid fractions and the dihedral angles were controlled using brucite added in the capsule bottom and oxalic acid dihydrate mixed with SiO_2 powder. 3D images were obtained using synchrotron X-ray microtomography at BL20XU experimental hutch2 of SPring-8. Regardless of dihedral angles (CO_2 content in fluids), both cross-sectional area and 3D images of samples showed grain-scale fluid localization which would be formed by pore fluid coalescence induced by grain growth. Computed permeabilities using numerical model, LaMEM (7) were almost consistent with laboratory measurements by (3) but more than one order of magnitude lower than a numerical model by (2). This would indicate that localized fluids extensively reduce permeability by reducing the diameter of fluid tubes along grain edges, which would suggest transport of water into Earth’ s deep interior by the subducting slab.

Reference:
1. von Bargen and Waff. 1986, J. Geophys. Res. 91, 9261–9276.
2. Rudge, J.F. 2018, Proc. R. Soc. Lond. A 474, 20170639.
3. Wark and Watson. 1998, Earth Planet. Sci. Lett. 164, 591–605.
4. Faul, U.H. 1997, J. Geophys. Res. 102, 10299–10311.
5. Walte et al. 2003, Geology 2003 31, 1009-1012.
6. Yoshino and Watson. 2005, Earth Planet. Sci. Lett. 235, 453–468.
7. Kaus et al. 2016, NIC Symposium 2016

Keywords: Permeability, Quartz, Grain growth, Dihedral angle, Fluid segregation

©2019. Japan Geoscience Union. All Right Reserved.

Pargasite stability in the upper mantle at H_2O-undersaturated conditions

*Marija Putak Juricek[1], Hans Keppler[1]

1. BGI

Amphibole is the most commonly occurring hydrous mineral in mantle xenoliths and the majority of upper mantle amphiboles have compositions close to pargasite end member. Previous experimental work has demonstrated that pargasite stability is sensitive to variations in bulk alkali and water content of the starting material. While it has been successfully shown that addition of more alkali leads to stabilization of pargasite to higher P and T, the effect of water on amphibole stability is not so straightforward.

At H_2O-saturated conditions, alkali elements partition strongly into aqueous fluid and become less available for crystallization of amphibole. As a result, amphibole seemingly becomes stable at higher P and T when less H_2O is added to the starting material. This observation led to the hypothesis that pargasite may be a ubiquitous phase in the upper mantle, which is believed to contain only several hundred ppm of H_2O. However, most of the previous studies determined pargasite stability at H_2 O-saturated conditions where solid phases coexist with an aqueous fluid during experiments. Since such environments are not representative of the nearly dry upper mantle, the purpose of this study is to investigate pargasite stability at H_2O-undersaturated conditions.

Because of the high specific surface area of powders, adsorption of atmospheric H_2O on fine grained starting materials prevents attaining H_2O-undersaturation by adding small amounts of water to the sample. Instead, H_2O-undersaturated conditions may be precisely controlled by diluting the water in the sample with another component. Under such conditions, solid phases are expected to coexist with a low water activity fluid throughout the experiment. As molecular nitrogen is mostly insoluble in upper mantle minerals, it can be used to adjust the water activity of the fluid to a desired low value.

All experiments were performed in a piston cylinder apparatus. The samples for H_2O-undersaturated experiments were prepared by adding silver azide (AgN_3) and brucite to a synthetic peridotite mixture. In several experiments water was added directly as $H_2O_{(l)}$. The amount of water was kept constant in all experiments (1 wt. percent) and the molar fraction of water in the N_2-H_2O fluid was adjusted to the desired value by weighing an appropriate amount of AgN_3, which decomposed to metallic silver and molecular nitrogen during heating. In H_2O-saturated experiments, no silver azide was added to the peridotite mixture. Experimental products were analyzed using JEOL JXA-8200 electron microprobe.

Preliminary results show that pargasite is not stable in equilibrium with fluids diluted to X_{H2O}=0.1 at pressures above 1 GPa. At H_2O-saturated conditions pargasite stability field can extend to pressures of 4 GPa and above 1100 ℃, depending on bulk alkali and water contents. Results from experiments at X_{H2O} =0.1 and X_{H2O}=1 suggest that pargasite can exist only in regions of the upper mantle which have been affected by high water activity fluids, such as areas in the vicinity of subduction zones. The ambient nominally anhydrous upper mantle, better represented by experiments at H_2O-undersaturated conditions, is not expected to contain pargasite.

Keywords: pargasite, stability, upper, mantle

©2019. Japan Geoscience Union. All Right Reserved.

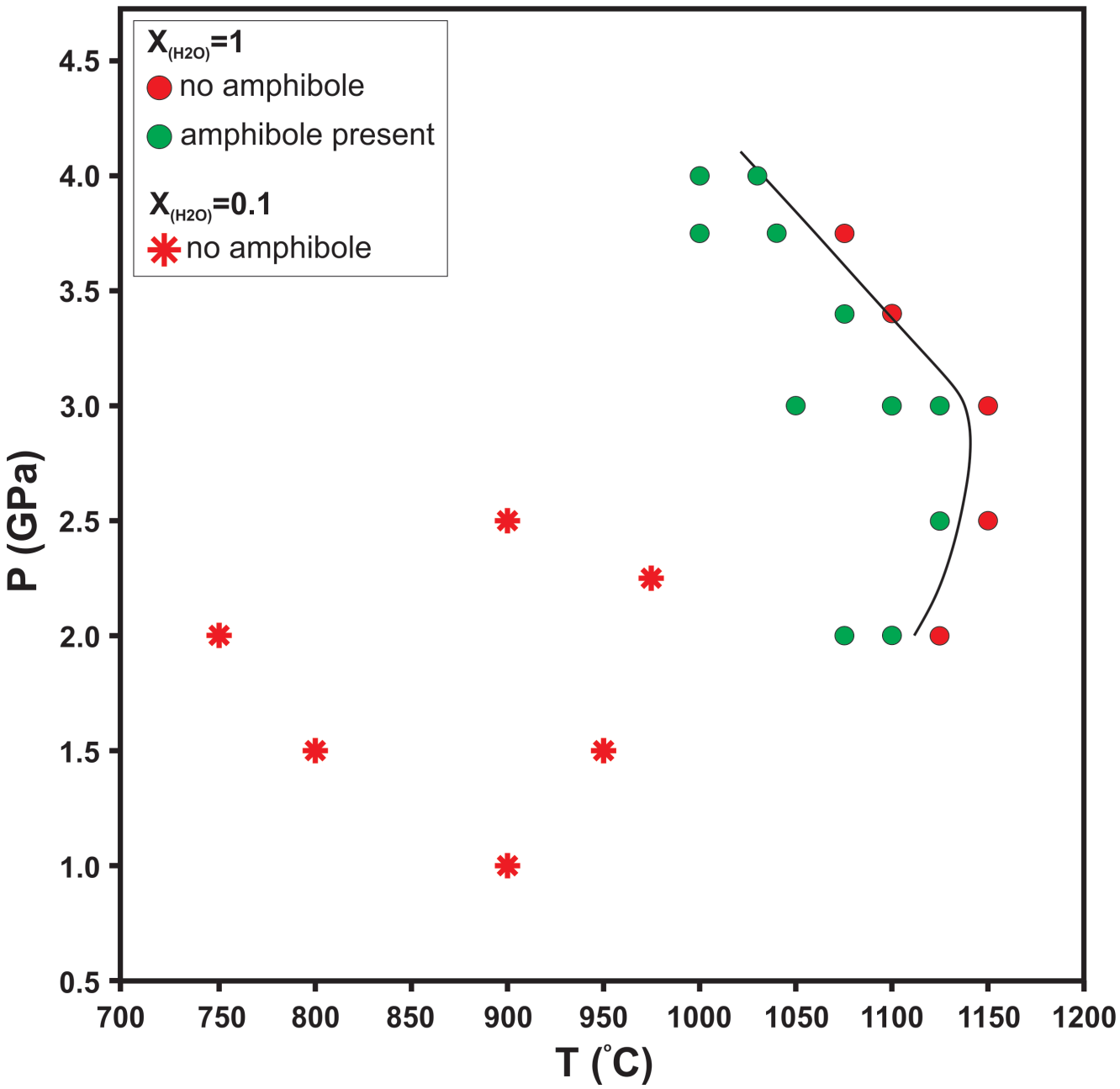

©2019. Japan Geoscience Union. All Right Reserved.

Constraining the water content at the top of the mantle transition zone with the elasticity of wadsleyite and olivine

*Zhongqing Wu[1]

1. University of Science and Technology of China

Zhongqing Wu[a,b,*], Wenzhong Wang[a,b], Michael J. Walter[c] ,Ye Peng[a,b], Simon Redfern[d],

[a] Laboratory of Seismology and Physics of Earth’ s Interior, School of Earth and Space Sciences, University of Science and Technology of China, Hefei, Anhui 230026, China

[b] Mengcheng National Geophysical Observatory, Anhui, China

[c]School of Earth Sciences, University of Bristol, Bristol BS8 1RJ, UK

[d]Department of Earth Science, University of Cambridge, Cambridge CB2 3EQ, UK

The water content in the mantle transition zone (MTZ) exerts a controlling influence on the dynamical and chemical evolution of Earth, but is poorly known. In principle the water content at the top of the transition zone can be inferred by comparing the velocity and density contrasts across the 410-km seismic discontinuity with predictions based on the phase transition of olivine to wadsleyite. The high-quality elastic data of at pressure and temperature (PT) conditions of the transition zone are crucial but are very challenge for experiments to obtain. Calculating these elastic data at high PT conditions in conventional method are also very expensive. Instead, these elastic data were calculated using the method of Wu and Wentzcovitch (2011), which reduces the computational workload to tenth of the conventional method. All calculations for two phases were conducted using the same computational details as far as possible, which guarantees that the velocity and density differences between two phases have very high precise. All these calculated elastic data agree well with the available experimental data. The iron and water effect on the elasticity are also well described.

With these high-quality elastic data covered the PT condition of the transition zone, we analyze the water and wadsleyite content at the top of the transition zone. We found that the water content of wadsleyite at the top of the transition zone can be well constrained when density and velocities jumps are considered together. For a pyrolitic mantle composition with ~60% olivine, our best fit is ~ 0.5 wt% water at the top of the transition zone. If the transition zone is dry, as suggested by some electrical conductivity models, the upper mantle may only contain ~ 50% olivine.

Wu, Z., Wentzcovitch, R.M., 2011. Quasiharmonic thermal elasticity of crystals: An analytical approach. Phys. Rev. B - Condens. Matter Mater. Phys. 83, 1–8. doi:10.1103/PhysRevB.83.184115

©2019. Japan Geoscience Union. All Right Reserved.

Single crystal elasticity of Fe-bearing phase E by Brillouin spectroscopy

*Niccolo Satta[1], Hauke Marquardt [2], Alexander Kurnosov[1], Tiziana Boffa Ballaran [1], Johannes Buchen[3], Catherine McCammon[1], Takaaki Kawazoe[4]

1. Bayerisches Geoinstitut, University of Bayreuth, 95440 Bayreuth, Germany, 2. Department of Earth Sciences, University of Oxford, South Parks Road, Oxford, UK., 3. Seismological Laboratory, California Institute of Technology, Pasadena, CA 91125, USA., 4. Department of Earth and Planetary Systems Science, Hiroshima University, Hiroshima 739-8526, Japan.

Earth’s deep water cycle plays a key role for the dynamic evolution of our planet and the development of habitable conditions. Surface water can be transported to Earth’s mantle by subduction of oceanic lithosphere. Experimental investigations have shown that water can be efficiently stored in Dense Hydrous Magnesium Silicates (DHMS) in cold subducting slabs. However, quantification of the incoming water budget based on the interpretation of seismological observations is hampered by a lack of elasticity measurements of DHMSs. Here, we report single-crystal elasticity measurements of Fe-bearing phase E, a DHMS that is stable at pressures and temperature of Earth’s mantle transition zone. A very low bulk modulus has been reported for phase E, suggesting that it might produce seismic velocity heterogeneities detectable by seismological investigations. However, the shear modulus of phase E has not been quantified.

We synthesized Fe-bearing phase E single crystals in a multi-anvil apparatus. Chemical composition as well as crystal structure have been determined using electron microprobe analysis, Mössbauer spectroscopy, and single-crystal X-ray diffraction. We derived the full elastic stiffness tensor by Brillouin spectroscopy on two single crystals of selected orientations. We found phase E to have both the lowest bulk modulus and shear modulus among the DHMSs at ambient conditions. Phase E shows very low compressional and shear velocities especially when compared to the other principal minerals likely present in subducting slabs after serpentine breakdown. Modelling of seismic velocities in dry and hydrated upper mantle and transition zone rocks suggests that the presence of even small amounts of phase E can appreciably lower seismic wave velocities. Phase E could be used as seismological indicator for water stored at depth in subducting scenarios. The elasticity of phase E under mantle conditions will be explored in future research.

Keywords: Brillouin scattering, Phase E, Seismic wave velocities

©2019. Japan Geoscience Union. All Right Reserved.

Discovery of two hexagonal phases in (Fe,Al)OOH under the P-T conditions of the deep lower mantle

*Lu Liu[1,2], Li Zhang[1], Hongsheng Yuan[1]

1. Center for High Pressure Science and Technology Advanced Research, 2. University of Science and Technology of China

Deep water can cause a series of complex seismological phenomena by changing the density and thermal stability of lower mantle components. δ-H solid solution phase (AlOOH-$MgSiO_2(OH)$) is stable at lower mantle conditions[1],because the crystallographic frameworks of the phase H is similar to that of the δ-AlOOH phase, with very strong hydrogen bonds[2,3]. δ-AlOOH and ε-FeOOH can also form solid solution[4] (δ - ε solution). It is reasonable to infer that δ - ε solid solution may have similar thermal stability as that of H- δ solution, considering their similar crystal structure[5]. In our experiments, we synthesized the δ - ε solution at 79GPa and 1600K in a laser-heated diamond anvil cell. As the temperature increases to 2100k, the orthorhombic δ - ε solution transformed into a hexagonal-structured phase. By combining powder X-ray diffraction techniques with multigrain indexation[6], we determined its hexagonal lattice with a=b=10.019Å and c=2.614Å. At 79GPa and 2400K, the hexagonal phase transforms into another hexagonal phase, with the lattice parameters of a=b=2.733Å and c=9.343Å. The discovery of these two new phases may provide new insights into the deep-water storage.

References
1.Ohira I, Ohtani E, Sakai T, et al. Stability of a hydrous δ-phase, AlOOH-$MgSiO_2(OH)_2$, and a mechanism for water transport into the base of lower mantle[J].Earth and Planetary Science Letters, 2014, 401: 12-17.
2.Ohtani, E., Amaike, Y., Kamada, S., Sakamaki, T. and Hirao, N. Stability of hydrous phase H $MgSiO_4H_2$ under lower mantle conditions. Geophys. Res. Lett. 41, -8287 (2014).
3.Nishi M,Kuwayama Y,Tsuchiya J,et al.The pyrite-type high-pressure form of FeOOH[J]. Nature,2017,54(7662):205-208.
4.T Kawazoe,I Ohira,T Ishii et al. Single crystal synthesis of δ-(Al,Fe)OOH American Mineralogist. Volume 102, pages 1953–1956, (2017)
5.Gleason A E,Quiroga C E,Suzuki A,et al.Symmetrization driven spin transition in ε-FeOOH at high pressure[J]. Earth and Planetary Science Letters, 2013, 379: 49-55.
6.Zhang L,Yuan H,Meng Y,et al.Discovery of a hexagonal ultradense hydrous phase in (Fe, Al) OOH[J]. Proceedings of the National Academy of Sciences,2018,115(12):2908-2911.

Keywords: High temperature and high pressure experiment, hydrous phase, diamond anvil cell

©2019. Japan Geoscience Union. All Right Reserved.

Effect of grid resolution on tectonic regimes in global-scale convection models

*Enrico Marzotto[1], Marcel Thielmann[1], Gregor Golabek[1]

1. Bayerisches Geoinstitut

Global-scale convection models using a visco-plastic rheology coupled with a temperature-dependent viscosity usually show different tectonic regimes: mobile, episodic or stagnant lid.

In the mobilelidregime, the lid is continuously subducting into the mantle (plate-like behavior). The episodic lid regime is characterized by the stability of the lid until sufficiently large lithospheric stresses break it, causing rapid resurfacing. Finally the stagnant lid regime is defined by an undeformable lid that does not participate in convection

In numerical simulations these three types of regimes can be obtained by varying some target parameters such as: temperature-dependency of viscosity and yield stress.

The yield stress in particular is a key parameter because it sets the stress necessary to cause plastic yielding, hence, in a visco-plastic rheology, the stress necessary to break the cold surface regions. A high yield stress will result in a stagnant lid. On the other hand, a low yield stress causes a weak lid that is constantly broken and sinks into the mantle.Despite the key importance of physical parameters, also numerical parameters have an effect on the tectonic regime, determining different outcomes justby changing the grid resolution.

Here we use the code StagYY (*Tackley, 2008*) in a 2D spherical annulus geometry (*Hernlund & Tackley, 2008*) to determine the resolution-dependent tectonic regime for different yield stresses in global-scale convection models. To assess the effect of grid resolution on lid behavior we use 16 different resolutions keeping all physical parameters unchanged. To make sure that steady state has been reached each simulation is run for 15 Gyrs. Tested resolutions vary from 128x32 to 1024x256 grid points. To understand this influence on the tectonic regime we study the resolution within the lid requiring an appropriate lid definition, based on the thermal and velocity field. Our results show that there is a correspondence between low radial resolution and mobile lid regime and that low aspect ratio cells (azimuthal to radial grid spacing) favor a plate-like behavior of the lid, while for large aspect ratios the mobile lid regime is persistent.

This work is the first part of a larger project, aiming to studyslab stagnation and hydration of the mantle transition zone (MTZ) using self-consistent global-scale mantle convection models, where subducting slabs carry water from the surface into the Earth’ s interior and potentially hydrate the MTZ. We expect that our previous work packages will help us to obtain realistic slab ponding in the MTZ, so we can study the hydration state of this region over time.

References:

Tackley, P. J. (2008). Modelling compressible mantle convection with large viscosity contrasts in a

©2019. Japan Geoscience Union. All Right Reserved.

three-dimensional spherical shell using the yin-yang grid. *Phys. Earth Planet. Int.* 171, 7-18.

Hernlund, J. W. and P. J. Tackley (2008). Modeling mantle convection in the spherical annulus. *Phys. Earth Planet. Int.* 171, 48-54

Keywords: Geodynamical Modelling, StagYY, Grid Resolution

©2019. Japan Geoscience Union. All Right Reserved.

A 3-D crust and uppermost mantle electrical conductivity model of subduction zone beneath NE Japan

*Masahiro Ichiki[1,2], Toshiki Kaida[1], Yasuo Ogawa[3]

1. Graduate School of Science, Tohoku University, 2. International Research Institute of Disaster Science, 3. School of Science, Tokyo Institute of Technology

The crustal fluids beneath NE Japan is originated from dehydration of subducting Pacific slab or from convection in the backarc mantle, as is shown by seismic tomography [e.g. Zhao, 2017]. We investigated the fluid transportation paths from upper mantle to crust of subduction zone using electrical conductivity exploration.

We expanded electromagnetic field observation sites (96 sites) to northern part of NE Japan and obtained magnetotelluric responses and geomagnetic transfer functions in the period range of 20 –30720 seconds (22 periods) by BIRRP code [Chave and Thomson, 2004]. We used WSINV3D [Siripunvaraporn and Egbert, 2009] to invert those responses into three dimensional electrical resistivity model.

The preliminary model gives normalized root mean square misfit 5.87. A prominent conductor appears in the crust to uppermost mantle and the conductor spreads towards backarc direction. In our previous model [Ichiki et al., 2015], we found the overturned shape conductor towards backarc direction in the mantle wedge beneath central part of NE Japan. This study has found it beneath northern part NE Japan as well.

Those imply the crustal fluid and/or melt is transported along the pathway that is the plate boundary beneath the volcanic front to the backarc crust. The fluid transportation can explain the presence of enigmatic backarc volcano in the NE Japan. In this presenation, we speculate and discuss evolution of this pathway in geological time on the basis of the chlonological data of igneous rocks [Yoshida et al., 2013].

Acknouwledgement: This study is financially supported by KAKEN-HI No.26109006.

Keywords: electrical conductivity, resistivity, magnetotelluric, subduction zone

©2019. Japan Geoscience Union. All Right Reserved.

The conditions of sublithospheric diamond formation constrained from ferric iron-rich exsolution from ferropericlase inclusions.

*Caterina Melai[1], Daniel Frost[1], Tiziana Boffa Ballaran[1], Catherine McCammon[1]

1. Bayerisches Geoinstitute

Ferropericlase is apparently one of the more common inclusions to be found in sub-lithospheric diamonds, which are considered to form in the convecting mantle. Although relatively rare, these inclusions have been examined in a number of studies in the hope of providing information on the formation conditions of such deep diamonds, which could potentially be in the transition zone or lower mantle. The wide range of oxide Fe/(Fe+Mg) ratios found has raised the idea that they may form through the oxidation of iron metal. During TEM investigations, however, evidence for the exsolution of Fe_2O_3-rich phases such as magnesioferrite have been found, which implies that a more complex scenario may be involved. Ferropericlase-magnesiowüstite diamond inclusions are most likely some of the deepest available samples from the mantle and they potentially provide the most direct evidence for deep mantle carbon transport processes. The ferric iron contents of such inclusions alone may not provide a direct estimate for the oxygen fugacity at which the inclusions were trapped, particularly if pressure has a strong effect on the fo_2 - Fe^{3+}/Fe_{tot} relationship. However, using experimental data it is possible to determine the oxygen fugacity at which the exsolution observed in the diamond inclusions occurred and coupled with the oxide Fe^{3+}/Fe_{tot} ratio this could be used to estimate the pressure of formation.

The ferropericlase- magnesioferrite system has been investigated by several studies at room pressure but the stability field of the two components has been shown to become more complicated at high pressure due to the formation of mixed valence oxides. We have combined experimental measurements with thermodynamic modelling in order to address two main questions: at which P, T, fO_2 conditions do Fe_2O_3 -rich phases exsolve from ferropericlase? And what is the maximum Fe^{3+}/Fe_{tot} ratio of ferropericlase. To answer these questions, multianvil experiments have been performed between 6 –25 GPa and 1200-1800˚C using a starting composition of $(Mg_{86}Fe_{14})O$ plus 20 % Fe_2O_3. Pt powder was added to the experiments to act as a redox sensor and minor amounts of Ni, Cr, Mn and Na were also added. Samples were then analyzed with the scanning electron microscope, electron microprobe, Mössbauer spectroscopy and X-ray diffraction. In the recovered experiments ferropericlase coexists with magnetite-magnesioferrite solid solution up to 10 GPa and $Mg_2Fe_2O_5$-Fe_4O_5 solid solution at higher pressures. In the calculation of the oxygen fugacity a ferropericlase model in the FeO-$Fe_{2/3}O$-MgO system was employed and exchange of Mg and Fe^{2+} in magnetite was accounted for. Oxygen fugacities at which the phases coexist can be calculated in the magnetite-magnesioferrite field using three different equilibria and a quite simple ferropericlase mixing model results in calculated oxygen fugacities that are within 0.1 log units of each other for all three equilibria. The results show that magnetite-magnesioferrite solid solution should not be in equilibrium with ferropericlase in the diamond stability field. Our results imply that the exsolution of Fe^{3+} rich phases observed in natural samples likely occurred at pressures corresponding to the transition zone or deeper.

©2019. Japan Geoscience Union. All Right Reserved.

Probing the variation of the oxygen fugacity in diamond anvil cells using the Fe-Ir alloy as redox sensor

*Serena Dominijanni[1], Catherine McCammon[1], Leonid Dubrovinsky[1], Dan Frost[1], Nobuyoshi Miyajima[1]

1. Bayerisches Geoinstitut

Understanding the oxygen fugacity (fO_2) in diamond anvil cells (DACs) is an important issue for many reasons, among them reconciling contradictory results that have been obtained for carbonate studies (Cerantola et al., 2017; Dorfman et al., 2018) that might be due to different redox conditions during the experiments. We therefore investigated the fO_2 conditions during DAC experiments using powder X-ray diffraction (beamlines ID15b and ID27) and energy-domain Synchrotron Mössbauer Source (SMS) spectroscopy (beamline ID18) at the European Synchrotron Radiation Facility (Grenoble, France). Double sided laser heating experiments (Aprilis et al., 2017) were carried out at high pressure and temperature using a mixture of synthetic ferropericlase ($Mg_{0.75}Fe_{0.25}$)O and pure iridium powder as a sliding redox sensor (Borisov and Palme, 2000; Swartzendruber, 1984; Taylor et al., 1992). The Fe content in the Fe-Ir alloy, together with the amount of FeO in ferropericlase, allows a calculation of fO_2 during the experiments (Stagno et al., 2011; Woodland and O'Neill, 1997). Preliminary results from powder X-ray diffraction data show that, after heating, an Fe-Ir metal alloy that can be indexed in the Fm-3m space group is formed by the reaction of pure Ir and Fe from ferropericlase according to the reaction:

(Mg,Fe)O + Ir --> (Mg,Fe)O + (Fe,Ir)

The compressibility of the Fe-Ir alloy and ferropericlase was measured up to ~ 60 GPa and SMS data were collected before and after heating. X-ray diffraction results coupled with energy-dispersive X-ray spectroscopy (EDS) measurements and a simple thermodynamic model indicate that the redox conditions during the DAC experiments were close to the iron-wüstite (IW) buffer, although some inhomogeneity was observed. Further chemical analyses and additional experiments are ongoing to understand the variation of oxygen fugacity in a DAC during laser heating.

Keywords: oxygen fugacity , redox sensor, diamond anvil cell

©2019. Japan Geoscience Union. All Right Reserved.

Goethite behavior at Earth's lower mantle conditions

*Egor Gennadievich Koemets[1], Maxim Bykov[1], George Aprilis[2], Timofey Fedotenko[2], Stella Chariton[1], Saiana Khandarkhaeva[1], Iuliia Koemets[1], Marcel Thielmann[1], Natalia Dubrovinsaia[2], Leonid Dubrovinsky[1]

1. BGI (Bayerisches Geoinstitut), Universität Bayreuth, Germany, 2. Material Physics and Technology at Extreme Conditions, Laboratory of Crystallography, Universität Bayreuth, Germany

Water and water-bearing species have a strong impact on numerous processes in Earth’ s interiors. Presence of water affects chemical and physical properties of mantle minerals, changes melting temperatures, sound velocities and viscosity of materials, and causing different global phenomena such as, for example, arc volcanism and plate tectonics. Thereby, the deep Earth’ s regions enriched with water are crucial for understanding our planet’ s geodynamics and geochemistry. Still, mechanisms of water circulation between geospheres remain poorly understood. Recent studies suggest that goethite present in Banded Iron Formations (BIFs) may transfer some quantities of water to the deep Earth interiors with subducting slabs. It was reported that goethite remains stable in the sinking slab until it reaches the base of a lower mantle. By the meaning of in situ powder XRD it was revealed that at pressures corresponding to the depths ~1500-1800 km and moderately high temperatures goethite undergoes a phase transition to form a novel stable pyrite-type phase FeO_2H_x with $0 \leqq x \leqq 1$ (named as Py-phase). Thus, goethite and its HP pyrite-type form became a candidate for water and/or hydrogen transfer and storage to the lower mantle and the core-mantle boundary. Using laser-heating in diamond anvil cells we performed a series of experiments on an investigation of goethite (as a starting material) stability at P-T conditions covering possible range in subducting slabs. By the meaning of sensitive in situ single-crystal XRD in DACs we registered decomposition of goethite and formation of known (such as ι-Fe_2O_3, η-Fe_2O_3, a high-pressure orthorhombic form of Fe_3O_4, Fe_5O_7) and novel iron-oxygen compounds. Results of structure solution and refinement established these compounds to be orthorhombic Fe_7O_{10} and hexagonal non-stoichiometric phase $Fe_{6.31}O_9$. Our results suggest that FeOOH cannot transport water into the deep of Earth’ s mantle.

Keywords: Goethite, Diamond anvil cell, High Pressure, Single-crystal XRD, Subducting slabs

©2019. Japan Geoscience Union. All Right Reserved.

The oxygen content of sulphides in the mantle and a geothermometer for diamond formation

*Sumith Abeykoon[1], Dan Frost[1], Vera Laurenz[1]

1. Bayerisches Geoinstitut, University of Bayreuth

Sulphides are ubiquitous accessory minerals in mantle rocks and form the most prevalent type of inclusion in diamonds. Diamond sulphide inclusions are trapped as sulphide melts that crystallise on cooling to form Fe-Ni monosulphide solid solution (MSS) and ultimately recrystallizes to assemblages containing pyrrhotite, $Fe_{(1-x)}S$ (x = 0 to 0.2), pentlandite, $(Fe,Ni)_9S_8$, and sometimes pyrite (FeS_2). Sulphide inclusions are also found in many xenoliths but those which are hosted by diamonds provide potentially the most pristine samples from the lithospheric mantle and deeper. Previous experiments indicate that oxygen partitions into sulphide melts and although sparse, some measurements of natural sulphide inclusions from mantle xenoliths indeed show measurable and in some cases relatively high oxygen concentrations. If the parameters that control sulphide oxygen concentration can be determined then they could be potentially used to understand conditions in the mantle and in particular in sublithospheric diamonds. The oxygen content of sulphides separating to the core during core formation could have also influenced the oxygen fugacity of the early mantle.
We have measured the oxygen contents of sulphide melts within experimentally produced mantle assemblages at high pressures and temperatures. A series of multi-anvil experiments were conducted to equilibrate a peridotite assemblage with molten sulphide (FeS) at pressures between 3 –11 GPa and temperatures of 1300 ˚C –1700 ˚C. The effects of pressure, temperature, oxygen fugacity and composition have been investigated. Oxygen fugacity was determined in some experiments by saturating the sulphide in Ir to produce a separate Ir-Fe metal alloy, for which the Fe content is a function of oxygen fugacity. The results show that sulphide melt oxygen contents can range up to 16 weight % FeO, at mantle conditions. Moreover, the content of oxygen in the sulphide is found to be not controlled by fO_2 or fS_2, which is in disagreement with previous experimental studies conducted at ambient pressure conditions. The experiments indicate that the oxygen concentration is mainly controlled by the FeO activity in coexisting silicates phases and the temperature, although further work is still required to calibrate effects of Ni and Cu. In order to fit the data and to account for the FeO dependence, we developed a thermodynamic model using an end-member equilibrium between olivine, pyroxene and FeO in the sulphide melt. The resulting relationship can be used as a geothermometer based on sulphide inclusion oxygen contents and could be particularly useful for determining diamond formation temperatures for sub lithospheric diamonds.

Keywords: Sulfide, Oxygen, Geothermometer

©2019. Japan Geoscience Union. All Right Reserved.

[E] Poster | M (Multidisciplinary and Interdisciplinary)：M-IS Intersection

Thu. May 30, 2019 10:45 AM - 12:15 PM JST | Thu. May 30, 2019 1:45 AM - 3:15 AM UTC | Poster Hall International Exhibition Hall8, Makuhari Messe_9

[M-IS03] Evolution and variability of the Asian monsoon in Cenozoic global climate changes

convener:Masanobu Yamamoto(Faculty of Environmental Earth Science, Hokkaido University), Ryuji Tada(Department of Earth and Planetary Science, Graduate School of Science, The Univeristy of Tokyo)

The Asian Monsoon (AM) is a part of interhemispheric atmospheric phenomena that is driven by the thermal gradient between ocean and land. Contrasts of insolation, heat content and latent heat transfer between ocean and land may have affected the behavior of the AM in the past, but the proxy records are occasionally controversial and do not show a clear picture of the AM variability. Recent proxy and modeling studies suggest that glacial pCO2 cycles could be related to the position of southern westerlies, which is sensitive to interhemispheric heat imbalance. Because monsoon is driven by the heat imbalance, knowledge on the variability of the AM is important to understand the behavior of the global climate system. In this session, presentations on the reconstruction of long-term AM variability from various archives such as IODP expedition cores, discussion on its forcing, and the roles of the AM in global climate changes are welcome.

[MIS03-P01] Asian dust source variability since 10 Ma based on grain size specific mineral composition at IODP Site U1425 in the Japan Sea

*Mui Fa Alison Lee[1], Tomohisa Irino[1] (1.Faculty of Environmental Earth Science, Hokkaido University)

[MIS03-P02] Sources and formation environment of biomass burning products in Pliocene and Pleistocene marine sediments in the Japan Sea

*Song Lu[1], Youhei Yamashita[2], Tomohisa Irino[2] (1.Graduate School of Environmental Science, Hokkaido University , 2.Faculty of Environmental Earth Science, Hokkaido University)

[MIS03-P03] Variation of mineral dust flux in peat at a high moor on the Mt. Daisetsu during Holocene

*Tomohisa Irino[1], Keisuke Hirai[1], Osamu Seki[1], James Hooper[2], Samuel Marx[2] (1.Hokkaido University, 2.University of Wollongong)

[MIS03-P04] Variations in sea surface environments recorded by algal biomarkers in the Japan Sea off the western coast of Hokkaido (IODP Site U1422) over the last 250 ka

*Asako Suzuki[1], Ken Sawada[2], Satoshi Furota[3], Yaeko Igarashi[4], Tomohisa Irino[5] (1.Graduate School of Science, Hokkaido University, 2.Department of Earth and Planetary Sciences, Faculty of Science, Hokkaido University, 3.Japan Agency for Marine-Earth Science and Technology, 4.Institute for Paleoenvironment of Northern Regions, 5.Faculty of Environmental Earth Science, Hokkaido University)

[MIS03-P05] **Decadal oscillation in hydrogen stable isotope ratio of long chain fatty acids in Lake Suigetsu sediment core**

*Masaya Inagaki[1], Masanobu Yamamoto[1,2], Takeshi Nakagawa[3] (1.Graduate School of Environmental Science, Hokkaido University, 2.Faculty of Environmental Earth Science, Hokkaido University, 3.Research Center for Palaeoclimatology, Ritsumeikan University)

[MIS03-P06] **Amplitude modulation of sea surface temperature variability in the Bay of Bengal by 400-kyr eccentricity cycle**

*Masanobu Yamamoto[1], Yuko Tsuchiya[1], Steven Clemens[2] (1.Faculty of Environmental Earth Science, Hokkaido University, 2.Department of Earth, Planetary and Environmental Sciences, Brown University)

Asian dust source variability since 10 Ma based on grain size specific mineral composition at IODP Site U1425 in the Japan Sea

*Mui Fa Alison Lee[1], Tomohisa Irino[1]

1. Faculty of Environmental Earth Science, Hokkaido University

Sediments at Integrated Ocean Drilling Program (IODP) Site U1425 in the Japan Sea is under the strong influence of westerly jet stream and winter monsoon wind which transporting a significant amount of aeolian dust from both Taklamakan deserts and Gobi deserts. Aeolian dust from Taklamakan showed very high content of quartz (60-90%) and less plagioclase (5-40%) than from NE Chinese deserts and Loess (Gobi). The lower value of half height width (FWHM) of illite peak in X-ray diffraction (XRD) profile can be used as an indicator higher illite crystallinity. A decreasing trend of illite FWHM (increasing trend of the crystalinity) towards the core of the fold and thrust anticline has been recognized (Robinson et al. 1990; Orozco et al. 1998). Illite is also predominant component of the Chinese loess, and its highly crystallized nature has been interpreted to indicate that the illite was not formed at surface temperature and may have originated from a low temperature metamorphic environment.

In order to reconstruct a long-term changes in dust sources and transport pathways of Asian dust utilizing knowledges above, we examined mineral composition of IODP Site U1425 located at the central Japan Sea. The sediment samples were separated into >4 μm (silt) and <4 μm (clay) fractions by repeated pipette method. Both fractions were used for powder XRD analysis and peak heights of diagnostic peaks of major minerals were regarded as relative abundance of the minerals. FWHM and chemical index of illite were also examined.

In general, a very high quartz content found at Site U1425 may indicate sediments are aeolian source from Taklamakan deserts and higher plagioclase (albite) may infer dust source from Gobi deserts. Intervals around 9.5 Ma, 8.3 Ma, 7.9 Ma and 4.5 Ma showed very high quartz content and less albite at Site U1425, which indicate increases in dust supplied from Taklamakan than Gobi deserts due to stronger westerly wind. During Pliocene to early Pleistocene (4.2-2Ma), Taklamakan dust is still dominant, however the increasing influence of Gobi dust is recognized at 4.1 and 3.4Ma. On the other hand, an abrupt increase of the ratio of albite to quartz from 0.2 at 4.5 Ma to 0.8 at 4.1 Ma is found, which also shows another maximum at 0.6 Ma. In general, increase of albite abundance in sediments at Site U1425 during Pleistocene indicates the increasing dust supplied from NE China and Gobi deserts and the strengthened winter monsoon.

FWHM (crystallinity) of illite in silt fraction at Site U1425 showed low values (high crystallinity) with narrow range around 0.2˚2θ during Pleistocene. The illite chemistry index showed values below 0.4 and genrerally around 0.3 during Pleistocene, which represents (Fe, Mg)-rich illites (biotite) characterized for physically eroded or unweathered rocks. The highly crystallized and Fe–Mg rich illites in the silt fraction at Site U1425 in the Japan Sea suggests their aeolian origin which may be derived from pre-existing sediments which eroded from low-grade metamorphic rocks in the northern regions of the Tibetan Plateau. In a longer time-scale, higher crystallinity and lower chemistry index of illite in silt fractions occurred in similar timing at 9.3 Ma and 6.6-2.7 Ma which could be correlated with the active regional uplift and tectonic activities of the northeastern margin of the Tibetan Plateau. Possible changes in source of illite indicates frequent plate tectonic activities near the Taklamakan deserts of North Tibet plateau especially from 6.6-2.7Ma.

©2019. Japan Geoscience Union. All Right Reserved.

Keywords: Aeolian dust, Taklamakan deserts, Quartz, Feldspar , Illite, Gobi deserts

©2019. Japan Geoscience Union. All Right Reserved.

Sources and formation environment of biomass burning products in Pliocene and Pleistocene marine sediments in the Japan Sea

*Song Lu[1], Youhei Yamashita[2], Tomohisa Irino[2]

1. Graduate School of Environmental Science, Hokkaido University , 2. Faculty of Environmental Earth Science, Hokkaido University

Behavior of black carbon (BC) is crucial for the earth surface environment because it could cause global warming by absorbing sunlight in the atmosphere. BC is originated from incomplete combustion of biomass or fossil fuels. Combustion in natural processes is incomplete due to local limitation of oxygen during the fire, which leads to the formation of organic fire residues. Robustness of BC to degradation in the natural environment enables us to use BC as a proxy to study the driving force of frequency and burning temperatures of past wildfire events. But the previous fire researches (paleoclimate rather than modern ecology) did not discuss the control factors for burning temperature or try to rebuild the fire temperature. Objective of this study is to understand factors controlling the thermal/optical/chemical characters of BC with burning temperature, provenance and aging in relation to the variabilities of vegetation in the hinterland. For these purposes, BC was quantified as elemental carbon (EC) in coarse (>2 μm) and fine (<2 μm) fractions of sediment samples using a thermal optical transmittance (TOT) method, and their burning temperatures were estimated for bulk samples through measurement of composition of benzene polycarboxylic acids (BPCAs), molecular markers of fire residues, determined with High Performance Liquid Chromatography (HPLC). In order to examine the relationship between burning temperature and BPCA composition, selected plants were experimentally charred to obtain standard charcoal samples. We also applied TOT and BPCA methods to marine sediments such as the surface sediments collected during KR15-10 cruise off the Wakasa Bay and 63 samples between 0 and 203 m CCSF-D were selected from IODP Site U1423 in the northeastern Japan Sea which covered the last 4.3 Myr. Size dependencies of EC contents and thermal properties will be compared with the contents and composition of BPCAs to examine the influence of sources, transport pathways, and burning temperatures of BCs contained in marine sediments.

Keywords: biomass burning, elemental carbon, benzene polycarboxylic acid

©2019. Japan Geoscience Union. All Right Reserved.

Variation of mineral dust flux in peat at a high moor on the Mt. Daisetsu during Holocene

*Tomohisa Irino[1], Keisuke Hirai[1], Osamu Seki[1], James Hooper[2], Samuel Marx[2]

1. Hokkaido University, 2. University of Wollongong

Mt. Daisetsu, Hokkaido, Japan is located just below the northern route of Asian dust transport and receives a significant amount of dust which dies snow surface brown in spring time every year. This area is also characterized by well-developed high moors on the mountains covering the last 4000 - 7500 yrs, which would continuously record the history of climate change during the middle to late Holocene. Peat collected from these high moor could be also a suitable material for a precise age determination using the radio carbon, and its inorganic fraction might consist of aeolian dust of continental origin and volcanic materials of the local origin which could be easily distinguished from each other.

Asian dust transported to the northern Japan may have a different source from those transported to the southwestern Japan. In spite of this, many of previous dust studies for Asian dust deposition in Japan have been conducted for the paleo-archives collected from the southern area. Therefore, it is necessary to reconstruct the composition and flux of Asian dust transported to the northern Japan in order to understand the spatio-temporal variability of westerly that could have significant influence on the climate in east Asia.

We collected peat cores from the high moor in Mt. Daisetsuzan area, and measured the mineral composition contained in peat. After heat treatment of peat samples, we conducted X-ray diffraction (XRD) analysis on the ash fraction and semi-quantified the minerals. Quartz, illite, and chlorite showed positive correlation among others, while various feldspars showed another positive correlation among others independent from quartz. Amorphous materials exhibited a variability different from quartz or feldspars. High ash content was associated with high feldspars or amorphous. Comparing these mineral compositions with those of aeolian dust deposited in this area and the local riverbed materials, we judged that the inorganic fraction could be explained by mixtures of aeolian dust and two kinds (crystalline and amorphous) of local volcanic materials.

We applied statistical unmixing of these mineral assemblage using PARAFAC algorithm on XRD profiles. Quantification of subcomponents such as Asian dust and local volcanic materials enabled us to estimate the variation of dust flux to this northern region for the last 5000 years. Comparison of our results with previous works for dust depositional history in southwestern region around Japan shows an antiphase variation of dust fluxes between north and south, which suggests the change in meandering pattern or pathway of westerly jet trasporting Asian dust.

Keywords: Asian dust, peat, Mt. Daisetsu, Holocene

©2019. Japan Geoscience Union. All Right Reserved.

Variations in sea surface environments recorded by algal biomarkers in the Japan Sea off the western coast of Hokkaido (IODP Site U1422) over the last 250 ka

*Asako Suzuki[1], Ken Sawada[2], Satoshi Furota[3], Yaeko Igarashi[4], Tomohisa Irino[5]

1. Graduate School of Science, Hokkaido University, 2. Department of Earth and Planetary Sciences, Faculty of Science, Hokkaido University, 3. Japan Agency for Marine-Earth Science and Technology, 4. Institute for Paleoenvironment of Northern Regions, 5. Faculty of Environmental Earth Science, Hokkaido University

The Japan Sea is a marginal sea that is closed by four straits, and the surface and deep waters are characterized by the Tsushima Warm Current (TWC), and Japan Sea Proper Water, respectively. In glacial-interglacial cycle, the sea surface environment in the Japan Sea has repeatedly changed by sea level fluctuation. It is reported that intense cooling of surface waters in the northern Japan Sea occurred caused by intensification of the East Asian Winter Monsoon (EAWM), but there have been few researches in this area. Thus, we analyzed algal biomarkers of a sediment core from the site U1422 (northern Japan Sea) of IODP Exp. 346 for the last 250ka. In particular, we apply the paleothermometer using long-chain alkyl diols, which are thought to be produced by diatoms and eustigmatophyte algae in addition to a proxy for sea surface temperature (SST based on alkenones, which are produced by haptophyte algae. The long-chain alkyl diols were also used as the proxies for upwelling intensity and inflow of fresh water, and thus, can provide multiple information for reconstruction of marine paleoenvironment.

The sediment cores studied were recovered at Site U1422 in the northern part of the Japan Basin (the Japan Sea off the western coast of Hokkaido) at 43°45.99’ N, 138°49.99’ E by Integrated Ocean Drilling Program (IODP) Expedition 346. We focus the duration from the MIS 8 to the present (-ca. 250ka). Lipids were extracted with dichloromethane/methanol, and separated to aliphatic, aromatic and polar fractions. Lipids were identified and quantified by GC-MS and GC-FID.

The SSTs based on alkenones and alkyl diols basically fluctuated along the glacial-interglacial cycles. The alkenone-based SSTs were found to be much higher than the diol-based SSTs during the MIS 2-3. The reasons of the differences are likely to be high contribution of distinctive alkenone producer during these stages. In our study, we calculated not only $U^{K'}_{37}$ but also the index containing tetra-unsaturated alkenone (U^{K}_{37}) in the SST estimate, because the tetra-unsaturated alkenone is abundantly detected in several samples. The U^{K}_{37}-based SSTs generally tend to be lower than those estimated by $U^{K'}_{37}$.

Diol Indices 1 and 2, which are proxies of upwelling intensity, are overall low levels. These results indicate that consistent upwelling system is hardly developed in the northern Japan Sea. However, the indices increase in the MIS 2, implying that vertical mixing was promoted as a result of the surface cooling in this stage. Moreover, the C_{32} 1, 15-diol ratio, which is considered as an indicator of fresh water input into marine environment, tended to increase at the transition periods, such as the glacial to interglacial periods. These results suggest that fresh water arisen by melting of snows and ices accumulated on lands was flowing into the Japan Sea through the rivers during these transitions. The increasing spikes of the diol-based fresh water index are also observed during the glacial periods. This can be attributed to the fresh waters arisen by sea ice melting that came from the northward and/or affected by the inflow of TWC as a result of sea-level falling.

©2019. Japan Geoscience Union. All Right Reserved.

Keywords: Northern Japan Sea, Algal biomarker, Alkenone, Diol, East Asian Monsoon, Quaternary

©2019. Japan Geoscience Union. All Right Reserved.

Decadal oscillation in hydrogen stable isotope ratio of long chain fatty acids in Lake Suigetsu sediment core

*Masaya Inagaki[1], Masanobu Yamamoto[1,2], Takeshi Nakagawa[3]

1. Graduate School of Environmental Science, Hokkaido University, 2. Faculty of Environmental Earth Science, Hokkaido University, 3. Research Center for Palaeoclimatology, Ritsumeikan University

Japanese weathers are affected by the Pacific Decadal Oscillation (PDO), monsoon, and El Niño Southern Oscillation. In this study, we analyzed the hydrogen isotopes of long chain n-fatty acids in sediment cores from Lake Suigetsu in Fukui Prefecture, and reconstructed variability in the isotopic ratio of precipitation from 1362 to 1662 CE and from1852 to 2017 CE. Hydrogen isotopic composition (δ D) showed decadal oscillation ranging from ~-170‰ to ~-120‰. Between 1362 and 1662 CE, this oscillation corresponded to the decadal oscillation seen in the UK37’ -based sea surface temperature (SST) in Beppu Bay. Higher SST corresponded to higher δ D. Because the SST in Beppu Bay corresponds to the PDO, we suppose that variability in the δ D of long chain n-fatty acids in Lake Suigetsu reflected the isotopic ratio of precipitation that responded to the PDO. In Nagoya, the isotope ratio of precipitation is governed by the position of Baiu front. When Baiu front is developed north of Nagoya, the isotope ratio is high. When Baiu front is south of Nagoya, isotope ratio is low (Kurita et al., 2015 Climate of the Past). This suggest that the position of the Baiu front was linked to the PDO from 1362 to 1662 CE. In the conditions of the negative PDO (high SST in Beppu Bay), the Baiu front was tended to be located north of Lake Suigetsu.

Keywords: PDO, isotopic ratio of precipitation, climate change

©2019. Japan Geoscience Union. All Right Reserved.

Amplitude modulation of sea surface temperature variability in the Bay of Bengal by 400-kyr eccentricity cycle

*Masanobu Yamamoto[1], Yuko Tsuchiya[1], Steven Clemens[2]

1. Faculty of Environmental Earth Science, Hokkaido University, 2. Department of Earth, Planetary and Environmental Sciences, Brown University

We generated a 1.7 kyr-resolution TEX_{86}-based sea surface temperature (SST) record from the International Ocean Discovery Program Site U1446 in the Bay of Bengal during the last 1.46 Myr. The SST varied synchronously with LR04 benthic foraminifera $\delta^{18}O$ and deep water $\delta^{13}C$. The cyclicity changed from 41-kyr to 100-kyr around 900 ka. The amplitude of SST variation responded to the 400-kyr cycles of eccentricity. Higher amplitude corresponded to low eccentricity. This suggests that eccentricity forced climate variability independently of the shift of cyclicity of glacial cycles across the Mid-Pleistocene Transition.

Keywords: Bay of Bengal, Sea surface temperature, Mid-Pleistocene Transition

©2019. Japan Geoscience Union. All Right Reserved.

[E] Poster | M (Multidisciplinary and Interdisciplinary)：M-IS Intersection

Thu. May 30, 2019 5:15 PM - 6:30 PM JST | Thu. May 30, 2019 8:15 AM - 9:30 AM UTC | Poster Hall International Exhibition Hall8, Makuhari Messe_34

[M-IS03] Evolution and variability of the Asian monsoon in Cenozoic global climate changes

convener:Masanobu Yamamoto(Faculty of Environmental Earth Science, Hokkaido University), Ryuji Tada(Department of Earth and Planetary Science, Graduate School of Science, The Univeristy of Tokyo)

The Asian Monsoon (AM) is a part of interhemispheric atmospheric phenomena that is driven by the thermal gradient between ocean and land. Contrasts of insolation, heat content and latent heat transfer between ocean and land may have affected the behavior of the AM in the past, but the proxy records are occasionally controversial and do not show a clear picture of the AM variability. Recent proxy and modeling studies suggest that glacial pCO2 cycles could be related to the position of southern westerlies, which is sensitive to interhemispheric heat imbalance. Because monsoon is driven by the heat imbalance, knowledge on the variability of the AM is important to understand the behavior of the global climate system. In this session, presentations on the reconstruction of long-term AM variability from various archives such as IODP expedition cores, discussion on its forcing, and the roles of the AM in global climate changes are welcome.

[MIS03-P01] Asian dust source variability since 10 Ma based on grain size specific mineral composition at IODP Site U1425 in the Japan Sea

*Mui Fa Alison Lee[1], Tomohisa Irino[1] (1.Faculty of Environmental Earth Science, Hokkaido University)

[MIS03-P02] Sources and formation environment of biomass burning products in Pliocene and Pleistocene marine sediments in the Japan Sea

*Song Lu[1], Youhei Yamashita[2], Tomohisa Irino[2] (1.Graduate School of Environmental Science, Hokkaido University , 2.Faculty of Environmental Earth Science, Hokkaido University)

[MIS03-P03] Variation of mineral dust flux in peat at a high moor on the Mt. Daisetsu during Holocene

*Tomohisa Irino[1], Keisuke Hirai[1], Osamu Seki[1], James Hooper[2], Samuel Marx[2] (1.Hokkaido University, 2.University of Wollongong)

[MIS03-P04] Variations in sea surface environments recorded by algal biomarkers in the Japan Sea off the western coast of Hokkaido (IODP Site U1422) over the last 250 ka

*Asako Suzuki[1], Ken Sawada[2], Satoshi Furota[3], Yaeko Igarashi[4], Tomohisa Irino[5] (1.Graduate School of Science, Hokkaido University, 2.Department of Earth and Planetary Sciences, Faculty of Science, Hokkaido University, 3.Japan Agency for Marine-Earth Science and Technology, 4.Institute for Paleoenvironment of Northern Regions, 5.Faculty of Environmental Earth Science, Hokkaido University)

[MIS03-P05] **Decadal oscillation in hydrogen stable isotope ratio of long chain fatty acids in Lake Suigetsu sediment core**

*Masaya Inagaki[1], Masanobu Yamamoto[1,2], Takeshi Nakagawa[3] (1.Graduate School of Environmental Science, Hokkaido University, 2.Faculty of Environmental Earth Science, Hokkaido University, 3.Research Center for Palaeoclimatology, Ritsumeikan University)

[MIS03-P06] **Amplitude modulation of sea surface temperature variability in the Bay of Bengal by 400-kyr eccentricity cycle**

*Masanobu Yamamoto[1], Yuko Tsuchiya[1], Steven Clemens[2] (1.Faculty of Environmental Earth Science, Hokkaido University, 2.Department of Earth, Planetary and Environmental Sciences, Brown University)

Asian dust source variability since 10 Ma based on grain size specific mineral composition at IODP Site U1425 in the Japan Sea

*Mui Fa Alison Lee[1], Tomohisa Irino[1]

1. Faculty of Environmental Earth Science, Hokkaido University

Sediments at Integrated Ocean Drilling Program (IODP) Site U1425 in the Japan Sea is under the strong influence of westerly jet stream and winter monsoon wind which transporting a significant amount of aeolian dust from both Taklamakan deserts and Gobi deserts. Aeolian dust from Taklamakan showed very high content of quartz (60-90%) and less plagioclase (5-40%) than from NE Chinese deserts and Loess (Gobi). The lower value of half height width (FWHM) of illite peak in X-ray diffraction (XRD) profile can be used as an indicator higher illite crystallinity. A decreasing trend of illite FWHM (increasing trend of the crystalinity) towards the core of the fold and thrust anticline has been recognized (Robinson et al. 1990; Orozco et al. 1998). Illite is also predominant component of the Chinese loess, and its highly crystallized nature has been interpreted to indicate that the illite was not formed at surface temperature and may have originated from a low temperature metamorphic environment.

In order to reconstruct a long-term changes in dust sources and transport pathways of Asian dust utilizing knowledges above, we examined mineral composition of IODP Site U1425 located at the central Japan Sea. The sediment samples were separated into >4 μm (silt) and <4 μm (clay) fractions by repeated pipette method. Both fractions were used for powder XRD analysis and peak heights of diagnostic peaks of major minerals were regarded as relative abundance of the minerals. FWHM and chemical index of illite were also examined.

In general, a very high quartz content found at Site U1425 may indicate sediments are aeolian source from Taklamakan deserts and higher plagioclase (albite) may infer dust source from Gobi deserts. Intervals around 9.5 Ma, 8.3 Ma, 7.9 Ma and 4.5 Ma showed very high quartz content and less albite at Site U1425, which indicate increases in dust supplied from Taklamakan than Gobi deserts due to stronger westerly wind. During Pliocene to early Pleistocene (4.2-2Ma), Taklamakan dust is still dominant, however the increasing influence of Gobi dust is recognized at 4.1 and 3.4Ma. On the other hand, an abrupt increase of the ratio of albite to quartz from 0.2 at 4.5 Ma to 0.8 at 4.1 Ma is found, which also shows another maximum at 0.6 Ma. In general, increase of albite abundance in sediments at Site U1425 during Pleistocene indicates the increasing dust supplied from NE China and Gobi deserts and the strengthened winter monsoon.

FWHM (crystallinity) of illite in silt fraction at Site U1425 showed low values (high crystallinity) with narrow range around 0.2˚2θ during Pleistocene. The illite chemistry index showed values below 0.4 and genrerally around 0.3 during Pleistocene, which represents (Fe, Mg)-rich illites (biotite) characterized for physically eroded or unweathered rocks. The highly crystallized and Fe–Mg rich illites in the silt fraction at Site U1425 in the Japan Sea suggests their aeolian origin which may be derived from pre-existing sediments which eroded from low-grade metamorphic rocks in the northern regions of the Tibetan Plateau. In a longer time-scale, higher crystallinity and lower chemistry index of illite in silt fractions occurred in similar timing at 9.3 Ma and 6.6-2.7 Ma which could be correlated with the active regional uplift and tectonic activities of the northeastern margin of the Tibetan Plateau. Possible changes in source of illite indicates frequent plate tectonic activities near the Taklamakan deserts of North Tibet plateau especially from 6.6-2.7Ma.

©2019. Japan Geoscience Union. All Right Reserved.

Keywords: Aeolian dust, Taklamakan deserts, Quartz, Feldspar , Illite, Gobi deserts

©2019. Japan Geoscience Union. All Right Reserved.

Sources and formation environment of biomass burning products in Pliocene and Pleistocene marine sediments in the Japan Sea

*Song Lu[1], Youhei Yamashita[2], Tomohisa Irino[2]

1. Graduate School of Environmental Science, Hokkaido University , 2. Faculty of Environmental Earth Science, Hokkaido University

Behavior of black carbon (BC) is crucial for the earth surface environment because it could cause global warming by absorbing sunlight in the atmosphere. BC is originated from incomplete combustion of biomass or fossil fuels. Combustion in natural processes is incomplete due to local limitation of oxygen during the fire, which leads to the formation of organic fire residues. Robustness of BC to degradation in the natural environment enables us to use BC as a proxy to study the driving force of frequency and burning temperatures of past wildfire events. But the previous fire researches (paleoclimate rather than modern ecology) did not discuss the control factors for burning temperature or try to rebuild the fire temperature. Objective of this study is to understand factors controlling the thermal/optical/chemical characters of BC with burning temperature, provenance and aging in relation to the variabilities of vegetation in the hinterland. For these purposes, BC was quantified as elemental carbon (EC) in coarse (>2 μm) and fine (<2 μm) fractions of sediment samples using a thermal optical transmittance (TOT) method, and their burning temperatures were estimated for bulk samples through measurement of composition of benzene polycarboxylic acids (BPCAs), molecular markers of fire residues, determined with High Performance Liquid Chromatography (HPLC). In order to examine the relationship between burning temperature and BPCA composition, selected plants were experimentally charred to obtain standard charcoal samples. We also applied TOT and BPCA methods to marine sediments such as the surface sediments collected during KR15-10 cruise off the Wakasa Bay and 63 samples between 0 and 203 m CCSF-D were selected from IODP Site U1423 in the northeastern Japan Sea which covered the last 4.3 Myr. Size dependencies of EC contents and thermal properties will be compared with the contents and composition of BPCAs to examine the influence of sources, transport pathways, and burning temperatures of BCs contained in marine sediments.

Keywords: biomass burning, elemental carbon, benzene polycarboxylic acid

©2019. Japan Geoscience Union. All Right Reserved.

Variation of mineral dust flux in peat at a high moor on the Mt. Daisetsu during Holocene

*Tomohisa Irino[1], Keisuke Hirai[1], Osamu Seki[1], James Hooper[2], Samuel Marx[2]

1. Hokkaido University, 2. University of Wollongong

Mt. Daisetsu, Hokkaido, Japan is located just below the northern route of Asian dust transport and receives a significant amount of dust which dies snow surface brown in spring time every year. This area is also characterized by well-developed high moors on the mountains covering the last 4000 - 7500 yrs, which would continuously record the history of climate change during the middle to late Holocene. Peat collected from these high moor could be also a suitable material for a precise age determination using the radio carbon, and its inorganic fraction might consist of aeolian dust of continental origin and volcanic materials of the local origin which could be easily distinguished from each other.

Asian dust transported to the northern Japan may have a different source from those transported to the southwestern Japan. In spite of this, many of previous dust studies for Asian dust deposition in Japan have been conducted for the paleo-archives collected from the southern area. Therefore, it is necessary to reconstruct the composition and flux of Asian dust transported to the northern Japan in order to understand the spatio-temporal variability of westerly that could have significant influence on the climate in east Asia.

We collected peat cores from the high moor in Mt. Daisetsuzan area, and measured the mineral composition contained in peat. After heat treatment of peat samples, we conducted X-ray diffraction (XRD) analysis on the ash fraction and semi-quantified the minerals. Quartz, illite, and chlorite showed positive correlation among others, while various feldspars showed another positive correlation among others independent from quartz. Amorphous materials exhibited a variability different from quartz or feldspars. High ash content was associated with high feldspars or amorphous. Comparing these mineral compositions with those of aeolian dust deposited in this area and the local riverbed materials, we judged that the inorganic fraction could be explained by mixtures of aeolian dust and two kinds (crystalline and amorphous) of local volcanic materials.

We applied statistical unmixing of these mineral assemblage using PARAFAC algorithm on XRD profiles. Quantification of subcomponents such as Asian dust and local volcanic materials enabled us to estimate the variation of dust flux to this northern region for the last 5000 years. Comparison of our results with previous works for dust depositional history in southwestern region around Japan shows an antiphase variation of dust fluxes between north and south, which suggests the change in meandering pattern or pathway of westerly jet trasporting Asian dust.

Keywords: Asian dust, peat, Mt. Daisetsu, Holocene

©2019. Japan Geoscience Union. All Right Reserved.

Variations in sea surface environments recorded by algal biomarkers in the Japan Sea off the western coast of Hokkaido (IODP Site U1422) over the last 250 ka

*Asako Suzuki[1], Ken Sawada[2], Satoshi Furota[3], Yaeko Igarashi[4], Tomohisa Irino[5]

1. Graduate School of Science, Hokkaido University, 2. Department of Earth and Planetary Sciences, Faculty of Science, Hokkaido University, 3. Japan Agency for Marine-Earth Science and Technology, 4. Institute for Paleoenvironment of Northern Regions, 5. Faculty of Environmental Earth Science, Hokkaido University

The Japan Sea is a marginal sea that is closed by four straits, and the surface and deep waters are characterized by the Tsushima Warm Current (TWC), and Japan Sea Proper Water, respectively. In glacial-interglacial cycle, the sea surface environment in the Japan Sea has repeatedly changed by sea level fluctuation. It is reported that intense cooling of surface waters in the northern Japan Sea occurred caused by intensification of the East Asian Winter Monsoon (EAWM), but there have been few researches in this area. Thus, we analyzed algal biomarkers of a sediment core from the site U1422 (northern Japan Sea) of IODP Exp. 346 for the last 250ka. In particular, we apply the paleothermometer using long-chain alkyl diols, which are thought to be produced by diatoms and eustigmatophyte algae in addition to a proxy for sea surface temperature (SST based on alkenones, which are produced by haptophyte algae. The long-chain alkyl diols were also used as the proxies for upwelling intensity and inflow of fresh water, and thus, can provide multiple information for reconstruction of marine paleoenvironment.

The sediment cores studied were recovered at Site U1422 in the northern part of the Japan Basin (the Japan Sea off the western coast of Hokkaido) at 43°45.99’ N, 138°49.99’ E by Integrated Ocean Drilling Program (IODP) Expedition 346. We focus the duration from the MIS 8 to the present (-ca. 250ka). Lipids were extracted with dichloromethane/methanol, and separated to aliphatic, aromatic and polar fractions. Lipids were identified and quantified by GC-MS and GC-FID.

The SSTs based on alkenones and alkyl diols basically fluctuated along the glacial-interglacial cycles. The alkenone-based SSTs were found to be much higher than the diol-based SSTs during the MIS 2-3. The reasons of the differences are likely to be high contribution of distinctive alkenone producer during these stages. In our study, we calculated not only $U^{K'}_{37}$ but also the index containing tetra-unsaturated alkenone (U^{K}_{37}) in the SST estimate, because the tetra-unsaturated alkenone is abundantly detected in several samples. The U^{K}_{37}-based SSTs generally tend to be lower than those estimated by $U^{K'}_{37}$.

Diol Indices 1 and 2, which are proxies of upwelling intensity, are overall low levels. These results indicate that consistent upwelling system is hardly developed in the northern Japan Sea. However, the indices increase in the MIS 2, implying that vertical mixing was promoted as a result of the surface cooling in this stage. Moreover, the C_{32} 1, 15-diol ratio, which is considered as an indicator of fresh water input into marine environment, tended to increase at the transition periods, such as the glacial to interglacial periods. These results suggest that fresh water arisen by melting of snows and ices accumulated on lands was flowing into the Japan Sea through the rivers during these transitions. The increasing spikes of the diol-based fresh water index are also observed during the glacial periods. This can be attributed to the fresh waters arisen by sea ice melting that came from the northward and/or affected by the inflow of TWC as a result of sea-level falling.

©2019. Japan Geoscience Union. All Right Reserved.

Keywords: Northern Japan Sea, Algal biomarker, Alkenone, Diol, East Asian Monsoon, Quaternary

©2019. Japan Geoscience Union. All Right Reserved.

Decadal oscillation in hydrogen stable isotope ratio of long chain fatty acids in Lake Suigetsu sediment core

*Masaya Inagaki[1], Masanobu Yamamoto[1,2], Takeshi Nakagawa[3]

1. Graduate School of Environmental Science, Hokkaido University, 2. Faculty of Environmental Earth Science, Hokkaido University, 3. Research Center for Palaeoclimatology, Ritsumeikan University

Japanese weathers are affected by the Pacific Decadal Oscillation (PDO), monsoon, and El Niño Southern Oscillation. In this study, we analyzed the hydrogen isotopes of long chain n-fatty acids in sediment cores from Lake Suigetsu in Fukui Prefecture, and reconstructed variability in the isotopic ratio of precipitation from 1362 to 1662 CE and from1852 to 2017 CE. Hydrogen isotopic composition (δ D) showed decadal oscillation ranging from ~-170‰ to ~-120‰. Between 1362 and 1662 CE, this oscillation corresponded to the decadal oscillation seen in the UK37’ -based sea surface temperature (SST) in Beppu Bay. Higher SST corresponded to higher δ D. Because the SST in Beppu Bay corresponds to the PDO, we suppose that variability in the δ D of long chain n-fatty acids in Lake Suigetsu reflected the isotopic ratio of precipitation that responded to the PDO. In Nagoya, the isotope ratio of precipitation is governed by the position of Baiu front. When Baiu front is developed north of Nagoya, the isotope ratio is high. When Baiu front is south of Nagoya, isotope ratio is low (Kurita et al., 2015 Climate of the Past). This suggest that the position of the Baiu front was linked to the PDO from 1362 to 1662 CE. In the conditions of the negative PDO (high SST in Beppu Bay), the Baiu front was tended to be located north of Lake Suigetsu.

Keywords: PDO, isotopic ratio of precipitation, climate change

©2019. Japan Geoscience Union. All Right Reserved.

Amplitude modulation of sea surface temperature variability in the Bay of Bengal by 400-kyr eccentricity cycle

*Masanobu Yamamoto[1], Yuko Tsuchiya[1], Steven Clemens[2]

1. Faculty of Environmental Earth Science, Hokkaido University, 2. Department of Earth, Planetary and Environmental Sciences, Brown University

We generated a 1.7 kyr-resolution TEX_{86}-based sea surface temperature (SST) record from the International Ocean Discovery Program Site U1446 in the Bay of Bengal during the last 1.46 Myr. The SST varied synchronously with LR04 benthic foraminifera $\delta^{18}O$ and deep water $\delta^{13}C$. The cyclicity changed from 41-kyr to 100-kyr around 900 ka. The amplitude of SST variation responded to the 400-kyr cycles of eccentricity. Higher amplitude corresponded to low eccentricity. This suggests that eccentricity forced climate variability independently of the shift of cyclicity of glacial cycles across the Mid-Pleistocene Transition.

Keywords: Bay of Bengal, Sea surface temperature, Mid-Pleistocene Transition

©2019. Japan Geoscience Union. All Right Reserved.

[E] Poster | M (Multidisciplinary and Interdisciplinary)：M-IS Intersection

Thu. May 30, 2019 10:45 AM - 12:15 PM JST | Thu. May 30, 2019 1:45 AM - 3:15 AM UTC | Poster Hall International Exhibition Hall8, Makuhari Messe_10

[M-IS04] Interdisciplinary studies on pre-earthquake processes

convener:Katsumi Hattori(Department of Earth Sciences, Graduate School of Science, Chiba University), JANN-YENQ Liu(Institute of Space Science, National Central University, Taiwan), Dimitar Ouzounov(Center of Excellence in Earth Systems Modeling & Observations (CEESMO) , Schmid College of Science & Technology Chapman University, Orange, California, USA), Qinghua Huang(Peking University)

This session expands the interdisciplinary discussions on preparation process of earthquake and earthquake predictability by presenting the latest progress in studying the physically based pre-earthquake phenomena. New observations from space and ground have provided
evidences, which may enhance better understanding of tectonic activity. The session anticipates talks that include but not limited to observations and analyses of seismic, electrical, electromagnetic, electro-chemical and thermodynamic processes related to stress changes in the lithosphere along with their statistical and physical validation. Presentations on the latest observational results associated with major earthquakes obtained by different methodologies are welcomed. The topics of the session are as follows but not limited.

-General discussion on earthquake preparation process and the physics of pre-earthquake signals

- Theory, modeling, laboratory experiments, computational simulation for generation and propagation of pre-earthquake signals and their connection with seismic cycle

 - Multi-parameter observations, detection, and validation of pre-earthquake signals

 - Cross-disciplinary studies, practical and technical approaches for better understanding of earthquake preparation processes and their connection with seismicity

[MIS04-P01] Statistical analysis and Evaluation of ULF seismo-magnetic phenomena at Kakioka, Japan, during 1983-2017

*Kei Takahashi[1], Katsumi Hattori[2], Peng Han[3] (1.Faculty of Science, Chiba University, 2.Graduate School of Science, Chiba University, 3.Southern University of Science and Technology, China)

[MIS04-P02] Pre-seismic anomalies on Earth’s magnetic field and ionosphere electron density using Swarm data

*Amune Yamazaki[1], Katsumi Hattori[1], Rui Song[1] (1.Chiba University)

[MIS04-P03] Measurement of radon density in the atmosphere at Okayama, Kochi, Choshi and Kiyosumi, II

*Tohru Okabayashi[1], Kiyotaka Ninagawa[2], Isao Yamamoto[3], Katsumi Hattori[4], Chie Yoshino[4], Haruna Kojima[4], Nobuhiro Maeda (1.Department of Merical Risk and Crisis Management, Faculty of Risk and Crisis Management, Chiba Institute of Science, 2.Faculty of Science, Okayama University of Science, 3.Falcuty of Engineering, Okayama University of Science, 4.Graduate school of Science, Chiba University)

[MIS04-P04] Possible anomalous changes in solar quiet-daily geomagnetic variation *Sq* related to the 2011 off the Pacific coast of Tohoku earthquake (Mw 9.0)

*Xiaocan Liu[1], Katsumi Hattori[2,3], Peng Han[4], Huaran Chen[1] (1.Institute of geophysics China Earthquake Administrition, 2.Graduate School of Science, Chiba University, Chiba, Japan, 3. Center for Environmental Remote Sensing, Chiba University, Chiba, Japan, 4.Department of Earth and Space Sciences, Southern University of Science and Technology, ShenZhen, China)

[MIS04-P05] Co-seismic geomagnetic fluctuations and atmospheric disturbances during the 2018 M6.2 Hualien Earthquake

*Chun-Rong Chen[1], JANN-YENQ Liu[1] (1.Graduate Institute of Space Science, National Central University)

[MIS04-P06] Multi-sensor monitoring network for earthquake precursor study near subduction zone at Boso, Japan

*Katsumi Hattori[1], Chie Yoshino[1], WEIYUN XIE[2], Sanaka Saito[2], Haruna Kojima[2], Rui Song[2], Peng Han[3], Toru Mogi[4], Tada-nori Goto[5], Ichi Takumi[6], Hiroshi Yasukawa[7], Motoaki Mouri[8], Jun Izutsu[9], Tadashi Takano[10], Chihiro Yamanaka[11], Masashi Kamogawa[12], Yoshiaki Ando[13], JANN-YENQ Liu[14], Dimitar Ouzounov[15], Valery Tramutoli[16] (1.Department of Earth Sciences, Graduate School of Science, Chiba University, 2.Graduate School of Science and Engineering, Chiba University, 3.Southern University of Science and Technology, China, 4.Hokkaido University, 5.Kyoto University, 6.Nagoya Institute of Technology, 7.Aichi Prefectural University, 8.Aichi University, 9.Chubu University, 10.Nihon University, 11.Osaka University, 12.Tokyo Gakugei University, 13.The University of Electro-Communications, 14.National Central University, Taiwan, 15.Chapman University, US, 16.University of Basilicagta, Italy)

[MIS04-P07] Transient Effects in Atmosphere and Ionosphere Associated with 2018 Mw 7.5 Sulawesi Indonesia Earthquake and Triggered Tsunami and Volcano Activities

★Invited Papers

*Dimitar Ouzounov[1], Sergey Pulinets[2], Dmitry Davidenko[2], Alexander Rozhnoi[3], Maria Solovieva[3], Tiger Liu[4] (1.Center of Excellence in Earth Systems Modeling & Observations (CEESMO) , Schmid College of Science & Technology Chapman University, Orange, California, USA, 2.Space Research Institute, RAS, Moscow, Russia, 3.The Schmidt Institute of Physics of the Earth, RAS, Moscow, Russia, 4.Center for Astronautical Physics and Engineering, National Central University, Taoyuan City, Taiwan)

[MIS04-P08] Seismicity change and b value variation prior to the Wenchuan earthquake (*Ms 8.0*)

*Peng Han[1], Rui Wang[1], Ying Chang[1], Miao Miao[1], Haixia Shi[2], Lingyuan Meng[2], Xuemei Zhang[2], Weiyun Xie[3], Katsumi Hattori[3] (1.Southern University of Science and Technology, Shenzhen, China, 2.China Earthquake Networks Center, Beijing 100045, China, 3.Chiba University, Chiba, Japan)

Statistical analysis and Evaluation of ULF seismo-magnetic phenomena at Kakioka, Japan, during 1983-2017

*Kei Takahashi[1], Katsumi Hattori[2], Peng Han[3]

1. Faculty of Science, Chiba University, 2. Graduate School of Science, Chiba University, 3. Southern University of Science and Technology, China

To clarify and verify the ultralow frequency (ULF) seismo-magnetic phenomena, we have performed statistical studies on the geomagnetic data observed at the Kakioka (KAK) station, Japan, during 1983-2017. We investigated the energy of ULF geomagnetic signals of the frequency around 0.01 Hz using wavelet transform analysis. To minimize the influences of artificial noises and global magnetic perturbations, we used only the geomagnetic data observed at midnight time (LT 2:30 A.M. to 4:00 A.M.).We define the geomagnetic anomalies when the Z components of geomagnetic data exceeds median + 1.5 IQR, where IQR is the interquartile range. Considering that ionospheric disturbances may also lead to enhancements in the Z component, we exclude the anomaly when the energy of H component exceeds median + 3.0 IQR. Statistical analysis of superposed epoch analysis have indicated that ULF magnetic anomalies are more likely to appear before sizable isolated earthquake events (Es parameter which is higher than 8th power of 10 and no earthquake events during ±45 days) rather than after them, especially 6-10 days before the events. Finally, we have evaluated the precursory information of ULF geomagnetic signals for local sizable earthquakes using Molchan’ s error diagram. The above results have indicated that the ULF seismo-magnetic phenomena at Kakioka clearly contain precursory information and have a possibility of improving forecasting of large earthquakes.

©2019. Japan Geoscience Union. All Right Reserved.

Pre-seismic anomalies on Earth’s magnetic field and ionosphere electron density using Swarm data

*Amune Yamazaki[1], Katsumi Hattori[1], Rui Song[1]

1. Chiba University

An earthquake is a rapid release of stress in the lithosphere and often leads to serious damages on human lives and society. Even though the short-time forecast of earthquake is important, it is not achieved yet. However, many electromagnetic phenomena that may be related to seismic activity have been reported recently. The satellite, one of the useful tools to observe these phenomena, can cover the global areas and can collect a large amount of data related to earthquakes which have large magnitude worldwide in short time. The Swarm satellites mission started to operate on November 22, 2013 by European Space Agency, with the constellation of three satellites (A, B, C) The anomalies preceded to the Ecuador earthquake in 2016 have been reported using the Swarm data. In this paper, in order to validate these results using the magnetic vector Y data by VFM and electron density data by Langmuir probe, we have analyzed the Swarm data related the M6.3~6.9 earthquakes occurred at Lombok Island, Indonesia, in July 28, August 5, and 19, 2018. The study area is a 1000 km square from the epicenter of 20180805 earthquake and the analyzed period is from May 28 to September 27, 2018. In this paper we report night-time orbit data at 18:00-6:00 LT.

As results, we found the following tendencies; (1) positive anomalies on magnetic Y vector about 1-2 weeks before the earthquakes and (2) negative anomalies on electron density from 1 week to 1 month before the earthquakes. We performed the same analysis to the data on the same period in 2016 and 2017 for reference when there were no M6+ earthquakes. We found that the number of anomaly track is only abruptly increased in the short period from the end of June to July in 2018, and that the trend is not able to be found in 2016 and 2017. From this unique trend in 2018, it is suggestive of the existence of the relation between the local seismic activity and in-situ satellite anomalies in the magnetic field and electron density in Lombok area.

©2019. Japan Geoscience Union. All Right Reserved.

Measurement of radon density in the atmosphere at Okayama, Kochi, Choshi and Kiyosumi, II

*Tohru Okabayashi[1], Kiyotaka Ninagawa[2], Isao Yamamoto[3], Katsumi Hattori[4], Chie Yoshino[4], Haruna Kojima[4], Nobuhiro Maeda

1. Department of Merical Risk and Crisis Management, Faculty of Risk and Crisis Management, Chiba Institute of Science, 2. Faculty of Science, Okayama University of Science, 3. Falcuty of Engineering, Okayama University of Science, 4. Graduate school of Science, Chiba University

We report continuous measurement of radon density in atmosphere at Okayama for three years, Kochi, Choshi and Kiyosumi for two years. An increase of radon density in groundwater at Nishinomiya city [1] and in atmosphere [2] at the southern part of Hyogo Prefecture Earthquake in 1995 were reported, respectively. In the case of Tohoku Region Pacific Coast Earthquake, the data obtained the exhaust air monitor that peak duration was long and the peak decreased rapidly before earthquake has been reported at the radiation facility of Fukushima Medical College in Fukushima [3]. On the other hand, a PIN photodiode have been developed and used as a high sensitive alpha ray detector in Super Kamiokande [4]. Since 2016, we also made an experimental setup using PIN photodiode, and measured the radon density in atmosphere. Using a Si PIN photodiode (S3204-09, unsealed, Hamamatsu Photodiode K.K.) as an alpha ray detector, we constructed radon detection setup combined with aluminum pot as an air accumulator, H4083 (Hamamatsu) as a charge amplifier, C4900-01 (Hamamatsu) as a high voltage power supply module, a pulse shaped amplifier with time constant of 10 msec, a multi channel analyzer (MCA-LiteN), and a PC as a data analysis. Obtained alpha spectra of atmosphere showed 4 peaks originated from ^{218}Po, ^{214}Po and ^{210}Po of U series, and ^{212}Po of Th series. Since 2017, we newly started to measure at Kochi, Choshi and Kiyosumi using our apparatus. Details of observed data are discussed in addition the data at Okayama since 2016.

[1] Igarashi G., Saeki S., Takahata N., Sumikawa K., Tasaka S., Sasaki Y., Takahashi M. and Sano Y. : Ground-water radon anomaly before the Kobe earthquake in Japan, Science, 269, 60-61, 1995.
[2] Yasuoka, Y. and Shinogi, M.: Anomaly in atmospheric radon concentration: a possible precursor of the 1995 Kobe, Japan, earthquake. Health Physics, 72, 759-761, 1997.
[3] Nagahama H., Yasuoka Y., Suzuki T., and Homma Y.: Radon Variation in the Air Before the 2011 Tohoku Earthquake (Mw =9.0), Programme and Abstracts, A32-09, The Seismological Society of Japan. 2011, Fall Meeting.
[4] Nemoto, M., Tasaka S., Hori H., Okumura K., Kajita T., and Takeuchi Y. : Development of High Sensitive Radon Detector with Electrostatic Collection. Radioisotopes, 46, 710-719, 1997 (Japanese).

Keywords: radon, atmosphere, earthquake prediction

©2019. Japan Geoscience Union. All Right Reserved.

Possible anomalous changes in solar quiet-daily geomagnetic variation *Sq* related to the 2011 off the Pacific coast of Tohoku earthquake (Mw 9.0)

*Xiaocan Liu[1], Katsumi Hattori[2,3], Peng Han[4], Huaran Chen[1]

1. Institute of geophysics China Earthquake Administrition, 2. Graduate School of Science, Chiba University, Chiba, Japan, 3. Center for Environmental Remote Sensing, Chiba University, Chiba, Japan, 4. Department of Earth and Space Sciences, Southern University of Science and Technology, ShenZhen, China

Seismo-electromagnetic researches have been studied for decades (e.g. Hayakawa and Fujinawa, 1994; Hayakawa and Molchanov, 2002, 2008,2013; Hattori, 2004, Hattori, et al., 2004a, 2004b; Hayakawa et al., 2007;, Hattori et al., 2013; Han et al., 2011, 2014, 2015, 2016, 2017; Huang QH et al., 2011, 2015; Du A, Huang Q et al., 2002, Rong YM et al., 2012, Yuan G.P., Zhang X.M. et al. 2015), and the geomagnetic diurnal variation (GDV) is a stable variation of the geomagnetic field that can be used to detect possible anomalous changes associated with large earthquakes.

We investigated data observed at 20 geomagnetic observatories at longitudes of 130˚E to 150˚E between 2009 and 2012 to detect possible anomalous changes in the geomagnetic solar quiet daily variation (Sq) related to the 2011 off the Pacific coast of Tohoku earthquake (Mw 9.0) occurred on March 11, 2011 in Japan. We selected the 5 quiet days every month and analyzed three component magnetic data with 1 min resolution using the natural orthogonal component (NOC) method to identify Sq variations from observations, and performed the spherical harmonic analysis (SHA) to separate the internal and the external equivalent Sq current systems of Je and Ji. We obtained that, Je and Ji are distorted near the epicenter area on two geomagnetic quiet days of January 23 and 27, 2011. They are about two months before the earthquake. Then, we made backward computation on the external and internal parts of the SHA model geomagnetic fields, Be and Bi, to determine the possible anomalous magnetic field variations at each station. Results show significant differences in daily variation for all components on January 23 and 27, 2011. The other days, we could not recognize any apparent anomalous behaviors, except known secular, seasonal, and solar activity dependences. A possible connection between this anomaly and the very strong Tohoku earthquake, which followed only one and half month after the geomagnetic anomaly is of highest interest for the research on earthquake precursors.

Keywords: geomagnetic solar quiet daily variation (Sq), natural orthogonal component (NOC) method, spherical harmonic analysis (SHA), the 2011 off the Pacific coast of Tohoku earthquak

©2019. Japan Geoscience Union. All Right Reserved.

Co-seismic geomagnetic fluctuations and atmospheric disturbances during the 2018 M6.2 Hualien Earthquake

*Chun-Rong Chen[1], JANN-YENQ Liu[1]

1. Graduate Institute of Space Science, National Central University

The strong ground motion of 6 February 2018 M6.2 Hualien Earthquake triggered a series of co-seismic geomagnetic fluctuations and seismo-traveling atmospheric disturbances (STADs) signatures in infrasonic waves and micro-pressures upon the seismic wave arrival. Networks of 9 QuakeFinder systems, 3 infrasound systems, 2 tiltmeters, 2 micro-barometers, and 11 co-located seismometers are used in this study. Each QuakeFinder system consists of a 3-axes induction magnetometer, an air conductivity sensor, a geophone, and temperature/relative humidity sensors. Co-seismic signatures clearly appear in the induction magnetometers, infrasound systems, and micro-barometers data. The magnetometers register both high- and low-frequency pulsations. Geomagnetic fluctuations occur upon the seismic wave arrival but last a longer duration, while the STADs lag their co-located seismic waves by about 15-45 seconds. The long-lasting fluctuations recorded by both induction and fluxgate magnetometers suggest that the ground/underground water motion play an important role, which is further conformed by low-frequency fluctuations in the tiltmeter data. In general, the amplitude of geomagnetic fluctuations decays as away from the epicenter. However, unusual large co-seismic geomagnetic fluctuations are detected over areas of the abnormal seismic intensity level and/or the magnetic underground structure with anomalously high susceptibilities.

Keywords: Geomagnetic, QuakeFinder, Infrasound, micro-Barometer, Tiltmeter

©2019. Japan Geoscience Union. All Right Reserved.

Multi-sensor monitoring network for earthquake precursor study near subduction zone at Boso, Japan

*Katsumi Hattori[1], Chie Yoshino[1], WEIYUN XIE[2], Sanaka Saito[2], Haruna Kojima[2], Rui Song[2], Peng Han[3], Toru Mogi[4], Tada-nori Goto[5], Ichi Takumi[6], Hiroshi Yasukawa[7], Motoaki Mouri[8], Jun Izutsu[9], Tadashi Takano[10], Chihiro Yamanaka[11], Masashi Kamogawa[12], Yoshiaki Ando[13], JANN-YENQ Liu[14], Dimitar Ouzounov[15], Valery Tramutoli[16]

1. Department of Earth Sciences, Graduate School of Science, Chiba University, 2. Graduate School of Science and Engineering, Chiba University, 3. Southern University of Science and Technology, China, 4. Hokkaido University, 5. Kyoto University, 6. Nagoya Institute of Technology, 7. Aichi Prefectural University, 8. Aichi University, 9. Chubu University, 10. Nihon University, 11. Osaka University, 12. Tokyo Gakugei University, 13. The University of Electro-Communications, 14. National Central University, Taiwan, 15. Chapman University, US, 16. University of Basilicagta, Italy

New observations from ground and space have provided multiple evidences of pre-earthquake signals and the latest studies show their statistical significance, repeatability, and universality. In this project, to understand the preparation process of large earthquakes and slow-slip events in subduction zone, especially to clarify the nucleation stage of the earthquake cycle, we plan to establish a dense observation network in Boso, Japan, where large subduction earthquakes are expected soon. Since the subsurface fluid flow may play an important role in the preparation process of subduction activities, we intend to employ electromagnetic approaches including oceanic and continental MT survey to monitor the underground resistivity structure which is sensitive to the dynamics of fluid. Other geophysical monitoring such as ULF geomagnetic and geoelectrical observations, radon measurements, and inland GPS movements, TIR, and OLR will be incorporated to help to understand the preparation process and evaluate the applicability of various pre-earthquake signals towards short term earthquake forecasting. We call this idea “sensor WEB”. We will show the state of the art and some results in our presentation.
This study is supported by Grand-in-Aids for Scientific Research of Japan Society for Promotion of Science (26249060).

©2019. Japan Geoscience Union. All Right Reserved.

Transient Effects in Atmosphere and Ionosphere Associated with 2018 Mw 7.5 Sulawesi Indonesia Earthquake and Triggered Tsunami and Volcano Activities

*Dimitar Ouzounov[1], Sergey Pulinets[2], Dmitry Davidenko[2], Alexander Rozhnoi[3], Maria Solovieva[3], Tiger Liu[4]

1. Center of Excellence in Earth Systems Modeling & Observations (CEESMO) , Schmid College of Science & Technology Chapman University, Orange, California, USA, 2. Space Research Institute, RAS, Moscow, Russia, 3. The Schmidt Institute of Physics of the Earth, RAS, Moscow, Russia, 4. Center for Astronautical Physics and Engineering, National Central University, Taoyuan City, Taiwan

We analyze retrospectively the transient variations of four different physical parameters of atmosphere/ionosphere during the time of M7.5 od Sept 28, 2018 in Indonesia namely: (i) thermodynamic proprieties in the lower atmosphere, (ii) outgoing earth radiation (OLR) at the TOA, (ii) GPS/TEC and (iv) the very-low-frequency (VLF/LF) signals at the receiving station in Petropavlovsk-Kamchatski (RTK, Russia). We found that in the second part of September 2018 a rapid augment of satellite observed earth radiation in the atmosphere and the anomaly located in close vicinity to the future M7.5 epicenter reached the maximum on Sept 21-22. The GPS/TEC data analysis indicates an augment and variation in electron density reaching a maximum value during the Sept 26-27 periods. Two VLF/LF crossing wave paths - NWC-RTK and JJY-RTK, have shown abnormal behavior of signals during on days Sept 26-28 two days before the earthquake. Our results show coherence between the appearance of pre-earthquake transient’ s effects in atmosphere and ionosphere (with a short time-lag, from hours up to a few days) and the occurrence of 2018 M7.5 in Indonesia. Traveling ionospheric tsunami disturbances (TITDs) in the total electron content (TEC) induced by tsunami waves of the 28 September 2018 Mw 7.5 Sulawesi Indonesia earthquake are detected by of seven ground-based receivers of the global positioning system (GPS) in South Asia, Oceanic, Pacific areas. It is found that the origin is about 100 km North of the epicenter and the horizontal speed is of about 187 m/s.

The pre-earthquake nature of the signals in atmosphere and ionosphere were revealed by simultaneous analysis of satellite, GPS/TEC and VLF/LF observations and suggest that they follow a general temporal-spatial evolution pattern, which has been seen in other large earthquakes worldwide.

Keywords: earthquake, tsunami, volcano, precursor, GPS/TEC, thermal anomaly

©2019. Japan Geoscience Union. All Right Reserved.

Seismicity change and b value variation prior to the Wenchuan earthquake (*Ms 8.0*)

*Peng Han[1], Rui Wang[1], Ying Chang[1], Miao Miao[1], Haixia Shi[2], Lingyuan Meng[2], Xuemei Zhang[2], Weiyun Xie[3], Katsumi Hattori[3]

1. Southern University of Science and Technology, Shenzhen, China, 2. China Earthquake Networks Center, Beijing 100045, China, 3. Chiba University, Chiba, Japan

The Gutenberg-Richter Law describes frequency-magnitude distribution of earthquakes. A number of studies have shown that the slope (b value) of the relationship between frequency and magnitude decreased before large earthquakes. Based on the analysis of the earthquake catalog from January, 2000 to April, 2008, we have investigated seismicity change and b value variation prior to the *Ms* 8.0 Wenchuan earthquake. The results show clear drops of both monthly and quarterly frequency of earthquakes during 2005-2006. The b value exhibits a long-term decrease trend since 2002, and reaches to the minimum just before the onset of the main shock. The temporal variation of b value is quite similar to that prior to the *Mw* 9.0 Tohoku earthquake in Japan, which may reflect the stress evolution during the preparation process of large earthquakes. These results indicate that the b value is an important indicator of an impending great earthquake, and has high potential in terms of predicting a future large quake.

Keywords: Wenchuan earthquake, b value, seismicity

©2019. Japan Geoscience Union. All Right Reserved.

[E] Poster | M (Multidisciplinary and Interdisciplinary)：M-IS Intersection

Thu. May 30, 2019 5:15 PM - 6:30 PM JST | Thu. May 30, 2019 8:15 AM - 9:30 AM UTC | Poster Hall International Exhibition Hall8, Makuhari Messe_35

[M-IS04] Interdisciplinary studies on pre-earthquake processes

convener:Katsumi Hattori(Department of Earth Sciences, Graduate School of Science, Chiba University), JANN-YENQ Liu(Institute of Space Science, National Central University, Taiwan), Dimitar Ouzounov(Center of Excellence in Earth Systems Modeling & Observations (CEESMO) , Schmid College of Science & Technology Chapman University, Orange, California, USA), Qinghua Huang(Peking University)

This session expands the interdisciplinary discussions on preparation process of earthquake and earthquake predictability by presenting the latest progress in studying the physically based pre-earthquake phenomena. New observations from space and ground have provided
evidences, which may enhance better understanding of tectonic activity. The session anticipates talks that include but not limited to observations and analyses of seismic, electrical, electromagnetic, electro-chemical and thermodynamic processes related to stress changes in the lithosphere along with their statistical and physical validation. Presentations on the latest observational results associated with major earthquakes obtained by different methodologies are welcomed. The topics of the session are as follows but not limited.

-General discussion on earthquake preparation process and the physics of pre-earthquake signals

- Theory, modeling, laboratory experiments, computational simulation for generation and propagation of pre-earthquake signals and their connection with seismic cycle

 - Multi-parameter observations, detection, and validation of pre-earthquake signals

 - Cross-disciplinary studies, practical and technical approaches for better understanding of earthquake preparation processes and their connection with seismicity

[MIS04-P01] Statistical analysis and Evaluation of ULF seismo-magnetic phenomena at Kakioka, Japan, during 1983-2017

*Kei Takahashi[1], Katsumi Hattori[2], Peng Han[3] (1.Faculty of Science, Chiba University, 2.Graduate School of Science, Chiba University, 3.Southern University of Science and Technology, China)

[MIS04-P02] Pre-seismic anomalies on Earth's magnetic field and ionosphere electron density using Swarm data

*Amune Yamazaki[1], Katsumi Hattori[1], Rui Song[1] (1.Chiba University)

[MIS04-P03] Measurement of radon density in the atmosphere at Okayama, Kochi, Choshi and Kiyosumi, II

*Tohru Okabayashi[1], Kiyotaka Ninagawa[2], Isao Yamamoto[3], Katsumi Hattori[4], Chie Yoshino[4], Haruna Kojima[4], Nobuhiro Maeda (1.Department of Merical Risk and Crisis Management, Faculty of Risk and Crisis Management, Chiba Institute of Science, 2.Faculty of Science, Okayama University of Science, 3.Falcuty of Engineering, Okayama University of Science, 4.Graduate school of Science, Chiba University)

[MIS04-P04] Possible anomalous changes in solar quiet-daily geomagnetic variation *Sq* related to the 2011 off the Pacific coast of Tohoku earthquake (Mw 9.0)

*Xiaocan Liu[1], Katsumi Hattori[2,3], Peng Han[4], Huaran Chen[1] (1.Institute of geophysics China Earthquake Administrition, 2.Graduate School of Science, Chiba University, Chiba, Japan, 3. Center for Environmental Remote Sensing, Chiba University, Chiba, Japan, 4.Department of Earth and Space Sciences, Southern University of Science and Technology, ShenZhen, China)

[MIS04-P05] Co-seismic geomagnetic fluctuations and atmospheric disturbances during the 2018 M6.2 Hualien Earthquake

*Chun-Rong Chen[1], JANN-YENQ Liu[1] (1.Graduate Institute of Space Science, National Central University)

[MIS04-P06] Multi-sensor monitoring network for earthquake precursor study near subduction zone at Boso, Japan

*Katsumi Hattori[1], Chie Yoshino[1], WEIYUN XIE[2], Sanaka Saito[2], Haruna Kojima[2], Rui Song[2], Peng Han[3], Toru Mogi[4], Tada-nori Goto[5], Ichi Takumi[6], Hiroshi Yasukawa[7], Motoaki Mouri[8], Jun Izutsu[9], Tadashi Takano[10], Chihiro Yamanaka[11], Masashi Kamogawa[12], Yoshiaki Ando[13], JANN-YENQ Liu[14], Dimitar Ouzounov[15], Valery Tramutoli[16] (1.Department of Earth Sciences, Graduate School of Science, Chiba University, 2.Graduate School of Science and Engineering, Chiba University, 3.Southern University of Science and Technology, China, 4.Hokkaido University, 5.Kyoto University, 6.Nagoya Institute of Technology, 7.Aichi Prefectural University, 8.Aichi University, 9.Chubu University, 10.Nihon University, 11.Osaka University, 12.Tokyo Gakugei University, 13.The University of Electro-Communications, 14.National Central University, Taiwan, 15.Chapman University, US, 16.University of Basilicagta, Italy)

[MIS04-P07] Transient Effects in Atmosphere and Ionosphere Associated with 2018 Mw 7.5 Sulawesi Indonesia Earthquake and Triggered Tsunami and Volcano Activities

★Invited Papers

*Dimitar Ouzounov[1], Sergey Pulinets[2], Dmitry Davidenko[2], Alexander Rozhnoi[3], Maria Solovieva[3], Tiger Liu[4] (1.Center of Excellence in Earth Systems Modeling & Observations (CEESMO) , Schmid College of Science & Technology Chapman University, Orange, California, USA, 2.Space Research Institute, RAS, Moscow, Russia, 3.The Schmidt Institute of Physics of the Earth, RAS, Moscow, Russia, 4.Center for Astronautical Physics and Engineering, National Central University, Taoyuan City, Taiwan)

[MIS04-P08] Seismicity change and b value variation prior to the Wenchuan earthquake (*Ms 8.0*)

*Peng Han[1], Rui Wang[1], Ying Chang[1], Miao Miao[1], Haixia Shi[2], Lingyuan Meng[2], Xuemei Zhang[2], Weiyun Xie[3], Katsumi Hattori[3] (1.Southern University of Science and Technology, Shenzhen, China, 2.China Earthquake Networks Center, Beijing 100045, China, 3.Chiba University, Chiba, Japan)

Statistical analysis and Evaluation of ULF seismo-magnetic phenomena at Kakioka, Japan, during 1983-2017

*Kei Takahashi[1], Katsumi Hattori[2], Peng Han[3]

1. Faculty of Science, Chiba University, 2. Graduate School of Science, Chiba University, 3. Southern University of Science and Technology, China

To clarify and verify the ultralow frequency (ULF) seismo-magnetic phenomena, we have performed statistical studies on the geomagnetic data observed at the Kakioka (KAK) station, Japan, during 1983-2017. We investigated the energy of ULF geomagnetic signals of the frequency around 0.01 Hz using wavelet transform analysis. To minimize the influences of artificial noises and global magnetic perturbations, we used only the geomagnetic data observed at midnight time (LT 2:30 A.M. to 4:00 A.M.).We define the geomagnetic anomalies when the Z components of geomagnetic data exceeds median + 1.5 IQR, where IQR is the interquartile range. Considering that ionospheric disturbances may also lead to enhancements in the Z component, we exclude the anomaly when the energy of H component exceeds median + 3.0 IQR. Statistical analysis of superposed epoch analysis have indicated that ULF magnetic anomalies are more likely to appear before sizable isolated earthquake events (Es parameter which is higher than 8th power of 10 and no earthquake events during ±45 days) rather than after them, especially 6-10 days before the events. Finally, we have evaluated the precursory information of ULF geomagnetic signals for local sizable earthquakes using Molchan’ s error diagram. The above results have indicated that the ULF seismo-magnetic phenomena at Kakioka clearly contain precursory information and have a possibility of improving forecasting of large earthquakes.

©2019. Japan Geoscience Union. All Right Reserved.

Pre-seismic anomalies on Earth’s magnetic field and ionosphere electron density using Swarm data

*Amune Yamazaki[1], Katsumi Hattori[1], Rui Song[1]

1. Chiba University

An earthquake is a rapid release of stress in the lithosphere and often leads to serious damages on human lives and society. Even though the short-time forecast of earthquake is important, it is not achieved yet. However, many electromagnetic phenomena that may be related to seismic activity have been reported recently. The satellite, one of the useful tools to observe these phenomena, can cover the global areas and can collect a large amount of data related to earthquakes which have large magnitude worldwide in short time. The Swarm satellites mission started to operate on November 22, 2013 by European Space Agency, with the constellation of three satellites (A, B, C) The anomalies preceded to the Ecuador earthquake in 2016 have been reported using the Swarm data. In this paper, in order to validate these results using the magnetic vector Y data by VFM and electron density data by Langmuir probe, we have analyzed the Swarm data related the M6.3~6.9 earthquakes occurred at Lombok Island, Indonesia, in July 28, August 5, and 19, 2018. The study area is a 1000 km square from the epicenter of 20180805 earthquake and the analyzed period is from May 28 to September 27, 2018. In this paper we report night-time orbit data at 18:00-6:00 LT.

As results, we found the following tendencies; (1) positive anomalies on magnetic Y vector about 1-2 weeks before the earthquakes and (2) negative anomalies on electron density from 1 week to 1 month before the earthquakes. We performed the same analysis to the data on the same period in 2016 and 2017 for reference when there were no M6+ earthquakes. We found that the number of anomaly track is only abruptly increased in the short period from the end of June to July in 2018, and that the trend is not able to be found in 2016 and 2017. From this unique trend in 2018, it is suggestive of the existence of the relation between the local seismic activity and in-situ satellite anomalies in the magnetic field and electron density in Lombok area.

©2019. Japan Geoscience Union. All Right Reserved.

Measurement of radon density in the atmosphere at Okayama, Kochi, Choshi and Kiyosumi, II

*Tohru Okabayashi[1], Kiyotaka Ninagawa[2], Isao Yamamoto[3], Katsumi Hattori[4], Chie Yoshino[4], Haruna Kojima[4], Nobuhiro Maeda

1. Department of Merical Risk and Crisis Management, Faculty of Risk and Crisis Management, Chiba Institute of Science, 2. Faculty of Science, Okayama University of Science, 3. Falcuty of Engineering, Okayama University of Science, 4. Graduate school of Science, Chiba University

We report continuous measurement of radon density in atmosphere at Okayama for three years, Kochi, Choshi and Kiyosumi for two years. An increase of radon density in groundwater at Nishinomiya city [1] and in atmosphere [2] at the southern part of Hyogo Prefecture Earthquake in 1995 were reported, respectively. In the case of Tohoku Region Pacific Coast Earthquake, the data obtained the exhaust air monitor that peak duration was long and the peak decreased rapidly before earthquake has been reported at the radiation facility of Fukushima Medical College in Fukushima [3]. On the other hand, a PIN photodiode have been developed and used as a high sensitive alpha ray detector in Super Kamiokande [4]. Since 2016, we also made an experimental setup using PIN photodiode, and measured the radon density in atmosphere. Using a Si PIN photodiode (S3204-09, unsealed, Hamamatsu Photodiode K.K.) as an alpha ray detector, we constructed radon detection setup combined with aluminum pot as an air accumulator, H4083 (Hamamatsu) as a charge amplifier, C4900-01 (Hamamatsu) as a high voltage power supply module, a pulse shaped amplifier with time constant of 10 msec, a multi channel analyzer (MCA-LiteN), and a PC as a data analysis. Obtained alpha spectra of atmosphere showed 4 peaks originated from ^{218}Po, ^{214}Po and ^{210}Po of U series, and ^{212}Po of Th series. Since 2017, we newly started to measure at Kochi, Choshi and Kiyosumi using our apparatus. Details of observed data are discussed in addition the data at Okayama since 2016.

[1] Igarashi G., Saeki S., Takahata N., Sumikawa K., Tasaka S., Sasaki Y., Takahashi M. and Sano Y. : Ground-water radon anomaly before the Kobe earthquake in Japan, Science, 269, 60-61, 1995.
[2] Yasuoka, Y. and Shinogi, M.: Anomaly in atmospheric radon concentration: a possible precursor of the 1995 Kobe, Japan, earthquake. Health Physics, 72, 759-761, 1997.
[3] Nagahama H., Yasuoka Y., Suzuki T., and Homma Y.: Radon Variation in the Air Before the 2011 Tohoku Earthquake (Mw =9.0), Programme and Abstracts, A32-09, The Seismological Society of Japan. 2011, Fall Meeting.
[4] Nemoto, M., Tasaka S., Hori H., Okumura K., Kajita T., and Takeuchi Y. : Development of High Sensitive Radon Detector with Electrostatic Collection. Radioisotopes, 46, 710-719, 1997 (Japanese).

Keywords: radon, atmosphere, earthquake prediction

©2019. Japan Geoscience Union. All Right Reserved.

Possible anomalous changes in solar quiet-daily geomagnetic variation *Sq* related to the 2011 off the Pacific coast of Tohoku earthquake (Mw 9.0)

*Xiaocan Liu[1], Katsumi Hattori[2,3], Peng Han[4], Huaran Chen[1]

1. Institute of geophysics China Earthquake Administrition, 2. Graduate School of Science, Chiba University, Chiba, Japan, 3. Center for Environmental Remote Sensing, Chiba University, Chiba, Japan, 4. Department of Earth and Space Sciences, Southern University of Science and Technology, ShenZhen, China

Seismo-electromagnetic researches have been studied for decades (e.g. Hayakawa and Fujinawa, 1994; Hayakawa and Molchanov, 2002, 2008,2013; Hattori, 2004, Hattori, et al., 2004a, 2004b; Hayakawa et al., 2007;, Hattori et al., 2013; Han et al., 2011, 2014, 2015, 2016, 2017; Huang QH et al., 2011, 2015; Du A, Huang Q et al., 2002, Rong YM et al., 2012, Yuan G.P., Zhang X.M. et al. 2015), and the geomagnetic diurnal variation (GDV) is a stable variation of the geomagnetic field that can be used to detect possible anomalous changes associated with large earthquakes.

We investigated data observed at 20 geomagnetic observatories at longitudes of 130˚E to 150˚E between 2009 and 2012 to detect possible anomalous changes in the geomagnetic solar quiet daily variation (Sq) related to the 2011 off the Pacific coast of Tohoku earthquake (Mw 9.0) occurred on March 11, 2011 in Japan. We selected the 5 quiet days every month and analyzed three component magnetic data with 1 min resolution using the natural orthogonal component (NOC) method to identify Sq variations from observations, and performed the spherical harmonic analysis (SHA) to separate the internal and the external equivalent Sq current systems of Je and Ji. We obtained that, Je and Ji are distorted near the epicenter area on two geomagnetic quiet days of January 23 and 27, 2011. They are about two months before the earthquake. Then, we made backward computation on the external and internal parts of the SHA model geomagnetic fields, Be and Bi, to determine the possible anomalous magnetic field variations at each station. Results show significant differences in daily variation for all components on January 23 and 27, 2011. The other days, we could not recognize any apparent anomalous behaviors, except known secular, seasonal, and solar activity dependences. A possible connection between this anomaly and the very strong Tohoku earthquake, which followed only one and half month after the geomagnetic anomaly is of highest interest for the research on earthquake precursors.

Keywords: geomagnetic solar quiet daily variation (Sq), natural orthogonal component (NOC) method, spherical harmonic analysis (SHA), the 2011 off the Pacific coast of Tohoku earthquak

©2019. Japan Geoscience Union. All Right Reserved.

Co-seismic geomagnetic fluctuations and atmospheric disturbances during the 2018 M6.2 Hualien Earthquake

*Chun-Rong Chen[1], JANN-YENQ Liu[1]

1. Graduate Institute of Space Science, National Central University

The strong ground motion of 6 February 2018 M6.2 Hualien Earthquake triggered a series of co-seismic geomagnetic fluctuations and seismo-traveling atmospheric disturbances (STADs) signatures in infrasonic waves and micro-pressures upon the seismic wave arrival. Networks of 9 QuakeFinder systems, 3 infrasound systems, 2 tiltmeters, 2 micro-barometers, and 11 co-located seismometers are used in this study. Each QuakeFinder system consists of a 3-axes induction magnetometer, an air conductivity sensor, a geophone, and temperature/relative humidity sensors. Co-seismic signatures clearly appear in the induction magnetometers, infrasound systems, and micro-barometers data. The magnetometers register both high- and low-frequency pulsations. Geomagnetic fluctuations occur upon the seismic wave arrival but last a longer duration, while the STADs lag their co-located seismic waves by about 15-45 seconds. The long-lasting fluctuations recorded by both induction and fluxgate magnetometers suggest that the ground/underground water motion play an important role, which is further conformed by low-frequency fluctuations in the tiltmeter data. In general, the amplitude of geomagnetic fluctuations decays as away from the epicenter. However, unusual large co-seismic geomagnetic fluctuations are detected over areas of the abnormal seismic intensity level and/or the magnetic underground structure with anomalously high susceptibilities.

Keywords: Geomagnetic, QuakeFinder, Infrasound, micro-Barometer, Tiltmeter

©2019. Japan Geoscience Union. All Right Reserved.

Multi-sensor monitoring network for earthquake precursor study near subduction zone at Boso, Japan

*Katsumi Hattori[1], Chie Yoshino[1], WEIYUN XIE[2], Sanaka Saito[2], Haruna Kojima[2], Rui Song[2], Peng Han[3], Toru Mogi[4], Tada-nori Goto[5], Ichi Takumi[6], Hiroshi Yasukawa[7], Motoaki Mouri[8], Jun Izutsu[9], Tadashi Takano[10], Chihiro Yamanaka[11], Masashi Kamogawa[12], Yoshiaki Ando[13], JANN-YENQ Liu[14], Dimitar Ouzounov[15], Valery Tramutoli[16]

1. Department of Earth Sciences, Graduate School of Science, Chiba University, 2. Graduate School of Science and Engineering, Chiba University, 3. Southern University of Science and Technology, China, 4. Hokkaido University, 5. Kyoto University, 6. Nagoya Institute of Technology, 7. Aichi Prefectural University, 8. Aichi University, 9. Chubu University, 10. Nihon University, 11. Osaka University, 12. Tokyo Gakugei University, 13. The University of Electro-Communications, 14. National Central University, Taiwan, 15. Chapman University, US, 16. University of Basilicagta, Italy

New observations from ground and space have provided multiple evidences of pre-earthquake signals and the latest studies show their statistical significance, repeatability, and universality. In this project, to understand the preparation process of large earthquakes and slow-slip events in subduction zone, especially to clarify the nucleation stage of the earthquake cycle, we plan to establish a dense observation network in Boso, Japan, where large subduction earthquakes are expected soon. Since the subsurface fluid flow may play an important role in the preparation process of subduction activities, we intend to employ electromagnetic approaches including oceanic and continental MT survey to monitor the underground resistivity structure which is sensitive to the dynamics of fluid. Other geophysical monitoring such as ULF geomagnetic and geoelectrical observations, radon measurements, and inland GPS movements, TIR, and OLR will be incorporated to help to understand the preparation process and evaluate the applicability of various pre-earthquake signals towards short term earthquake forecasting. We call this idea “sensor WEB”. We will show the state of the art and some results in our presentation.
This study is supported by Grand-in-Aids for Scientific Research of Japan Society for Promotion of Science (26249060).

©2019. Japan Geoscience Union. All Right Reserved.

Transient Effects in Atmosphere and Ionosphere Associated with 2018 Mw 7.5 Sulawesi Indonesia Earthquake and Triggered Tsunami and Volcano Activities

*Dimitar Ouzounov[1], Sergey Pulinets[2], Dmitry Davidenko[2], Alexander Rozhnoi[3], Maria Solovieva[3], Tiger Liu[4]

1. Center of Excellence in Earth Systems Modeling & Observations (CEESMO) , Schmid College of Science & Technology Chapman University, Orange, California, USA, 2. Space Research Institute, RAS, Moscow, Russia, 3. The Schmidt Institute of Physics of the Earth, RAS, Moscow, Russia, 4. Center for Astronautical Physics and Engineering, National Central University, Taoyuan City, Taiwan

We analyze retrospectively the transient variations of four different physical parameters of atmosphere/ionosphere during the time of M7.5 od Sept 28, 2018 in Indonesia namely: (i) thermodynamic proprieties in the lower atmosphere, (ii) outgoing earth radiation (OLR) at the TOA, (ii) GPS/TEC and (iv) the very-low-frequency (VLF/LF) signals at the receiving station in Petropavlovsk-Kamchatski (RTK, Russia). We found that in the second part of September 2018 a rapid augment of satellite observed earth radiation in the atmosphere and the anomaly located in close vicinity to the future M7.5 epicenter reached the maximum on Sept 21-22. The GPS/TEC data analysis indicates an augment and variation in electron density reaching a maximum value during the Sept 26-27 periods. Two VLF/LF crossing wave paths - NWC-RTK and JJY-RTK, have shown abnormal behavior of signals during on days Sept 26-28 two days before the earthquake. Our results show coherence between the appearance of pre-earthquake transient’ s effects in atmosphere and ionosphere (with a short time-lag, from hours up to a few days) and the occurrence of 2018 M7.5 in Indonesia. Traveling ionospheric tsunami disturbances (TITDs) in the total electron content (TEC) induced by tsunami waves of the 28 September 2018 Mw 7.5 Sulawesi Indonesia earthquake are detected by of seven ground-based receivers of the global positioning system (GPS) in South Asia, Oceanic, Pacific areas. It is found that the origin is about 100 km North of the epicenter and the horizontal speed is of about 187 m/s.

The pre-earthquake nature of the signals in atmosphere and ionosphere were revealed by simultaneous analysis of satellite, GPS/TEC and VLF/LF observations and suggest that they follow a general temporal-spatial evolution pattern, which has been seen in other large earthquakes worldwide.

Keywords: earthquake, tsunami, volcano, precursor, GPS/TEC, thermal anomaly

©2019. Japan Geoscience Union. All Right Reserved.

Seismicity change and b value variation prior to the Wenchuan earthquake (*Ms 8.0*)

*Peng Han[1], Rui Wang[1], Ying Chang[1], Miao Miao[1], Haixia Shi[2], Lingyuan Meng[2], Xuemei Zhang[2], Weiyun Xie[3], Katsumi Hattori[3]

1. Southern University of Science and Technology, Shenzhen, China, 2. China Earthquake Networks Center, Beijing 100045, China, 3. Chiba University, Chiba, Japan

The Gutenberg-Richter Law describes frequency-magnitude distribution of earthquakes. A number of studies have shown that the slope (b value) of the relationship between frequency and magnitude decreased before large earthquakes. Based on the analysis of the earthquake catalog from January, 2000 to April, 2008, we have investigated seismicity change and b value variation prior to the *Ms* 8.0 Wenchuan earthquake. The results show clear drops of both monthly and quarterly frequency of earthquakes during 2005-2006. The b value exhibits a long-term decrease trend since 2002, and reaches to the minimum just before the onset of the main shock. The temporal variation of b value is quite similar to that prior to the *Mw* 9.0 Tohoku earthquake in Japan, which may reflect the stress evolution during the preparation process of large earthquakes. These results indicate that the b value is an important indicator of an impending great earthquake, and has high potential in terms of predicting a future large quake.

Keywords: Wenchuan earthquake, b value, seismicity

©2019. Japan Geoscience Union. All Right Reserved.

[E] Poster | M (Multidisciplinary and Interdisciplinary)：M-IS Intersection

Thu. May 30, 2019 3:30 PM - 5:00 PM JST | Thu. May 30, 2019 6:30 AM - 8:00 AM UTC | Poster Hall International Exhibition Hall8, Makuhari Messe_19

[M-IS06] Conservation of geoparks, natural geosites and cultural heritage: weathering process and damage assessment

convener:Chiaki T. Oguchi(Institute for Environmental Science and Technology, Graduate School of Science and Engineering, Saitama University), Tetsuya Waragai(Graduate School of Science and Engineering, Nihon University), Kuniyasu Mokudai(Tohoku Gakuin University), Magdalini Theodoridou(School of Engineering, Cardiff University)

Geoparks, world heritage sites, natural geosites and cultural heritage structures are considered important natural and/or cultural heritage properties. They have been exposed to weathering not only in geologic time frame but also in human time scale, thus rocks and geological materials are often facing deterioration. In order to preserve these sites conservation measures should be considered. Several studies have taken place on this topic involving a wide range of research fields, such as geomorphology, engineering geology, geoarchaeology, conservation science, geoconservation, materials science, petrophysics, geochemistry, geotechnical engineering etc. However, our knowledge on many aspects is still limited. The session welcomes contributions, presenting original research, discussions as well as case studies on documentation, measurement and monitoring techniques, experimental procedures, predictive models, damage assessment, etc. Papers from all research fields are invited dealing with the broad topic of geosites and cultural heritage.

[MIS06-P01] The artistic qualities of religion reliefs in Taya-cave.Japan

*OGATA KEISUKE[1] (1.TSURUMI UNIVERSITY)

[MIS06-P02] Effect of stress concentration on the Weathering Mechanism of Sandstone Pillars of Angkor Wat, Cambodia by means of numerical simulation

*Takato Takemura[1], Tetsuya Waragai[2] (1.Nihon Univ., 2.Nihon University)

[MIS06-P03] Meaning to preserve evidence of large scale landslide

*Kuniyasu Mokudai[1], Hidekazu Sato[2] (1.Japan Geoservice Incorporated, 2.Mt. Kurikoma Area Geopark)

The artistic qualities of religion reliefs in Taya-cave.Japan

*OGATA KEISUKE[1]

1. TSURUMI UNIVERSITY

The Yaya-csve is located within the Jōsenji-Temle in Taya Town,Sakae ward,Yokohama-shi,Kanagawa Prefecture.The cave is called “Yuga-dou”,which is thought to be the present form in the Edo period, when the Kamakura period entered monks drills as a training ground. As for the religious relief carved in the cave, it is presumed from the record of “Koukoku-chishi” that it was produced for about 20years from 1842 to1862. In addition, “Sekiguchi diary” contains articles on visiting caves in 1859.

Subjects of reliefs are divided into the following areas in order of the route, and about 300 are engraved over 250 meters in total length.

First area:A and Un lions, Up and Doun dragon, Gold wing bird. Ceiling family crest.

Second area:Zodiac image. Ceiling three bats.

Third area:Chichibu 33 Kannon sacred place. Karyou-binga.

Fourth area:Asahina-benzaiten.

Fifth area:Saigoku 33 Kannon sacred place.

Sixth area:Sone Tenman-gū shrine and Takasago pine.

Seventh area:Yakuyoke Kobō-daishi master.

Eighth area:Taizōkai-shugi-mandala. Ceiling crane hemp leaf pattern.

Ninth area:Ichigan Kobō-daishi master. Shikoku 88 sacred place.

Tenth area:Shikoku 88 sacred place. 49in-shugi-mandala. Four Gorin tower.

Eleventh area:Godai-myouou.

Twelfth area:Water Kobō-daishi master. Sadasan one Turtle. Kouya-san Ishidoumaru. Unchū-kuyou bodhisattva.

Thirteenth area:18Rakan.

Fourteenth area:Iwaya-Fudou.

Fifteenth area:Bandou 33 Kannon sacred place.

Regrading the style, religious subjecks such as the Saigoku, bandou, Chichibu 33 Kannon sacred place,

©2019. Japan Geoscience Union. All Right Reserved.

Shikoku 88 sacred place and shugi-mandala are also perfunctory aspects, but “Sone Tenman-gū shrine and Takasago pine” and “Sadasan one Turtle” and 18-Rakan etc are the sculptures with high artistic and strong paintertly elements.

The faith in the 18th century was diverse, especially the common people went around the whole countey sacred place. Also for each of those who can not visit the sacred place a mini sacred place of each sacred place was established in various places. The Taya-cave near the Tokaido must also have collected the faith of the common people as a mini sacred place.

Taya-cave is currently designated as a registered cultural property of Yokohama City as a historic site in 1990. However, due to years of deterioration, it is becoming difficult to preserve and maintain the current situation. Therefore, in 2017 the Taya-cave preservation execution committee was established, we aim to conduct a basic survey in each department of cultural property, engineering and environmental studies, revalidate its value, preserve it as VR digital data in the future, to make it public and utilize.
In 2018, under the auspices of the Japan Society for the Promotion of Science(JSPS), collaborative research with the Italian ISSM/CNR Laboratory began, and in 2019 the research was continued with the subsidy of the Asahi Shimbun Cultural Foundation.

Keywords: History of Jōsenji-Temle and Taya-cave., On the time of religion haut-reliefs prodactionin in Taya-cave., Types and artistic religious reliefs in Taya-cave., From of common people’s belief in Japan in the 18th century., Preservation of Taya-cave and its future use.

©2019. Japan Geoscience Union. All Right Reserved.

Effect of stress concentration on the Weathering Mechanism of Sandstone Pillars of Angkor Wat, Cambodia by means of numerical simulation

*Takato Takemura[1], Tetsuya Waragai[2]

1. Nihon Univ., 2. Nihon University

Since Angkor Wat is located in a tropical monsoon climate, the sandstone building materials are strongly affected by weathering related to high temperatures, heavy rainfall and intense solar radiation. Weathering damage can be observed on a number of pillars, however, the outer pillars exhibit little weathering damage compared to the inner pillars, even though the outer pillars are more exposed to the rain and sunlight than the inner pillars. To understand the effect of stress concentration on the weathering sandstone pillars, we carried out the measurement of the degree of weathering damage of pillars, in-situ measurement of humidity and temperature change near the pillar and the numerical simulation for structural analysis.As a result, the weathering damage is not necessarily only due to the wetting-drying cycle. Since relatively large compressive stress is applied to the base of the inner pillar where the weathering damage is large, therefore, the weathering rate could be accelerated by the compressive stress concentration.

Keywords: Angkor Wat, Stress concentration

©2019. Japan Geoscience Union. All Right Reserved.

Meaning to preserve evidence of large scale landslide

*Kuniyasu Mokudai[1], Hidekazu Sato[2]

1. Japan Geoservice Incorporated, 2. Mt. Kurikoma Area Geopark

There are many mountainous area in Japanese islands. In mountainous area, many natural hazards occured. Visualization of landslide is necessary in order to understand the slope process in the mountains to non-experts. At Mt. Kurikoma Mountain area Geopark, we have been engaged in conservation of large-scale landslide landform, education and information dissemination activities. In order to preserve the landslide phenomenon which is the cause of the slope disaster, a scientific understanding of the landform is necessary. Furthermore, it is necessary to restructure the view of nature of the concerned parties.

Keywords: large scale landslide, geopark, geoconservation

©2019. Japan Geoscience Union. All Right Reserved.

[E] Poster | M (Multidisciplinary and Interdisciplinary)：M-IS Intersection

Thu. May 30, 2019 5:15 PM - 6:30 PM JST | Thu. May 30, 2019 8:15 AM - 9:30 AM UTC | Poster Hall International Exhibition Hall8, Makuhari Messe_36

[M-IS06] Conservation of geoparks, natural geosites and cultural heritage: weathering process and damage assessment

convener:Chiaki T. Oguchi(Institute for Environmental Science and Technology, Graduate School of Science and Engineering, Saitama University), Tetsuya Waragai(Graduate School of Science and Engineering, Nihon University), Kuniyasu Mokudai(Tohoku Gakuin University), Magdalini Theodoridou(School of Engineering, Cardiff University)

Geoparks, world heritage sites, natural geosites and cultural heritage structures are considered important natural and/or cultural heritage properties. They have been exposed to weathering not only in geologic time frame but also in human time scale, thus rocks and geological materials are often facing deterioration. In order to preserve these sites conservation measures should be considered. Several studies have taken place on this topic involving a wide range of research fields, such as geomorphology, engineering geology, geoarchaeology, conservation science, geoconservation, materials science, petrophysics, geochemistry, geotechnical engineering etc. However, our knowledge on many aspects is still limited. The session welcomes contributions, presenting original research, discussions as well as case studies on documentation, measurement and monitoring techniques, experimental procedures, predictive models, damage assessment, etc. Papers from all research fields are invited dealing with the broad topic of geosites and cultural heritage.

[MIS06-P01] The artistic qualities of religion reliefs in Taya-cave.Japan

*OGATA KEISUKE[1] (1.TSURUMI UNIVERSITY)

[MIS06-P02] Effect of stress concentration on the Weathering Mechanism of Sandstone Pillars of Angkor Wat, Cambodia by means of numerical simulation

*Takato Takemura[1], Tetsuya Waragai[2] (1.Nihon Univ., 2.Nihon University)

[MIS06-P03] Meaning to preserve evidence of large scale landslide

*Kuniyasu Mokudai[1], Hidekazu Sato[2] (1.Japan Geoservice Incorporated, 2.Mt. Kurikoma Area Geopark)

The artistic qualities of religion reliefs in Taya-cave.Japan

*OGATA KEISUKE[1]

1. TSURUMI UNIVERSITY

The Yaya-csve is located within the Jōsenji-Temle in Taya Town,Sakae ward,Yokohama-shi,Kanagawa Prefecture.The cave is called “Yuga-dou”,which is thought to be the present form in the Edo period, when the Kamakura period entered monks drills as a training ground. As for the religious relief carved in the cave, it is presumed from the record of “Koukoku-chishi” that it was produced for about 20years from 1842 to1862. In addition, “Sekiguchi diary” contains articles on visiting caves in 1859.

Subjects of reliefs are divided into the following areas in order of the route, and about 300 are engraved over 250 meters in total length.

First area:A and Un lions, Up and Doun dragon, Gold wing bird. Ceiling family crest.

Second area:Zodiac image. Ceiling three bats.

Third area:Chichibu 33 Kannon sacred place. Karyou-binga.

Fourth area:Asahina-benzaiten.

Fifth area:Saigoku 33 Kannon sacred place.

Sixth area:Sone Tenman-gū shrine and Takasago pine.

Seventh area:Yakuyoke Kobō-daishi master.

Eighth area:Taizōkai-shugi-mandala. Ceiling crane hemp leaf pattern.

Ninth area:Ichigan Kobō-daishi master. Shikoku 88 sacred place.

Tenth area:Shikoku 88 sacred place. 49in-shugi-mandala. Four Gorin tower.

Eleventh area:Godai-myouou.

Twelfth area:Water Kobō-daishi master. Sadasan one Turtle. Kouya-san Ishidoumaru. Unchū-kuyou bodhisattva.

Thirteenth area:18Rakan.

Fourteenth area:Iwaya-Fudou.

Fifteenth area:Bandou 33 Kannon sacred place.

Regrading the style, religious subjecks such as the Saigoku, bandou, Chichibu 33 Kannon sacred place,

©2019. Japan Geoscience Union. All Right Reserved.

Shikoku 88 sacred place and shugi-mandala are also perfunctory aspects, but “Sone Tenman-gū shrine and Takasago pine” and “Sadasan one Turtle” and 18-Rakan etc are the sculptures with high artistic and strong paintertly elements.

The faith in the 18th century was diverse, especially the common people went around the whole countey sacred place. Also for each of those who can not visit the sacred place a mini sacred place of each sacred place was established in various places. The Taya-cave near the Tokaido must also have collected the faith of the common people as a mini sacred place.

Taya-cave is currently designated as a registered cultural property of Yokohama City as a historic site in 1990. However, due to years of deterioration, it is becoming difficult to preserve and maintain the current situation. Therefore, in 2017 the Taya-cave preservation execution committee was established, we aim to conduct a basic survey in each department of cultural property, engineering and environmental studies, revalidate its value, preserve it as VR digital data in the future, to make it public and utilize.
In 2018, under the auspices of the Japan Society for the Promotion of Science(JSPS), collaborative research with the Italian ISSM/CNR Laboratory began, and in 2019 the research was continued with the subsidy of the Asahi Shimbun Cultural Foundation.

Keywords: History of Jōsenji-Temle and Taya-cave., On the time of religion haut-reliefs prodactionin in Taya-cave., Types and artistic religious reliefs in Taya-cave., From of common people’s belief in Japan in the 18th century., Preservation of Taya-cave and its future use.

©2019. Japan Geoscience Union. All Right Reserved.

Effect of stress concentration on the Weathering Mechanism of Sandstone Pillars of Angkor Wat, Cambodia by means of numerical simulation

*Takato Takemura[1], Tetsuya Waragai[2]

1. Nihon Univ., 2. Nihon University

Since Angkor Wat is located in a tropical monsoon climate, the sandstone building materials are strongly affected by weathering related to high temperatures, heavy rainfall and intense solar radiation. Weathering damage can be observed on a number of pillars, however, the outer pillars exhibit little weathering damage compared to the inner pillars, even though the outer pillars are more exposed to the rain and sunlight than the inner pillars. To understand the effect of stress concentration on the weathering sandstone pillars, we carried out the measurement of the degree of weathering damage of pillars, in-situ measurement of humidity and temperature change near the pillar and the numerical simulation for structural analysis.As a result, the weathering damage is not necessarily only due to the wetting-drying cycle. Since relatively large compressive stress is applied to the base of the inner pillar where the weathering damage is large, therefore, the weathering rate could be accelerated by the compressive stress concentration.

Keywords: Angkor Wat, Stress concentration

©2019. Japan Geoscience Union. All Right Reserved.

Meaning to preserve evidence of large scale landslide

*Kuniyasu Mokudai[1], Hidekazu Sato[2]

1. Japan Geoservice Incorporated, 2. Mt. Kurikoma Area Geopark

There are many mountainous area in Japanese islands. In mountainous area, many natural hazards occured. Visualization of landslide is necessary in order to understand the slope process in the mountains to non-experts. At Mt. Kurikoma Mountain area Geopark, we have been engaged in conservation of large-scale landslide landform, education and information dissemination activities. In order to preserve the landslide phenomenon which is the cause of the slope disaster, a scientific understanding of the landform is necessary. Furthermore, it is necessary to restructure the view of nature of the concerned parties.

Keywords: large scale landslide, geopark, geoconservation

©2019. Japan Geoscience Union. All Right Reserved.

[E] Poster | M (Multidisciplinary and Interdisciplinary) : M-IS Intersection

Thu. May 30, 2019 3:30 PM - 5:00 PM JST | Thu. May 30, 2019 6:30 AM - 8:00 AM UTC | Poster Hall International Exhibition Hall8, Makuhari Messe_20

[M-IS07] Astrobiology

convener:Hikaru Yabuta(Hiroshima University, Department of Earth and Planetary Systems Science), Seiji Sugita(Department of Earth and Planetary Science, Graduate School of Science Sciece, The University of Tokyo), Misato Fukagawa(National Astronomical Observatory of Japan), Fujishima Kosuke(Tokyo Institute of Technology, Earth-Life Science Institute)

Twenty years have passed since when the field of Astrobiology, which aims to unveil the origins, evolution, and habitability of life by integrating multidisciplinary fields, was established. Individual themes related to Astrobiology, such as chemical evolution in the early Solar System, formation of planetary system, prebiotic chemistry in the early Earth, evolution of life in the Earth's history, extremophile, and habitable planetary environments, has been studied by the knowledge and methods from the multiple fields, which has enabled us to explain "Where we came from" in some ways. However, despite an overwhelming number of investigations and discussions through gathering of the scientists from different fields, there has remained the long-standing unsolved question: How did abiotic materials gain biological function in the Earth and elsewhere in universe? There is still a large gap between prebiotic organic chemistry and biochemistry toward Origins of Life and planetary habitability. Therefore, the JpGU Astrobiology session focuses on pathfinding of "integration of astronomy, geoscience, and biochemistry", which will face an increasing need for the future Astrobiology. In order to enhance our understanding of "What is life", we propose to discuss the biochemical events linked with planetary systems, which is beyond the knowledge in a test tube, by an integration of exoplanets and molecular biology, etc. Through this approach, we will lead the discussions and developments of life-detection strategies for the future exploration of life in universe.

[MIS07-P01] Exoplanets Revealed by High-Precision Infrared Doppler Technique Using IRD: Large Exploration for Planets around Cool M-type Stars Begins

*Masayuki Kuzuhara[1,3], Bunei Sato[4], Motohide Tamura[2,1,3], Takayuki Kotani[1,3,5], Nagayoshi Ohashi[3,6], Masashi Omiya[1,3], Teruyuki Hirano[4], Hiroki Harakawa[6,3,1], Wako Aoki[3,5], Norio Narita[2,1], Yasunori Hori[1,3], Akitoshi Ueda[3,5], Akihiko Fukui[2], Hiroyuki Tako Ishikawa[5,3], Ishizuka Masato[2], Takashi Kurokawa[1,7], Nobuhiko Kusakabe[1,3], Tomoyuki Kudo[6,3,1], Eiichiro Kokubo[3], Mihoko Konishi[1,3], Tadashi Nakajima[1,3,5], Jun Nishikawa[3,5,1], Masahiro Ogihara[3], Takuma Serizawa[7] (1.Astrobiology Center of NINS, 2.The University of Tokyo, Graduate School of Science, 3.National Astronomical Observatory of Japan, 4.Tokyo Institute of Technology, 5.SOKENDAI, 6.Subaru Telescope, 7.Tokyo University of Agriculture and Technology)

[MIS07-P02] Discrimination of organic compounds and mineral particles by fluorescent microscopy for the detection of Martian life.

*Tomoka Okada[1], Yoshitaka Yoshimura[2], Atsuo Miyakawa[3], Yuka Murano[3], Shin-ichi Yokobori[3], Akihiko Yamagishi[3], Kensei Kobayashi[1], Yoko Kebukawa[1] (1.YOKOHAMA National university, 2.Tamagawa University, 3.Tokyo University of Pharmacy and Life Sciences)

[MIS07-P03] Morphological and spectroscopic characteristics of organic matter in Banded Iron Formation, Barberton Greenstone Belt, South Africa

*Hiroki Amemiya[1], Ryo Nakajima[1], Yoko Ohtomo[1], Tsubasa Otake[1], Tsutomu Sato[1] (1.Division of sustainable Resources Engineering, Faculty of Engineering, Hokkaido University)

[MIS07-P04] Understanding peptide sequence selectivity on iron sulfide (FeS) nanoparticle surfaces

*Fujishima Kosuke[1], Norio Kitadai[1], Kenji Kasama[1] (1.Earth-Life Science Institute, Tokyo Institute of Technology)

[MIS07-P05] A process model of L-homochiral peptides formation initiated with L-alanine

*Toratane Munegumi[1], Taisuke Yamaga[1] (1.Department of Science Education, Naruto University of Education)

[MIS07-P06] Possible Formation of Amino Acids and Carboxylic Acids in Slightly-Reducing Primitive Earth Atmospheres

*Miei Kinoshita[1], Shintaro Ikeda[1], Kimitaka Kawamura[2], Bhagawati Kunwar[2], Hitoshi Fukuda[3], Yoshiyuki Oguri[3], Hiromi Shibata[4], Junichi Takahashi[1], Vladimir Airapetian[5], Yoko Kebukawa[1], Kensei Kobayashi[1] (1.Yokohama National University, 2.Chubu University, 3.Tokyo Institute of Technology, 4.Osaka University, 5.NASA Goddard SFC)

[MIS07-P07] Application of Machine learning and software development for initial analysis in the TANPOPO mission

*Kyoko Okudaira[1], Yuto Toda[1], Takashi Sonoke[1], Yuichi Yaguchi[1], Masashi Yoshida[1], Junya Imani[2], Satoshi Sasaki[3], Hajime Yano[4], Hirohide Demura[1], Makoto Tabata[5], Akihiko Yamagishi[6] (1.The University of Aizu, 2.YUKI Precision, 3.Tokyo University of Technology, 4.JAXA, 5.Chiba University, 6.Tokyo University of Pharmacy and Life Science)

[MIS07-P08] Structure analysis of the hyper velocity impact tracks of the particles captured by silica aerogel on the International Space Station

*Mizuho Nishi[1], Akira Tsuchiyama[1], Hajime Yano[2], Hikaru Yabuta[3], Kyoko Okudaira[4], Junya Matsuno[1], Masayuki Uesugi[5], Uesugi Kentaro[5], Nakano Tukasa[6], Takaaki Noguchi[7], MITA Hajime[8], Akihiko Yamagishi[9] (1.Kyoto University, 2.Institute of Space and Astronautical Science, Japan Aerospace Exploration Agency, 3.Hiroshima University, 4.The University of Aizu, 5.JASRI/SPring-8, 6.National Institute of Advanced Industrial Science and Technology, 7.Kyusyu University, 8.Fukuoka Institute of Technology, 9.Tokyo University of Pharmacy and Life Science)

[MIS07-P09] High-Angular-Resolution Observations of Protoplanetary Disks

*Misato Fukagawa[1] (1.National Astronomical Observatory of Japan)

[MIS07-P10] Characterization of high molecular weight amino acid precursors formed in interstellar ice analog

*Soushi Kuramoto[1], Tomohito Sato[1], Hitoshi Fukuda[2], Yoshiyuki Oguri[2], Kotaro Kondo[2], Hiromi Shibata[3], Yoko Kebukawa[1], Kensei Kobayashi[1], Satoshi Yoshida[4] (1.Yokohama National University, 2.Tokyo Institute of Technology, 3.University of Osaka, 4.National Institutes for Quantum Radiological Science and Technology)

[MIS07-P11] Theoretical elucidation of prebiotic formation processes into nucleobases

*Yu Komatsu[1,2], Taiki Suzuki[1,2] (1.Astrobiology Center, 2.National Astronomical Observatory of Japan)

[MIS07-P12] Formation Process of A Glycine's Precursor Candidate, CH3NH2

*Taiki Suzuki[1,2], Liton Majumdar[3], Masatoshi Ohishi[2] (1.National Institutes of Natural Sciences Astrobiology Center, 2.National Astronomical Observatory of Japan, 3.NASA Jet Propulsion Laboratory (JPL))

[MIS07-P13] Numerical study on the stellar atmosphere & wind of Cool Stars

*Takahito Sakaue[1], Kazunari Shibata[1] (1.Kyoto University)

[MIS07-P14] Design of space exposure experiments of organic matter in Tanpopo 2

*Takuya Yokoo[1], tomohito sato[1], Itsuki Sakon[2], Kazumichi Nakagawa[3], Hajime Yano[4], Miki Nakayama[5], Hajime Mita[5], Yoko Kebukawa[1], Kensei Kobayashi[1] (1.Yokohama National University, 2.University of Tokyo, 3.Kobe University, 4.JAXA, 5.Fukuoka Institute of Technology)

Exoplanets Revealed by High-Precision Infrared Doppler Technique Using IRD: Large Exploration for Planets around Cool M-type Stars Begins

*Masayuki Kuzuhara[1,3], Bunei Sato[4], Motohide Tamura[2,1,3], Takayuki Kotani[1,3,5], Nagayoshi Ohashi[3,6], Masashi Omiya[1,3], Teruyuki Hirano[4], Hiroki Harakawa[6,3,1], Wako Aoki[3,5], Norio Narita[2,1], Yasunori Hori[1,3], Akitoshi Ueda[3,5], Akihiko Fukui[2], Hiroyuki Tako Ishikawa[5,3], Ishizuka Masato[2], Takashi Kurokawa[1,7], Nobuhiko Kusakabe[1,3], Tomoyuki Kudo[6,3,1], Eiichiro Kokubo[3], Mihoko Konishi[1,3], Tadashi Nakajima[1,3,5], Jun Nishikawa[3,5,1], Masahiro Ogihara[3], Takuma Serizawa[7]

1. Astrobiology Center of NINS, 2. The University of Tokyo, Graduate School of Science, 3. National Astronomical Observatory of Japan, 4. Tokyo Institute of Technology, 5. SOKENDAI, 6. Subaru Telescope, 7. Tokyo University of Agriculture and Technology

Planets outside the Solar system, so-called exoplanets, are promising as a new window for astrobiology. Among those, planets orbiting cool M-type stars (main-sequence stars with effective temperatures less than about 3000 K) have the great potential to push forward astrobiological studies on exoplanets. The habitable zone (HZ) is the zone where liquid water is sustainable on the surfaces of planets. It is expected that the HZs around cooler stars come closer to the parent stars (Kopparapu et al. 2013, ApJ 765, 131). In addition, the recent exoplanet observations performed by the *Kepler* space telescope have revealed that the occurrence rate of small exoplanets similar to Earth increases as the effective temperatures of stars decrease (e.g., Mulders et al. 2015, ApJ 798, 112). Furthermore, the Doppler technique, one of primary methods for exoplanet observations, can more easily find a planet with the orbit closer to its parent star. Accordingly, targeting cool M-type stars provides a significant advantage in the observations of rocky planets in HZs based on the Doppler technique. Also, the snow line around a cool M-type star is close to the star; this is intriguing in terms of the planet formation process.
Nevertheless, the exoplanet observations for cool M-type stars have not been advanced compared with those for hotter stars, due to their faintness. In particular, the low brightness of a cool M-type star at optical wavelengths makes it problematic to observe its planet based on visible light, which has been mostly used in exoplanet observations. We have therefore developed the InfraRed Doppler (IRD) instrument, which is a high-dispersion spectrograph to enable the exoplanet observations using the high-precision Doppler technique at near-infrared (Kotani et al. 2018, Proc. of the SPIE 10702, 1070211). Near-infrared light is suited for observing cool M-type stars, since their peak flux is located in a near-infrared region. One of bottlenecks to achieve high-precision measurements using the near-infrared Doppler technique is the lack of a reference source that enables us to correctly calibrate a measurement fluctuation caused by the instability of an observation instrument. We use a laser frequency comb (LFC) generated by the system that has been newly developed for IRD as a reference source to calibrate IRD measurements. An LFC spectrum has a number of emission lines with fine sampling intervals and is observed simultaneously with a stellar spectrum, so it works as a correct wavelength calibrator for the stellar spectrum. After our laboratory performance verifications of IRD with its LFC system (Kuzuhara et al. 2018, Proc. of the SPIE 10702, 1070260), the IRD operation started on the Subaru Telescope, whose large primary mirror enables high-sensitivity observations even for cool M-type stars. The use of IRD with the Subaru Telescope significantly helps the discoveries and characterizations of exoplanets around cool M-type stars.
We have planned a large survey for planets around cool M-type stars with IRD on the Subaru Telescope, which actually begins on February, 2019. In this survey, we monitor 60 M-type stars over 175 nights

©2019. Japan Geoscience Union. All Right Reserved.

allocated for 5 years. Our pre-survey simulation prospects more than 60 planet detections; those discoveries include a few dozen Earth-like planets, among which some are expected to locate within HZs. Thus, the IRD survey provides important contributions on improving our current understanding of planet formation models for low-mass stars like cool M-type stars, as well as the provisions of samples for exoplanet characterizations using the future large telescopes such as TMT. Here, we report the result of our ongoing on-sky tests to evaluate the IRD performances such as its measurement precision and stability. Furthermore, we explain the above large program in detail: our science goals, and the target selection and observation strategy for the goals are provided.

Keywords: Exoplanet, Doppler technique, Habitable Zone, IRD, planet formation, M-type star

©2019. Japan Geoscience Union. All Right Reserved.

Discrimination of organic compounds and mineral particles by fluorescent microscopy for the detection of Martian life.

*Tomoka Okada[1], Yoshitaka Yoshimura[2], Atsuo Miyakawa[3], Yuka Murano[3], Shin-ichi Yokobori[3], Akihiko Yamagishi[3], Kensei Kobayashi[1], Yoko Kebukawa[1]

1. YOKOHAMA National university, 2. Tamagawa University, 3. Tokyo University of Pharmacy and Life Sciences

The Viking mission searched life on Mars in 1976, but did not find apparent biological activities[1)]. However, the detection sensitivity of the Viking instrument (GC-MS) has been found to be low, suggesting that organic compounds could exist on Martian surface. Recently the MSL Curiosity by NASA detected organic compounds[2)]. The Phoenix mission discovered H_2O ice[3)] and possible liquid water flows were found at RSL (Recurring Slope Lineae) by MRO (Mars Reconnaissance Orbiter)[4)]. These findings suggested that life might exist on Martian surface.

We have proposed a life search program on the surface of Mars with a fluorescence microscope[5)]. This microscope is called Life detection Microscope (LDM) which detects microorganisms in more than 100 times higher sensitivity than the Viking GC-MS. In this program, we plan to use two fluorescent dyes SYTO 24 and propidium iodide (PI) in LDM. SYTO24 permeates cell membrane and stains organic compounds. PI also stains organic compounds such as nucleic acids, but it doesn’t permeate cell membrane. Therefore, the combination of these two dyes makes it possible to differentiate the organic compounds surrounded by membranes (living cells) and dead cells.

However, there are some mineral particles have autofluorescence, possibly detected as false positives. In this research, in order to discriminate organic compounds from mineral particles, the autofluorescence of minerals were measured under various conditions.

Various kind of mineral specimens were finely ground with a glass pen washed with ethanol. Fluorescent images were obtained with a fluorescence microscope and a digital camera and their fluorescent intensities were measured by image analysis. We also examined fluorescent spectra of mineral particles using a diffraction grating. The results showed the fluorescent intensities and spectra of mineral particles were clearly different from the stained organic compounds. These methods would be useful to detect organic compounds among mineral particles.

1) Navarro-Gonzalez, R., *et al.,* 2006, *PNAS*, 103: 16089-16094. 2) Freissient, C., *et al*., 2015, *J. Geophys. Res. Planets,* 120: 495-514. 3) Feldman, W. C., *et al.,* 2002. *Science*, 297, 75-78. 4) McEwen A. S, *et al.,* 2011, *Science,* 333: 740-743. 5) Yamagishi, A., *et al*., 2010, *Bio. Sci. Space,* 24: 67-82.

Keywords: Mars, Fluorescent microscope, Life Detection

©2019. Japan Geoscience Union. All Right Reserved.

Morphological and spectroscopic characteristics of organic matter in Banded Iron Formation, Barberton Greenstone Belt, South Africa

*Hiroki Amemiya[1], Ryo Nakajima[1], Yoko Ohtomo[1], Tsubasa Otake[1], Tsutomu Sato[1]

1. Division of sustainable Resources Engineering, Faculty of Engineering, Hokkaido University

The emergence of cyanobacteria has been postulated to cause an increase in Earth’ s atmospheric oxygen concentration ~2.45 Ga and oxidation of ferrous iron in a seawater, facilitating the formation of Banded Iron Formations (BIFs) in the Proterozoic era. On the other hand, iron precipitation process in the Archean is still controversial. Previous studies suggest that anoxygenic iron-oxidizing bacteria and/or free oxygen produced by cyanobacteria, was responsible for iron oxidation before ~2.45 Ga. Organic matter preserved in BIFs may provide insights into the iron oxidation process and biological evolution in Archean. However, authenticity of Archaean organic matter has to be first clarified for further investigations due to possible later contamination. Here, we investigated morphological and spectroscopic characteristics of organic matter in ~3.2 Ga BIFs in Sheba mine, Moodies Group, Barberton Green stone Belt, South Africa to estimate the chemical structure combined with a contamination check using Raman spectroscopy.

Organic matter was collected by two different methods: extraction by acid treatment of powder samples and pick up with a micro-manipulator from thin sections. When Raman spectra were obtained using 532 nm wavelength laser, acid-treated organic matter showed two peaks ~1350 and ~1580 cm^{-1} corresponding to disordered and ordered carbon structures, whereas micro-sampled organic matter shows no detectable peak with a high background. Because yellow-green fluorescence was observed in micro-sampled organic matter using a Fluorescence microscope, the fluorescence likely causes a high background in the Raman spectra. Therefore, 785 nm wavelength laser was applied for micro-sampled organic matter. Calculated metamorphic temperature from the Raman spectra obtained by acid-treated and micro-sampled organic matter was from 400 to 540˚C, which is consist with greenschist facies of the Barberton Greenstone Belt. This indicates that the organic matter is not a later contamination. Chemical mapping with an Electron Probe Micro Analyzer shows that micro-sampled organic matter is predominately comprised of carbon with slight contribution of nitrogen (< 0.1wt%). Infrared spectra of the organic matter show absorption peaks corresponding to N-O, C-O, and C=O bonds, suggesting that organic matter remains their functional groups in the structure. Based on the morphology and microstructure observed by Field Emission- Scanning Electron Microscope, the organic matter may have been derived from biofilm because of similarity in the morphology as well as the large size (20 –50 μm). Furthermore, the micro-sampled organic matter has a rough surface while the acid-treated organic matter has a smooth one, which may be due to damages by acid-treatment. Our results suggest that micro-sampling is suitable to observe the detailed morphological and structural features of organic matter preserved in Archean sedimentary rocks.

Keywords: Archean, Microfossils, Barberton Greenstone Belt, Raman spectroscopy, Infrared spectroscopy

©2019. Japan Geoscience Union. All Right Reserved.

Understanding peptide sequence selectivity on iron sulfide (FeS) nanoparticle surfaces

*Fujishima Kosuke[1], Norio Kitadai[1], Kenji Kasama[1]

1. Earth-Life Science Institute, Tokyo Institute of Technology

The emergence and evolution of functional biopolymers on Earth is one of the unsolved key questions regarding the origin of life. Amongst various building blocks of polymers, amino acids are prebiotically abundant and different plausible paths toward forming polypeptides have been previously shown in the context of early Earth environment. However, relationship between a specific geochemical environment and the types of biopolymers that could retain or to propergate in that condition is not yet fully systematically explored. Hence, we have prepared random octapeptide library with a combination of limited set of amino acids (Gly, Ile, His, Asp, Cys, Arg) as a probe to explore the sequence selectivity of iron sulfide (FeS) nanoparticles as a simulant of the geochemical settings that once existed at the deep-sea floor or the surface of early Earth. Experiment was carried out by mixing the FeS nanoparticles and random peptides in pure H_2O solution inside the anoxic chamber to allow adsorption under moderate temperature/pH condition. After extensive rinsing step, peptides that remain bound to the FeS nanoparticles were analyzed directly by MALDI-MS/MS to retrieve sequence information. We will discuss the latest sequence results obtained from screening and discuss sequence selective feature of FeS and its relevance to the iron-sulfur cluster known as a fundamental cofactor in biology.

Keywords: Iron sulfide, peptide adsorption, MALDI-MS/MS, iron-sulfur cluster

©2019. Japan Geoscience Union. All Right Reserved.

A process model of L-homochiral peptides formation initiated with L-alanine

*Toratane Munegumi[1], Taisuke Yamaga[1]

1. Department of Science Education, Naruto University of Education

Hydrogen abstraction from L-alanine by hydroxy radical facilitates alkylation on β-carbon of alanine as well as retention of L-chirality. The reaction rate constant of hydrogen abstraction ($k=6.21\times10^{7}\ M^{-1}s^{-1}$) on β-carbon was about 3.7 times faster than that ($k=1.7\times10^{7}\ M^{-1}s^{-1}$) on α-carbon. The fact supports that alkylation proceeds faster than racemization, and the chirality of product amino acids will be hold. Similar alkylation of oligopeptides will also proceed with a lower level epimerization than alkylation. This research discusses how the lower reaction rate of epimerization than alkylation lead homochiral peptides.

Keywords: L-alanine, peptides, homochirality

©2019. Japan Geoscience Union. All Right Reserved.

Possible Formation of Amino Acids and Carboxylic Acids in Slightly-Reducing Primitive Earth Atmospheres

*Miei Kinoshita[1], Shintaro Ikeda[1], Kimitaka Kawamura[2], Bhagawati Kunwar[2], Hitoshi Fukuda[3], Yoshiyuki Oguri[3], Hiromi Shibata[4], Junichi Takahashi[1], Vladimir Airapetian[5], Yoko Kebukawa[1], Kensei Kobayashi[1]

1. Yokohama National University, 2. Chubu University, 3. Tokyo Institute of Technology, 4. Osaka University, 5. NASA Goddard SFC

Since 1950s, a large number of laboratory experiments have been performed to examine possible formation of bioorganic compounds such as amino acids in primitive Earth atmosphere. Earlier experiments with strongly reducing gas mixtures containing large molar ratio of methane and ammonia, and it was reported that efficient production of amino acids and other important organics were formed in it by spark discharges and other energy sources. It is now estimated, however, that the early Earth atmosphere was only slightly reducing [1]: N_2 and CO_2were the major atmospheric constituents, together with some small amount of reducing carbon species like CH_4 and/or CO. Simulation experiments suggested, however, that amino acid formation was restricted under these conditions [2]. We reported that cosmic rays could facilitate chemical reactions with less reducing model of primitive atmosphere such as a mixture of CO_2, CO, $N_2$and H_2O [3]. However these energy sources have been ignored in experiments with initiation of prebiotic chemistry [4]. Here, we examine possible formation of amino acids from slightly reducing gas mixtures by applying high-energy protons to simulate the action of cosmic rays.

We conducted three sets of laboratory experiments using energetic particles, spark discharge and UV light as dominant energy sources. In these sets of experiments we used 400 mL of gas mixture of N_2, $CO_2$and CH_4introduced to a Pyrex tube together with 5 mL of pure water under 350 Torr of N2 and 350 Torr of mixtures with varied mixing ratios of $CH_4$and CO_2. In order to simulate possible roles of cosmic rays, the gas mixture was irradiated with 2.5 MeV proton beam produced in the Tandem accelerator at Tokyo Tech, Japan. We also exposed the same composition of gas mixtures to spark discharges by using a Tesla coil to simulate lightning. The gas mixtures were also irradiated with UV light (l> 190 nm) from a xenon lamp. Each product was acid-hydrolyzed and was subjected to amino acid analysis by HPLC and GC/MS, both after derivatization. Carboxylic acids were determined by GC/MS after derivatization. Starting and resulting gas mixtures were analyzed with a quadrupole mass spectrometer.

Amino acids were detected in the hydrolyzed products when gas mixtures of N_2, CO_2, $CH_4$and H_2O were irradiated with 2.5 MeV protons at the initial the molar ratio of methane (r_{CH4}) in the starting gas mixture as low as 0.5 %. On the other hand, amino acids were detected only when $r_{CH4}$was greater than 15 % in the case of spark discharges. The experiments with UV irradiation source did not yield amino acids or their precursors even when $r_{CH4}$was 50 %. Very little amino acids were detected in all the products before hydrolysis. It was shown that not free amino acids but amino acid precursors were formed in selected experiments.

Carboxylic acids including formic acid, oxalic acid and glyoxylic acid were detected from unhydrolized products derived from N_2-CO_2gas mixtures exposed to spark discharges and proton irradiation. We show that some free carboxylic acids could be formed in non-reducing atmospheres as well as slightly reducing atmospheres either by proton irradiation or by spark discharges. It was suggested that the mechanism of formation of amino acid precursors from N_2-CO_2-CH_4-H_2O mixtures was quite different from that of

©2019. Japan Geoscience Union. All Right Reserved.

carboxylic acids.

Lightning and solar UV have been considered important energy sources for prebiotic synthesis in primitive Earth atmosphere. We here showed that lightning and solar UV could not singularly synthesize important N-containing organics such as amino acids from slightly reducing primitive Earth atmosphere. On the other hand, cosmic ray could have been an important energy source to synthesize amino acid precursors even if primitive Earth atmosphere was only slightly reducing. It would be of interest to examine whether there are synergetic effects among cosmic rays, UV and thundering.

References:

[1] H. Kuwahara and S. Sugita, *Icarus,* **257**,290-301 (2015).

[2] H. Kuwahara *et al.,Orig. Life Evol. Biosph.,* **42**,533-541(2012).

[3] K. Kobayashi *et al.*, *Orig. Life Evol. Biosph.* **28**, 155-165 (1998).

[4] S. L. Miller and H. C. Urey, *Science,* **130**,245-251 (1957).

Keywords: Primitive Earth Atmospheres, Amino Acids, Solar Energetic Particles

©2019. Japan Geoscience Union. All Right Reserved.

Application of Machine learning and software development for initial analysis in the TANPOPO mission

*Kyoko Okudaira[1], Yuto Toda[1], Takashi Sonoke[1], Yuichi Yaguchi[1], Masashi Yoshida[1], Junya Imani[2], Satoshi Sasaki[3], Hajime Yano[4], Hirohide Demura[1], Makoto Tabata[5], Akihiko Yamagishi[6]

1. The University of Aizu, 2. YUKI Precision, 3. Tokyo University of Technology, 4. JAXA, 5. Chiba University, 6. Tokyo University of Pharmacy and Life Science

One of the goals of the TANPOPO mission is collecting cosmic dust and space debris on the International Space Station [1]. Ultra-low density material “silica aerogel” panels are used as capture media [2]. These panels retrieved from the space are sent to the laboratory and initial analysis has been conducted by a system called “CLOXS”.

CLOXS efficiently covers the processes (1) Automatic imaging the entire panel, 2) Search for penetration track candidates, 3) Mapping of track candidates, 4) Shape data acquisition of tracks, and 5) Automatic sample cutting) up to sample allocation to researchers. However, to reduce researchers’ time and effort, improvement of the software and automation of some processes are required.

In this study, application of machine learning in discrimination of objects in aerogel images taken by CLOXS is mainly reported. The research goal is to classify objects in the images into tracks and dirt using machine learning.

There are morphological varieties in the objects. As for both tracks and dirt, they are classified into 4 types respectively in this study.

Since the contrast of the images are low, the first step of our approach is preprocessing of the images. We compared the results of *Contrast Stretching* and *CLAHE* (Contrast Limited Adaptive Histogram Equalization).

Learning data and test data are prepared respectively, to compare the case that the images are categorized into 4 types and the case that the images of all types are dealt altogether.

Convolutional Neural Network (CNN) is used as a method of machine learning. *Python* is used as programing Language.

In conclusion, as for image processing, *CLAHE* showed higher accuracy when tracks were judged to be tracks, and *Contrast Stretching* was found to yield a better result for dirt. It is probably because, in *Contrast Stretching*, *CNN* was not sufficiently highlighted to capture features, and *CLAHE* was able to improve the contrast sufficiently.

Regarding separating the types of tracks and dirt, the accuracy rate was higher when tracks were categorized into different types and learned.

Although further evaluation and improvements might be needed, our accuracy rates meet the mission requirements, that is, the percentage of identifying track as track should be more than 95 %, while the percentage of identifying dirt as dirt should be more than 70 % (that of NOT identifying true track as dirt

©2019. Japan Geoscience Union. All Right Reserved.

should be less than 30 %).

[1] A. Yamagishi et al., “Tanpopo: Astrobiology exposure and micrometeoroid capture experiments - proposed experiments at the exposure facility of ISS-JEM”, *Trans. JSASS. Aerospace Tech. Jpn.* vol. 12, No. ists29, p. Tk_49-Tk_55, 2014.

[2] M. Tabata, et al. “Ultralow-density double-layer silica aerogel fabrication for the intact capture of cosmic dust in low-Earth orbits” *J. Sol-Gel Sci. Technol.* 77(2), 325-334, 2016.

Keywords: TANPOPO mission, Astrobiology, Initial analysis, Machine learning, Software development

©2019. Japan Geoscience Union. All Right Reserved.

Structure analysis of the hyper velocity impact tracks of the particles captured by silica aerogel on the International Space Station

*Mizuho Nishi[1], Akira Tsuchiyama[1], Hajime Yano[2], Hikaru Yabuta[3], Kyoko Okudaira[4], Junya Matsuno[1], Masayuki Uesugi[5], Uesugi Kentaro[5], Nakano Tukasa[6], Takaaki Noguchi[7], MITA Hajime[8], Akihiko Yamagishi[9]

1. Kyoto University, 2. Institute of Space and Astronautical Science, Japan Aerospace Exploration Agency, 3. Hiroshima University, 4. The University of Aizu, 5. JASRI/SPring-8, 6. National Institute of Advanced Industrial Science and Technology, 7. Kyusyu University, 8. Fukuoka Institute of Technology, 9. Tokyo University of Pharmacy and Life Science

In Japan's first astrobiology experiment “Tanpopo”, attempts have been made to capture cosmic dust by installing ultra-low-density silica aerogel at the Japanese Experiment Module “Kibo” of the International Space Station (ISS) [1]. This mission was conducted with the aim of verifying the hypothesis that the origin of life was supplied from outside the earth [2]. Silica aerogel had been used in NASA’s cometary dust sample return mission “Stardust” [3]. Impact tracks formed by collision of cometary dust against aerogel were classified into 3 types, A, B and C, based on their shapes [4]. The track shapes have useful information for estimating the size and density of dust particles [5]. The purposes of this research are (1) to find impact tracks formed by cosmic dust in Tanpopo aerogel and (2) to describe the three-dimensional shapes of impact tracks with different origins (cosmic dust and space debris) and finally to clarify the relation between the track shape and the origin.

At SPring-8 BL47XU, three-dimensional shapes were obtained with imaging absorption tomography for 8 impact tracks (D1-231, D1-298, D1-362, E1-200, E1-304, F1-328, F1-389, F1-623), which were found in Tanpopo aerogel faced to the space direction. The imaging experiments were made at 7, 8, 9 keV with the voxel size of 0.24 or 0.465 μm. CT images at 8 keV were used to extract track shapes. Track length (L_t), maximum track diameter (D_m), aspect ratio, and other shape properties were obtained. These values were compared with Stardust tracks. Dual-energy tomography (DET) [6] was applied to estimate the materials of particles captured in the tracks. Another track (E2-000) was observed only with an optical microscope. For D1-231, D1-298, D1-362 and E2-000, the aerogel was compressed and real solid particles in the tracks were searched with an optical microscope.

The 9 tracks in total were classified into 5 types based on their shapes. Type 1 (E2-000) is a track formed by cosmic dust, where two pyroxene particles were identified at the tip of the track [7]. The track shape resembles Stardust type B track, but its entrance widely spreads. Type 2 (D1-231) is somewhat similar to Stardust type A track. Type 3 (E1-200 and E1-304) is a track having abundant cracks developed on the wall with a narrow entrance. Type 4 (F1-328 and F1-389) is extremely asymmetrical in its shape and has cracks similar to Type 3. Type 5 (D1-362 and F1-623) is a bowl-shaped track with a large entrance. The relationship between L_t and D_m of these tracks was almost the same as that of Stardust tracks except for Type 5. However, their specific shapes of Types 2, 3 and 4 are significantly different from Stardust tracks. The cracks of these tracks are similar to those seen at the end of Stardust type A and B tracks, indicating that they were formed by a relatively low-speed impact. Similar tracks to Type 5 were reported in the aerogel in the exposure experiment on the Mir Station. They may be due to high-speed collision of weakly-adhered aggregates [8]. From the quantitative analysis of such impact tracks, there is a possibility of obtaining knowledge about new parameter areas which could not be obtained by conventional research. DET results showed that most of fine particles in the tracks do not contain Fe and Ni. Low values of their

©2019. Japan Geoscience Union. All Right Reserved.

linear absorption coefficients are smaller than that of cosmic dust. They should be formed by impact of weekly-adhered aggregates that were broken into very small pieces by the impact and mixed with condensed aerogel. Two particles with relatively high linear absorption coefficient were confirmed in D1-231 and D1-362. They were confirmed by and optical microscope after compressing.

[1] Yamagishi A. et al. 2012. Space Utiliz Res, 28, 220. [2] Chyba C. & Sagan C. 1992. Nature, 355, 125. [3] Brownlee D. et al. 2006. Science, 314, 1711. [4] Hörz et al. 2006. Science, 314, 1716. [5] Tsuchiyama A. et al. 2009. Meteoritics & Planetary Science, 44, 1203. [6] Tsuchiyama A. 2013. Geochimica et Cosmochimica Acta 116, 5. [7] Noguchi T., 2018, Private message. [8] Hörz and Zolensky, 2000, Icarus 147, 559.

Keywords: Tanpopo mission, Cosmic dust

©2019. Japan Geoscience Union. All Right Reserved.

High-Angular-Resolution Observations of Protoplanetary Disks

*Misato Fukagawa[1]

1. National Astronomical Observatory of Japan

The recent progress in understanding of planet-formation process will be reviewed based on the results obtained at high angular resolution with astronomical facilities such as the Atacama Large Millimeter/submillimeter Array (ALMA). Circumstellar disk structures around young stars are birthplaces of planets. The physical and chemical condition in such protoplanetary disks can be linked to some extent to the planetary environment (e.g., atmospheric composition) where further chemical reactions might lead to formation of building blocks of life. This presentation includes the topics on detailed disk density structures at ~5-au or better resolution, gas detections in the later stages of disks where the collisional events in the planetary systems may happen, detections of organic molecules, and the prospects on disk observations in future.

Keywords: Exoplanets, Astronomy

©2019. Japan Geoscience Union. All Right Reserved.

Characterization of high molecular weight amino acid precursors formed in interstellar ice analog

*Soushi Kuramoto[1], Tomohito Sato[1], Hitoshi Fukuda[2], Yoshiyuki Oguri[2], Kotaro Kondo[2], Hiromi Shibata[3], Yoko Kebukawa[1], Kensei Kobayashi[1], Satoshi Yoshida[4]

1. Yokohama National University, 2. Tokyo Institute of Technology, 3. University of Osaka, 4. National Institutes for Quantum Radiological Science and Technology

It is suggested that extraterrestrial organic compounds are important for chemical evolution toward the generation of the first life on the Earth. Bioorganic compounds such as amino acids were found in hydrolyzed extracts of meteorite [1]. The products before hydrolysis referred to as “amino acid precursors” were, however, little known. It has been sometimes claimed that a-amino acids found in meteorites were formed by the Strecker synthesis. If so, aminonitriles and amino acid amides are the precursors, but they have not identified as major precursors yet. Extraterrestrial amino acid precursors were probably synthesized in molecular cloud environments or small celestial bodies. We irradiated possible interstellar media, such as mixture of carbon monoxide, ammonia and water to simulate possible reactions among interstellar media in dense clouds. The irradiation products were analyzed by HPLC and mass spectrometry.

A gaseous mixture (CO and NH_3) was sealed in a Pyrex glass tube with liquid water. The gaseous mixture was irradiated with 2.5 MeV protons from a Tandem accelerator at Tokyo Institute of Technology. Total quantity of electricity was 2 mC. The name of the irradiation products is hereafter called CAW. CAW was fractionated by cation exchange HPLC into several fractions to discriminate the fractions with glycine amide or aminoacetonitrile (the Strecker-type precursors) and those without them. Each fraction was hydrolyzed with 6M HCl at 110 ˚C for 24h and was subjected to amino acid analysis. Molecular weights of CAW were estimated by ultrafiltration (molecular weight cut off: 3000), gel filtration (column: Shodex OHpak SB-802.5 HQ) and mass spectrometry by ESI-TOF-MS.

It was shown that glycine was rarely detected in the fractions with the Strecker-type simple amino acid precursors (aminoacetonitrile, glycine amide). It was suggested that the CAW (an interstellar organics analogue) contained complex amino acid precursors with molecular weights of some thousands. Compared with molecular weights standards (authentic proteins), molecular weights of CAW were estimated 6000 or more by gel filtration chromatography. Peaks of m/z = 1000 or over were detected by mass spectrometry. These results strongly suggested that complex amino acid precursors with large molecular weights could be directly generated from small molecules such as CO in interstellar environments. We are now trying to characterize amino acid precursors formed in interstellar ice analogue (frozen mixture of CH3OH, NH3 and H2O [2]) by heavy ions irradiation.

[1] K. A. Kvenvolden *et al.*, *Nature* 228, 923 (1970).

[2] K. Kobayashi *et al.*, *Electr. Commun.* Jpn. 91, 293 (2008).

Keywords: Chemical evolution, interstellar ice, the Strecker synthesis, amino acid precursor

©2019. Japan Geoscience Union. All Right Reserved.

Theoretical elucidation of prebiotic formation processes into nucleobases

*Yu Komatsu[1,2], Taiki Suzuki[1,2]

1. Astrobiology Center, 2. National Astronomical Observatory of Japan

As argued [1], the comets and meteorites may have provided a large amount of prebiotic molecules to the Early Earth. However, where and how such organic molecules were built is still controversial.

Recently, volatile glycine (NH2CH2COOH) has been detected in the coma of comet 67P/Churyumov-Gerasimenko by the ROSINA mass spectrometer [2], with giving us clues to glycine's interstellar origin. Moreover, in addition to various amino acids, nucleobases, such as purine, uracil, guanine, and xanthine have been identified in the meteorite (e.g., [3]). These studies suggest the formation of prebiotic molecules in the extreme condition prior to the early Earth chemistry.

If prebiotic molecules are built from small atoms or radicals in the cold ISM, the prebiotic molecules must have almost barrier-less formation paths. On the other hand, the bombardment of comets and/or asteroids would have provided very high temperature condition for chemical reactions, which may have led to the decomposition and formation of further complex prebiotic molecules. To understand the formation processes, the quantum chemical calculation is a powerful tool. The previous quantum chemical calculation has already reported the promising chemical paths to amino acids and nucleobases (e.g., [4]).

Here we investigated the possible pathway of pyrimidine, purine, uracil and thymine by the automated exploration of chemical reaction pathways. We have already discovered key dissociations for each molecule. For example, uracil and thymine, the pyrimidine type of nucleobase, have lower barriers to dissociate into an isocyanic acid, which corresponds to the previous laboratory experience, and the rest molecule. Pyrimidine and purine, which are skeleton structures of nucleobases and do not poses any oxygen atoms, have high barriers, implying to require high temperature environment like the bombardment, even though we did not exclude all possibilities of radical reactions. Detailed discussions will be provided on our poster.

References

[1] Ehrenfreund (2002), Rep. Prog. Phys. 65 1427

[2] Altwegg et al. (2016), Sci, 2, e1600285

[3] Simomiya et al. (1990), Geo, 24,343

[4] Ferus et al. (2015), PNAS, 112, 7109

Keywords: Prebiotic Chemistry, Quantum Chemistry, DNA /RNA, Interstellar Chemistry

©2019. Japan Geoscience Union. All Right Reserved.

©2019. Japan Geoscience Union. All Right Reserved.

Formation Process of A Glycine's Precursor Candidate, CH3NH2

*Taiki Suzuki[1,2], Liton Majumdar[3], Masatoshi Ohishi[2]

1. National Institutes of Natural Sciences Astrobiology Center, 2. National Astronomical Observatory of Japan, 3. NASA Jet Propulsion Laboratory (JPL)

As [1] argued, the comets and meteorites may have provided a large amount of prebiotic molecules to the early Earth. An attempt to understand the origins of life must necessarily begin with detailed studies of the formation and evolution of complex organic molecules (COMs), products of complex chemistry that most likely starts in molecular clouds and continues within the protoplanetary disk.
Since the amino acids are the essential building blocks of life, the search for amino acids and their complex organic precursors at different stages of star and planet formation is one of the exciting topics in modern astronomy. Recently, volatile glycine (NH_2CH_2COOH) was detected in the coma of comet 67P/Churyumov-Gerasimenko by the ROSINA mass spectrometer [2], also giving clues about glycine's interstellar origin. However, the survey observations of glycine toward ISM have been not successful. Therefore, revealing the formation pathways to glycine is important for astrochemistry and astrobiology not only to know the promising glycine-rich sources for future surveys but also to understand the general chemical evolution of N-bearing molecules in the ISM.
In this context, we performed the chemical modeling study for the high-mass star, with the possible formation processes of glycine with theoretically and/or experimentally suggested formation paths [3]. We suggested that glycine was efficiently formed through the following reactions: First, the hydrogenation process to HCN leads to the formation of CH_2NH and CH_3NH_2 on interstellar grain surface (HCN + 2H => CH_2NH, and then CH_2NH + 2H => CH_3NH_2). Then, the destruction of CH_3NH_2 by radicals will form CH_2NH_2. Finally, CH_2NH_2 and COOH radical react to form glycine. For this test, a key molecule would be CH_3OH, whose formation process is well known. Both experiments and theoretical works suggested that CH_3OH is built via grain surface hydrogenation processes to CO (CO + 2H => H_2CO, and then H_2CO + 2H => CH_3OH). If CH_3NH_2 is also produced through hydrogenation process, “CH_3NH_2/CH_3OH” ratio should be well reproduced by the modeling. However, it was difficult to test this formation process due to the very limited number of previous CH3NH2 observations.
With this motivation, we performed the observation of CH_3NH_2 and CH_3OH with ALMA toward high mass star-forming regions, G10.47+0.03, NGC6334I, W51 e1/e2, and G31.41+0.3. As a result, both of CH_3OH and CH_3NH_2 were detected toward all sources. The molecular abundances were derived with rotation diagram method. The high excitation temperatures of 100 and 200 K and compact distributions suggest that CH_3NH_2 emissions originate from the hot and dense regions. The observed molecular abundance ratio, “CH_3NH_2/CH_3OH” ranges from 0.2 to 2.1. The low “CH_3NH_2/CH_3OH” ratio of 0.2 is close to our modeling, supporting that CH_3NH_2 is the product of the hydrogenation process in those sources. However, the higher “CH_3NH_2/CH_3OH” ratio of nearly two, observed toward NGC6334I MM1, could not be reproduced with our modeling under the possible parameter range. Thus, our chemical modeling would not correctly reproduce the physics or chemistry of such CH_3NH_2-rich sources. Further studies of such sources will enable us to promote our knowledge of glycine chemistry and provide us with promising sources for future glycine surveys.

Citations:
[1] Ehrenfreund (2002), Rep. Prog. Phys. 65 1427

©2019. Japan Geoscience Union. All Right Reserved.

[2] Altwegg et al. (2016), Sci, 2, e1600285
[3] Suzuki et al, (2018), ApJ, 825, 51

Keywords: radio astronomy, chemical modeling, prebiotic molecules

©2019. Japan Geoscience Union. All Right Reserved.

Numerical study on the stellar atmosphere & wind of Cool Stars

*Takahito Sakaue[1], Kazunari Shibata[1]

1. Kyoto University

Cool stars offer the good opportunities to investigate what environments the Earth-like exoplanets are in, and how they are affected by the host star. TRAPPIST-1 is an ultracool dwarf; the spectral type is M8V (T_{eff} =2559K) with the lower mass of 0.08M_{sun} (radius = 0.11R_{sun}). The star is confirmed to have seven planets (Gillon et al. 2017) and thus greatly interested in not only by stellar astrophysics but also by astrobiology. Here, we report the results of one-dimensional magnetohydrodynamic (MHD) simulation of the stellar wind from TRAPPIST-1. Several solar wind theories, which have been examined observationally, are applied to the case of TRAPPIST-1. Among them, it is the plausible idea that the dissipation of the incompressible MHD wave leads to the heating and driving the stellar wind. For instance, Garraffo et al. 2017 succeeded in the three-dimensional MHD simulation of the stellar wind from TRAPPIST-1, by extending their solar wind model in which the incompressible MHD wave is exhausted by the turbulent dissipation. The incompressible MHD wave, on the other hand, is also affected not only by the turbulent dissipation but also by the nonlinear mode coupling, which leads to the formation of the shock wave and consequently contribute to heating the wind. This nonlinear process has been well investigated to account for the dynamics of the lower solar atmosphere (Kudoh & Shibata 1999) and driving the solar wind (Suzuki & Inutsuka 2005), but not discussed for the stellar wind from TRAPPIST-1. In this study, therefore, we performed the one-dimensional MHD simulation to consider the nonlinear process of the incompressible MHD wave leading to the shock formation, and succeeded in reproducing the stellar wind from TRAPPIST-1.

Keywords: stellar wind, cool stars, TRAPPIST-1

©2019. Japan Geoscience Union. All Right Reserved.

Design of space exposure experiments of organic matter in Tanpopo 2

*Takuya Yokoo[1], tomohito sato[1], Itsuki Sakon[2], Kazumichi Nakagawa[3], Hajime Yano[4], Miki Nakayama[5], Hajime Mita[5], Yoko Kebukawa[1], Kensei Kobayashi[1]

1. Yokohama National University, 2. University of Tokyo, 3. Kobe University, 4. JAXA, 5. Fukuoka Institute of Technology

1. Introduction

Large number of organic compounds have been discovered in molecular clouds and in meteorites. Some of organic compounds required for emergence of life are thought to be synthesized in space. Then, meteorites and interplanetary dust particles could deliver them to the Earth. The first Japanese astrobiology space experiment called “Tanpopo” was conducted to study this hypothesis[1].
The objective of the Tanpopo Mission is to understand bi-directional propagation of microorganisms and organic matter between the Earth and space. In other words, in the Tanpopo Mission, we examine whether life exists only on the earth by evaluating whether microorganisms can escape into space and whether organic matter can reach to the Earth from outer space.
As one of subthemes in this project, amino acids and their precursor compounds including complex interstellar organic matter analog were directly exposed to outer space by utilizing the International Space Station (ISS), and recoveries of these organics were measured to understand degradation of organic compounds under the environment of the outer space. In the Tanpopo experiment, hexatriacontane (HTC) was used to prevent the sample from sublimation during exposure to space at the ISS. However, HTC absorbs ultraviolet light with a wavelength of 160 nm or less. To understand the effects of shorter wavelength UV, the next space experiment "Tanpopo 2" applies a new design for direct exposure of organic compounds without HTC and optical windows. In addition to the aluminum plate same as the one used in Tanpopo, the silicon substrates are also used for exposure the sample to space, in the organic matter exposure experiment of “Tanpopo 2 “. In the Tanpopo Mission, glycine, hydantoin, isovaline, ethylmethylhydantoin, CAW (complex organic matter produced from proton beam irradiation to CO, NH_3, H_2O mixture) were used, and glycine and CAW showed relatively high recoveries [2]. In "Tanpopo 2", glycine and CA (proton beam irradiation product to CO, NH_3 mixture) on the silicon substrates will be directly exposed to space in addition to the same compounds on the same aluminum plate used in the Tanpopo. The recovered samples will be analyzed by FT-IR, XANES, and SEM, in addition to amino acid analysis.
Here we report the design of the space experiment such as preparation method of the space experiment sample.

2. Experimental

(1) A gas mixture of CO (350 Torr) and NH_3 (350 Torr) and a silicon plate (10 mmϕ) were placed in a glass container, and the gas mixture was irradiated with 2.5 MeV proton beam from a tandem accelerator to deposit organic matter on the plate.
(2) The thickness of the organic matter (CA) film on the silicon plate was measured using a three-dimensional microscope.
(3) Structural analysis of organic matter (CA) on the silicon plate was also carried out using FT-IR.
(4) Amino acid analysis was carried out by cation exchange HPLC after hydrolyzing silicon plate with CA with 6 M hydrochloric acid at 110 ˚C for 24 hours.

©2019. Japan Geoscience Union. All Right Reserved.

(5) Glycine is planned to be deposited on a silicon substrate by a vacuum vapor deposition equipment (Fukuoka Institute of Technology).

3. Results and Discussion

The CA deposition thickness was approximately 8 μm, but more sample thickness would be required due to potential loss of the organic materials by atomic oxygen present in low Earth orbit during exposure. Thus, we decided to use non-polished Si substrates instead of polished Si substrate. Because the sample can be kept in the bottom of indentations on the rough surface of non-polished substrate, even if a part of sample surface is lost.
Amino acid analyses of CA by cation exchanged HPLC showed, various amino acids including aspartic acid, threonine, glycine, alanine, -aminoisobutyric acid and serine were detected after acid hydrolysis. Glycine was particularly abundant, whose yield was 827 ±7 nmol from a single CA deposited Si substrate.

4. Conclusions

We will conduct the durability test of our samples on the silicon substrate including the vibration test, cooling test, heating test before launch in 2019 with the space X company to the ISS. We are planning to conduct various analyses from recovered samples. The recovery and degradation of these samples will make a further leap forward our understanding of the possible delivery of organic matter from interplanetary dust particles to the early Earth.

5. References

[1] A. Yamagishi, H. Yano, K. Okudaira, K. Kobayashi, S. Yokobori, M. Tabata, H. Kawai, *Biol. Sci. Space*, **21** : 67-75 (2007).
[2] K. Kobayashi *et al.*, 2018 JpGU meeting, Chiba (2018).

©2019. Japan Geoscience Union. All Right Reserved.

[E] Poster | M (Multidisciplinary and Interdisciplinary) : M-IS Intersection

Thu. May 30, 2019 5:15 PM - 6:30 PM JST | Thu. May 30, 2019 8:15 AM - 9:30 AM UTC | Poster Hall International Exhibition Hall8, Makuhari Messe_37

[M-IS07] Astrobiology

convener:Hikaru Yabuta(Hiroshima University, Department of Earth and Planetary Systems Science), Seiji Sugita(Department of Earth and Planetary Science, Graduate School of Science Sciece, The University of Tokyo), Misato Fukagawa(National Astronomical Observatory of Japan), Fujishima Kosuke(Tokyo Institute of Technology, Earth-Life Science Institute)

Twenty years have passed since when the field of Astrobiology, which aims to unveil the origins, evolution, and habitability of life by integrating multidisciplinary fields, was established. Individual themes related to Astrobiology, such as chemical evolution in the early Solar System, formation of planetary system, prebiotic chemistry in the early Earth, evolution of life in the Earth's history, extremophile, and habitable planetary environments, has been studied by the knowledge and methods from the multiple fields, which has enabled us to explain "Where we came from" in some ways. However, despite an overwhelming number of investigations and discussions through gathering of the scientists from different fields, there has remained the long-standing unsolved question: How did abiotic materials gain biological function in the Earth and elsewhere in universe? There is still a large gap between prebiotic organic chemistry and biochemistry toward Origins of Life and planetary habitability. Therefore, the JpGU Astrobiology session focuses on pathfinding of "integration of astronomy, geoscience, and biochemistry", which will face an increasing need for the future Astrobiology. In order to enhance our understanding of "What is life", we propose to discuss the biochemical events linked with planetary systems, which is beyond the knowledge in a test tube, by an integration of exoplanets and molecular biology, etc. Through this approach, we will lead the discussions and developments of life-detection strategies for the future exploration of life in universe.

[MIS07-P01] Exoplanets Revealed by High-Precision Infrared Doppler Technique Using IRD: Large Exploration for Planets around Cool M-type Stars Begins

*Masayuki Kuzuhara[1,3], Bunei Sato[4], Motohide Tamura[2,1,3], Takayuki Kotani[1,3,5], Nagayoshi Ohashi[3,6], Masashi Omiya[1,3], Teruyuki Hirano[4], Hiroki Harakawa[6,3,1], Wako Aoki[3,5], Norio Narita[2,1], Yasunori Hori[1,3], Akitoshi Ueda[3,5], Akihiko Fukui[2], Hiroyuki Tako Ishikawa[5,3], Ishizuka Masato[2], Takashi Kurokawa[1,7], Nobuhiko Kusakabe[1,3], Tomoyuki Kudo[6,3,1], Eiichiro Kokubo[3], Mihoko Konishi[1,3], Tadashi Nakajima[1,3,5], Jun Nishikawa[3,5,1], Masahiro Ogihara[3], Takuma Serizawa[7] (1.Astrobiology Center of NINS, 2.The University of Tokyo, Graduate School of Science, 3.National Astronomical Observatory of Japan, 4.Tokyo Institute of Technology, 5.SOKENDAI, 6.Subaru Telescope, 7.Tokyo University of Agriculture and Technology)

[MIS07-P02] Discrimination of organic compounds and mineral particles by fluorescent microscopy for the detection of Martian life.

*Tomoka Okada[1], Yoshitaka Yoshimura[2], Atsuo Miyakawa[3], Yuka Murano[3], Shin-ichi Yokobori[3], Akihiko Yamagishi[3], Kensei Kobayashi[1], Yoko Kebukawa[1] (1.YOKOHAMA National university, 2.Tamagawa University, 3.Tokyo University of Pharmacy and Life Sciences)

[MIS07-P03] Morphological and spectroscopic characteristics of organic matter in Banded Iron Formation, Barberton Greenstone Belt, South Africa

*Hiroki Amemiya[1], Ryo Nakajima[1], Yoko Ohtomo[1], Tsubasa Otake[1], Tsutomu Sato[1] (1.Division of sustainable Resources Engineering, Faculty of Engineering, Hokkaido University)

[MIS07-P04] Understanding peptide sequence selectivity on iron sulfide (FeS) nanoparticle surfaces

*Fujishima Kosuke[1], Norio Kitadai[1], Kenji Kasama[1] (1.Earth-Life Science Institute, Tokyo Institute of Technology)

[MIS07-P05] A process model of L-homochiral peptides formation initiated with L-alanine

*Toratane Munegumi[1], Taisuke Yamaga[1] (1.Department of Science Education, Naruto University of Education)

[MIS07-P06] Possible Formation of Amino Acids and Carboxylic Acids in Slightly-Reducing Primitive Earth Atmospheres

*Miei Kinoshita[1], Shintaro Ikeda[1], Kimitaka Kawamura[2], Bhagawati Kunwar[2], Hitoshi Fukuda[3], Yoshiyuki Oguri[3], Hiromi Shibata[4], Junichi Takahashi[1], Vladimir Airapetian[5], Yoko Kebukawa[1], Kensei Kobayashi[1] (1.Yokohama National University, 2.Chubu University, 3.Tokyo Institute of Technology, 4.Osaka University, 5.NASA Goddard SFC)

[MIS07-P07] Application of Machine learning and software development for initial analysis in the TANPOPO mission

*Kyoko Okudaira[1], Yuto Toda[1], Takashi Sonoke[1], Yuichi Yaguchi[1], Masashi Yoshida[1], Junya Imani[2], Satoshi Sasaki[3], Hajime Yano[4], Hirohide Demura[1], Makoto Tabata[5], Akihiko Yamagishi[6] (1.The University of Aizu, 2.YUKI Precision, 3.Tokyo University of Technology, 4.JAXA, 5.Chiba University, 6.Tokyo University of Pharmacy and Life Science)

[MIS07-P08] Structure analysis of the hyper velocity impact tracks of the particles captured by silica aerogel on the International Space Station

*Mizuho Nishi[1], Akira Tsuchiyama[1], Hajime Yano[2], Hikaru Yabuta[3], Kyoko Okudaira[4], Junya Matsuno[1], Masayuki Uesugi[5], Uesugi Kentaro[5], Nakano Tukasa[6], Takaaki Noguchi[7], MITA Hajime[8], Akihiko Yamagishi[9] (1.Kyoto University, 2.Institute of Space and Astronautical Science, Japan Aerospace Exploration Agency, 3.Hiroshima University, 4.The University of Aizu, 5.JASRI/SPring-8, 6.National Institute of Advanced Industrial Science and Technology, 7.Kyusyu University, 8.Fukuoka Institute of Technology, 9.Tokyo University of Pharmacy and Life Science)

[MIS07-P09] High-Angular-Resolution Observations of Protoplanetary Disks

*Misato Fukagawa[1] (1.National Astronomical Observatory of Japan)

[MIS07-P10] Characterization of high molecular weight amino acid precursors formed in interstellar ice analog

*Soushi Kuramoto[1], Tomohito Sato[1], Hitoshi Fukuda[2], Yoshiyuki Oguri[2], Kotaro Kondo[2], Hiromi Shibata[3], Yoko Kebukawa[1], Kensei Kobayashi[1], Satoshi Yoshida[4] (1.Yokohama National University, 2.Tokyo Institute of Technology, 3.University of Osaka, 4.National Institutes for Quantum Radiological Science and Technology)

[MIS07-P11] Theoretical elucidation of prebiotic formation processes into nucleobases

*Yu Komatsu[1,2], Taiki Suzuki[1,2] (1.Astrobiology Center, 2.National Astronomical Observatory of Japan)

[MIS07-P12] Formation Process of A Glycine's Precursor Candidate, CH3NH2

*Taiki Suzuki[1,2], Liton Majumdar[3], Masatoshi Ohishi[2] (1.National Institutes of Natural Sciences Astrobiology Center, 2.National Astronomical Observatory of Japan, 3.NASA Jet Propulsion Laboratory (JPL))

[MIS07-P13] Numerical study on the stellar atmosphere & wind of Cool Stars

*Takahito Sakaue[1], Kazunari Shibata[1] (1.Kyoto University)

[MIS07-P14] Design of space exposure experiments of organic matter in Tanpopo 2

*Takuya Yokoo[1], tomohito sato[1], Itsuki Sakon[2], Kazumichi Nakagawa[3], Hajime Yano[4], Miki Nakayama[5], Hajime Mita[5], Yoko Kebukawa[1], Kensei Kobayashi[1] (1.Yokohama National University, 2.University of Tokyo, 3.Kobe University, 4.JAXA, 5.Fukuoka Institute of Technology)

Exoplanets Revealed by High-Precision Infrared Doppler Technique Using IRD: Large Exploration for Planets around Cool M-type Stars Begins

*Masayuki Kuzuhara[1,3], Bunei Sato[4], Motohide Tamura[2,1,3], Takayuki Kotani[1,3,5], Nagayoshi Ohashi[3,6], Masashi Omiya[1,3], Teruyuki Hirano[4], Hiroki Harakawa[6,3,1], Wako Aoki[3,5], Norio Narita[2,1], Yasunori Hori[1,3], Akitoshi Ueda[3,5], Akihiko Fukui[2], Hiroyuki Tako Ishikawa[5,3], Ishizuka Masato[2], Takashi Kurokawa[1,7], Nobuhiko Kusakabe[1,3], Tomoyuki Kudo[6,3,1], Eiichiro Kokubo[3], Mihoko Konishi[1,3], Tadashi Nakajima[1,3,5], Jun Nishikawa[3,5,1], Masahiro Ogihara[3], Takuma Serizawa[7]

1. Astrobiology Center of NINS, 2. The University of Tokyo, Graduate School of Science, 3. National Astronomical Observatory of Japan, 4. Tokyo Institute of Technology, 5. SOKENDAI, 6. Subaru Telescope, 7. Tokyo University of Agriculture and Technology

Planets outside the Solar system, so-called exoplanets, are promising as a new window for astrobiology. Among those, planets orbiting cool M-type stars (main-sequence stars with effective temperatures less than about 3000 K) have the great potential to push forward astrobiological studies on exoplanets. The habitable zone (HZ) is the zone where liquid water is sustainable on the surfaces of planets. It is expected that the HZs around cooler stars come closer to the parent stars (Kopparapu et al. 2013, ApJ 765, 131). In addition, the recent exoplanet observations performed by the *Kepler* space telescope have revealed that the occurrence rate of small exoplanets similar to Earth increases as the effective temperatures of stars decrease (e.g., Mulders et al. 2015, ApJ 798, 112). Furthermore, the Doppler technique, one of primary methods for exoplanet observations, can more easily find a planet with the orbit closer to its parent star. Accordingly, targeting cool M-type stars provides a significant advantage in the observations of rocky planets in HZs based on the Doppler technique. Also, the snow line around a cool M-type star is close to the star; this is intriguing in terms of the planet formation process.
Nevertheless, the exoplanet observations for cool M-type stars have not been advanced compared with those for hotter stars, due to their faintness. In particular, the low brightness of a cool M-type star at optical wavelengths makes it problematic to observe its planet based on visible light, which has been mostly used in exoplanet observations. We have therefore developed the InfraRed Doppler (IRD) instrument, which is a high-dispersion spectrograph to enable the exoplanet observations using the high-precision Doppler technique at near-infrared (Kotani et al. 2018, Proc. of the SPIE 10702, 1070211). Near-infrared light is suited for observing cool M-type stars, since their peak flux is located in a near-infrared region. One of bottlenecks to achieve high-precision measurements using the near-infrared Doppler technique is the lack of a reference source that enables us to correctly calibrate a measurement fluctuation caused by the instability of an observation instrument. We use a laser frequency comb (LFC) generated by the system that has been newly developed for IRD as a reference source to calibrate IRD measurements. An LFC spectrum has a number of emission lines with fine sampling intervals and is observed simultaneously with a stellar spectrum, so it works as a correct wavelength calibrator for the stellar spectrum. After our laboratory performance verifications of IRD with its LFC system (Kuzuhara et al. 2018, Proc. of the SPIE 10702, 1070260), the IRD operation started on the Subaru Telescope, whose large primary mirror enables high-sensitivity observations even for cool M-type stars. The use of IRD with the Subaru Telescope significantly helps the discoveries and characterizations of exoplanets around cool M-type stars.
We have planned a large survey for planets around cool M-type stars with IRD on the Subaru Telescope, which actually begins on February, 2019. In this survey, we monitor 60 M-type stars over 175 nights

©2019. Japan Geoscience Union. All Right Reserved.

allocated for 5 years. Our pre-survey simulation prospects more than 60 planet detections; those discoveries include a few dozen Earth-like planets, among which some are expected to locate within HZs. Thus, the IRD survey provides important contributions on improving our current understanding of planet formation models for low-mass stars like cool M-type stars, as well as the provisions of samples for exoplanet characterizations using the future large telescopes such as TMT. Here, we report the result of our ongoing on-sky tests to evaluate the IRD performances such as its measurement precision and stability. Furthermore, we explain the above large program in detail: our science goals, and the target selection and observation strategy for the goals are provided.

Keywords: Exoplanet, Doppler technique, Habitable Zone, IRD, planet formation, M-type star

©2019. Japan Geoscience Union. All Right Reserved.

Discrimination of organic compounds and mineral particles by fluorescent microscopy for the detection of Martian life.

*Tomoka Okada[1], Yoshitaka Yoshimura[2], Atsuo Miyakawa[3], Yuka Murano[3], Shin-ichi Yokobori[3], Akihiko Yamagishi[3], Kensei Kobayashi[1], Yoko Kebukawa[1]

1. YOKOHAMA National university, 2. Tamagawa University, 3. Tokyo University of Pharmacy and Life Sciences

The Viking mission searched life on Mars in 1976, but did not find apparent biological activities[1)]. However, the detection sensitivity of the Viking instrument (GC-MS) has been found to be low, suggesting that organic compounds could exist on Martian surface. Recently the MSL Curiosity by NASA detected organic compounds[2)]. The Phoenix mission discovered H_2O ice[3)] and possible liquid water flows were found at RSL (Recurring Slope Lineae) by MRO (Mars Reconnaissance Orbiter)[4)]. These findings suggested that life might exist on Martian surface.

We have proposed a life search program on the surface of Mars with a fluorescence microscope[5)]. This microscope is called Life detection Microscope (LDM) which detects microorganisms in more than 100 times higher sensitivity than the Viking GC-MS. In this program, we plan to use two fluorescent dyes SYTO 24 and propidium iodide (PI) in LDM. SYTO24 permeates cell membrane and stains organic compounds. PI also stains organic compounds such as nucleic acids, but it doesn’t permeate cell membrane. Therefore, the combination of these two dyes makes it possible to differentiate the organic compounds surrounded by membranes (living cells) and dead cells.

However, there are some mineral particles have autofluorescence, possibly detected as false positives. In this research, in order to discriminate organic compounds from mineral particles, the autofluorescence of minerals were measured under various conditions.

Various kind of mineral specimens were finely ground with a glass pen washed with ethanol. Fluorescent images were obtained with a fluorescence microscope and a digital camera and their fluorescent intensities were measured by image analysis. We also examined fluorescent spectra of mineral particles using a diffraction grating. The results showed the fluorescent intensities and spectra of mineral particles were clearly different from the stained organic compounds. These methods would be useful to detect organic compounds among mineral particles.

1) Navarro-Gonzalez, R., *et al.,* 2006, *PNAS*, 103: 16089-16094. 2) Freissient, C., *et al*., 2015, *J. Geophys. Res. Planets,* 120: 495-514. 3) Feldman, W. C., *et al.,* 2002. *Science*, 297, 75-78. 4) McEwen A. S, *et al.,* 2011, *Science,* 333: 740-743. 5) Yamagishi, A., *et al*., 2010, *Bio. Sci. Space,* 24: 67-82.

Keywords: Mars, Fluorescent microscope, Life Detection

©2019. Japan Geoscience Union. All Right Reserved.

Morphological and spectroscopic characteristics of organic matter in Banded Iron Formation, Barberton Greenstone Belt, South Africa

*Hiroki Amemiya[1], Ryo Nakajima[1], Yoko Ohtomo[1], Tsubasa Otake[1], Tsutomu Sato[1]

1. Division of sustainable Resources Engineering, Faculty of Engineering, Hokkaido University

The emergence of cyanobacteria has been postulated to cause an increase in Earth’ s atmospheric oxygen concentration ~2.45 Ga and oxidation of ferrous iron in a seawater, facilitating the formation of Banded Iron Formations (BIFs) in the Proterozoic era. On the other hand, iron precipitation process in the Archean is still controversial. Previous studies suggest that anoxygenic iron-oxidizing bacteria and/or free oxygen produced by cyanobacteria, was responsible for iron oxidation before ~2.45 Ga. Organic matter preserved in BIFs may provide insights into the iron oxidation process and biological evolution in Archean. However, authenticity of Archaean organic matter has to be first clarified for further investigations due to possible later contamination. Here, we investigated morphological and spectroscopic characteristics of organic matter in ~3.2 Ga BIFs in Sheba mine, Moodies Group, Barberton Green stone Belt, South Africa to estimate the chemical structure combined with a contamination check using Raman spectroscopy.

Organic matter was collected by two different methods: extraction by acid treatment of powder samples and pick up with a micro-manipulator from thin sections. When Raman spectra were obtained using 532 nm wavelength laser, acid-treated organic matter showed two peaks ~1350 and ~1580 cm^{-1} corresponding to disordered and ordered carbon structures, whereas micro-sampled organic matter shows no detectable peak with a high background. Because yellow-green fluorescence was observed in micro-sampled organic matter using a Fluorescence microscope, the fluorescence likely causes a high background in the Raman spectra. Therefore, 785 nm wavelength laser was applied for micro-sampled organic matter. Calculated metamorphic temperature from the Raman spectra obtained by acid-treated and micro-sampled organic matter was from 400 to 540˚C, which is consist with greenschist facies of the Barberton Greenstone Belt. This indicates that the organic matter is not a later contamination. Chemical mapping with an Electron Probe Micro Analyzer shows that micro-sampled organic matter is predominately comprised of carbon with slight contribution of nitrogen (< 0.1wt%). Infrared spectra of the organic matter show absorption peaks corresponding to N-O, C-O, and C=O bonds, suggesting that organic matter remains their functional groups in the structure. Based on the morphology and microstructure observed by Field Emission- Scanning Electron Microscope, the organic matter may have been derived from biofilm because of similarity in the morphology as well as the large size (20 –50 μm). Furthermore, the micro-sampled organic matter has a rough surface while the acid-treated organic matter has a smooth one, which may be due to damages by acid-treatment. Our results suggest that micro-sampling is suitable to observe the detailed morphological and structural features of organic matter preserved in Archean sedimentary rocks.

Keywords: Archean, Microfossils, Barberton Greenstone Belt, Raman spectroscopy, Infrared spectroscopy

©2019. Japan Geoscience Union. All Right Reserved.

Understanding peptide sequence selectivity on iron sulfide (FeS) nanoparticle surfaces

*Fujishima Kosuke[1], Norio Kitadai[1], Kenji Kasama[1]

1. Earth-Life Science Institute, Tokyo Institute of Technology

The emergence and evolution of functional biopolymers on Earth is one of the unsolved key questions regarding the origin of life. Amongst various building blocks of polymers, amino acids are prebiotically abundant and different plausible paths toward forming polypeptides have been previously shown in the context of early Earth environment. However, relationship between a specific geochemical environment and the types of biopolymers that could retain or to propergate in that condition is not yet fully systematically explored. Hence, we have prepared random octapeptide library with a combination of limited set of amino acids (Gly, Ile, His, Asp, Cys, Arg) as a probe to explore the sequence selectivity of iron sulfide (FeS) nanoparticles as a simulant of the geochemical settings that once existed at the deep-sea floor or the surface of early Earth. Experiment was carried out by mixing the FeS nanoparticles and random peptides in pure H_2O solution inside the anoxic chamber to allow adsorption under moderate temperature/pH condition. After extensive rinsing step, peptides that remain bound to the FeS nanoparticles were analyzed directly by MALDI-MS/MS to retrieve sequence information. We will discuss the latest sequence results obtained from screening and discuss sequence selective feature of FeS and its relevance to the iron-sulfur cluster known as a fundamental cofactor in biology.

Keywords: Iron sulfide, peptide adsorption, MALDI-MS/MS, iron-sulfur cluster

©2019. Japan Geoscience Union. All Right Reserved.

A process model of L-homochiral peptides formation initiated with L-alanine

*Toratane Munegumi[1], Taisuke Yamaga[1]

1. Department of Science Education, Naruto University of Education

Hydrogen abstraction from L-alanine by hydroxy radical facilitates alkylation on β-carbon of alanine as well as retention of L-chirality. The reaction rate constant of hydrogen abstraction ($k=6.21\times10^{7}\ M^{-1}s^{-1}$) on β-carbon was about 3.7 times faster than that ($k=1.7\times10^{7}\ M^{-1}s^{-1}$) on α-carbon. The fact supports that alkylation proceeds faster than racemization, and the chirality of product amino acids will be hold. Similar alkylation of oligopeptides will also proceed with a lower level epimerization than alkylation. This research discusses how the lower reaction rate of epimerization than alkylation lead homochiral peptides.

Keywords: L-alanine, peptides, homochirality

©2019. Japan Geoscience Union. All Right Reserved.

Possible Formation of Amino Acids and Carboxylic Acids in Slightly-Reducing Primitive Earth Atmospheres

*Miei Kinoshita[1], Shintaro Ikeda[1], Kimitaka Kawamura[2], Bhagawati Kunwar[2], Hitoshi Fukuda[3], Yoshiyuki Oguri[3], Hiromi Shibata[4], Junichi Takahashi[1], Vladimir Airapetian[5], Yoko Kebukawa[1], Kensei Kobayashi[1]

1. Yokohama National University, 2. Chubu University, 3. Tokyo Institute of Technology, 4. Osaka University, 5. NASA Goddard SFC

Since 1950s, a large number of laboratory experiments have been performed to examine possible formation of bioorganic compounds such as amino acids in primitive Earth atmosphere. Earlier experiments with strongly reducing gas mixtures containing large molar ratio of methane and ammonia, and it was reported that efficient production of amino acids and other important organics were formed in it by spark discharges and other energy sources. It is now estimated, however, that the early Earth atmosphere was only slightly reducing [1]: N_2 and CO_2were the major atmospheric constituents, together with some small amount of reducing carbon species like CH_4 and/or CO. Simulation experiments suggested, however, that amino acid formation was restricted under these conditions [2]. We reported that cosmic rays could facilitate chemical reactions with less reducing model of primitive atmosphere such as a mixture of CO_2, CO, $N_2$and H_2O [3]. However these energy sources have been ignored in experiments with initiation of prebiotic chemistry [4]. Here, we examine possible formation of amino acids from slightly reducing gas mixtures by applying high-energy protons to simulate the action of cosmic rays.

We conducted three sets of laboratory experiments using energetic particles, spark discharge and UV light as dominant energy sources. In these sets of experiments we used 400 mL of gas mixture of N_2, $CO_2$and CH_4introduced to a Pyrex tube together with 5 mL of pure water under 350 Torr of N2 and 350 Torr of mixtures with varied mixing ratios of $CH_4$and CO_2. In order to simulate possible roles of cosmic rays, the gas mixture was irradiated with 2.5 MeV proton beam produced in the Tandem accelerator at Tokyo Tech, Japan. We also exposed the same composition of gas mixtures to spark discharges by using a Tesla coil to simulate lightning. The gas mixtures were also irradiated with UV light (l> 190 nm) from a xenon lamp. Each product was acid-hydrolyzed and was subjected to amino acid analysis by HPLC and GC/MS, both after derivatization. Carboxylic acids were determined by GC/MS after derivatization. Starting and resulting gas mixtures were analyzed with a quadrupole mass spectrometer.

Amino acids were detected in the hydrolyzed products when gas mixtures of N_2, CO_2, $CH_4$and H_2O were irradiated with 2.5 MeV protons at the initial the molar ratio of methane (r_{CH4}) in the starting gas mixture as low as 0.5 %. On the other hand, amino acids were detected only when $r_{CH4}$was greater than 15 % in the case of spark discharges. The experiments with UV irradiation source did not yield amino acids or their precursors even when $r_{CH4}$was 50 %. Very little amino acids were detected in all the products before hydrolysis. It was shown that not free amino acids but amino acid precursors were formed in selected experiments.

Carboxylic acids including formic acid, oxalic acid and glyoxylic acid were detected from unhydrolized products derived from N_2-CO_2gas mixtures exposed to spark discharges and proton irradiation. We show that some free carboxylic acids could be formed in non-reducing atmospheres as well as slightly reducing atmospheres either by proton irradiation or by spark discharges. It was suggested that the mechanism of formation of amino acid precursors from N_2-CO_2-CH_4-H_2O mixtures was quite different from that of

©2019. Japan Geoscience Union. All Right Reserved.

carboxylic acids.

Lightning and solar UV have been considered important energy sources for prebiotic synthesis in primitive Earth atmosphere. We here showed that lightning and solar UV could not singularly synthesize important N-containing organics such as amino acids from slightly reducing primitive Earth atmosphere. On the other hand, cosmic ray could have been an important energy source to synthesize amino acid precursors even if primitive Earth atmosphere was only slightly reducing. It would be of interest to examine whether there are synergetic effects among cosmic rays, UV and thundering.

References:

[1] H. Kuwahara and S. Sugita, *Icarus,* **257**,290-301 (2015).

[2] H. Kuwahara *et al.,Orig. Life Evol. Biosph.,* **42**,533-541(2012).

[3] K. Kobayashi *et al.*, *Orig. Life Evol. Biosph.* **28**, 155-165 (1998).

[4] S. L. Miller and H. C. Urey, *Science,* **130**,245-251 (1957).

Keywords: Primitive Earth Atmospheres, Amino Acids, Solar Energetic Particles

©2019. Japan Geoscience Union. All Right Reserved.

Application of Machine learning and software development for initial analysis in the TANPOPO mission

*Kyoko Okudaira[1], Yuto Toda[1], Takashi Sonoke[1], Yuichi Yaguchi[1], Masashi Yoshida[1], Junya Imani[2], Satoshi Sasaki[3], Hajime Yano[4], Hirohide Demura[1], Makoto Tabata[5], Akihiko Yamagishi[6]

1. The University of Aizu, 2. YUKI Precision, 3. Tokyo University of Technology, 4. JAXA, 5. Chiba University, 6. Tokyo University of Pharmacy and Life Science

One of the goals of the TANPOPO mission is collecting cosmic dust and space debris on the International Space Station [1]. Ultra-low density material “silica aerogel” panels are used as capture media [2]. These panels retrieved from the space are sent to the laboratory and initial analysis has been conducted by a system called “CLOXS”.

CLOXS efficiently covers the processes (1) Automatic imaging the entire panel, 2) Search for penetration track candidates, 3) Mapping of track candidates, 4) Shape data acquisition of tracks, and 5) Automatic sample cutting) up to sample allocation to researchers. However, to reduce researchers’ time and effort, improvement of the software and automation of some processes are required.

In this study, application of machine learning in discrimination of objects in aerogel images taken by CLOXS is mainly reported. The research goal is to classify objects in the images into tracks and dirt using machine learning.

There are morphological varieties in the objects. As for both tracks and dirt, they are classified into 4 types respectively in this study.

Since the contrast of the images are low, the first step of our approach is preprocessing of the images. We compared the results of *Contrast Stretching* and *CLAHE* (Contrast Limited Adaptive Histogram Equalization).

Learning data and test data are prepared respectively, to compare the case that the images are categorized into 4 types and the case that the images of all types are dealt altogether.

Convolutional Neural Network (CNN) is used as a method of machine learning. *Python* is used as programing Language.

In conclusion, as for image processing, *CLAHE* showed higher accuracy when tracks were judged to be tracks, and *Contrast Stretching* was found to yield a better result for dirt. It is probably because, in *Contrast Stretching*, *CNN* was not sufficiently highlighted to capture features, and *CLAHE* was able to improve the contrast sufficiently.

Regarding separating the types of tracks and dirt, the accuracy rate was higher when tracks were categorized into different types and learned.

Although further evaluation and improvements might be needed, our accuracy rates meet the mission requirements, that is, the percentage of identifying track as track should be more than 95 %, while the percentage of identifying dirt as dirt should be more than 70 % (that of NOT identifying true track as dirt

©2019. Japan Geoscience Union. All Right Reserved.

should be less than 30 %).

[1] A. Yamagishi et al., “Tanpopo: Astrobiology exposure and micrometeoroid capture experiments - proposed experiments at the exposure facility of ISS-JEM”, *Trans. JSASS. Aerospace Tech. Jpn.* vol. 12, No. ists29, p. Tk_49-Tk_55, 2014.

[2] M. Tabata, et al. “Ultralow-density double-layer silica aerogel fabrication for the intact capture of cosmic dust in low-Earth orbits” *J. Sol-Gel Sci. Technol.* 77(2), 325-334, 2016.

Keywords: TANPOPO mission, Astrobiology, Initial analysis, Machine learning, Software development

©2019. Japan Geoscience Union. All Right Reserved.

Structure analysis of the hyper velocity impact tracks of the particles captured by silica aerogel on the International Space Station

*Mizuho Nishi[1], Akira Tsuchiyama[1], Hajime Yano[2], Hikaru Yabuta[3], Kyoko Okudaira[4], Junya Matsuno[1], Masayuki Uesugi[5], Uesugi Kentaro[5], Nakano Tukasa[6], Takaaki Noguchi[7], MITA Hajime[8], Akihiko Yamagishi[9]

1. Kyoto University, 2. Institute of Space and Astronautical Science, Japan Aerospace Exploration Agency, 3. Hiroshima University, 4. The University of Aizu, 5. JASRI/SPring-8, 6. National Institute of Advanced Industrial Science and Technology, 7. Kyusyu University, 8. Fukuoka Institute of Technology, 9. Tokyo University of Pharmacy and Life Science

In Japan's first astrobiology experiment “Tanpopo”, attempts have been made to capture cosmic dust by installing ultra-low-density silica aerogel at the Japanese Experiment Module “Kibo” of the International Space Station (ISS) [1]. This mission was conducted with the aim of verifying the hypothesis that the origin of life was supplied from outside the earth [2]. Silica aerogel had been used in NASA’s cometary dust sample return mission “Stardust” [3]. Impact tracks formed by collision of cometary dust against aerogel were classified into 3 types, A, B and C, based on their shapes [4]. The track shapes have useful information for estimating the size and density of dust particles [5]. The purposes of this research are (1) to find impact tracks formed by cosmic dust in Tanpopo aerogel and (2) to describe the three-dimensional shapes of impact tracks with different origins (cosmic dust and space debris) and finally to clarify the relation between the track shape and the origin.

At SPring-8 BL47XU, three-dimensional shapes were obtained with imaging absorption tomography for 8 impact tracks (D1-231, D1-298, D1-362, E1-200, E1-304, F1-328, F1-389, F1-623), which were found in Tanpopo aerogel faced to the space direction. The imaging experiments were made at 7, 8, 9 keV with the voxel size of 0.24 or 0.465 μm. CT images at 8 keV were used to extract track shapes. Track length (L_t), maximum track diameter (D_m), aspect ratio, and other shape properties were obtained. These values were compared with Stardust tracks. Dual-energy tomography (DET) [6] was applied to estimate the materials of particles captured in the tracks. Another track (E2-000) was observed only with an optical microscope. For D1-231, D1-298, D1-362 and E2-000, the aerogel was compressed and real solid particles in the tracks were searched with an optical microscope.

The 9 tracks in total were classified into 5 types based on their shapes. Type 1 (E2-000) is a track formed by cosmic dust, where two pyroxene particles were identified at the tip of the track [7]. The track shape resembles Stardust type B track, but its entrance widely spreads. Type 2 (D1-231) is somewhat similar to Stardust type A track. Type 3 (E1-200 and E1-304) is a track having abundant cracks developed on the wall with a narrow entrance. Type 4 (F1-328 and F1-389) is extremely asymmetrical in its shape and has cracks similar to Type 3. Type 5 (D1-362 and F1-623) is a bowl-shaped track with a large entrance. The relationship between L_t and D_m of these tracks was almost the same as that of Stardust tracks except for Type 5. However, their specific shapes of Types 2, 3 and 4 are significantly different from Stardust tracks. The cracks of these tracks are similar to those seen at the end of Stardust type A and B tracks, indicating that they were formed by a relatively low-speed impact. Similar tracks to Type 5 were reported in the aerogel in the exposure experiment on the Mir Station. They may be due to high-speed collision of weakly-adhered aggregates [8]. From the quantitative analysis of such impact tracks, there is a possibility of obtaining knowledge about new parameter areas which could not be obtained by conventional research. DET results showed that most of fine particles in the tracks do not contain Fe and Ni. Low values of their

©2019. Japan Geoscience Union. All Right Reserved.

linear absorption coefficients are smaller than that of cosmic dust. They should be formed by impact of weekly-adhered aggregates that were broken into very small pieces by the impact and mixed with condensed aerogel. Two particles with relatively high linear absorption coefficient were confirmed in D1-231 and D1-362. They were confirmed by and optical microscope after compressing.

[1] Yamagishi A. et al. 2012. Space Utiliz Res, 28, 220. [2] Chyba C. & Sagan C. 1992. Nature, 355, 125. [3] Brownlee D. et al. 2006. Science, 314, 1711. [4] Hörz et al. 2006. Science, 314, 1716. [5] Tsuchiyama A. et al. 2009. Meteoritics & Planetary Science, 44, 1203. [6] Tsuchiyama A. 2013. Geochimica et Cosmochimica Acta 116, 5. [7] Noguchi T., 2018, Private message. [8] Hörz and Zolensky, 2000, Icarus 147, 559.

Keywords: Tanpopo mission, Cosmic dust

©2019. Japan Geoscience Union. All Right Reserved.

High-Angular-Resolution Observations of Protoplanetary Disks

*Misato Fukagawa[1]

1. National Astronomical Observatory of Japan

The recent progress in understanding of planet-formation process will be reviewed based on the results obtained at high angular resolution with astronomical facilities such as the Atacama Large Millimeter/submillimeter Array (ALMA). Circumstellar disk structures around young stars are birthplaces of planets. The physical and chemical condition in such protoplanetary disks can be linked to some extent to the planetary environment (e.g., atmospheric composition) where further chemical reactions might lead to formation of building blocks of life. This presentation includes the topics on detailed disk density structures at ~5-au or better resolution, gas detections in the later stages of disks where the collisional events in the planetary systems may happen, detections of organic molecules, and the prospects on disk observations in future.

Keywords: Exoplanets, Astronomy

©2019. Japan Geoscience Union. All Right Reserved.

Characterization of high molecular weight amino acid precursors formed in interstellar ice analog

*Soushi Kuramoto[1], Tomohito Sato[1], Hitoshi Fukuda[2], Yoshiyuki Oguri[2], Kotaro Kondo[2], Hiromi Shibata[3], Yoko Kebukawa[1], Kensei Kobayashi[1], Satoshi Yoshida[4]

1. Yokohama National University, 2. Tokyo Institute of Technology, 3. University of Osaka, 4. National Institutes for Quantum Radiological Science and Technology

It is suggested that extraterrestrial organic compounds are important for chemical evolution toward the generation of the first life on the Earth. Bioorganic compounds such as amino acids were found in hydrolyzed extracts of meteorite [1]. The products before hydrolysis referred to as “amino acid precursors” were, however, little known. It has been sometimes claimed that a-amino acids found in meteorites were formed by the Strecker synthesis. If so, aminonitriles and amino acid amides are the precursors, but they have not identified as major precursors yet. Extraterrestrial amino acid precursors were probably synthesized in molecular cloud environments or small celestial bodies. We irradiated possible interstellar media, such as mixture of carbon monoxide, ammonia and water to simulate possible reactions among interstellar media in dense clouds. The irradiation products were analyzed by HPLC and mass spectrometry.

A gaseous mixture (CO and NH_3) was sealed in a Pyrex glass tube with liquid water. The gaseous mixture was irradiated with 2.5 MeV protons from a Tandem accelerator at Tokyo Institute of Technology. Total quantity of electricity was 2 mC. The name of the irradiation products is hereafter called CAW. CAW was fractionated by cation exchange HPLC into several fractions to discriminate the fractions with glycine amide or aminoacetonitrile (the Strecker-type precursors) and those without them. Each fraction was hydrolyzed with 6M HCl at 110 ˚C for 24h and was subjected to amino acid analysis. Molecular weights of CAW were estimated by ultrafiltration (molecular weight cut off: 3000), gel filtration (column: Shodex OHpak SB-802.5 HQ) and mass spectrometry by ESI-TOF-MS.

It was shown that glycine was rarely detected in the fractions with the Strecker-type simple amino acid precursors (aminoacetonitrile, glycine amide). It was suggested that the CAW (an interstellar organics analogue) contained complex amino acid precursors with molecular weights of some thousands. Compared with molecular weights standards (authentic proteins), molecular weights of CAW were estimated 6000 or more by gel filtration chromatography. Peaks of m/z = 1000 or over were detected by mass spectrometry. These results strongly suggested that complex amino acid precursors with large molecular weights could be directly generated from small molecules such as CO in interstellar environments. We are now trying to characterize amino acid precursors formed in interstellar ice analogue (frozen mixture of CH3OH, NH3 and H2O [2]) by heavy ions irradiation.

[1] K. A. Kvenvolden *et al.*, *Nature* 228, 923 (1970).

[2] K. Kobayashi *et al.*, *Electr. Commun.* Jpn. 91, 293 (2008).

Keywords: Chemical evolution, interstellar ice, the Strecker synthesis, amino acid precursor

©2019. Japan Geoscience Union. All Right Reserved.

Theoretical elucidation of prebiotic formation processes into nucleobases

*Yu Komatsu[1,2], Taiki Suzuki[1,2]

1. Astrobiology Center, 2. National Astronomical Observatory of Japan

As argued [1], the comets and meteorites may have provided a large amount of prebiotic molecules to the Early Earth. However, where and how such organic molecules were built is still controversial.

Recently, volatile glycine (NH2CH2COOH) has been detected in the coma of comet 67P/Churyumov-Gerasimenko by the ROSINA mass spectrometer [2], with giving us clues to glycine's interstellar origin. Moreover, in addition to various amino acids, nucleobases, such as purine, uracil, guanine, and xanthine have been identified in the meteorite (e.g., [3]). These studies suggest the formation of prebiotic molecules in the extreme condition prior to the early Earth chemistry.

If prebiotic molecules are built from small atoms or radicals in the cold ISM, the prebiotic molecules must have almost barrier-less formation paths. On the other hand, the bombardment of comets and/or asteroids would have provided very high temperature condition for chemical reactions, which may have led to the decomposition and formation of further complex prebiotic molecules. To understand the formation processes, the quantum chemical calculation is a powerful tool. The previous quantum chemical calculation has already reported the promising chemical paths to amino acids and nucleobases (e.g., [4]).

Here we investigated the possible pathway of pyrimidine, purine, uracil and thymine by the automated exploration of chemical reaction pathways. We have already discovered key dissociations for each molecule. For example, uracil and thymine, the pyrimidine type of nucleobase, have lower barriers to dissociate into an isocyanic acid, which corresponds to the previous laboratory experience, and the rest molecule. Pyrimidine and purine, which are skeleton structures of nucleobases and do not poses any oxygen atoms, have high barriers, implying to require high temperature environment like the bombardment, even though we did not exclude all possibilities of radical reactions. Detailed discussions will be provided on our poster.

References

[1] Ehrenfreund (2002), Rep. Prog. Phys. 65 1427

[2] Altwegg et al. (2016), Sci, 2, e1600285

[3] Simomiya et al. (1990), Geo, 24,343

[4] Ferus et al. (2015), PNAS, 112, 7109

Keywords: Prebiotic Chemistry, Quantum Chemistry, DNA /RNA, Interstellar Chemistry

©2019. Japan Geoscience Union. All Right Reserved.

©2019. Japan Geoscience Union. All Right Reserved.

Formation Process of A Glycine's Precursor Candidate, CH3NH2

*Taiki Suzuki[1,2], Liton Majumdar[3], Masatoshi Ohishi[2]

1. National Institutes of Natural Sciences Astrobiology Center, 2. National Astronomical Observatory of Japan, 3. NASA Jet Propulsion Laboratory (JPL)

As [1] argued, the comets and meteorites may have provided a large amount of prebiotic molecules to the early Earth. An attempt to understand the origins of life must necessarily begin with detailed studies of the formation and evolution of complex organic molecules (COMs), products of complex chemistry that most likely starts in molecular clouds and continues within the protoplanetary disk.
Since the amino acids are the essential building blocks of life, the search for amino acids and their complex organic precursors at different stages of star and planet formation is one of the exciting topics in modern astronomy. Recently, volatile glycine (NH_2CH_2COOH) was detected in the coma of comet 67P/Churyumov-Gerasimenko by the ROSINA mass spectrometer [2], also giving clues about glycine's interstellar origin. However, the survey observations of glycine toward ISM have been not successful. Therefore, revealing the formation pathways to glycine is important for astrochemistry and astrobiology not only to know the promising glycine-rich sources for future surveys but also to understand the general chemical evolution of N-bearing molecules in the ISM.
In this context, we performed the chemical modeling study for the high-mass star, with the possible formation processes of glycine with theoretically and/or experimentally suggested formation paths [3]. We suggested that glycine was efficiently formed through the following reactions: First, the hydrogenation process to HCN leads to the formation of CH_2NH and CH_3NH_2 on interstellar grain surface (HCN + 2H => CH_2NH, and then CH_2NH + 2H => CH_3NH_2). Then, the destruction of CH_3NH_2 by radicals will form CH_2NH_2. Finally, CH_2NH_2 and COOH radical react to form glycine. For this test, a key molecule would be CH_3OH, whose formation process is well known. Both experiments and theoretical works suggested that CH_3OH is built via grain surface hydrogenation processes to CO (CO + 2H => H_2CO, and then H_2CO + 2H => CH_3OH). If CH_3NH_2 is also produced through hydrogenation process, “CH_3NH_2/CH_3OH” ratio should be well reproduced by the modeling. However, it was difficult to test this formation process due to the very limited number of previous CH3NH2 observations.
With this motivation, we performed the observation of CH_3NH_2 and CH_3OH with ALMA toward high mass star-forming regions, G10.47+0.03, NGC6334I, W51 e1/e2, and G31.41+0.3. As a result, both of CH_3OH and CH_3NH_2 were detected toward all sources. The molecular abundances were derived with rotation diagram method. The high excitation temperatures of 100 and 200 K and compact distributions suggest that CH_3NH_2 emissions originate from the hot and dense regions. The observed molecular abundance ratio, “CH_3NH_2/CH_3OH” ranges from 0.2 to 2.1. The low “CH_3NH_2/CH_3OH” ratio of 0.2 is close to our modeling, supporting that CH_3NH_2 is the product of the hydrogenation process in those sources. However, the higher “CH_3NH_2/CH_3OH” ratio of nearly two, observed toward NGC6334I MM1, could not be reproduced with our modeling under the possible parameter range. Thus, our chemical modeling would not correctly reproduce the physics or chemistry of such CH_3NH_2-rich sources. Further studies of such sources will enable us to promote our knowledge of glycine chemistry and provide us with promising sources for future glycine surveys.

Citations:
[1] Ehrenfreund (2002), Rep. Prog. Phys. 65 1427

©2019. Japan Geoscience Union. All Right Reserved.

[2] Altwegg et al. (2016), Sci, 2, e1600285
[3] Suzuki et al, (2018), ApJ, 825, 51

Keywords: radio astronomy, chemical modeling, prebiotic molecules

©2019. Japan Geoscience Union. All Right Reserved.

Numerical study on the stellar atmosphere & wind of Cool Stars

*Takahito Sakaue[1], Kazunari Shibata[1]

1. Kyoto University

Cool stars offer the good opportunities to investigate what environments the Earth-like exoplanets are in, and how they are affected by the host star. TRAPPIST-1 is an ultracool dwarf; the spectral type is M8V (T_{eff} =2559K) with the lower mass of 0.08M_{sun} (radius = 0.11R_{sun}). The star is confirmed to have seven planets (Gillon et al. 2017) and thus greatly interested in not only by stellar astrophysics but also by astrobiology. Here, we report the results of one-dimensional magnetohydrodynamic (MHD) simulation of the stellar wind from TRAPPIST-1. Several solar wind theories, which have been examined observationally, are applied to the case of TRAPPIST-1. Among them, it is the plausible idea that the dissipation of the incompressible MHD wave leads to the heating and driving the stellar wind. For instance, Garraffo et al. 2017 succeeded in the three-dimensional MHD simulation of the stellar wind from TRAPPIST-1, by extending their solar wind model in which the incompressible MHD wave is exhausted by the turbulent dissipation. The incompressible MHD wave, on the other hand, is also affected not only by the turbulent dissipation but also by the nonlinear mode coupling, which leads to the formation of the shock wave and consequently contribute to heating the wind. This nonlinear process has been well investigated to account for the dynamics of the lower solar atmosphere (Kudoh & Shibata 1999) and driving the solar wind (Suzuki & Inutsuka 2005), but not discussed for the stellar wind from TRAPPIST-1. In this study, therefore, we performed the one-dimensional MHD simulation to consider the nonlinear process of the incompressible MHD wave leading to the shock formation, and succeeded in reproducing the stellar wind from TRAPPIST-1.

Keywords: stellar wind, cool stars, TRAPPIST-1

©2019. Japan Geoscience Union. All Right Reserved.

Design of space exposure experiments of organic matter in Tanpopo 2

*Takuya Yokoo[1], tomohito sato[1], Itsuki Sakon[2], Kazumichi Nakagawa[3], Hajime Yano[4], Miki Nakayama[5], Hajime Mita[5], Yoko Kebukawa[1], Kensei Kobayashi[1]

1. Yokohama National University, 2. University of Tokyo, 3. Kobe University, 4. JAXA, 5. Fukuoka Institute of Technology

1. Introduction

Large number of organic compounds have been discovered in molecular clouds and in meteorites. Some of organic compounds required for emergence of life are thought to be synthesized in space. Then, meteorites and interplanetary dust particles could deliver them to the Earth. The first Japanese astrobiology space experiment called “Tanpopo” was conducted to study this hypothesis[1].
The objective of the Tanpopo Mission is to understand bi-directional propagation of microorganisms and organic matter between the Earth and space. In other words, in the Tanpopo Mission, we examine whether life exists only on the earth by evaluating whether microorganisms can escape into space and whether organic matter can reach to the Earth from outer space.
As one of subthemes in this project, amino acids and their precursor compounds including complex interstellar organic matter analog were directly exposed to outer space by utilizing the International Space Station (ISS), and recoveries of these organics were measured to understand degradation of organic compounds under the environment of the outer space. In the Tanpopo experiment, hexatriacontane (HTC) was used to prevent the sample from sublimation during exposure to space at the ISS. However, HTC absorbs ultraviolet light with a wavelength of 160 nm or less. To understand the effects of shorter wavelength UV, the next space experiment "Tanpopo 2" applies a new design for direct exposure of organic compounds without HTC and optical windows. In addition to the aluminum plate same as the one used in Tanpopo, the silicon substrates are also used for exposure the sample to space, in the organic matter exposure experiment of “Tanpopo 2 “. In the Tanpopo Mission, glycine, hydantoin, isovaline, ethylmethylhydantoin, CAW (complex organic matter produced from proton beam irradiation to CO, NH_3, H_2O mixture) were used, and glycine and CAW showed relatively high recoveries [2]. In "Tanpopo 2", glycine and CA (proton beam irradiation product to CO, NH_3 mixture) on the silicon substrates will be directly exposed to space in addition to the same compounds on the same aluminum plate used in the Tanpopo. The recovered samples will be analyzed by FT-IR, XANES, and SEM, in addition to amino acid analysis.
Here we report the design of the space experiment such as preparation method of the space experiment sample.

2. Experimental

(1) A gas mixture of CO (350 Torr) and NH_3 (350 Torr) and a silicon plate (10 mmϕ) were placed in a glass container, and the gas mixture was irradiated with 2.5 MeV proton beam from a tandem accelerator to deposit organic matter on the plate.
(2) The thickness of the organic matter (CA) film on the silicon plate was measured using a three-dimensional microscope.
(3) Structural analysis of organic matter (CA) on the silicon plate was also carried out using FT-IR.
(4) Amino acid analysis was carried out by cation exchange HPLC after hydrolyzing silicon plate with CA with 6 M hydrochloric acid at 110 ˚C for 24 hours.

©2019. Japan Geoscience Union. All Right Reserved.

(5) Glycine is planned to be deposited on a silicon substrate by a vacuum vapor deposition equipment (Fukuoka Institute of Technology).

3. Results and Discussion

The CA deposition thickness was approximately 8 μm, but more sample thickness would be required due to potential loss of the organic materials by atomic oxygen present in low Earth orbit during exposure. Thus, we decided to use non-polished Si substrates instead of polished Si substrate. Because the sample can be kept in the bottom of indentations on the rough surface of non-polished substrate, even if a part of sample surface is lost.
Amino acid analyses of CA by cation exchanged HPLC showed, various amino acids including aspartic acid, threonine, glycine, alanine, -aminoisobutyric acid and serine were detected after acid hydrolysis. Glycine was particularly abundant, whose yield was 827 ±7 nmol from a single CA deposited Si substrate.

4. Conclusions

We will conduct the durability test of our samples on the silicon substrate including the vibration test, cooling test, heating test before launch in 2019 with the space X company to the ISS. We are planning to conduct various analyses from recovered samples. The recovery and degradation of these samples will make a further leap forward our understanding of the possible delivery of organic matter from interplanetary dust particles to the early Earth.

5. References

[1] A. Yamagishi, H. Yano, K. Okudaira, K. Kobayashi, S. Yokobori, M. Tabata, H. Kawai, *Biol. Sci. Space*, **21** : 67-75 (2007).
[2] K. Kobayashi *et al.*, 2018 JpGU meeting, Chiba (2018).

©2019. Japan Geoscience Union. All Right Reserved.

[E] Poster | M (Multidisciplinary and Interdisciplinary)：M-AG Applied Geosciences

Thu. May 30, 2019 10:45 AM - 12:15 PM JST | Thu. May 30, 2019 1:45 AM - 3:15 AM UTC | Poster Hall International Exhibition Hall8, Makuhari Messe_11

[M-AG38] Satellite Land Physical Processes Monitoring at Medium/High/Very High Resolution

convener:Jean-Claude Roger(University of Maryland College Park), Shinichi Sobue(Japan Aerospace Exploration Agency), Eric Vermote(NASA Goddard Space Flight Center)

We solicit papers on the land physical processes monitoring. In particular, it will include the inversion and use of land products from medium, high, and very high spatial resolution. For the last years, medium, high, and very high resolutions became a useful and a powerful toll for Earth studies. Topics of interest mainly include (not limited to):
- New developments for data processing, including atmospheric correction and cloud screening;
- Analysis and correction of directional effects in land surface reflectances;
- Use of time series of surface reflectances for land monitoring, including land cover classification and crop yield prediction (including data integration and data harmonization);
- Development and use of new vegetation indices (i.e. red edge) and other products for agriculture applications;
- Theoretical studies for sensors capabilities enhancements to future sensors at high/medium resolutions;
- Use of products in agricultural monitoring applications (such as crop area, crop type, crop growing, yield estimation and prediction, damage assessment);
- Agriculture monitoring algorithm description;
- Evaluation or validation of potential products with ground measurements, official statistics;
- International initiative to enhance Earth-Observing-based agricultural information.

Depending on outcome, we think about a special issue.

[MAG38-P01] Improving the AVHRR LTDR BRDF correction

*Jose Luis Villaescusa[1,2], Belen Franch[1,2], Jean-Claude Roger[1,2], Eric Vermote[2] (1.University of Maryland College Park, 2.NASA Goddard Space Flight Center)

[MAG38-P02] Winter wheat yield model based on remote sensing data

*Belen Franch[1,2], Eric Vermote[2,1], Sergii Skakun[1,2], Jean-Claude Roger[1,2], Inbal Becker-Reshef[1], Chris Justice[1] (1.Department of Geographical Sciences, University of Maryland, 2.NASA Goddard Space Flight Center)

[MAG38-P03] Agricultural monitoring from Optical and SAR data

*Andrés Eduardo Santamaría-Artigas[1,2], Sergii Skakun[1,2], Belen Franch[1,2], Jean-Claude Roger[1,2], Eric Vermote[2] (1.University of Maryland College Park, 2.NASA Goddard Space Flight Center)

[MAG38-P04] Eco-hydrological modeling using field-based and Earth Observations to assess water use efficiency and support agricultural water resources management

pierre Guillevic[2,1], *Jean-Claude Roger[1,2] (1.University of Maryland, College Park, USA, 2.NASA Goddard Space flight Center, Greenbelt, USA)

[MAG38-P05] Detecting and quantifying forest dynamics using SAR time-series data in Indonesia

*Pedro Rodriguez-Veiga[1,2,3], Narumasa Tsutsumida[3] (1.Centre for Landscape and Climate Research, University of Leicester, Leicester, UK, 2.NERC National Centre for Earth Observation (NCEO), Leicester, UK, 3.Graduate School of Global Environmental Studies, Kyoto University, Japan)

Improving the AVHRR LTDR BRDF correction

*Jose Luis Villaescusa[1,2], Belen Franch[1,2], Jean-Claude Roger[1,2], Eric Vermote[2]

1. University of Maryland College Park, 2. NASA Goddard Space Flight Center

The Advanced Very High Resolution Radiometer (AVHRR) sensors aboard the different NOAA satellites provide a unique global remote sensing dataset that ranges from the 1980s to the present. Using these data, the NASA funded Long Term Data Record (LTDR) project aims to develop a quality and consistent Climate Data Record (CDR) of AVHRR data with the use of the Moderate Resolution Imaging Spectrometer (MODIS) instrument as a reference. This product retrieves the BRDF corrected land surface reflectance using the VJB method (Vermote et al., 2009), which corrects the anisotropic effects by obtaining Volumetric (V) and Geometrical (R) parameters, defined in the Roujean model (Roujean et al., 1992), as a function of the Normalized Difference Vegetation Index (NDVI). Inaccuracies regarding the AVHRR atmospheric correction and calibration in the red band for the pre-MODIS era (1982-2000), propagate towards the surface reflectance’ s BRDF correction. However, with the use of the less noisy Near-Infrared (NIR) band we can reduce said errors by finding an empirical relationship between the red-NIR V and R parameters. This study aims to find said relationship using the MODIS sensor, which is an already established and accurate product (Justice et al., 2002; Liang et al., 2002), to then apply it to the noisy AVHRR data and reduce the BRDF errors in the red band.

Keywords: AVHRR, VJB, MODIS, BRDF, LTDR

©2019. Japan Geoscience Union. All Right Reserved.

Winter wheat yield model based on remote sensing data

*Belen Franch[1,2], Eric Vermote[2,1], Sergii Skakun[1,2], Jean-Claude Roger[1,2], Inbal Becker-Reshef[1], Chris Justice[1]

1. Department of Geographical Sciences, University of Maryland, 2. NASA Goddard Space Flight Center

Accurate and timely crop yield forecasts are critical for making informed agricultural policies and investments, as well as increasing market efficiency and stability. Earth observation data from space can contribute to agricultural monitoring, including crop yield assessment and forecasting. This work presents a new EO-based empirical winter wheat yield model. It is based on the un-mixing of the wheat signal from a coarse resolution EO data at 1 km by using yearly crop type masks to a pure wheat signal (100% of wheat within the pixel). *This wheat signal is used to calibrate the model using as inputs the seasonal amplitude and length of the Difference Vegetation Index (DVI) peak extracted from Moderate Resolution Imaging Spectroradiometer (MODIS) data and the average of the evaporative fraction (EF) 30 days after the peak. The three regressors proposed are focused on the reproduction stage of the wheat (DVI amplitude and length) and the grain filling process (EF 30-days average). The model is calibrated at subnational level using historical statistics from 2001 to 2016. In each administrative unit, a different calibration coefficient (based on all possible combination of the three regressors in a linear model) is selected depending on the statistical significance of each variable. The model was applied to estimate the national and subnational winter wheat yield in the United States, Ukraine, Russia and France from 2001 to 2017. At the subnational level the model shows very good performance with a coefficient of determination higher than 0.7 and Root Mean Square Error (RMSE) lower than 15%. At the national level the model provides a strong coefficient of determination higher than 0.8 and a RMSE lower than 8%, which demonstrates good performance of the models at this scale. Additionally, it was also able to capture low winter wheat yields during years with extreme weather events, for example 2002 in US and 2003 in Ukraine.*

Keywords: Yield model, MODIS , agriculture

©2019. Japan Geoscience Union. All Right Reserved.

Agricultural monitoring from Optical and SAR data

*Andrés Eduardo Santamaría-Artigas[1,2], Sergii Skakun[1,2], Belen Franch[1,2], Jean-Claude Roger[1,2], Eric Vermote[2]

1. University of Maryland College Park, 2. NASA Goddard Space Flight Center

Vegetation indices derived from optical remote sensing data are a valuable source of information for agricultural monitoring. However, cloud cover over some areas reduces the number of valid observations, which can difficult the detection of changes in crop condition. In this context, synthetic aperture radar (SAR) systems are an interesting alternative due to their low sensitivity to clouds. In this work, we analyze the relationship between SAR backscatter from Sentinel-1 and vegetation indices derived from the Harmonized Landsat-8 Sentinel-2 (HLS) product with data from the year 2017 over 6 land cover classes in Ukraine: Winter crops, summer crops, bare land, grasslands, forest, and water. Results show that SAR data from Sentinel-1 could be used to complement optical indices for certain land covers. In the case of winter crops (rapeseed and wheat), the ratio between Sigma-0 VV and VH polarization showed the highest relationship with the Normalized Difference Vegetation Index (NDVI) while for summer crops (maize, sugar beet, sunflower, and soybean) the highest relationship was shown by the Sigma-0 VH polarization and NDVI. Further work is being developed to exploit more complex SAR models which account for other variables that affect the backscatter signal such as soil moisture.

Keywords: agricultural monitoring, crop condition, synthetic aperture radar, HLS, normalized difference vegetation index

©2019. Japan Geoscience Union. All Right Reserved.

Eco-hydrological modeling using field-based and Earth Observations to assess water use efficiency and support agricultural water resources management

pierre Guillevic[2,1], *Jean-Claude Roger[1,2]

1. University of Maryland, College Park, USA, 2. NASA Goddard Space flight Center, Greenbelt, USA

The objective of this NASA project is to develop an integrated modeling platform using Earth Observations to simulate large-scale hydrological processes and food production in support of water use decision and agricultural policy. The decision tool will provide timely and relevant assessments of crop growth, agricultural water use and available water supply from local to regional scales, with the capability to predict the impact of different climate and water resources management scenarios on food production. The approach is based on the use of field and Earth observations to calibrate an eco-hydrological model, and climate simulations to forecast crop condition and yield through the crop season. The expected primary outcomes and results for stakeholders is potential best water management practices to improve water use efficiency and prevent excessive losses of water and nitrogen to the environment. These will be provided to in-country end-users within various relevant Ministries and Departments, in order to inform regional and national decisions. Changing precipitation patterns, droughts of increasing duration and severity and growing demand for food have significant implications on water management practices, spurring an increased need for irrigation in a sustainable manner and better monitoring of water resources for the agricultural sector in general. Understanding the context and water resource constraints that stakeholders and smallholder farmers face in climate sensitive regions is critical to target and understand the potential impact of water use management. We focus on a diverse set of regional pilot cases in Argentina, South Africa, Tanzania and the United States that are representative of a range of agricultural systems, water issues and climate impacts. The application is integrated in the GEOGLAM project, an existing widely-used web-based platform which will aid synthesizing the project outcomes and expert domain knowledge to provide timely and actionable water resources and crop condition information to assist local, regional and national water management decisions. At the end, the application will be interactive and will offer the end-user organizations the possibility to submit new water resource management scenarios online for impact evaluation.

Earth Observations are critical to characterize and monitor the different components of agricultural ecosystems and change (forests, croplands and marginal lands availability, for example) across temporal and spatial scales. Satellite data in the shortwave, thermal infrared and microwave spectral domains from US (MODIS, VIIRS, Landsat, SMAP) and European (Sentinel 1 and 2) sensors will be used to characterize changes in land surfaces and water use from 2000 to the present in support of agricultural planning decisions. In a research context, the potential of new satellite missions (i.e., ECOSTRESS, SWOT and SAOACOM) to derive surface hydrology information will be evaluated. The Agricultural Policy/Environmental eXtender (APEX) watershed model is proposed as the modeling tool to understand the biophysical and human-decision processes associated with the food-energy-water nexus. Model simulations will use climate data from the NASA Goddard Earth Observing System Model (GEOS-5) Atmosphere-Ocean General Circulation Model: MERRA-2 for simulation of past conditions and seasonal (6-month) forecasts for projections in the future. The study focus on large, key agricultural regions where agricultural ecosystems are vulnerable to demographic expansion and/or climate variability and change including drought and flood events.

©2019. Japan Geoscience Union. All Right Reserved.

Keywords: water resources, hydrologycal modelling , remote sensing

©2019. Japan Geoscience Union. All Right Reserved.

Detecting and quantifying forest dynamics using SAR time-series data in Indonesia

*Pedro Rodriguez-Veiga[1,2,3], Narumasa Tsutsumida[3]

1. Centre for Landscape and Climate Research, University of Leicester, Leicester, UK, 2. NERC National Centre for Earth Observation (NCEO), Leicester, UK, 3. Graduate School of Global Environmental Studies, Kyoto University, Japan

Satellite Earth Observation (EO) data allows the generation of forest disturbance maps that can improve greenhouse gas (GHG) monitoring at local and national scales, and provide information that can be used for land use planning and management. Mapping forest biomass stocks, deforestation, forest degradation and enhancement is crucial in order to determine the loss of carbon stocks due to disturbances (e.g. deforestation, fires) or the gain due to new forest or growth. Time-series observations identify decreasing or increasing trends of aboveground biomass carbon, and separate anthropogenic related changes from seasonal changes of vegetation. This is important for understanding the terrestrial carbon cycle and for supporting better forest management and policies. This study uses time-series data from L-band Synthetic Aperture Radar (SAR) JAXA’s ALOS PALSAR and ALOS-2 PALSAR-2 to quantify carbon loss and gain trajectories (emission / sequestration) of existing forests in West Java (Indonesia).

Keywords: deforestation, SAR, time-series, forest dynamics

©2019. Japan Geoscience Union. All Right Reserved.

[E] Poster | M (Multidisciplinary and Interdisciplinary)：M-AG Applied Geosciences

Thu. May 30, 2019 5:15 PM - 6:30 PM JST | Thu. May 30, 2019 8:15 AM - 9:30 AM UTC | Poster Hall International Exhibition Hall8, Makuhari Messe_43

[M-AG38] Satellite Land Physical Processes Monitoring at Medium/High/Very High Resolution

convener:Jean-Claude Roger(University of Maryland College Park), Shinichi Sobue(Japan Aerospace Exploration Agency), Eric Vermote(NASA Goddard Space Flight Center)

We solicit papers on the land physical processes monitoring. In particular, it will include the inversion and use of land products from medium, high, and very high spatial resolution. For the last years, medium, high, and very high resolutions became a useful and a powerful toll for Earth studies. Topics of interest mainly include (not limited to):
- New developments for data processing, including atmospheric correction and cloud screening;
- Analysis and correction of directional effects in land surface reflectances;
- Use of time series of surface reflectances for land monitoring, including land cover classification and crop yield prediction (including data integration and data harmonization);
- Development and use of new vegetation indices (i.e. red edge) and other products for agriculture applications;
- Theoretical studies for sensors capabilities enhancements to future sensors at high/medium resolutions;
- Use of products in agricultural monitoring applications (such as crop area, crop type, crop growing, yield estimation and prediction, damage assessment);
- Agriculture monitoring algorithm description;
- Evaluation or validation of potential products with ground measurements, official statistics;
- International initiative to enhance Earth-Observing-based agricultural information.

Depending on outcome, we think about a special issue.

[MAG38-P01] Improving the AVHRR LTDR BRDF correction

*Jose Luis Villaescusa[1,2], Belen Franch[1,2], Jean-Claude Roger[1,2], Eric Vermote[2] (1.University of Maryland College Park, 2.NASA Goddard Space Flight Center)

[MAG38-P02] Winter wheat yield model based on remote sensing data

*Belen Franch[1,2], Eric Vermote[2,1], Sergii Skakun[1,2], Jean-Claude Roger[1,2], Inbal Becker-Reshef[1], Chris Justice[1] (1.Department of Geographical Sciences, University of Maryland, 2.NASA Goddard Space Flight Center)

[MAG38-P03] Agricultural monitoring from Optical and SAR data

*Andrés Eduardo Santamaría-Artigas[1,2], Sergii Skakun[1,2], Belen Franch[1,2], Jean-Claude Roger[1,2], Eric Vermote[2] (1.University of Maryland College Park, 2.NASA Goddard Space Flight Center)

[MAG38-P04] Eco-hydrological modeling using field-based and Earth Observations to assess water use efficiency and support agricultural water resources management

pierre Guillevic[2,1], *Jean-Claude Roger[1,2] (1.University of Maryland, College Park, USA, 2.NASA Goddard Space flight Center, Greenbelt, USA)

[MAG38-P05] Detecting and quantifying forest dynamics using SAR time-series data in Indonesia

*Pedro Rodriguez-Veiga[1,2,3], Narumasa Tsutsumida[3] (1.Centre for Landscape and Climate Research, University of Leicester, Leicester, UK, 2.NERC National Centre for Earth Observation (NCEO), Leicester, UK, 3.Graduate School of Global Environmental Studies, Kyoto University, Japan)

Improving the AVHRR LTDR BRDF correction

*Jose Luis Villaescusa[1,2], Belen Franch[1,2], Jean-Claude Roger[1,2], Eric Vermote[2]

1. University of Maryland College Park, 2. NASA Goddard Space Flight Center

The Advanced Very High Resolution Radiometer (AVHRR) sensors aboard the different NOAA satellites provide a unique global remote sensing dataset that ranges from the 1980s to the present. Using these data, the NASA funded Long Term Data Record (LTDR) project aims to develop a quality and consistent Climate Data Record (CDR) of AVHRR data with the use of the Moderate Resolution Imaging Spectrometer (MODIS) instrument as a reference. This product retrieves the BRDF corrected land surface reflectance using the VJB method (Vermote et al., 2009), which corrects the anisotropic effects by obtaining Volumetric (V) and Geometrical (R) parameters, defined in the Roujean model (Roujean et al., 1992), as a function of the Normalized Difference Vegetation Index (NDVI). Inaccuracies regarding the AVHRR atmospheric correction and calibration in the red band for the pre-MODIS era (1982-2000), propagate towards the surface reflectance’ s BRDF correction. However, with the use of the less noisy Near-Infrared (NIR) band we can reduce said errors by finding an empirical relationship between the red-NIR V and R parameters. This study aims to find said relationship using the MODIS sensor, which is an already established and accurate product (Justice et al., 2002; Liang et al., 2002), to then apply it to the noisy AVHRR data and reduce the BRDF errors in the red band.

Keywords: AVHRR, VJB, MODIS, BRDF, LTDR

©2019. Japan Geoscience Union. All Right Reserved.

Winter wheat yield model based on remote sensing data

*Belen Franch[1,2], Eric Vermote[2,1], Sergii Skakun[1,2], Jean-Claude Roger[1,2], Inbal Becker-Reshef[1], Chris Justice[1]

1. Department of Geographical Sciences, University of Maryland, 2. NASA Goddard Space Flight Center

Accurate and timely crop yield forecasts are critical for making informed agricultural policies and investments, as well as increasing market efficiency and stability. Earth observation data from space can contribute to agricultural monitoring, including crop yield assessment and forecasting. This work presents a new EO-based empirical winter wheat yield model. It is based on the un-mixing of the wheat signal from a coarse resolution EO data at 1 km by using yearly crop type masks to a pure wheat signal (100% of wheat within the pixel). *This wheat signal is used to calibrate the model using as inputs the seasonal amplitude and length of the Difference Vegetation Index (DVI) peak extracted from Moderate Resolution Imaging Spectroradiometer (MODIS) data and the average of the evaporative fraction (EF) 30 days after the peak. The three regressors proposed are focused on the reproduction stage of the wheat (DVI amplitude and length) and the grain filling process (EF 30-days average). The model is calibrated at subnational level using historical statistics from 2001 to 2016. In each administrative unit, a different calibration coefficient (based on all possible combination of the three regressors in a linear model) is selected depending on the statistical significance of each variable. The model was applied to estimate the national and subnational winter wheat yield in the United States, Ukraine, Russia and France from 2001 to 2017. At the subnational level the model shows very good performance with a coefficient of determination higher than 0.7 and Root Mean Square Error (RMSE) lower than 15%. At the national level the model provides a strong coefficient of determination higher than 0.8 and a RMSE lower than 8%, which demonstrates good performance of the models at this scale. Additionally, it was also able to capture low winter wheat yields during years with extreme weather events, for example 2002 in US and 2003 in Ukraine.*

Keywords: Yield model, MODIS , agriculture

©2019. Japan Geoscience Union. All Right Reserved.

Agricultural monitoring from Optical and SAR data

*Andrés Eduardo Santamaría-Artigas[1,2], Sergii Skakun[1,2], Belen Franch[1,2], Jean-Claude Roger[1,2], Eric Vermote[2]

1. University of Maryland College Park, 2. NASA Goddard Space Flight Center

Vegetation indices derived from optical remote sensing data are a valuable source of information for agricultural monitoring. However, cloud cover over some areas reduces the number of valid observations, which can difficult the detection of changes in crop condition. In this context, synthetic aperture radar (SAR) systems are an interesting alternative due to their low sensitivity to clouds. In this work, we analyze the relationship between SAR backscatter from Sentinel-1 and vegetation indices derived from the Harmonized Landsat-8 Sentinel-2 (HLS) product with data from the year 2017 over 6 land cover classes in Ukraine: Winter crops, summer crops, bare land, grasslands, forest, and water. Results show that SAR data from Sentinel-1 could be used to complement optical indices for certain land covers. In the case of winter crops (rapeseed and wheat), the ratio between Sigma-0 VV and VH polarization showed the highest relationship with the Normalized Difference Vegetation Index (NDVI) while for summer crops (maize, sugar beet, sunflower, and soybean) the highest relationship was shown by the Sigma-0 VH polarization and NDVI. Further work is being developed to exploit more complex SAR models which account for other variables that affect the backscatter signal such as soil moisture.

Keywords: agricultural monitoring, crop condition, synthetic aperture radar, HLS, normalized difference vegetation index

©2019. Japan Geoscience Union. All Right Reserved.

Eco-hydrological modeling using field-based and Earth Observations to assess water use efficiency and support agricultural water resources management

pierre Guillevic[2,1], *Jean-Claude Roger[1,2]

1. University of Maryland, College Park, USA, 2. NASA Goddard Space flight Center, Greenbelt, USA

The objective of this NASA project is to develop an integrated modeling platform using Earth Observations to simulate large-scale hydrological processes and food production in support of water use decision and agricultural policy. The decision tool will provide timely and relevant assessments of crop growth, agricultural water use and available water supply from local to regional scales, with the capability to predict the impact of different climate and water resources management scenarios on food production. The approach is based on the use of field and Earth observations to calibrate an eco-hydrological model, and climate simulations to forecast crop condition and yield through the crop season. The expected primary outcomes and results for stakeholders is potential best water management practices to improve water use efficiency and prevent excessive losses of water and nitrogen to the environment. These will be provided to in-country end-users within various relevant Ministries and Departments, in order to inform regional and national decisions. Changing precipitation patterns, droughts of increasing duration and severity and growing demand for food have significant implications on water management practices, spurring an increased need for irrigation in a sustainable manner and better monitoring of water resources for the agricultural sector in general. Understanding the context and water resource constraints that stakeholders and smallholder farmers face in climate sensitive regions is critical to target and understand the potential impact of water use management. We focus on a diverse set of regional pilot cases in Argentina, South Africa, Tanzania and the United States that are representative of a range of agricultural systems, water issues and climate impacts. The application is integrated in the GEOGLAM project, an existing widely-used web-based platform which will aid synthesizing the project outcomes and expert domain knowledge to provide timely and actionable water resources and crop condition information to assist local, regional and national water management decisions. At the end, the application will be interactive and will offer the end-user organizations the possibility to submit new water resource management scenarios online for impact evaluation.

Earth Observations are critical to characterize and monitor the different components of agricultural ecosystems and change (forests, croplands and marginal lands availability, for example) across temporal and spatial scales. Satellite data in the shortwave, thermal infrared and microwave spectral domains from US (MODIS, VIIRS, Landsat, SMAP) and European (Sentinel 1 and 2) sensors will be used to characterize changes in land surfaces and water use from 2000 to the present in support of agricultural planning decisions. In a research context, the potential of new satellite missions (i.e., ECOSTRESS, SWOT and SAOACOM) to derive surface hydrology information will be evaluated. The Agricultural Policy/Environmental eXtender (APEX) watershed model is proposed as the modeling tool to understand the biophysical and human-decision processes associated with the food-energy-water nexus. Model simulations will use climate data from the NASA Goddard Earth Observing System Model (GEOS-5) Atmosphere-Ocean General Circulation Model: MERRA-2 for simulation of past conditions and seasonal (6-month) forecasts for projections in the future. The study focus on large, key agricultural regions where agricultural ecosystems are vulnerable to demographic expansion and/or climate variability and change including drought and flood events.

©2019. Japan Geoscience Union. All Right Reserved.

Keywords: water resources, hydrologycal modelling , remote sensing

©2019. Japan Geoscience Union. All Right Reserved.

Detecting and quantifying forest dynamics using SAR time-series data in Indonesia

*Pedro Rodriguez-Veiga[1,2,3], Narumasa Tsutsumida[3]

1. Centre for Landscape and Climate Research, University of Leicester, Leicester, UK, 2. NERC National Centre for Earth Observation (NCEO), Leicester, UK, 3. Graduate School of Global Environmental Studies, Kyoto University, Japan

Satellite Earth Observation (EO) data allows the generation of forest disturbance maps that can improve greenhouse gas (GHG) monitoring at local and national scales, and provide information that can be used for land use planning and management. Mapping forest biomass stocks, deforestation, forest degradation and enhancement is crucial in order to determine the loss of carbon stocks due to disturbances (e.g. deforestation, fires) or the gain due to new forest or growth. Time-series observations identify decreasing or increasing trends of aboveground biomass carbon, and separate anthropogenic related changes from seasonal changes of vegetation. This is important for understanding the terrestrial carbon cycle and for supporting better forest management and policies. This study uses time-series data from L-band Synthetic Aperture Radar (SAR) JAXA’s ALOS PALSAR and ALOS-2 PALSAR-2 to quantify carbon loss and gain trajectories (emission / sequestration) of existing forests in West Java (Indonesia).

Keywords: deforestation, SAR, time-series, forest dynamics

©2019. Japan Geoscience Union. All Right Reserved.

[E] Poster | M (Multidisciplinary and Interdisciplinary)：M-AG Applied Geosciences

Thu. May 30, 2019 3:30 PM - 5:00 PM JST | Thu. May 30, 2019 6:30 AM - 8:00 AM UTC | Poster Hall International Exhibition Hall8, Makuhari Messe_25

[M-AG40] CTBT IMS Technologies for Detecting Nuclear Explosion and Their Applications to Earth Science

convener:Nurcan Meral Ozel(Comprehensive Nuclear-Test-Ban Treaty Organization), Hiroyuki Matsumoto(Japan Agency for Marine-Earth Science and Technology), Yosuke Naoi(Japan Atomic Energy Agency)

The Comprehensive Nuclear-Test-Ban Treaty Organization (CTBTO) was founded in 1996 in response to the adaption of the Treaty in 1996 by the United Nations General Assembly, which bans nuclear explosions on the Earth's surface, in the atmosphere, underwater and underground. The Treaty has a unique and comprehensive verification regime to make sure that no nuclear explosion goes undetected. The regime is supported by International Monitoring Systems (IMS) composed of the four state-of-art technologies; 1) Seismic, 2) Hydroacoustic, 3) Infrasound, and 4) Radionuclide, by the International Data Centre (IDC), and by the On-Site Inspections (OSI).
IMS will, when complete, consists of 337 facilities worldwide to monitor the planet for signs of nuclear explosion. Around 90 % of the facilities are in operation and sending the data to the IDC in Vienna, Austria.
The huge amount of data collected by the stations can be used for other purposes such as civil and scientific applications in addition to detecting nuclear explosions. They can provide Tsunami Warning centres with near real-time information about an underwater earthquake. During the Fukushima Daiichi Power Plant accident, in March 2011, the IMS network's radionuclide stations tracked the dispersion of radioactivity on a global scale. The data could also help better understand the oceans, volcanos, climate change, the movement of marine mammals, and many other issues.
This session will provide the overview of CTBTO and its IMS, the scientific discussion on each technology, and its outcomes. The session welcomes young scientists and engineers who are interested in four IMS technologies.

[MAG40-P01] Overview of the Japanese National Data Centre-1 (NDC-1)

*RYOHEI EMURA[1], Takayuki Otsu[1], Toyomi Sakamoto[1], Soshi Iwata[1], Takanari Fujii[1], Mami Nogami[1], Makiko Iwakuni[1], Masashi Motohashi[1] (1.Japan Weather Association)

[MAG40-P02] Challenging to utilize the infrasound technologies for civil and science application

*Masashi Motohashi[1], Nobuo Arai[2], Takayuki Otsu[1], Mami Nogami[1], Makiko Iwakuni[1], Ryohei Emura[1] (1.Japan Weather Association, 2.Disaster Mitigation Research Center, Nagoya Unicersity)

[MAG40-P03] CTBT IMS hydroacoustic signal detections from the Ioto volcanic island in the northwest Pacific Ocean

*Hiroyuki Matsumoto[1,2], Mario Zampolli[1], Georgios Haralabus[1], Jerry Stanley[1], James Mattila[1], Nurcan Meral Ozel[1] (1.Comprehensive Nuclear-Test-Ban Treaty Organization (CTBTO), 2.Japan Agency for Marine-Earth Science and Technology (JAMSTEC))

[MAG40-P04] Installation of a floating hydrophone system within the SOFAR channel

*Hiroko Sugioka[1], Masayuki Obayashi[2] (1.Kobe University, 2.JAMSTEC)

[MAG40-P05] Fin whale signals observed at S-net seismic stations

*Takeshi Nakamura[1], Ryoichi Iwase[2] (1.National Research Institute for Earth Science and Disaster Resilience, 2.Japan Agency for Marine-Earth Science and Technology)

[MAG40-P06] Implementation of integrated observation from seafloor through atmosphere – past, current, and future plans

*Keisuke Ariyoshi[1], Akira Nagano[1], Hiroyuki Matsumoto[1], Nurcan Meral Ozel[2] (1.Japan Agency for Marine-Earth Science and Technology, 2.Comprehensive Nuclear-Test-Ban Treaty Organization)

Overview of the Japanese National Data Centre-1 (NDC-1)

*RYOHEI EMURA[1], Takayuki Otsu[1], Toyomi Sakamoto[1], Soshi Iwata[1], Takanari Fujii[1], Mami Nogami[1], Makiko Iwakuni[1], Masashi Motohashi[1]

1. Japan Weather Association

Japan Weather Association (JWA) is working as the Comprehensive Nuclear-Test-Ban Treaty (CTBT) National Data Centre-1 (NDC-1) of Japan which is in charge of analysis on waveform data, operation and maintenance of seismic and infrasound stations in Japan. There are two main roles of NDC-1: 1: technical adviser to the national authority (MOFA) from the view point of seismic and infrasound analysis, and 2: station operator of IMS stations (PS22, AS51-AS55 and IS30). And there are three main activities of NDC-1 as technical adviser: 1: if the suspicious event would occur, we would try to clarify its characteristics and report its results to the MOFA via the secretariat, 2: we sometimes do 1-week integrated operational exercise hosted by the secretariat on the assumption that the situation would be, and 3: we are paying efforts to improve our analytical capability of SHI data and explanation capability by using the national exercises.

This poster introduces the integrated operational exercise and the event discrimination analysis results of the 6th DPRK nuclear test as of the real analysis results in particular.

The integrated operational exercise is conducted by NDCs, integrating the data and analysis addressed by NDCs, and reporting to the CTBT National Operating System of Japan. These exercises have been implemented 27 times since 2009 and 30areas were selected for regions and countries. And our event discrimination analysis takes mainly three methods: 1: regional P/S ratio, 2: P/S spectral ratio and 3: mb: Ms.

Keywords: CTBT, National Data Centre, seismic, infrasound, waveform analysis, event discrimination analysis

©2019. Japan Geoscience Union. All Right Reserved.

Challenging to utilize the infrasound technologies for civil and science application

*Masashi Motohashi[1], Nobuo Arai[2], Takayuki Otsu[1], Mami Nogami[1], Makiko Iwakuni[1], Ryohei Emura[1]

1. Japan Weather Association, 2. Disaster Mitigation Research Center, Nagoya Unicersity

Japan Weather Association (JWA) is working as the Comprehensive Nuclear-Test-Ban Treaty (CTBT) National Data Centre-1 (NDC-1) of Japan which is in charge of analysis on waveform data, operation and maintenance of infrasound and seismic stations in Japan.

We observed infrasonic signals two times from underground nuclear test in DPRK. From the perspective of nuclear test monitoring, it is important to analyze and study the infrasonic signals from a variety of natural phenomena to discriminate the signal from explosion. On the other hand, that kind of studies are also important for civil and science application of infrasound technologies. We also observed infrasound from large tsunami at the time of 2011 off the Pacific coast of Tohoku Earthquake. If the signals from such hazardous phenomena can be detected immediately, it will be very helpful to alert the occurrence of disaster or approach of hazardous phenomena.

This triggered us to build our own observation network in Japan. We are challenging to utilize the infrasound technologies for civil and science application as well as nuclear test monitoring.

Keywords: Barometer, Infrasound, CTBT

©2019. Japan Geoscience Union. All Right Reserved.

CTBT IMS hydroacoustic signal detections from the Ioto volcanic island in the northwest Pacific Ocean

*Hiroyuki Matsumoto[1,2], Mario Zampolli[1], Georgios Haralabus[1], Jerry Stanley[1], James Mattila[1], Nurcan Meral Ozel[1]

1. Comprehensive Nuclear-Test-Ban Treaty Organization (CTBTO), 2. Japan Agency for Marine-Earth Science and Technology (JAMSTEC)

In-situ observation in terms of seismicity suggested that the volcanic activity of Ioto (formerly Iwojima), a volcanic island offshore Japan in the northwest Pacific Ocean increased in early September in 2018. Discolored waters and a splash were confirmed in the nearshore by a local flyover observation. Although these visual signs evidenced a connection between undersea eruptions and recorded seismic activity, there still remained uncertainty as to what portion of the *in-situ* recorded seismic activity was associated with volcanic tremors vs. undersea eruptive events.
During the same period, a large number of underwater acoustic (hydroacoustic) signals were recorded by the Comprehensive Nuclear-Test-Ban Treaty’s (CTBT) International Monitoring System (IMS) hydroacoustic (HA) station HA11 Wake Island. A set of three hydrophone sensors forming a triplet makes it possible to compute the back-azimuth uniquely for wave packets with a good signal-to-noise ratio. We analyzed the data of the IMS hydrophone triplets during the month of September 2018 and compared them with *in-situ* seismic observations in Ioto for the same period.
The IMS hydrophone triplet data made it possible to discriminate the hydroacoustic signals associated with the Ioto volcanic activity. The direction-of-arrival (DOA) was estimated during the entire period of relatively high volcanic activity using cross-correlation analysis. The arrivals from Ioto at the IMS HA station and the *in-situ* observations showed good correlation. The present study suggests that two-thirds of the arrivals of hydroacoustec signals were associated with volcanic tremors and one-third with the undersea eruptions.

Keywords: Internataional Monitoring System (IMS), Hydrophone triplet, Ioto

©2019. Japan Geoscience Union. All Right Reserved.

Installation of a floating hydrophone system within the SOFAR channel

*Hiroko Sugioka[1], Masayuki Obayashi[2]

1. Kobe University, 2. JAMSTEC

Unequal geographical data coverage continues to fundamentally limit the quality of tomographic reconstructions of seismic wave speeds in the interior of the Earth. Only at great cost can geophysicists overcome the difficulties of placing seismographs on the two thirds of the Earth’ s surface that is covered by oceans. The lack of spatial data coverage strongly hampers the determination of the structure of the Earth in the uncovered regions. Therefore, three-dimensional Earth models are marked by blank spots in areas where little or no information can be obtained. Improving this problem requires the observation of seismic waves in the oceans. Ocean bottom seismometers are capable of addressing the coverage gap, but they are expensive to manufacture and deploy using vessels.

Oceanographers had designed robotic floating instruments, floats that spend their lives at depth but surface periodically, using a pump and bladder, to make temperature and salinity profile measurements (the large-scale international Argo project). Such low-cost Sounding Oceanographic Lagrangian Observers (SOLO) (Davis et al., 2001) could be equipped with a hydrophone to record water pressure variations induced by compressional waves. Such a floating seismometer would surface upon detection of a useful seismic event, determine a GPS location, and transmit the waveforms to a satellite, which is nicknamed MERMAID for ‘mobile earthquake recorder in marine areas by independent divers’. The great promise of this technology has been demonstrated since the first voyage in 2003, clearly illustrates its contributions to global seismology.

We installed five MERMAID floats in the South Pacific Ocean in late December of 2018 to early January of 2019 during the MR18-06 Leg 1 cruise from Japan to Chile using the R/V Mirai of JAMSTEC under an international project of SPPIM (South Pacific Plume Imaging with MERMAIDs). The launching locations for MERMAIDs are (01-42.256N,146-12.472W), (03-19.696S, 139-31.973W), (15-55.626S, 120-07.688W), (18-31.285S, 114-57.378W) and (20-59.832S, 109-59.513W), respectively. All floats have been drifting to almost west since the deployment as recording to transfer the land at sea surface every 10 days. So far, MERMAID detected several seismic events, for example, the Mw 6.8 Brazil deep focus earthquake at depth of 575 km on January 5. MERMAID recorded a clear incoming P-wave whose precise arrival time can be determined to within a fraction of a second. In addition to recording teleseismic P-waves, they would pick up hydroacoustic phases (T-waves) trapped waves propagating in the SOFAR (Sound Fixing and Ranging) channel. They might be complementary to the global seismic network including CTBTO stations to recognize unknown enigmatic events.

Keywords: SOFAR channel, Hydroacoustic waves

©2019. Japan Geoscience Union. All Right Reserved.

Fin whale signals observed at S-net seismic stations

*Takeshi Nakamura[1], Ryoichi Iwase[2]

1. National Research Institute for Earth Science and Disaster Resilience, 2. Japan Agency for Marine-Earth Science and Technology

Real-time earthquake and tsunami seafloor station network called “S-net” (Seafloor observation network for earthquakes and tsunamis along the Japan Trench) was developed by National Research Institute for Earth Science and Disaster Resilience (NIED) in water depths of 100-7,830 m in northeastern Japan. The network consists of 150 observation stations off Boso to Kushiro and Aomori areas (Kanazawa et al., 2016; Uehira et al. 2016; Mochizuki et al., 2016). Each station has seismic sensors and pressure gauges to observe broadband signals from seismic event and tsunami. In this study, we show fin whale signals detected from the S-net data and present the seasonal variation of the signals and the migratory behavior of the whales.

We analyzed seismic station data of S-net from 2016 to 2018. We found characteristic signals with the spectral peak in the frequency bands of 15-25 Hz. One of remarkable features in the signals is that the band width that can be identified as signal is limited in a very narrow range; the signal level is very low or below the noise level in the frequency bands of less than 10 Hz that are typical bands in seismic waves and T-phases. Another feature is that the signals have a short duration of about 1 second and are repeatedly found at regular intervals of several tens of seconds. These are consistent with the features of acoustic signals from fin whales as found in observation data at IMS hydroacoustic stations (e.g., Lawrence, 2004) and also as shown in previous studies such as Iwase (2014) and Sugioka et al. (2015) that analyzed seafloor station data off the Kushiro-Tokachi cable sensor system. We thus assume that the characteristic signals observed at S-net stations are ones associated with fin whale activities. Most of the signals were detected at stations off Kushiro and Aomori areas in cold winter. The signals were also detected at stations deployed in the outer rise area. We suppose that integrated scientific studies across marine biology to geophysics using S-net data could contribute to developing our understandings of various signal sources observed in seafloor areas and of ecological behavior of marine mammals and also to real-time monitoring of their activities and safe navigation of ships by the monitoring.

Keywords: seafloor observation, S-net, fin whale

©2019. Japan Geoscience Union. All Right Reserved.

Implementation of integrated observation from seafloor through atmosphere –past, current, and future plans

*Keisuke Ariyoshi[1], Akira Nagano[1], Hiroyuki Matsumoto[1], Nurcan Meral Ozel[2]

1. Japan Agency for Marine-Earth Science and Technology, 2. Comprehensive Nuclear-Test-Ban Treaty Organization

The authors have challenged to promote our understandings of global dynamics associated with ocean physics particularly by the simultaneous observation through the seafloor to the atmosphere. We have initiated the total station using both D/V ‘Chikyu’ and the seafloor observatory network ‘DONET’ in the Nankai trough. This total station has clarified the Kuroshio current variation in this region by using both the ambient pressure at DONET and the surface current measurement at D/V ‘Chikyu’. This observation performed at the point where D/V ‘Chikyu’ was in operation for a few months, and therefore there still remained some difficulties to extend to areal and long-term observation. Now, we try to extend our proposed total station to the nearshore network from the point of view of not only scientific application but also civil use for natural disaster mitigation such as earthquake, tsunami, and high-tide caused by storm. On the other hand, a global permanent observation network has been developed and operated by the Comprehensive Nuclear-Test-Ban Treaty Organization (CTBTO) since the 2000s as the International Monitoring System (IMS) regime for the real-time monitoring of nuclear explosion’s test in the underground, underwater, and above surface up to the atmosphere. Four technologies with over 330 stations will cover the entire Earth after certification of all of stations. Three categories of geophysical observations of four technologies such as seismic (50 primary and 120 auxiliary stations), infrasound (60 stations), and hydro-acoustic (11 stations) network operated globally may be beneficial and of interest for our proposed integrated observations. In the presentation, we introduce the preliminary results on our integrated observation of total stations and our drawing blue print of future plans.

Keywords: seismic observation, seafloor cabled network, disaster mitigation

©2019. Japan Geoscience Union. All Right Reserved.

[E] Poster | M (Multidisciplinary and Interdisciplinary)：M-AG Applied Geosciences

Thu. May 30, 2019 5:15 PM - 6:30 PM JST | Thu. May 30, 2019 8:15 AM - 9:30 AM UTC | Poster Hall International Exhibition Hall8, Makuhari Messe_45

[M-AG40] CTBT IMS Technologies for Detecting Nuclear Explosion and Their Applications to Earth Science

convener:Nurcan Meral Ozel(Comprehensive Nuclear-Test-Ban Treaty Organization), Hiroyuki Matsumoto(Japan Agency for Marine-Earth Science and Technology), Yosuke Naoi(Japan Atomic Energy Agency)

The Comprehensive Nuclear-Test-Ban Treaty Organization (CTBTO) was founded in 1996 in response to the adaption of the Treaty in 1996 by the United Nations General Assembly, which bans nuclear explosions on the Earth's surface, in the atmosphere, underwater and underground. The Treaty has a unique and comprehensive verification regime to make sure that no nuclear explosion goes undetected. The regime is supported by International Monitoring Systems (IMS) composed of the four state-of-art technologies; 1) Seismic, 2) Hydroacoustic, 3) Infrasound, and 4) Radionuclide, by the International Data Centre (IDC), and by the On-Site Inspections (OSI).
IMS will, when complete, consists of 337 facilities worldwide to monitor the planet for signs of nuclear explosion. Around 90 % of the facilities are in operation and sending the data to the IDC in Vienna, Austria.
The huge amount of data collected by the stations can be used for other purposes such as civil and scientific applications in addition to detecting nuclear explosions. They can provide Tsunami Warning centres with near real-time information about an underwater earthquake. During the Fukushima Daiichi Power Plant accident, in March 2011, the IMS network's radionuclide stations tracked the dispersion of radioactivity on a global scale. The data could also help better understand the oceans, volcanos, climate change, the movement of marine mammals, and many other issues.
This session will provide the overview of CTBTO and its IMS, the scientific discussion on each technology, and its outcomes. The session welcomes young scientists and engineers who are interested in four IMS technologies.

[MAG40-P01] Overview of the Japanese National Data Centre-1 (NDC-1)

*RYOHEI EMURA[1], Takayuki Otsu[1], Toyomi Sakamoto[1], Soshi Iwata[1], Takanari Fujii[1], Mami Nogami[1], Makiko Iwakuni[1], Masashi Motohashi[1] (1.Japan Weather Association)

[MAG40-P02] Challenging to utilize the infrasound technologies for civil and science application

*Masashi Motohashi[1], Nobuo Arai[2], Takayuki Otsu[1], Mami Nogami[1], Makiko Iwakuni[1], Ryohei Emura[1] (1.Japan Weather Association, 2.Disaster Mitigation Research Center, Nagoya Unicersity)

[MAG40-P03] CTBT IMS hydroacoustic signal detections from the Ioto volcanic island in the northwest Pacific Ocean

*Hiroyuki Matsumoto[1,2], Mario Zampolli[1], Georgios Haralabus[1], Jerry Stanley[1], James Mattila[1], Nurcan Meral Ozel[1] (1.Comprehensive Nuclear-Test-Ban Treaty Organization (CTBTO), 2.Japan Agency for Marine-Earth Science and Technology (JAMSTEC))

[MAG40-P04] Installation of a floating hydrophone system within the SOFAR channel

*Hiroko Sugioka[1], Masayuki Obayashi[2] (1.Kobe University, 2.JAMSTEC)

[MAG40-P05] Fin whale signals observed at S-net seismic stations

*Takeshi Nakamura[1], Ryoichi Iwase[2] (1.National Research Institute for Earth Science and Disaster Resilience, 2.Japan Agency for Marine-Earth Science and Technology)

[MAG40-P06] Implementation of integrated observation from seafloor through atmosphere – past, current, and future plans

*Keisuke Ariyoshi[1], Akira Nagano[1], Hiroyuki Matsumoto[1], Nurcan Meral Ozel[2] (1.Japan Agency for Marine-Earth Science and Technology, 2.Comprehensive Nuclear-Test-Ban Treaty Organization)

Overview of the Japanese National Data Centre-1 (NDC-1)

*RYOHEI EMURA[1], Takayuki Otsu[1], Toyomi Sakamoto[1], Soshi Iwata[1], Takanari Fujii[1], Mami Nogami[1], Makiko Iwakuni[1], Masashi Motohashi[1]

1. Japan Weather Association

Japan Weather Association (JWA) is working as the Comprehensive Nuclear-Test-Ban Treaty (CTBT) National Data Centre-1 (NDC-1) of Japan which is in charge of analysis on waveform data, operation and maintenance of seismic and infrasound stations in Japan. There are two main roles of NDC-1: 1: technical adviser to the national authority (MOFA) from the view point of seismic and infrasound analysis, and 2: station operator of IMS stations (PS22, AS51-AS55 and IS30). And there are three main activities of NDC-1 as technical adviser: 1: if the suspicious event would occur, we would try to clarify its characteristics and report its results to the MOFA via the secretariat, 2: we sometimes do 1-week integrated operational exercise hosted by the secretariat on the assumption that the situation would be, and 3: we are paying efforts to improve our analytical capability of SHI data and explanation capability by using the national exercises.

This poster introduces the integrated operational exercise and the event discrimination analysis results of the 6th DPRK nuclear test as of the real analysis results in particular.

The integrated operational exercise is conducted by NDCs, integrating the data and analysis addressed by NDCs, and reporting to the CTBT National Operating System of Japan. These exercises have been implemented 27 times since 2009 and 30areas were selected for regions and countries. And our event discrimination analysis takes mainly three methods: 1: regional P/S ratio, 2: P/S spectral ratio and 3: mb: Ms.

Keywords: CTBT, National Data Centre, seismic, infrasound, waveform analysis, event discrimination analysis

©2019. Japan Geoscience Union. All Right Reserved.

Challenging to utilize the infrasound technologies for civil and science application

*Masashi Motohashi[1], Nobuo Arai[2], Takayuki Otsu[1], Mami Nogami[1], Makiko Iwakuni[1], Ryohei Emura[1]

1. Japan Weather Association, 2. Disaster Mitigation Research Center, Nagoya Unicersity

Japan Weather Association (JWA) is working as the Comprehensive Nuclear-Test-Ban Treaty (CTBT) National Data Centre-1 (NDC-1) of Japan which is in charge of analysis on waveform data, operation and maintenance of infrasound and seismic stations in Japan.

We observed infrasonic signals two times from underground nuclear test in DPRK. From the perspective of nuclear test monitoring, it is important to analyze and study the infrasonic signals from a variety of natural phenomena to discriminate the signal from explosion. On the other hand, that kind of studies are also important for civil and science application of infrasound technologies. We also observed infrasound from large tsunami at the time of 2011 off the Pacific coast of Tohoku Earthquake. If the signals from such hazardous phenomena can be detected immediately, it will be very helpful to alert the occurrence of disaster or approach of hazardous phenomena.

This triggered us to build our own observation network in Japan. We are challenging to utilize the infrasound technologies for civil and science application as well as nuclear test monitoring.

Keywords: Barometer, Infrasound, CTBT

©2019. Japan Geoscience Union. All Right Reserved.

CTBT IMS hydroacoustic signal detections from the Ioto volcanic island in the northwest Pacific Ocean

*Hiroyuki Matsumoto[1,2], Mario Zampolli[1], Georgios Haralabus[1], Jerry Stanley[1], James Mattila[1], Nurcan Meral Ozel[1]

1. Comprehensive Nuclear-Test-Ban Treaty Organization (CTBTO), 2. Japan Agency for Marine-Earth Science and Technology (JAMSTEC)

In-situ observation in terms of seismicity suggested that the volcanic activity of Ioto (formerly Iwojima), a volcanic island offshore Japan in the northwest Pacific Ocean increased in early September in 2018. Discolored waters and a splash were confirmed in the nearshore by a local flyover observation. Although these visual signs evidenced a connection between undersea eruptions and recorded seismic activity, there still remained uncertainty as to what portion of the *in-situ* recorded seismic activity was associated with volcanic tremors vs. undersea eruptive events.
During the same period, a large number of underwater acoustic (hydroacoustic) signals were recorded by the Comprehensive Nuclear-Test-Ban Treaty’s (CTBT) International Monitoring System (IMS) hydroacoustic (HA) station HA11 Wake Island. A set of three hydrophone sensors forming a triplet makes it possible to compute the back-azimuth uniquely for wave packets with a good signal-to-noise ratio. We analyzed the data of the IMS hydrophone triplets during the month of September 2018 and compared them with *in-situ* seismic observations in Ioto for the same period.
The IMS hydrophone triplet data made it possible to discriminate the hydroacoustic signals associated with the Ioto volcanic activity. The direction-of-arrival (DOA) was estimated during the entire period of relatively high volcanic activity using cross-correlation analysis. The arrivals from Ioto at the IMS HA station and the *in-situ* observations showed good correlation. The present study suggests that two-thirds of the arrivals of hydroacoustec signals were associated with volcanic tremors and one-third with the undersea eruptions.

Keywords: Internataional Monitoring System (IMS), Hydrophone triplet, Ioto

©2019. Japan Geoscience Union. All Right Reserved.

Installation of a floating hydrophone system within the SOFAR channel

*Hiroko Sugioka[1], Masayuki Obayashi[2]

1. Kobe University, 2. JAMSTEC

Unequal geographical data coverage continues to fundamentally limit the quality of tomographic reconstructions of seismic wave speeds in the interior of the Earth. Only at great cost can geophysicists overcome the difficulties of placing seismographs on the two thirds of the Earth’ s surface that is covered by oceans. The lack of spatial data coverage strongly hampers the determination of the structure of the Earth in the uncovered regions. Therefore, three-dimensional Earth models are marked by blank spots in areas where little or no information can be obtained. Improving this problem requires the observation of seismic waves in the oceans. Ocean bottom seismometers are capable of addressing the coverage gap, but they are expensive to manufacture and deploy using vessels.

Oceanographers had designed robotic floating instruments, floats that spend their lives at depth but surface periodically, using a pump and bladder, to make temperature and salinity profile measurements (the large-scale international Argo project). Such low-cost Sounding Oceanographic Lagrangian Observers (SOLO) (Davis et al., 2001) could be equipped with a hydrophone to record water pressure variations induced by compressional waves. Such a floating seismometer would surface upon detection of a useful seismic event, determine a GPS location, and transmit the waveforms to a satellite, which is nicknamed MERMAID for ‘mobile earthquake recorder in marine areas by independent divers’. The great promise of this technology has been demonstrated since the first voyage in 2003, clearly illustrates its contributions to global seismology.

We installed five MERMAID floats in the South Pacific Ocean in late December of 2018 to early January of 2019 during the MR18-06 Leg 1 cruise from Japan to Chile using the R/V Mirai of JAMSTEC under an international project of SPPIM (South Pacific Plume Imaging with MERMAIDs). The launching locations for MERMAIDs are (01-42.256N,146-12.472W), (03-19.696S, 139-31.973W), (15-55.626S, 120-07.688W), (18-31.285S, 114-57.378W) and (20-59.832S, 109-59.513W), respectively. All floats have been drifting to almost west since the deployment as recording to transfer the land at sea surface every 10 days. So far, MERMAID detected several seismic events, for example, the Mw 6.8 Brazil deep focus earthquake at depth of 575 km on January 5. MERMAID recorded a clear incoming P-wave whose precise arrival time can be determined to within a fraction of a second. In addition to recording teleseismic P-waves, they would pick up hydroacoustic phases (T-waves) trapped waves propagating in the SOFAR (Sound Fixing and Ranging) channel. They might be complementary to the global seismic network including CTBTO stations to recognize unknown enigmatic events.

Keywords: SOFAR channel, Hydroacoustic waves

©2019. Japan Geoscience Union. All Right Reserved.

Fin whale signals observed at S-net seismic stations

*Takeshi Nakamura[1], Ryoichi Iwase[2]

1. National Research Institute for Earth Science and Disaster Resilience, 2. Japan Agency for Marine-Earth Science and Technology

Real-time earthquake and tsunami seafloor station network called “S-net” (Seafloor observation network for earthquakes and tsunamis along the Japan Trench) was developed by National Research Institute for Earth Science and Disaster Resilience (NIED) in water depths of 100-7,830 m in northeastern Japan. The network consists of 150 observation stations off Boso to Kushiro and Aomori areas (Kanazawa et al., 2016; Uehira et al. 2016; Mochizuki et al., 2016). Each station has seismic sensors and pressure gauges to observe broadband signals from seismic event and tsunami. In this study, we show fin whale signals detected from the S-net data and present the seasonal variation of the signals and the migratory behavior of the whales.

We analyzed seismic station data of S-net from 2016 to 2018. We found characteristic signals with the spectral peak in the frequency bands of 15-25 Hz. One of remarkable features in the signals is that the band width that can be identified as signal is limited in a very narrow range; the signal level is very low or below the noise level in the frequency bands of less than 10 Hz that are typical bands in seismic waves and T-phases. Another feature is that the signals have a short duration of about 1 second and are repeatedly found at regular intervals of several tens of seconds. These are consistent with the features of acoustic signals from fin whales as found in observation data at IMS hydroacoustic stations (e.g., Lawrence, 2004) and also as shown in previous studies such as Iwase (2014) and Sugioka et al. (2015) that analyzed seafloor station data off the Kushiro-Tokachi cable sensor system. We thus assume that the characteristic signals observed at S-net stations are ones associated with fin whale activities. Most of the signals were detected at stations off Kushiro and Aomori areas in cold winter. The signals were also detected at stations deployed in the outer rise area. We suppose that integrated scientific studies across marine biology to geophysics using S-net data could contribute to developing our understandings of various signal sources observed in seafloor areas and of ecological behavior of marine mammals and also to real-time monitoring of their activities and safe navigation of ships by the monitoring.

Keywords: seafloor observation, S-net, fin whale

©2019. Japan Geoscience Union. All Right Reserved.

Implementation of integrated observation from seafloor through atmosphere –past, current, and future plans

*Keisuke Ariyoshi[1], Akira Nagano[1], Hiroyuki Matsumoto[1], Nurcan Meral Ozel[2]

1. Japan Agency for Marine-Earth Science and Technology, 2. Comprehensive Nuclear-Test-Ban Treaty Organization

The authors have challenged to promote our understandings of global dynamics associated with ocean physics particularly by the simultaneous observation through the seafloor to the atmosphere. We have initiated the total station using both D/V ‘Chikyu’ and the seafloor observatory network ‘DONET’ in the Nankai trough. This total station has clarified the Kuroshio current variation in this region by using both the ambient pressure at DONET and the surface current measurement at D/V ‘Chikyu’. This observation performed at the point where D/V ‘Chikyu’ was in operation for a few months, and therefore there still remained some difficulties to extend to areal and long-term observation. Now, we try to extend our proposed total station to the nearshore network from the point of view of not only scientific application but also civil use for natural disaster mitigation such as earthquake, tsunami, and high-tide caused by storm. On the other hand, a global permanent observation network has been developed and operated by the Comprehensive Nuclear-Test-Ban Treaty Organization (CTBTO) since the 2000s as the International Monitoring System (IMS) regime for the real-time monitoring of nuclear explosion’s test in the underground, underwater, and above surface up to the atmosphere. Four technologies with over 330 stations will cover the entire Earth after certification of all of stations. Three categories of geophysical observations of four technologies such as seismic (50 primary and 120 auxiliary stations), infrasound (60 stations), and hydro-acoustic (11 stations) network operated globally may be beneficial and of interest for our proposed integrated observations. In the presentation, we introduce the preliminary results on our integrated observation of total stations and our drawing blue print of future plans.

Keywords: seismic observation, seafloor cabled network, disaster mitigation

©2019. Japan Geoscience Union. All Right Reserved.